frontiers | Research Topics

Adaptive nutrient management systems for plant nutrition: optimization, profitability, and ecosystem assessment

Edited by
Henry Yabbey Sintim, Khurram Shahzad and Xinhua Yin Yin

Published in
Frontiers in Plant Science

ISSN 1664-8714
ISBN 978-2-8325-6175-1
DOI 10.3389/978-2-8325-6175-1

About Frontiers

Frontiers is more than just an open access publisher of scholarly articles: it is a pioneering approach to the world of academia, radically improving the way scholarly research is managed. The grand vision of Frontiers is a world where all people have an equal opportunity to seek, share and generate knowledge. Frontiers provides immediate and permanent online open access to all its publications, but this alone is not enough to realize our grand goals.

Frontiers journal series

The Frontiers journal series is a multi-tier and interdisciplinary set of open-access, online journals, promising a paradigm shift from the current review, selection and dissemination processes in academic publishing. All Frontiers journals are driven by researchers for researchers; therefore, they constitute a service to the scholarly community. At the same time, the *Frontiers journal series* operates on a revolutionary invention, the tiered publishing system, initially addressing specific communities of scholars, and gradually climbing up to broader public understanding, thus serving the interests of the lay society, too.

Dedication to quality

Each Frontiers article is a landmark of the highest quality, thanks to genuinely collaborative interactions between authors and review editors, who include some of the world's best academicians. Research must be certified by peers before entering a stream of knowledge that may eventually reach the public - and shape society; therefore, Frontiers only applies the most rigorous and unbiased reviews. Frontiers revolutionizes research publishing by freely delivering the most outstanding research, evaluated with no bias from both the academic and social point of view. By applying the most advanced information technologies, Frontiers is catapulting scholarly publishing into a new generation.

What are Frontiers Research Topics?

Frontiers Research Topics are very popular trademarks of the *Frontiers journals series*: they are collections of at least ten articles, all centered on a particular subject. With their unique mix of varied contributions from Original Research to Review Articles, Frontiers Research Topics unify the most influential researchers, the latest key findings and historical advances in a hot research area.

Find out more on how to host your own Frontiers Research Topic or contribute to one as an author by contacting the Frontiers editorial office: frontiersin.org/about/contact

Adaptive nutrient management systems for plant nutrition: optimization, profitability, and ecosystem assessment

Topic editors
Henry Yabbey Sintim — The University of Georgia, Tifton Campus, United States
Khurram Shahzad — Lasbela University of Agriculture, Water and Marine Sciences, Pakistan
Xinhua Yin Yin — The University of Tennessee, Knoxville, United States

Citation
Sintim, H. Y., Shahzad, K., Yin, X. Y., eds. (2025). *Adaptive nutrient management systems for plant nutrition: optimization, profitability, and ecosystem assessment*. Lausanne: Frontiers Media SA. doi: 10.3389/978-2-8325-6175-1

Table of contents

frontiers | Frontiers in Plant Science

ORIGINAL RESEARCH
published: 19 May 2022
doi: 10.3389/fpls.2022.863211

Evaluating Decision Support Tools for Precision Nitrogen Management on Creeping Bentgrass Putting Greens

Qiyu Zhou and Douglas J. Soldat**

Department of Soil Science, University of Wisconsin-Madison, Madison, WI, United States

Nitrogen (N) is the most limiting nutrient for turfgrass growth. Few tools or soil tests exist to help managers guide N fertilizer decisions. Turf growth prediction models have the potential to be useful, but the lone turfgrass growth prediction model only takes into account temperature, limiting its accuracy. This study investigated the ability of a machine learning (ML)-based turf growth model using the random forest (RF) algorithm (ML-RF model) to improve creeping bentgrass (*Agrostis stolonifera*) putting green management by estimating short-term clipping yield. This method was compared against three alternative N application strategies including (1) PACE Turf growth potential (GP) model, (2) an experience-based method for applying N fertilizer (experience-based method), and (3) the experience-based method guided by a vegetative index, normalized difference red edge (NDRE)-based method. The ML-RF model was built based on a set of variables including 7-day weather, evapotranspiration (ET), traffic intensity, soil moisture content, N fertilization rate, NDRE, and root zone type. The field experiment was conducted on two sand-based research greens in 2020 and 2021. The cumulative applied N fertilizer was 281 kg ha^{-1} for the PACE Turf GP model, 190 kg ha^{-1} for the experience-based method, 140 kg ha^{-1} for the ML-RF model, and around 75 kg ha^{-1} NDRE-based method. ML-RF model and NDRE-based method were able to provide customized N fertilization recommendations on different root zones. The methods resulted in different mean turfgrass qualities and NDRE. From highest to lowest, they were PACE Turf GP model, experience-based, ML-RF model, and NDRE-based method, and the first three methods produced turfgrass quality over 7 (on a scale from 1 to 9) and NDRE value over 0.30. N fertilization guided by the ML-RF model resulted in a moderate amount of fertilizer applied and acceptable turfgrass performance characteristics. This application strategy is based on the N cycle and has the potential to assist turfgrass managers in making N fertilization decisions for creeping bentgrass putting greens.

Keywords: turfgrass, precision nitrogen management, decision support tool, nitrogen use efficiency, machine learning, random forest

OPEN ACCESS

Edited by:
Gregorio Egea, University of Seville, Spain

Reviewed by:
Karl Guillard, University of Connecticut, United States
Roxana Vidican, University of Agricultural Sciences and Veterinary Medicine of Cluj-Napoca, Romania

***Correspondence:**
Qiyu Zhou
qzhou53@wisc.edu
Douglas J. Soldat
djsoldat@wisc.edu

Specialty section:
This article was submitted to Plant Nutrition, a section of the journal Frontiers in Plant Science

Received: *26 January 2022*
Accepted: *20 April 2022*
Published: *19 May 2022*

Citation:
Zhou Q and Soldat DJ (2022) Evaluating Decision Support Tools for Precision Nitrogen Management on Creeping Bentgrass Putting Greens. Front. Plant Sci. 13:863211. doi: 10.3389/fpls.2022.863211

INTRODUCTION

Well-managed turfgrass systems that include golf courses can provide many beneficial environmental services to our society (Lonsdorf et al., 2021). However, natural resources, which include soil, water, and air, are negatively affected by the intensive use and production of agrochemicals. In turfgrass systems, especially on the highly maintained golf courses and athletic fields, agrochemicals are used to achieve desired aesthetics and functions. Nitrogen (N) fertilizer is applied in amounts greater than all other nutrients. US golf courses used 55,333 Mg N fertilizer annually (Gelernter et al., 2016). These N inputs pose potentially significant nonpoint source pollution risks (Bock and Easton, 2020). Optimizing the N application rate is one of the most effective ways to improve turfgrass management and reduce its potentially negative environmental impacts.

Maintenance of a high-quality playing surface of a golf course takes priority over maximizing turfgrass yield as is common for agricultural crops. Specifically, golf course putting greens are the main focus for most golf course managers (Hammond and Hudson, 2007); therefore, putting greens usually receive the most resource inputs and energy use per unit area (Gelernter et al., 2016). N is the most limiting nutrient for turfgrass, is an important driver of plant growth, and plays an important role in the visual quality of the surface. Relatively high N fertilization rates result in verdant and aesthetically pleasing playing surfaces. However, the rapid growth induced by relatively high N fertilization increases thatch and soil organic matter which reduces the function (e.g., ball roll speed) and aesthetics of putting greens (Meinhold et al., 1973; Murray and Juska, 1977; Throssell, 1981; Gaussoin et al., 2013). On the other hand, putting greens receiving relatively low rates of N fertilization can be slow to recover from ball marks and wear damage from foot traffic which encourages weed invasion (Beard, 1972).

Other nutrient application decisions, such as potassium, phosphate, calcium, magnesium, and so on., can be guided by soil testing (Murphy and Murphy, 2010; Landschoot, 2017). However, most commercial soil testing laboratories do not offer tests for estimating available N in soil. Tests for N exist, but they are often not quick nor cost-effective. Furthermore, plant-available N in the soil is affected by weather, so the N release pattern varies during the growing season. Lacking a tool or test, N application recommendations for golf courses putting greens are often based solely on turfgrass managers' experience and observations of turf quality. Annual recommended N fertilization amounts for golf course putting greens generally range from 49 to 195 kg ha^{-1} y^{-1} (Murphy and Murphy, 2010; Landschoot, 2017). Applying N fertilizer based on turfgrass visual performance might be warranted for turfgrass showing signs of inadequate N such as chlorosis, decreased density and growth, and slower recovery from abiotic and biotic stresses. However, golf turf managers prefer to avoid these negative responses and therefore regularly make fertilization applications to turfgrass that is performing optimally. This could result in overapplication because optimally performing turfgrass may perform well with optimum and above-optimum N. It is clear that a more objective N application strategy is needed to maximize N fertilizer efficiency.

Turfgrass visual quality assessment has been widely used as a standard to evaluate turfgrass response to various management practices. It involves a subjective visual evaluation of a turfgrass stand on a scale of 1 to 9 (where 1 represents completely dead turf, 6 represents the minimally acceptable quality, and 9 represents ideal turfgrass quality) based on the evaluator's mental integration of turfgrass color, uniformity, and shoot density (Beard, 1972). With the recent development and increasing availability of sensor technology, turfgrass professionals are able to utilize spectral reflectance data obtained from proximal and remote sensors to subjectively quantify turfgrass response to various practices, including N fertilization. Spectral reflectance is measured with given wavelengths of light, and studies (Trenholm et al., 1999; Bell et al., 2002; Fitz–Rodríguez and Choi, 2002; Keskin et al., 2008) have shown that spectral reflectance could be well correlated with visual quality for turfgrass species maintained under different management practices. Spectral reflectance is sensitive to N fertilization of turfgrasses (Caturegli et al., 2016; Guillard et al., 2016) and therefore has the potential to serve as an objective measurement of turfgrass performance. For example, spectral reflectance has been used to detect chlorophyll concentration and has also been shown to have a good correlation with plant N status (Horler et al., 1983; Steven and Clark, 2013). However, few studies have evaluated the feasibility of making N application decisions solely based on spectral reflectance measurement of turfgrass on golf course putting greens, and these measurements are likely to play a larger role in the precision management of turfgrass in the future.

Precision turfgrass management aims to provide optimal management of pests, fertilizer, salinity, cultivation, and irrigation (Stowell and Gelernter, 2006; Carrow et al., 2007; Bell and Xiong, 2008; Krum et al., 2010). Precision N management is a branch of precision turfgrass management that seeks to match N supply with turfgrass N demand spatially and temporally to maximize turfgrass function and minimize nutrient loss from the turf system. On sand-based putting green soils, the N cycle can be simplified using a few assumptions. Potential N loss by denitrification, volatilization, runoff, and leaching is expected to be negligible or quite low when best management practices are used (Snyder et al., 1984; Morton et al., 1988; Gross et al., 1990; Miltner et al., 1996; Erickson et al., 2001, 2008). This leaves clipping removal as the primary output of N, and fertilization as the primary input (assuming negligible input from irrigation water sources and atmospheric deposition). Moreover, Zhou and Soldat (2021a) concluded that tissue N of putting green creeping bentgrass spanned 2.5 and 5% during the growing season under typical conditions with an average of 3.9%. The optimal N fertilization rate (input) can be estimated by quantifying the N outputs (clipping mass x clipping tissue N concentration). This requires accurate estimates or measurements of turfgrass clipping yield, so that optimal N fertilizer inputs can be estimated.

The turfgrass growth potential (GP) model was developed by Gelernter and Stowell (2005) to aid decision-making related to fall overseeding on golf courses. Later, the turfgrass GP model was recognized as a tool for determining monthly or annual turfgrass N requirements based on the turfgrass growth potential (Woods, 2013), and this tool is used by turfgrass managers to guide N fertilization application decisions. The turfgrass GP model uses average air temperature to estimate turfgrass growth potential which spans 0 to 100%. For cool-season grasses, the model assumes that the optimal average air temperature for growth is 20°C (growth potential = 100%); as the temperature deviates from 20°C, the growth potential will decrease correspondingly until the growth potential reaches 0% at 0 and 40°C. The turfgrass GP model assumes that N should be applied to match the turfgrass' growth potential. An obvious pitfall with this method is that turfgrass growth is determined by complex physiological processes including genetic potential, environmental, and edaphic factors in addition to air temperature. For example, foot traffic stress, which is one of the most common stresses on golf course putting greens (Beard, 1972; Carrow and Martin Petrovic, 1992), can result in turf damage and reduced turf quality and clipping yield (Shearman et al., 1974; Shearman and Beard, 1975; Carrow and Martin Petrovic, 1992; Bilgili and Acikgoz, 2007). Water availability is another important factor of turfgrass growth. Limited access to water results in reduced root growth (Beard and Daniel, 1965), and excessive irrigation has been shown to also be detrimental to turfgrass growth and visual quality (Beard, 1972; DaCosta and Huang, 2006). Although the turfgrass GP model is useful for understanding how temperature may influence growth across regional or larger scales, at the local scale, a more detailed model could be useful for making more accurate predictions of turfgrass growth and corresponding N need.

In precision agriculture, crop growth models are widely used to guide N applications based on crop N demand to ensure increased N use efficiency. These models often estimate crop N needs by accounting for soil-plant processes, environmental conditions, and interactions with various management practices. A common approach for building a crop growth model is to use historical data to empirically predict future crop yield *via* machine learning (ML) (Jaikla et al., 2008; Brdar et al., 2011; Fukuda et al., 2013; Kuwata and Shibasaki, 2015; Everingham et al., 2016; Zhang et al., 2019; Van Klompenburg et al., 2020). Because of the differences in managing agriculture crops compared to turfgrass as well as the differing goals between agricultural production and turfgrass management, the utility of ML to aid turfgrass management decisions needs to be tested. Zhou and Soldat (2021b) developed turfgrass growth models with an ML approach and reported that the random forest (RF) algorithm was the best among those algorithms that tested for predicting creeping bentgrass clipping production on golf course putting green. The ML-RF turfgrass growth model inputs included daily weather, evapotranspiration (ET), soil moisture content, number of rounds of play, root zone type, N fertilization inputs, and NDRE. The aims of this study were to (1) evaluate the feasibility of the turfgrass ML-RF growth prediction model for improving N management and (2) compare how various N application strategies and decision support tools in terms of N applied and turfgrass performance characteristics. Specifically, the study evaluated two turfgrass growth models for guiding N fertilization: the PACE Turf growth potential model and an ML-RF growth prediction model against two more traditional approaches to N fertilizer management: the standard experience-based approach (which is the current standard for putting green fertilization) and an experience-based approach modified by reflectance measurements.

METHODS AND MATERIALS

Study Sites

The study was conducted at the University of Wisconsin-Madison O.J. Noer Turfgrass Research and Education Facility located in Verona, WI, USA. Field experiments were conducted on two different sand-based putting green root zones in 2020 and 2021 using the same plots in each year. Both research greens were constructed according to USGA recommendations (U.S. Golf Association, 2004) in 2000. Root zone characteristics are reported in **Table 1**. Both greens were established in 2011 with "Focus" creeping bentgrass (*Agrostis stolonifera*), which is the most commonly planted cool-season grass species used on golf courses putting greens in this region. Research plots were irrigated daily to replace 70% of reference ET as estimated by an on-site weather station. The research greens were topdressed with 0.6 m^3 ha^{-1} of sand approximately every 3 weeks during the growing seasons. Hollow tine cultivation was conducted once near the end of each growing season (September), and the cores were removed and holes filled with topdressing sand. Disease and other pests were monitored and controlled as needed. A total of four N treatments along with a non-fertilized control treatment were imposed on both root zones, and a detailed description of the four treatments can be found in Section Nitrogen Application Strategies. The experiment was set out as a completely randomized design with four replicates, and each plot measured 1.2 m by 2.4 m.

Turfgrass Data Collection

Clipping was collected from both research greens during 2020 and 2021 approximately every other day between 9:00 and 12:00 (weather permitting) by mowing a 1.9 m pass down the center of each plot using a 0.54-m-wide walking greens mower (Toro Co., Bloomington, Minnesota, USA). Before each clipping collection, 0.27-m wide alleys were mowed at the top and bottom of each plot perpendicular to the collection pass. This was done to reduce the variability associated with starting and stopping the mower. The effective clipping collection area for each plot was 1 m^2. Turfgrass was maintained at 3.2 mm during the research period for both research greens. Clippings were brushed from the mower bucket into paper bags, which were then placed in an oven set to 50°C for at least 48 h. Sand and other debris were removed from the dried clippings using the water method described in Kreuser et al. (2011). NDRE of each plot was also recorded prior to each clipping collection event. In this study, to quantify the estimated N uptake of creeping bentgrass, we assumed that the tissue N concentration was 3.9% throughout the research.

TABLE 1 | Soil chemical properties of two putting green root zones.

Root zones ID	Depth	SOM [θ]	P [ϕ]	K	Ca	Mg	CEC [ξ]	pH
	(cm)	(g kg^{-1})	(mg kg^{-1})				(cmol kg^{-1})	
A	0–5	0.7	25.9	40.7	586.6	133.1	3.0	7.7
	5–10	0.5	24.1	17.2	429.9	101.6	3.0	7.5
B	0–5	1.2	64.2	91.6	1210.0	295.8	8.0	7.5
	5–10	0.6	17.0	25.5	578.5	143.6	4.0	7.3

[θ] *SOM, soil organic matter by loss on ignition (360°C for 2 h) (Davies, 1974).*
[ϕ] *Nutrients extracted via Mehlich-3 (Mehlich, 1984).*
[ξ] *CEC, cation exchange capacity via summation of extracted cations.*

Nitrogen Application Strategies

Traditional N Fertilization Plan (Experience-Based)

Traditionally, N fertilization rates are based on manager experience, observations, and recommendations from local services or organizations. In this region, golf course putting greens typically receive between 100 and 250 kg N ha^{-1} y^{-1}. At the O.J. Noer Turfgrass Research Facility, it would be typical for the station manager to apply 10 kg ha^{-1} every other week during the ∼30-week growing season to putting green plots, for a total of ∼150 kg ha^{-1} N per season. Therefore, for this study, the traditional N fertilization plan treatment utilized a 10 kg ha^{-1} application every other week during the growing season, which approximately spanned the period of May to October. Urea was used as the N source and was dissolved and sprayed as a liquid at a nozzle pressure of 40 psi. using a CO_2 pressurized boom sprayer equipped with two XR Teejet 8004 VS nozzles.

Turfgrass Vegetative Index-Guided N Fertilization Method (NDRE-Based)

Another N treatment in the study used the normalized difference red edge (NDRE) obtained from the handheld proximal sensor (Rapid SCAN CS-45, Holland Scientific Inc., Lincoln, NE) to guide N application. NDRE is calculated using the combination of near-infrared red light (±800 nm) and red-edge band (±720 nm). NDRE is designed for crops with relatively high canopy density because the red edge band is able to penetrate deeper through the plant canopy. To calibrate the sensor and use spectral reflectance to guide N fertilization, the spectral reflectance readings from the turfgrass area are compared with the readings from reference strips, and then, fertilizer decisions are made according to the relationship between the two readings (Blackmer and Schepers, 1995; Raun et al., 2008; Samborski et al., 2009; Holland and Schepers, 2013; Guillard et al., 2021). One of the types of reference strips for spectral reflectance is called the virtual reference concept (Holland and Schepers, 2013). This method requires obtaining the spectral reflectance references from uniform research areas in the field where the turfgrass looks the greenest (well-fertilized) and the least green (under-fertilized) by visual observation. Based on the relationship between NDRE and N rate of well-fertilized and under-fertilized turf, a N fertilizer recommendation for turfgrass would be made based on the NDRE reading of an unknown area. In the study, we followed a similar approach but with some adjustments. Instead of finding the greenest and least green strip, we aimed to maintain the turfgrass at a minimally acceptable visual turfgrass quality. Therefore, the reference strips were the turfgrass research areas at a visual quality of ∼6. The mean NDRE on turfgrass areas with a quality of 6 was 0.28. Therefore, if the mean NDRE of the treatment for the preceding 14 days was > 0.28, and then, no additional N fertilizer was added; otherwise, additional N fertilizer was applied at 10 kg ha^{-1}. NDRE was collected by scanning the research plot approximately 1 m above the canopy and was measured three times each week during the growing season prior to each clipping collection.

Growth Potential (GP) Model (PACE Turf GP Model)

The GP model was presented as equation (1) (Woods, 2013). N fertilization for this treatment was applied every other week (consistent with all other treatments in this study), and the N application rate was determined by the GP (which is a percentage) multiplying by a maximum daily N use rate and multiplying that by the number of days since the last fertilization event. For this study, the maximum daily N use rate was determined to be 3.2 g m^{-2} d^{-1} based on growth and tissue N data collected on the same root zone during the 2019 growing season. This translates to a maximum N fertilization amount of 17.5 kg ha^{-1} every 2 weeks. The amount of N applied to each event was corrected by the GP of the previous 14 days.

$$GP = \frac{1}{e^{0.5(\frac{T-T_0}{var})^2}} \quad (1)$$

where

e: 2.718

T: local daily average temperature; °C

T_0: optimal temperature for turfgrass growth; 20°C for cool-season grass

Var: adjust the change in GP as temperature moves away from T_0; 5.5 for cool-season grass.

Machine Learning-Random Forest (ML-RF) Model

For the final N treatment, we used an RF algorithm for predicting turfgrass clipping yield using ML (Zhou and Soldat, 2021b). The model was constructed using clipping yield data

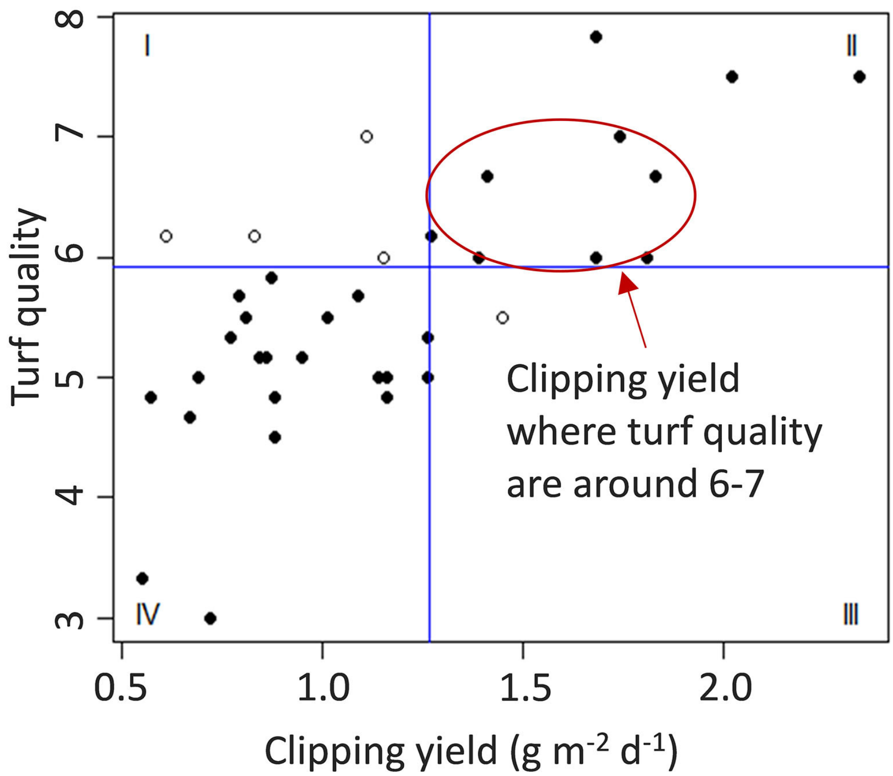

FIGURE 1 | Relationship between creeping bentgrass dry clipping yield and turf quality where the clipping and turf quality were collected in 2018 at the University of Wisconsin–Madison turfgrass research facility, Verona WI, USA. Turf quality was evaluated on a scale from 1 to 9 where 1 represents completely dead turf, 6 represents the minimally acceptable quality, and 9 represents ideal turfgrass quality.

collected in 2019 and 2020, where clipping data collected in 2019 were used to train the model to predict 2020's turfgrass clipping production, and clipping yield data collected in 2019 and 2020 were used to train the model to predict the 2021 turfgrass clipping production. Variable inputs when making predictions included (1) 3-day average soil moisture content (%) which was the average soil moisture content on the clipping collection event and the one before, soil moisture content was measured by time-domain reflectometry with 7.6-cm rods (FieldScout TDR 350, Spectrum Technologies, Aurora, Illinois, USA); (2) average weekly traffic intensities (round wk^{-1}); (3) NDRE; (4) categorical value representing the root zone of the two putting greens; (5) days between mowing events; (6) daily weather variables obtained from the nearest weather station reported on Weather Underground (an open online real-time weather information website). These variables included daily maximum temperature (Tmax) (°C), minimum temperature (Tmin) (°C), average temperature (Tavg) (°C), precipitation (precip) (mm), maximum relative humidity (RHmax) (%), minimum relative humidity (RHmin) (%), average relative humidity (RHavg) (%), and average wind speed (Windavg) (km h^{-1}); and (7) ET (mm) from a local weather station. A detailed description of the processes of choosing the input variables and detail about building and validating the model was presented by Zhou and Soldat (2021b).

The goal of using ML-RF growth model to guide N application was to accurately predict turfgrass clipping production and then make N fertilization decisions to maintain the clipping production within a target range. As maintaining a good quality of turfgrass is still the ultimate goal of turfgrass management, target clipping production was determined by making observations about the relationship between clipping production and turf quality (**Figure 1**). We selected our target clipping production range to coincide with visual turfgrass quality between 6 and 7, which required the daily clipping production to be between 1.25 and 1.6 g m^{-2} d^{-1}. The N fertilization decision used the following logic: (1) if the predicted 2-week cumulative clipping production was between 17.5 and 22.5 g m^{-2}, the N fertilization rate would replace the N removed as estimated by the model predicted clipping yield multiplied by the estimated average tissue N concentration (3.9%); (2) if the predicted clipping yield was > 17.5 g m^{-2} 2 wks^{-1}, then the N fertilization rate was determined using the median clipping yield (20 g m^{-2} 2 wks^{-1}) of the ideal clipping removal range multiplied by the estimated average tissue N concentration (3.9%). If the model predicted clipping yield in excess of 22.5 g m^{-2} for a given 2-week period, then no N fertilizer would be added. However, this

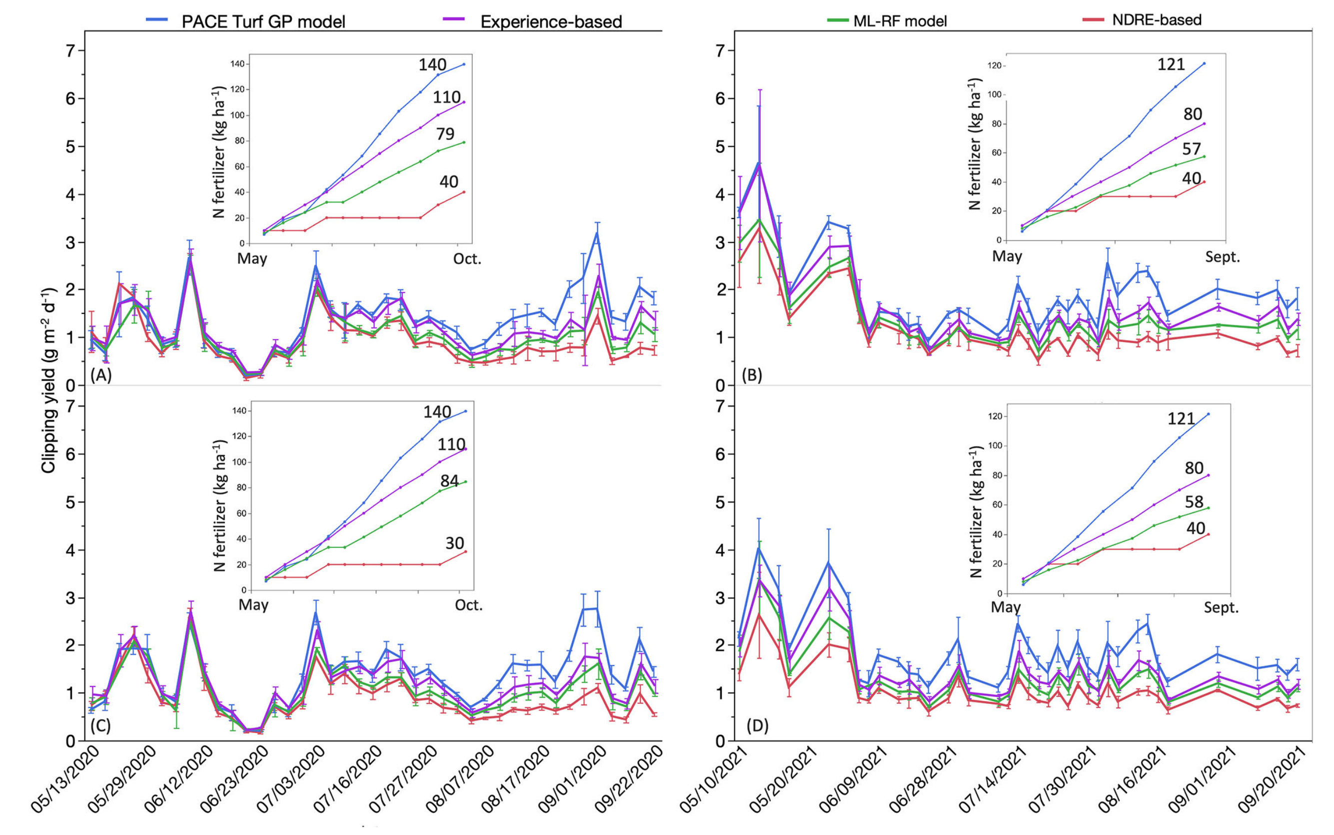

FIGURE 2 | Creeping bentgrass clipping yield response to four nitrogen (N) application strategies, which include PACE Turf growth potential (GP) model, traditional N fertilization plan (experience-based), machine learning-random forest (ML-RF) method, and vegetative index-based strategy (NDRE-based). **(A)** creeping bentgrass growth response on root zone A, data collected in 2020. **(B)** bentgrass growth response on root zone A, data collected in 2021. **(C)** bentgrass growth response on root zone B, data collected in 2020. **(D)** bentgrass growth response on root zone B, data collected in 2021. Inserted figures in each panel represent the cumulative N fertilizer usage for each year on each root zone. Error bars indicate standard deviation.

only occurred one time during the study period (July 2021), and the predicted clipping yield was in the range of 17.5 to 22.5 g m^{-2} 2 wks^{-1} for the majority of the study except at the beginning of each year's data collection, where the estimated clipping yield was lower than the target range.

Statistical Analysis

Statistical analysis was conducted using ANOVA for clipping yield, NDRE, turfgrass quality, cumulative clipping yield overall 2 years and N use efficiency (NUE) using JMP software (version 15.0, SAS Institute Inc., USA). Data collected from 2020 to 2021 were pooled and analyzed collectively. Years were considered as a random effect in this study. Treatment means were separated using Fisher's protected least significant difference (LSD) using a *p*-value of 0.05. Box plots were made to represent the distribution of the ratio of predicted clipping and actual clippings. The box plots were set at maximum values, 75th (the upper quartile), median, 25th (the lower quartile), and minimum. Pearson correlation was conducted to quantify the correlation between clipping yield and NDRE.

RESULTS

The 2-year creeping bentgrass growth response to the four N application strategies and corresponding N fertilizer inputs is presented in **Figure 2**. Generally, there was greater clipping production when the turfgrass received greater N fertilization rates. In this study, the PACE Turf GP model resulted in the greatest amount of N fertilizer applied, followed by the experience-based method. The ML-RF model recommended the third most N fertilizer inputs, and creeping bentgrass clipping production from that method was also lower than the previous two N fertilization strategies. The NDRE-based strategy resulted in the least N fertilizer use and lowest clipping production on both root zones in both years. The creeping bentgrass growth response to four N application plans on both root zones had a similar trend, as N is one of the major contributions to turfgrass growth; however, there was a different growth pattern in each year, likely as a result of the different weather and soil conditions (i.e., temperature, moisture) in each year. Interestingly, creeping bentgrass clipping yield responses to the four N application strategies were similar during

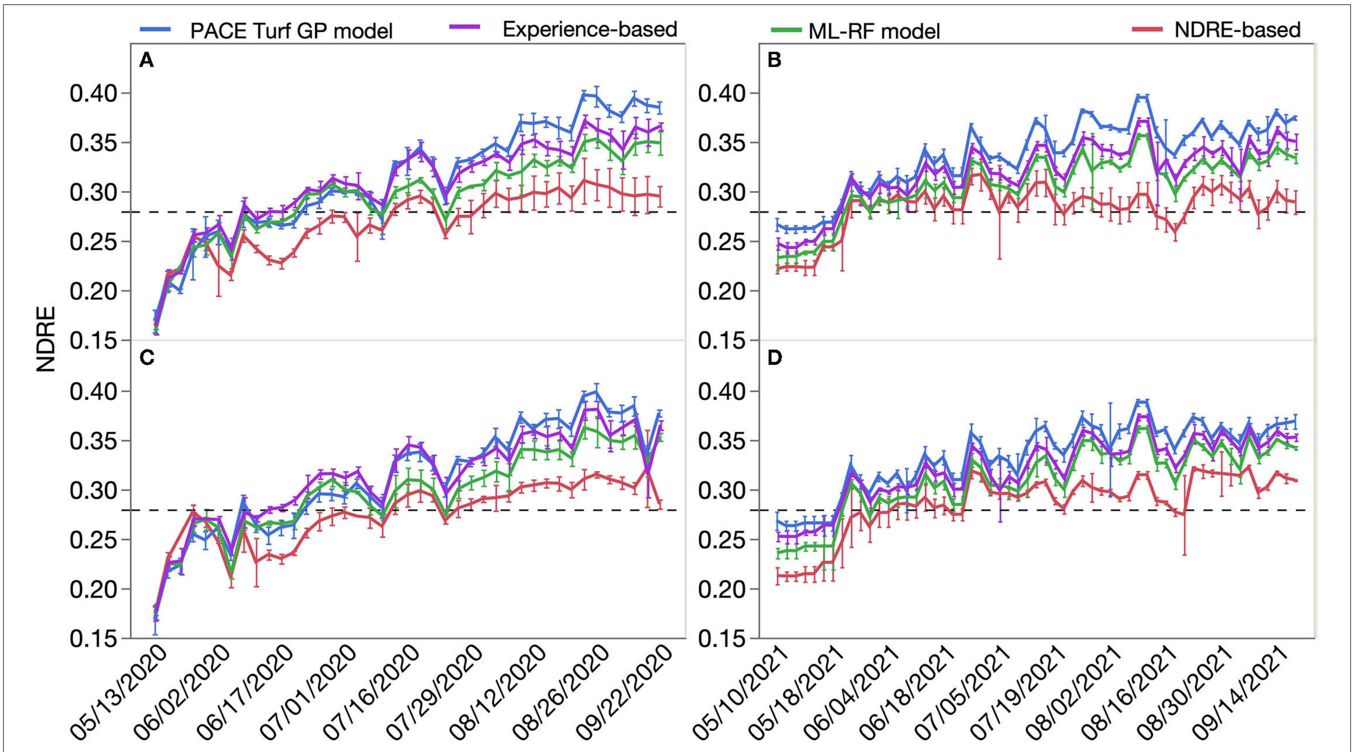

FIGURE 3 | NDRE readings of creeping bentgrass response to four nitrogen (N) application strategies: the PACE Turf growth potential (GP) model, traditional N fertilization plan (experience-based), machine learning-random forest (ML-RF) model, and vegetative index (NDRE)-based strategy). **(A)** NDRE readings on root zone A in 2020. **(B)** NDRE readings on root zone A in 2021. **(C)** NDRE readings on root zone B in 2020. **(D)** NDRE readings on root zone B in 2021. The dashed line is the NDRE decision threshold of 0.28. Error bars indicate standard deviation.

the first 5 weeks of the experiment even though different N fertilization rates were applied during this time. Turfgrass growth showed a delayed response to N fertilization. Creeping bentgrass NDRE readings under the four N fertilization treatments are presented in **Figure 3**. Similar to the growth response, plots that received N fertilizer recommendation following the PACE Turf GP model had the highest NDRE readings, followed by the experience-based method, ML-RF model, and the NDRE-based N fertilization strategy. The trends in NDRE readings on both greens and both years were similar, which implied that N fertilizer inputs were the primary driver of differences in NDRE readings. At the end of each season, PACE Turf GP model method had ∼20% greater NDRE compared to the NDRE-based method, which represented the highest and lowest N fertilization amounts. The difference in the season-end NDRE readings between the PACE Turf GP model and ML-RF model was ∼10%, and the difference between the PACE Turf GP model and the traditional N fertilization strategy was ∼5%. Additionally, although there was no overall significant difference in creeping bentgrass clipping yield among the four N treatments in the first 5 weeks of the field experiment, there were significant differences in NDRE readings which demonstrated that N fertilization had an immediate impact on creeping bentgrass canopy characteristics. The creeping bentgrass readings were above the reference reading (0.28) among the four N treatments more times in 2021 than in 2020.

The 2-year mean creeping bentgrass clipping yield, NDRE, and turf quality response to four N treatments, as well the 2-year cumulative N fertilizer usage, clipping yield, and NUE, are presented in **Table 2**. There was no significant difference in clipping yield, NDRE, and turfgrass quality between the two root zones within the same N treatment. Turfgrass that received N treatments followed by the PACE Turf GP model produced significantly higher clipping yield, NDRE readings, and turf visual quality. The experience-based model produced the second most clipping yield, NDRE, and turf quality, followed by the ML-RF model and the NDRE-based N fertilization plan.

The 2-year cumulative clipping yield from the non-fertilized control treatments on root zones A and B was 64.9 and 60.4 g m^{-2} 2 yrs^{-1}, respectively. NUEs were highest (near 70%) on both root zones receiving N fertilization according to the NDRE-based method. NUEs were around 45% on the root zones following the ML-RF N fertilization method and were about 40% following the experience-based method. NUEs were lowest when using PACE Turf GP model method (34%). The PACE Turf GP model and experience-based methods do not customize N fertilization recommendations on different root zones, whereas the ML-RF model and the NDRE-based method are able to account for root zone properties. The experience-based method resulted in 32% less N fertilizer than the GP method, and the ML-RF model applied 52 and 49% less N fertilizer on root zones A and B, respectively, than the GP method. The NDRE-based method

TABLE 2 | The 2-year mean creeping bentgrass clipping yield, NDRE, and turfgrass quality responses to four nitrogen (N) application strategies on two research putting greens.

Root zone ID	N app. strategies	Clipping (g m^{-2} d^{-1})	NDRE	Turf quality†	Sum of N fertilizer$^{¤}$ (kg ha^{-1} 2yrs^{-1})	Sum of clipping (g m^{-2} 2yrs^{-1})	NUE$^{\mu}$ (%)
A	PACE Turf GP$^{\Theta}$	1.63 a‡	0.328 a	7.6 a	281	297.5 a	33.1 d
	Experience$^{\beta}$	1.38 b	0.315 b	7.4 ab	190	251.6 b	39.3 bc
	ML-RF approach$^{\alpha}$	1.20 c	0.302 c	7.2 b	136	216.7 c	44.6 b
	NDRE-based$^{\Gamma}$	1.02 d	0.277 d	6.1 c	80	184.2 d	60.0 a
B	PACE Turf GP	1.62 a	0.326 a	7.5 a	281	288.9 a	32.5 d
	Experience	1.32 b	0.318 b	7.4 ab	190	240.1 b	37.8 cd
	ML-RF approach	1.17 c	0.306 c	7.2 b	142	213.9 c	43.2 bc
	NDRE-based	0.96 d	0.282 d	6.2 c	70	174.9 d	65.4 a

$^{\Theta}$*PACE Turf growth potential model-guided N application strategy.*
$^{\beta}$*Traditional N application plan.*
$^{\alpha}$*Machine learning (random forest) growth model-guided N application strategy.*
$^{\Gamma}$*Turfgrass vegetative index (NDRE)-based N application strategy.*
‡*Within each column, means sharing the letter are not statistically different according to Fisher's protected LSD test ($\alpha = 0.05$).*
†*Turf quality is evaluated on a scale from 1 to 9 where 1 represents completely dead turf, 6 represents the minimally acceptable quality, and 9 represents ideal turfgrass quality.*
$^{¤}$ *Overall, N fertilizer use on the research plots in this study in 2020 and 2021.*
$^{\mu}$*NUE, nitrogen use efficiency, calculated by (N uptake by plant-N uptake by plant from non-fertilizer control plot)/2-year N fertilizer applied.*

resulted in 72 and 75% less N fertilizer on root zones A and B, respectively, than the GP method.

The PACE Turf GP model and ML-RF model were the two approaches to making N application decisions based on turfgrass growth rate. **Figure 4** presents the prediction accuracy of 2-week cumulative clipping yield using the two models. The ratio of predicted and observed clipping yield was near 1 with the ML-RF model, and therefore, it accurately predicted creeping bentgrass clipping yield on both research greens. The ratio of predicted to actual clipping yield with the PACE Turf GP method was much larger than ML-RF model ratio (2.5 and 2.7 for research root zones A and B, respectively). The range of the ratio when using the PACE Turf GP model spanned 1.7 to 3.2 for root zone A and 1.6 to 3.1 for root zone B. The range of the ratio when using ML-RF model spanned 0.6 to 1.2 for both root zones, and if the first clipping collection event of each year was excluded, the range of the ratio improved to 0.8 to 1.2.

Among four treatments, there were significant but weak correlations between daily clipping yield and NDRE across 2 years (**Figure 5**), where the correlation coefficient ranged from −0.20 to 0.15. Interestingly, the PACE Turf model had a weak positive correlation between daily clipping yield and NDRE, whereas the three other treatments all appeared to have negative correlation between daily clipping yield and NDRE.

DISCUSSION

Averaged over two seasons, we recovered 34–71% of applied N in clippings among the four N application strategies. According to Miltner et al. (1996), about 35% of applied N fertilizer was recovered in Kentucky bluegrass (*Poa pratensis*) clippings, and the majority of the rest of the applied N was immobilized in thatch and soil. We did not attempt to quantify the fate of the remaining fertilizer N in this study, and the long and short-term fate of the un-recovered N requires further investigation, but lower N recovery does not necessarily imply N leaching losses, and greater recovery of applied N is generally desirable assuming performance goals are being met.

The ML-RF model more accurately predicted creeping bentgrass clipping yield than the GP method and therefore more accurately estimated N removal from mowing. During the 2-year field experiment in Verona WI, USA, the average air temperature during the study period was 18.7°C in 2020 and 20.1°C in 2021 which both were near the optimum temperature for cool-season grass. Therefore, the N fertilization rates applied based on the GP model maintained the turfgrass growth at or close to the maximum growth rate that we selected based on the 2019 growing season (not necessarily the genetic maximum growth potential of the grass). A lower fertilization rate would have resulted with this method if we had selected a lower "maximum" growth rate. Therefore, calibration of the PACE Turf GP model may improve its utility as a decision support tool for nutrient applications. The GP model is simpler to use than the ML-RF model and therefore may have a wider reach.

Vegetation indices such as NDRE and NDVI have been evaluated as methods to guide N fertilization or quantify turfgrass response to fertilization (Kruse et al., 2006; Bremer et al., 2011a; Lee et al., 2011; López-Bellido et al., 2012; Inguagiato and Guillard, 2016; Guillard et al., 2021). Our study demonstrated that there was a weak correlation between creeping bentgrass clipping yield and NDRE. This implied that NDRE would also have a weak correlation with turfgrass growth and N uptake. Interestingly, we observed a weak positive correlation between daily clipping yield and NDRE when the N rate was based on the PACE Turf GP model (relatively higher N), whereas the correlation became negative once the N application rates

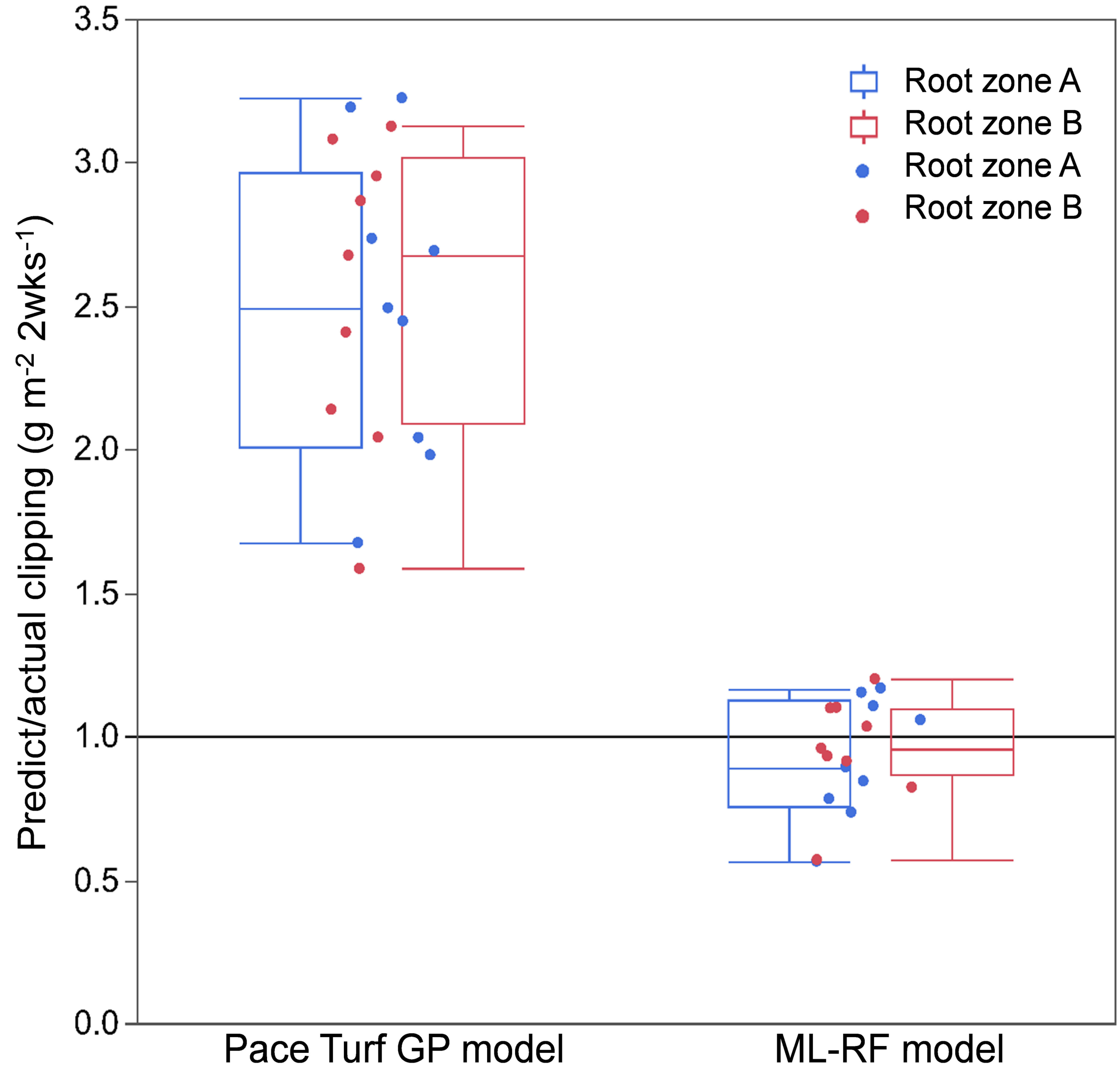

FIGURE 4 | Creeping bentgrass growth prediction accuracy of PACE Turf growth potential (GP) model and machine learning-random forest (ML-RF) model. Blue boxes and dots represent data collected on root zone A and red boxes and dots represent data collected on root zone B. The boxplots were set at maximum, 75th (the upper quartile), median, and 25th (the lower quartile), and minimum.

were lower (experience-based, ML-RF model, and NDRE-based methods). Studies have concluded that NDRE has much stronger correlations with some turfgrass growth characteristics such as turfgrass biomass (Marín et al., 2020) and turfgrass N status (Guillard et al., 2021). These studies applied a wider range of N rates which resulted in large variation in turfgrass growth. In this study, N fertilizer was applied at a relatively smaller range, and this could be the reason for the weak correlation between NDRE and turfgrass clipping yield.

Additionally, NDRE and other vegetative indices can be affected by many variables in the field, such as canopy density (Bremer et al., 2011b), turfgrass water status (Caturegli et al., 2020), plant colorants (Obear et al., 2017), and other stresses (Fenstermaker-Shaulis et al., 1997; Badzmierowski et al., 2019). Because these stresses can be independent of plant N status, using NDRE to make N fertilization decisions could be oversimplistic. In contrast, the machine learning growth prediction model was designed for sand-based greens and uses a simplified N cycle to make fertilizer recommendations. This method requires collecting and tracking clipping yield for calibration purposes and is only practical for golf course putting greens. For other parts of a golf course, such as fairways where it may not be practical to measure clipping yield and are under less stress than putting greens, using NDRE or other vegetative indices to guide N application decision could be more appropriate.

The ML-RF model in this study relied on the previous years' clipping yield as well as the current year's weather data, management practices, and vegetative indices. It was able to

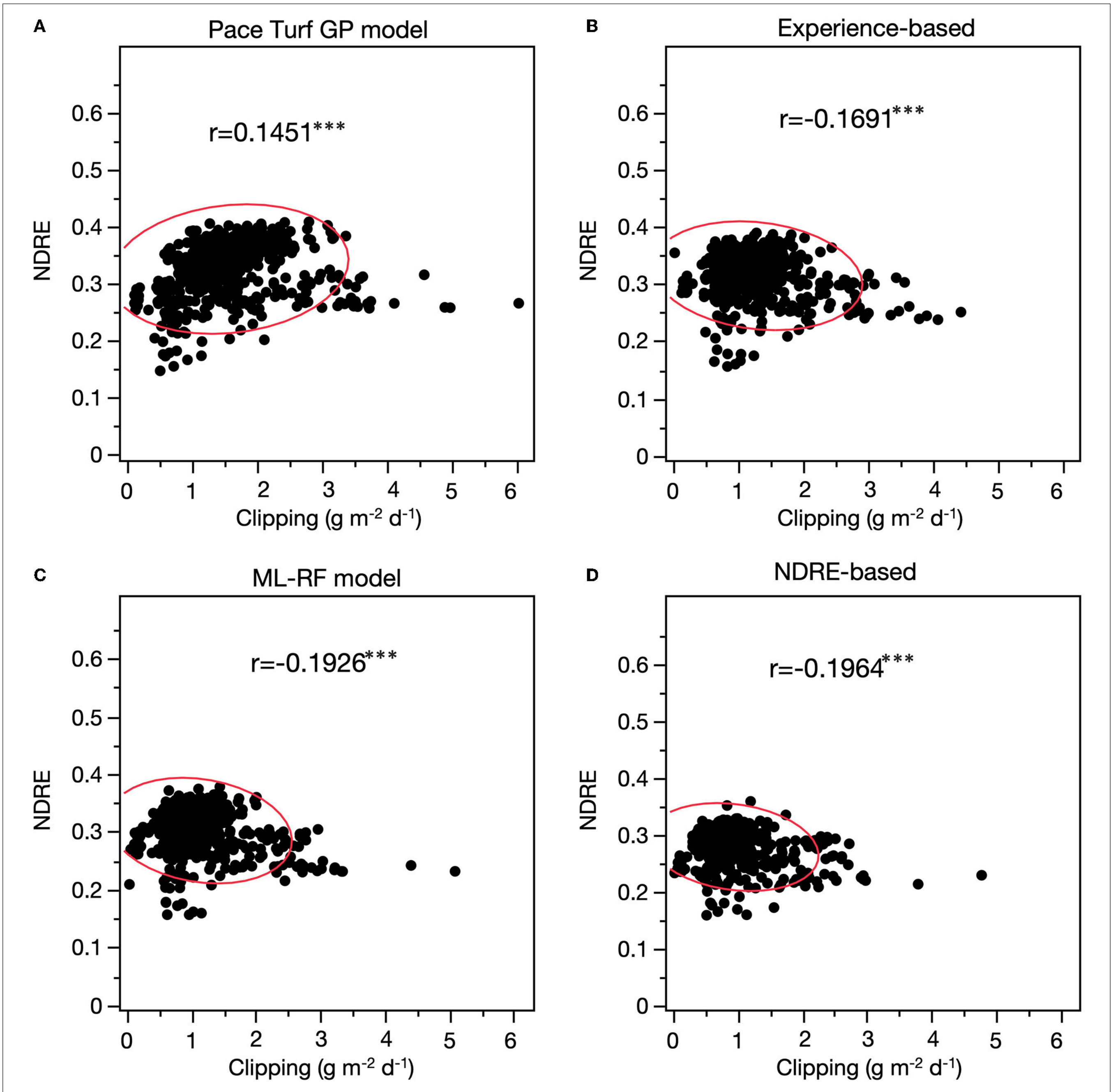

FIGURE 5 | Pearson correlation between vegetative index (NDRE) and corresponding creeping bentgrass clipping yield, where the turfgrass was fertilized using different strategies **(A)**. PACE Turf GP model: using the PACE Turf growth potential model; **(B)** experience-based: traditional N fertilization plan that is based on turfgrass quality and manager's experience; **(C)** ML-RF model: machine learning-random forest growth prediction model; **(D)** NDRE-based: vegetative index (NDRE)-guided N fertilization. The red lines illustrate the 95% prediction.

provide site-specific N recommendations for turfgrass planted in different soil conditions, different micro-climates, and under different management practices. The model also resulted in reduced N input compared to the traditional experience-based method and resulted in acceptable turfgrass quality. Similar studies (Engel et al., 1999; Long et al., 2000) also employed precision N management by monitoring and estimating N and as a result increased crop quality, yield, and economic profit. The ML-RF N application strategy proposed in this study is anchored in the N cycle and allows turfgrass managers to adjust the target clipping yield or clipping volume to meet different performance goals.

Ericsson et al. (2012, 2013) concluded that 3.1 to 3.5% leaf N concentration was sufficient to achieve a good turfgrass color and quality in most turfgrasses, including bentgrass and fescues (*Festuca spp.*). They also concluded that turfgrass with 60% of maximum growth would be sufficient to produce good turfgrass playing quality. The drawbacks to such a generalized approach include the need to frequently send leaf tissue to the laboratory for leaf N analysis, knowledge of the maximum growth rate, and measuring turfgrass yield to compare against that maximum growth rate. In contrast, the ML-RF model could help turfgrass managers to make clipping yield predictions based on weather data and management practice input without spending time on clipping collection aside from the calibration period. However, the ML-RF model does not yet exist in a user-friendly graphical interface, so one would need to be created for it to become widely used. A user-friendly decision support tool would be able to automatically process the data input without the need for knowledge of coding from end-users, additionally, it would predict turfgrass clipping yield of each golf course greens for the next weeks depending on the management practices, environment, and weather data input. The decision support tool would provide N fertilizer recommendations for the next N application event based on predicted clipping yield.

Many turfgrass managers of golf courses are beginning to recognize the benefits of regularly measuring grass growth by tracking clipping volume of golf course putting greens, and adjusting N fertilization based on the collected clipping. Precision N fertilization application has the potential to provide economic (i.e., reduced N fertilization input and other resource inputs, such as labor and energy) and environmental benefits (i.e., reduced N leaching and gaseous losses). However, there is not enough research, including economic research and environmental assessment, to evaluate precision N management and compare with the experience-based method which has been widely used. A better understanding of the economic and environmental outcomes from precision N management could help turfgrass managers choose optimized N fertilization methods.

CONCLUSION

Sustainable turfgrass systems integrate the goals of environmentally friendly and economic profitability. Among other resource inputs on turfgrass systems, the efficient and effective use of N fertilizer is one of the main drivers for improving sustainability, and proper N fertilization is in the economic interest of those in the golf and turfgrass industry. Our proposed precision N management attempts to help golf courses optimize N fertilizer use while maintaining quality standards on putting greens. Several N fertilizer management strategies were evaluated on golf course creeping bentgrass putting greens. The results demonstrated that a ML-RF method was able to significantly reduce N fertilizer usage and increase N use efficiency while maintaining high-quality turfgrass relative to the traditional method for fertilization. Whereas, the ML-RF and PACE Turf GP methods were both based on turfgrass growth predictions, the ML-RF method was able to more accurately estimate clipping removal and therefore may be useful for helping turfgrass managers to tie N fertilization decisions to the N cycle, rather than simply basing decisions on experience and visual observations.

DATA AVAILABILITY STATEMENT

The original contributions presented in the study are included in the article/supplementary material, further inquiries can be directed to the corresponding authors.

AUTHOR CONTRIBUTIONS

QZ and DS designed the study and conducted field experiments. QZ performed data analysis, built the prediction model, and wrote the manuscript. DS provided critical insights, edited, and revised the manuscript. Both authors reviewed the manuscript and agreed with the submission.

FUNDING

This work was partially funded by the United States Golf Association (Grant #: 2019-10-680), the Wisconsin Golf Course Superintendents Association, and the Wisconsin Turfgrass Association.

ACKNOWLEDGMENTS

We thank Nick Bero, Mike Katz, Travis Miller, Dimi Scweitzer, Abigail Chapman, Megan Hart, Britta Welsch, and Dimitrios Pavlou for their help with turfgrass clipping collection and processing. We thank Carol Duffy for the help with manuscript preparation. We thank Michael Bekken for help with reviewing the paper and providing suggestions. We thank the United States Golf Association, the Wisconsin Turfgrass Association, and the Wisconsin Golf Course Superintendents Association for providing partial financial assistance for this project.

REFERENCES

Badzmierowski, M. J., McCall, D. S., and Evanylo, G. (2019). Using hyperspectral and multispectral indices to detect water stress for an urban turfgrass system. *Agron*. 9, 439. doi: 10.3390/agronomy9080439

Beard, J. (1972). *Turfgrass: Science and culture*. NJ: Prentice-Hall, Englewood Cliffs.

Beard, J. B., and Daniel, W. H. (1965). Effect of temperature and cutting on the growth of creeping bentgrass (Agrostis palustris Huds.) roots 1. *Agro. J.* 57, 249–250. doi: 10.2134/agronj1965.00021962005700030006x

Bell, G. E., Martin, D. L., Wiese, S. G., Dobson, D. D., Smith, M. W., Stone, M. L., et al. (2002). Vehicle-mounted optical sensing: An objective means for evaluating turf quality. *Crop Sci*. 42, 197–201. doi: 10.2135/cropsci2002.1970

Bell, G. E., and Xiong, X. (2008). "The history, role, and potential of optical sensing for practical turf management." in: *Handbook of turfgrass management and physiology*, ed M. Pessarakli (Boca Raton, FL: CRC Press), p. 641–660. doi: 10.1201/9781420006483.ch36

Bilgili, U., and Acikgoz, E. (2007). Effect of nitrogen fertilization on quality characteristics of four turf mixtures under different wear treatments. *J. Plant Nutr*. 30, 1139–1152. doi: 10.1080/01904160701394600

Blackmer, T. M., and Schepers, J. S. (1995). Use of a chlorophyll meter to monitor nitrogen status and schedule fertigation for corn. *J. Prod. Agric*. 8, 56–60. doi: 10.2134/jpa1995.0056

Bock, E. M., and Easton, Z. M. (2020). Export of nitrogen and phosphorus from golf courses: A review. *J. Environ. Manage*. 55, 109817. doi: 10.1016/j.jenvman.2019.109817

Brdar, S., Culibrk, D., Marinkovic, B., Crnobarac, J., and Crnojevic, V. (2011). "Support vector machines with features contribution analysis for agricultural yield prediction." in: Second *International Workshop on Sensing Technologies in Agriculture, Forestry and Environment (EcoSense 2011)* (Belgrade, Serbia). p. 43–47

Bremer, D. J., Lee, H., Su, K., and Keeley, S. J. (2011a). Relationships between normalized difference vegetation index and visual quality in cool-season turfgrass: I. Variation among species and cultivars. *Crop Sci*. 51, 2212–2218. doi: 10.2135/cropsci2010.12.0728

Bremer, D. J., Lee, H., Su, K., and Keeley, S. J. (2011b). Relationships between normalized difference vegetation index and visual quality in cool-season turfgrass: II. Factors affecting NDVI and its component reflectances. *Crop Sci*. 51, 2219–2227. doi: 10.2135/cropsci2010.12.0729

Carrow, R. N., Cline, V., and Krum, J. (2007). "Monitoring spatial variability in soil properties and turfgrass stress: Applications and protocols." in: *Proceedings of 28th international irrigation show*. p. 641–645.

Carrow, R. N., and Martin Petrovic, A. (1992). Effects of traffic on turfgrasses. *Turfgrass*. 32, 285–330. doi: 10.2134/agronmonogr32.c9

Caturegli, L., Corniglia, M., Gaetani, M., Grossi, N., Magni, S., Migliazzi, M., et al. (2016). Unmanned aerial vehicle to estimate nitrogen status of turfgrasses. *PloS ONE*. 11, e0158268. doi: 10.1371/journal.pone.0158268

Caturegli, L., Matteoli, S., Gaetani, M., Grossi, N., Magni, S., Minelli, A., et al. (2020). Effects of water stress on spectral reflectance of bermudagrass. *Sci. Rep*. 10, 1–12. doi: 10.1038/s41598-020-72006-6

DaCosta, M., and Huang, B. (2006). Minimum water requirements for creeping, colonial, and velvet bentgrasses under fairway conditions. *Crop Sci*. 46, 81–89. doi: 10.2135/cropsci2005.0118

Davies, B. E. (1974). Loss-on-ignition as an estimate of soil organic matter. *Soil Sci. Soc. Am. J*. 38, 150–151. doi: 10.2136/sssaj1974.03615995003800010046x

Engel, R. E., Long, D. S., Carlson, G. R., and Meirer, C. (1999). Method for precision nitrogen management in spring wheat: I Fundamental relationships. *Precis. Agric*. 1, 327–338. doi: 10.1023/A:1009929226268

Erickson, J. E., Cisar, J. L., Snyder, G. H., Park, D. M., and Williams, K. E. (2008). Does a mixed-species landscape reduce inorganic-nitrogen leaching compared to a conventional St. Augustinegrass lawn? *Crop Sci*. 48, 1586–1594. doi: 10.2135/cropsci2007.09.0515

Erickson, J. E., Cisar, J. L., Volin, J. C., and Snyder, G. H. (2001). Comparing nitrogen runoff and leaching between newly established St. Augustinegrass turf and an alternative residential landscape. *Crop Sci*. 41, 1889–1895. doi: 10.2135/cropsci2001.1889

Ericsson, T., Blomback, K., and Kvalbein, A. (2013). *Precision Fertilisation–From Theory to Practice*. Available online at: http://sterf.golf.se

Ericsson, T., Blombäck, K., and Neumann, A. (2012). Demand-driven fertilization. Part I: Nitrogen productivity in four high-maintenance turf grass species. *Acta Agric. Scand.-B Soil Plant Sci*. 62, 113–121. doi: 10.1080/09064710.2012.682735

Everingham, Y., Sexton, J., Skocaj, D., and Inman-Bamber, G. (2016). Accurate prediction of sugarcane yield using a random forest algorithm. *Agron. Sustain. Dev*. 36, 27. doi: 10.1007/s13593-016-0364-z

Fenstermaker-Shaulis, L. K., Leskys, A., and Devitt, D. A. (1997). Utilization of remotely sensed data to map and evaluate turfgrass stress associated with drought. *J.Turfgrass Manag*. 2, 65–81. doi: 10.1300/J099v02n01_06

Fitz–Rodríguez, E., and Choi, C. Y. (2002). Monitoring turfgrass quality using multispectral radiometry. *Trans. ASAE*. 45, 865. doi: 10.13031/2013.8839

Fukuda, S., Spreer, W., Yasunaga, E., Yuge, K., Sardsud, V., and Müller, J. (2013). Random Forests modelling for the estimation of mango (Mangifera indica L. cv. Chok Anan) fruit yields under different irrigation regimes. *Agric. Water Manag*. 116,142–150. doi: 10.1016/j.agwat.2012.07.003

Gaussoin, R. E., Berndt, W. L., Dockrell, C. A., and Drijber, R. A. (2013). Characterization, development, and management of organic matter in turfgrass systems. *Turfgrass: Biology, use, and management*. 56, 425–456. doi: 10.2134/agronmonogr56.c12

Gelernter, W., and Stowell, L. (2005). Improved overseeding programs 1. The role of weather. *Golf Course Manage*. 73, 108–113.

Gelernter, W. D., Stowell, L. J., Johnson, M. E., and Brown, C. D. (2016). Documenting trends in nutrient use and conservation practices on US golf courses. *Crop. Forage Turfgrass Manag*. 2, 1–10. doi: 10.2134/cftm2016.04.0032

Gross, C. M., Angle, J. S., and Welterlen, M. S. (1990). Nutrient and sediment losses from turfgrass ASA, CSSA and SSSA. 19, 663–668. doi: 10.2134/jeq1990.00472425001900040006x

Guillard, K., Fitzpatrick, R. J. M., and Burdett, H. (2016). Can frequent measurement of normalized difference vegetative index and soil nitrate guide nitrogen fertilization of Kentucky bluegrass sod? *Crop Sci*. 56, 827–836. doi: 10.2135/cropsci2015.06.0347

Guillard, K., Miele, K. M., Sürer, I., and Morris, T. F. (2021). Guiding fall fertilization of cool-season turfgrass lawns with NDVI sufficiency index. *Crop Sci*. 61, 784–803. doi: 10.1002/csc2.20301

Hammond, R. A., and Hudson, M. D. (2007). Environmental management of UK golf courses for biodiversity—attitudes and actions. *Landsc. Urban Plan*. 83, 127–136. doi: 10.1016/j.landurbplan.2007.03.004

Holland, K. H., and Schepers, J. S. (2013). Use of a virtual-reference concept to interpret active crop canopy sensor data. *Precis. Agric*. 14, 71–85. doi: 10.1007/s11119-012-9301-6

Horler, D. N. H., Dockray, M., and Barber, J. (1983). The red edge of plant leaf reflectance. *Int. J. Remote Sens*. 4, 273–288. doi: 10.1080/01431168308948546

Inguagiato, J. C., and Guillard, K. (2016). Foliar N concentration and reflectance meters to guide N fertilization for anthracnose management of annual bluegrass putting green turf. *Crop Sci*. 56, 3328–3337. doi: 10.2135/cropsci2015.12.0765

Jaikla, R., Auephanwiriyakul, S., and Jintrawet, A. (2008). "Rice yield prediction using a support vector regression method," in *Proceedoings of the 5th International Conference Electrical Engineering/Electronics, Computer, Telecommunications and Information Technology* (Piscataway, NJ: IEEE). doi: 10.1109/ECTICON.2008.4600365

Keskin, M., Han, Y. J., Dodd, R. B., and Khalilian, A. (2008). Reflectance-based sensor to predict visual quality ratings of turfgrass plots. *Appl. Eng*. 24, 855–860. doi: 10.13031/2013.25355

Kreuser, W. C., Fish, M. P., Soldat, D. J., and Bauer, S. (2011). Removing sand from putting green clipping samples substantially reduces clipping weight measurement error. *Crop Sci*. 51, 1268–1273. doi: 10.2135/cropsci2010.10.0592

Krum, J. M., Carrow, R. N., and Karnok, K. (2010). Spatial mapping of complex turfgrass sites: Site-specific management units and protocols. *Crop Sci*. 50, 301–315. doi: 10.2135/cropsci2009.04.0173

Kruse, J. K., Christians, N. E., and Chaplin, M. H. (2006). Remote sensing of nitrogen stress in creeping bentgrass. *Agron. J*. 98, 1640–1645. doi: 10.2134/agronj2006.0022

Kuwata, K., and Shibasaki, R. (2015). "Estimating crop yields with deep learning and remotely sensed data." in: *2015 IEEE International Geoscience and Remote Sensing Symposium (IGARSS)*. Milan: IEEE. 858–861 doi: 10.1109/IGARSS.2015.7325900

Landschoot, P. (2017). *Turfgrass fertilization–A basic guide for professional turfgrass managers. Doc. UC184*. Penn State Extension, Penn State Univ., University Park, State College, PA..

Lee, H., Bremer, D. J., Su, K., and Keeley, S. J. (2011). Relationships between NDVI and visual quality in turfgrasses: Effects of mowing height. *Crop Sci*. 51, 323–332. doi: 10.2135/cropsci2010.05.0296

Long, D. S., Engel, R. E., and Carlson, G. R. (2000). Method for precision nitrogen management in spring wheat: II. Implementation. *Precis. Agric*. 2, 25–38. doi: 10.1023/A:1009980432643

Lonsdorf, E. V., Nootenboom, C., Janke, B., and Horgan, B. P. (2021). Assessing urban ecosystem services provided by green infrastructure: Golf courses in the Minneapolis-St. Paul metro area. *Landsc. Urban Plan*. 208, 104022. doi: 10.1016/j.landurbplan.2020.104022

López-Bellido, R. J., López-Bellido, L., Fernández-García, P., López-Bellido, J. M., Muñoz-Romero, V., López-Bellido, P. J., et al. (2012). Nitrogen remote diagnosis in a creeping bentgrass golf green. *Eur. J. Agron*. 37, 23–30. doi: 10.1016/j.eja.2011.10.001

Marín, J., Yousfi, S., Mauri, P. V., Parra, L., Lloret, J., and Masaguer, A. (2020). RGB vegetation indices, NDVI, and biomass as indicators to evaluate C3 and C4 turfgrass under different water conditions. *Sustainability.* 12, 2160. doi: 10.3390/su12062160

Mehlich, A. (1984). Mehlich 3 soil test extractant: A modification of Mehlich 2 extractant. *Commun. Soil Sci. Plant Anal.* 15, 1409–1416. doi: 10.1080/00103628409367568

Meinhold, V. H., Duble, R. L., Weaver, R. W., and Holt, E. C. (1973). Thatch Accumulation in Bermudagrass Turf in Relation to Management[1]. *Agron. J.* 65, 833–835.

Miltner, E. D., Branham, B. E., Paul, E. A., and Rieke, P. E. (1996). Leaching and mass balance of 15N-labeled urea applied to a Kentucky bluegrass turf. *Crop Sci*. 36, 1427–1433. doi: 10.2135/cropsci1996.0011183X003600060001x

Morton, T. G., Gold,A. J., and Sullivan, W.M. (1988). Influence of overwatering and fertilization on nitrogen losses from home lawns. *American Society of Agronomy, Crop Science Society of America, and Soil Science Society of America*. 17, 124–130. doi: 10.2134/jeq1988.00472425001700010019x

Murphy, J. A., and Murphy, S. L. (2010). *Best Management Practices for Nutrient Management of Turf in New Jersey*. Rutgers University, New Brunswick, NJ. Cooperative Extension, Bulletin E327.

Murray, J. J., and Juska, F. V. (1977). Effect of Management Practices on Thatch Accumulation, Turf Quality, and Leaf Spot Damage in Common Kentucky Bluegrass[1]. *Agronomy J.* 69, 365–369. doi: 10.2134/agronj1977.00021962006900030008x

Obear, G. R., Kreuser, W. C., Hubbard, K., DeBels, B., and Soldat, D. J. (2017). Plant colorants interfere with reflectance-based vegetation indices. *Crop Sci*. 57, 595–601. doi: 10.2135/cropsci2016.05.0440

Raun, W. R., Solie, J. B., Taylor, R. K., Arnall, D. B., Mack, C. J., and Edmonds, D. E. (2008). Ramp calibration strip technology for determining midseason nitrogen rates in corn and wheat. *Agron. J.* 100, 1088–1093. doi: 10.2134/agronj2007.0288N

Samborski, S. M., Tremblay, N., and Fallon, E. (2009). Strategies to make use of plant sensors-based diagnostic information for nitrogen recommendations. *Agron. J.* 101, 800–816. doi: 10.2134/agronj2008.0162Rx

Shearman, R. C., and Beard, J. B. (1975). Turfgrass Wear Tolerance Mechanisms: II. Effects of Cell Wall Constituents on Turfgrass Wear Tolerance[1]. *Agron. J.* 67, 211–215. doi: 10.2134/agronj1975.00021962006700020010x

Shearman, R. C., Beard, J. B., Hansen, C. M., and Apaclla, R. (1974). Turfgrass Wear Simulator for Small Plot Investigations[1]. *Agron. J.* 66, 332–334. doi: 10.2134/agronj1974.00021962006600020043x

Snyder, G. H., Augustin, B. J., and Davidson, J. M. (1984). Moisture Sensor-Controlled Irrigation for Reducing N Leaching in Bermudagrass Turf[1]. *Agron. J.* 76, 964–969. doi: 10.2134/agronj1984.00021962007600060023x

Steven, M. D., and Clark, J. A. (2013). *Applications of remote sensing in agriculture*. London: Elsevier.

Stowell, L., and Gelernter, W. (2006). Sensing the future. *Golf Course Management*. 74, 107–110.

Throssell, C. S. (1981). *Management factors affecting putting green speed* (Master's thesis). State College, PA: Pennsylvania State University.

Trenholm, L. E., Carrow, R. N., and Duncan, R. R. (1999). Relationship of multispectral radiometry data to qualitative data in turfgrass research. *Crop Sci*. 39, 763–769. doi: 10.2135/cropsci1999.0011183X003900030025x

U.S. Golf Association (2004). *USGA recommendations for a method of putting green construction*. USGA: Far Hills, NJ, USA.

Van Klompenburg, T., Kassahun, A., and Catal, C. (2020). Crop yield prediction using machine learning: A systematic literature review. *Comput. Electron. Agric*. 177, 105709. doi: 10.1016/j.compag.2020.105709

Woods, M. (2013). *Using temperature to predict turfgrass growth potential (GP) and to estimate turfgrass nitrogen use*. Bangkok: Asian Turfgrass Publication.

Zhang, Z., Jin, Y., Chen, B., and Brown, P. (2019). California almond yield prediction at the orchard level with a machine learning approach. *Front. Plant Sci*. 10, 809. doi: 10.3389/fpls.2019.00809

Zhou, Q., and Soldat, D. (2021b). Creeping bentgrass yield prediction with machine learning models. *Front. Plant Sci*. 12, 749854 doi: 10.3389/fpls.2021.749854

Zhou, Q., and Soldat, D. J. (2021a). Influence of foot traffic, irrigation, nitrogen (N) fertilization, and weather factors on creeping bentgrass "Focus"(Agrostis stolonifera L.) tissue N content. *Int. Turfgrass Soc. Res. J.* 2021, 1–5. doi: 10.1002/its2.88

Conflict of Interest: The authors declare that the research was conducted in the absence of any commercial or financial relationships that could be construed as a potential conflict of interest.

Publisher's Note: All claims expressed in this article are solely those of the authors and do not necessarily represent those of their affiliated organizations, or those of the publisher, the editors and the reviewers. Any product that may be evaluated in this article, or claim that may be made by its manufacturer, is not guaranteed or endorsed by the publisher.

TYPE Original Research
PUBLISHED 19 December 2023
DOI 10.3389/fpls.2023.1324820

An appropriate ammonium: nitrate ratio promotes the growth of centipedegrass: insight from physiological and micromorphological analyses

Dong-Li Hao[1], Jin-Yan Zhou[2], Ling Li[1], Jia Qu[1,3], Xiao-Hui Li[1], Rong-Rong Chen[1], Wei-Yi Kong[1], Dan-Dan Li[1], Jian-Jian Li[1], Hai-Lin Guo[1], Jian-Xiu Liu[1], Jun-Qin Zong[1*] and Jing-Bo Chen[1*]

[1]The National Forestry and Grassland Administration Engineering Research Center for Germplasm Innovation and Utilization of Warm-Season Turfgrasses, Jiangsu Key Laboratory for the Research and Utilization of Plant Resources, Institute of Botany, Jiangsu Province and Chinese Academy of Sciences (Nanjing Botanical Garden Mem. Sun Yat-Sen), Nanjing, China, [2]Department of Agronomy and Horticulture, Jiangsu Vocational College of Agriculture and Forest, Jurong, China, [3]Sanya Nanfan Research Institute of Hainan University, Sanya, China

Reasonable nitrogen fertilizer application is an important strategy to maintain optimal growth of grasslands, thereby enabling them to better fulfil their ecological functions while reducing environmental pollution caused by high nitrogen fertilizer production and application. Optimizing the ammonium (NH_4^+):nitrate (NO_3^-) ratio is a common approach for growth promotion in crops and vegetables, but research on this topic in grass plants has not received sufficient attention. Centipedegrass, which is widely used in landscaping and ecological protection, was used as the experimental material. Different NH_4^+:NO_3^- ratios (0: 100, 25:75, 50:50, 75:25, 100:0) were used as the experimental treatments under hydroponic conditions. By monitoring the physiological and morphological changes under each treatment, the appropriate NH_4^+:NO_3^- ratio for growth and its underlying mechanism were determined. As the proportion of ammonium increased, the growth showed a “bell-shaped” response, with the maximum biomass and total carbon and nitrogen accumulation achieved with the NH_4^+:NO_3^- ratio of 50:50 treatment. Compared with the situation where nitrate was supplied alone, increasing the ammonium proportion increased the whole plant biomass by 93.2%, 139.7%, 59.0%, and 30.5%, the whole plant nitrogen accumulation by 44.9%, 94.6%, 32.8%, and 54.8%, and the whole plant carbon accumulation by 90.4%, 139.9%, 58.7%, and 26.6% in order. As a gateway for nitrogen input, the roots treated with an NH_4^+:NO_3^- ratio of 50:50 exhibited the highest ammonium and nitrate uptake rate, which may be related to the maximum total root length, root surface area, average root diameter, root volume, and largest root xylem vessel. As a gateway for carbon input, leaves treated with an NH_4^+:NO_3^- ratio of 50:50 exhibited the highest stomatal aperture, stomatal conductance, photosynthetic rate, transpiration rate, and photosynthetic products. The NH_4^+:NO_3^- ratio of 50:50 treatment had the largest stem xylem vessel area.

Check for updates

OPEN ACCESS

EDITED BY
Henry Yabbey Sintim,
The University of Georgia, United States

REVIEWED BY
Mohammad Shah Jahan,
Sher-e-Bangla Agricultural University, Bangladesh
Krishan K. Verma,
Guangxi Academy of Agricultural Sciences, China

*CORRESPONDENCE
Jun-Qin Zong
zongjq1980@163.com
Jing-Bo Chen
chenjb19@163.com

RECEIVED 20 October 2023
ACCEPTED 05 December 2023
PUBLISHED 19 December 2023

CITATION
Hao D-L, Zhou J-Y, Li L, Qu J, Li X-H, Chen R-R, Kong W-Y, Li D-D, Li J-J, Guo H-L, Liu J-X, Zong J-Q and Chen J-B (2023) An appropriate ammonium: nitrate ratio promotes the growth of centipedegrass: insight from physiological and micromorphological analyses. *Front. Plant Sci.* 14:1324820. doi: 10.3389/fpls.2023.1324820

This structure and force caused by transpiration may synergistically facilitate root-to-shoot nutrient translocation. Notably, the change in stomatal opening occurred in the early stage (4 hours) of the NH_4^+:NO_3^- ratio treatments, indicating that stomates are structures that are involved in the response to changes in the root NH_4^+:NO_3^- ratio. In summary, we recommend 50:50 as the appropriate NH_4^+:NO_3^- ratio for the growth of centipedegrass, which not only improves the nitrogen use efficiency but also enhances the carbon sequestration capacity.

KEYWORDS

NH4 +:NO3 -ratio, stomatal aperture, root and stem structure, nitrogen use efficiency, carbon sequestration, centipedegrass

1 Introduction

Grasslands are known as barriers for ecological protection, contributors to soil formation, atmospheric filters, green granaries, and climate regulators. Globally, grasslands store 306-330 Pg C and are the main terrestrial carbon storage system, accounting for one-third of total terrestrial carbon storage (Tang et al., 2018). Maintaining the fine growth of grasslands is a precondition for them to fulfil their ecological functions (Smith, 2014). The extensive application of nitrogen fertilizer is the most important nutrient guarantee for the high yield and quality of grasslands (Li et al., 2022). However, 1) 70% of China's nitrogen fertilizer production is dependent on coal rather than natural gas, thereby producing much more CO_2 than developed countries. 2) Nitrogen use efficiency in China is 30%-40% (Hao et al., 2023), and the remaining portion either enters groundwater leading to pollution or escapes into the air in the form of N_2O, causing ozone layer destruction and exacerbating global warming (Ravishankara et al., 2009). N_2O can exist in the atmosphere for a long time (>120 years), and its greenhouse effect is 265-300 times that of equivalent CO_2. Nitrogen fertilizer application is the main source of N_2O emissions, which accounts for 44% of atmospheric N_2O emissions caused by human activity and 77% of N_2O emissions caused by soil (Akiyama et al., 2009). Grasslands account for 17-30% of the total natural soil emissions (Xu et al., 2018). Previous studies have shown that an average increase of 5% to 15% in nitrogen use efficiency can reduce N_2O emissions by 30% (Akiyama et al., 2009). Therefore, the key to controlling grassland N_2O emissions is to improve the nitrogen use efficiency of grass plants. 3) Excessive application of nitrogen fertilizer leads to a sharp decrease in soil organic matter and a serious decline in soil carbon storage and control (Khan et al., 2007), which restricts the soil carbon pool, the largest carbon pool in the biosphere, from playing a role in stabilizing carbon and fixing carbon. 4) Grasslands can intercept lost nitrogen fertilizer in farmland soil and alleviate a series of environmental problems, such as water eutrophication and atmospheric active nitrogen pollution, caused by low nitrogen fertilizer utilization efficiency in farmland (Shaddox et al., 2016). 5) The improvement of nitrogen use efficiency in grass plants would strengthen the ecological functions of grasslands, such as carbon sequestration and carbon sinks. Improving the nitrogen use efficiency of grass plants is a necessary strategy to achieve a double-win of ensuring stable growth of grassland and reducing the negative environmental effects caused by high nitrogen fertilizer production and application.

Ammonium and nitrate are the two main forms of inorganic nitrogen in soil. Many studies have shown that under the same applied concentration, the appropriate ammonium (NH_4^+): nitrate (NO_3^-) ratio promotes plant growth and improves nitrogen use efficiency. Notably, those studies mainly concentrate on Chinese cabbage (Chen et al., 2005; Hu et al., 2017), strawberry (Tabatabaei et al., 2006), cabbage (Zhang et al., 2007), tomato (Liu et al., 2017), maize (Wang et al., 2019b), coffee (Carr et al., 2020), purple coneflower (Ahmadi et al., 2021a; Ahmadi et al., 2021b; Ahmadi et al., 2022), pecan (Chen et al., 2021), soybean (Raza et al., 2021), Chinese kale (Wang et al., 2021), wheat (Yang et al., 2021), blueberry (Zhang et al., 2021), flowering Chinese cabbage (Zhu et al., 2021), lettuce (Du et al., 2022), and blackberry (Wei et al., 2023), with little attention given to grass plants. The growth promotion triggered by an appropriate NH_4^+:NO_3^- ratio is attributed to the accumulation of more carbon and nitrogen (Chen et al., 2005), a higher leaf area and photosynthetic rate (Tabatabaei et al., 2006; Hu et al., 2017; Liu et al., 2017; Wang et al., 2019b; Carr et al., 2020; Raza et al., 2021; Zhang et al., 2021), a higher chlorophyll concentration (Liu et al., 2017; Raza et al., 2021), increased auxin synthesis (Wang et al., 2019b), improved absorption of $H_2PO_4^-$, K^+, Ca^{2+}, and Mg^{2+} nutrients and a suitable proportion of nitrogen assimilation and storage (Zhang et al., 2007; Carr et al., 2020), improved root growth and root/shoot ratio (Ahmadi et al., 2021b; Raza et al., 2021; Zhang et al., 2021), or maintenance of the pH value and NH_4^+:NO_3^- ratios of the nutrient solution (Wang et al., 2021; Zhu et al., 2021). However, information regarding the role of plant micromorphological structure in growth promotion and the early-stage response of the above physiological parameters to the changes of different NH_4^+:NO_3^- ratios is still lacking. Based on the above background knowledge, centipedegrass, which is used as a typical landscape and ecological restoration grass, was used in this study as the experimental material. By monitoring the physiological and morphological changes under different NH_4^+:NO_3^- ratio treatments, the appropriate NH_4^+:NO_3^- ratio for growth and its underlying mechanism were determined. The recommended NH_4^+:NO_3^- ratio would facilitate the growth of grass, enabling it to better function in ecological protection. This practice would simultaneously alleviate a series of environmental problems caused by low nitrogen use efficiency.

2 Materials and methods

2.1 Plant growth condition

Stolons of the centipedegrass were collected from field plots in the turfgrass nursery in Nanjing Botanical Garden Mem. Sun Yat-Sen, China. The stolon with the top three nodes was obtained by cutting off from these stolons and cultured in water for 7 days to allow root emergence (Xu et al., 2023). Then, uniform seedlings were subjected to different NH_4^+:NO_3^- ratio treatments under hydroponic conditions. The nutrient solutions were composed of 0.5 mM nitrogen (with different NH_4^+:NO_3^- ratios), 0.3 mM KH_2PO_4, 0.35 mM K_2SO_4, 1 mM $CaCl_2$, 1 mM $MgSO_4.7H_2O$, 20 μM EDTA-Fe, 20 μM H_3BO_3, 9 μM $MnCl_2.4H_2O$, 0.77 μM $ZnSO_4.7H_2O$, 0.32 μM $CuSO_4.5H_2O$, and 0.39 μM $Na_2MoO_4.2H_2O$. The NH_4^+:NO_3^- ratio treatments were 0:100, 25:75, 50:50, 75:25, and 100:0. Each treatment contained 3 replicates. Each replicate included 12 seedlings planted in 3 L of nutrient solution. The pH of the nutrient solution was 5.5. The nutrient solution was renewed every three days. The room temperature was 28 °C, the relative humidity was 70%, the photosynthetic photon flux density was 500 $\mu mol \cdot m^{-2} \cdot s^{-1}$, and the photoperiod was 12 h/12 h (day/night). The seedlings were harvested after one month of treatment.

2.2 Growth parameter determination

The root parameters were obtained through a root scanner. Briefly, the root system was cut from the plant and then put into the sample plate without blocking each other. Four parameters, including total root length, root surface area, root volume, and average root diameter, were obtained by a root scanner. The plant height and internode length were measured with a ruler. The stem diameters were measured using a Vernier calliper. The number of nodes was obtained by counting.

2.3 Histochemical staining

The roots in the mature zone (5 cm from the root tip) and the 5th stems of centipedegrass that received one month of treatment were used for the staining test. The experimental procedure is referred to in the following literature (Wang et al., 2019c). First, small pieces of the roots and stems were immersed in a solution containing phosphate buffer (pH 7.2) and 2.5% glutaraldehyde (4° C, overnight). Following dehydration with ethanol and infiltration with epoxy propane, the samples were soaked and embedded in paraffin. A 1 μm sample was obtained by using a Leica ultramicrotome. After deparaffinization with xylene and washing with ethanol, the samples were stained in 1% safranin-O for 2 h and dehydrated with different concentration gradients of ethanol (50%, 70%, and 80%) for 5 s, respectively. Then, the samples received 15 s of 0.5% fast green staining. Following washing with 95% ethanol and 100% ethanol, the sections were mounted using neutral balsam. Safranin-O stained the xylem vessel red; fast green stained the phloem sieve tube green. The structures of the samples were photographed using the Mshot Image Analysis system under a light microscope at 5x and 40x magnification. The number of vascular bundles was directly counted, and the area of the large xylem vessels was measured by the Mshot Image Analysis system.

2.4 Stomatal aperture and photosynthetic parameters

The second leaves from the top of the centipedegrass were taken and cultivated under different NH_4^+:NO_3^- ratio treatments. Then, the leaves were placed in 0.5% KCl (pH 5.8) for 1.5 h. The solution clinging to the leaves was then carefully wiped off, nail polish was applied on the leaf surface, and temporary slides were created when the nail polish was dry. Photos were taken using the Mshot Image Analysis system under 40x magnification, and measurements of the length and width of the stomata were conducted by ImageJ software. The stomatal aperture was obtained by width/length. Each treatment contained data from at least 45 stomata.

Gas-exchange measurements were conducted in the totally expanded top second leaves of plants receiving different nutrient treatments using a Li-COR 6800 portable photosynthesis system. The rate of CO_2 assimilation (Pn), transpiration rate (Tr), and stomatal conductance (gs) were determined under light-saturated conditions with a photosynthetic photon flux density (PPFD) of 1200 $\mu mol\ m^{-2}\ s^{-1}$ at 25°C and with a reference CO_2 concentration of 400 ppm.

2.5 Carbon and nitrogen content

After one month of treatment, the roots were soaked in a 0.1 mM $CaSO_4$ solution for 5 minutes to exchange the ions adsorbed on the roots. Then, the roots and shoots were harvested. Following 30 minutes of 105 °C and 3 d of 80 °C drying, the dry weight of the plants was determined by a balance. The dry sample was powdered using a ball mill and then passed through a 0.425 mm sieve. Each sample containing 0.05 g of the uniform powder was set into a carbon and nitrogen element analyser for the carbon and nitrogen contents determination. Total root carbon content = root carbon content × root dry weight. Total shoot carbon content = shoot carbon content × shoot dry weight. Whole plant carbon content = total root carbon content + total shoot carbon content. Similarly, the total root nitrogen content, total shoot nitrogen content, and whole plant nitrogen content are obtained.

2.6 Ammonium and nitrate uptake rates

The method used for determining ammonium and nitrate uptake rates was based on our previous reports (Hao et al., 2020). Briefly, centipedegrass plants were subjected to nitrogen starvation (by cultivation in a nutrient solution without nitrogen) for 3 days followed by one month of different NH_4^+:NO_3^- ratio treatments. Then, the roots were soaked in a 0.1 mM $CaSO_4$ solution for 5 minutes to exchange the ions sticking to the root. After cleaning with water, the roots were placed into an ammonium uptake solution containing 0.1 mM NH_4Cl and 0.1 mM $CaSO_4$ (pH 5.5) or a nitrate uptake solution containing 0.1 mM $NaNO_3$ and 0.1 mM $CaSO_4$ (pH 5.5) for 1 hour. Each seedling was carefully placed in a 250 mL container, and its roots were immersed in either 200 mL of ammonium uptake solution or nitrate uptake solution. The residual fluid was then collected, and the fresh weight of the corresponding roots was simultaneously measured. The concentrations of ammonium and nitrate retained in the uptake solution were determined by Nessler's reagent method (for ammonium, #S26016) and the sulfonamide colorimetric method (for nitrate, #R30301-100T) according to the manufacturer's instructions (Shanghai Yuanye Biological Technology Company, China), respectively. The nitrogen absorption rate was determined with the following equation: nitrogen absorption rate = (initial concentration – sample concentration) × volume/(absorption time × root weight).

2.7 Glutamine, fructose, glucose, sucrose, and starch content determinations

Glutamine (Gln) content was determined by the high-performance liquid chromatography (HPLC) method (Pilot et al., 2004). The contents of fructose, glucose, sucrose, and starch were determined according to the instructions of the Nanjing Jiancheng Company reagent kit (#MB-W-B501 for fructose, #MB-W-B500 for glucose, #MB-W-B502 for sucrose, #MB-W-C400 for starch). A colorimetric method was used. The determination of fructose, glucose, sucrose, and starch content was performed at wavelengths of 480 nm, 505 nm, 480 nm, and 620 nm, respectively.

2.8 Statistical analysis and graph drawing

All the data were analysed using one-way analysis of variance (ANOVA) followed by Duncan's *post hoc* multiple comparisons tests ($P < 0.05$). Figures were drawn by GraphPad Prism 9.5. Data are expressed as the mean ± standard error (SE) of at least three measurements.

3 Results

3.1 Plant growth

Under hydroponic conditions, a of five NH_4^+:NO_3^- ratios (0:100; 25:75; 50:50; 75:25; 100:0) with a constant total nitrogen concentration was set to study the effect of changing the NH_4^+:NO_3^- ratio on the growth of centipedegrass. The results showed that as the proportion of ammonium increased, the growth response showed a "bell-shaped" pattern (first increasing and then decreasing), achieving the maximum growth effect at an NH_4^+:NO_3^- ratio of 50:50 (Figure 1A). With the increase in the ammonium proportion, the total root length, total root surface area, average diameter, and root volume all showed a trend of first increasing and then decreasing. The maximum root growth parameters were obtained at an NH_4^+:NO_3^- ratio of 50:50 (Figures 1B-E). Compared with the situation under the supply of only nitrate nitrogen, the total root length increased by 49.2%, 73.6%, -12.8%, and -6.7% (Figure 1B), the total root surface area increased by 26.6%, 34.0%, -9.9%, and -3.4% (Figure 1C), the average root diameter increased by 39.9%, 77.1%, 30.4%, and 30.6% (Figure 1D), and the root volume increased by 81.1%, 223.3%, -8.4%, and -4.2% (Figure 1E) with the increase in the proportion of ammonium. The plant height and number of stem nodes also showed a trend of first increasing and then decreasing with an increasing proportion of ammonium, reaching their maximum values at NH_4^+:NO_3^- ratios of 50:50 and 25:75 (Figures 1F, G). Compared with the situation where only nitrate was supplied, the plant height increased by 73.7%, 94.5%, 41.4%, and 42.1% after the proportion of ammonium increased (Figure 1F); the number of stem nodes increased by 56.3%, 57.2%, 24.5%, and 32.4% (Figure 1G). As the proportion of ammonium increased, the diameter and internode length of the 3^{rd}, 4^{th}, and 5^{th} stem nodes showed a trend of first increasing and then decreasing. The NH_4^+:NO_3^- ratio of 50:50 treatment had the largest stem diameter and internode length (Figures 1H, I). Compared with the situation where only nitrate was supplied, the diameter of the 3^{rd} stem nodes increased by 14.1%, 22.7%, 9.2%, and 17.5%, the diameter of the 4^{th} stem nodes increased by 10.9%, 21.2%, -0.2%, and 7.0%, and the diameter of the 5^{th} stem nodes increased by 10.4%, 22.7%, 6.1%, and 8.0% (Figure 1H). The internode length of the 3^{rd} stem nodes increased by 3.58%, 31.5%, -4.9%, and 15.1%, the internode length of the 4^{th} stem nodes increased by -3.2%, 22.4%, -6.1%, and 15.6%, and the internode length of the 5^{th} stem nodes increased by -3.6%, 18.4%, -0.7%, and 12.1% (Figure 1I).

3.2 Micromorphological structure

Because the growth of the root and stem was regulated by the treatment of different NH_4^+:NO_3^- ratios (Figure 1D; Figure 1H), the root and stem were cross-cut to observe their micromorphological structure changes. The results showed that the number and area of xylem vessels in the root mature zone showed a trend of first increasing and then decreasing with increasing ammonium proportion. The NH_4^+:NO_3^- ratio of 50:50 treatment had the largest number and area of root xylem vessels (Figures 2A-C). Compared with only nitrate supplied, increasing the proportion of ammonium increased the number of root xylem vessels by 17.1%, 37.1%, 34.3%, and 5.7%, respectively (Figure 2B), and increased the

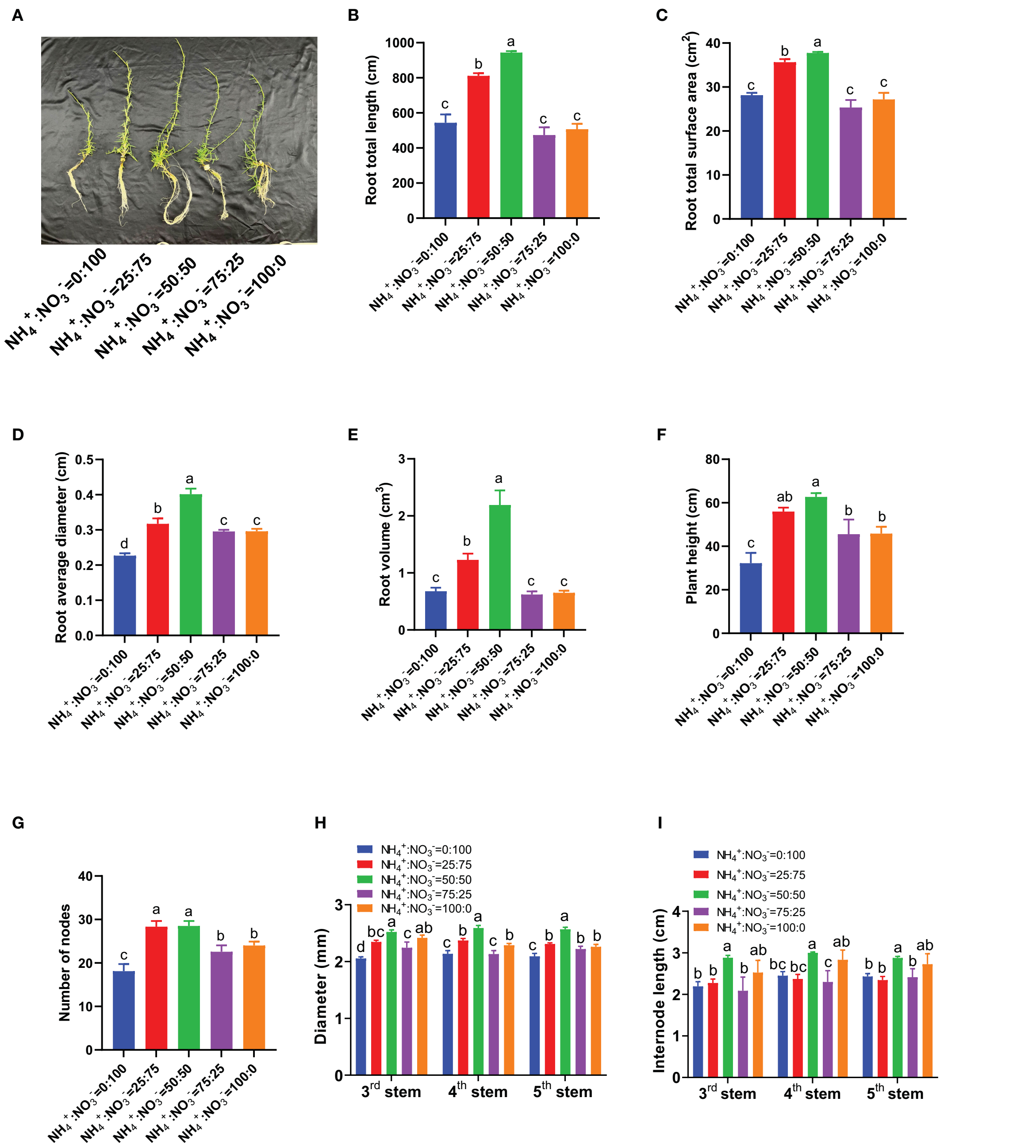

FIGURE 1
Growth parameters of centipedegrass that received one month of different NH_4^+:NO_3^- ratio treatments. **(A)**, Photos of growth. **(B)**, Root total length. **(C)**, Root total surface area. **(D)**, Root average diameter. **(E)**, Root volume. **(F)**, Plant height. **(G)**, Numbers of nodes. **(H)**, Diameter of the 3rd, 4th, and 5th stems. **(I)**, Internode length of the 3rd, 4th, and 5th stems. N=4 for Panels **(B–E)**, n=8 for Panels **(F–I)**. The different letters above the columns represent significant differences between treatments (P < 0.05).

xylem vessel area by 7.7%, 65.2%, 32.3%, and 1.3%, respectively (Figure 2C). The number and area of xylem vessels in the stem also showed a trend of first increasing and then decreasing with increasing ammonium proportion. The NH_4^+:NO_3^- ratio of 50:50 and 25:75 treatments had the largest number and area of stem xylem vessels (Figures 2D-F). Compared with the only nitrate supplied, increasing the proportion of ammonium increased the number of stem xylem vessels by 10.6%, 14.6%, -13.1%, and -4.0% (Figure 2E) and increased the stem xylem vessel area by 131.5%, 150.9%, 46.3%, and 51.7% (Figure 2F).

3.3 Biomass, carbon, and nitrogen content

With the increase in the ammonium proportion, the biomass showed a trend of first increasing and then decreasing. The NH_4^+:NO_3^- ratio of 50:50 treatment had the maximum biomass of roots, shoots, and whole plants (Figure 3A). Compared with the situation where nitrate was supplied alone, increasing the ammonium proportion increased the root biomass by 48.6%, 218.4%, 9.9%, and 19.0%, the shoot biomass by 96.1%, 134.6%, 62.2%, and 31.2%, and the whole plant biomass by 93.2%, 139.7%, 59.0%, and 30.5%

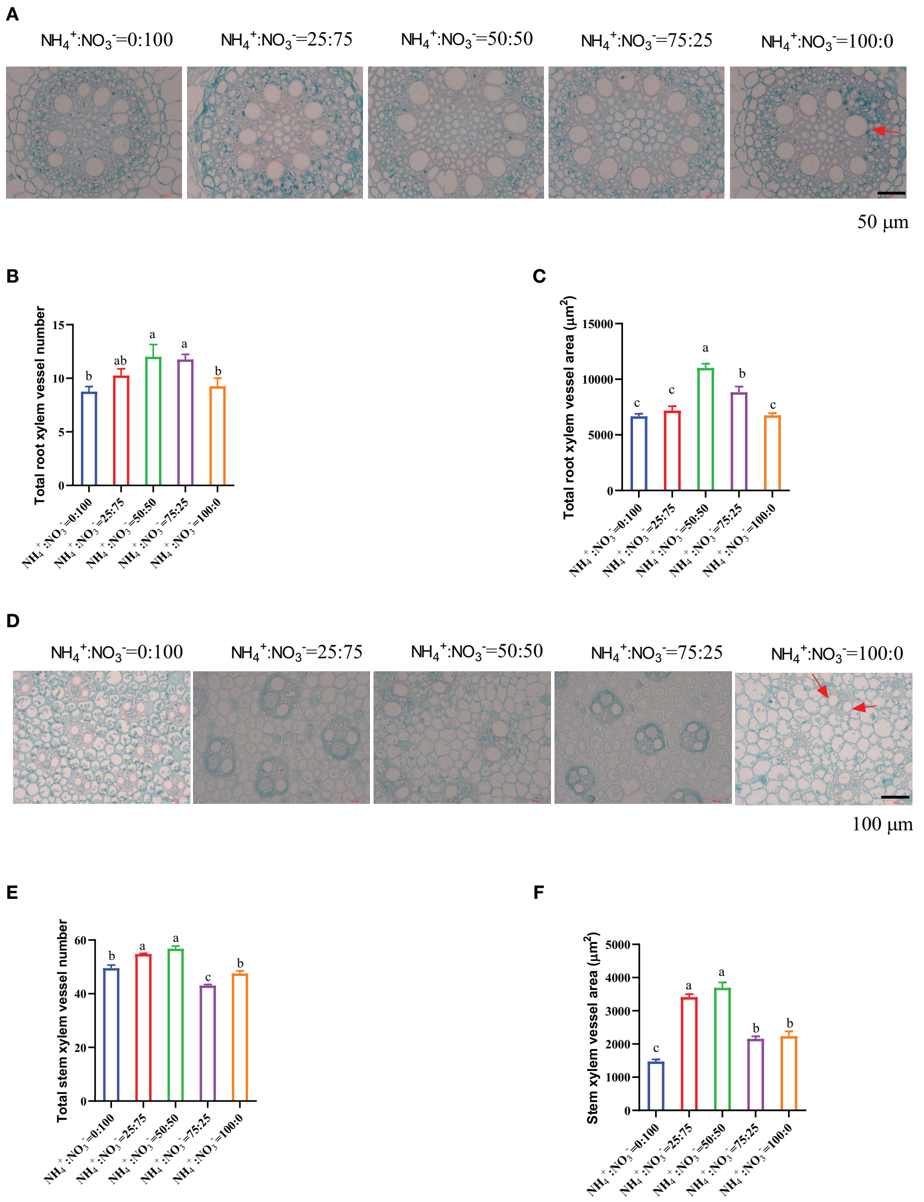

FIGURE 2
Cross-sections of the roots and stems that received one month of different NH_4^+:NO_3^- ratio treatments. **(A–C)**, Cross section of root mature zone **(A)**, total xylem vessel number **(B)**, and total xylem vessel **(C)**. **(D–F)**, Cross section of the 5th stem **(D)**, total stem xylem vessel number **(E)**, and stem xylem vessel area **(F)**. N=4 for Panels **B**, **C**, and **E**, n=16 for Panel **(F)** The red arrows in **(A, D)** indicate the root vessel and stem vessel, respectively. The different letters above the columns represent significant differences between treatments (P < 0.05).

(Figure 3A). The nitrogen accumulation, carbon accumulation, and carbon-nitrogen ratio also showed a trend of first increasing and then decreasing with increasing ammonium proportion. The NH_4^+:NO_3^- ratio of 50:50 treatment showed the highest nitrogen accumulation, carbon accumulation, and carbon-nitrogen ratio (Figures 3B-D). Compared with only nitrate being supplied, increasing the ammonium proportion increased the root nitrogen accumulation by 9.0%, 90.1%, -25.5%, and 48.1%, the shoot nitrogen accumulation by 50.4%, 95.3%, 41.8%, and 55.9%, and the whole plant nitrogen accumulation by 44.9%, 94.6%, 32.8%, and 54.8% (Figure 3B). Compared with the situation where only nitrate was supplied, increasing the ammonium proportion increased the root carbon accumulation by 34.8%, 200.2%, 0.1%, and 13.8%, the shoot carbon accumulation by 94.2%, 135.8%, 62.8%, and 27.5%, and the whole plant carbon accumulation by 90.4%, 139.9%, 58.7%, and 26.6% (Figure 3C). Compared with the situation where nitrate was supplied alone, increasing the ammonium proportion increased the root carbon:nitrogen ratio by 27.7%, 126.1%, 49.9%, and 12.4% and the shoot carbon:nitrogen ratio by 8.3%, 48.7%, 15.9%, and -24.3% (Figure 3D).

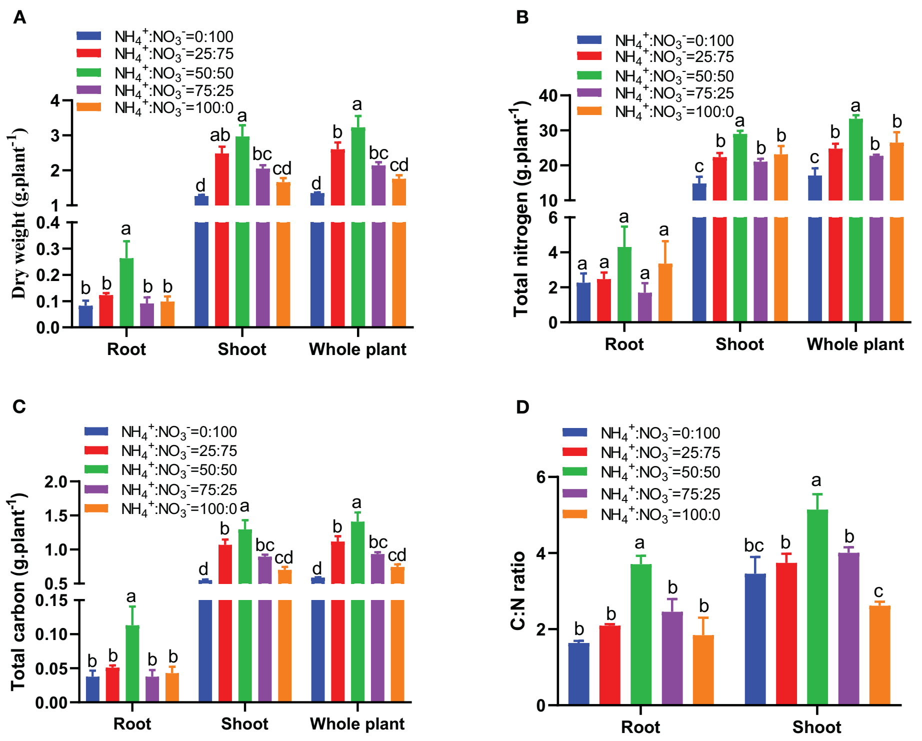

FIGURE 3
The biomass, carbon, and nitrogen accumulation in centipedegrass that received one month of different NH_4^+:NO_3^- ratio treatments. **(A)**, Biomass. **(B)**, Nitrogen accumulation. **(C)**, Carbon accumulation. **(D)**, Carbon **(C)** nitrogen (N) ratio. N=4. The different letters above the columns represent significant differences between treatments (P < 0.05).

3.4 Nitrogen uptake and assimilation

Since roots are the main pathway of nitrogen input, we first measured the absorption rate of ammonium nitrate by roots that received different NH_4^+:NO_3^- ratio treatments. The results showed that as the proportion of ammonium increased, the absorption rates of ammonium and nitrate showed a trend of first increasing and then decreasing. The maximum absorption rates of ammonium and nitrate were observed under the NH_4^+:NO_3^- ratio of 50:50 treatment (Figures 4A, B). No matter NH_4^+ or NO_3^-, they need to be first assimilated into Gln through the GS-GOGAT pathway. The first nitrogen assimilation product Gln in roots and leaves also showed a trend of first increasing and then decreasing with increasing ammonium proportion. The highest Gln content was observed under the NH_4^+:NO_3^- ratio of 50:50 treatment (Figures 4C, D). Compared with the situation where nitrate was supplied alone, increasing the ammonium proportion increased the root total Gln content by 66.1%, 245.9%, 31.0%, and 24.2% (Figure 4C) and the shoot total Gln content by 37.2%, 46.5%, -3.2%, and -45.3% (Figure 4D).

3.5 Carbon uptake and assimilation

The stomata located on the leaves are the gateway for plant carbon input. We monitored the stomatal aperture under different NH_4^+:NO_3^- ratio treatments and found that the stomatal aperture showed a trend of first increasing and then decreasing with increasing proportions of ammonium, reaching the maximum stomatal opening at an NH_4^+:NO_3^- ratio of 50:50 (Figure 5A). The trend of stomatal conductance measurement data is consistent with that of stomatal aperture measurement data, reaching the maximum stomatal conductance at an NH_4^+:NO_3^- ratio of 50:50 (Figure 5B). Compared with the situation where only nitrate was supplied, increasing the ammonium proportion increased the stomatal conductance by 39.6%, 87.2%, 3.4%, and -3.4% (Figure 5B). Consistent with the trend of changes in stomatal aperture/conductance, both the photosynthetic rate and transpiration rate showed a trend of first increasing and then decreasing with increasing ammonium proportion, reaching the maximum photosynthetic rate and transpiration rate at an NH_4^+:NO_3^- ratio of 50:50 (Figures 5C, D). Compared with the situation where nitrate was supplied alone, increasing the ammonium proportion increased the photosynthetic rate by 52.7%, 106.3%, -1.0%, and 6.8% (Figure 5C) and the transpiration rate by 35.3%, 65.6%, 1.5%, and -1.9% (Figure 5D).

Considering that soluble sugar and starch are the main photosynthetic products, we measured these parameters under different NH_4^+:NO_3^- ratio treatments. The results showed that the contents of fructose, glucose, sucrose, and starch in roots and leaves showed a trend of first increasing and then decreasing with increasing ammonium proportion. NH_4^+:NO_3^- ratio of 50:50 had the highest content of fructose, glucose, sucrose, and starch (Figures 6A-H). Compared with the situation where only nitrate

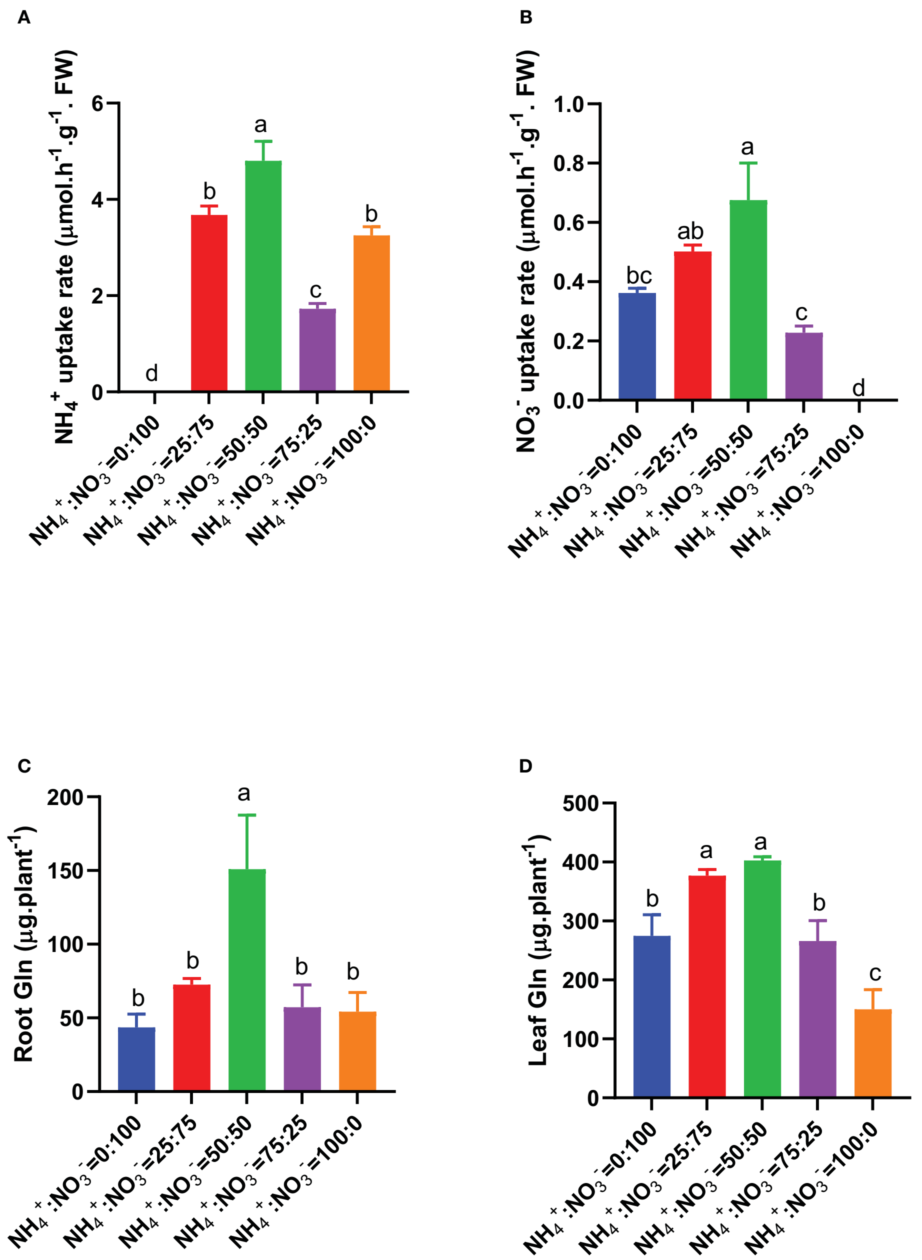

FIGURE 4
Ammonium and nitrate uptake rates in centipedegrass that received one month of different NH_4^+:NO_3^- ratio treatments. **(A)**, Ammonium uptake rate. **(B)**, Nitrate uptake rate. **(C, D)**, Total Gln in the roots and leaves. N=4. The different letters above the columns represent significant differences between treatments ($P < 0.05$).

was supplied, increasing the ammonium proportion increased the content of fructose in roots by 32.3%, 227.9%, 4.9%, and 20.1% (Figure 6A), the content of fructose in leaves by 54.4%, 122.2%, 8.8%, and 11.9% (Figure 6B), the content of glucose in roots by 30.3%, 171.1%, -7.3%, and 8.6% (Figure 6C), the content of glucose in leaves by 20.6%, 221.4%, -2.7%, and 84.8% (Figure 6D), the content of sucrose in roots by 48.3%, 218.5%, 9.3%, and 19.5% (Figure 6E), the content of sucrose in leaves by 31.8%, 71.3%, 8.3%, and -22.8% (Figure 6F), the content of starch in roots by 46.9%, 215.1%, 8.5%, and 17.8% (Figure 6G), and the content of starch in leaves by 31.0%, 97.9%, 7.2%, and -3.7% (Figure 6H).

3.6 Early stage response of stomata

In view of the key roles of stomata and photosynthesis in carbon input and assimilation, we monitored the early-stage response of these parameters to different NH_4^+:NO_3^- ratio treatments. The results showed that 4 hours after being treated with different NH_4^+:NO_3^- ratios, the NH_4^+:NO_3^- ratio of 50:50 treatment had the largest stomatal aperture, and this situation was maintained with the extension of treatment time (48 hours) (Figure 7A). At the two time points of 4 hours and 48 hours, the stomatal aperture under the NH_4^+:NO_3^- ratio of 50:50 treatment increased by 52.8% and 30.6% and by 52.8% and 38.5%, respectively,

10.3389/fpls.2023.1324820

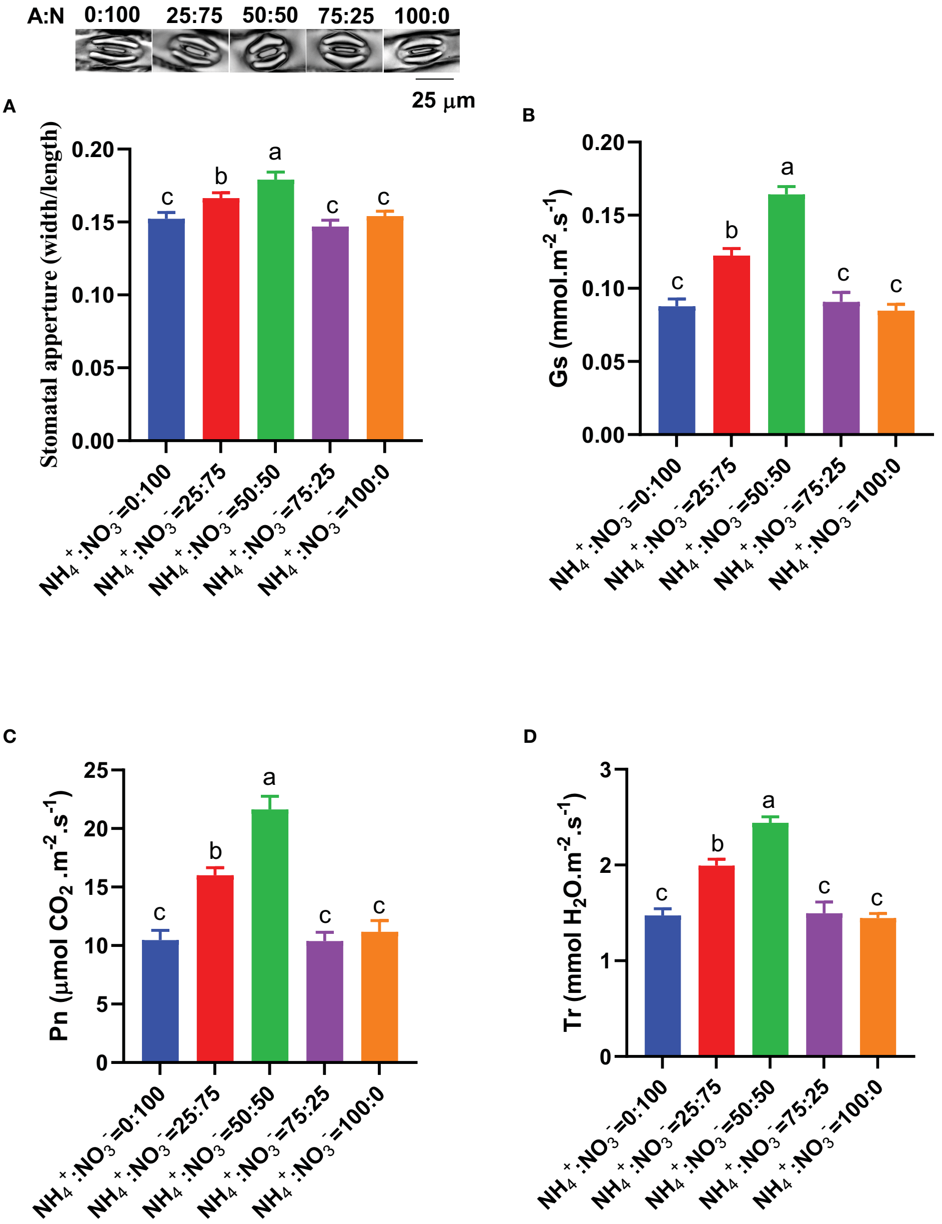

FIGURE 5
Stomatal aperture and photosynthetic parameters in centipedegrass that received one month of different NH_4^+:NO_3^- ratio treatments. **(A)**, Representative photos of stomata (upper) and statistical results of stomatal aperture (lower). **(B)**, Stomatal conductance (Gs). **(C)**, Photosynthetic rate (Pn). **(D)**, Transpiration rate (Tr). N>80 for Panel **(A)**. n=4 for Panels **(B–D)**. The different letters above the columns represent significant differences between treatments ($P < 0.05$).

compared to those under only nitrate or only ammonium conditions (Figure 7A). The stomatal conductance also showed similar response characteristics: the maximum stomatal conductance was reached at the NH_4^+:NO_3^- ratio of 50:50 treatment, which increased by 85.7% and 117.1%, respectively, compared to those under only nitrate and only ammonium treatments (Figure 7B). The photosynthetic rate reached its maximum under the NH_4^+:NO_3^- ratio of 50:50 treatment, which increased by 142.0% and 113.6% compared to those under only nitrate or only ammonium conditions, respectively (Figure 7C). The transpiration rate reached its maximum under the NH_4^+:NO_3^- ratio of 50:50 treatment, which increased by 126.1% and 151.2% compared to those under only nitrate or only ammonium conditions, respectively (Figure 7D).

4 Discussion

4.1 Appropriate NH_4^+:NO_3^- ratio promotes the growth and improves the carbon sequestration ability and nitrogen use efficiency of centipedegrass

The appropriate NH_4^+:NO_3^- ratio promotes plant growth, and different species require different optimal NH_4^+:NO_3^- ratios. For example, the optimal NH_4^+:NO_3^- ratio is 0:100 for yellow flag (Chang et al., 2010) and wheat (Yang et al., 2021); 25:75 for Chinese cabbage cultivars (Chen et al., 2005; Zhu et al., 2021), strawberry (Tabatabaei et al., 2006), tomato (Liu et al., 2017),

10.3389/fpls.2023.1324820

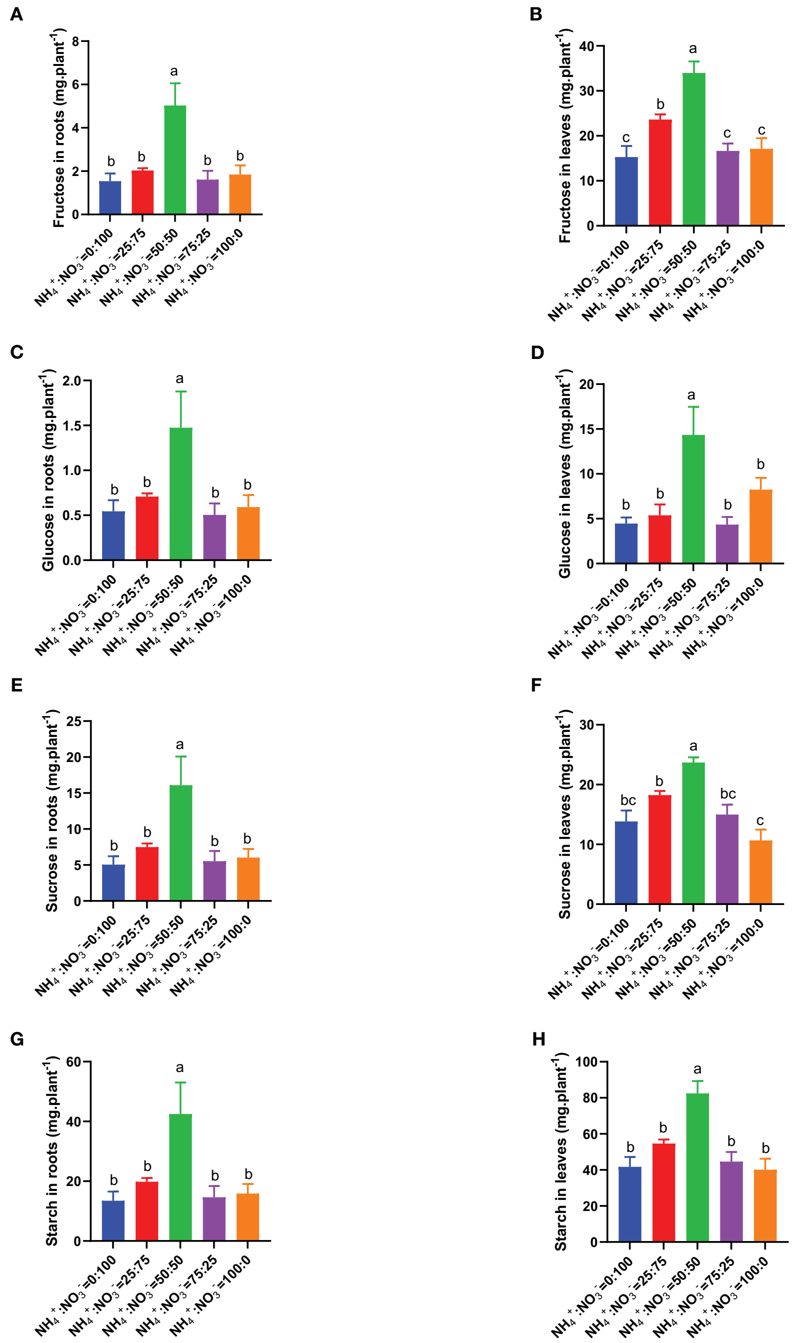

FIGURE 6
Total soluble sugars and starch in centipedegrass that received one month of different NH_4^+:NO_3^- ratio treatments. **(A, B)**, Total fructose content in the roots **(A)** and leaves **(B)**. **(C, D)**, Total glucose content in the roots **(C)** and leaves **(D)**. **(E, F)**, Total sucrose content in the roots **(E)** and leaves **(F)**. **(G, H)**, Total sucrose content in the roots **(G)** and leaves **(H)**. N=4. The different letters above the columns represent significant differences between treatments (P < 0.05).

Chinese kale (Wang et al., 2021), and lettuce (Du et al., 2022); 50:50 for cabbage (Zhang et al., 2007), Sweet flag (Chang et al., 2010), coffee (Carr et al., 2020), soybean (Raza et al., 2021), and blackberry (Wei et al., 2023); 75:25 for pecan (Chen et al., 2021); and 83:17 for blueberry (Zhang et al., 2021). In this study, the effects of different NH_4^+:NO_3^- ratios on the growth parameters of centipedegrass were monitored and the NH_4^+:NO_3^- ratio of 50:50 treatment had the highest biomass and carbon and nitrogen accumulation (Figure 3).

We recommend an NH_4^+:NO_3^- ratio of 50:50 as the optimal NH_4^+:NO_3^- ratio for the production of centipedegrass. The reason for this phenomenon is as follows. 1) Roots, the gateway for nitrogen input, have the maximal ammonium and nitrate absorption capacity, which is closely related to the better root architecture under this treatment (Figure 1; Figure 4). Certainly, the possibility that the increased expression abundance of transporters responsible for ammonium and nitrate uptake contributes to the maximal

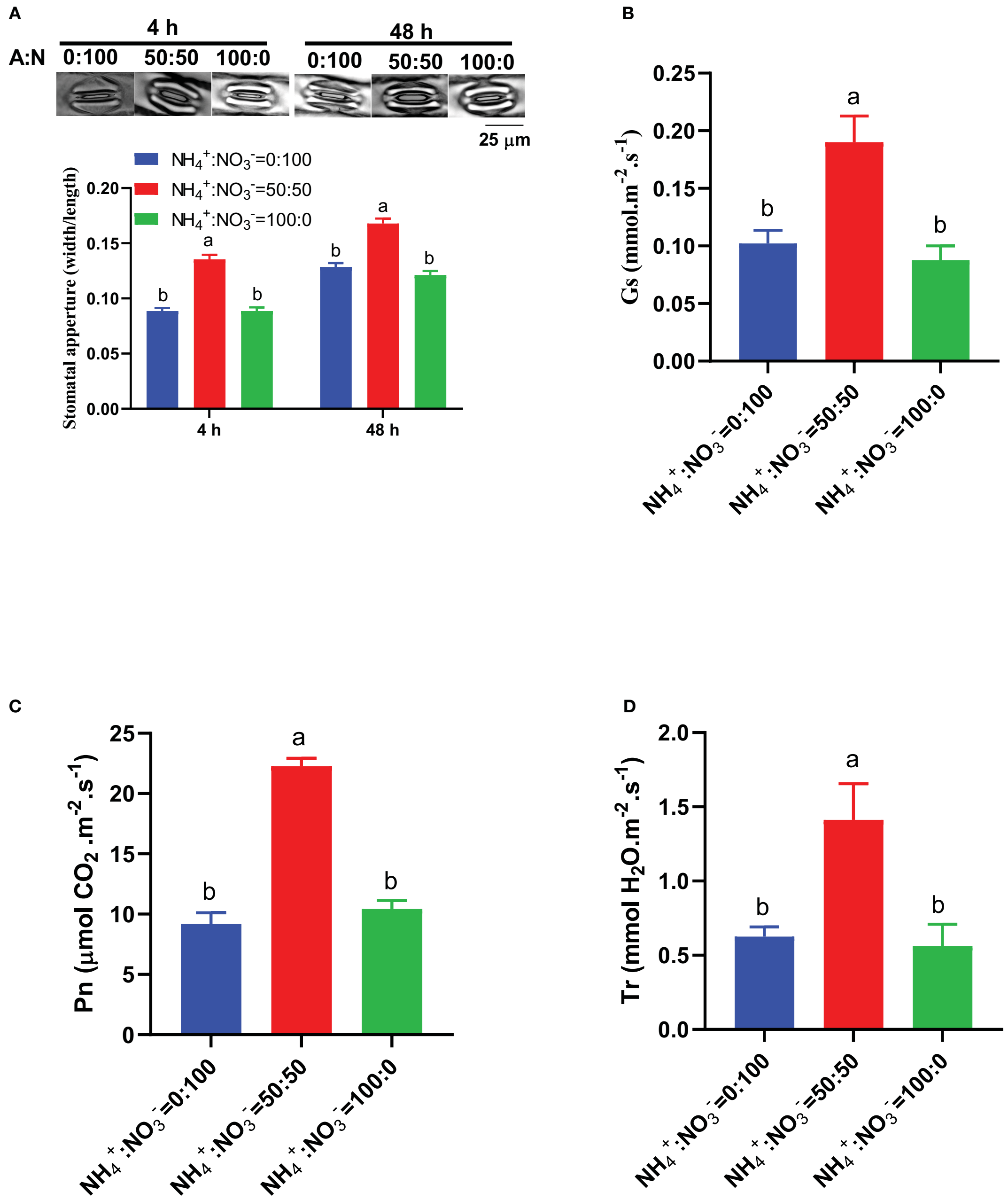

FIGURE 7
The early stage response of stomata and photosynthetic parameters to different NH_4^+:NO_3^- ratio treatments. **(A)**, Representative photos of stomata (upper) and statistical results of stomatal aperture (lower) in leaves that received 4 h and 48 h of treatments. **(B–D)**, Stomatal conductance (Gs) **(B)**, photosynthetic rate (Pn) **(C)**, and transpiration rate (Tr) **(D)** in leaves that received 48 hours of treatments. N>70 for Panel **(A)**. n=4 for Panels **(B–D)**. The different letters above the columns represent significant differences between treatments ($P < 0.05$).

nitrogen uptake capacity cannot be ruled out. In addition to the improvement of nitrogen absorption capacity, the NH_4^+:NO_3^- ratio of 50:50 has the strongest nitrogen assimilation ability, which is confirmed by the highest Gln (the first product of nitrogen assimilation) accumulation (Figure 4). As an essential element, the improvement of both the absorption and utilization capacity of nitrogen is beneficial for plant growth. The enhanced nitrogen assimilation ability requires more energy and carbon skeleton, which were come from the enhanced carbon absorption and assimilation ability mentioned below. 2) Leaves, the gateway for carbon input, have the highest photosynthetic capacity and content of carbohydrates (fructose, glucose, sucrose, starch), which is closely related to the largest stomatal aperture under this treatment (Figures 5, 6). The photosynthetic rate reflects the ability of plants to assimilate CO_2. The higher the photosynthetic rate demonstrates a stronger ability of plants to assimilate CO_2. The photosynthetic products of CO_2 assimilation are sugars, which are composed of monosaccharides (glucose, fructose), disaccharides (sucrose), and polysaccharides (starch). Therefore, the NH_4^+:NO_3^- ratio of 50:50 resulted in the highest photosynthetic rate, resulting in the maximum photosynthetic products. This is similar to the result of the maximum sugar accumulation in corn under the optimal NH_4^+:NO_3^- ratio (Wang et al., 2019b). Since more than 90% of the dry matter accumulation in plants comes from photosynthesis, the increase in photosynthetic rate and products is beneficial for plant growth. 3) The NH_4^+:NO_3^- ratio of 50:50 treatment showed the largest stem xylem vessel area and transpiration rate (Figure 2; Figure 5). The NH_4^+:NO_3^- ratio of 50:50 treatment had the highest transpiration rate, which provides plants with greater transpiration pull and facilitates the root-to-shoot translocation of water and inorganic salts from the enlarged stem xylem vessel. Among the three explanations, the stronger photosynthetic capacity and better root architecture are consistent with many reports of appropriate NH_4^+:NO_3^- ratios promoting plant growth (Tabatabaei et al., 2006; Hu et al., 2017; Liu et al., 2017; Wang et al., 2019b; Carr et al., 2020; Raza et al., 2021; Zhang et al., 2021). There is still a lack of information regarding the response of the micromorphological structure of roots and stems to changes in the NH_4^+:NO_3^- ratio. This study was the first to report the effect of different NH_4^+:NO_3^- ratios on the micromorphological structure of roots and stems. The NH_4^+:NO_3^- ratio of 50:50 treatment had the highest number of root xylem vessels, root xylem vessel area, stem xylem vessel number, and stem xylem vessel area (Figure 2). Given that a larger root and stem xylem vessel area is conducive to the loading of water and inorganic salts in the roots and their root-to-shoot translocation (Albornoz et al., 2020) and that the NH_4^+:NO_3^- ratio of 50:50 treatment had the highest transpiration rate, the greater transpiration pull and the enlarged stem xylem vessel facilitated nutrient uptake and translocation.

The mean biomass carbon density of grasslands (4.8 Mg C ha^{-1}) in China is significantly lower than the global average level (7.2 Mg C ·ha^{-1}) (Tang et al., 2018), indicating that grasslands in China still have high carbon sequestration potential. In this study, the maximum carbon accumulation was achieved under the NH_4^+:NO_3^- ratio of 50:50 treatment, which significantly improved the carbon sequestration capacity, reaching an increased amplitude of 140% when compared with the parameter under only nitrate treatment (Figure 3). This appropriate NH_4^+:NO_3^- ratio is efficient in enhancing the carbon sequestration capacity of grasslands. The reason for the maximum carbon accumulation achieved under the NH_4^+:NO_3^- ratio of 50:50 treatment is attributed to the maximum stomatal aperture, stomatal conductivity, maximum photosynthetic rate, and maximum soluble sugar and starch content (Figures 5, 6). Numerous reports have shown that an appropriate NH_4^+:NO_3^- ratio improves the photosynthetic rate (Tabatabaei et al., 2006; Hu et al., 2017; Liu et al., 2017; Wang et al., 2019b; Carr et al., 2020; Raza et al., 2021; Zhang et al., 2021). The underlying mechanism is related to the maximum and effective quantum yield of PSII, improved activities of Calvin cycle enzymes, increased levels of mRNA relative expression of several genes involved in the Calvin cycle (Hu et al., 2017; Raza et al., 2021), improved gas exchanges (Raza et al., 2021), and higher chlorophyll pigments. The positive correlation between photosynthetic rate and stomatal aperture/conductance observed in this study further confirms the above conclusion (Figure 5). The increase in stomatal opening occurred in the early stages of treatment (4 hours) (Figure 7), indicating that the change in stomatal opening is crucial for the improved photosynthetic rate. Whether other factors affecting the photosynthetic rate changed in the early stages of NH_4^+:NO_3^- ratio treatment, thereby regulating the photosynthetic rate, needs further experimental evidence.

The improvement of nitrogen use efficiency can effectively reduce a series of environmental problems caused by large nitrogen fertilizer production and application. The maximum nitrogen accumulation was achieved under the NH_4^+:NO_3^- ratio of 50:50 treatment, which significantly improved the nitrogen use efficiency compared to other NH_4^+:NO_3^- ratio treatments (Figure 3). We recommend an NH_4^+:NO_3^- ratio of 50:50 as the optimal NH_4^+:NO_3^- ratio to improve nitrogen use efficiency. The highest nitrogen accumulation was attributed to the highest root ammonium, nitrate uptake rate, and assimilation ability (Figure 4). The NH_4^+:NO_3^- ratio of 50:50 treatment resulted in the largest root surface area and total root length (Figure 1). The root architecture plays an essential role in nitrogen uptake (Meister et al., 2014). The root length and surface area are important for nitrogen acquisition and a large root system is associated with higher nitrogen acquisition (Sattelmacher et al., 1990), since these parameters reflect the contact area between the plant root system and the external nutrient solution. The larger the total root length and root surface area would lead to a greater contact area between the plant and the rhizosphere nutrient, which is more conducive to nutrient absorption under the NH_4^+:NO_3^- ratio of 50:50 treatment. In addition, an increase in the area of the root xylem vessel is also beneficial for nutrient loading in the roots (Figure 2). The absorption rate of ammonium was much higher than that of nitrate (Figure 4), indicating that centipedegrass has a preference for ammonium. This may reflect an adaptation of centipedegrass to its acidic soil growth environment, similar to the situation in other plants (Daryanto et al., 2019). The NH_4^+:NO_3^- ratio of 50:50 treatment had the highest Gln content, which may be closely related to the maximum photosynthetic rate and the largest amount of photosynthetic products, providing the carbon skeleton and energy needed for nitrogen assimilation (Li et al., 2020).

4.2 Stomata are the structures that respond to root ammonium nitrate ratio treatment at the early stage

Carbon-nitrogen synergy is beneficial for plant growth (Wang et al., 2019a). Carbon metabolism provides energy and carbon skeletons for nitrogen metabolism. Nitrogen, as a component of amino acids, proteins, nucleic acids, phospholipids, enzymes, ATP, chlorophyll, and hormones, significantly regulates carbon metabolism (Lawlor, 2002). The main reason for plant growth inhibition under ammonium supply alone is photosynthetic inhibition-induced carbon deficiency (Yang et al., 2020). The discovery in this study that ammonium treatment alone had the smallest carbon accumulation and carbon-nitrogen ratio once again supports this conclusion (Figure 3). Compared with other NH_4^+:NO_3^- ratio treatments, the NH_4^+:NO_3^- ratio of 50:50 treatment showed the highest stomatal opening and photosynthetic rate,

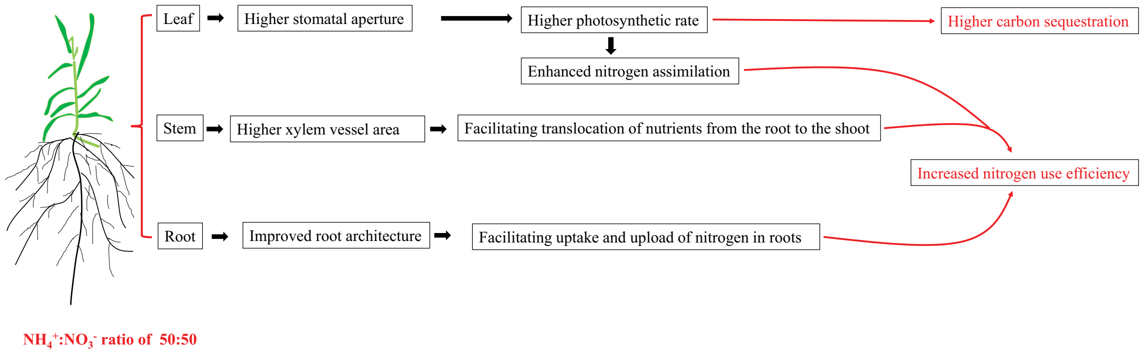

FIGURE 8
A mode explaining the growth promotion caused by the appropriate NH_4^+:NO_3^- ratio treatment. Under the appropriate NH_4^+:NO_3^- ratio treatment, the changes in root architecture allow a more favourable absorption of nitrogen and its loading into the root xylem. The greater transpiration pull triggered by greater transpiration and the larger stem xylem vessel synergistically facilitated the root-to-shoot translocation of nutrients. The increase in leaf stomatal opening increases the photosynthetic rate, increases carbon absorption and assimilation, and promotes nitrogen assimilation. The synergistic changes in the structure and physiological functions of the three organs of roots, stems, and leaves caused by the appropriate NH_4^+:NO_3^- ratio together improve the nitrogen use efficiency and carbon sequestration capacity of centipedegra.

resulting in the highest carbon accumulation and carbon-nitrogen ratio (Figure 3). Considering that photosynthesis is the main source of plant carbon, the maximum photosynthetic rate under the NH_4^+:NO_3^- ratio of 50:50 treatment is the main reason for its maximum carbon accumulation and carbon-nitrogen ratio under this treatment. Numerous studies have reported the key role of enhanced photosynthetic capacity in promoting plant growth under appropriate NH_4^+:NO_3^- ratio treatments. Notably, those measurements were obtained after long-term NH_4^+:NO_3^- ratio treatment (>12 days) (Tabatabaei et al., 2006; Wang et al., 2019b; Zhang et al., 2021). This study was the first to show that in the early stages of treatment (4 hours), stomata began to respond to the root NH_4^+:NO_3^- ratio supply (Figure 7). Manipulating stomata is a promising focus for improving the nitrogen use efficiency of centipedegrass.

5 Conclusion

We recommend 50:50 as the appropriate NH_4^+:NO_3^- ratio for the growth of centipedegrass, which not only improves the nitrogen use efficiency but also enhances the carbon sequestration capacity. Both of which facilitate the achievement of carbon neutrality. The synergistic effect of physiological and structural aspects on various parts of roots, stems, and leaves is the main reason for this phenomenon. Briefly, the changes in root architecture allow a more favourable absorption of nitrogen and its loading into the root xylem. The greater transpiration pull triggered by greater transpiration and the larger stem xylem vessel synergistically facilitated the root-to-shoot translocation of nutrients. The increase in leaf stomatal opening increases the photosynthetic rate, increases carbon absorption and assimilation, and promotes nitrogen assimilation. The synergistic changes in the structure and physiological functions of the three organs of roots, stems, and leaves caused by the appropriate NH_4^+:NO_3^- ratio together improve the nitrogen use efficiency and carbon sequestration capacity of centipedegrass (Figure 8). Considering that stomatal aperture is sensitive to the root NH_4^+:NO_3^- ratio treatment, manipulating stomata is a promising strategy for improving the nitrogen use efficiency of centipedegrass.

Data availability statement

The original contributions presented in the study are included in the article/supplementary material. Further inquiries can be directed to the corresponding authors.

Author contributions

DH: Data curation, Methodology, Writing – original draft. JZ: Methodology, Writing – review & editing. LL: Writing – review & editing. JQ: Methodology, Writing – review & editing. XL: Writing – review & editing. RC: Writing – review & editing. WK: Writing – review & editing. DL: Writing – review & editing. JL: Writing – review & editing. HG: Writing – review & editing. JL: Writing – review & editing. JZ: Supervision, Writing – review & editing. JC: Supervision, Writing – review & editing.

Funding

The author(s) declare financial support was received for the research, authorship, and/or publication of this article. The authors are grateful for the financial support provided by the Jiangsu Provincial Double-Innovation Doctor Program (Grant No. JSSCBS20221643), the Jiangsu Institute of Botany Talent Fund (Grant No. JIBTF202210), the Natural Science Foundation of Jiangsu Province (BK20210162), the Scientific and Technological Innovation Fund of Carbon Emissions Peak and Neutrality of Jiangsu Provincial Department of Science and Technology (Grant No. BE2022304), the Program for the Young Innovative Talents of Jiangsu Vocational College of Agriculture and Forest (Grant No.

2021kj26), and the National Nature Science Foundation of China (32102424).

Conflict of interest

The authors declare that the research was conducted in the absence of any commercial or financial relationships that could be construed as a potential conflict of interest.

Publisher's note

All claims expressed in this article are solely those of the authors and do not necessarily represent those of their affiliated organizations, or those of the publisher, the editors and the reviewers. Any product that may be evaluated in this article, or claim that may be made by its manufacturer, is not guaranteed or endorsed by the publisher.

References

Ahmadi, F., Samadi, A., Sepehr, E., Rahimi, A., and Shabala, S. (2021a). Optimizing hydroponic culture media and NO(3)(-)/NH(4)(+) ratio for improving essential oil compositions of purple coneflower (EChinacea purpurea L.). *Sci. Rep.* 11, 8009. doi: 10.1038/s41598-021-87391-9

Ahmadi, F., Samadi, A., Sepehr, E., Rahimi, A., and Shabala, S. (2021b). Perlite particle size and NO3-/NH4+ ratio affect growth and chemical composition of purple coneflower (EChinacea purpurea L.) in hydroponics. *Ind. Crop Prod.* 162, 113285. doi: 10.1016/j.indcrop.2021.113285

Ahmadi, F., Samadi, A., Sepehr, E., Rahimi, A., and Shabala, S. (2022). Cell-type-specific H+-ATPase activity and antioxidant enzymes improve the EChinacea purpurea L. Moench tolerance to salinity stress at different NO3-/NH4+ ratios. *Ind. Crop Prod.* 186, 115199. doi: 10.1016/j.indcrop.2022.115199

Akiyama, H., Yan, X., and Yagi, K. (2009). Evaluation of effectiveness of enhanced-efficiency fertilizers as mitigation options for N2O and NO emissions from agricultural soils: meta-analysis. *Global Change Biol.* 16, 1837–1846. doi: 10.1111/j.1365-2486.2009.02031.x

Albornoz, F., Pérez-Donoso, A. G., Leigh Urbina, J., Monasterio, M., Gómez, M., and Steinfort, Ú. (2020). Nitrate transport rate in the xylem of tomato plants grafted onto a vigorous rootstock. *Agronomy* 10, 182. doi: 10.3390/agronomy10020182

Carr, N. F., Boaretto, R. M., and Mattos, D. (2020). Coffee seedlings growth under varied NO3–:NH4+ ratio: Consequences for nitrogen metabolism, amino acids profile, and regulation of plasma membrane H+-ATPase. *Plant Physiol. Biochem.* 154, 11–20. doi: 10.1016/j.plaphy.2020.04.042

Chang, J., Liu, D., Cao, H., Chang, S. X., Wang, X., Huang, C., et al. (2010). NO3–/NH4 + ratios affect the growth and N removal ability of Acorus calamus and Iris pseudacorus in a hydroponic system. *Aquat. Bot.* 93, 216–220. doi: 10.1016/j.aquabot.2010.08.002

Chen, W., Luo, J. K., and Shen, Q. R. (2005). Effect of NH4+-N/NO3–N ratios on growth and some physiological parameters of chinese cabbage cultivars. *Pedosphere* 15, 310–318.

Chen, M., Zhu, K., Tan, P., Liu, J., Xie, J., Yao, X., et al. (2021). Ammonia–nitrate mixture dominated by NH4+–N promoted growth, photosynthesis and nutrient accumulation in pecan (Carya illinoinensis). *Forests* 12, 1808. doi: 10.3390/f12121808

Daryanto, S., Wang, L., Gilhooly, W. P., and Jacinthe, P.-A. (2019). Nitrogen preference across generations under changing ammonium nitrate ratios. *J. Plant Ecol.* 12, 235–244. doi: 10.1093/jpe/rty014

Du, K., Zhang, J., Han, Y., Hao, J., Qin, X., Liu, C., et al. (2022). Effects of varying NO3$^-$:NH4+ ratios on lettuce (Lactuca sativa L.) nitrogen metabolism. *Pak. J. Bot.* 54, 2081–2088. doi: 10.30848/PJB2022-6(37

Hao, D., Li, X., Kong, W., Chen, R., Liu, J., Guo, H., et al. (2023). Phosphorylation regulation of nitrogen, phosphorus, and potassium uptake systems in plants. *Crop J.* 11, 1034–1047. doi: 10.1016/j.cj.2023.06.003

Hao, D. L., Zhou, J. Y., Yang, S. Y., Huang, Y. N., and Su, Y. H. (2020). Functional and regulatory characterization of three AMTs in maize roots. *Front. Plant Sci.* 11. doi: 10.3389/fpls.2020.00884

Hu, L., Liao, W., Dawuda, M. M., Yu, J., and Lv, J. (2017). Appropriate NH4 +: NO3 – ratio improves low light tolerance of mini Chinese cabbage seedlings. *BMC Plant Biol.* 17, 1–14. doi: 10.1186/s12870-017-0976-8

Khan, S. A., Mulvaney, R. L., Ellsworth, T. R., and Boast, C. W. (2007). The myth of nitrogen fertilization for soil carbon sequestration. *J. Environ. Qual.* 36, 1821–1832. doi: 10.2134/jeq2007.0099

Lawlor, D. W. (2002). Carbon and nitrogen assimilation in relation to yield: mechanisms are the key to understanding production systems. *J. Exp. Bot.* 53, 773–787. doi: 10.1093/jexbot/53.370.773

Li, D., Liu, J., Guo, H., Zong, J., Li, J., Wang, J., et al. (2022). Effects of low nitrogen supply on nitrogen uptake, assimilation and remobilization in wild Bermudagrass. *Plant Physiol. Biochem.* 191, 34–41. doi: 10.1016/j.plaphy.2022.09.019

Li, Y., Zhou, J., Hao, D., Yang, S., and Su, Y. (2020). Arabidopsis under ammonium over-supply: Characteristics of ammonium toxicity in relation to the activity of ammonium transporters. *Pedosphere* 30, 314–325. doi: 10.1016/S1002-0160(20)60011-X

Liu, G., Du, Q., and Li, J. (2017). Interactive effects of nitrate-ammonium ratios and temperatures on growth, photosynthesis, and nitrogen metabolism of tomato seedlings. *Sci. Hortic.* 214, 41–50. doi: 10.1016/j.scienta.2016.09.006

Meister, R., Rajani, M. S., Ruzicka, D., and Schachtman, D. P. (2014). Challenges of modifying root traits in crops for agriculture. *Trends Plant Sci.* 19, 779–788. doi: 10.1016/j.tplants.2014.08.005

Pilot, G., Stransky, H., Bushey, D. F., Pratelli, R., Ludewig, U., Wingate, V. P., et al. (2004). Overexpression of GLUTAMINE DUMPER1 leads to hypersecretion of glutamine from Hydathodes of Arabidopsis leaves. *Plant Cell* 16, 1827–1840. doi: 10.1105/tpc.021642

Ravishankara, A. R., Daniel, J. S., and Portmann, R. W. (2009). Nitrous oxide (N2O): the dominant ozone-depleting substance emitted in the 21st century. *Science* 326, 123–125. doi: 10.1126/science.1176985

Raza, A., Asghar, M. A., Hussain, S., Bin, C., Shafiq, I., Ahmad, I., et al. (2021). Optimal NH(4) (+) /NO(3) (-) ratios enhance the shade tolerance of soybean seedlings under low light conditions. *Plant Biol.* 23, 464–472. doi: 10.1111/plb.13219

Sattelmacher, B., Klotz, F., and Marschner., H. (1990). Influence of the nitrogen level on root growth and morphology of two potato varieties differing in nitrogen acquisition. *Plant Soil* 123, 131–137. doi: 10.1007/BF00011258

Shaddox, T. W., Unruh, J. B., and Trenholm, L. E. (2016). Nitrate leaching from soluble nitrogen applied to 'Floratam' St. Augustinegrass and common centipedegrass during dormancy. *Crop Sci.* 56, 837–844. doi: 10.2135/cropsci2015.02.0104

Smith, P. (2014). Do grasslands act as a perpetual sink for carbon? *Global Change Biol.* 20, 2708–2711. doi: 10.1111/gcb.12561

Tabatabaei, S. J., Fatemi, L. S., and Fallahi, E. (2006). Effect of ammonium: nitrate ratio on yield, calcium concentration, and photosynthesis rate in strawberry. *J. Plant Nutr.* 29, 1273–1285. doi: 10.1080/01904160600767575

Tang, X., Zhao, X., Bai, Y., Tang, Z., Wang, W., Zhao, Y., et al. (2018). Carbon pools in China's terrestrial ecosystems: New estimates based on an intensive field survey. *Proc. Natl. Acad. Sci. U. S. A.* 115, 4021–4026. doi: 10.1073/pnas.1700291115

Wang, Y. X., Teng, R. M., Wang, W. L., Wang, Y., Shen, W., and Zhuang, J. (2019c). Identification of genes revealed differential expression profiles and lignin accumulation during leaf and stem development in tea plant (Camellia sinensis (L.) O. Kuntze). *Protoplasma* 256, 359–370. doi: 10.1007/s00709-018-1299-9

Wang, P., Wang, Z., Pan, Q., Sun, X., Chen, H., Chen, F., et al. (2019b). Increased biomass accumulation in maize grown in mixed nitrogen supply is mediated by auxin synthesis. *J. Exp. Bot.* 70, 1859–1873. doi: 10.1093/jxb/erz047

Wang, P., Wang, Z.-K., Sun, X.-C., Mu, X.-H., Chen, H., Chen, F.-J., et al. (2019a). Interaction effect of nitrogen form and planting density on plant growth and nutrient uptake in maize seedlings. *J. Integr. Agric.* 18, 1120–1129. doi: 10.1016/S2095-3119(18)61977-X

Wang, Y., Zhang, X., Liu, H., Sun, G., Song, S., and Chen, R. (2021). High NH4 +/NO3– ratio inhibits the growth and nitrogen uptake of chinese kale at the late growth stage by ammonia toxicity. *Horticulturae* 8, 8. doi: 10.3390/horticulturae8010008

Wei, Z., Yang, H., Duan, Y., Wu, W., Lyu, L., and Li, W. (2023). Physiological and metabolomic analyses reveal the effects of different NH4+:NO3– ratios on blackberry fruit quality. *Sci. Hortic.* 318, 112124. doi: 10.1016/j.scienta.2023.112124

Xu, R., Wang, Y., Wang, Y., Niu, H., Liu, Y., and Zhuang, Q. (2018). Estimating N2O emissions from soils under natural vegetation in China. *Plant Soil* 434, 271–287. doi: 10.1007/s11104-018-3856-6

Xu, X., Wang, H., Zhang, B., Zhang, L., Li, X., Hao, D., et al. (2023). Micromorphological and physiological responses of two contrasting centipedegrass (Eremochloa ophiuroides (Munro) hack.) genotypes in response to aluminum toxicity. *J. Soil Sci. Plant Nutr.* 23, 2174–2189. doi: 10.1007/s42729-023-01171-0

Yang, S., Hao, D., Jin, M., Li, Y., Liu, Z., Huang, Y., et al. (2020). Internal ammonium excess induces ROS-mediated reactions and causes carbon scarcity in rice. *BMC Plant Biol.* 20, 143. doi: 10.1186/s12870-020-02363-x

Yang, D., Zhao, J., Bi, C., Li, L., and Wang, Z. (2021). Transcriptome and proteomics analysis of wheat seedling roots reveals that increasing NH(4) (+)/NO(3) (-) ratio induced root lignification and reduced nitrogen utilization. *Front. Plant Sci.* 12. doi: 10.3389/fpls.2021.797260

Zhang, F.-C., Kang, S.-Z., Li, F.-S., and Zhang, J.-H. (2007). Growth and major nutrient concentrations in brassica campestris supplied with different NH4+/NO3- ratios. *J. Integr. Plant Biol.* 49, 455–462. doi: 10.1111/j.1744-7909.2007.00373.x

Zhang, Y. Y., Tian, J. P., Cui, J., Hong, Y. H., and Luan, Y. S. (2021). Effects of different NH4+/NO3- ratios on the photosynthetic and physiology responses of blueberry (Vaccinium spp.) seedlings growth. *J. Plant Nutr.* 44, 854–864. doi: 10.1080/01904167.2021.1871754

Zhu, Y., Qi, B., Hao, Y., Liu, H., Sun, G., Chen, R., et al. (2021). Appropriate NH(4) (+)/NO(3) (-) ratio triggers plant growth and nutrient uptake of flowering chinese cabbage by optimizing the ph value of nutrient solution. *Front. Plant Sci.* 12. doi: 10.3389/fpls.2021.656144

frontiers | Frontiers in Plant Science

TYPE Original Research
PUBLISHED 06 March 2024
DOI 10.3389/fpls.2024.1344022

Check for updates

OPEN ACCESS

EDITED BY
Levent Ozturk,
Sabancı University, Türkiye

REVIEWED BY
Jie Jin,
North China Electric Power University, China
Hafiz Mohkum Hammad,
Muhammad Nawaz Shareef University of Agriculture, Pakistan

*CORRESPONDENCE
Henry Y. Sintim
hsintim@uga.edu

RECEIVED 24 November 2023
ACCEPTED 20 February 2024
PUBLISHED 06 March 2024

CITATION
Amissah S, Ankomah G, Lee RD, Perry CD, Washington BJ, Porter WM, Virk S, Bryant CJ, Vellidis G, Harris GH, Cabrera M, Franklin DH, Diaz-Perez JC and Sintim HY (2024) Assessing corn recovery from early season nutrient stress under different soil moisture regimes. *Front. Plant Sci.* 15:1344022. doi: 10.3389/fpls.2024.1344022

Assessing corn recovery from early season nutrient stress under different soil moisture regimes

Solomon Amissah[1], Godfred Ankomah[1], Robert D. Lee[1], Calvin D. Perry[2], Bobby J. Washington[2], Wesley M. Porter[1], Simerjeet Virk[1], Corey J. Bryant[1,3], George Vellidis[1], Glendon H. Harris[1], Miguel Cabrera[4], Dorcas H. Franklin[4], Juan C. Diaz-Perez[5] and Henry Y. Sintim[1*]

[1]Department of Crop and Soil Sciences, University of Georgia, Tifton, GA, United States, [2]C. M. Stripling Irrigation Research Park, University of Georgia, Camilla, GA, United States, [3]Delta Research and Extension Center, Mississippi State University, Stoneville, MS, United States, [4]Department of Crop and Soil Sciences, University of Georgia, Athens, GA, United States, [5]Department of Horticulture, University of Georgia, Tifton, GA, United States

Corn (*Zea mays*) biomass accumulation and nutrient uptake by the six-leaf collar (V6) growth stage are low, and therefore, synchronizing nutrient supply with crop demand could potentially minimize nutrient loss and improve nutrient use efficiency. Knowledge of corn's response to nutrient stress in the early growth stages could inform such nutrient management. Field studies were conducted to assess corn recovery from when no fertilizer application is made until the V6 growth stage, and thereafter, applying fertilizer rates as those in non-stressed conditions. The early season nutrient stress and non-stress conditions received the same amount of nutrients. As the availability of nutrients for plant uptake is largely dependent on soil moisture, corn recovery from the early season nutrient stress was assessed under different soil moisture regimes induced via irrigation scheduling at 50% and 80% field capacity under overhead and subsurface drip irrigation (SSDI) systems. Peanut (*Arachis hypogaea*) was the previous crop under all conditions, and the fields were under cereal rye (*Secale cereale*) cover crop prior to planting corn. At the V6 growth stage, the nutrient concentrations of the early season-stressed crops, except for copper, were above the minimum threshold of sufficiency ranges reported for corn. However, the crops showed poor growth, with biomass accumulation being reduced by over 50% compared to non-stressed crops. Also, the uptake of all nutrients was significantly lower under the early season nutrient stress conditions. The recovery of corn from the early season nutrient stress was low. Compared to non-stress conditions, the early season nutrient stress caused 1.58 Mg ha^{-1} to 3.4 Mg ha^{-1} yield reduction. The percent yield reduction under the SSDI system was 37.6-38.2% and that under the overhead irrigation system was 11.7-13%. The high yield reduction from the early season nutrient stress under the SSDI system was because of water stress conditions in the topsoil soil layer. The findings of the study suggest ample nutrient supply in the early season growth stage is critical for corn production, and thus, further studies are recommended to determine the optimum nutrient supply for corn at the initial growth stages.

KEYWORDS

adaptive nutrient management, nutrient stress, nutrient dilution effects, soil moisture, residual soil nutrients, corn productivity

1 Introduction

Optimum plant nutrition is required to sustain plant health and productivity, especially for a high-input crop such as corn (*Zea mays*). Application of fertilizer to meet plant nutritional needs is therefore very critical in regions with highly weathered soil conditions. Oxisols and Ultisols, for instance, are highly weathered soils commonly found in tropical and subtropical regions. They are characterized by low organic matter, strong acidity, and poor native fertility because of rapid mineralization rates, intense weathering of primary minerals, and leaching of essential base cations (Juo and Franzluebbers, 2003; Chesworth et al., 2008; Weil and Brady, 2017; Nunes et al., 2019). This makes fertilizer a major input cost in corn production in the region. Moreover, instability in the supply and prices of fertilizers observed in recent years poses a lot of concern (Singh and Tan, 2022; Amissah et al., 2023b). Several fertilizers exceeded record prices in 2008, which affected the profit margin for growers (Singh and Tan, 2022). It is therefore imperative to optimize nutrient management in corn production.

Adaptive nutrient management that synchronizes nutrient supply with crop demand could increase nutrient use efficiency and minimize nutrient losses through runoff, leaching, ammonia volatilization, and denitrification (Esfandbod et al., 2017; Shahzad et al., 2018, 2019a; Amissah et al., 2023a). Crop nutrient uptake is low at the initial stages of growth, increasing towards the reproductive stage (Bender et al., 2013; Ciampitti and Vyn, 2014). A study conducted at two locations in the state of Illinois in the United States showed that by the six-leaf collar (V6) growth stage, <15% of macro- and micronutrients had been taken up by corn when compared to the total uptake at maturity (Bender et al., 2013). Also, biomass accumulation by the V6 stage was <5%. In conventional nutrient management, almost all the fertilizer rates are applied before planting or at the initial stages of planting, except for nitrogen, which is usually split-applied. In the southeast United States, with characteristic high rainfall and temperatures, fertilizers applied at the initial stages of growth are susceptible to losses, especially when the vegetation cover is minimal. Knowledge of corn recovery to early season nutrient stress could be used to better synchronize nutrient application with crop demand.

As corn is a high-input crop, it requires substantial levels of nutrients and water to sustain productivity. Moreover, the amount of water present in the soil largely affects the solubility and availability of applied mineral nutrients to crops (Pan et al., 2011; Sintim et al., 2015, 2016; Kusi et al., 2021b). Thus, there is a vital relationship between plant nutrient uptake and the status of soil water (Misra and Tyler, 2000; Djaman et al., 2013). Higher nutrient uptake levels have mainly been observed under adequate or fully irrigated conditions, while lower nutrient uptake is typical under water-limiting conditions (Setiyono et al., 2010; Djaman et al., 2013; Faloye et al., 2019). For instance, Djaman and Irmak (2018) observed reduced nitrogen (N) uptake when corn was irrigated below 75% of fully-irrigated treatment, with the fully-irrigated treatment being irrigation scheduling at 60% of total available water. The authors observed similar results for phosphorus (P) (Djaman and Irmak, 2018). Also, Seiffert et al. (1995) observed reduced potassium (K) uptake in corn with decreasing soil water content. The root length and K influx were also reduced by about 50% under the low soil water conditions (Seiffert et al., 1995). The lower nutrient uptake under water stress is usually due to decreased nutrient transport by mass flow and diffusion (Seiffert et al., 1995; Buljovcic and Engels, 2001; Djaman and Irmak, 2018). Thus, nutrients that are preferentially taken up by the mass flow pathway tend to restrict plant growth the most under dry conditions.

After nutrient uptake, plants assimilate, translocate, or remobilize nutrients, which determines nutrient use efficiency (Masclaux-Daubresse et al., 2010; Sintim et al., 2015, 2016). Moisture stress conditions have a negative impact on transpiration rate and stomatal conductance, ultimately impacting photosynthesis and nutrient assimilation and translocation (Masclaux-Daubresse et al., 2010; Fahad et al., 2017). Plants under moisture stress also have poor growth due to impaired cell growth as a result of reduced turgor pressure (Hussain et al., 2008). Irrigation is therefore an important management practice to supplement crop water demand. Overhead irrigation is a widely used irrigation method, which supplies water over the top of the plant canopy or soil surface. High amounts of water can be lost under overhead irrigation systems via evaporation and surface runoff, especially during the early growth stages with little to no soil cover. There has been increased interest in subsurface drip irrigation (SSDI), which entails supplying water through drip tapes installed below the soil surface. The method effectively reduces water loss via evaporation and surface runoff (Colaizzi et al., 2004; Hassanli et al., 2009). The different modes of water supply in overhead and

SSDI irrigation systems change the soil moisture dynamics, and thus, different amounts of water may be needed to maintain the soil moisture content at a similar level. For corn production, irrigation scheduling at 50% field capacity (FC-50) is recommended as the standard to maximize net economic returns (Kisekka et al., 2016). However, the crop may experience some moisture stress. A study observed a significant yield difference in corn irrigated at FC-50 and 75% field capacity, with the FC-50 resulting in lower yields (Kebede et al., 2014).

Also, corn is particularly sensitive to nutrient stress in the early season, causing it to transition through its developmental stages quickly (Silva and Uchida, 2000; Grant et al., 2001; Roth et al., 2023). Thus, starter fertilizer, especially via band placement at 5.08 cm below the soil and 5.08 cm to the side of plant rows, is often applied at planting to induce early-season plant growth. However, the use of starter fertilizer does not always translate into better yield, especially under warm soil conditions, medium to high soil nutrient test levels, or when legume is the previous crop (Hoeft, 2000; Mallarino, 2015). There is limited information on whether corn will recover fully from nutrient stress in the early season under non-moisture stress conditions. Thus, the objective of the study was to assess corn recovery from early-season nutrient stress under different soil moisture regimes.

2 Materials and methods

2.1 Experimental site

Field experiments were established in 2021 and 2022 at the University of Georgia Stripling Irrigation Research Park in Camilla, GA (31°16'45.86"N, 84°17'29.65" W). The soil at the experimental site was Lucy loamy sand, classified as Loamy, kaolinitic, thermic Arenic Kandiudults, with an average sand, silt, and clay content of 90.7%, 3.2%, and 6.1%, respectively, at the 0-15 cm depth. The climate at the experimental site is subtropical, having average annual maximum, mean, and minimum air temperatures of 26.0°C, 19.4°C, and 12.8°C, respectively, with an annual rainfall of 1,314 mm and 98 average rainy days (Georgia AEMN, 2023). The minimum, average, and maximum air temperatures were 10.3°C, 20°C, and 27.7°C, respectively, in 2021, and 9.10°C, 19.7°C, and 28.1°C, respectively, in 2022. Annual rainfall was 1,419 mm in 2021 and 1,100 mm in 2022. Total rainfall received during the corn growing season (between planting and harvest) was 791 mm in 2021 and 629 mm in 2022.

2.2 Experimental approach

The field experiment entailed two irrigation scheduling thresholds [FC-50 and 80% field capacity (FC-80)], and two nutrient stress conditions [early season nutrient stress (ESN-stress) and non-nutrient stress (NN-stress)]. The treatment factors were laid in a split-plot randomized complete block design with four replications, and the experiment was established under two separate fields, with one field being equipped with an overhead irrigation system and the other field being equipped with an SSDI system. The two fields were 50 m apart in 2021 and 200 m apart in 2022. The irrigation schedules were the main plot factors, while the nutrient stress levels were the subplot factors.

The NN-stress entailed periodic nutrient application to ensure plant tissue nutrient levels were within recommended sufficiency levels for corn (Baker et al., 2000). The ESN-stress entailed no nutrient application until the V6 growth stage, after which the plots received a similar nutrient application as the NN-stress. The nutrient rates not supplied to the ESN-stress at the early stage were provided between the V6 and V7 growth stages. Thus, both nutrient stress levels received the same nutrient rates. Granular sources of nutrients were used as pre-plant fertilizer sources, and they were applied with a drop spreader, whereas in-season nutrient applications were by use of liquid side-dress applicators and injection through irrigation systems. Nutrient rates and main nutrient sources applied are presented in Table 1. Corn growth stage identification followed the University of Georgia Extension guideline (Bryant, 2021).

The irrigation schedule was determined by utilizing Teros 12 moisture sensors (METER Group, Inc., Pullman, WA, USA) initially installed at (a) 20 cm deep and 15 cm to the side of the plant row, and (b) 30 cm deep and 25 cm to the side of plant row to monitor soil moisture dynamics. The sensors were connected to a Zentra datalogger which was used to wirelessly transmit hourly soil moisture data. However, the sensors could not detect low rainfall events well. Thus, additional sensors and data loggers were obtained and installed at 10 cm deep and 15 to the side of plant rows, except for the FC-80 treatment under the SSDI system in 2021 due to limited supply. The available water holding capacity of the soil was calculated as the difference in water content at -33 kPa and -1500 kPa (Klute, 1986). Table 2 provides the amount of irrigation water supplied under the different irrigation scheduling and application methods.

2.3 Experimental field management

A lateral irrigation unit was used for the overhead irrigation system and had variable rate irrigation application capabilities. The SSDI system was set up by installing Netafim Typhoon drip tapes (Netafim Irrigation, Inc., Fresno, CA, USA) in the middle of plant rows at 30 cm soil depth. The fields were under cereal rye (*Secale cereale*) cover crop, and peanut (*Arachis hypogaea*) was the previous cash crop in both years. The cover crop was terminated by spraying Glyphosate [N-(phosphonomethyl) glycine] at the manufacturer-recommended rates, and the fields were prepared by strip-tilling to a depth of 30.5–45.7 cm before planting in March each year. The plot size was 12.2 m long by 5.49 m wide under the SSDI and 12.8 m long by 7.32 m wide under the overhead irrigation. Corn hybrid A6499STX by AgriGold was planted at the seeding rate of 88,958 seeds ha^{-1} and row spacing of 91.4 cm. Besides study treatments, standard agronomic and pest management recommendations by the University of Georgia Cooperative Extension were followed throughout the season to manage the experimental sites (Bryant, 2021).

TABLE 1 Total nutrient rates and main nutrient sources applied in 2021 and 2022.

Nutrients	Rates in 2021	Rates in 2022	Main nutrient sources
	kg ha^{-1}	kg ha^{-1}	
N	336	303	Urea; Urea ammonium nitrate solution
P_2O_5	252	121	Diammonium phosphate; Ammonium polyphosphate solution
K_2O	280	280	Potassium chloride; Potassium nitrate
Mg	5.60	5.60	Magnesium oxy-sulfate; Magnesium nitrate solution
Ca	11.2	5.60	Calcium chloride; Calcium sulfate; Calcium nitrate solution
S	11.2	11.2	Potassium sulfate; Ammonium thiosulfate solution
B	0.56	1.12	Fertilizer borate derived from Ulexite; Borosol® 10 solution
Zn	1.12	1.68	Zinc oxysulfate; Zinc nitrate solution
Mn	1.68	3.36	Manganese sucrate; Manganese nitrate solution
Fe	1.68	2.24	Iron sucrate; Iron nitrate solution
Cu	0.56	0.56	Copper sulfate; Copper nitrate solution
Mo	0.00	0.22	Sodium molybdate solution

2.4 Data collection

Initial nutrient levels of the soil were determined by sampling soils at 0-15 cm depth and sending them to the Waters Agricultural Laboratories, Inc. in Camilla, GA for analyses following standard procedures. Nitrate-N was measured with the automated flow injection analysis system (FIAlyzer-1000, FIAlab Instruments, Inc., Seattle, WA, USA) after extraction in a 2 M KCl solution. Extractable P, K, calcium (Ca), magnesium (Mg), iron (Fe), manganese (Mn), zinc (Zn), boron (B), and copper (Cu) were measured with an inductively coupled plasma optical emission spectrophotometer (ICP-OES; iCAP™ 6000 Series, Thermo Fisher Scientific, Cambridge, United Kingdom) after extraction with Mehlich I solution, and sulfur (S) was measured after extraction with monocalcium phosphate.

Before nutrient application in the ESN-stress plots, aboveground tissue samples were collected at the V6 growth stage within a uniform 1-m long strip of every plot and oven-dried, with oven set to 78°C until constant weight, to determine plant biomass. Nutrient analyses of the biomass samples were performed at the H.SINTIM LAB of the University of Georgia campus in Tifton, GA, following standard procedures. A 2400 Series II CHNS/O Elemental Analyzer (PerkinElmer U.S. LLC, Shelton, CT, USA) was used to measure the total N. Also, Avio 200 ICP-OES (PerkinElmer U.S. LLC, Shelton, CT, USA) was used to measure total P, K, Ca, Mg, S, Fe, Mn, Zn, B, Cu, and molybdenum (Mo) after sample digestion in nitric acid and hydrogen peroxide mixture using DigiPREP MS digestion block (SCP Science, Montreal, QC, Canada). Plant height (measured from the soil surface to the tallest leaf); ear height (measured from the soil surface to the base of the ear); ear length (length of the cob); ear diameter (measured from the center of the cob with grain intact); and ear grain rows (number of rows of corn grains on the cobs); and thousand seed weight (TSW) were determined at physiological maturity from plants within a uniform 1-m long strip. Also, the plants were partitioned into seeds and stover and dried in an oven to constant weight, and the weights were used to calculate the harvest index. The entire length of two rows of every plot was harvested with a plot combine harvester to obtain the seed weight and moisture content. The grain yield was determined at 155 g kg^{-1} moisture content.

2.5 Statistical analyses

The collected data were analyzed using a linear mixed model with the 'lme4' package in R (Bates et al., 2015). Separate statistical analyses were performed for the studies under the overhead irrigation and SSDI systems. The irrigation scheduling and nutrient stress factors were considered fixed effects, and year and block were considered random effects. Homoscedasticity of variance and assumptions of normality of residuals were assessed, and where appropriate, data transformation was performed using the Box-Cox transformation or the square root transformation methods. Separation of means was performed using the least square means and adjusted Tukey multiple comparison procedures with the 'emmeans' package in R (Lenth, 2018), and the significance level of all analyses was assessed at $P = 0.05$. The actual means and standard error of the data are reported in the tables and figures, which were followed by the mean separation letters obtained from the analyses. This approach avoids the need to back-transform data which sometimes produces values that are not consistent with the actual data.

TABLE 2 Irrigation water supplied (in mm) under the different irrigation scheduling and application methods in 2021 and 2022.

Irrigation	——— FC-50 ———		——— FC-80 ———	
	2021	2022	2021	2022
Overhead	172	240	226	446
SSDI	117	244	189	470

SSDI, Subsurface drip irrigation; FC-50, Irrigation triggered at 50% field capacity; FC-80, Irrigation triggered at 80% field capacity.

3 Results and discussion

3.1 Initial soil nutrients

Initial nutrient concentrations of the soil are presented in Table 3. The initial NO_3-N levels were generally low despite peanut, a legume, being the previous crop. However, the initial levels of the other nutrients were above the low threshold of the soil test classification for corn by the University of Georgia Extension, except for Zn in 2021 in the SSDI field (UGA-AESL, 2023). Nitrogen is usually not included in routine soil tests in the region because available forms of nitrogen do not accumulate (Kissel and Sonon, 2008; Hurisso et al., 2018). The sandy nature and high rainfall conditions in the region cause the available forms of nitrogen to readily leach, which could explain why low initial NO_3-N levels were observed. Moreover, the use of rye cover crops could have depleted the soil of NO_3-N. In addition, soils were sampled in late February, when temperatures were still low; thus, the peanut crop residuals may have not been sufficiently mineralized by the time of sampling (Grzyb et al., 2020; Shahzad et al., 2022; Amissah et al., 2023b). Mineralization of crop residues depends on several abiotic and biotic factors, including temperature, rainfall, soil properties, the chemical composition of crop residues, and the structure and composition of microbial communities (Whalen, 2014; Shahzad et al., 2019b; Grzyb et al., 2020; Sintim et al., 2022a; b).

3.2 Soil water dynamics

Soil moisture recharge at the 30-cm depth of the overhead irrigation at FC-50 was low during the mid-season in 2021. This triggered more irrigation under the overhead irrigation in 2021. The difference in irrigation water amount between the FC-50 and FC-80 of the overhead system was 54 mm in 2021 and 206 mm in 2022. Under the SSDI system, when soil moisture values of the sensors installed at 10 cm depth in 2021 and at 10 cm and 20 cm depths in 2022 are compared with those installed at the 30 cm depth, it can be seen that the sensors at the shallower depths could not detect irrigation events (Figure 1). The sensors were, however, able to detect rainfall events, demonstrating that the sensors were functional. As a result, the topsoil layer of the SSDI field was mostly below the permanent wilting point during the growing season, regardless of the irrigation scheduling threshold. In contrast, water content at the topsoil layer of the overhead irrigation was high, except for a single occasion when the water content under the FC-50 of the overhead irrigation went below the permanent wilting point in 2022. This was due to a technical constraint that delayed irrigation at the experiment station.

The inability of the soil moisture sensors at the topsoil layer to detect irrigation events under the SSDI system could be attributed to the configuration of the soil profile. The field has a top sandy layer underlaid by kaolinite clay minerals in the subsoil. Clay minerals have a larger surface area and more negative matric potential than sand (Jury and Horton, 2004). The drip tapes were installed at a 30-cm depth, which was at the interface of the sandy and clayey soil layer. Thus, the irrigation water would preferentially move downwards due to the higher capillarity of the clay layer and the downward exertion of the force of gravity (Abu-Zeid and El-Aal, 2017; Kroes et al., 2018; Rambabu et al., 2023). Irrigation water will only redistribute upwards to maintain equilibrium under very wet subsoil conditions.

3.3 Tissue nutrient concentration at the vegetative stage

The *P*-values of the main effects and interaction effects of irrigation schedule and nutrient stress on the concentration of plant nutrients at the vegetative stage are presented in Supplementary Table S1. The effects of the irrigation schedule on nutrient concentration were significant for only N under both the overhead and SSDI. Averaged across the fertility treatments under both irrigation scheduling methods, the FC-80 had a higher nutrient concentration, with a 6.07% and 7.65% increase in nutrient concentration under the overhead and SSDI, respectively, compared to the FC-50 (Table 4). The effects of nutrient stress on nutrient concentration were significant for N, P, Mg, Ca, Zn, Mn, and Mo under the overhead irrigation and for N, Ca, B, Zn, Mn, Cu, Fe, and Mo under the SSDI. The ESN-stress increased the concentrations of Mg, Ca, and Mo by 14.0%, 13.1%, and 30.5%, respectively, under the overhead irrigation and the concentrations of Ca, B, and Mo by 15.6%, 14.0%, and 63.3%, respectively, under the SSDI. In contrast, the NN-stress increased the concentrations of N, P, Zn, and Mn by 26.4%, 22.3%, 28.7%, and 100%,

TABLE 3 Initial nutrient status of the overhead and subsurface drip irrigation (SSDI) experimental field soil at 0-15 cm depth in 2021 and 2022.

Year	NO_3-N	P	K	Mg	Ca	S	B	Zn	Mn	Fe	Cu
	Overhead (kg ha^{-1})										
2021	2.04	81.5	152	103	980	9.20	0.60	5.30	40.1	28.0	0.80
2022	1.96	81.5	152	103	979	9.25	0.62	5.30	40.1	28.0	0.78
	SSDI (kg ha^{-1})										
2021	1.60	38.1	76.8	62.7	800	10.1	0.28	1.35	19.6	10.1	4.99
2022	0.78	119	106	121	1131	24.6	0.31	6.11	43.1	26.1	1.12

Soil NO_3-N was measured after extraction with 2 M KCl solution; soil P, K, Ca, Mg, Fe, Mn, Zn, B, and Cu were measured after Mehlich I extraction; and soil S was measured after extraction with monocalcium phosphate.

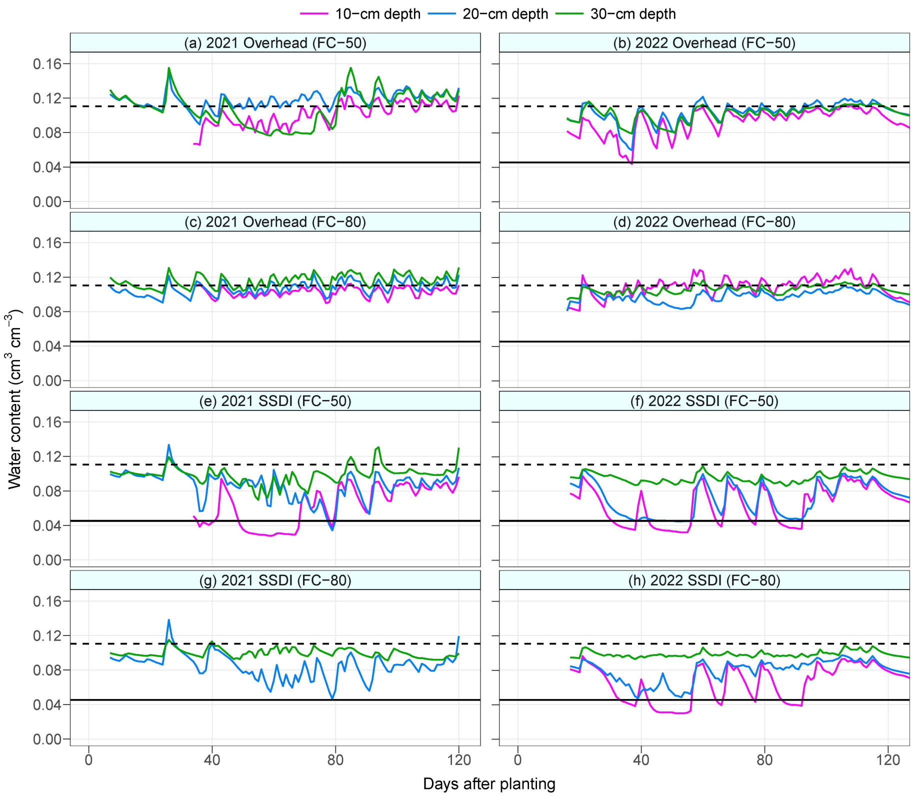

FIGURE 1
Mean daily soil water content at 10-cm, 20-cm, and 30-cm depths in 2021 **(A, C, E, G)** and 2022 **(B, D, F, H)**. Black solid and dashed horizontal lines indicate the permanent wilting point and field capacity of the soil, respectively. SSDI, Subsurface drip irrigation; FC-50, Irrigation triggered at 50% field capacity; FC-80, Irrigation triggered at 80% field capacity.

respectively, under the overhead irrigation and N, Zn, Mn, Cu, and Fe by 17.2%, 20.6%, 35.7%, 55.7%, and 20.7%, respectively, under the SSDI (Table 4). The interaction between irrigation schedule and nutrient stress was significant for only N under the overhead irrigation method, with the reduction in N concentration from ESN-stress being more severe under the FC-50 than under the FC-80 (24.3% vs. 17.4%). Similar observations were made under the SSDI (17.7% vs. 12.0%), except the interaction term was not significant.

The greater reduction in N concentration from ESN-stress under the FC-50 could suggest water content at 50% of the soil's field capacity was not sufficient to solubilize high amount of N. Water stress can drastically reduce the concentration of N since the amount of nutrients a plant can take depends on the volume of water available (Saud et al., 2017; Plett et al., 2020). The ESN-stress had almost all the plant tissue nutrient concentrations above the low threshold of the reference nutrient sufficiency ranges (NSR) reported in the Southern Cooperative Series Bulletin (SCSB) #394 (Baker et al., 2000), a publication of a regional collaboration that provides nutrient sufficiency ranges (NSRs) for plant analyses in the southern region of the United States (Baker et al., 2000). Only Cu, under the ESN-stress of the FC-80 for both overhead irrigation and SSDI, had concentrations below the NSR reported in the SCSB publication.

Nutrient concentration is affected by biomass accumulation, and hence, crops with good growth could have lower nutrient concentrations than those with poor growth, even though the actual nutrient uptake may be greater (Plénet and Lemaire, 1999; Adee et al., 2016; Rosa et al., 2019). The effect is commonly termed as 'nutrient dilution effects.' Therefore, nutrient concentration alone is not an adequate way to compare nutrient availability to crops. Research work by Amissah et al. (2023a) to assess the nutrient sufficiency ranges of corn in the SCSB publication showed some plots had more than 95% relative biomass at the V6-V7 growth stage even though the Cu levels were below the lower threshold. The findings highlighted that corn can tolerate lower Cu levels than reported. Moreover, Amissah et al. (2023a) observed that 25.4% of samples with all nutrient concentrations above the lower threshold even had relative biomass <50% and the effects were not due to the accumulation of nutrients at toxic levels. Thus, the thresholds of some nutrients can be higher or lower than what is currently reported, especially with the breeding of new corn varieties that are high-yielding and expected to require more nutrients (Bender et al., 2013).

3.4 Biomass and nutrient uptake at the vegetative stage

The *P*-values of the main effects and interaction effects of irrigation schedule and nutrient stress on plant biomass and

TABLE 4 Effects of irrigation schedule and nutrient stress on nutrient concentrations of corn biomass sampled at the vegetative stage under overhead irrigation and SSDI systems.

Irrigation schedule	Nutrient stress	N	P	K	Mg	Ca	S	B	Zn	Mn	Fe	Cu	Mo
		————— g kg^{-1} —————						————— mg kg^{-1} —————					
——— Overhead ———													
FC-50	ESN-stress	34.6 ± 1.3a	4.00 ± 0.12ab	55.61 ± 0.93a	2.38 ± 0.12b	6.65 ± 0.24a	2.28 ± 0.19a	11.1 ± 0.4a	25.9 ± 1.7a	75.4 ± 5.2a	81.9 ± 10.3a	5.18 ± 0.48a	2.91 ± 0.41b
FC-50	NN-stress	45.7 ± 1.6c	4.63 ± 0.32bc	56.15 ± 1.26a	2.05 ± 0.12a	5.85 ± 0.13ab	2.36 ± 0.18a	10.8 ± 0.4a	32.1 ± 2.8b	151.4 ± 31.5b	89.8 ± 16.3a	5.68 ± 0.13a	2.09 ± 0.43a
FC-80	ESN-stress	38.5 ± 2.2b	3.79 ± 0.08a	55.85 ± 1.42a	2.34 ± 0.11ab	6.50 ± 0.20a	2.27 ± 0.16a	11.3 ± 0.3a	24.1 ± 2.0a	73.0 ± 4.1a	78.2 ± 16.1a	4.90 ± 0.38a	2.63 ± 0.42ab
FC-80	NN-stress	46.6 ± 1.8c	4.89 ± 0.29c	57.10 ± 1.55a	2.09 ± 0.18ab	5.77 ± 0.31b	2.32 ± 0.18a	10.7 ± 0.5a	32.3 ± 2.6b	145.5 ± 35.1b	87.7 ± 15.6a	5.56 ± 0.26a	2.15 ± 0.39a
——— SSDI ———													
FC-50	ESN-stress	34.9 ± 2.2a	4.45 ± 0.18a	47.7 ± 2.1b	2.58 ± 0.23a	6.65 ± 0.56b	2.11 ± 0.13a	17.2 ± 0.7c	28.1 ± 4.6a	102.2 ± 6.4a	75.5 ± 9.6a	5.42 ± 0.72ab	2.87 ± 0.24b
FC-50	NN-stress	42.4 ± 1.0bc	4.75 ± 0.09a	49.1 ± 1.3a	2.49 ± 0.20a	5.58 ± 0.25a	2.18 ± 0.14a	14.6 ± 0.7a	31.7 ± 4.8b	151.5 ± 24.9b	91.9 ± 7.6b	6.72 ± 1.08ab	1.86 ± 0.26a
FC-80	ESN-stress	39.0 ± 0.9ab	4.40 ± 0.18a	46.0 ± 2.0b	2.61 ± 0.22a	6.44 ± 0.55b	2.22 ± 0.19a	16.2 ± 0.6bc	26.7 ± 3.6a	93.1 ± 12.6a	78.0 ± 8.1a	4.93 ± 0.33a	3.04 ± 0.26b
FC-80	NN-stress	44.3 ± 1.7c	4.55 ± 0.20a	48.9 ± 2.1a	2.40 ± 0.17a	5.74 ± 0.30a	2.36 ± 0.19a	14.8 ± 0.4ab	34.3 ± 6.5b	152.7 ± 32.7b	93.3 ± 8.2b	7.33 ± 1.14b	1.76 ± 0.29a

Within the irrigation application method (overhead or SSDI) and nutrient element, means not sharing any letter are significantly different using the least squares means and adjusted Tukey multiple comparisons ($P < 0.05$). Values represent the mean ± standard error. SSDI, Subsurface drip irrigation; FC-50, Irrigation triggered at 50% field capacity; FC-80, Irrigation triggered at 80% field capacity; ESN-stress, early season nutrient stress; NN-stress, reduced nutrient stress.

10.3389/fpls.2024.1344022

nutrient uptake at the vegetative stage are presented in Supplementary Table S2. The effects of the nutrient stress on biomass were significant for both the overhead irrigation and the SSDI. The effects of the irrigation schedule and the interaction effects between the irrigation schedule and nutrient stress were not significant. Averaged over the irrigation schedule, the biomass of NN-stress was 2× greater than the biomass of ESN-stress under the overhead irrigation and 2.6× greater under the SSDI (Table 5). Supplementary Figure S1 is a drone image of the SSDI field showing poor growth in the ESN-stress plots. The more severe effects of ESN-stress under the SSDI were likely because of the dry conditions experienced at the topsoil layer. Water regulates the transport of nutrients to the plant (Smethurst, 2004; Plett et al., 2020). Water stress will, therefore, lead to reduced uptake of water and nutrients and subsequently impact stomatal opening and absorption of carbon dioxide for photosynthesis. The effect will reduce growth, resulting in reduced biomass accumulation and partitioning (Chatzistathis and Therios, 2013; Bárzana and Carvajal, 2020; Pandey et al., 2021; Yan et al., 2023).

In contrast to the results observed for nutrient concentration at the vegetative stage, the effects of nutrient stress on nutrient uptake were significant for all nutrients under both the overhead irrigation and the SSDI (Table 5). Under both irrigation scheduling methods, the ESN-stress caused a reduction in nutrient uptake. Irrigation scheduling significantly impacted the uptake of N, K, Mg, and Ca under overhead irrigation but not under the SSDI (Table 5). The interaction of irrigation scheduling and nutrient stress did not significantly impact nutrient uptake at the vegetative stage. Under the overhead irrigation, the ESN-stress caused a general reduction in nutrients. The nutrient uptake for the FC-50 irrigation scheduling method was higher than the FC-80, with the differences being significant for the N, K, Mg, and Ca under the overhead irrigation system. A similar trend was observed under the SSDI except for the uptake of S, Zn, and Cu where they were rather higher under the FC-80.

Reduction in nutrient uptake for the ESN-stress suggests the residual nutrients in the soil and mineralization of the peanut crop residues, which was the previous cash crop, could not supply adequate nutrients to corn by the V6 growth stage. Peanut is a leguminous crop that fixes atmospheric nitrogen, and it typically has 46 kg ha^{-1} to 80 kg ha^{-1} nitrogen in the aboveground biomass (Meso et al., 2007; Mulvaney et al., 2017). Moreover, peanuts are a good scavenger of residual nutrients in the soil, and thus, the decomposition of peanut residues can be a good source of nutrients for succeeding crops (Crusciol et al., 2021; Jat et al., 2023). The availability of nutrients from peanut residues to succeeding crops, is however, dependent on several management and environmental factors, including tillage operations, planting time, temperature, rainfall, soil properties, and the structure and composition of microbial communities (Whalen, 2014; Shahzad et al., 2019b; Grzyb et al., 2020; Sintim et al., 2022a; b).

Nutrient uptake of corn by the V6 growth stage was reported to be <15% of the total taken up by maturity (Karlen et al., 1988; Bender et al., 2013; Ciampitti and Vyn, 2013; Ciampitti et al., 2013). Despite the reduced nutrient uptake of corn in the early season, the results of the study demonstrate that nutrient supply must be optimum to sustain plant health and growth. Stress at any of the developmental stages of corn can affect biomass accumulation (Bender et al., 2013; Ciampitti et al., 2013). In contrast to corn, early-season nutrient stress (no nutrient application from planting to the square stage) was found to have no adverse effects on cotton growth and yield (Amissah et al., 2023b). Unlike corn, cotton is an indeterminate crop and can exhibit a high degree of plasticity in growth (Atkin et al., 2006; Rochester et al., 2012; Li et al., 2020; Kusi et al., 2021a; Amissah et al., 2023b).

3.5 Yield and growth parameters at maturity

The interaction effects of irrigation schedule and nutrient stress were not significant on grain yield under both the overhead irrigation and SSDI systems (Supplementary Table S3). The main effects of the irrigation schedule on grain yield were significant under just the SSDI system, but the main effects of nutrient stress on grain yield were significant under both the overhead and SSDI systems. Compared to the NN-stress, the ESN-stress caused a yield reduction of 1.58 Mg ha^{-1} (11.7%) and 1.86 Mg ha^{-1} (13.0%), respectively, for the FC-50 and FC-80 under the overhead irrigation system, and 2.95 Mg ha^{-1} (38.2%) and 3.4 Mg ha^{-1} (37.6%), respectively, for the FC-50 and FC-80 under the SSDI when compared to the NN-stress (Figures 2A, B). Under the SSDI, the FC-50 caused a 3.07 Mg ha^{-1} (16.7%) reduction in grain yield compared to the FC-80. Also, under the overhead irrigation, the FC-50 caused a 1.79 Mg ha^{-1} (5.9%) reduction in grain yield compared to the FC-80, but the difference was not significant as already noted.

Unlike grain yield, the main effects of the irrigation schedule were not significant on the plant height under both the overhead irrigation and SSDI systems. The main effects of nutrient stress were, however, significant on the plant height under the SSDI system (Supplementary Table S3). The ESN-stress significantly decreased plant height compared to the NN-stress under both FC-50 (by 9.38%) and FC-80 (by 6.43%) (Figures 2C, D). Under the overhead irrigation, the FC-80 also resulted in increased plant height compared to the FC-50, albeit the differences were not significant. The main effects of nutrient stress were significant on the stover under both the overhead irrigation and SSDI systems, but the main effects of the irrigation schedule were significant under just the SSDI system (Supplementary Table S3). Compared to the NN-stress, the ESN-stress decreased the stover by 29.9% (FC-50) and 21.9% (FC-80) under the overhead irrigation and by 34.6% (FC-50) and 31.6% (FC-80) under the SSDI (Figures 2E, F).

In contrast, the ESN-stress increased the harvest index over the NN-stress under both the overhead irrigation and SSDI systems (Supplementary Table S3 and Figures 2G, H). Although the differences were statistically significant, the magnitude was quite marginal, with the ESN-stress increasing harvest index over the NN-stress by just 3.3% (FC-50) and 2.8% (FC-80) under the overhead irrigation and by 3.1% (FC-50) and 3.9% (FC-80) under the SSDI (Figures 2E, F). The main effects of the irrigation schedule, and the interaction effects of the irrigation schedule and nutrient stress, were not significant on the TSW under both the overhead

TABLE 5 Effects of irrigation schedule and nutrient stress on corn biomass and nutrient uptake at the vegetative stage under overhead irrigation and SSDI systems.

Irrigation schedule	Nutrient stress	Biomass	N	P	K	Mg	Ca	S	B	Zn	Mn	Fe	Cu	Mo
		———— kg ha^{-1} ————							———— g ha^{-1} ————					
———— Overhead ————														
FC-50	ESN-stress	214 ± 25a	7.55 ± 1.1a	0.85 ± 0.10a	11.9 ± 1.4a	0.52 ± 0.08ab	1.39 ± 0.13a	0.46 ± 0.03a	2.38 ± 0.29a	5.34 ± 0.54a	15.6 ± 1.4a	16.0 ± 1.4a	1.14 ± 0.20a	0.68 ± 0.16ab
FC-50	NN-stress	483 ± 38b	21.8 ± 1.3c	2.29 ± 0.29b	27.0 ± 1.9c	0.98 ± 0.07c	2.81 ± 0.19c	1.16 ± 0.16b	5.22 ± 0.44b	15.9 ± 2.23b	78.6 ± 19.5b	45.1 ± 9.5b	2.77 ± 0.26b	0.93 ± 0.14b
FC-80	ESN-stress	197 ± 20a	7.71 ± 1.0a	0.75 ± 0.08a	10.9 ± 1.1a	0.42 ± 0.09a	1.29 ± 0.15a	0.43 ± 0.04a	2.24 ± 0.26a	4.54 ± 0.35a	14.0 ± 1.2a	14.3 ± 2.7a	0.95 ± 0.11a	0.55 ± 0.13a
FC-80	NN-stress	356 ± 22b	14.5 ± 2.3b	1.76 ± 0.17b	20.3 ± 1.4b	0.74 ± 0.08bc	2.05 ± 0.18b	0.82 ± 0.08b	3.80 ± 0.30b	11.5 ± 1.12b	46.4 ± 13.5ab	31.3 ± 6.0ab	1.98 ± 0.17b	0.76 ± 0.14ab
———— SSDI ————														
FC-50	ESN-stress	176 ± 31a	6.09 ± 1.4a	0.79 ± 0.15a	8.69 ± 1.71a	0.41 ± 0.05a	1.11 ± 0.17a	0.35 ± 0.05a	2.92 ± 0.43a	4.21 ± 0.48a	17.8 ± 2.86a	13.8 ± 3.3a	0.86 ± 0.10a	0.53 ± 0.12ab
FC-50	NN-stress	443 ± 41b	15.3 ± 2.5b	2.10 ± 0.19b	21.58 ± 1.87b	1.15 ± 0.19b	2.52 ± 0.31b	1.00 ± 0.15b	6.57 ± 0.81b	15.08 ± 3.24b	71.9 ± 16.33b	40.2 ± 4.8b	3.22 ± 0.76b	0.79 ± 0.10b
FC-80	ESN-stress	153 ± 20a	5.52 ± 1.1a	0.66 ± 0.07a	7.25 ± 1.14a	0.38 ± 0.03a	0.94 ± 0.10a	0.32 ± 0.03a	2.43 ± 0.26a	3.64 ± 0.19a	14.4 ± 2.38a	12.9 ± 2.5a	0.73 ± 0.08a	0.48 ± 0.09a
FC-80	NN-stress	417 ± 45b	15.0 ± 2.6b	1.94 ± 0.28b	20.05 ± 1.86b	1.03 ± 0.16b	2.46 ± 0.38b	1.04 ± 0.18b	6.25 ± 0.80b	16.2 ± 4.32b	70.4 ± 19.63b	38.8 ± 5.7b	3.38 ± 0.78b	0.66 ± 0.07ab

Within the irrigation application method (overhead or SSDI) and nutrient element, means not sharing any letter are significantly different using the least squares means and adjusted Tukey multiple comparisons ($P < 0.05$). Values represent the mean ± standard error. SSDI, Subsurface drip irrigation; FC-50, Irrigation triggered at 50% field capacity; FC-80, Irrigation triggered at 80% field capacity; ESN-stress, early season nutrient stress; NN-stress, reduced nutrient stress.

10.3389/fpls.2024.1344022

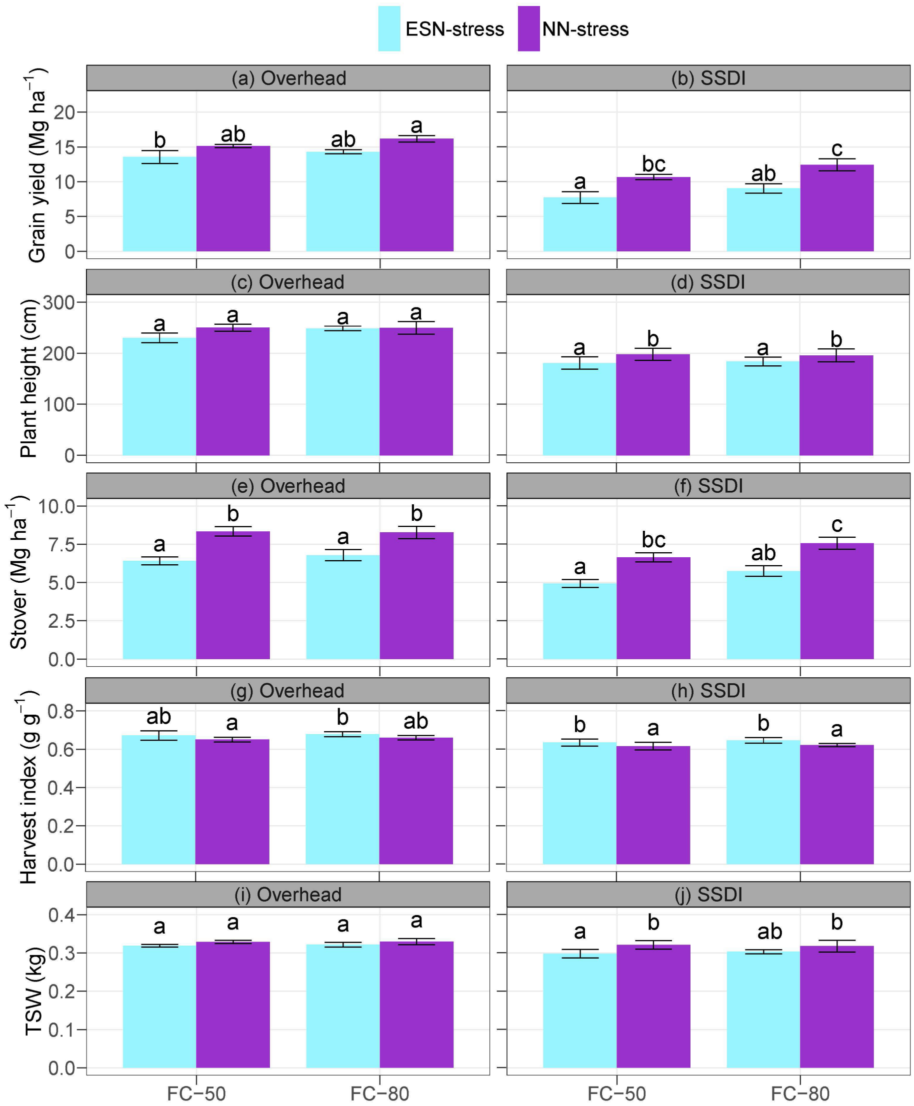

FIGURE 2
Effects of irrigation schedule and nutrient stress on corn yield **(A, B)** and growth parameters **(C–J)** at maturity under overhead irrigation and SSDI systems. Within the irrigation application method (overhead or SSDI) and measurement variable, bar plots of means not sharing any letter are significantly different using the least squares means and adjusted Tukey multiple comparisons ($P < 0.05$). Error bars indicate standard errors of the mean (n = 4). SSDI, Subsurface drip irrigation; FC-50, Irrigation triggered at 50% field capacity; FC-80, Irrigation triggered at 80% field capacity; ESN-stress, early season nutrient stress; NN-stress, reduced nutrient stress; TSW, Thousand seed weight.

irrigation and SSDI systems (Supplementary Table S3 and Figures 2I, J). However, the main effects of nutrient stress were significant on the TSW under the SSDI. The ESN-stress decreased the TSW by 7.77% under the FC-50 and by 4.80% under the FC-80 compared to the NN-stress.

As already noted, yield reduction from the early season nutrient stress under the SSDI system was fairly high. The results could be due to the dry conditions of the topsoil layer under the SSDI field, evident by the soil moisture sensors (Akıncı and Lösel, 2012; Bárzana and Carvajal, 2020; Sah et al., 2020). The soil moisture sensors at the 10-cm depth of the SSDI field showed the water content was below the permanent wilting point for a prolonged period. Reduced nutrient uptake due to drought stress can result in a reduction in cell expansion, stunted growth, and increased susceptibility to pests and diseases, all of which will eventually lead to reduced biomass, yield, stover, and TSW as observed in this study (Hussain et al., 2019; Bárzana and Carvajal, 2020). The inability of corn to fully recover from the early season nutrient stress highlights the sensitivity of corn in the early season. Studies show that stress conditions cause corn to transition through its developmental stages quickly (Silva and Uchida, 2000; Grant et al., 2001; Roth et al., 2023). The ESN-stress, however, resulted in a higher harvest index than the NN-stress. Harvest index is a measure of the efficiency of plant biomass partitioned to the grain (Smith et al., 2018; Porker et al., 2020). Prevailing environmental conditions can cause an increase or decrease in the harvest index of corn. Generally, crops survive stress by reducing the length of the vegetative stage, which limits the growth of the vegetative parts to partition photo-assimilates to the seeds (Unkovich et al., 2010; Cohen et al., 2021).

3.6 Ear development

The main effects of irrigation schedule and the interaction effects of irrigation schedule and nutrient stress were not significant on the ear height, ear length, ear diameter, and grain rows. However, the main effects of nutrient stress had significant impacts on ear length, ear diameter, and ear grain rows under the overhead irrigation and on the ear diameter and ear grain rows under the SSDI (Supplementary Table S3). Compared to the NN-stress, the ESN-stress resulted in a general reduction in all the measured ear development parameters, ranging from 1.7% to 20% reduction in ear height, 2.4% to 8.7% reduction in ear length, 6.2% to 11.4% reduction in ear grain rows, and 2.6% to 5.9% reduction in ear diameter across the overhead irrigation and SSDI systems (Figure 3). The results indicate the early season nutrient stress affected the source and sink dynamics. The use of nutrients entails uptake, assimilation, translocation, and remobilization during senescence (Masclaux-Daubresse et al., 2010; Sintim et al., 2015, 2016). As already mentioned, nutrient stress can cause the plant to shorten the vegetative stage and progress to the reproductive stage (Silva and Uchida, 2000; Grant et al., 2001; Roth et al., 2023). Thus, plants may not accumulate adequate nutrients at the vegetative stage to translocate and remobilize, which could subsequently impact the ear development of corn, as observed in the ESN-stress plots (Unkovich et al., 2010; Cohen et al., 2021).

4 Conclusions

Inducing early season nutrient stress in corn by delaying fertilizer application until the V6 growth stage resulted in biomass accumulation that was reduced by over 50% than non-stressed crops even though all plots received the same nutrient amount. Consequently, the uptake of all nutrients was significantly lower under the early season nutrient stress conditions. Soil moisture levels affected the severity of the early season nutrient stress on N accumulation, with a greater reduction in N concentration from the early season nutrient stress being more severe under the FC-50

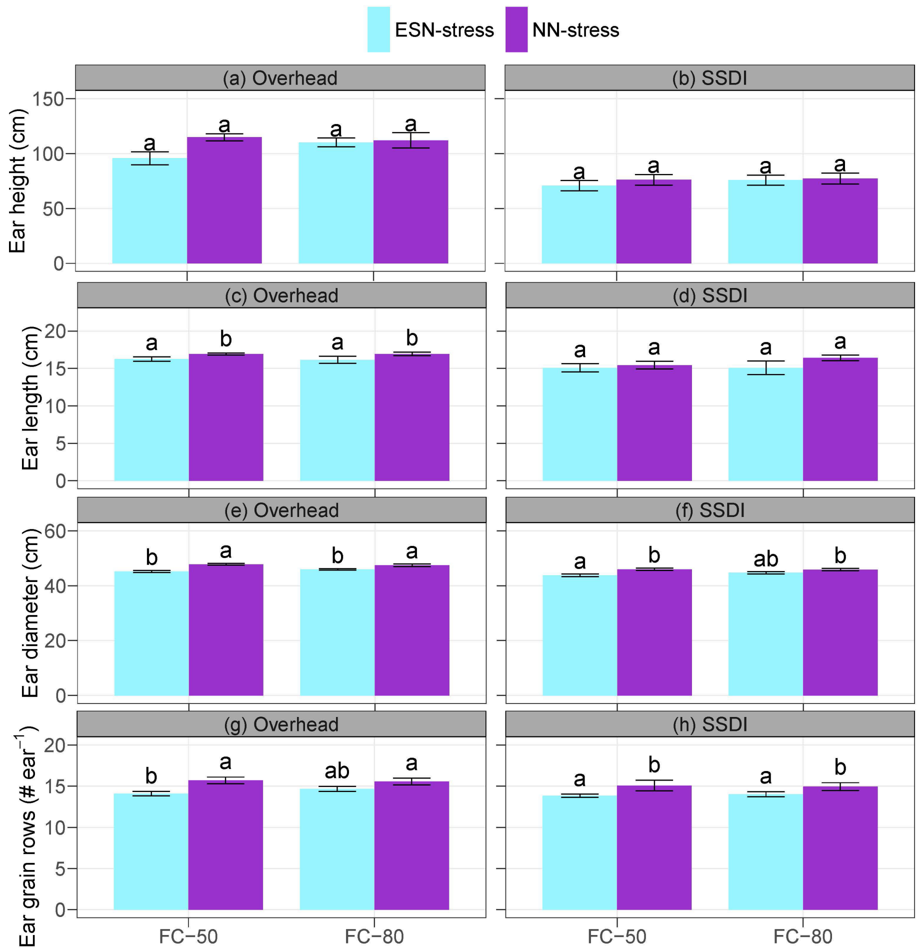

FIGURE 3
Effects of irrigation schedule and nutrient stress on corn ear development **(A–H)** under overhead irrigation and SSDI systems. Within the irrigation application method (overhead or SSDI) and measurement variable, bar plots of means not sharing any letter are significantly different using the least squares means and adjusted Tukey multiple comparisons ($P < 0.05$). Error bars indicate standard errors of the mean (n = 4). SSDI, Subsurface drip irrigation; FC-50, Irrigation triggered at 50% field capacity; FC-80, Irrigation triggered at 80% field capacity; ESN-stress, early season nutrient stress; NN-stress, reduced nutrient stress.

than under the FC-80 (17.7-×4.3% vs. 12.0-17.4%). Overall, corn recovery from the early season nutrient stress was low, with the early season nutrient stress causing yield reduction of 1.58 Mg ha^{-1} (11.7%) and 1.86 Mg ha^{-1} (13.0%), respectively, for the FC-50 and FC-80 under the overhead irrigation system, and 2.95 Mg ha^{-1} (38.2%) and 3.4 Mg ha^{-1} (37.6%), respectively, for the FC-50 and FC-80 under the SSDI when compared to non-stress conditions. The findings of the study highlight that although corn has low nutrient requirement at the early growth stage, it should not be allowed to undergo nutrient stress in the early season as it will not fully recover, resulting in poor growth and reduced yield potential. Further studies are also needed to determine the optimum nutrient supply for corn at the initial growth stages.

Data availability statement

The raw data supporting the conclusions of this article will be made available by the authors, without undue reservation.

Author contributions

SA: Conceptualization, Data curation, Formal Analysis, Investigation, Methodology, Visualization, Writing – original draft, Writing – review and editing. GA: Data curation, Investigation, Methodology, Writing – review and editing. RL: Conceptualization, Funding acquisition, Writing – review and editing. CP: Data curation, Funding acquisition, Investigation, Methodology, Resources, Validation, Writing – review and editing. BW: Data curation, Investigation, Methodology, Resources, Writing – review and editing. WP: Conceptualization, Funding acquisition, Writing – review and editing. SV: Funding acquisition, Writing – review and editing. CB: Data curation, Writing – review and editing. GV: Funding acquisition, Writing – review and editing. GH: Supervision, Writing – review and editing. MC: Supervision, Writing – review and editing. DF: Supervision, Writing – review and editing. JD-P: Supervision, Writing – review and editing. HS: Conceptualization, Data curation, Formal Analysis, Funding acquisition, Investigation, Methodology, Project administration, Resources, Supervision, Validation, Visualization, Writing – original draft, Writing – review and editing.

Funding

The author(s) declare that financial support was received for the research, authorship, and/or publication of this article. Financial support for the research was provided by the Georgia Corn Commission (Award numbers AWD00012993 and AWD00014394). Funding was further provided by the USDA National Institute for Food and Agriculture through Hatch project 1026085.

Acknowledgments

We appreciate the staff of the University of Georgia Stripling Irrigation Research Park for their support with land preparation, irrigation, and other agronomic management of the crops. We also thank Benjamin Agyei, Russel Deal, and Noah Garner for assisting with sample processing and data collection.

Conflict of interest

The authors declare that the research was conducted in the absence of any commercial or financial relationships that could be construed as a potential conflict of interest.

Publisher's note

All claims expressed in this article are solely those of the authors and do not necessarily represent those of their affiliated organizations, or those of the publisher, the editors and the reviewers. Any product that may be evaluated in this article, or claim that may be made by its manufacturer, is not guaranteed or endorsed by the publisher.

Supplementary material

The Supplementary Material for this article can be found online at: https://www.frontiersin.org/articles/10.3389/fpls.2024.1344022/full#supplementary-material

References

Abu-Zeid, M. M., and El-Aal, A. K. A. (2017). Effect of salinity of groundwater on the geotechnical properties of some Egyptian clay. *Egypt J. Pet.* 26, 643–648. doi: 10.1016/j.ejpe.2016.09.003

Adee, E., Hansel, F. D., Ruiz Diaz, D. A., and Janssen, K. (2016). Corn response as affected by planting distance from the center of strip-till fertilized rows. *Front. Plant Sci.* 7. doi: 10.3389/fpls.2016.01232

Akıncı, Ş., and Lösel, D. M. (2012). *Plant Water-Stress Response Mechanisms, Water Stress*. Ed. P. I. Md. M. Rahman (Rijeka, Croatia: InTech). Available at: http://www.intechopen.com/books/water-stress/plant-water-stress-response-mechanisms, ISBN: 978-953-307-963-9.

Amissah, S., Ankomah, G., Agyei, B. K., Lee, R. D., Harris, G. H., Cabrera, M., et al. (2023a). Nutrient sufficiency ranges for corn at the early growth stage: Implications for nutrient management. *Plants* 12, 713. doi: 10.3390/plants12040713

Amissah, S., Baidoo, M., Agyei, B. K., Ankomah, G., Black, R. A., Perry, C. D., et al. (2023b). Early and late season nutrient stress conditions: Impact on cotton productivity and quality. *Agronomy* 13, 64. doi: 10.3390/agronomy13010064

Atkin, O. K., Loveys, B. R., Atkinson, L. J., and Pons, T. L. (2006). Phenotypic plasticity and growth temperature: understanding interspecific variability. *J. Exp. Bot.* 57, 267–281. doi: 10.1093/jxb/erj029

Baker, W. H., Bell, P. F., Campbell, C. R., Cox, F. R., Donohue, S. J., Gascho, G. J., et al. (2000). *Reference sufficiency ranges for plant analysis in the southern region of the United States*. Ed. C. R. Campbell (Fayetteville, AR, USA: Southern Cooperative Series Bulletin #394, Southern Extension Research Activities).

Bárzana, G., and Carvajal, M. (2020). Genetic regulation of water and nutrient transport in water stress tolerance in roots. *J. Biotechnol.* 324, 134–142. doi: 10.1016/j.jbiotec.2020.10.003

Bates, D., Maechler, M., Bolker, B., and Walker, S. (2015). Fitting linear mixed-effects models using lme4. *J. Stat. Software* 67, 1–48. doi: 10.18637/jss.v067.i01

Bender, R. R., Haegele, J. W., Ruffo, M. L., and Below, F. E. (2013). Nutrient uptake, partitioning, and remobilization in modern, transgenic insect-protected maize hybrids. *Agron. J.* 105, 161–170. doi: 10.2134/agronj2012.0352

Bryant, C. (2021). *Corn growth & development. Georgia Corn Production Guide* (Athens, GA, USA: University of Georgia Extension).

Buljovcic, Z., and Engels, C. (2001). Nitrate uptake ability by maize roots during and after drought stress. *Plant Soil* 229, 125–135. doi: 10.1023/A:1004879201623/METRICS

Chatzistathis, T., and Therios, I. (2013). *How Soil Nutrient Availability Influences Plant Biomass and How Biomass Stimulation Alleviates Heavy Metal Toxicity in Soils: The Cases of Nutrient Use Efficient Genotypes and Phytoremediators, Respectively*. Ed. M. D. Matovic (Rijeka: IntechOpen).

Chesworth, W., Spaargaren, O., Hadas, A., Groenevelt, P. H., Otero, X. L., Ferreira, T. O., et al. (2008). "Tropical soils," in *Encyclopedia of Soil Science*. Ed. W. Chesworth (Springer Netherlands, Dordrecht), 793–803.

Ciampitti, I., Camberato, J. J., Murrell, T. S., and Vyn, T. (2013). Maize nutrient accumulation and partitioning in response to plant density and nitrogen rate: I. macronutrients. *Agron. J.* 105, 783–795. doi: 10.2134/agronj2012.0467

Ciampitti, I., and Vyn, T. (2013). Maize nutrient accumulation and partitioning in response to plant density and nitrogen rate: II. calcium, magnesium, and micronutrients. *Agron. J.* 105, 1645–1657. doi: 10.2134/agronj2013.0126

Ciampitti, I. A., and Vyn, T. J. (2014). Nutrient sufficiency concepts for modern corn hybrids: impacts of management practices and yield levels. *Crop Manage.* 13, CM–2013-0022-RS. doi: 10.2134/CM-2013-0022-RS

Cohen, I., Zandalinas, S. I., Huck, C., Fritschi, F. B., and Mittler, R. (2021). Meta-analysis of drought and heat stress combination impact on crop yield and yield components. *Physiol. Plant* 171, 66–76. doi: 10.1111/ppl.13203

Colaizzi, P. D., Schneider, A. D., Evett, S. R., and Howell, T. A. (2004). Comparison of SDI, LEPA, and spray irrigation performance for grain sorghum. *Trans. Am. Soc Agric. Eng.* 47, 1477–1492. doi: 10.13031/2013.17628

Crusciol, C. A. C., Portugal, J. R., Bossolani, J. W., Moretti, L. G., Fernandes, A. M., Garcia, J. L. N., et al. (2021). Dynamics of macronutrient uptake and removal by modern peanut cultivars. *Plants* 10, 2167. doi: 10.3390/plants10102167

Djaman, K., and Irmak, S. (2018). Evaluation of critical nitrogen and phosphorus models for maize under full and limited irrigation conditions. *Ital. J. Agron.* 13, 80–92. doi: 10.4081/IJA.2017.958

Djaman, K., Irmak, S., Martin, D. L., Ferguson, R. B., and Bernards, M. L. (2013). Plant nutrient uptake and soil nutrient dynamics under full and limited irrigation and rainfed maize production. *Agron. J.* 105, 527–538. doi: 10.2134/agronj2012.0269

Esfandbod, M., Phillips, I. R., Miller, B., Rashti, M. R., Lan, Z. M., Srivastava, P., et al. (2017). Aged acidic biochar increases nitrogen retention and decreases ammonia volatilization in alkaline bauxite residue sand. *Ecol. Eng.* 98, 157–165. doi: 10.1016/j.ecoleng.2016.10.077

Fahad, S., Bajwa, A. A., Nazir, U., Anjum, S. A., Farooq, A., Zohaib, A., et al. (2017). Crop production under drought and heat stress: Plant responses and management options. *Front. Plant Sci.* 8. doi: 10.3389/fpls.2017.01147

Faloye, O. T., Alatise, M. O., Ajayi, A. E., and Ewulo, B. S. (2019). Effects of biochar and inorganic fertiliser applications on growth, yield and water use efficiency of maize under deficit irrigation. *Agric. Water Manage.* 217, 165–178. doi: 10.1016/j.agwat.2019.02.044

Georgia AEMN (2023) Georgia Automated Environmental Monitoring Network. (Griffin, GA, USA: University of Georgia). Available online at: www.Georgiaweather.net (Accessed 15 March 2023).

Grant, C. A., Flaten, D. N., Tomasiewicz, D. J., and Sheppard, S. C. (2001). The importance of early season phosphorus nutrition. *Can. J. Plant Sci.* 81, 211–224. doi: 10.4141/P00-093

Grzyb, A., Wolna-Maruwka, A., and Niewiadomska, A. (2020). Environmental factors affecting the mineralization of crop residues. *Agronomy* 10, 1951. doi: 10.3390/agronomy10121951

Hassanli, A. M., Ebrahimizadeh, M. A., and Beecham, S. (2009). The effects of irrigation methods with effluent and irrigation scheduling on water use efficiency and corn yields in an arid region. *Agric. Water Manage.* 96, 93–99. doi: 10.1016/j.agwat.2008.07.004

Hoeft, R. (2000). *Will starter fertilizer increase corn yield?* (Urbana, IL, USA: University of Illinois Extension).

Hurisso, T. T., Moebius-Clune, D. J., Culman, S. W., Moebius-Clune, B. N., Thies, J. E., and van Es, H. M. (2018). Soil protein as a rapid soil health indicator of potentially available organic nitrogen. *Agric. Environ. Lett.* 3, 1–5. doi: 10.2134/ael2018.02.0006

Hussain, M., Malik, M. A., Farooq, M., Ashraf, M. Y., and Cheema, M. A. (2008). Improving drought tolerance by exogenous application of glycinebetaine and salicylic acid in sunflower. *J. Agron. Crop Sci.* 194, 193–199. doi: 10.1111/j.1439-037X.2008.00305.x

Hussain, H. A., Men, S., Hussain, S., Chen, Y., Ali, S., Zhang, S., et al. (2019). Interactive effects of drought and heat stresses on morpho-physiological attributes, yield, nutrient uptake and oxidative status in maize hybrids. *Sci. Rep.* 9, 1–12. doi: 10.1038/s41598-019-40362-7

Jat, R. A., Jain, N. K., Yadav, R. S., Reddy, K. K., Choudhary, R. R., Zala, P. V., et al. (2023). System-based integrated nutrient management improves productivity, profitability, energy use efficiency and soil quality in peanut-wheat cropping sequence in light black soils. *Sustain* 15, 1361. doi: 10.3390/su15021361

Juo, A. S. R., and Franzluebbers, K. (2003). *Tropical soils: Properties and management for sustainable agriculture* (New York, USA: Oxford Academic). doi: 10.1093/oso/9780195115987.001.0001

Jury, W. A., and Horton, R. (2004). *Soil physics. 6th ed*. Eds. W. Jury and R. Horton (New York, United States: John Wiley & Sons).

Karlen, D. L., Flannery, R. L., and Sadler, E. J. (1988). Aerial accumulation and partitioning of nutrients by corn. *Agron. J.* 80, 232–242. doi: 10.2134/agronj1988.00021962008000020018x

Kebede, H., Sui, R., Fisher, D. K., Reddy, K. N., Bellaloui, N., Molin, W. T., et al. (2014). Corn yield response to reduced water use at different growth stages. *Agric. Sci.* 5, 1305–1315. doi: 10.4236/as.2014.513139

Kisekka, I., Aguilar, J. P., Rogers, D. H., Holman, J., O'Brien, D. M., and Klocke, N. (2016). Assessing deficit irrigation strategies for corn using simulation. *Trans. ASABE* 59, 303–317. doi: 10.13031/issn.2151-0032

Kissel, D. E., and Sonon, L. S. (2008). *Soil test handbook for Georgia* (Athens, GA, USA: University of Georgia Cooperative Extension).

Klute, A. (1986). "Water retention: Laboratory methods," in *Methods of Soil Analysis: Part 1—Physical and Mineralogical Methods* (Madison, WI: American Society of Agronomy; Soil Science Society of America), 635–662. doi: 10.2136/sssabookser5.1.2ed

Kroes, J., Supit, I., Van Dam, J., Van Walsum, P., and Mulder, M. (2018). Impact of capillary rise and recirculation on simulated crop yields. *Hydrol. Earth Syst. Sci.* 22, 2937–2952. doi: 10.5194/hess-22-2937-2018

Kusi, N. Y. O., Lewis, K. L., Morgan, G. D., Ritchie, G. L., Deb, S. K., Stevens, R. D., et al. (2021a). Cotton cultivar response to potassium fertilizer application in Texas' southern high plains. *Agron. J.* 113, 5436–5453. doi: 10.1002/agj2.20807

Kusi, N. Y. O., Stevens, W. B., Sintim, H. Y., Garcia y Garcia, A., and Mesbah, A. O. (2021b). Phosphorus fertilization and enhanced efficiency products effects on sugarbeet. *Ind. Crops Prod.* 171, 113887. doi: 10.1016/j.indcrop.2021.113887

Lenth, R. (2018). *emmeans: Estimated Marginal Means, aka Least-Squares Means* (Vienna, Austria: R package version 1.1.2).

Li, B., Tian, Q., Wang, X., Han, B., Liu, L., Kong, X., et al. (2020). Phenotypic plasticity and genetic variation of cotton yield and its related traits under water-limited conditions. *Crop J.* 8, 966–976. doi: 10.1016/j.cj.2020.02.003

Mallarino, A. P. (2015). *Starter Fertilization Sometimes Boosts Corn Yield | Integrated Crop Management* (Ames, IA, USA: Iowa State University Extension and Outreach).

Masclaux-Daubresse, C., Daniel-Vedele, F., Dechorgnat, J., Chardon, F., Gaufichon, L., and Suzuki, A. (2010). Nitrogen uptake, assimilation and remobilization in plants: challenges for sustainable and productive agriculture. *Ann. Bot.* 105, 1141–1157. doi: 10.1093/aob/mcq028

Meso, B., Balkcom, K. S., Wood, C. W., and Adams, J. F. (2007). Nitrogen contribution of peanut residue to cotton in a conservation tillage system. *J. Plant Nutr.* 30, 1153–1165. doi: 10.1080/01904160701394618

Misra, A., and Tyler, G. (2000). Effect of wet and dry cycles in calcareous soil on mineral nutrient uptake of two grasses, Agrostis stolonifera L. and Festuca ovina L. *Plant Soil* 224, 297–303. doi: 10.1023/A:1004866730187/METRICS

Mulvaney, M. J., Balkcom, K. S., Wood, C. W., and Jordan, D. (2017). Peanut residue carbon and nitrogen mineralization under simulated conventional and conservation tillage. *Agron. J.* 109, 696–705. doi: 10.2134/agronj2016.04.0190

Nunes, M. R., Denardin, J. E., Vaz, C. M. P., Karlen, D. L., and Cambardella, C. A. (2019). Lime movement through highly weathered soil profiles. *Environ. Res. Commun.* 1, 1–15. doi: 10.1088/2515-7620/ab4eba

Pan, X., Lada, R., Caldwell, C. D., and Falk, K. C. (2011). Photosynthetic and growth responses of Camelina sativa (L.) Crantz to varying nitrogen and soil water status. *Photosynthetica* 49, 316–320. doi: 10.1007/s11099-011-0035-x

Pandey, R., Vengavasi, K., and Hawkesford, M. J. (2021). Plant adaptation to nutrient stress. *Plant Physiol. Rep.* 26, 583–586. doi: 10.1007/s40502-021-00636-7

Plénet, D., and Lemaire, G. (1999). Relationships between dynamics of nitrogen uptake and dry matter accumulation in maize crops. *Determination Crit. N concentration. Plant Soil* 216, 65–82. doi: 10.1023/A:1004783431055/METRICS

Plett, D. C., Ranathunge, K., Melino, V. J., Kuya, N., Uga, Y., and Kronzucker, H. J. (2020). The intersection of nitrogen nutrition and water use in plants: New paths toward improved crop productivity. *J. Exp. Bot.* 71, 4452–4468. doi: 10.1093/jxb/eraa049

Porker, K., Straight, M., and Hunt, J. R. (2020). Evaluation of G × E × M interactions to increase harvest index and yield of early sown wheat. *Front. Plant Sci.* 11. doi: 10.3389/fpls.2020.00994

Rambabu, G. V., Bridjesh, P., Prabhu Kishore, N., and Shiva Sai, N. (2023). Design and development of a drip irrigation system. *Mater. Today Proc.* doi: 10.1016/j.matpr.2023.06.349

Rochester, I. J., Constable, G. A., Oosterhuis, D. M., and Errington, M. (2012). "Nutritional requirements of cotton during flowering and fruiting," in *Flowering and Fruiting in Cotton*. Eds. D. M. Oosterhuis and J. T. Cothren (The Cotton Foundation, Cordova, TN, United States), 35–50.

Rosa, A. T., Diaz, D. A. R., Hansel, F. D., Sebastian, J. S. V., and Adee, E. A. (2019). Genotypic variation on root growth and nutrient uptake in corn and soybean. *Agrosystems Geosci. Environ.* 2, 1–12. doi: 10.2134/age2019.03.0018

Roth, R., Harris, G., Sintim, H., Porter, W., Mallard, J., Hall, D., et al. (2023). *Georgia Corn Production Guide* Vol. 2023 (Athens, GA, USA: University of Georgia Extension).

Sah, R. P., Chakraborty, M., Prasad, K., Pandit, M., Tudu, V. K., Chakravarty, M. K., et al. (2020). Impact of water deficit stress in maize: Phenology and yield components. *Sci. Rep.* 10, 1–15. doi: 10.1038/s41598-020-59689-7

Saud, S., Fahad, S., Yajun, C., Ihsan, M. Z., Hammad, H. M., Nasim, W., et al. (2017). Effects of nitrogen supply on water stress and recovery mechanisms in Kentucky bluegrass plants. *Front. Plant Sci.* 8. doi: 10.3389/fpls.2017.00983

Seiffert, S., Kaselowsky, J., Jungk, A., and Claassen, N. (1995). Observed and calculated potassium uptake by maize as affected by soil water content and bulk density. *Agron. J.* 87, 1070–1077. doi: 10.2134/agronj1995.00021962008700060007x

Setiyono, T. D., Walters, D. T., Cassman, K. G., Witt, C., and Dobermann, A. (2010). Estimating maize nutrient uptake requirements. *F. Crop Res.* 118, 158–168. doi: 10.1016/j.fcr.2010.05.006

Shahzad, K., Abid, M., and Sintim, H. Y. (2018). Wheat productivity and economic implications of biochar and inorganic nitrogen application. *Agron. J.* 110, 2259–2267. doi: 10.2134/agronj2018.01.0055

Shahzad, K., Abid, M., Sintim, H. Y., Hussain, S., and Nasim, W. (2019a). Tillage and biochar effects on wheat productivity under arid conditions. *Crop Sci.* 59, 1–9. doi: 10.2135/cropsci2018.08.0485

Shahzad, K., Bary, A. I., Collins, D. P., Chalker-Scott, L., Abid, M., Sintim, H. Y., et al. (2019b). Carbon dioxide and oxygen exchange at the soil-atmosphere boundary as affected by various mulch materials. *Soil Tillage Res.* 194, 104335. doi: 10.1016/j.still.2019.104335

Shahzad, K., Sintim, H. Y., Ahmad, F., Abid, M., and Nasim, W. (2022). "Importance of carbon sequestration in the context of climate change," in *Building Climate Resilience in Agriculture*. Eds. W. N. Jatoi, M. Mubeen, A. Ahmad, M. A. Cheema, Z. Lin, et al (Springer, Cham, Switzerland), 385–401.

Silva, J., and Uchida, R. (2000). *Plant Nutrient Management in Hawaii's Soils, Approaches for Tropical and Subtropical Agriculture* (Manoa, HI, United States: University of Hawaii).

Singh, S., and Tan, H. H. (2022). *High natural gas prices could lead to spike in food costs through fertilizer link* (London, United Kingdom: S&P Global Platts).

Sintim, H. Y., Adjesiwor, A. T., Zheljazkov, V. D., Islam, M. A., and Obour, A. K. (2016). Nitrogen application in Sainfoin under rain-fed conditions in wyoming: productivity and cost implications. *Agron. J.* 108, 294–300. doi: 10.2134/agronj2015.0317

Sintim, H. Y., Shahzad, K., Bary, A. I., Collins, D. P., Myhre, E. A., Flury, M., et al. (2022a). Differential gas exchange and soil microclimate dynamics under biodegradable plastic, polyethylene, and paper mulches. *Ital. J. Agron.* 17, 1979. doi: 10.4081/ija.2022.1979

Sintim, H. Y., Shahzad, K., and Yin, X. (2022b). Editorial: Innovative agricultural practices to improve soil health and sustain food production. *Front. Sustain. Food Syst.* 6. doi: 10.3389/fsufs.2022.1055636

Sintim, H. Y., Zheljazkov, V. D., Obour, A. K., Garcia y Garcia, A., and Foulke, T. K. (2015). Influence of nitrogen and sulfur application on camelina performance under dryland conditions. *Ind. Crops Prod.* 70, 253–259. doi: 10.1016/j.indcrop.2015.03.062

Smethurst, P. (2004). "Nutritional Physiology of Trees," in *TREE PHYSIOLOGY*. Ed. J.B.T.-E. Burley (Elsevier, Oxford), 1616–1622. doi: 10.1016/B0-12-145160-7/00103-4

Smith, M. R., Rao, I. M., and Merchant, A. (2018). Source-sink relationships in crop plants and their influence on yield development and nutritional quality. *Front. Plant Sci.* 871. doi: 10.3389/fpls.2018.01889

UGA-AESL (2023). *UGFertex: Prescription Lime and Nutrient Guidelines for Agronomic Crops. UGFertex Version 3.1* (Athens, GA, USA: University of Georgia Agricultural and Environmental Services Laboratories, University of Georgia).

Unkovich, M., Baldock, J., and Forbes, M. (2010). *Variability in Harvest Index of Grain Crops and Potential Significance for Carbon Accounting: Examples from Australian Agriculture. 1st ed* (Amsterdam, The Netherlands: Academic Press, Elsevier Inc) 173–219. doi: 10.1016/S0065-2113(10)05005-4

Weil, R. R., and Brady, N. C. (2017). *The Nature and Properties of Soils. 15th ed* (Upper Saddle River, NJ, USA: Pearson Press).

Whalen, J. K. (2014). Managing soil biota-mediated decomposition and nutrient mineralization in sustainable agroecosystems. *Adv. Agric.* 2014, 1–13. doi: 10.1155/2014/384604

Yan, S., Weng, B., Jing, L., and Bi, W. (2023). How soil nutrient availability influences plant biomass and how biomass stimulation alleviates heavy metal toxicity in soils: the cases of nutrient use efficient genotypes and phytoremediators, respectively. *Front. Plant Sci.* 14. doi: 10.3389/fpls.2023.1118131

frontiers | Frontiers in Plant Science

TYPE Original Research
PUBLISHED 23 April 2024
DOI 10.3389/fpls.2024.1379485

OPEN ACCESS

EDITED BY
Khurram Shahzad,
Lasbela University of Agriculture, Water and Marine Sciences, Pakistan

REVIEWED BY
Tajamul Hussain,
Oregon State University, United States
Kailou Liu,
Jiangxi Institute of Red Soil, China

*CORRESPONDENCE
Youjun Li
lyj@haust.edu.cn
Ming Huang
huangming_2003@126.com

†These authors have contributed equally to this work and share first authorship

RECEIVED 31 January 2024
ACCEPTED 03 April 2024
PUBLISHED 23 April 2024

CITATION
Zhang J, Li S, Jiang P, Wang R, Guo J, Xiao H, Wu J, Shaaban M, Li Y and Huang M (2024) Organic fertilizer substituting 20% chemical N increases wheat productivity and soil fertility but reduces soil nitrate-N residue in drought-prone regions. *Front. Plant Sci.* 15:1379485. doi: 10.3389/fpls.2024.1379485

Organic fertilizer substituting 20% chemical N increases wheat productivity and soil fertility but reduces soil nitrate-N residue in drought-prone regions

Jun Zhang[1,2†], Shuang Li[1†], Peipei Jiang[1], Rongrong Wang[1], Jinhua Guo[1], Huishu Xiao[1], Jinzhi Wu[1], Muhammad Shaaban[1], Youjun Li[1*] and Ming Huang[1*]

[1]College of Agriculture, Henan University of Science and Technology, Luoyang, Henan, China,
[2]College of Biopharmaceutical and Food Engineering, Shangluo University, Shangluo, Shaanxi, China

Organic fertilizer substitution is an effective measure for increasing both the quantity and quality of wheat grain while reducing chemical fertilizer input. However, the effects of reducing nitrogen (N) fertilizer combined with organic fertilizer substitution on grain yield, grain protein content and protein yield, plant N accumulation and translocation, N use efficiency, soil fertility, N apparent surplus and nitrate-N residue in rain-fed drought-prone areas remains limited. In this study, field experiments were conducted over four consecutive seasons (2019-2023) at two sites with four treatments: zero N application (ZN), farmer N application (FN), reduced 20% N of FN (RN), and organic fertilizer substituting 20% N of RN (OSN). The results showed that compared with the ZN treatment, the FN, RN and OSN treatments increased grain yield and its components, grain protein content and protein yield, aboveground N accumulation at the anthesis and maturity stages, pre-anthesis N translocation, post-anthesis N accumulation, N use efficiency, soil fertility. Compared with RN and FN, OSN increased grain yield by 17.12% and 15.03%, grain protein yield by 3.31% and 17.15%, grain N accumulation by 17.78% and 15.58%, and N harvest index by 2.63% and 4.45% averaged across years and sites, respectively. Moreover, OSN increased the contents of organic matter, total N, available P and available K in both 0-20 and 20-40 cm soil layers, decreased N apparent surplus and nitrate-N residue in 0-100 cm, and pH in both 0-20 and 20-40 cm soil layer. Fundamentally, this study suggests that integrating a 20% reduction N from conventional farmer practices with the utilization of organic fertilizer to replace 20% of the chemical N fertilizer (OSN) represents an effective strategy. This approach shows promise in enhancing wheat grain yield, grain protein yield, and N use efficiency. Additionally, it supports the improvement of soil fertility while simultaneously reducing soil nitrate-N residues and the apparent surplus of N in rain-fed drought-prone regions.

KEYWORDS

dryland, organic fertilizer substitution, grain yield, grain protein, N use efficiency, soil fertility, nitrate-N residue

1 Introduction

Wheat (*Triticum aestivum* L.) is one of the most important staple cereals worldwide, providing approximately 20% of the global calorie and protein supply (Zhong et al., 2019). Therefore, boosting wheat yield and quality plays an important role in food safety. In China, wheat accounted for 20.4% of the total crop area and 24.3% of the total food crop production (National Bureau of Statistics, 2020). Despite this, around 1/3 of wheat production emanates from China's rain-fed drylands—regions characterized by aridity, semi-aridity, and humid drought-prone (Wu et al., 2023b). In these regions, precipitation is the main water sources for wheat growth, and the seasonal unevenness of rainfall causes the grain production potential to decrease by up to 60-70% (Ren et al., 2010; Zhang et al, 2020); meanwhile, water limitation during wheat growth stages hinders nutrient uptake from the soil by plants, thereby resulting in wheat quality fluctuation including protein content under different rainfall patterns. For example, in the Heyang County, where belongs to typical dryland in China, the wheat protein content in humid year is 8.3% and 5.2% lower than that in dry year and normal year, respectively (Liu P. Z. et al., 2021). Nevertheless, nutrient shortfalls impose significant constraints of crop production in these regions (Zhang X. Q. et al., 2023). On the pursuit of the targets for high yield and high quality, the mass even excessive chemical fertilizer was applied to wheat field to minimize the limitation of water and nutrients, which leads to the low efficiency and great environmental risk (Bom et al., 2018; Lu et al., 2022; Nadeem et al., 2022). Therefore, it is imperative to improve fertilization practices to increase grain and protein yield, and resource efficiency and reduce the environmental risk for sustainable wheat production in rain-fed drought-prone areas.

Nitrogen (N), one of the most important macro elements for crop growth and development (Makino, 2011; Jones et al., 2013), plays an important role in uplifting the grain yield and quality wheat (Tilman et al., 2011; McLellan et al., 2018). To boost wheat productivity, high quantities of manufactured N are used in China and throughout the world (Wang et al., 2023). Liu et al. (2018) concluded that a scientific N application was beneficial to root growth, alleviates the negative impact to some extent, and thus promotes water and N uptake by wheat to increase the grain yield in drought-prone areas. However, applying excessive amounts of N fertilizer is not conducive to high-yielding and high-efficient production of wheat (Bappa et al., 2014; Yang et al., 2021). In rain-fed wheat production, the recommended N rate is between 150 and 250 kg ha^{-1}, but generally the N rate is more than 225 kg ha^{-1} in farmer production (Zhang et al., 2019; Luo et al., 2020). These long-term improper applications of N fertilizer have caused low N use efficiency and high risk of nitrate-N residue (Zhou J. Y. et al., 2016; Bom et al., 2018). Thus, fertilization strategies that provide food security and environmental sustainability through optimizing the application rate of chemical N fertilizer are urgently required (Peng et al., 2017; Wang et al., 2020; Ren et al., 2023). Cao et al. (2023) found that 20% reduction of N application had the highest wheat yield in plastic film mulching maize-no-tillage wheat rotation system. While Zhang et al., (2023) concluded that reduced 20% the application rate of chemical N fertilizer did not significantly decrease wheat yield in rice-wheat cropping system. These studies showed that reduced 20% of N fertilizer may maintain or even increase wheat yield, and it is feasible in practice.

Organic fertilizer substitution is an effectively technique to coordinate with soil fertility and crop production (Saudy et al., 2020; Abd-Elrahman et al., 2022). Many studies have shown that organic fertilizer substitution can increase soil organic matter content, promote soil fertility, and improve crop yield. Xia et al. (2017) showed substituting organic fertilizer for chemical fertilizer increased crop productivity by 6.8%. He et al. (2022) found that organic fertilizer substitution increased soil organic matter, alkali-hydrolyzable N, available phosphorus (P) and available potassium (K) in both low fertility soil and high fertility soil. Abbasi and Tahir (2012) concluded that organic fertilizer substituting 25% chemical N fertilizer could ensure wheat yield stability, promote N uptake, and increase N utilization by 20%. Wu et al., 2023a found that organic fertilizer substituting 33% chemical N fertilizer significantly increased wheat protein content and protein yield by 8.0% and 6.3%, respectively. With the advancement of China's "Zero Growth of Chemical Fertilizer" action in recently years, the organic fertilizer substitution techniques become more widely used in agricultural production (Wang et al., 2021), which is favorable for the local fertilizer management converted towards more sustainable practice. However, the impacts of organic fertilizer substitution varied markedly owing to the great differences of wheat production regions in climate conditions, cropping systems and fertilization methods (Zhang et al., 2015; Lv et al., 2023), thus suitable fertilizer management practices should be further explored and carefully adapted and adopted, taking advantages of local resources (Tan et al., 2013; Liu et al., 2019).

In practice, only a minority of farmers opt to use organic fertilizer for food crops, particularly in dryland wheat production areas. This reluctance can be attributed to several factors. Primarily, the limited availability of organic fertilizer and its relatively high cost mean it is predominantly used for high-profit crops such as organically grown food, vegetables, and fruits, rather than for grain crops (Zhang Q. R. et al., 2020; Shi and Yang, 2023). Additionally, organic fertilizers often do not show immediate benefits, in contrast to the readily observable impact of chemical fertilizers on crop growth and yield formation (Case et al., 2017; Li et al., 2021). Furthermore, research on organic fertilizer lags behind that of chemical fertilizers, which restricts the application and broader adoption of organic alternatives (Ju and Zhang, 2021; Shi and Yang, 2023). This situation highlights the imperative for more comprehensive studies to examine the effects of substituting organic for chemical fertilizers on winter wheat productivity. Such research would offer robust field demonstrations to encourage farmers in rain-fed, drought-prone areas to adopt organic fertilization methods.

Within these contexts, our study proposed that integrating reduced N of farmer practice with organic fertilizer substituting could optimize N productivity in winter wheat and reduce soil nitrate-N residue. A 4-year experiment was employed in two sites in a semi-humid, drought-prone region. The objectives were to (1) quantify the impact of reduced N of farmer practice, organic fertilizer substituting on wheat yield, protein content and yield and N use efficiency, and (2) evaluate their effects on soil fertility, N apparent surplus and nitrate-N residue, and (3) identify an optimal agronomic strategy that synergizes wheat productivity, soil fertility and nitrate-N residue in these challenging environments.

2 Materials and methods

2.1 Experimental site description

An experiment was performed 4 years from October 2019 to June 2023 in two sites—Mengjin (34°49′N, 112°35′E) and Luoning (34°47′N, 111°71′E) in Luoyang, the typical rain-fed drought-prone area (junction of the Loess Plateau and the Huang-Huai-Hai Plain), China. The altitude of Mengjin site and Luoning site are 262 m and 560 m, respectively. During the present study, the annual average temperature and precipitation of Mengjin site were 14.6°C and 610.2 mm, and that of Luoning site were 13.7°C and 552.9 mm, respectively (Figure 1). Winter wheat-summer maize is the typical cropping system in Mengjin and winter wheat-summer fallow in Luoning. The soils of both the two sites are classified as brown soil. At the initiation of the experiment in 2019, the basic soil properties (0-40 cm layer) are listed in Table 1.

2.2 Experimental design and field management

The present study was conducted from October 2021 to June 2023. A completely randomized block design was used, with three replicates for each treatment. The plots were 72.0 m^2 (10.0 m×7.2 m) and 25.2 m^2 (7 m×3.6 m) in Mengjin and Luoning, with a 1.2 m wide buffer strip between the plots to avoid effects of nutrients accorded the plots. Four treatments were used: (1) zero N application (ZN); (2) farmer N application (FN) as local farmer practice; (3) reduced N application (RN), 20% reduction of N fertilizer based on FN, and (4) organic fertilizer substituting 20% N of reduced N application (OSN). All treatments received same amount P and K fertilizers (P_2O_5 90 kg ha^{-1}, K_2O 60 kg ha^{-1}). The application rate of chemical N in FN was 192 kg ha^{-1} and 172 kg ha^{-1} in Mengjin and Luoning, respectively. In OSN, the application rate of chemical N was 122.9 kg ha^{-1} and 110.1 kg ha^{-1}, and the application amount of organic fertilizer was 706.6 kg ha^{-1} and 633.0 kg ha^{-1} in Mengjin and Luoning, respectively. N, P, K fertilizers were urea (N, 46%), triple superphosphate (P_2O_5, 12%) and potassium sulfate (K_2O, 50%), respectively. Organic fertilizer (N, 2.6%; P_2O_5, 1.5%; K_2O, 2.5%; organic matter, 50%; living bacteria count ≥20 million g^{-1}) was provided by Luoyang Qihe Ecological Agricultural Technology Co., Ltd. (Luoyang, Henan, China). All fertilizers were broadcasted in the corresponding plots as basal fertilizer. Wheat (*Triticum aestivum* L.) cultivars Zhoumai 27 and Luohan 22 were used in Mengjin and Luoning, respectively. In each growing season, wheat was sown in middle or late October, depending on weather conditions, at a seedling rate of 225 kg ha^{-1}, and harvested in late May or early June. Weeds, pests, and diseases were controlled with herbicides and pesticides according to local practices.

2.3 Measurements and methods

2.3.1 Grain yield and yield components

At maturity, three quadrats covering 1 m^2 (1m×1m) were randomly harvested from each plot and threshed after air-drying. Grains from the three quadrats of same plot were mixed and weighed, and then 50 ± 5 g grains were oven-dried at 70°C to constant weight to determine the moisture contents in grain. Grain yield was standardized at a 12.5% moisture content. Before harvest, spike number was counted from the two 1 m double rows of each plot. Grain number per spike was determined by calculating grains of 50 randomly selected spikes from the two 1 m double rows. The 1000-grain weight was calculated by weighing 1000 grains of each sample.

2.3.2 N accumulation, translocation, and distribution

At anthesis, 300 stems of relatively uniform were marked in each plot. After that, the 50 marked stems were manually sampled by cutting aboveground parts at the anthesis and maturity stages, and organs were separated into leaves, stem+sheaths, and spikes (further separated into grain and glume+axis at maturity). All

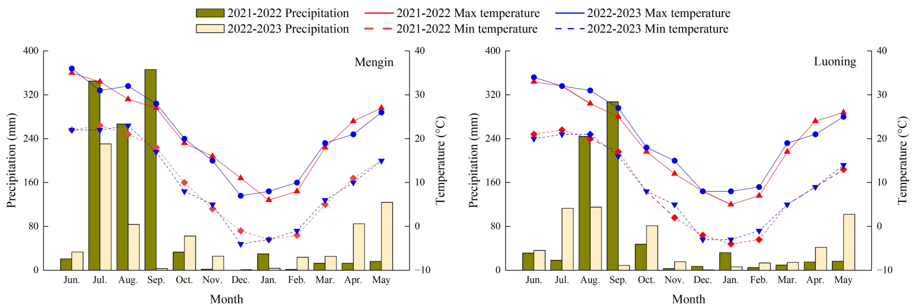

FIGURE 1
Monthly precipitation during the experiment.

TABLE 1 Basic soil properties of the top 0-40 cm soil layers.

Site	Soil layer (cm)	Organic matter (g kg^{-1})	Total N (g kg^{-1})	Nitrate-N (mg kg^{-1})	Available P (mg kg^{-1})	Available K (mg kg^{-1})	pH
Mengjin	0-20	14.71	1.17	12.05	19.38	139.74	7.54
	20-40	10.74	0.85	8.99	5.64	106.87	7.41
Luoning	0-20	12.72	0.73	7.83	15.68	197.57	7.26
	20-40	9.56	0.54	5.91	3.15	136.71	7.23

samples were first dried at 105°C for 30 min, and then at 70°C until constant weight to measure the aboveground biomass (kg ha^{-1}). N concentration was determined by milling the dried samples, passing through a 0.25mm sieve, and then the total N concentration was digested by H_2SO_4-H_2O_2 and examined using a high-resolution digital colorimeter auto analyzer 3 (AA3, SEAL Company, Germany). The N accumulation in different organs was N concentration multiplied by the dry weight of the corresponding organ.

The calculation formula was as follows (Yu et al., 2023; Li J. J. et al., 2023):

(1) Pre-anthesis N translocation amount (kg ha^{-1}) = N accumulation of vegetative organs at anthesis – N accumulation of vegetative organs at maturity;

(2) Contribution rate of pre-anthesis N translocation amount to grain (%) = Pre-anthesis N translocation amount/grain N accumulation at maturity×100;

(3) Post-anthesis N accumulation amount (kg ha^{-1}) = Grain N accumulation at maturity – shoot N accumulation at anthesis;

(4) Contribution rate of post-anthesis N accumulation amount to grain (%) = Post-anthesis N accumulation/grain N accumulation at maturity×100;

(5) N harvest index (%) = Grain N accumulation at maturity/ Shoot N accumulation at maturity×100.

2.3.3 Grain protein content and protein yield

The protein content and protein yield were calculated as follows (Huang et al., 2021):

(6) Protein content (%) = Grain N concentration×5.7;

(7) Protein yield (kg ha^{-1}) = Protein content×grain dry matter amount.

2.3.4 Calculation of N use efficiency and N apparent surplus

The N use efficiency was calculated as follows (Huang et al., 2021; Zhang S. M. et al., 2023):

(8) N grain production efficiency (kg kg^{-1}) = Grain yield/Shoot N accumulation at maturity×100;

(9) N uptake efficiency (kg kg^{-1}) = Shoot N accumulation at maturity/N application rate;

(10) N agronomy efficiency (kg kg^{-1}) = (Grain yield under N application treatment – grain yield under ZN treatment)/N application rate;

(11) N recovery efficiency (%) = (Shoot N accumulation amount under N application treatment – Shoot N accumulation amount under ZN treatment)/N application rate×100;

(12) N partial factor productivity (kg kg^{-1}) = Grain yield under N application treatment/N application rate.

The N apparent surplus was calculated as follows (Li et al., 2015):

(13) N apparent surplus (kg ha^{-1}) = N application rate – Grain N accumulation at maturity.

2.3.5 Soil sampling and analysis

Soil samples were taken 3 days after harvesting in 2023. Five soil subsamples from 0 to 100 cm depth with 20 cm increments were randomly collected from each plot using a soil drill (4.0 cm in diameter). After removing visible roots and stones, the fresh soil subsamples were thoroughly mixed to get a composite soil sample. About 300 g soil was collected for soil fertility analysis and the rest was stored in a freezer at -20°C for nitrate-N residue analysis within 7 days. The sample for soil fertility was air-dried and then passed through 2.0 mm sieve. The determination methods of soil fertility were performed according to Chen et al. (2017). External heating with potassium dichromate was used to determine organic matter. Total N was quantified with Kjeldahl digestion and examined using a high-resolution digital colorimeter auto analyzer 3 (AA3, SEAL Company, Germany). The 0.5 mol L^{-1} $NaHCO_3$-molybdeenum blue colorimetric method was used to measure available P. The 1 mol L^{-1} ammonium acetate-flame spectrophotometry method was used to measure available K. The soil pH (1:8 soil: water ratio) was measured using a digital pH meter (PHSJ-4F, Leici Company, China). The nitrate-N residue was quantified with the method described by Dai et al. (2015). Briefly, fresh soil samples weighing 5.0 g were extracted with 50 mL of 1.0 mol L^{-1} KCl after shaking for 1h, and then nitrate-N concentration was measured by a high-resolution digital colorimeter auto analyzer 3 (AA3, SEAL Company, Germany). The nitrate-N residues in each soil layer were calculated as follows:

(14) Nitrate-N residue (kg ha^{-1}) = $H_i \times D_i \times C_i \times 0.1$. Where Hi is the soil thickness of the i layer (cm), Di is the soil bulk density (g cm^{-3}), Ci is the nitrate-N concentration (mg kg^{-1}) in the corresponding soil layer and 0.1 is the conversion coefficient.

2.4 Statistical analysis

Data were analyzed using Microsoft Excel 2010 (Microsoft Windows, Redmond, DC, USA) and SPSS 18.0 (IBM, Corp., Chicago, IL, USA). The differences test was performed by the Duncan's test at a 0.05 probability level. Principal component analysis was performed on the measured indexes using SPSS 18.0 and a graphical presentation was generated using Origin 2024 (Origin Lab Corporation, Northampton, USA).

3 Results

3.1 Grain yield and yield components

Table 2 presented year (Y) and treatment (T) extremely significantly but not site (S) affected the grain yield, spike number and grain number per spike, and significantly affected 1000-grain weight, the interaction of S and Y, Y and T, and S, T and Y extremely significantly affected on grain number per spike; while the interaction of S and Y significantly affected on 1000-grain weight. Compared with ZN, FN, RN and OSN significantly increased wheat grain yield, spike number and grain number per spike in both years and sites. Compared with FN, RN did not significantly decrease wheat yield, spike number and grain number per spike except grain number per spike in Mengjin and spike number in Luoning in 2022-2023. Compared with RN and FN, the grain yield, spike number, grain number per spike and 1000-grain weight under OSN increased by 17.12% and 15.03%, 11.11% and 7.21%, 6.45% and 2.95%, 1.41% and 1.03%, respectively, averaged across years and sites.

3.2 N accumulation

The year (Y), treatment (T), interaction of S and year (Y), and interaction of S, T and Y extremely significantly affected N accumulation at anthesis and maturity, and the N accumulation

TABLE 2 Effects of different treatments on wheat yield and its components of winter wheat in 2021-2023.

Site	Year	Treatment	Grain yield/ (kg ha^{-1})	Spike number/ (10^{4} ha^{-1})	Grain number per spike	1000-grain weight (g)
Mengjin	2021-2022	ZN	3820 c	411.3 c	28.5 c	39.2 b
		FN	5450 b	476.9 b	33.6 ab	41.0 a
		RN	5373 b	460.8 b	32.9 b	42.0 a
		OSN	6214 a	516.3 a	34.6 a	42.3 a
	2022-2023	ZN	3634 c	398.1 c	26.8 c	39.8 b
		FN	5170 b	431.7 b	37.2 a	41.7 a
		RN	5088 b	415.6 b	35.5 b	41.4 a
		OSN	6038 a	465.2 a	37.7 a	41.7 a
Luoning	2021-2022	ZN	3540 c	398.1 c	26.8 c	39.6 a
		FN	5101 b	431.7 b	32.5 ab	40.4 a
		RN	5057 b	415.6 b	31.5 b	39.7 a
		OSN	5803 a	465.2 a	33.3 a	40.6 a
	2022-2023	ZN	3472 c	366.0 d	29.9 c	39.3 b
		FN	4985 b	406.9 b	35.8 ab	42.4 a
		RN	4824 b	393.8 c	34.6 b	41.8 ab
		OSN	5761 a	427.3 a	37.6 a	42.6 a
Sources of variance (*F*-value)		Site (S)	22.91	51.63	0.57	0.23
		Year (Y)	19.27**	116.68**	186.97**	6.61*
		Treatment (T)	806.77**	48.84**	26.81**	19.59*
		S×Y	2.21	2.26	16.49**	6.17*
		Y×T	0.76	2.04	11.71**	0.61
		S×T	4.66	0.85	0.66	0.25
		S×T×Y	0.09	2.40	8.07**	1.99

ZN, FN, RN and OSN indicated zero N application, farmer N application, 20% reduction of N fertilizer based on FN and organic fertilizer substituting 20% N of RN, respectively. Different lowercase letters within the same year and the same column indicate significant differences at P<0.05 among treatments. * and ** indicate significant difference at P<0.05 and P<0.01, respectively.

at anthesis and maturity showed the same order of ZN<RN<FN<OSN in both years and sites (Figure 2). Compared with ZN, FN, RN and OSN increased N accumulation by 72.51%, 63.22% and 82.06% at anthesis and by 72.44%, 66.50% and 90.12% at maturity in Mengjin, respectively; and by 81.35%, 70.97% and 91.99% and by 82.79%, 76.15% and 103.01% in Luoning, averaged across years. These results showed that OSN significantly increased accumulation N at anthesis and maturity, compared with FN and RN. However, RN reduced N accumulation by 5.57% and 3.54% at anthesis and maturity compared with FN, averaged across years and sites.

3.3 Pre-anthesis N translocation, post-anthesis N accumulation and N harvest index

As shown in Table 3, year (Y), treatment (T) significantly affected the characteristics of pre-anthesis N translocation, post-anthesis N accumulation and N harvest index, and the intersection of S×Y, Y×T, S×T×Y extremely significantly affected N harvest index. Compared with ZN, FN, RN, OSN increased pre-anthesis N translocation amount, post-anthesis N accumulation amount, and contribution rate of post-anthesis N accumulation amount to grain, and thus increased the N accumulation amount in grain, but decreased the N harvest index. Compared with FN and RN, OSN significantly increased N accumulation amount in grain by 14.57% and 16.84% in Mengjin and by 16.59% and 18.70% in Luoning averaged across years, respectively, and thus significantly increased the N harvest index. Compared with FN and RN, OSN increased the N harvest index by 3.91% and 2.30% in Mengjin and by 4.96% and 2.91% in Luoning averaged across years, respectively.

3.4 Grain protein content and protein yield

Figure 3 reveals year (Y), treatment (T) extremely significantly affected protein content and protein yield in the both years and sites. Compared with ZN, the protein content under FN, RN and OSN significantly increased by 19.45%, 6.67% and 7.25%, as well as protein yield significantly increased by 71.01%, 50.03% and 76.61% averaged across years and sites, respectively. Compared with FN, RN and OSN significantly decreased the protein content by 11.71% and 10.18%, respectively, while RN significantly decreased protein yield by 12.23%, but OSN increased protein yield by 3.31% averaged across years and sites.

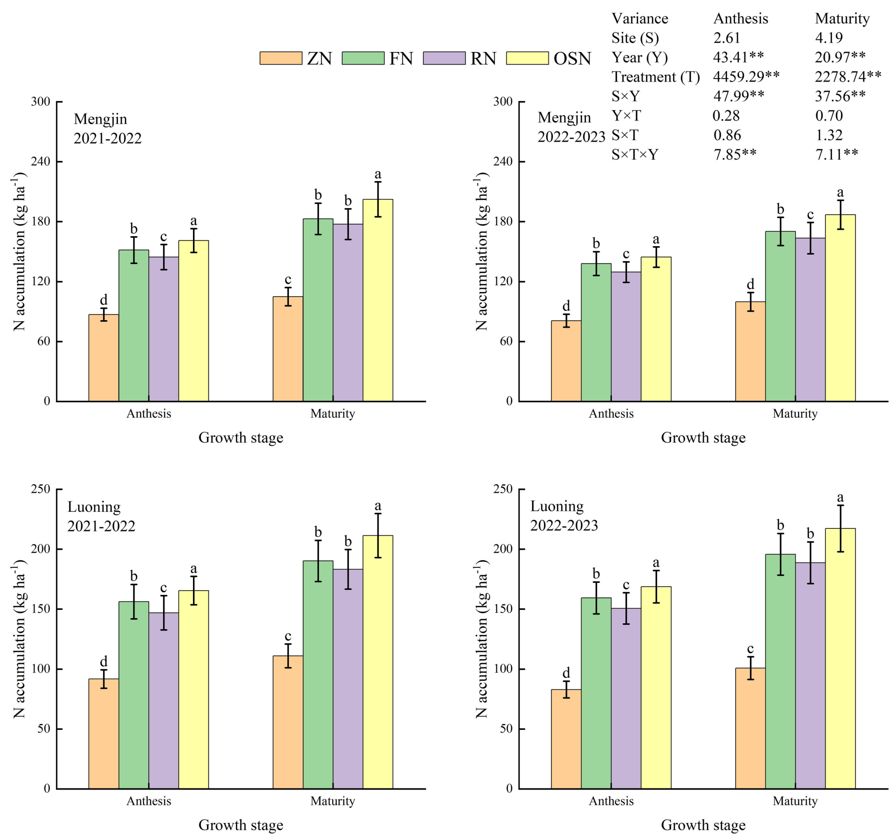

FIGURE 2
Effects of different treatments on N accumulation at anthesis and maturity of winter wheat in 2021-2023. ZN, FN, RN and OSN indicated zero N application, farmer N application, 20% reduction of N fertilizer based on FN and organic fertilizer substituting 20% N of RN, respectively. Lowercase letters above bars within the same growth stage indicate significant difference among treatments (*P*<0.05). * and ** indicate significant difference at *P*<0.05 and *P*<0.01, respectively.

TABLE 3 Effects of different treatments on N translocation, N accumulation and N harvest index of winter wheat in 2021-2023.

Site	Year	Treatment	Pre-anthesis N		Post-anthesis N		N accumulation amount in grain (kg ha^{-1})	N harvest index (%)
			Translocation Amount (kg ha^{-1})	Contribution rate to grain (%)	Accumulation amount (kg ha^{-1})	Contribution rate to grain (%)		
Mengjin	2021-2022	ZN	64.99 d	78.31 a	17.99 c	21.69 c	82.99 c	79.05 a
		FN	99.77 b	76.15 b	31.25 b	23.85 b	131.02 b	71.65 d
		RN	95.64 c	74.38 bc	32.94 b	25.62 ab	128.58 b	72.43 c
		OSN	108.71 a	72.53 c	41.17 a	27.47 a	149.89 a	74.06 b
	2022-2023	ZN	61.01 d	76.36 a	18.89 c	23.64 c	79.90 c	80.09 a
		FN	93.05 b	74.29 ab	32.20 b	25.71 bc	125.25 b	73.58 d
		RN	88.81 c	72.37 bc	33.91 b	27.63 ab	122.71 b	75.08 c
		OSN	101.29 a	70.49 c	42.41 a	29.51 a	143.70 a	76.85 b
Luoning	2021-2022	ZN	68.52 d	78.01 a	19.31 c	21.99 c	87.83 c	79.13 a
		FN	103.69 b	75.35 ab	33.92 b	24.65 bc	137.61 b	72.34 d
		RN	98.96 c	73.17 bc	36.29 b	26.83 ab	135.25 b	73.82 c
		OSN	112.95 a	71.09 c	45.94 a	28.91 a	158.89 a	75.14 b
	2022-2023	ZN	62.78 c	77.81 a	17.90 c	22.19 b	80.68 c	80.03 a
		FN	104.13 b	74.10 ab	36.40 b	25.90 ab	140.53 b	71.76 d
		RN	99.86 b	72.38 b	38.11 b	27.62 a	137.96 b	73.09 c
		OSN	116.87 a	70.64 c	48.57 a	29.36 a	165.44 a	76.12 b
Sources of variance (*F*-value)		Site (S)	4.96	0.08	301.80	0.08	9.54	0.03
		Year (Y)	26.73**	13.30**	3.92	13.29**	6.00*	153.32*
		Treatment (T)	947.43**	2685.30**	472.04**	3167.58**	735.01**	146.43**
		S×Y	24.69**	2.24	0.09	2.25	16.03**	116.37**
		Y×T	1.08	0.02	0.67	0.02	1.90	8.32**
		S×T	1.18	1.05	6.02	1.05	2.06	0.23
		S×T×Y	5.11	0.26	0.56	0.26	5.07**	14.28**

ZN, FN, RN and OSN indicated zero N application, farmer N application, 20% reduction of N fertilizer based on FN and organic fertilizer substituting 20% of RN, respectively. Values within the same year and the same column followed by different lowercase letters indicate significant differences(P<0.05) among treatments. * and ** indicate significant difference at P<0.05 and P<0.01, respectively.

3.5 N use efficiency and N apparent surplus

N use efficiency and N apparent surplus was significantly affected by year (Y), Site (S), treatment (T), and their interactions (Table 4). Compared with FN and RN, OSN increased N grain production efficiency except Luoning site in 2021-2022, and there were no significant differences between FN and RN. Compared with FN, RN and OSN increased N uptake efficiency, N agronomy efficiency, N recovery efficiency and N partial factor productivity, while RN and OSN decreased N apparent surplus. Compared with RN, OSN significantly increased N uptake efficiency, N agronomy efficiency, N recovery efficiency and N partial factor productivity by 15.22%, 59.47%, 35.93% and 17.12%, averaged across years and sites; and decreased N apparent surplus by 45.82% in Mengjin and 168.43% in Luoning across years. These results showed that OSN could increase winter wheat N use efficiency and decrease N apparent surplus in drought-prone area.

3.6 Soil fertility

Soil fertility was significantly affected by the 4-year located fertilization in both sites (Figure 4). Compared with the initial value, ZN significantly decreased the organic matter and total N but increased pH in both 0-20 cm and 20-40 cm soil layers. The overall trend of organic matter, total N, available P and available K among treatments was ZN<RN<FN<OSN in both soil layers. Compared with FN, RN decreased the contents of organic matter, total N, available P, available K by 6.93%, 4.95%, 4.71% and 4.65%, respectively, in 0-20 cm soil layer, and by 4.69%, 11.08%, 15.02% and 11.21% in 20-40 cm soil layer, averaged across sites. However,

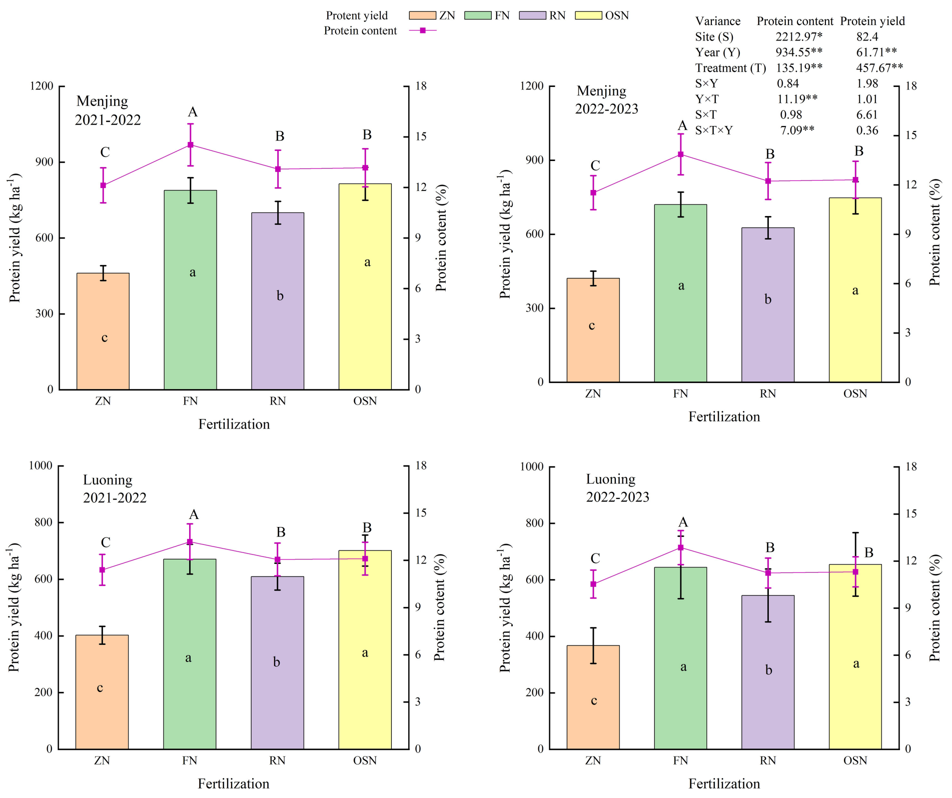

FIGURE 3
Effects of different treatments on grain protein content and protein yield of winter wheat in 2021-2023. ZN, FN, RN and OSN indicated zero N application, farmer N application, 20% reduction of N fertilizer based on FN and organic fertilizer substituting 20% N of RN, respectively. Different uppercase and lowercase letters indicate that significant difference at *P*<0.05 among treatments, respectively for protein content and protein yield.

OSN increased the contents of organic matter, total N, available P and available K in 0-20 cm soil layer by 17.30%, 12.95%, 9.92% and 7.82% and in 20-40 cm soil layer by 12.17%, 25.82%, 21.85% and 23.03% compared with RN. While compared with RN, OSN decreased pH in 0-20 cm and in 20-40 cm soil layer.

3.7 Nitrate-N residue

As shown in Figure 5, the nitrate-N residue in 0-100 cm soil depth were 23.57 kg ha^{-1}, 84.69 kg ha^{-1}, 61.62 kg ha^{-1} and 55.77 kg ha^{-1} in Mengjin and 20.47 kg ha^{-1}, 78.68 kg ha^{-1}, 57.09 kg ha^{-1} and 52.73 kg ha^{-1} in Luoning under ZN, OSN, RN and FN, respectively. The ZN showed the lowest nitrate-N residue while FN showed the highest value in each soil layer. Except for 0-20 cm soil layer of both sites and in 60-80 cm soil layer in Mengjin, the nitrate-N residue in 0-100 soil layer of OSN was lower than that of RN, with the average decrease of 20.37% in Mengjin and 12.78% in Luoning across soil layers, indicating that OSN had a beneficial effect on reducing nitrate-N residue.

3.8 Comprehensive evaluation

Principal component analysis was used to evaluate the comprehensive effects of different treatments (Table 5). The results showed that the N fertilization effects could be explained by the two principal components, with the cumulative contribution rate of 96.82% (Mengjin) and 96.03% (Luoning). The first principal component mainly included grain yield and its components, N translocation and accumulation amount, N accumulation amount in grain, protein content, soil fertility and nitrate-N residue in 0-100 cm soil layer. The second principal component mainly included N harvest index, protein yield and pH in 20-40 cm soil layer. Based on the evaluation formula ($y=0.8785C_1+0.0884C_2$, Mengjin; $y=0.8619C_1+0.0871C_2$, Luoning), the comprehensive score of each treatment could be calculated (Figure 6). The comprehensive score ranked as OSN>FN>RN>ZN, meaning OSN had a good comprehensive effect on wheat production, soil fertility and soil nitrate-N residue.

4 Discussion

4.1 Effects of organic fertilizer substitution on wheat grain yield, protein content and protein yield

Substituting chemical fertilizers with organic alternatives is a crucial strategy for enhancing crop yields. However, the effectiveness of this approach varies according to the rates of substitution (Shen et al., 2020; He et al., 2022). A meta-analysis revealed that replacing

TABLE 4 Effects of different treatments on N use efficiency and N apparent surplus of winter wheat in 2021-2023.

Site	Year	Treatment	N use efficiency					N apparent surplus (kg ha^{-1})
			N grain production efficiency (kg kg^{-1})	N uptake efficiency (kg kg^{-1})	N agronomy efficiency (kg kg^{-1})	N recovery efficiency (%)	N partial factor productivity (kg kg^{-1})	
Mengjin	2021-2022	ZN	36.43 a	—	—	—	—	—
		FN	29.84 c	0.95 b	8.49 b	40.55 b	28.38 c	60.98 a
		RN	30.30 bc	1.03 b	9.03 b	42.17 b	31.24 b	43.42 b
		OSN	30.74 b	1.18 a	13.92 a	56.61 a	36.13 a	22.11 c
	2022-2023	ZN	36.47 a	—	—	—	—	—
		FN	30.40 c	0.89 c	7.99 b	36.73 b	26.93 c	66.75 a
		RN	31.17 bc	0.95 b	8.45 b	37.05 b	29.58 b	49.29 b
		OSN	32.28 b	1.09 a	13.97 a	50.71 a	35.10 a	28.30 c
Luoning	2021-2022	ZN	32.15 a	—	—	—	—	
		FN	27.04 b	1.11 c	9.08 b	46.07 b	29.65 c	27.72 a
		RN	27.79 b	1.21 b	9.98 b	47.51 b	33.27 b	16.75 a
		OSN	27.66 b	1.39 a	14.89 a	66.06 a	38.17 a	-6.89 b
	2022-2023	ZN	34.44 a	—	—	—	—	—
		FN	25.46 c	1.14 c	8.80 b	55.21 b	28.98 c	24.80 a
		RN	25.56 c	1.24 b	9.98 b	57.86 b	31.74 b	14.04 a
		OSN	26.51 b	1.43 a	15.06 a	76.64 a	37.90 a	-13.44 b
Sources of variance (*F*-value)		Site (S)	31.41	17.61	746.89*	3.63	55.25	47.97
		Year (Y)	150	21.41**	2.14	56.73**	17.34**	0.33
		Treatment (T)	54.28*	3415.77**	189.63**	12822.38**	318.87**	1513.30**
		S×Y	24.46**	171.91**	0.01	493.44**	1.10	9.34 **
		Y×T	9.21**	0.34	1.20	0.09	1.07	0.12
		S×T	0.19	22.58*	1.01	11.15	4.27	8.14
		S×T×Y	20.06***	1.04	0.20	2.39	0.16	0.18

ZN, FN, RN and OSN indicated zero N application, farmer N application, 20% reduction of N fertilizer based on FN and organic fertilizer substituting 20% N of RN, respectively. Lowercase letters within the same year and the same column followed by different indicate significant differences (P<0.05) among treatments. * and ** indicate significant difference at P<0.05 and P<0.01, respectively.

up to 30% of chemical fertilizers with organic ones can lead to an increase in wheat yields. Nevertheless, when the substitution rate surpasses 30%, the beneficial effects on wheat yield become observable only after a decade or more (Li et al., 2021). The present 4-year and 2-site experiment found that the organic fertilizer substituted 20% of chemical N fertilizer (OSN) could optimized winter wheat yield components and improved grain yield. This was consistent with previous the studies in winter wheat-summer maize cropping system (Shen et al., 2020) and wheat-fallow fallow cropping system (He et al., 2022), which showed that the substitution of 20% chemical N fertilizer with organic fertilizer could improve wheat yield. These findings suggest that the substitution with organic fertilizers not only accelerates the release of nutrients from chemical fertilizers (Li W. X. et al., 2023) but also leverages the slow-release properties of organic fertilizer nutrients. This dual action enhances nutrient absorption and utilization by wheat throughout its entire growth stage (Yang et al., 2020), ultimately leading to higher yields. Moreover, compared to the FN application, the RN application achieved a relatively stable yield despite a 20% reduction in N. This outcome indicates that current N application rates by farmers could be decreased by at least 20% without compromising yields. The present study also found that, compared with FN and RN, OSN significantly increased spike number and grain number per spike; however, it did not affect the 1000-grain weight. These results demonstrated that OSN increased yield by greatly improving spike number and grain number per spike. The main reason may be the organic fertilizer induces the relatively sufficient nutrients and optimal water supply, boosts the growth development and spike differentiation, and finally improves the spike number and grain number per spike (Zhang Q. R. et al., 2020).

10.3389/fpls.2024.1379485

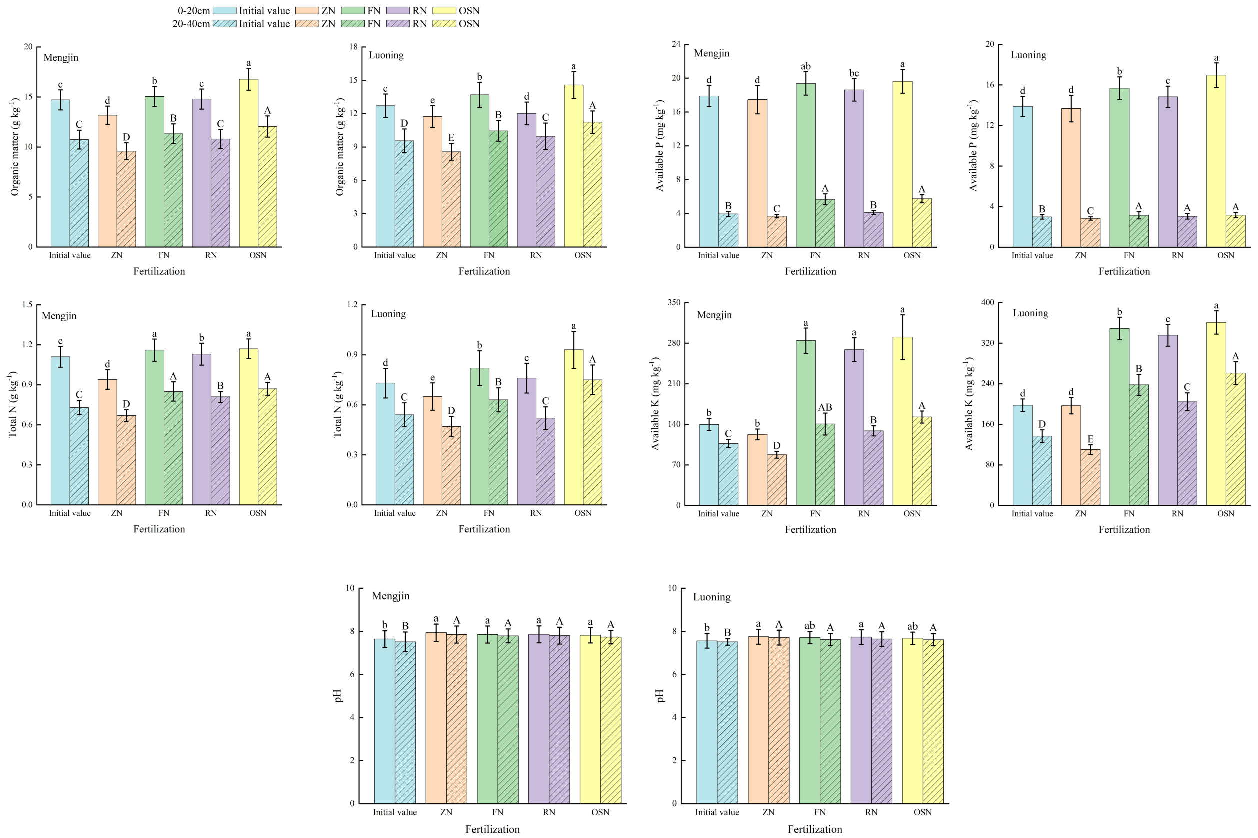

FIGURE 4
Effects of different treatments on content of organic matter, total N, available P, available K and pH in 0-20 cm and 20-40 cm soil layers at maturity of winter wheat in 2022-2023. ZN, FN, RN and OSN indicated zero N application, farmer N application, 20% reduction of N fertilizer based on FN and organic fertilizer substituting 20% N of RN, respectively. Different lowercase and uppercase letters indicate that significant difference (P<0.05) among treatments in 0-20 cm and 20-40 cm soil layer, respectively.

Protein is an important index to evaluate wheat grain quality. The present study found that, compared with FN, the grain protein content under RN and OSN significantly decreased, which was consistent with the results of Han et al. (2022). These results showed that reduced N fertilizer (20%) had a negative impact on wheat quality in drought-prone area. The reason may be because the amount of N requirement for high-protein was higher than that of high-yield (Ghimire et al., 2021). Conversely, these results indicated that the current N application rate of farmers is reasonable for high-quality production, which was mainly due to the recommended fertilization guidance in China in the past 20 years (Xu et al., 2021). Besides, compared with RN, OSN did not increase the protein content while significantly increased grain yield, meaning that the improvement of OSN on grain yield was prior to that on protein content (Li W. X. et al., 2023). Conversely, some studies have found that organic fertilizer substitution increased protein content (Xia et al., 2017). The variability of the effeteness among studies might be related to organic fertilizer type and substitution ratio. Additionally, the significant increase in grain yield helped to reach the highest protein yield under OSN, which indicated that it is feasible for OSN to realize a high protein yield based on the higher yield.

4.2 Effects of organic fertilizer substitution on plant N accumulation, translocation, and distribution

Wheat yield and grain protein content are regulated not only by the pre-anthesis stored-N translocation in vegetative organs, but also by post-anthesis N absorption, accumulation, and translocation (Jones et al., 2013; Zhou B. W. et al., 2016). In this study, the OSN notably enhanced N accumulation at both anthesis and maturity stages compared to the FN and RN treatments. These results could be related to the ability of OSN to improve precipitation storage effectiveness, mitigate soil water depletion (Zhang Q. R. et al., 2020), and stimulate plant growth and nutrient content (Thomas et al., 2019). Consequently, this led to the highest N accumulation in the aboveground parts and grains, as shown in Table 3. These results are in line with other studies reporting positive effects of organic fertilizer substitution on cereal crops (Saikia et al., 2015; Lv et al., 2023). This could be attributed to OSN offering a better synchronization between N supply and demand, while also contributing to an increase in the size of the grain sink. (Pei et al., 2020). Besides, the source-traits such as aboveground dry matter accumulation, leaf photosynthesis also responded to organic

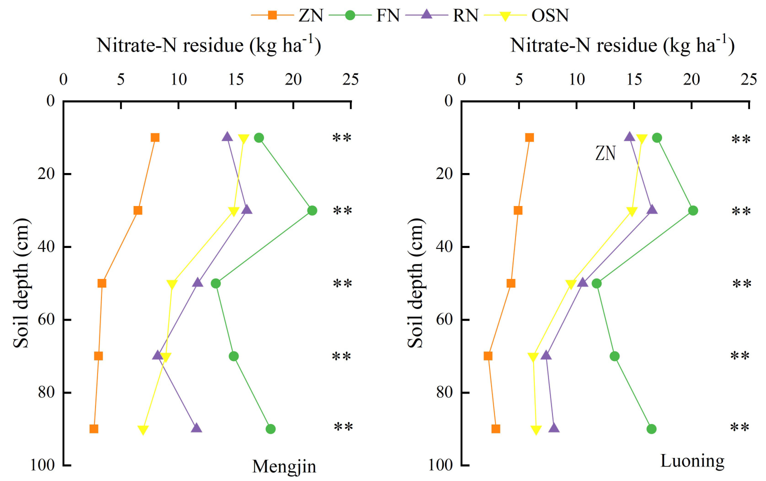

FIGURE 5
Effects of different treatments on nitrate-N residue in 0-100 cm soil layer at maturity of wheat in 2022-2023 at maturity. ZN, FN, RN and OSN indicated zero N application, farmer N application, 20% reduction of N fertilizer based on FN and organic fertilizer substituting 20% N of RN, respectively. ** indicate that significant differences at *P*<0.01 among treatments within the same soil layer.

fertilizer substitution (Saikia et al., 2015). In addition, ONS delayed leaf senescence, extended duration of source activity, thus increased the contribution rate of post-anthesis dry matter and N accumulation to grain (Pan et al., 2022). This is maybe explained why OSN improved the characteristics of N accumulation and translocation, and increased N harvest index, finally achieving synergistic improvement of grain yield and protein yield.

4.3 Effects of organic fertilizer substitution on N use efficiency and N apparent surplus

N use efficiency is an important index to measure the rationality of fertilization measures (Shen et al., 2020; Yin et al., 2021). In this study, compared with FN and RN, OSN increased N uptake efficiency, N agronomy efficiency, N recovery efficiency and N partial factor productivity increased averaged across years and sites, which was consistence with the results of He et al. (2022) and Lv et al. (2023). These findings could be attributed to several factors: (1) OSN addressed the soil nutrient imbalance caused by the prolonged excessive use of chemical fertilizers (Yang et al., 2018); (2) OSN enhanced soil microbial activity and bettered the micro-ecological environment by elevating the soil's carbon-to-nitrogen ratio (Liu et al., 2022); (3) The consistent nutrient release from organic fertilizers ensured a steady nutrient availability throughout the growing season (Liu J. A. et al., 2021). OSN obtained a reasonable N grain production efficiency, N agronomy efficiency and N partial factor productivity, with the average of 29.30 kg kg^{-1}, 14.46 kg kg^{-1} and 36.83 kg kg^{-1}, respectively, these indexes fall into the reasonable range of above indexes for 30-60 kg kg^{-1}, 10-30 kg kg^{-1} and 40-70 kg kg^{-1}, respectively, according to Dobermann (2005) documented. However, the N recovery efficiency in this study was 62.51%, obviously higher than 30-50% reported by Dobermann (2005). This was maybe ascribed the accumulative effect of long-term zero N application under ZN, leaded to lower N accumulation and higher N recovery efficiency.

N apparent surplus is often employed to reflect the N input-output balance of a field, farm or for a specific region (Li W. X. et al., 2023; Sapkota and Takele, 2023). Li T. Y. et al., (2020) reported that the reasonable threshold of N apparent surplus in farmland was 40 kg ha^{-1}. In the present study, N apparent surplus under FN and RN were 63.87 kg ha^{-1} and 46.36 kg ha^{-1} in Menjin across years. This indicated that reduced 20% N based on the local farmer practice (FN) still lead to a little higher N apparent surplus in Mengjin. While in Luoning, the N apparent surplus of FN and RN were 26.26 kg ha^{-1} and 25.40 kg ha^{-1} across years, which were below the threshold value at 40 kg ha^{-1}. Compared with RN, OSN decreased the N apparent surplus remarkably, under which the average N apparent surplus was 25.21 kg ha^{-1} in Mengjin and -10.17 kg ha^{-1} in Luoning, both of that were lower than the reasonable threshold of 40 kg ha^{-1} reported by Li Y. H. et al., (2020). These may be due to the OSN induced improvement of soil properties and soil water-holding capability (Yang et al., 2018; Liu P. Z. et al., 2021), leading to a remarkable increase of wheat growth and shoot N uptake, and finally resulting in an over-consumption of soil N (Yue et al., 2012; Ju and Zhang, 2021). Additionally, this study also found that due to the lower N input and slightly higher grain N output in Luoning, resulting in N apparent surplus was lower than that in Mengjin. Particularly, the N apparent surplus under OSN in Luoning was negative value. Therefore, the over-low N apparent surplus should be pay attention when the OSN technique employed in rain-fed, drought-prone areas.

4.4 Effects of organic fertilizer substitution on soil fertility and nitrate-N residue

Evaluation of soil fertility is of great significance to improve farmland quality (Li et al., 2024). In this study, owing to four-year

TABLE 5 Score coefficient and contribution rate of principal component.

Indexes	Mengjin		Luoning	
	Component 1 (C_1)	Component 2 (C_2)	Component 1 (C_1)	Component 2 (C_2)
Grain yield	0.043	-0.074	0.043	0.048
Spike number	0.041	-0.119	0.041	0.136
Grain number per spike	0.043	0.042	0.044	-0.013
1000-grain weight	0.042	-0.028	0.044	-0.035
N accumulation of anthesis	0.043	0.030	0.043	-0.055
N accumulation of maturity	0.044	-0.004	0.044	-0.021
Pre-anthesis N translocation amount	0.044	-0.009	0.044	-0.002
Contribution rate of pre-anthesis N translocation amount	-0.038	0.203	-0.039	-0.113
Post-anthesis N accumulation amount	0.042	-0.116	0.042	0.083
Contribution rate of post-anthesis N accumulation amount	0.038	-0.203	0.039	0.113
N accumulation amount in grain	0.043	-0.046	0.043	0.028
N harvest index	-0.035	-0.238	-0.032	0.303
Protein yield	0.029	0.319	0.028	-0.295
Protein content	0.043	0.044	0.044	-0.051
N grain production efficiency	-0.039	-0.162	-0.040	0.166
Organic matter in 0-20 cm soil layer	0.041	-0.146	0.038	0.125
Organic matter in 20-40 cm soil layer	0.043	-0.055	0.044	0.055
Total N in 0-20 cm soil layer	0.043	0.061	0.042	0.119
Total N in 20-40 cm soil layer	0.043	0.036	0.039	0.163
Available P in 0-20 cm soil layer	0.043	0.025	0.042	0.124
Available P in 20-40 cm soil layer	0.037	0.047	0.043	-0.064
Available K in 0-20 cm soil layer	0.043	0.064	0.043	-0.081
Available K in 20-40 cm soil layer	0.044	-0.002	0.044	-0.017
Nitrate-N residue in 0-100 cm soil layer	-0.044	0.030	-0.041	-0.150
pH in 0-20 cm soil layer	-0.040	0.155	-0.044	0.049
pH in 20-40 cm soil layer	0.034	0.272	0.035	-0.272
Eigenvalue	22.918	2.256	22.760	2.209
Contribution rate (%)	88.146	8.677	87.538	8.496
Cumulative contribution rate (%)	88.146	96.823	87.538	96.034

no N application, ZN significantly decreased organic matter, total N, available P and available K except for available P and available K in 0-20 cm soil layer. Also, compared with FN, except for available P and available K in 0-20 cm and available K in Mengjin, the content of organic matter, total N, available P and available K in both 0-20 cm and 20-40 cm soil layer under RN were significantly decreased. These results indicated that ZN and RN went against the maintenance and/or improvement of soil fertility. Favorably, compared with FN, OSN could not only increase the content of organic matter, but also maintained or increased the content of total N, available P and available K in 0-20 cm and 20-40 soil layer. Additionally, available P and available K under ZN showed no significant decrease in 0-20 cm soil layer compared with initial value. This may be because the straw was fully returned to the field, which improved soil phosphorus availability and led to a great number of free potassium ions in straw entered the soil (Zhang et al., 2021; Zhang Y. et al., 2023). Besides, compared with RN, OSN decreased pH in both 0-20 cm and 20-40 cm soil layer. In organic

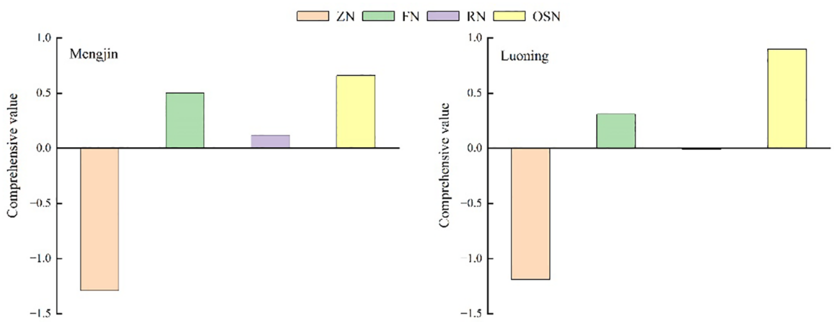

FIGURE 6
Comprehensive score of different fertilization treatment. ZN, FN, RN and OSN indicated no N application, farmer N application, 20% reduction of N fertilizer based on FN and organic fertilizer substituting 20% N of RN, respectively.

fertilizer, organic acids containing phenolic hydroxyl and carboxyl groups could butter soil acidity (Garcıía-Gil et al., 2004) and decrease soil pH (Zhang Q. R. et al., 2020), which created a favorable condition for root growth and increased yield (Shen et al., 2020; Zhao et al., 2023).

Nitrate-N residues present in the soil were susceptible to leaching, denitrification and emission if the level exceeds the safe threshold (Wen et al., 2016). Thus, soil nitrate-N residue in 0-100 cm soil layer is usually used to evaluate the sustainability of nutrient management practice (Yang et al., 2020). In this study, the nitrate-N residue under RN in the 0-100 cm soil layer reduced by 22.34 kg ha^{-1} averaged across the sites when compared with FN, indicating that nitrate-N residues could be decreased to a reasonable level by reducing the N rate. Similar results also reported in northern India (Lenka et al., 2013), where the nitrate-N residue in 0-120 cm soil layer could decrease by 62 kg ha^{-1} when the N application rate was reduced from 180 kg ha^{-1} to 120 kg ha^{-1}. Besides, the nitrate-N residue of OSN in the 0-100 cm soil layer was reduced by 5.11 kg ha^{-1} (8.61%) averaged cross the sites compared with RN, this was in line with the results of Zhang Q. R. et al., (2020). The significant improvement of soil physical and chemical properties and microbial activity, which led to effectively utilized soil nitrate-N by crop, maybe explained why less nitrate-N residue was left under OSN (Zhang Q. R. et al., 2020). In addition, in this study, RN and OSN showed the suitable nitrate-N residues, which were 59.36 kg ha^{-1} and 54.25 kg ha^{-1} across sites, respectively. This residue was around the safe threshold of 50 kg ha^{-1} reported by Zhou and Butterbach-Bahl (2014) and 55 kg ha^{-1} demonstrated by Huang et al. (2017), indicating that RN and OSN can achieve the aim of controlling soil nitrate-N residues in dryland areas.

4.5 Solutions to enhance the application of organic fertilizer substitution for wheat production in drought-prone areas

In China, agricultural land is dominated by 200-300 million smallholders (Yin et al., 2021), and around 1/3 of wheat production emanates from China's rain-fed drought-prone areas (Wu et al., 2023b). However, only a small number of farmlands have been applied organic fertilizer in these areas, so it is necessary to optimize the policy measures to enhance organic fertilizer substitution in wheat production (Case et al., 2017; Li et al., 2021). If subsidies are provided according to organic fertilizer application rather than the wheat planting area, it will improve the enthusiasm of smallholders to apply this suitable fertilizer management practice (Li T. Y. et al., 2020). Furthermore, enhancing experiments, demonstrations, and training on the substitution of chemical fertilizers with organic alternatives in major wheat-producing regions will also support farmers in adopting this technique. This represents a crucial aspect of our continued efforts in the coming years.

5 Conclusion

The results of the present 4-year and 2-site experiment showed that compared with FN and RN, OSN increased grain yield by 17.12% and 15.03%, grain protein yield by 3.31% and 17.15%, grain N accumulation by 17.78% and 15.58%, N harvest index by 2.63% and 4.45% averaged across years and sites, respectively. Besides, OSN significantly increased N use efficiency, as well as soil fertility in both 0-20 cm and 20-40 cm soil layer, while decreased nitrate-N residue in 0-100 cm soil layer by 33.59% and 8.61%, and decreased N apparent surplus by 34.48% and 100.09% compared with FN and RN, respectively. In conclusion, our study revealed that OSN increased grain yield, protein yield and N use efficiency via optimizing wheat N characteristics and soil fertility, and reduced nitrate-N residue and N apparent surplus, thus OSN could be adopted as the suitable fertilization practice to improve grain yield and quality and maintain sustainable agricultural production in rain-fed drought-prone areas.

Data availability statement

The original contributions presented in the study are included in the article/supplementary material. Further inquiries can be directed to the corresponding authors.

Author contributions

JZ: Writing – original draft, Writing – review & editing, Conceptualization, Data curation, Formal analysis. SL: Data curation, Formal analysis, Writing – original draft. PJ: Investigation, Writing – original draft, Validation. RW: Writing – original draft, Investigation, Validation. JG: Writing – original draft, Investigation, Validation. HX: Validation, Investigation, Writing – original draft. JW: Project administration, Resources, Writing – review & editing. YL: Writing – review & editing, Funding acquisition, Project administration, Supervision. MS: Writing – review & editing, Validation. MH: Funding acquisition, Project administration, Supervision, Writing – review & editing, Resources.

Funding

The author(s) declare financial support was received for the research, authorship, and/or publication of this article. This study was financially supported by National Key Research and Development Program of China (under Grant No. 2022YFD2300800), the Science and Technology Research Project of Henan, China (under Grant No. 222102110087; 232102111009).

Conflict of interest

The authors declare that the research was conducted in the absence of any commercial or financial relationships that could be construed as a potential conflict of interest.

Publisher's note

All claims expressed in this article are solely those of the authors and do not necessarily represent those of their affiliated organizations, or those of the publisher, the editors and the reviewers. Any product that may be evaluated in this article, or claim that may be made by its manufacturer, is not guaranteed or endorsed by the publisher.

References

Abbasi, M. K., and Tahir, M. M. (2012). Economizing nitrogen fertilizer in wheat through combinations with organic manures in Kashmir, Pakistan. *Agron. J.* 104, 169–177. doi: 10.2134/agronj2011.0264

Abd-Elrahman, S. H., Saudy, H. S., El–Fattah, D. A. A., and Hashem, F. A. E. (2022). Effect of irrigation water and organic fertilizer on reducing nitrate accumulation and boosting lettuce productivity. *J. Soil Sci. Plant Nutt.* 22, 2144–2155. doi: 10.1007/s42729-022-00799-8

Bappa, D., Chakraborty, D., Singh, V. K., Aggarwal, P., Singh, R., Dwivedi, B. S., et al. (2014). Effect of integrated nutrient management practice on soil aggregate properties, its stability and aggregate-associated carbon content in an intensive rice–wheat system. *Soil Till. Res.* 136, 9–18. doi: 10.1016/j.still.2013.09.009

Bom, F., Nunes, I., Raymond, N. S., Hansen, V., Bonnichsen, L., Magid, J., et al. (2018). Long-term fertilisation form, level and duration affect the diversity, structure and functioning of soil microbial communities in the field. *Soil Biol. Biochem.* 122, 91–103. doi: 10.1016/j.soilbio.2018.04.003

Cao, Y. G., Xu, L. L., Chai, Q., Hu, F. L., Yin, W., Fan, Z. L., et al. (2023). Water use characteristics of wheat rotated after no tillage plastic film mulching maize with reduced water and nitrogen. *Sci. Agric. Sin.* 56, 2660–2672. doi: 10.3864/j.issn.0578-1752.2023.14.003

Case, S. D. C., Oelofse, M., Hou, Y., Oenema, O., and Jensen, L. S. (2017). Farmer perceptions and use of organic waste products as fertilisers–A survey study of potential benefits and barriers. *Agr. Syst.* 151, 84–95. doi: 10.1016/j.agsy.2016.11.012

Chen, Y. L., Li, X., Liu, J. T., Yuan, M. Z., Liu, S. T., Jiang, W., et al. (2017). Changes in bacterial community of soil induced by long-term straw returning. *Sci. Agr.* 74, 349–356. doi: 10.1590/1678-992X-2016-0025

Dai, J., Wang, Z. H., Li, F. C., He, G., Wang, S., Li, Q., et al. (2015). Optimizing nitrogen input by balancing winter wheat yield and residual nitrate-N in soil in a long-term dryland field experiment in the Loess Plateau of China. *Field Crop Res.* 181, 32–41. doi: 10.1016/j.fcr.2015.06.014

Dobermann, A. R. (2005). *Nitrogen use efficiency-state of the art* (Lincoln, USA: Agronomy-Faculty Publications), 316.

Garcıía-Gil, J. C., Ceppi, S. B., Velasco, M. I., Polo, A., and Senesi, N. (2004). Long-term effects of amendment with municipal solid waste compost on the elemental and acidic functional group composition and pH-buffer capacity of soil humic acids. *Geoderma* 121, 135–142. doi: 10.1016/j.geoderma.2003.11.004

Ghimire, D., Das, S., Mueller, N. D., Creech, C. F., Santra, D., Baenziger, P. S., et al. (2021). Effects of cultivars and nitrogen management on wheat grain yield and protein. *Agron. J.* 113, 4348–4368. doi: 10.1002/agj2.20836

Han, Y., Lv, F. L., Lin, X. D., Zhang, C. Y., Sun, B. H., Yang, X. Y., et al. (2022). Crop yield and nutrient efficiency under organic manure substitution fertilizer in a double cropping system: A 6-year field experiment on an anthrosol. *Agronomy* 12, 2047. doi: 10.3390/agronomy12092047

He, H., Peng, M. W., Lu, W. D., Hou, Z. N., and Li, J. H. (2022). Commercial organic fertilizer substitution increases wheat yield by improving soil quality. *Sci. Total. Environ.* 851, 158132. doi: 10.1016/j.scitotenv.2022.158132

Huang, M., Wang, Z. H., Luo, L. C., Wang, S., Hui, X. L., He, G., et al. (2017). Soil testing at maturity to enhance productivity and reduce nitrate residues in dryland wheat production. *Field Crop Res.* 212, 153–164. doi: 10.1016/j.fcr.2017.07.011

Huang, M., Wu, J. Z., Li, Y. J., Fu, G. Z., Zhao, K. N., Zhang, Z. W., et al. (2021). Effects of tillage practices and nitrogen fertilizer application rates on grain yield, protein content in winter wheat and soil nitrate residue in dryland. *Acta Agron. Sin.* 54, 5206–5219. doi: 10.3864/j.issn.0578-1752.2021.24.004

Jones, D. L., Clode, P. L., Kilburn, M. R., Stockdale, E. A., and Murphy, D. V. (2013). Competition between plant and bacterial cells at the microscale regulates the dynamics of nitrogen acquisition in wheat (*Triticum aestivum*). *New Phytol.* 200, 796–807. doi: 10.1111/nph.12405

Ju, X. T., and Zhang, C. (2021). The principles and indicators of rational N fertilization. *Acta Pedol. Sin.* 58, 1–13. doi: 10.11766/trxb202006220322

Lenka, S., Singh, A. K., and Lenka, N. K. (2013). Soil water and nitrogen interaction effect on residual soil nitrate and crop nitrogen recovery under maize–wheat cropping system in the semi-arid region of northern India. *Agr. Ecosyst. Environ.* 179, 108–115. doi: 10.1016/j.agee.2013.08.001

Li, J. J., Ma, H. Y., Ma, H. L., Lei, F., He, D. H., Huang, X. L., et al. (2023). Comprehensive effects of N reduction combined with biostimulants on N use efficiency and yield of the winter wheat–summer maize rotation system. *Agronomy* 13, 2319. doi: 10.3390/agronomy13092319

Li, T. Y., Zhang, W. F., Cao, H., Ying, H. B., Zhang, Q. S., Ren, S. Y., et al. (2020). Region-specific nitrogen management indexes for sustainable cereal production in China. *Environ. Res. Commun.* 2, 075002. doi: 10.1088/2515-7620/aba12d

Li, W. X., Huang, K., Chai, T. H., Li, Y. P., Shi, X. J., Tang, L., et al. (2023). Effects of replacing chemical fertilizers with bio-organic fertilizers on wheat yield and quality and soil quality. *J. Hebei. Agric. Sci.* 27, 60–65. doi: 10.12148/hbnykx.20230011

Li, Y. B., Li, J., Li, S., and Tian, X. (2015). Effects of reducing nitrogen application on crops yields, nutrients uptake and utilization with straw incorporation. *Agric. Res. Arid. Areas.* 33, 79–84,152. doi: 10.16302/j.cnki.1000-7601.2015.01.013

Li, Y. H., Wu, X. P., He, G., and Wang, Z. H. (2020). Benefits of yield, environment and economy from substituting fertilizer by manure for wheat production of China. *Sci. Agric. Sin.* 53, 4879–4890. doi: 10.3864/j.issn.0578-1752.2020.23.013

Li, Y., Wei, J. L., Ma, L., Wu, X. B., Zheng, F. L., Cui, R. Z., et al. (2024). Enhancing wheat yield through microbial organic fertilizer substitution for partial chemical fertilization: regulation of nitrogen conversion and utilization. *J. Soil. Sci. Plant Nutt.* 24, 1–9. doi: 10.1007/s42729-023-01597-6

Li, Z. D., Jiao, Y. Q., Yin, J., Li, D., Wang, B. B., Zhang, K. L., et al. (2021). Productivity and quality of banana in response to chemical fertilizer reduction with bio-organic fertilizer: Insight into soil properties and microbial ecology. *Agr. Ecosys. Environ.* 322, 107659. doi: 10.1016/j.agee.2021.107659

Liu, H. W., Du, X. F., Li, Y. B., Han, X., Li, B., Zhang, X. K., et al. (2022). Organic substitutions improve soil quality and maize yield through increasing soil microbial diversity. *J. Clean. Prod.* 347, 131323. doi: 10.1016/j.jclepro.2022.131323

Liu, W. X., Ma, G., Wang, C. Y., Wang, J. R., Lu, H. F., Li, S. S., et al. (2018). Irrigation and nitrogen regimes promote the use of soil water and nitrate nitrogen from deep soil layers by regulating root growth in wheat. *Front. Plant Sci.* 9. doi: 10.3389/fpls.2018.00032

Liu, J. A., Shu, A. P., Song, W. F., Shi, W. C., Li, M. C., Zhang, W. X., et al. (2021). Long-term organic fertilizer substitution increases rice yield by improving soil properties and regulating soil bacteria. *Geoderma* 404, 115287. doi: 10.1016/j.geoderma.2021.115287

Liu, H. Y., Zhang, A. P., Yang, S. Q., Xing, L., and Yang, Z. L. (2019). Construction and evaluation of a soil nitrogen surplus index system for the wheat maize rotation system in Shandong Province, China: A case study of Dezhou City. *J. Agro-Environ. Sci.* 38, 1321–1329. doi: 10.11654/jaes.2018-1158

Liu, P. Z., Zhou, D., Guo, X. Y., Yu, Q., Zhang, Y. H., Li, H. Y., et al. (2021). Response of water use and yield of dryland winter wheat to nitrogen application under different rainfall patterns. *Sci. Agric. Sin.* 54, 3065–3076. doi: 10.3864/j.issn.0578-1752.2021.14.012

Lu, J. S., Ma, L. H., Hu, T. T., Geng, C. M., and Yan, S. C. (2022). Deficit drip irrigation based on crop evapotranspiration and precipitation forecast improves water-use efficiency and grain yield of summer maize. *J. Sci. Food Agr.* 102, 653–663. doi: 10.1002/jsfa.11394

Luo, W. H., Shi, Z. J., Wang, X. M., Li, J., and Wang, R. (2020). Effects of water saving and nitrogen reduction on soil nitrate nitrogen distribution, water and nitrogen use efficiencies of winter wheat. *Acta Agron. Sin.* 46, 924–936. doi: 10.3724/SP.J.1006.2020.91060

Lv, M., Huang, M., Zhao, K. N., Gu, X. X., Li, S. Q., Wang, J. T., et al. (2023). Effects of partial substitution of organic fertilizer for synthetic n fertilizer on yield and N use efficiencies in a semiarid winter wheat-summer maize rotation. *Agronomy* 13, 2281. doi: 10.3390/agronomy13092281

Makino, A. (2011). Photosynthesis, grain yield, and nitrogen utilization in rice and wheat. *Plant Physiol.* 155, 125–129. doi: 10.1104/pp.110.165076

McLellan, E. L., Cassman, K. G., Eagle, A. J., Woodbury, P. B., Sela, S., Tonitto, C., et al. (2018). The nitrogen balancing act: tracking the environmental performance of food production. *BioScience* 68, 194–203. doi: 10.1093/biosci/bix164

Nadeem, M. Y., Zhang, J., Zhou, Y., Ahmad, S., Ding, Y., and Li, G. (2022). Quantifying the impact of reduced nitrogen rates on grain yield and nitrogen use efficiency in the wheat and rice rotation system of the Yangtze river region. *Agronomy* 12, 920. doi: 10.3390/agronomy12040920

National Bureau of Statistics (2020). *China Statistical Yearbook* (Beijing, China: China Statistics Press).

Pan, Y. H., Guo, J. J., Fan, L. Y., Ji, Y., Liu, Z., Wang, F., et al. (2022). The source–sink balance during the grain filling period facilitates rice production under organic fertilizer substitution. *Eur. J. Agron.* 134, 126468. doi: 10.1016/j.eja.2022.126468

Pei, X. X., Dang, J. Y., Zhang, D. Y., Zhang, J., and Cheng, M. F. (2020). Effects of organic substitution on the yield and nutrient absorption and utilization of wheat under chemical fertilizer reduction. *Plant Nutr. Fert. Sci.* 26, 1768–1781. doi: 10.11674/zwyf.20197

Peng, Z. P., Liu, Y. N., Li, Y. C., Abawi, Y., Wang, Y. Q., Men, M. X., et al. (2017). Responses of nitrogen utilization and apparent nitrogen loss to different control measures in the wheat and maize rotation system. *Front. Plant Sci.* 8. doi: 10.3389/fpls.2017.00160

Ren, X., Chen, X., and Jia, Z. (2010). Effect of rainfall collecting with ridge and furrow on soil moisture and root growth of corn in semiarid northwest China. *J. Agron. Crop Sci.* 196, 109–122. doi: 10.1111/j.1439-037X.2009.00401

Ren, K. Y., Sun, Y., Zou, H. Q., Li, D. J., Lu, C. G., Duan, Y. H., et al. (2023). Effect of replacing synthetic nitrogen fertilizer with animal manure on grain yield and nitrogen use efficiency in China: a meta-analysis. *Front. Plant Sci.* 14. doi: 10.3389/fpls.2023.1153235

Saikia, P., Bhattacharya, S. S., and Baruah, K. K. (2015). Organic substitution in fertilizer schedule: Impacts on soil health, photosynthetic efficiency, yield and assimilation in wheat grown in alluvial soil. *Agr. Ecosyst. Environ.* 203, 102–109. doi: 10.1016/j.agee.2015.02.003

Sapkota, T. B., and Takele, R. (2023). Improving nitrogen use efficiency and reducing nitrogen surplus through best fertilizer nitrogen management in cereal production: The case of India and China. *Adv. Agron.* 178, 233–294. doi: 10.1016/bs.agron.2022.11.006

Saudy, H. S., Hamed, M. F., Abd El-Momen, W. R., and Hussein, H. (2020). Nitrogen use rationalization and boosting wheat productivity by applying packages of humic, amino acids, and microorganisms. *Commun. Soil Sci. Plan.* 51, 1036–1047. doi: 10.1080/00103624.2020.1744631

Shen, C. W., Yuan, J. P., Li, X. H., Zhang., S. L., Ren, X. J., Wang, F., et al. (2020). Improving winter wheat N utilization efficiency and soil fertility through replacement of chemical N by 20% organic manure. *Plant Nutr. Fert. Sci.* 26, 1395–1406. doi: 10.11674/zwyf.19504

Shi, Z., and Yang, Z. (2023). Influence of social captical on farmers' willingness and behavior to apply organic fertilizer: Analysis of mediation effect based on information availability. *J. China Agric. Univ.* 28, 279–294. doi: 10.11841/j.issn.1007-4333.2023.11.23

Tan, D. S., Jiang, L. H., Tan, S. Y., Zheng, F. L., Xu, Y., Cui, R. Z., et al. (2013). An in *situ* study of inorganic nitrogen flow under different fertilization treatments on a wheat–maize rotation system surrounding Nansi Lake, China. *Agr. Water. Manage.* 123, 45–54. doi: 10.1016/j.agwat.2013.03.011

Thomas, C. L., Acquah, G. E., Whitmore, A. P., McGrath, S. P., and Haefele, S. M. (2019). The effect of different organic fertilizers on yield and soil and crop nutrient concentrations. *Agronomy* 9, 776. doi: 10.3390/agronomy9120776

Tilman, D., Balzer, C., Hill, J., and Befort, B. L. (2011). Global food demand and the sustainable intensification of agriculture. *P. Natl. Acad. Sci.* 108, 20260–20264. doi: 10.1073/pnas.1116437108

Wang, L., Lu, P. P., Ren, T., Liu, T., Geilfus, C. M., and Lu, J. W. (2020). Improved nitrogen efficiency in winter oilseed rape hybrid compared with the parental lines under contrasting nitrogen supply. *Ind. Crop Prod.* 155, 112777. doi: 10.1016/j.indcrop.2020.112777

Wang, L., Ma, L., Li, Y., Geilfus, C. M., Wei, J. L., Zheng, F. L., et al. (2023). Managing nitrogen for sustainable crop production with reduced hydrological nitrogen losses under a winter wheat–summer maize rotation system: an eight-season field study. *Front. Plant Sci.* 14, 1274943. doi: 10.3389/fpls.2023.1274943

Wang, J. B., Xie, J. H., Li, L. L., Luo, Z. Z., Zhang, R. Z., Wang, L. L., et al. (2021). The impact of fertilizer amendments on soil autotrophic bacteria and carbon emissions in maize field on the semiarid Loess Plateau. *Front. Microbiol.* 12. doi: 10.3389/fmicb.2021.664120

Wen, Z., H., W., Jianbo, S. H. E. N., Blackwell, M., Haigang, L. I., Bingqiang, Z. H. A. O., et al. (2016). Combined applications of nitrogen and phosphorus fertilizers with manure increase maize yield and nutrient uptake via stimulating root growth in a long-term experiment. *Pedosphere* 26, 62–73. doi: 10.1016/S1002-0160(15)60023-6

Wu, J. Z., Li, S. J., Li, G. Q., Huang, M., Fu, G. Z., Li, Y. J., et al. (2023b). Effects of irrigation and topdressing nitrogen at jointing stage on grain yield and quality of furrow-seeding wheat in dryland. *Acta Agric. Boreali-Sin.* 38, 100–107. doi: 10.7668/hbnxb.20193771

Wu, J. Z., Xiao, H. S., Guo, J. H., Huang, M., Zhao, K. M., Hou, Y. Q., et al. (2023a). Effects of straw returning combined with organic fertilizer replacing 1/3 chemical fertilizer on grain yield, grain protein and chemical fertilizer use efficiency in dryland maize-wheat double cropping system. *J. Soil Water Conserv.* 37, 319–326. doi: 10.13870/j.cnki.stbcxb.2023.04.039

Xia, L. L., Lam, S. K., Chen, D. L., Wang, J. Y., Tang, Q., and Yan, X. Y. (2017). Can knowledge-based N management produce more staple grain with lower greenhouse gas emission and reactive nitrogen pollution? A meta-analysis. *Global Change Biol.* 23, 1917–1925. doi: 10.1111/gcb.13455

Xu, X. P., He, P., Chuan, L. M., Liu, X. Y., Liu, Y. X., Zhang, J. J., et al. (2021). Regional distribution of wheat yield and chemical fertilizer requirements in China. *J. Integr. Agr.* 20, 2772–2780. doi: 10.1016/S2095-3119(20)63338-X

Yang, Y. J., Lei, T., Du, W., Liang, C. L., Li, H. D., and Lv, J. L. (2020). Substituting chemical fertilizer nitrogen with organic manure and comparing their nitrogen use efficiency and winter wheat yield. *J. Agr. Sci.* 158, 262–268. doi: 10.1017/s0021859620000544

Yang, X. D., Ni, K., Shi, Y. Z., Yi, X. Y., Zhang, Q. F., Fang, L., et al. (2018). Effects of long-term nitrogen application on soil acidification and solution chemistry of a tea plantation in China. *Agr. Ecosyst. Environ.* 252, 74–82. doi: 10.1016/j.agee.2017.10.004

Yang, M., Zhu, X. Q., Bai, Y., Sun, D., Zou, H. T., Fang, Y. T., et al. (2021). Coated controlled-release urea creates a win-win scenario for producing more staple grains and resolving N loss dilemma worldwide. *J. Clean. Prod.* 288, 125660. doi: 10.1016/j.jclepro.2020.125660

Yin, Y., Zhao, R., Yang, Y., Meng, Q., Ying, H., Cassman, K. G., et al. (2021). A steady-state N balance approach for sustainable smallholder farming. *P. Natl. A. Sci.* 118, 2106576118. doi: 10.1073/pnas.2106576118

Yu, H. L., Kan, M. X., Xu, Z. L., Ma., R. Q., Liu, A. K., Wang, D. M., et al. (2023). Yield and dry matter accumulation of wheat in response to spring irrigation water in uniform sowing and strip sowing. *Acta Agron. Sin.* 49, 2833–2844. doi: 10.3724/SP.J.1006.2023.21069

Yue, S. C., Meng, Q. F., Zhao, R. F., Ye, Y. L., Zhang, F. S., and Cui, Z. L. (2012). Change in nitrogen requirement with increasing grain yield for winter wheat. *Agronomy-Basel* 104, 1687–1693. doi: 10.2134/agronj2012.0232

Zhang, X., Davidson, E. A., Mauzerall, D. L., Searchinger, T. D., Dumas, P., and Shen, Y. (2015). Managing nitrogen for sustainable development. *Nature* 528, 51–59. doi: 10.1038/nature15743

Zhang, S. M., Duan, Z. Q., Gu, K. J., Zhang, C. H., and Zhang, H. G. (2023). Effects of reduced nitrogen fertilization on wheat yield, nutrient uptake and soil physicochemical properties under rice straw returning. *Soils* 55, 537–543. doi: 10.13758/j.cnki.tr.2023.03.010

Zhang, Y., Gao, Y., Zhang, Y., Huang, D. D., Chen, X. W., Zhang, S. X., et al. (2023). Effects of residue return on stoichiometric characteristics of soil carbon, nitrogen, phosphorus, potassium, and the maize yield in black soil of Northeast China. *Plant Nutr. Fert. Sci.* 29, 31–44. doi: 10.11674/zwyf.2022234

Zhang, Z. Y., Liu, D. B., Wu, M. Q., Xia, Y., Zhang, F. L., and Fan, X. P. (2021). Long-term straw returning improve soil K balance and potassium supplying ability under rice and wheat cultivation. *Sci. Rep.* 11, 22260. doi: 10.1038/s4159-021-01594-8

Zhang, X. Q., Sun, H. F., Wang, C., Zhang, J. N., and Zhou, S. (2023). Optimizing fertilizer management mitigated net greenhouse gas emissions in a paddy rice-upland wheat rotation system: A ten-year in *situ* observation of the Yangtze River Delta, China. *Agr. Ecosyst. Environ.* 356, 108640. doi: 10.1016/j.agee.2023.108640

Zhang, Y. L., Wang, R., Wang, H., Wang, S. L., Wang, X. L., and Li, J. (2019). Soil water use and crop yield increase under different long-term fertilization practices incorporated with two-year tillage rotations. *Agr. Water. Manage.* 221, 362–370. doi: 10.1016/j.agwat.2019.04.018

Zhang, Q. R., Xie, Y. H., Liu, T. L., Liu, K., Jiang, L. W., Cao, J., et al. (2020). Effects of organic fertilizers replacing chemical fertilizers on yield, nutrient use efficiency, economic and environmental benefits of dryland wheat. *Sci. Agric. Sin.* 53, 4866–4878. doi: 10.3864/j.issn.0578-1752.2020.23.012

Zhang, Z., Zhang, Y. L., Shi, Y., and Yu, Z. W. (2020). Optimized split nitrogen fertilizer increase photosynthesis, grain yield, nitrogen use efficiency and water use efficiency under water-saving irrigation. *Sci. Rep.* 10, 20310. doi: 10.1038/s41598-020-75388-9

Zhao, K. N., Wu, J. Z., Li, J. J., Tian, W. Z., Zhang, J., Li, F., et al. (2023). Effects of combined straw and organic fertilizer application as partial replacement for chemical fertilization on water use efficiency and soil nitrate residue. *Plant Nutr. Fert. Sci.* 28, 1770–1781. doi: 10.11674/zwyf.2022051

Zhong, Y. X., Wang, W. L., Huang, X., Liu, M. M., Hebelstrup, K. H., Yang, D. L., et al. (2019). Nitrogen topdressing timing modifies the gluten quality and grain hardness related protein levels as revealed by iTRAQ. *Food Chem.* 277, 135–144. doi: 10.1016/j.foodchem.2018.10.071

Zhou, M. H., and Butterbach-Bahl, K. (2014). Assessment of nitrate leaching loss on a yield-scaled basis from maize and wheat cropping systems. *Plant Soil* 374, 977–991. doi: 10.1007/s11104-013-1876-9

Zhou, J. Y., Gu, B. J., Schlesinger, W. H., and Ju, X. T. (2016). Significant accumulation of nitrate in Chinese semi-humid croplands. *Sci. Rep.* 6, 25088. doi: 10.1038/srep25088

Zhou, B. W., Serret, M. D., Elazab, A., Bort Pie, J., Araus, J. L., Aranjuelo, I., et al. (2016). Wheat ear carbon assimilation and nitrogen remobilization contribute significantly to grain yield. *J. Integr. Plant Biol.* 58, 914–926. doi: 10.1111/jipb.12478

frontiers | Frontiers in Plant Science

TYPE Original Research
PUBLISHED 29 April 2024
DOI 10.3389/fpls.2024.1354384

OPEN ACCESS

EDITED BY
Henry Yabbey Sintim,
The University of Georgia, Tifton,
United States

REVIEWED BY
Depeng Wang,
Linyi University, China
Xinpeng Xu,
Institute of Agricultural Resources and
Regional Planning (CAAS), China
Solomon Amissah,
University of Florida, United States

*CORRESPONDENCE
Yixiang Sun
sunyixiang@aaas.org.cn

RECEIVED 12 December 2023
ACCEPTED 03 April 2024
PUBLISHED 29 April 2024

CITATION
Yuan M, Wu G, Wang J, Liu C, Hu Y, Hu R, Zhou Y, Zhang X, Wang W and Sun Y (2024) Blended controlled-release nitrogen fertilizer increases rice post-anthesis nitrogen accumulation, translocation and nitrogen-use efficiency.
Front. Plant Sci. 15:1354384.
doi: 10.3389/fpls.2024.1354384

Blended controlled-release nitrogen fertilizer increases rice post-anthesis nitrogen accumulation, translocation and nitrogen-use efficiency

Manman Yuan[1], Gang Wu[1], Jiabao Wang[1], Chuang Liu[1], Yegong Hu[2], Run Hu[3], Yan Zhou[4], Xiangming Zhang[1], Wenjun Wang[1] and Yixiang Sun[1*]

[1]Key Laboratory of Nutrient Cycling, Resources and Environment of Anhui, Institute of Soil and Fertilizer, Anhui Academy of Agricultural Sciences, Hefei, China, [2]Agricultural Technology Promotion Center of Mingguang, Chuzhou, China, [3]Chizhou Academy of Agricultural Science, Chizhou, China, [4]Chaohu Agricultural Technology Promotion Center, Hefei, China

One-time application of blended controlled-release nitrogen fertilizer (CRN) has the potential to solve the difficulty of top-dressing fertilizer in the cultivation of rice and reduce the cost of CRN fertilizer application. However, its effects on rice dry matter and nitrogen (N) accumulation and translocation, yield and N-use efficiency (NUE) remain uncertain. Field experiments were carried out at three sites (Mingguang, Chaohu, and Guichi) in the Yangtze River Delta in China to compare the effects of the conventional split applications of urea and the blended CRN and on post-anthesis dry matter and N accumulation and translocation, yield, and NUE in rice at 0, 60, 120, 180, and 240 kg N ha^{-1}. The results showed that at the equal N application rates, compared under the conventional N fertilizer treatment, the blended CRN application significantly increased the rice yield by an average of 0.9-6.9%, mainly due to increase the number of spikelets per panicle. The highest yield achieved with blended CRN treatment occurred at 200 kg N ha^{-1}, with an NUE of 45.9%. Moreover, in comparison to the conventional N fertilizer, the blended CRN treatment increased pre-anthesis N translocation (Pre-NT) by 1.0-19.8%, and the contribution of pre-NT to grain N by 0.2-8.7%, and NUE by 3.2-28.4%. Meanwhile, the blended CRN treatment reduced labor costs by 1800 Yuan ha^{-1} and enhanced the economic gains by 21.5-68.8%. Therefore, one-time application of blended CRN $\leq$ 200 kg N ha^{-1} application rate improved rice yield, NUE, and economic profit compared to equivalent rates of split applied conventional N fertilizers.

KEYWORDS

economic return, yield, nitrogen translocation, post-anthesis nitrogen uptake, urea N type

1 Introduction

Rice is one of the most important food crops in the world, with approximately 50% of the world's population and more than 60% of China's population consuming rice as their staple food (Yamaji et al., 2017; Zhang et al., 2018a). It is estimated that by 2030, China will increase rice production by 20% to meet the needs of population growth (Zhang et al., 2018a). Nitrogen (N) is one of the essential nutrients for rice growth. Growers often achieve high rice yields by increasing the application of N fertilizers. China is the largest N fertilizer user in the world, consuming more than 30% of the world's N fertilizer (IFA, 2021). The Yangtze River Delta is one of the main rice production areas in China. The application rate of N fertilizer under farmers' conventional practice in the whole rice season is often above 300 kg N ha^{-1}. It is reported that the average rice N-use efficiency (NUE) is only 39% (Yu and Shi, 2015), which is 33.3-42.9% lower than that of the United States of America and Europe (Lassaletta et al., 2014; Yu et al., 2022). Excessive application of N fertilizer not only increases the production cost of rice, but also reduces NUE, and causes environmental problems such as soil acidification and water eutrophication (Congreves et al., 2021; Yuan et al., 2023).

Controlled-release nitrogen fertilizers (CRNs) have longer residence time in soil and are to synchronize N release with plant demand compared to conventional fertilizers. The CRNs applied at one-time can reduce 2-3 times of topdressing in rice cultivation, improve NUE, and reduce N runoff and leaching, and ammonia volatilization (Chen et al., 2020; Guo et al., 2019; Zhang et al., 2018a). The CRNs at the same N rate are more effective than the split application of urea at increasing crop yield and NUE (Lyu et al., 2021). For example, Zheng et al. (2020) reported that the rice yield and NUE of CRN-applied treatments were increased by 12.2% and 33.9%, respectively, when compared with conventional urea fertilizer treatment. Therefore, the application of CRNs to achieve simultaneous improvement of rice yield and NUE have become an important research topic.

Although CRNs increase rice yield and NUE, their agronomic and physiological mechanisms are still unclear. The grain yield of rice mainly depends on the post-anthesis accumulation of photosynthetic products and the transport and distribution efficiency of photosynthetic assimilates. It is generally believed that more than 60% of the rice grain grouting material comes from post-anthesis photosynthetic assimilates (Kumar et al., 2006; Deng et al., 2015). Moreover, the accumulation and redistribution of N metabolism and assimilation and their products in the rice vegetative and regenerating organs are also important factors affecting yield and even NUE (Cheng et al., 2010; Sun et al., 2012; Pal et al., 2017). The N uptake by rice from flowering to maturity is much lower than the total N accumulated in the grain at maturity (Mae and Ohira, 1981; Mae, 1997). About 68% of the N accumulated in vegetative organs, such as stems and leaves after flowering, are transported to the panicle for grain development (Pal et al., 2017). However, most of the above studies focused on the effect of urea on the accumulation and transport of photosynthates and N in rice (Kumar et al., 2006; Sun et al., 2012; Deng et al., 2015). The application rate, type and management of N fertilizer are known to affect rice photosynthate and N accumulation and translocation (Artacho et al., 2009; Wang et al., 2018). Therefore, it is necessary to fully understand the measure of application of CRNs and associated mechanisms to simultaneously improve rice yield and benefits.

Urea is currently the main fertilizer N source for rice. Therefore, the amount of CRNs or blended CRNs with urea applied is mainly determined by the amount of urea applied to rice (Wang et al., 2018; Lyu et al., 2021). We conducted a five-year field experiment to derive the application rate of blended CRNs for rice in the Chaohu watershed of the Yangtze River Delta in China (Yuan et al., 2023). The optimum N rate under the blended CRN treatment was determined to be 180-214 kg N ha^{-1} with one-time application, reducing the N rate by 32-64 kg N ha^{-1} compared with the conventional N fertilizer treatment. From an environmental perspective, it was elucidated that a significant reduction in ammonia volatilization in rice fields was the crucial cause for the increase in NUE under the blended CRN treatments (Yuan et al., 2023), but empirical evidence in rice agronomy and physiology is still lacking. Moreover, the data from one field site is insufficient to establish the optimal application rate of blended CRNs in the Yangtze River Delta (Yuan et al., 2023; Zhang et al., 2018b). Therefore, in this study, field experiments were conducted across three locations over two years to compare rice yield, NUE, pre-anthesis and post-anthesis biomass and N accumulation and translocation to grain yield between the blended CRN treatments and the conventional N fertilizer treatments. This study is expected to provide a physiological basis for the improvement of NUE and yield by the application of CRNs.

2 Materials and methods

2.1 Site description

Field experiments were carried out in the 2019 and 2020 rice seasons in Mingguang, Chaohu and Guichi counties in Anhui Province, located in the Yangtze River Delta, China, which belongs to the northern subtropical monsoon climate. The annual average temperature and precipitation are 15.2°C and 953 mm in Mingguang, 16.1°C and 1030 mm in Chaohu, and 16.1°C and 1400 mm in Guichi, respectively (Figures 1A, B). The physical and chemical properties of the topsoil (0-20 cm) in the experimental sites are shown in Table 1.

The CRNs (44.5% N) were purchased from Anhui Moith Agricultural Technology Co., Ltd. in China centered on a urea pellet coated with polyurethane. In this study, two N release periods of CRNs were used. Two CRNs with the N release periods of 40 and 90 days are abbreviated as CRN1 and CRN2, respectively. The N release characteristics of CRN1 and CRN2 in 25°C water and paddy fields for 42 and 100 days were measured in the 2019 (Yuan et al., 2023).

2.2 Experimental design

A split-plot design was used, with the main plot being the type of N fertilizer and its application method, and the subplot being N application rate. The numbers of main plot and subplot per

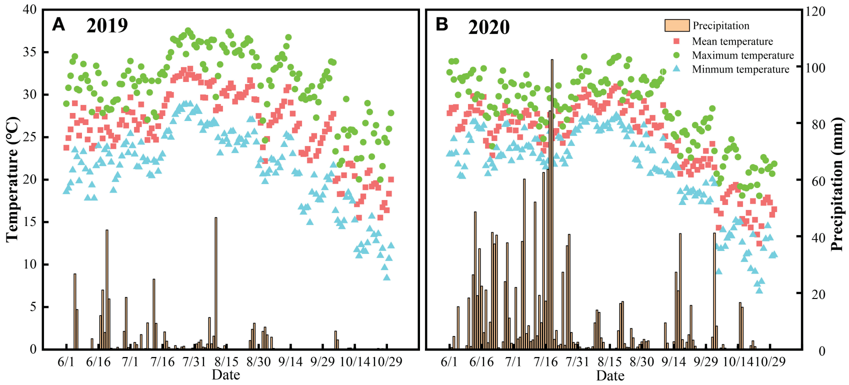

FIGURE 1
Temperature and precipitation in the rice season in 2019 **(A)** and 2020 **(B)**, respectively. The yellow bar chart represents daily precipitation, while the triangular, square, and circular point charts represent minimum, mean and maximum temperatures, respectively.

replicate were 2 and 5, respectively. The plot size was 5 m × 6 m. The main plot treatments were as follows: 1. blended CRN treatment: the conventional N fertilizer, CRN1 and CRN2 with a 4:3:3 ratio of the N rate applied at one-time, and 2. conventional N fertilizer treatment: the conventional N fertilizer applied at three times as basal, tillering and panicle fertilizer. The subplot treatments were N application rates at 0, 60, 120, 180, and 240 kg N ha^{-1}. The 0 rate was the same for both two main plot factors. Therefore, there were 9 treatments in the experiment. The amount and application method of N fertilizer in the different treatment are shown in Table 2. Triple superphosphate and potassium chloride were applied as basal fertilizers at a rate of 39 kg P ha^{-1} and 62 kg K ha^{-1}, respectively.

The rice variety and timing of the planting and management operations in this study are shown in Table 3. All rice varieties used in this study were high-yield super indica rice, which are commonly grown in the region. The spacing of transplanted rice was 0.30 m (length) by 0.13 m (width).

2.3 Sampling and measurements

At the anthesis and maturity, the number of tillers per unit area in each plot was measured. Based on the average number of tillers per hole, rice from three representative holes were selected for destructive sampling. The samples were divided into two parts: leaf and stem, and panicle. The panicle samples at maturity were used to determine the yield components, including the number of panicles (NP), the number of spikelets per panicle (NSP), seed-setting rate (SR), and 1000-grain weight (GW). Thereafter, the samples were dried at 105°C for 30 min and then dried continuously at 85°C for 48 h and weighed. The biomass weight was the sum of dry matter weight of shoots and panicles (Yuan et al., 2021). The dry matter samples were digested with H_2SO_4-H_2O_2. The N concentrations in the digests were determined by the Kjeldahl method (Bremner and Mulvaney, 1982).

At the final stage, the entire length of 20 rows of every plot was harvested manually to obtain the seed weight and moisture content. The rice grain yield was determined at 14% moisture content (Yang et al., 2006).

2.4 Calculation

The NUE was calculated according to the following equation (Sun et al., 2012):

$$\begin{aligned}\text{NUE}\,(\%) &= (\text{the whole N accumulation of rice under N} - \\ &\quad \text{application the whole Naccumulation of rice under} \\ &\quad \text{N0})/\text{N application rate} \times 100\end{aligned} \tag{1}$$

Based on the dry matter (DM) and N concentration, the accumulation and translocation parameters of DM and N after anthesis stage were calculated according to the following equations (Ntanos and Koutroubas, 2002; Jiang et al., 2004):

$$\begin{aligned}&\text{Pre}-\text{anthesis DM translocation (Pre}-\text{DMT, kg ha}^{-1}) = \\ &\quad \text{rice panicle and plant DM accumulation} \\ &\text{at anthesis stage}- \text{ rice plant DM accumulation at harvest}\end{aligned} \tag{2}$$

TABLE 1 Basic soil properties of three experimental sites before trial establishment.

Experimental site	Longitude	Latitude	pH	Total N (g kg^{-1})	Available P (mg kg^{-1})	Available K (mg kg^{-1})	Organic matter (g kg^{-1})
Mingguang	118°01′12″ E	32°58′40″ N	6.7	0.8	18.6	97.8	10.1
Chaohu	117°46′34″ E	31°39′14″ N	7.1	1.9	9.0	198.8	29.1
Guichi	117°19′21″ E	30°31′ 04″ N	5.6	1.7	6.1	83.2	15.4

TABLE 2 Experimental design and nitrogen fertilizer application measures.

Treatment	N application rate (kg N ha^{-1})	Type and ratio of N	N application rate in different growth stages (kg N ha^{-1})		
			Basal fertilizer	Tillering fertilizer	Panicle fertilizer
N0	0	—	—	—	—
N60	60	Urea 100%	30	18	12
N120	120	Urea 100%	60	36	24
N180	180	Urea 100%	90	54	36
N240	240	Urea 100%	120	72	48
CRN60	60	Urea: CRN1: CRN2 = 4: 3: 3	60	0	0
CRN120	120	Urea: CRN1: CRN2 = 4: 3: 3	120	0	0
CRN180	180	Urea: CRN1: CRN2 = 4: 3: 3	180	0	0
CRN240	240	Urea: CRN1: CRN2 = 4: 3: 3	240	0	0

The blended controlled-release nitrogen fertilizer (CRN) treatments are CRN60, CRN120, CRN180, CRN240. The conventional N fertilizer treatments are N60, N120, N180, N240.

$$\text{Pre} - \text{anthesis DM translocation efficiency (Pre} - \text{DMTE, \%)} = \text{Pre} - \text{DMT}/(\text{rice panicle and plant DM accumulation at anthesis stage}) \times 100 \tag{3}$$

$$\text{Post} - \text{anthesis DM accumulation (Post} - \text{DMA, kg ha}^{-1}) = \text{rice grain and plant DM accumulation at harvest} - \text{rice panicle and plant DM accumulation at anthesis stage} \tag{4}$$

$$\text{Contribution of pre} - \text{DMT or post} - \text{DMA to grain yield (DMC, \%)} = \text{Pre} - \text{DMT or Post} - \text{DMA/grain yield} \times 100 \tag{5}$$

$$\text{Pre} - \text{anthesis N translocation (Pre} - \text{NT, kg ha}^{-1}) = \text{rice panicle and plant N accumulation at heading stage} - \text{rice plant N accumulation at harvest} \tag{6}$$

$$\text{Pre} - \text{anthesis N translocation efficiency (Pre} - \text{NTE, \%)} = \text{Pre} - \text{NT}/(\text{rice panicle and plant N accumulation at anthesis stage}) \times 100 \tag{7}$$

$$\text{Post} - \text{anthesis N uptake (Post} - \text{NU, kg ha}^{-1}) = \text{rice grain and plant N accumulation at harvest} - \text{rice panicle and plant N accumulation at anthesis stage} \tag{8}$$

$$\text{Contribution of pre} - \text{NT or post} - \text{NU to grain N (NC, \%)} = \text{Pre} - \text{NT or Post} - \text{NU/rice grain N accumulation at harvest} \times 100 \tag{9}$$

Economic benefit calculation: the output value was calculated according to the average yield and the average price of rice sold in the 2019 and 2020 (2.5 Yuan kg^{-1}). The labor cost of rice fertilization was 900 Yuan ha^{-1} each time. The fertilizer cost was calculated according to the prices and amount of fertilizer. The average prices of urea, CRN, potassium and phosphorus fertilizer were 2.0, 2.8, 2.0 and 0.6 Yuan kg^{-1} in 2019 and 2020, respectively. The other rice production costs included seed cost, irrigation cost, and disease, pest and weed management costs, etc, which were the same under all the treatments for two years. Moreover, this study mainly focused on the impact of costs associated with the type and application method of N fertilizer on the economic benefits of rice. Therefore, the net economic benefit this study was a partial net economic benefit due to the fact that the other rice production costs was not calculated.

The net economic benefit was calculated according to the following equation:

$$\text{Net economic benefit} = \text{Output value} - \text{Labor cost} - \text{fertilizer cost} \tag{10}$$

2.5 Statistical analyses

Rice yield, NUE, and the accumulation and translocation parameters of dry matter and N after the anthesis stage were analyzed as split-plot analyses of variance (Equation 1), where the type and application method of N fertilizer were assigned as the main plot factor, and the N application rate as the sub-plot factor. The analyses were performed separately for each site and location, and differences in treatment means were assessed using the least significant difference test. Also, the relationships between parameters were analyzed by using the Pearson correlation method. The analyses were conducted with the SPSS 20.0 software (SPSS 22.0, IBM Corp., Armonk, NY, USA), and all analyses were reported as significant at $P \leq 0.05$. The figures were created using the Origin 2022 software (OriginLab Corp., Northampton, MA, USA).

3 Result

3.1 Yield

Compared to the conventional N fertilizer at the equal N application rate, the blended CRN treatments increased the grain

10.3389/fpls.2024.1354384

TABLE 3 Rice varieties and planting times (month/day) of sowing, transplanting and management operations at three experiment sites.

Experimental site	Year	Rice variety	Sowing	Transplanting	Basal fertilization	Tillering topdressing	Heading topdressing	Anthesis	Harvest
Mingguang	2019	Jingliangyou huazhan	5/3	6/5	6/5	6/12	7/11	7/28	9/17
	2020	Jingliangyou huazhan	5/2	6/2	6/2	6/9	7/8	7/25	9/13
Chaohu	2019	Chaoyou 1000	5/25	6/29	6/29	7/6	8/2	8/20	10/8
	2020	Chaoyou 1000	5/20	6/22	6/22	6/30	7/29	8/17	10/10
Guichi	2019	Jingliangyou huazhan	5/18	6/18	6/18	6/26	7/25	8/12	9/30
	2020	Jingliangyou huazhan	5/19	6/21	6/21	6/29	7/27	8/15	10/4

yield by an average of 0.9 - 6.7% at the three experiment sites across the two years (Figures 2A-F, $P< 0.05$). The rice yield increased significantly with the increase of N application rate (Figures 2A-F, $P< 0.01$) with no significant interaction of N type × rate (Figures 2A-F). The rice yield in 2020 was, on average, 18.3% lower than that in 2019. The N type had consistent effects on rice yields at the three experiment sites across the two years (Figures 2A-F).

The relationship between rice yield and N fertilizer rate can be simulated by a quadratic equation (Figures 2A-F). Under the blended CRN treatments, the highest average yield was 9604 kg ha^{-1} at 200 kg N ha^{-1} (Figures 2A-F). Compared with the conventional N fertilizer treatments, the maximum yield of the blended CRN treatments increased by 109-309 kg ha^{-1}, with an average increase of 1.6%, and the corresponding N application rate decreasing by 10-32 kg ha^{-1}, with an average decrease of 14.7% (Figures 2A-F).

3.2 Yield components

Compared with the conventional N fertilizer, the blended CRN application significantly increased the number of spikelets per panicle and seed-setting rate by averages of 1.6% and 2.0%, respectively. In contrast, the blended CRN application decreased the number of panicles by 2.0% (Table 4, $P< 0.05$). Increasing N application rate significantly increased these two parameters (Table 4, $P< 0.01$). The N type had consistent effects on rice components across the three experiment sites and two years (Table 4).

3.3 Nitrogen-use efficiency

With the equal N application rate, NUE was significantly higher under the blended CNR than the conventional N fertilizer treatments (Figures 3A-F, $P< 0.05$). The increases were 5.0-16.2%, 3.2-28.4%, 10.4-21.8%, and 4.7-18.7% at 60, 120, 180 and 240 kg N ha^{-1}, respectively. Increasing N application rate decreased NUE (Figures 3A-F, $P< 0.01$). There was no interaction between N type and rate on NUE (Figures 3A-F). The treatment effects on NUE followed similar trend at the three experiment sites over the two years (Figures 3A-F). According to the quadratic equation, the blended CNR treatments had 31.9% higher than the conventional N fertilizer treatments at the highest average grain yield.

3.4 Dry matter accumulation and translocation

Compared with the conventional N fertilizer, the use of blended CRN (Equation 2) significantly increased pre-anthesis DM translocation (Equation 3) (Pre-DMT), pre-anthesis N translocation efficiency (Equation 4) (Pre-DMTE), and the contribution of Pre-DMT to grain yield (Pre-DMC) by 0.8-36.7%, 0.4-25.3%, and 0.7-37.0%, respectively, but decreased the

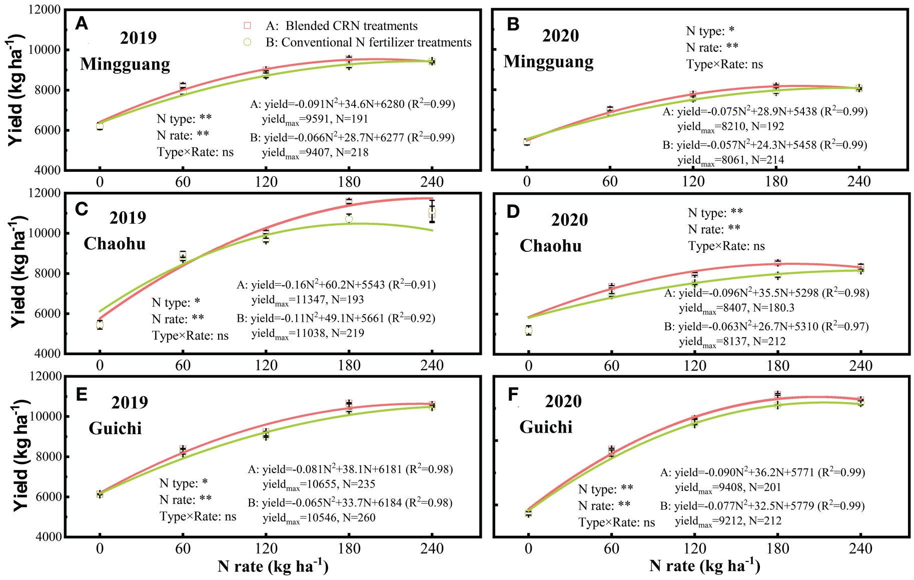

FIGURE 2
Rice yield under the treatments of blended controlled-release nitrogen fertilizer (CRN) (red square) and conventional N fertilizer treatments (green circle) applied at 0, 60, 120, 180, and 240 kg N ha^{-1} in 2019 and 2020 at Mingguang **(A, B)**, Chaohu **(C, D)** and Guichi **(E, F)** field sites, respectively. Statistically significant differences (*P*< 0.01**; *P*< 0.05*) and no significant differences (*P* > 0.05, ns) are shown. Values are the means ± SE (n=3).

contribution (Equation 5) of pre-anthesis DM accumulation to grain yield (Post-DMC) by 0.3-25.9% (Supplementary Table S1; Table 5, *P*<0.05). Increasing N dose significantly increased Pre-DMT, Post-DMA, Pre-DMTE and Pre-DMC (Supplementary Table S1, *P*<0.05), but decreased Post-DMC at Chaohu and Guichi experiment sites (Supplementary Table S1; Table 5, *P*< 0.05).

3.5 N accumulation and translocation

Compared with the conventional N fertilizer (Equation 6), the blended CRN increased the pre-anthesis N translocation (Pre-NT) and the contribution of pre-NT to grain N (Equation 9) (Pre-NC) by 1.0-19.8% and 0.2-8.7%, respectively, while decreased the contribution of post-anthesis N translocation to grain N (Equation 7) (Post-NC) by 1.0-24.8% (Supplementary Tables S2; Table 6, *P*< 0.05). The fertilizer (Equation 8) type did not affect the pre-anthesis N translocation efficiency (Pre-NTE) (Table 6, *P* > 0.05). Increasing N rate significantly increased the Pre-NT, post-anthesis N uptake (Post-NU), and Post-NC, but decreased Pre-NTE and the contribution of pre-NT to grain N (Pre-NC) by 0.1-23.6% and 0.1-20.0%, respectively (Supplementary Table S2; Table 6, *P*< 0.05). The effects of N type and dose on N accumulation and translocation were consistent across the three experiment sites over two years (Table 6).

3.6 Analysis of relationship

Dry matter and N accumulation, translocation, and utilization are closely related to yield and NUE. Rice yield was correlated positively with NP, NSP, Pre-DMT, Pre-DMC, Pre-NT, Post-NU, Post-NC but negatively with Pre-DMTE, Post-DMC, Pre-NTE, Pre-NC and NUE (Table 7, *P*<0.05). The NUE was correlated positively with Post-DMC and Pre-NC, but negatively with yield, NP, Pre-DMT, Pre-DMC, Post-NU and Post-NC (Table 7, *P*<0.05).

3.7 Economic benefit

The effects of N type and application rate on economic benefits were assessed by average yields across three sites over two years (Table 8). The N fertilization increased fertilizer cost, economic output and net economic benefit increased by 38.5-179.0%, 33.5-67.5% and 21.5-68.8%, respectively (Equation 10). Compared with the conventional N fertilization, the blended CRN treatments reduced the labor cost by 1800 Yuan ha^{-1}, but increased the fertilizer cost, economic output and net economic benefit by 4.5-9.8%, 0.2-5.2% and 8.8-15.3%, respectively. Using quadratic equation simulation, the highest net benefit was 21450 Yuan ha^{-1} under the blended CNR at an application rate of 189 kg ha^{-1} and NUE of 47.3%. In comparison, the highest net economic benefit was 19161 Yuan ha^{-1} under the conventional N fertilization at an application rate of 247 kg ha^{-1} and NUE of 31.9%. The blended CNR treatment had 11.9% higher net profit, but the applied N rate was 23.6% lower N dose and NUE was 50.4% higher NUE than the conventional N fertilization.

4 Discussion

4.1 Rice yield

The final yield of rice results from the translocation of pre-anthesis stored DM and post-anthesis accumulation of photosynthetic products (Kumar et al., 2006). Appropriate N

10.3389/fpls.2024.1354384

TABLE 4 The yield components of rice grown at Mingguang, Chaohu and Guichi field sites under the treatments of blended controlled-release nitrogen fertilizer (CRN) and conventional N fertilizer (N) applied at 0, 60, 120, 180, and 240 kg N ha^{-1} in 2019 and 2020.

Year / Location	Treatment	2019 NP ($\times10^4$ ha^{-1})	2019 NSP	2019 SR (%)	2019 GW (g)	2020 NP ($\times10^4$ ha^{-1})	2020 NSP	2020 SR (%)	2020 GW (g)
Mingguang	N0	200 ± 5.5	124 ± 2.3	82.1 ± 3.3	26.1 ± 0.3	183 ± 2.5	112 ± 2.1	87.1 ± 1.5	26.0 ± 0.1
	CRN60	241 ± 2.5	136 ± 4.0	85.7 ± 1.0	27.1 ± 0.6	241 ± 2.5	129 ± 3.8	87.4 ± 1.1	26.9 ± 0.6
	CRN120	257 ± 7.4	139 ± 2.8	87.4 ± 3.3	27.3 ± 0.2	257 ± 7.4	132 ± 2.6	89.1 ± 3.3	27.1 ± 0.2
	CRN180	265 ± 4.0	146 ± 3.3	89.0 ± 1.1	27.5 ± 0.2	263 ± 3.8	139 ± 3.2	90.8 ± 1.2	26.9 ± 0.4
	CRN240	257 ± 2.4	148 ± 4.4	88.9 ± 1.9	27.5 ± 0.2	257 ± 2.4	140 ± 4.8	90.7 ± 2.0	27.1 ± 0.2
	N60	239 ± 4.0	136 ± 6.7	83.4 ± 0.7	26.7 ± 0.2	237 ± 3.2	129 ± 6.4	85.1 ± 0.7	26.5 ± 0.2
	N120	252 ± 4.4	137 ± 1.8	86.7 ± 0.8	27.1 ± 0.2	249 ± 2.7	130 ± 1.7	88.4 ± 0.8	26.9 ± 0.2
	N180	273 ± 2.0	144 ± 2.8	87.2 ± 1.2	26.8 ± 0.2	269 ± 3.4	137 ± 2.7	88.0 ± 0.7	26.4 ± 0.3
	N240	293 ± 1.1	138 ± 1.9	84.7 ± 0.8	27.2 ± 0.0	276 ± 2.4	135 ± 2.6	86.4 ± 0.8	26.6 ± 0.2
	N type	*	*	*	ns	*	*	*	ns
	N rate	**	**	ns	**	**	**	ns	*
	Type×Rate	**	ns	ns	ns	**	ns	ns	ns
Chaohu	N0	178 ± 0.7	199 ± 3.7	79.9 ± 1.1	23.6 ± 0.1	161 ± 2.6	194 ± 5.9	71.3 ± 2.1	23.2 ± 0.1
	CRN60	215 ± 2.3	220 ± 0.8	80.0 ± 1.6	23.3 ± 0.3	183 ± 5.0	224 ± 2.1	70.0 ± 0.8	23.1 ± 0.1
	CRN120	227 ± 4.1	225 ± 1.3	83.3 ± 0.9	23.4 ± 0.1	199 ± 3.2	240 ± 4.4	70.4 ± 1.0	23.3 ± 0.2
	CRN180	244 ± 2.8	250 ± 1.3	84.1 ± 2.3	23.4 ± 0.2	230 ± 4.1	241 ± 3.4	68.9 ± 1.2	23.2 ± 0.2
	CRN240	255 ± 2.6	235 ± 2.6	81.4 ± 1.8	23.2 ± 0.3	250 ± 2.1	230 ± 6.3	65.9 ± 0.9	23.0 ± 0.1
	N60	213 ± 4.8	216 ± 2.7	81.6 ± 2.7	23.4 ± 0.3	188 ± 4.6	217 ± 3.1	67.7 ± 1.0	23.4 ± 0.1
	N120	223 ± 0.6	224 ± 6.3	79.8 ± 0.1	23.7 ± 0.3	204 ± 7.8	229 ± 5.9	68.6 ± 1.3	23.0 ± 0.1
	N180	242 ± 0.4	235 ± 6.7	84.9 ± 1.4	23.8 ± 0.1	238 ± 4.8	224 ± 2.7	68.7 ± 2.5	23.2 ± 0.2
	N240	257 ± 3.7	253 ± 1.9	79.3 ± 1.0	23.1 ± 0.3	251 ± 1.1	232 ± 9.6	64.8 ± 2.7	23.2 ± 0.2
	N type	*	*	*	ns	*	*	*	ns
	N rate	**	**	ns	ns	**	**	*	ns
	Type×Rate	ns	**	ns	ns	ns	ns	ns	ns
Guichi	N0	179 ± 3.2	204 ± 2.3	89.1 ± 0.5	23.5 ± 0.0	155 ± 3.2	212 ± 0.9	80.6 ± 0.9	23.0 ± 0.2
	CRN60	198 ± 3.2	208 ± 0.7	87.9 ± 1.1	23.4 ± 0.1	190 ± 3.0	215 ± 1.9	83.0 ± 1.2	23.0 ± 0.1
	CRN120	229 ± 6.6	211 ± 1.9	83.4 ± 1.5	23.4 ± 0.1	217 ± 2.4	222 ± 1.0	80.9 ± 0.7	23.0 ± 0.1
	CRN180	255 ± 2.0	217 ± 1.0	84.0 ± 0.6	23.5 ± 0.0	249 ± 1.8	208 ± 1.1	79.3 ± 0.1	23.0 ± 0.0
	CRN240	263 ± 3.2	209 ± 1.4	84.4 ± 0.7	23.4 ± 0.2	256 ± 3.0	201 ± 2.1	76.7 ± 0.5	22.9 ± 0.1
	N60	214 ± 1.5	211 ± 1.1	88.2 ± 0.6	23.4 ± 0.1	204 ± 2.5	216 ± 1.0	81.5 ± 0.6	23.0 ± 0.1
	N120	237 ± 2.0	213 ± 1.1	83.0 ± 0.7	23.5 ± 0.0	230 ± 3.6	219 ± 1.8	79.4 ± 0.4	23.0 ± 0.2
	N180	250 ± 1.5	219 ± 1.4	82.9 ± 0.9	23.5 ± 1.0	250 ± 2.4	201 ± 2.8	75.9 ± 1.8	23.0 ± 0.1
	N240	269 ± 2.6	209 ± 0.9	82.4 ± 0.5	23.4 ± 0.0	256 ± 1.4	198 ± 1.9	75.7 ± 0.5	22.9 ± 0.1
	N type	*	*	*	ns	**	*	*	ns
	N rate	**	**	**	**	**	**	**	**
	Type×Rate	ns	ns	ns	ns	*	ns	ns	ns

Statistically significant differences ($P < 0.01$**; $P < 0.05$*) and no statistical significance ($P > 0.05$, ns) are shown. Values are the means ± SEs (n=3). NP, NSP, SR, GW refer to the number of panicles, number of spikelets per panicle, seed-setting rate, 1000-grain weight, respectively.

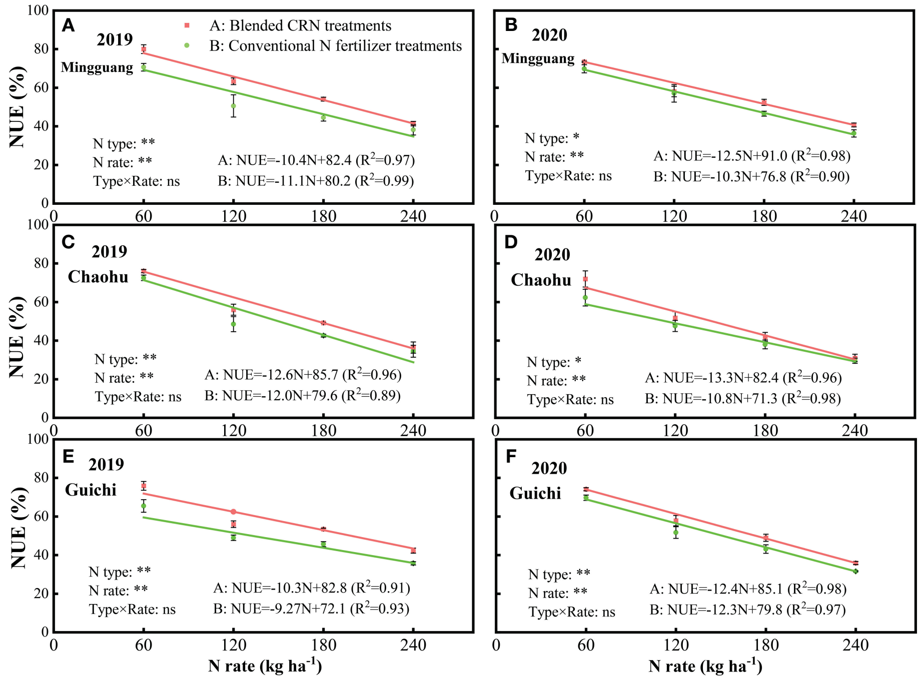

FIGURE 3
The N-use efficiency (NUE) under the treatments of blended controlled-release nitrogen fertilizer (CRN) (red) and conventional N fertilizer (green) applied at 0, 60, 120, 180, and 240 kg N ha^{-1} in 2019 and 2020 at Mingguang **(A, B)**, Chaohu **(C, D)** and Guichi **(E, F)** field sites, respective.

fertilizer type, rate and management can improve the photosynthetic rate and increase biomass and N accumulation and translocation, and hence yield (Artacho et al., 2009; Wang et al., 2018; Ju et al., 2021). The blended CRN treatment increased pre-anthesis DM translocation (Pre-DMT) and the contribution of Pre-DMT to grain yield (Pre-DMC) compared with the conventional N fertilizer treatment (Supplementary Tables S1, Table 5, *P*<0.05), which was consistent with the results of Wang et al. (2018). In addition, rice yield was positively correlated with Pre-DMT and Pre-DMC (Table 7, *P*<0.01), in agreement with the findings by Pal et al. (2017). This may be related to the fact that the blended CRN treatment decreased ineffective tillering to increase panicle number (Table 4), improved post-anthesis root function, especially cytokinin transport to leaves, and increased the accumulation of photosynthetic assimilates (Gu et al., 2017). The blended CRN might play a role in enhancing the sink and source sizes.

Rice yield also depends on yield components, including the number of panicles (NP), the number of spikelets per panicle (NSP), seed-setting rate (SR), and 1000-grain weight (GW). Previous studies have shown that one-time application of CRN increased NP, NSP, and SR of rice, thereby increasing yield (Guang et al., 2018; Wang et al., 2018). In this study, compared with the conventional urea use, one-time application of CRN significantly improved rice yield, mainly due to the increased NSP (Table 4). The positive correlation between NSP and yield in this study (Table 5) was consistent with previous studies (Artacho et al., 2009; Lan et al., 2021). Although the blended CRN treatment of significantly reduced the NP (Table 4), the contribution of the NP and NSP to rice yield is a trade-off process (Sui et al., 2013). Due to its slow N release at the tillering stage (Yuan et al., 2023), CRN decreased the NP of rice by 3.8-11.7% and increased the NSP by 11.8-21.8% during the heading stage compared to the common urea (Dun et al., 2023). Moreover, the lack of a significant N type effect on GW in this study (Table 4; *P*>0.05) was consistent with previous reports (Sui et al., 2013; Wang et al., 2018), suggesting that the GW is a stable trait determined by rice genotype.

4.2 Optimum N rate, NUE

Nitrogen fertilization is an important measure to promote sustainable crop production (Li et al., 2017). There is not a simple linear relationship between N application rate and rice yield but the one-variable quadratic can describe this relationship well (Ju et al., 2021). According to the quadratic equation, the optimal N application rate differed slightly for different rice varieties under the conventional N fertilization. The optimal N application rates for the highest yields of rice varieties HD-5 and YJ-8 under the conventional N fertilizer treatment were 255 and 261 kg ha^{-1}, respectively (Ju et al., 2021). Under the blended CRN treatment, this study obtained the average optimal N application rate of 200 kg ha^{-1}, which was lower than previous results. Wang et al. (2018) recommended the N application rate of 150 kg ha^{-1} for rice crop in the Yangtze River Basin of China to achieve a rice yield of approximately 7700 kg ha^{-1}. This yield was comparable to the rice

 10.3389/fpls.2024.1354384

TABLE 5 Pre-anthesis and post-anthesis dry matter (DM) accumulation and translocation of rice plants grown in the treatments of blended controlled-release nitrogen fertilizer (CRN) and conventional N fertilizer applied at 0, 60, 120, 180, and 240 kg N ha^{-1} in 2019 and 2020.

Year / Location	Treatment	2019 Pre-DMTE (%)	2019 Pre-DMC (%)	2019 Post-DMC (%)	2020 Pre-DMTE (%)	2020 Pre-DMC (%)	2020 Post-DMC (%)
Mingguang	N0	26.7 ± 3.3	23.9 ± 3.5	76.1 ± 3.5	26.8 ± 1.4	23.8 ± 1.4	76.2 ± 1.4
	CRN60	28.5 ± 0.6	35.3 ± 1.1	64.7 ± 1.1	30.3 ± 4.0	37.2 ± 1.4	62.8 ± 4.9
	CRN120	24.7 ± 3.6	29.7 ± 4.0	70.3 ± 4.0	29.8 ± 3.9	37.0 ± 3.0	63.0 ± 3.0
	CRN180	23.9 ± 1.3	31.6 ± 2.1	68.4 ± 2.1	26.4 ± 1.3	35.7 ± 1.8	64.3 ± 1.8
	CRN240	23.2 ± 1.9	32.6 ± 2.9	67.4 ± 2.9	24.8 ± 2.2	33.1 ± 3.1	66.9 ± 3.1
	N60	25.1 ± 3.3	30.2 ± 4.2	69.8 ± 4.2	28.4 ± 3.5	35.2 ± 4.5	64.8 ± 4.5
	N120	23.9 ± 2.4	29.5 ± 3.1	70.5 ± 3.1	26.4 ± 0.5	32.6 ± 0.6	67.4 ± 0.6
	N180	23.6 ± 1.6	29.2 ± 2.3	70.8 ± 2.3	23.5 ± 0.5	30.6 ± 0.9	69.4 ± 0.9
	N240	22.7 ± 1.4	30.1 ± 2.3	69.9 ± 2.3	24.4 ± 0.8	32.1 ± 1.3	67.9 ± 1.3
	N type	*	*	*	*	*	*
	N rate	ns	ns	ns	ns	**	**
	Type×Rate	ns	ns	ns	ns	ns	ns
Chaohu	N0	18.1 ± 0.9	21.8 ± 0.7	78.2 ± 0.7	17.5 ± 0.2	19.0 ± 0.3	81.0 ± 0.3
	CRN60	21.2 ± 0.8	25.5 ± 1.0	74.5 ± 1.0	23.2 ± 1.8	27.1 ± 0.8	72.9 ± 0.8
	CRN120	17.9 ± 1.2	20.6 ± 1.7	79.4 ± 1.7	27.9 ± 0.9	34.7 ± 1.9	65.3 ± 1.9
	CRN180	23.7 ± 1.4	29.9 ± 1.7	70.1 ± 1.7	27.2 ± 1.1	35.8 ± 1.9	64.2 ± 1.9
	CRN240	22.5 ± 1.2	27.4 ± 0.8	72.6 ± 0.8	23.7 ± 1.7	31.9 ± 1.7	68.1 ± 1.7
	N60	17.9 ± 1.0	21.6 ± 0.2	78.4 ± 0.2	21.7 ± 2.0	26.0 ± 2.0	74.0 ± 2.0
	N120	17.6 ± 1.0	19.4 ± 0.7	80.6 ± 0.7	24.1 ± 1.4	27.8 ± 0.4	72.2 ± 0.4
	N180	23.6 ± 2.0	27.8 ± 1.1	72.2 ± 1.1	23.7 ± 1.6	30.3 ± 0.3	69.7 ± 0.3
	N240	18.9 ± 1.7	24.0 ± 2.0	76.0 ± 2.0	23.3 ± 1.1	29.8 ± 2.0	70.2 ± 2.0
	N type	*	*	*	*	*	*
	N rate	*	*	*	**	**	**
	Type×Rate	ns	ns	ns	ns	ns	ns
Guichi	N0	12.6 ± 0.5	12.8 ± 0.6	87.2 ± 0.6	12.7 ± 1.2	15.4 ± 1.1	84.6 ± 1.1
	CRN60	17.7 ± 1.3	20.8 ± 1.7	79.2 ± 1.7	21.4 ± 0.8	26.1 ± 1.1	73.9 ± 1.1
	CRN120	21.2 ± 1.1	26.4 ± 1.3	73.6 ± 1.3	31.8 ± 1.2	46.4 ± 0.9	53.6 ± 0.9
	CRN180	31.7 ± 1.9	44.0 ± 2.5	56.0 ± 2.5	38.1 ± 2.4	59.2 ± 4.4	40.8 ± 4.4
	CRN240	31.2 ± 2.5	44.1 ± 4.1	55.9 ± 4.1	36.7 ± 1.0	58.0 ± 2.0	42.0 ± 2.0
	N60	15.0 ± 1.7	15.2 ± 2.1	84.8 ± 2.1	18.9 ± 3.9	23.5 ± 6.1	76.5 ± 6.1
	N120	18.3 ± 0.6	20.5 ± 0.5	79.5 ± 0.5	27.7 ± 0.9	38.1 ± 0.7	61.9 ± 0.7
	N180	27.4 ± 2.0	33.8 ± 2.4	66.2 ± 2.4	30.4 ± 1.2	44.9 ± 1.8	55.1 ± 1.8
	N240	30.8 ± 1.2	40.5 ± 1.1	59.5 ± 1.1	33.4 ± 0.6	51.1 ± 0.6	48.9 ± 0.6
	N type	**	**	**	**	**	**
	N rate	**	**	**	**	**	**
	Type×Rate	ns	ns	ns	ns	**	**

Statistically significant differences (P< 0.01**; P< 0.05*) and no statistical significance (P >0.05, ns) are shown. Values are the means ± SEs (n=3). Pre-DMTE, Pre-DMC, and Post-DMC refer to pre-anthesis DM translocation efficiency, contribution of pre-anthesis DM to grain yield, and contribution of post-anthesis DM accumulation to grain yield, respectively.

TABLE 6 Pre-anthesis and post-anthesis N accumulation and translocation of rice plants grown in the treatments of blended controlled-release nitrogen fertilizer (CRN) and conventional N fertilizer applied at 0, 60, 120, 180, and 240 kg N ha^{-1} in 2019 and 2020.

Year	Treatment	2019			2020		
Location		Pre-NTE (%)	Pre-NC (%)	Post-NC (%)	Pre-NTE (%)	Pre-NC (%)	Post-NC (%)
Mingguang	N0	64.5 ± 1.2	92.4 ± 1.2	7.6 ± 1.2	64.0 ± 0.8	91.1 ± 0.7	8.9 ± 0.7
	CRN60	62.9 ± 1.5	87.4 ± 0.3	12.6 ± 0.3	63.5 ± 1.6	88.4 ± 0.1	11.5 ± 0.1
	CRN120	58.9 ± 0.8	83.0 ± 1.2	17.0 ± 1.2	57.0 ± 0.8	83.0 ± 1.4	17.0 ± 1.4
	CRN180	55.7 ± 1.9	78.8 ± 1.4	21.2 ± 1.4	52.9 ± 1.6	79.1 ± 0.4	20.9 ± 0.4
	CRN240	49.0 ± 1.2	74.0 ± 1.8	26.0 ± 1.8	48.8 ± 1.3	72.7 ± 0.5	27.3 ± 0.5
	N60	62.3 ± 1.9	89.0 ± 0.3	11.0 ± 0.3	63.3 ± 2.0	88.6 ± 0.6	11.4 ± 0.6
	N120	60.0 ± 1.2	85.9 ± 1.1	14.1 ± 1.1	58.5 ± 0.5	83.4 ± 1.6	16.6 ± 1.6
	N180	55.4 ± 1.5	81.0 ± 1.9	19.0 ± 1.9	53.7 ± 1.4	81.1 ± 1.9	18.9 ± 1.9
	N240	49.5 ± 1.4	80.4 ± 0.7	19.6 ± 0.7	48.9 ± 1.5	75.0 ± 0.8	25.0 ± 0.8
	N type	ns	**	**	ns	*	*
	N rate	**	**	**	**	**	**
	Type×Rate	ns	ns	ns	ns	ns	ns
Chaohu	N0	65.8 ± 1.5	90.9 ± 0.1	9.4 ± 0.1	68.9 ± 0.5	91.2 ± 0.6	10.2 ± 0.6
	CRN60	62.8 ± 3.5	87.8 ± 0.5	12.2 ± 0.5	67.5 ± 1.0	88.7 ± 0.6	11.3 ± 0.6
	CRN120	65.2 ± 0.7	86.0 ± 0.5	14.0 ± 0.5	68.2 ± 0.5	85.7 ± 0.2	14.3 ± 0.2
	CRN180	63.8 ± 0.8	82.3 ± 0.4	17.7 ± 0.4	67.7 ± 0.9	82.0 ± 0.2	18.0 ± 0.2
	CRN240	63.0 ± 2.1	79.9 ± 0.6	20.1 ± 0.6	66.0 ± 1.7	80.4 ± 0.4	19.6 ± 0.4
	N60	63.2 ± 1.7	90.1 ± 0.3	9.3 ± 0.3	67.6 ± 2.2	91.1 ± 0.2	8.9 ± 0.4
	N120	65.2 ± 0.9	87.5 ± 0.7	12.5 ± 0.7	68.7 ± 1.7	88.2 ± 0.5	11.8 ± 0.5
	N180	64.7 ± 1.5	85.3 ± 0.3	14.7 ± 0.3	66.8 ± 3.7	85.6 ± 0.9	14.4 ± 0.9
	N240	63.0 ± 1.0	83.2 ± 0.8	16.8 ± 0.8	69.1 ± 1.5	83.6 ± 0.8	16.4 ± 0.8
	N type	ns	*	*	ns	**	**
	N rate	*	**	**	*	**	**
	Type×Rate	ns	ns	ns	ns	ns	ns
Guichi	N0	63.3 ± 0.7	91.3 ± 0.8	8.7 ± 0.8	60.8 ± 1.0	91.0 ± 0.9	9.0 ± 0.9
	CRN60	61.5 ± 0.4	88.2 ± 0.8	11.8 ± 0.8	58.7 ± 0.9	88.4 ± 0.5	11.6 ± 0.5
	CRN120	60.2 ± 0.4	85.9 ± 1.0	14.1 ± 1.0	56.7 ± 0.9	85.0 ± 0.4	15.0 ± 0.4
	CRN180	57.9 ± 0.7	82.8 ± 0.1	17.2 ± 0.1	55.2 ± 0.5	82.2 ± 0.6	17.8 ± 0.6
	CRN240	54.5 ± 0.4	78.7 ± 1.3	21.3 ± 1.3	53.8 ± 0.5	78.8 ± 0.2	21.2 ± 0.2
	N60	63.2 ± 0.3	89.0 ± 0.7	11.0 ± 0.7	57.4 ± 1.1	89.6 ± 0.8	10.4 ± 0.8
	N120	60.9 ± 0.2	87.7 ± 0.4	12.3 ± 0.4	56.8 ± 0.8	88.1 ± 0.5	11.9 ± 0.5
	N180	60.4 ± 0.3	85.4 ± 0.6	14.6 ± 0.6	56.7 ± 1.5	84.1 ± 0.1	15.9 ± 0.1
	N240	59.2 ± 2.0	82.3 ± 0.8	17.7 ± 0.8	54.4 ± 1.1	82.1 ± 0.2	17.9 ± 0.2
	N type	*	**	**	ns	**	**
	N rate	**	**	**	*	**	**
	Type×Rate	ns	*	*	ns	ns	ns

Statistically significant differences (P< 0.01**; P< 0.05*) and no statistical significance (P > 0.05, ns) are shown. Values are the means ± SEs (n=3). Pre-NTE, Pre-NC, and Post-NC refer to pre-anthesis N translocation efficiency, contribution of pre-anthesis N translocation to grain N, and contribution of post-anthesis N translocation to grain N, respectively.

TABLE 7 Pearson corrections among yield, the number of panicles (NP), number of spikelets per panicle (NSP), seed-setting rate (SR), 1000-grain weight (GW), pre-anthesis dry matter (DM) translocation (Pre-DMT), pre-anthesis DM translocation efficiency (Pre-DMTE), post-anthesis DM accumulation (Post-MDA), contribution of pre-DMT (Pre-MDC), contribution of post-DMA (Post-MDC), pre-anthesis N translocation (Pre-NT), pre-anthesis N translocation efficiency (Pre-NTE), post-anthesis N uptake (Post-NU), contribution of pre-NT to grain N (Pre-NC) and contribution of post-NU to grain N (Post-NC) and N-use efficiency (NUE) of rice plants grown under various treatments in the 2019 and 2020 seasons (n=162).

Index	Yield	NP	NSP	SR	GW	Pre-DMT	Pre-DMTE	Post-DMA	Pre-DMC	Post-DMC	Pre-NT	Pre-NTE	Post-NU	Pre-NC	Post-NC	NUE
Yield	1															
NP	0.66**	1														
NSP	0.35**	-0.29**	1													
SR	0.11	0.29**	-0.58**	1												
GW	-0.14	0.41**	-0.91**	0.59**	1											
Pre-DMT	0.58**	0.58**	0.12	-0.07	-0.13	1										
Pre-DMTE	-0.23**	0.44**	-0.18*	-0.07	0.11	0.84**	1									
Post-DMA	0.01	0.12	-0.21**	-0.01	0.44**	-0.40**	-0.27**	1								
Pre-DMC	0.32**	0.51**	-0.07	-0.11	0.01	0.94**	0.95**	-0.36**	1							
Post-DMC	-0.32**	-0.51**	0.07	0.11	-0.01	-0.94**	-0.95**	0.36**	-1.00**	1						
Pre-NT	0.85**	0.77**	0.11	0.10	0.13	0.53**	0.34**	0.18*	0.38**	-0.38**	1					
Pre-NTE	-0.20*	-0.52**	0.44**	-0.52**	-0.42**	-0.40**	-0.28**	0.26**	-0.37**	0.37**	-0.09	1				
Post-NU	0.64**	0.81**	-0.11	0.18*	0.29**	0.53**	0.33**	0.18*	0.43**	-0.43**	0.69**	-0.53**	1			
Pre-NC	-0.53**	-0.76**	0.15	-0.16*	-0.30**	-0.51**	-0.33**	-0.14	-0.44**	0.44**	-0.54**	0.61**	-0.98**	1		
Post-NC	0.53**	0.76**	-0.15	0.16*	0.30**	0.51**	0.33**	0.14	0.44**	-0.44**	0.54**	-0.61**	0.98**	-1.00**	1	
NUE	-0.43**	-0.61**	-0.20	0.25	0.13	-0.43**	-0.23	-0.27	-0.31**	0.31**	-0.02	0.15	-0.75**	0.62**	-0.14*	1

Statistical significant correlation (P < 0.01, **; P < 0.05, *) and no statistical significant correlation (P > 0.05, ns) are shown.

10.3389/fpls.2024.1354384

 10.3389/fpls.2024.1354384

yield of 7820 kg ha^{-1} at the N application rate of 60 kg ha^{-1} in our study, with the yield further increasing with increasing N dose to 120 and 180 kg ha^{-1} (8540 and 9420 kg ha^{-1}, respectively). The reason for such a discrepancy in yield response to N fertilization was related to the different rice varieties. Wang et al. (2018) tested indica varieties of rice, while this study used super hybrid rice varieties. At the equivalent N application rate, the yield of super hybrid rice was higher than that of indica rice (Hu et al., 2020; Zhu et al., 2020). Therefore, rice varieties and their yield potential should be considered when the N fertilizer program is formulated.

Intensive agricultural production in developing countries faces the dual challenge of ensuring sustained increases in crop yields and reducing the environmental risks of excessive fertilizer inputs (Chen et al., 2011). Changing N application methods, such as deep application and split application, or fertilizer type, has achieved simultaneous improvement in rice yield and NUE, mainly through reducing N losses such as NH_3 volatilization, N runoff and NO_3 leaching (Huang et al., 2019; Liu et al., 2016; Wang et al., 2018; Yuan et al., 2023). This and previous studies demonstrated that the single application of CRN improved NUE compared with the urea split application (Wang et al., 2018; Huang et al., 2019). This improved NUE was mainly due to the slow N release and longevity (40 and 90 d) of CRNs in the paddy fields.

The NUE is closely related to grain N accumulation, which could be derived via translocation of the pre-anthesis stored N and the post-anthesis uptake of soil N (Jiang et al., 2005; Wei et al., 2017). In this study, Pre-NC under the blended CRN treatment was 74.0-88.7% which was significantly higher than that under the conventional N fertilizer treatment (Table 6). The results implied that the blended CRN treatment was more conducive than the conventional N fertilizer treatment to enhancing the re-translocation of N from stems and leaves to grains. The increased yield and NUE under blended CRN fertilization had resulted from the increased Pre-NT (Table 6), improved photosynthetic rate, delayed leaf senescence, and increased post-anthesis carbon assimilation (Wu et al., 2018).

4.3 Economic benefit

Economic benefit is one of the important factors influencing farmers to adopt fertilizer management practices (Zhang et al., 2021). The relatively high price of CRNs limits their use in farming practices such as rice production (Naz and Sulaiman, 2016). However, this study suggested that the blended CRN treatments could improve the economic benefits for rice cultivation (Table 8). With accelerated urbanization, labor for agricultural cultivation has become expensive (Chen et al., 2014). Compared with the conventional N fertilization, the use of blended CRN could save labor costs. Under the blended CRN treatment, labor cost saving offset the increased fertilizer cost, which ultimately increased the profitability for the rice growers (Table 8). It appears to be an effective way to achieve high grain yield and NUE by optimizing the N management mode of CRN and urea blended application (Guo et al., 2019; Huang et al., 2019; Zhang et al., 2021).

5 Conclusions

At the equivalent N rate, the rice yield, NUE and economic benefit significantly increased under the blended CRN treatment. The quadratic equation estimated that the N rate for the highest yield under the blended CRN treatment was 200 kg ha^{-1} and NUE was 45.9%, which were 14.7% less and 31.9% more than those under the conventional N fertilizer treatment, respectively. The rice yield at the highest economic benefit was slightly below the highest yield. At the highest economic benefit under the blended CRN treatment, the N rate was 189 kg ha^{-1} and NUE was 47.3%, which were 23.6% less and 50.4% more than those under the conventional N fertilizer treatment, respectively. The increase in NUE was due to the increase in Pre-NT and Post-NC under the blended CRN fertilizer treatment. The increase in economic benefit was mainly due to the reduction in labor cost under the blended CRN fertilizer treatment. The application rate of the blended CRN at 189 kg N ha^{-1} is recommended for rice production in the Yangtze River Delta.

TABLE 8 The output values, labor and costs, and net economic benefits under the treatments of blended controlled-release nitrogen fertilizer (CRN) and conventional N fertilizer applied at 0, 60, 120, 180, and 240 kg N ha^{-1}.

Treatment	Average yield (kg ha^{-1})	Output value (Yuan ha^{-1})	Labor cost (Yuan ha^{-1})	Fertilizer cost (Yuan ha^{-1})	Net economic benefit (Yuan ha^{-1})
N0	5766	14415	900	675	12840
CRN60	7945	19861	900	977	17984
CRN120	8787	21968	900	1279	19789
CRN180	9660	24150	900	1581	21669
CRN240	9436	23589	900	1883	20806
N60	7696	19239	2700	935	15603
N120	8498	21246	2700	1195	17350
N180	9187	22968	2700	1455	18813
N240	9413	23533	2700	1715	19118

The data are average in the 2019 and 2020 seasons.

Data availability statement

The original contributions presented in the study are included in the article/Supplementary Material. Further inquiries can be directed to the corresponding authors.

Author contributions

MY: Data curation, Formal analysis, Investigation, Writing – original draft, Writing – review & editing, Conceptualization. GW: Formal analysis, Investigation, Writing – review & editing, Supervision. JW: Investigation, Writing – review & editing, Methodology, Project administration. CL: Software, Writing – review & editing, Formal analysis. YH: Resources, Writing – review & editing. RH: Resources, Writing – review & editing. YZ: Resources, Writing – review & editing. XZ: Investigation, Writing – review & editing. WW: Investigation, Writing – review & editing. YS: Conceptualization, Funding acquisition, Project administration, Writing – review & editing.

Funding

The author(s) declare financial support was received for the research, authorship, and/or publication of this article. The National Key Research & Development Program of China (No. 2023YFD1901102, No. 2022YFD2301403, No.2016YFD0200806), the Key Research & Development Program of Anhui Province (2023n06020019) and the Natural Science Foundation of Anhui Province (2108085QC124).

Acknowledgments

Many thanks go to Dr Caixian Tang of La Trobe University, Dr Jianguo Zhu, Dr Zubin Xie, Dr Chuang Cai of Institute of Soil Science, Chinese Academy of Sciences, Dr Xiaozhong Wang of Academy of Agricultural Sciences, Southwest University for revising the manuscript.

Conflict of interest

The authors declare that the research was conducted in the absence of any commercial or financial relationships that could be construed as a potential conflict of interest.

Publisher's note

All claims expressed in this article are solely those of the authors and do not necessarily represent those of their affiliated organizations, or those of the publisher, the editors and the reviewers. Any product that may be evaluated in this article, or claim that may be made by its manufacturer, is not guaranteed or endorsed by the publisher.

Supplementary material

The Supplementary Material for this article can be found online at: https://www.frontiersin.org/articles/10.3389/fpls.2024.1354384/full#supplementary-material

SUPPLEMENTARY TABLE 1
Pre-anthesis dry matter translocation (Pre-DMT) and post-anthesis dry matter accumulation (Post-DMA) of rice crop grown in the treatments of blended controlled-release nitrogen fertilizer (CRN) and conventional N fertilizer applied at 0, 60, 120, 180, and 240 kg N ha^{-1} in 2019 and 2020. Statistically significant differences (*P*< 0.01, **; *P*< 0.05, *) and no statistical significance (*P* > 0.05, ns) are shown. Values are the means ± SEs (n=3).

SUPPLEMENTARY TABLE 2
Pre-anthesis N translocation (Pre-NT) and post-anthesis N uptake (Post-NU) of rice grown in the treatments of blended controlled-release nitrogen fertilizer (CRN) and conventional N fertilizer applied at 0, 60, 120, 180, and 240 kg N ha^{-1} in 2019 and 2020. Statistically significant differences (*P*< 0.01, **; *P*< 0.05, *) and no statistical significance (*P* > 0.05, ns) are shown. Values are the means ± SEs (n=3).

References

Artacho, P., Bonomelli, C., and Meza, F. (2009). Nitrogen application in irrigated rice grown in Mediterranean conditions: effects on grain yield, dry matter production, nitrogen uptake, and nitrogen use efficiency. *J. Plant Nutr.* 32, 157–1593. doi: 10.1080/01904160903094339

Bremner, J. M., and Mulvaney, C. S. (1982). "Total nitrogen," in *Methods of soil science society of america journal*, vol. 328 . Eds. T. Page, J. M. Miller and D. R. Keeney (Madison, WI, USA: American Society of Agronomy), 595–642.

Chen, X., Cui, Z., Fan, M., Vitousek, P., Zhao, M., Ma, W., et al. (2014). Producing more grain with lower environmental costs. *Nature* 514, 486. doi: 10.1038/nature13609

Chen, X. P., Cui, Z. L., Vitousek, P. M., Cassman, K. G., Matson, P. A., Bai, J. S., et al. (2011). Integrated soil-crop system management for food security. *Proc. Natl. Acad. Sci. United States America* 108, 6399–6404.

Chen, Z., Wang, Q., Ma, J., Zou, P., and Jiang, L. (2020). Impact of controlled-release urea on rice yield, nitrogen use efficiency and soil fertility in a single rice cropping system. *Sci. Rep.* 10, 10432. doi: 10.1038/s41598-020-67110-6

Cheng, J., Jiang, H., Pan, X., Dai, T., and Cao, W. (2010). Effects of nitrogen rates on Post-anthesis accumulation and transfer of dry matter and nitrogen in rice with differential nitrogen nutrition efficiency. *Chin. Agric. Sci. Bull.* 26, 150–156.

Congreves, K. A., Otchere, O., Ferland, D., Farzadfar, S., Williams, S., and Arcand, M. M. (2021). Nitrogen use efficiency definitions of today and tomorrow. *Fronts Plant Sci.* 12, 912. doi: 10.3389/fpls.2021.637108

Deng, F., Wang, L., Ren, W. J., Mei, X. F., and Li, S. X. (2015). Optimized nitrogen managements and polyaspartic acid urea improved dry matter production and yield of indica hybrid rice. *Soil Tillage Res.* 145, 1–9. doi: 10.1016/j.still.2014.08.004

Dun, C. P., Wang, R., Mi, K. L., Zhang, Y. T., Zhang, H. P., Cui, P. Y., et al. (2023). One-time application of controlled-release bulk blending fertilizer enhanced yield quality and photosynthetic efficiency of late japonica rice. *J. Integr. Agric.* doi: 10.1016/j.jia.2023.10.007

Gu, J. F., Chen, Y., Zhang, H., Li, Z., and Yang, J. (2017). Canopy light and nitrogen distributions are related to grain yield and nitrogen use efficiency in rice. *Field Crops Res.* 206, 74–85. doi: 10.1016/j.fcr.2017.02.021

Guang, C., Tingting, C., Song, C., Chunmei, X., Xiufu, Z., and Danying, W. (2018). Polymer-coated urea application could produce more grain yield in "super" rice. *Agron. J.* 110, 246–259. doi: 10.2134/agronj2017.07.0400

Guo, J., Wang, Y., Blaylock, A. D., and Chen, X. (2019). Mixture of controlled release and normal urea to optimize nitrogen management for high-yielding (& 15 Mg ha^{-1}) maize. *Field Crops Res.* 204, 23–30.

Hu, J., Wang, D., Liu, K., Chu, G., Huang, L., Tian, X., et al. (2020). Inbred varieties outperformed hybrid rice varieties under dense planting with reducing nitrogen. *Sci. Rep.* 10, 8769. doi: 10.1038/s41598-020-65574-0

Huang, Q., Fan, X., Tang, S., Zhang, M., Huang, X., Yi, Q., et al. (2019). Seasonal differences in N release dynamic of controlled-released urea in paddy field and its impact on the growth of rice under double rice cropping system. *Soil Tillage Res.* 195, 104371. doi: 10.1016/j.still.2019.104371

IFA. (2021). *IFADATA statstics*. Paris: International Fertilizer Industry Association. http://www.fertilizer.org/ifa/HomePage/STATISTICS[EB/OL].

Jiang, L. G., Dai, T. B., Jiang, D., Cao, W. X., Gan, X. Q., and Wei, S. (2004). Characterizing physiological N-use efficiency as influenced by nitrogen management in three rice cultivars. *Field Crops Res.* 88, 239–250. doi: 10.1016/j.fcr.2004.01.023

Jiang, L. G., Dong, D. F., Gan, X. Q., and Wei, S. Q. (2005). Photosynthetic efficiency and nitrogen distribution under different nitrogen management and relationship with physiological N-use efficiency in three rice genotypes. *Plant Soil* 271, 321–328. doi: 10.1007/s11104-004-3116-9

Ju, C., Zhu, Y., Liu, T., and Sun, C. (2021). The effect of nitrogen reduction at different stages grain yield and nitrogen use efficiency for nitrogen efficient rice varieties. *Agronomy* 11, 462. doi: 10.3390/agronomy11030462

Kumar, R., Sarawgi, A. K., Ramos, C., Amarante, S. T., Ismail, A. M., and Wade, L. J. (2006). Partitioning of dry matter during drought stress in rainfed lowland rice. *Field Crops Res.* 96, 455–465. doi: 10.1016/j.fcr.2005.09.001

Lan, Y., Sui, X., Wang, J., Duan, Q., Wu, C., Ding, C., et al. (2021). Effects of nitrogen application rate on protein components and yield of low gluten rice. *Agriculture* 11, 302. doi: 10.3390/agriculture11040302

Lassaletta, L., Billen, G., Grizzetti, B., Anglade, J., and Garnier, J. (2014). 50 year trends in nitrogen use efficiency of world cropping systems: the relationship between yield and nitrogen input to cropland. *Environ. Res. Lett.* 9, 105011. doi: 10.1088/1748-9326/9/10/105011

Li, H., Hu, B., and Chu, C. (2017). Nitrogen use efficiency in crops: Lessons from Arabidopsis and rice. *J. Exp. Bot.* 68, 2477–2488. doi: 10.1093/jxb/erx101

Liu, Y., Gao, F., Yi, H., Yang, C., Zhang, R., Zhou, Y., et al. (2021). Recent advances in selective catalytic oxidation of nitric oxide (NO-SCO) in emissions with excess oxygen: a review on catalysts and mechanisms. *Environ. Sci. Pollut. R.* 28, 2549–2571.

Lyu, Y., Yang, X., Pan, H., Zhang, X., Cao, H., Ulgiati, S., et al. (2021). Impact of fertilization schemes with different ratios of urea to controlled release nitrogen fertilizer on environmental sustainability, nitrogen use efficiency and economic benefit of rice production: A study case from Southwest China. *J. Clean. Product.* 293, 126198. doi: 10.1016/j.jclepro.2021.126198

Mae, T. (1997). Physiological nitrogen efficiency in rice: Nitrogen utilization, photosynthesis, and yield potential. *Plant Soil* 196, 201–210. doi: 10.1023/A:1004293706242

Mae, T., and Ohira, K. (1981). The remobilization of nitrogen related to leaf growth and senescence in rice plants (Oryza sativa L.). *Plant Cell Physiol.* 22, 1067–1074.

Naz, M. Y., and Sulaiman, S. A. (2016). Slow release coating remedy for nitrogen loss from conventional urea: a review. *J. Controlled Release* 225, 109–120. doi: 10.1016/j.jconrel.2016.01.037

Ntanos, D. A., and Koutroubas, S. D. (2002). Dry matter and N accumulation and translocation for Indica and Japonica rice under Mediterranean conditions. *Field Crops Res.* 74, 93–101. doi: 10.1016/S0378-4290(01)00203-9

Pal, R., Mahajan, G., Sardana, V., and Chauhan, B. S. (2017). Impact of sowing date yield, dry matter and nitrogen accumulation, and nitrogen translocation in dry-seeded rice in North-West India. *Field Crops Res.* 206, 138–148. doi: 10.1016/j.fcr.2017.01.025

Sui, B., Feng, X., Tian, G., Hu, X., Shen, Q., and Guo, S. (2013). Optimizing nitrogen supply increases rice yield and nitrogen use efficiency by regulating yield formation factors. *Field Crops Res.* 150, 99–107. doi: 10.1016/j.fcr.2013.06.012

Sun, Y., Ma, J., Sun, Y., Hui, X., Yang, Z., Liu, S., et al. (2012). The effects of different water and nitrogen managements on yield and nitrogen use efficiency in hybrid rice of China. *Field Crops Res.* 127, 85–98. doi: 10.1016/j.fcr.2011.11.015

Wang, L., Xue, C., Pan, X., Chen, F., and Liu, Y. (2018). Application of controlled-release urea enhances grain yield and nitrogen use efficiency in irrigated rice in the Yangtze river basin, China. *Front. Plant Sci.* 9, 1–13. doi: 10.3389/fpls.2018.00999

Wei, H. H., Meng, T. Y., Li, C., Xu, K., Huo, Z. Y., Wei, H. Y., et al. (2017). Comparisons of grain yield and nutrient accumulation and translocation in high-yielding japonica/indica hybrids, indica hybrids, and japonica conventional varieties. *Field Crops Res.* 204, 101–109. doi: 10.1016/j.fcr.2017.01.001

Wu, H., Xiang, J., Zhang, Y., Zhang, Y., Peng, S., Chen, H., et al. (2018). Effects of post-anthesis nitrogen uptake and translocation on photosynthetic production and rice yield. *Sci. Rep.* 8, 12891. doi: 10.1038/s41598-018-31267-y

Yamaji, N., Takemoto, Y., Miyaji, T., Mitani-Ueno, N., Yoshida, K. T., and Ma, J. F. (2017). Reducing phosphorous accumulation in rice grains with an impaired transporter in the node. *Nature* 541, 92–99. doi: 10.1038/nature20610

Yang, L., Huang, J., Yang, H., Dong, G., Liu, G., Zhu, J., et al. (2006). Seasonal changes in the effects of free-air CO_2 enrichment (FACE) on dry matter production and distribution of rice (*Oryza sativa* L.). *Field Crops Res.* 98, 12–19. doi: 10.1016/j.fcr.2005.11.003

Yu, F., and Shi, W. M. (2015). Nitrogen use efficiencies of major grain crops in China in recent 10 years. *Acta Pedologica Sinica.* 52, 1311–1324. doi: 10.11766/trxb201501270058

Yu, X., Keitel, C., Zhang, Y., Wangeci, A. N., and Dijkstra, F. A. (2022). Global meta-analysis of nitrogen fertilizer use efficiency in rice, wheat and maize. *Agricult. Ecosyst. Environ.* 338, 108089. doi: 10.1016/j.agee.2022.108089

Yuan, M., Cai, C., Wang, X., Li, G., Wu, G., Wang, J., et al. (2021). Warm air temperatures increase photosynthetic acclimation to elevated CO_2 concentrations in rice under field conditions. *Field Crops Res.* 262, 108036. doi: 10.1016/j.fcr.2020.108036

Yuan, M., Sun, Y., Wu, G., Wang, J., Liu, C., Tang, T., et al. (2023). The optimum economic nitrogen rate of blended controlled-release nitrogen fertilizer or rice in the Chaohu watershed in the Yangtze River Delta, China. *Front. Plant Sci.* 14, 1144461. doi: 10.3389/fpls.2023.1144461

Zhang, L., Liang, Z., Hu, Y., Schmidhalter, U., and Chen, X. (2021). Integrated assessment of agronomic, environmental and ecosystem economic benefits of blending use of controlled-release and common urea in wheat production. *J. Clean. Product.* 287, 125572. doi: 10.1016/j.jclepro.2020.125572

Zhang, D., Wang, H., Pan, J., Luo, J., Liu, J., Gu, B., et al. (2018a). Nitrogen application rates need to be reduced for half of the rice paddy field in China. *Agricult. Ecosyst. Environ.* 265, 8–14. doi: 10.1016/j.agee.2018.05.023

Zhang, M., Yao, Y. L., Tian, Y. H., Ceng, K., Zhao, M., Zhao, M., et al. (2018b). Increasing yield and N use efficiency with organic fertilizer in Chinese intensive rice cropping systems. *Field Crops Res.* 227, 102–109. doi: 10.1016/j.fcr.2018.08.010

Zheng, Y., Han, X., Li, Y., Liu, S., Ji, J., and Tong, Y. (2020). Effects on mixed controlled release nitrogen fertilizer with rice straw biochar on rice yield and nitrogen balance in Northeast China. *Sci. Rep.* 10, 9452. doi: 10.1038/s41598-020-66300-6

Zhu, K., Zhou, Q., Shen, Y., Yan, J., Xu, Y., Wang, Z., et al. (2020). Agronomic and physiological performance of an indica-japonica rice variety with a high yield and high nitrogen use efficiency. *Crop Sci.* 60. doi: 10.1002/csc2.20150

frontiers | Frontiers in Plant Science

TYPE Original Research
PUBLISHED 01 July 2024
DOI 10.3389/fpls.2024.1377364

Check for updates

OPEN ACCESS

EDITED BY
Khurram Shahzad,
Lasbela University of Agriculture, Water and Marine Sciences, Pakistan

REVIEWED BY
Tajamul Hussain,
Oregon State University, United States
Shahid Hussain,
Bahauddin Zakariya University, Pakistan
Muhammad Atif Muneer,
Fujian Agriculture and Forestry University, China

*CORRESPONDENCE
Waqar Ahmed
ahmed.waqar1083@yahoo.com
Zhengxiong Zhao
zhaozx0801@163.com

[†]These authors have contributed equally to this work and share first authorship

RECEIVED 27 January 2024
ACCEPTED 10 June 2024
PUBLISHED 01 July 2024

CITATION
Li S, Jiang T, Ahmed W, Yang Y, Yang L, Zhang T, Mei F, Alharbi SA, Shan Q, Guo C and Zhao Z (2024) Deciphering the impact of nitrogen morphologies distribution on nitrogen and biomass accumulation in tobacco plants.
Front. Plant Sci. 15:1377364.
doi: 10.3389/fpls.2024.1377364

Deciphering the impact of nitrogen morphologies distribution on nitrogen and biomass accumulation in tobacco plants

Shichen Li[1†], Tao Jiang[1†], Waqar Ahmed[1*], Yingfen Yang[1], Linyuan Yang[1], Tao Zhang[1], Fupeng Mei[1], Sulaiman Ali Alharbi[2], Qu Shan[1], Cuilian Guo[1] and Zhengxiong Zhao[1*]

[1]Yunnan Agricultural University, Kunming, Yunnan, China, [2]Department of Botany & Microbiology College of Science, King Saud University, Riyadh, Saudi Arabia

Background and aims: Nitrogen (N) distribution in plants is intricately linked to key physiological functions, including respiration, photosynthesis, structural development, and nitrogen storage. However, the specific effects of different N morphologies on N accumulation and plant growth are poorly understood. Our research specifically focused on determining how different N morphologies affect N absorption and biomass accumulation.

Methods: This study elucidated the impact of different application rates (CK: 0 g N/plant; T1: 4 g N/plant; T2: 8 g N/plant) of N fertilizer on N and biomass accumulation in tobacco cultivars Hongda and K326 at different growth stages.

Results: Our findings emphasize the critical role of N distribution in various plant parts, including leaves, stems, and roots, in determining the complex mechanisms of N and biomass accumulation in tobacco. We found that in relation to total N, a greater ratio of water-soluble N (N_w) in leaves facilitated N accumulation in leaves. In contrast, an increased ratio of SDS (detergent)-insoluble N ($N_{in\text{-}SDS}$) in leaves and non-protein N (N_{np}) in roots hindered this increase. Additionally, our results indicate that a greater proportion of N_{np} in leaves has a negative impact on biomass accumulation in leaves. Furthermore, elevated levels of $N_{in\text{-}SDS}$, N_w, and N_{np} in roots, and N_{np} in leaves adversely affected biomass accumulation in tobacco leaves. The Hongda cultivar exhibited greater biomass and N accumulation abilities as compared to K326.

Conclusions: Our findings highlight the significant role of distribution of N morphologies on plant growth, as well as N and biomass accumulation in tobacco plants. Understanding N distribution allows farmers to optimize N application, minimizing environmental losses and maximizing yield for specific cultivars. These insights advance sustainable agriculture by promoting efficient resource use and reducing environmental impact.

KEYWORDS
Nicotiana tabacum, nitrogen use efficiency, water-soluble nitrogen, non-protein nitrogen, SDS-insoluble nitrogen

1 Introduction

Nitrogen (N) fertilizers contribute significantly to enhancing crop productivity and serve as a cornerstone for addressing global food security by substantially increasing crop yields (Cui et al., 2022). China is the world's largest fertilizer producer and consumer, and from 1978 to 2006, its fertilizer input contributed 56.18% of the increase in grain yield (Wang et al., 2022b). Previous studies have highlighted the direct correlation between N application, N uptake, and improved plant growth parameters, including tobacco plant height, leaf number, leaf area, and stem diameter by 61.04% (Haghighi et al., 2011; Li et al., 2021). Despite these advances, a comprehensive understanding of the intricate distribution of N across various plant organs remains limited. This knowledge gap calls for a thorough investigation of the effects of diverse N allocation ratios on N and biomass accumulation in tobacco plants, particularly under different N conditions, growth stages, and cultivars.

In plants, water-soluble N (N_w), SDS (detergent)-soluble N (N_s), SDS (detergent)-insoluble N ($N_{in\text{-}SDS}$), and non-protein N (N_{np}) are commonly distributed distinct N morphologies (Liu et al., 2018). Each of these N morphologies plays a specific role within plant leaves; for example, N_w primarily facilitates photosynthesis and storage functions (Qiang et al., 2023), N_s is predominantly linked to photosynthesis including electron transfer and light capture (Viola et al., 2022), $N_{in\text{-}SDS}$ is primarily present in cell wall proteins, which are assumed to contribute to the mechanical toughness of leaves and DNA integrity (Evans and Seemann, 1989; Takashima et al., 2004; Liu et al., 2018, 2023), and N_{np} is primarily involved in coordinating leaf expansion and photosynthetic activities (Liu et al., 2018).

Furthermore, the intricate relationship between N allocation and various agronomic measures, particularly N application, has been highlighted as the primary determinant of N distribution in leaves (Tian et al., 2023). High N application has been linked to increased N_s and N_w distributions in soybean and oilseed rape plants, which improves electron transfer, light capture, and overall plant growth (Qiang et al., 2023). It has been reported that increased N application could enhance the light-capturing ability of *Panax notoginseng* by optimizing the distribution of N_s (Cun et al., 2021). Comprehensive research is crucial for fully understanding the implications of N allocation across various plant organs, particularly at different growth stages and among different cultivars.

The influence of N morphology varied significantly across different growth stages. In earlier growth stages, a greater ratio of N_{np} has been observed to promote leaf development, whereas this ratio decreases during later growth stages when leaf expansion ceases (Liu et al., 2018). Qu et al. (2022) highlighted a decline in N_s and $N_{in\text{-}SDS}$ during the flowering to early fruiting stages compared to the seedling stages of cucumbers, indicating a dynamic beneficial impact of these N morphologies during the seedling stages, but adverse effects during the early fruiting stages. Similarly, N allocation also determined the distinct characteristics of cultivars; among different cultivars of pecans, the greater ratio of N_s and N_w in the cultivar YLC35 promoted greater photosynthetic N-use efficiency (Xu et al., 2022), which benefited the growth of plants (Qiang et al., 2023). Conversely, a greater ratio of $N_{in\text{-}SDS}$ in two different N environments adversely affected photosynthesis and respiration abilities in two canola plant cultivars (Liu et al., 2023). Our previous research also indicated that greater proportions of N_w and N_s can enhance N use efficiency, thereby benefiting both biomass and N accumulation (Li et al., 2023).

Understanding N accumulation and growth in tobacco is of utmost importance, considering its significant role in the rural economy of China (Sun et al., 2020). The present study primarily focused on N allocation in leaves, with limited insights into N distribution across different plant organs, morphological variations, and implications for crop growth and development under varying N conditions, growth stages, and cultivars (Hongda and K326). However, long-term unscientific fertilization not only affects yield but also seriously impacts the fragile ecological environment. This study aimed to bridge the existing knowledge gaps by investigating the relationships between N allocation and N and biomass accumulation across different plant organs in flue-cured tobacco cultivars at different growth stages (with a particular emphasis on the Hongda variety, which consistently accumulates more N and biomass under the same N application) under various treatments and at different growth stages. This study aimed to provide valuable insights for optimizing N fertilizer application, producing high-yield flue-cured tobacco leaves and reducing the ecological footprint.

Abbreviations: N, Nitrogen; N_w, Water-soluble nitrogen; N_s, SDS (detergent)-soluble nitrogen; $N_{in\text{-}SDS}$, SDS (detergent)-insoluble nitrogen; N_{np}, Non-protein nitrogen.

2 Materials and methods

2.1 Experimental site

The study was conducted during two growing seasons from May to September 2021 and 2022 in Yongping County, Dali Prefecture (25.6065°N, 100.2676°E), Yunnan, China. The area receives an average annual precipitation of approximately 919.0 mm and an average temperature of 16.7°C. The soil at the research site was classified as loam and had the following basic physical and chemical properties: 36.58 g kg^{-1} organic matter, 1.95 g kg^{-1} total nitrogen, 0.82 g kg^{-1} total phosphorus, 17.88 g kg^{-1} total potassium, 233.10 mg kg^{-1} available nitrogen, 49.34 mg kg^{-1} available phosphorus, and 236.00 mg kg^{-1} available potassium.

2.2 Experimental design and conditions

In an open-field pot experiment, we aimed to assess the impact of different N fertilizer application rates on N efficiency in two flue-cured tobacco cultivars (Hongda and K326). Seedlings of the tobacco cultivars Hongda and K326 were transplanted into pots (25 cm × 24 cm), each containing 15 kg of loam soil. To ensure adequate soil moisture, each pot was irrigated with 1,000 mL of water thrice a week. Pots were strategically positioned in the field, maintaining a plant × row spacing of approximately 110 cm × 55 cm, which is consistent with a planting density of 16,500 plants per hectare (Cai et al., 2021). Each treatment consisted of three biological replicates, with 30 plants per cultivar within each replicate. Experiments were performed under three different application rates of N fertilizer (Table 1). Fertilizers were applied as base and top dressings according to standards for tobacco production (Ahmed et al., 2022). At the time of transplantation, the following percentages of fertilizer were added: 80% N, 100% P, and 80% K. Twenty-one days after transplantation, the remaining 20% of the estimated N and K were applied as a top dressing. All management practices were performed according to the guidelines outlined in China's National Standards for the Tobacco Industry (Li et al., 2022).

2.3 Harvesting and sample analysis

Samples were collected at 25, 50, 75, 100, and 125 days after transplantation of tobacco seedlings. After being harvested, the tobacco plants were divided into five distinct parts: roots, stems, lower leaves, middle leaves, and upper leaves. Three tobacco plants per replicate were uprooted for each treatment at each growth stage. To remove excess soil, the plants were thoroughly rinsed with running water, as described by Hu et al. (2021). The fresh and dry weights of each plant part were recorded before and after curing. To ensure consistency, each plant part was dried at 105°C for 30 min, followed by drying at 75°C for 72 h as part of the curing process. Each dried plant part was sieved through a 2-mm mesh sieve before being crushed and digested with H_2SO_4-H_2O_2. According to the method outlined by Liu et al. (2018), the total N content of the digested plant material was determined through continuous flow analysis using an AA3 instrument (Seal Analytical Inc., Southampton, UK).

2.4 Nitrogen morphologies in tobacco

The N morphologies were assessed in frozen samples according to Takashima et al. (2004). Nitrogen was divided into four morphologies: water-soluble (N_w), non-protein nitrogen (N_{np}), SDS (detergent)-soluble nitrogen (N_s), and SDS (detergent)-insoluble nitrogen ($N_{in\text{-}SDS}$). One gram of each plant part, including leaves, roots, and stems, was cryogenically frozen in liquid N and subsequently homogenized with 1 mL of 100 mM sodium phosphate buffer [comprising 2 mM $MgCl_2$, 0.4 M d-sorbitol, 5 mM dithiothreitol (DTT), 5 mM iodoacetate, 10 mM NaCl, and 5 mM phenylmethylsulfonyl fluoride]. The supernatant N_w was separated by centrifuging at 12,000 × *g* at 4°C for 10 min. The residual samples were dissolved in 1 mL of phosphate buffer (containing 3% SDS) for 5 min at 90°C and then centrifuged at 5,500 × *g* for 8 min to collect the supernatant as N_s. The $N_{in\text{-}SDS}$ residues were purified by washing with anhydrous ethanol (20 mL) and filtered through medium-speed quantitative filter paper. The supernatant was mixed with an equal volume of 20% trichloroacetic acid, filtered through medium-speed quantitative filter paper, and thoroughly rinsed with anhydrous ethanol (20 mL) to denature the N compounds. Three distinct N morphologies were determined from the residue on the quantitative filter paper after natural air-drying and subsequent digestion using H_2SO_4-H_2O_2 following Thomas's method (Thomas et al., 1967). The N content of the digested solution was determined using continuous flow analysis (AA3; Seal Analytical Inc., Southampton, UK). The N_{np} content was calculated by subtracting the values of N_w, N_s, and $N_{in\text{-}SDS}$ from the total N content. Percentage of each N morphologies in each organs were calculated using the following equation:

$$\text{Each N morphologies in leaves (\%)} = \frac{\text{The content of each N morphologies in leaves} * \text{Biomass of leaves}}{\text{The total nitrogen accumulation of whole plant (sum of leaves, stems and roots)}} * 100\%$$

The calculation of N morphology in stems and roots was similar to that for leaves.

2.5 Statistical analysis

The data were statistically analyzed using SPSS (version 23.0; Armonk, NY, USA) for *Z* score, curve fitting analysis, and analysis of variance (two-way ANOVA). To evaluate significant differences between treatments, the least significant difference (LSD) test was applied, with significance set at $p < 0.05$. Graphical representations were created using OriginLab Version 2022 (Northampton, MA, USA) and further refined and compiled using Adobe Illustrator Version 2019 (San Jose, CA, USA).

3 Results

3.1 Nitrogen accumulation in the leaves of tobacco cultivars at different growth stages under different rates of N application

Figure 1 shows that higher levels of N application led to increased N accumulation in tobacco leaves during 125 d of

TABLE 1 Experimental conditions under different application rates of nitrogen fertilizer.

Treatments	Cultivars	N application per plant	P application per plant	K application per plant
CK	Hongda	No N fertilizer	2.5 g	10 g
	K326	No N fertilizer	2.5 g	10 g
T1	Hongda	4 g	2.5 g	10 g
	K326	4 g	2.5 g	10 g
T2	Hongda	8 g	2.5 g	10 g
	K326	8 g	2.5 g	10 g

N, nitrogen; P, phosphorus; K, potassium.

growth after transplantation in 2021 (Figure 1A) and 2022 (Figure 1B). During the initial 50 d following transplantation, CK exhibited 18.80% and 32.38% greater N accumulation in tobacco leaves than treatments T1 and T2, respectively, indicating that lower N application resulted in greater N accumulation during the early growth stages. However, at 75 d, higher levels of N application increased N accumulation in tobacco leaves, highlighting the dynamic response of tobacco plants to varying N levels at different growth stages. Additionally, at 125 d, N accumulation in CK was 63.36% and 45.65% lower than N accumulation in T1 and T2, respectively. The Hongda cultivar, known for its superior N efficiency, displayed 15.25% higher N accumulation in leaves than the K326 cultivar.

3.2 Biomass accumulation in tobacco leaves at different growth stages under different rates of N application

Figure 2 shows a strong correlation between N application and biomass accumulation in tobacco leaves in 2021 (Figure 2A) and 2022 (Figure 2B). This trend is closely correlated with the pattern observed for N accumulation in tobacco leaves. Higher levels of N application corresponded to increased tobacco leaf biomass, particularly at 125 d after transplantation. During the initial stages of tobacco growth (0–50 days after transplanting), CK exhibited 37.89% and 85.93% more biomass accumulation compared to T1 and T2 treatments, respectively. After 75 d of transplantation, higher levels of N application led to increased tobacco leaf biomass production. However after 125 d of transplantation, CK accumulated 56.25% and 44.07% lower biomass than T1 and T2, respectively. Moreover, the Hongda cultivar exhibited 18.23% greater tobacco leaf biomass production than the K326 cultivar under similar treatment conditions in both 2021 and 2022.

3.3 Variations in allocation ratios of different nitrogen morphologies in tobacco leaves at different growth stages under different N fertilizer treatments

The different application levels of N fertilizer at various growth stages across the two tobacco cultivars differently induced the distribution of various nitrogen morphologies within the tobacco plant parts (Table 2). A notable trend was observed throughout an extensive 2-year study: $N_{\text{in-SDS}}$ levels in tobacco leaves decreased with increased N application. Conversely, there was an overall increase in the levels of N_w, N_s, and N_{np} in the tobacco leaves in response to augmented N application. As the growth of the tobacco plants progressed, a noticeable decrease in the ratio of $N_{\text{in-SDS}}$ was observed, whereas the N_s and N_{np} ratios consistently increased. The Hongda cultivar exhibited greater ratios of N_w and N_s in leaves as compared to K326, but showed lower levels of N_{np}.

3.4 Variations in the ratios of different nitrogen morphologies in tobacco roots at various growth stages under different N fertilizer treatments

Different N application levels, growth stages, and cultivars led to distinct alterations in the distribution of nitrogen morphologies within tobacco roots (Table 3). Over 2 years, a collective decrease in the ratios of N_w, N_s, and N_{np} in tobacco roots was observed in response to increasing N application. Simultaneously, the proportion of $N_{\text{in-SDS}}$ decreased as the tobacco plants grew. In comparison to K326, the roots of the Hongda cultivar contained lower proportions of both $N_{\text{in-SDS}}$ and N_{np}.

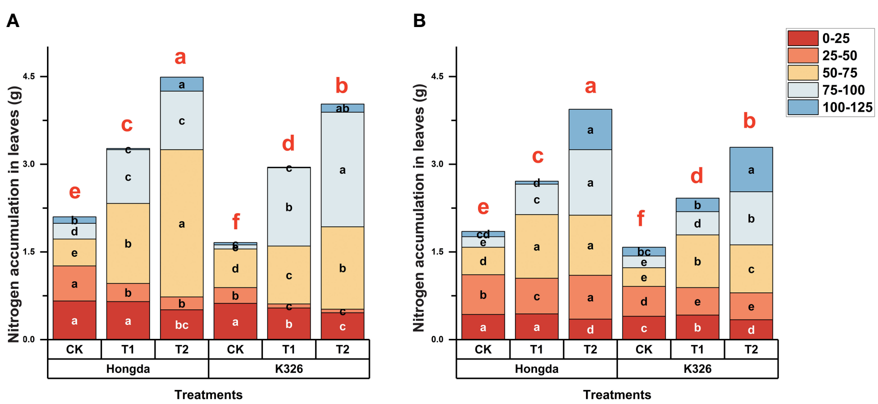

FIGURE 1
Stacked bar charts illustrating nitrogen accumulation in tobacco plants at different time intervals (0–25 d, 25–50 d, 50–75 d, 75–100 d, and 100–125 d) after transplantation. Here, control (CK): no N fertilizer (0 g/plant), medium (T1): 4 g/plant of pure N, and high (T2): 8 g/plant of pure N. The different colors represent the N accumulation at different growth stages. The total height of the bar demonstrates the difference in N accumulation at 125 d after transplanting. Lowercase letters within the same growth stage indicate significant differences among treatments according to the least significant difference test (LSD, $p < 0.05$). Specifically, after 125 days of transplantation, the significant differences among treatments are indicated by red lowercase letters above the bar chart (LSD; $p < 0.05$). **(A, B)** represent the results for 2021 and 2022, respectively.

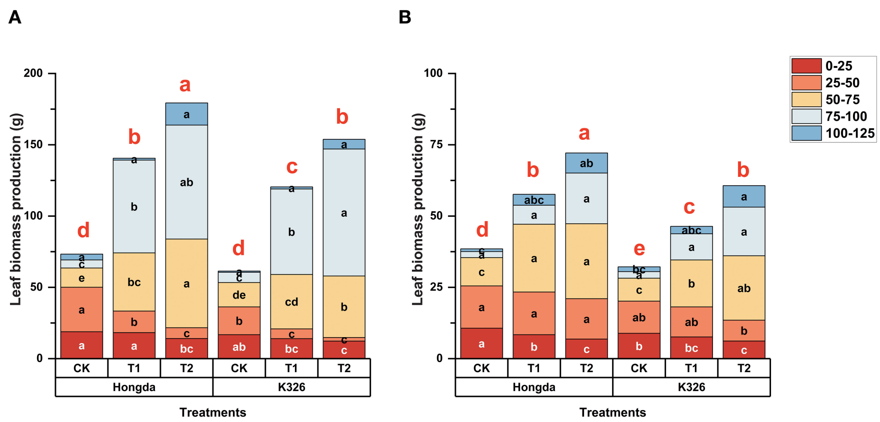

FIGURE 2
Stacked bar charts illustrating biomass accumulation in tobacco plants at different time intervals (0–25 d, 25–50 d, 50–75 d, 75–100 d, and 100–125 d) after transplantation. Here, control (CK): no N fertilizer (0 g/plant), medium (T1): 4 g/plant of pure N, and high (T2): 8 g/plant of pure N. The different colors represent the N accumulation at different growth stages. The total height of the bar demonstrates the difference in N accumulation at 125 d after transplantation. Lowercase letters within the same growth stage indicate significant differences among treatments according to the least significant difference test (LSD, $p < 0.05$). Specifically, after 125 days of transplantation, the significant differences among treatments are indicated by red lowercase letters above the bar chart (LSD; $p < 0.05$). **(A, B)** represent the results for 2021 and 2022, respectively.

3.5 Variations in the ratios of different nitrogen morphologies in the stem at various growth stages of tobacco plants under different treatments

The influence of N application, growth stage, and cultivar on the distribution of nitrogen morphologies within tobacco stems was apparent (Table 4). The analysis revealed a pronounced decline in the proportions of N_{np}, N_w, and N_s with increasing N application levels. Similarly, the ratio of N_{np} in the stems consistently decreased as the tobacco plants developed. Significant disparities between Hongda and K326 were noted, with Hongda demonstrating greater ratios of N_w and N_s in stems but lower proportions of N_{np} than K326.

3.6 Nitrogen distribution influences nitrogen accumulation in tobacco plants

To explore how various N morphologies affect N and biomass accumulation in flue-cured tobacco, we conducted a standardized data analysis using the Z score method (Supplementary Tables 1–4). A subsequent investigation into the influence of different N morphologies on N accumulation in flue-cured tobacco leaves (Figure 3; Table 5) indicated that increased proportions of N_w in leaves were associated with an increase in overall N accumulation. Moreover, greater proportions of $N_{in\text{-}SDS}$ in leaves and N_{np} in roots are linked to a reduction in overall N accumulation. A quadratic function accurately described the relationship between N_w and N accumulation in leaves, shedding light on the intricate dynamics. Notably, cubic curves accurately represented the relationship between N_{np} and N accumulation in roots, revealing a complex and nonlinear association between these factors. Similarly, the correlation between $N_{in\text{-}SDS}$ in leaves and N accumulation was effectively characterized by an exponential function, highlighting the intricate and nonlinear interplay between these variables. These findings underscore the multifaceted interactions between different N morphologies and biomass accumulation in flue-cured tobacco leaves, providing valuable insights into the underlying mechanisms that influence crop growth and development.

3.7 Effect of N distribution on biomass accumulation in tobacco plants

It became apparent that the presence of $N_{in\text{-}SDS}$, N_w, and N_{np} in roots and N_{np} in leaves hindered the accumulation of biomass in tobacco leaves (Figure 4; Table 6). Notably, the inhibitory effects of $N_{in\text{-}SDS}$ and N_{np} on roots and N_{np} on leaves did not follow a linear pattern despite their increasing proportions. Specifically, the relationship between $N_{in\text{-}SDS}$ in roots and biomass accumulation in leaves can be described as a cubic function, highlighting the intricate interplay between these variables. Similarly, the relationship between N_w in roots and N accumulation in leaves followed a linear function. Additionally, the association between N_{np} in roots and biomass accumulation in leaves can be described as a quadratic function, suggesting a complex interplay between these variables. Finally, the relationship between N_{np} and biomass accumulation in leaves can be described as a quadratic function, indicating a complex and nonlinear association between these factors. These functional relationships provide valuable insights into the dynamics of biomass distribution and accumulation in flue-cured tobacco leaves.

4 Discussion

Nitrogen (N) is a critical factor for the growth and development of plants and influences various metabolic functions and cellular processes that ultimately determine crop yield (Song et al., 2022).

10.3389/fpls.2024.1377364

TABLE 2 Allocation ratios of different nitrogen morphologies in tobacco leaves at different growth stages under various treatments.

Days after transplanting	Cultivars	Treatments	2021				2022			
			$N_{in\text{-}SDS}$ (%)	N_w (%)	N_s (%)	N_{np} (%)	$N_{in\text{-}SDS}$ (%)	N_w (%)	N_s (%)	N_{np} (%)
25	Hongda	CK	4.32a	53.37a	18.58b	13.76bc	12.80a	19.81a	37.74a	1.32d
		T1	10.81a	47.89a	26.24a	5.77c	10.39a	17.58a	34.50a	11.32c
		T2	6.50a	49.00a	19.93b	17.84bc	10.98a	15.50a	25.99b	22.74b
	K326	CK	15.30a	20.54b	12.31d	41.30a	13.92a	16.44a	35.30a	8.19cd
		T1	14.44a	32.22b	16.88bc	26.40b	11.79a	9.31b	32.39ab	24.35b
		T2	9.56a	20.47b	13.42cd	45.75a	11.09a	9.49b	19.02c	38.63a
50	Hongda	CK	7.22b	40.93abc	12.73a	16.19ab	14.56bc	21.85a	20.96bc	7.20c
		T1	6.90b	54.40a	10.73a	4.11ab	14.10bc	24.64a	23.18ab	3.85c
		T2	11.09ab	37.02bc	12.28a	21.94a	12.80c	22.14a	26.36a	6.53c
		CK	15.92a	41.21abc	13.48a	2.90b	12.51c	16.10b	18.13cd	18.22a
		T1	13.15ab	51.34ab	11.98a	1.68b	16.69b	22.11a	18.73bcd	13.86ab
		T2	10.37ab	37.03c	12.67a	16.75a	25.06a	16.98b	16.06d	8.68bc
75	Hongda	CK	2.49cd	27.77c	13.87b	8.29bc	17.75bc	20.44a	19.80a	11.57b
		T1	1.14d	37.59b	20.74a	1.29c	19.38b	17.46bc	18.41ab	7.43b
		T2	6.83bc	45.22a	12.98b	17.30b	7.62d	25.57a	20.23a	8.17b
	K326	CK	14.02a	24.23c	11.16bc	3.04bc	23.22a	18.32ab	16.20ab	9.43b
		T1	11.59ab	30.35c	14.63b	3.99bc	18.43bc	15.12c	16.33ab	20.37a
		T2	8.52ab	26.21c	8.32c	30.50a	16.43c	19.12ab	14.74b	14.00b
100	Hongda	CK	8.60a	21.53c	14.58a	4.99a	22.14b	19.57ab	15.66b	9.83b
		T1	8.79a	34.39ab	15.65a	4.22a	15.30c	21.88a	15.55b	8.43b
		T2	7.68a	38.40a	14.22a	11.14a	14.43c	22.83a	20.60a	2.94c
	K326	CK	8.96a	19.99c	12.58a	3.69a	22.41b	15.40c	13.33c	14.63a
		T1	10.86a	28.39bc	13.93a	8.52a	32.78a	16.34bc	13.42c	4.28c
		T2	8.13a	31.60ab	14.67a	13.09a	24.12b	20.35a	13.73c	3.85c

Control (CK): no N fertilizer (0 g/plant), medium (T1): 4 g/plant of pure N, and high (T2): 8 g/plant of pure N. Different lowercase letters within a column show the significant difference among treatments according to the least significant difference test (LSD; $p < 0.05$). $N_{in\text{-}SDS}$, SDS-insoluble nitrogen; N_s, SDS-soluble nitrogen; N_w, water-soluble nitrogen; and N_{np}, non-protein nitrogen.

TABLE 3 Allocation ratios of different nitrogen morphologies in tobacco roots at different growth stages under various treatments.

Days after transplanting	Cultivars	Treatments	2021				2022			
			$N_{in\text{-}SDS}$ (%)	N_w (%)	N_s (%)	N_{np} (%)	$N_{in\text{-}SDS}$ (%)	N_w (%)	N_s (%)	N_{np} (%)
25	Hongda	CK	0.72ab	3.35a	0.94a	1.40b	0.35b	6.86a	4.49a	5.16c
		T1	0.69ab	2.70ab	0.69abc	1.16b	0.38b	4.23c	3.34b	5.58c
		T2	0.33b	0.83d	0.37c	2.28ab	0.46b	5.70b	3.66ab	1.88d
	K326	CK	0.76ab	1.89bc	0.55bc	2.31ab	0.40b	4.31c	2.09c	10.20a
		T1	0.43ab	1.41cd	0.54bc	3.34a	0.39b	2.21d	1.21c	9.01ab
		T2	0.86a	2.86a	0.70ab	2.16ab	1.41a	3.51c	1.22c	7.64b
50	Hongda	CK	3.29b	4.30b	2.65a	0.86c	0.12d	5.25b	3.29a	0.23e
		T1	2.11d	3.17c	0.84c	1.86b	0.14cd	5.54a	2.14c	0.18e
		T2	2.36cd	3.28bc	1.84ab	0.32c	0.27bcd	1.55f	2.50b	0.39d
	K326	CK	5.23a	6.15a	2.47a	0.82c	0.32bc	2.89d	1.27d	5.22a
		T1	3.06bc	4.49b	1.87ab	1.75b	0.40b	3.54c	0.62e	4.09b
		T2	3.29b	3.77bc	1.44bc	4.25a	4.64a	2.34e	2.14c	0.92c
75	Hongda	CK	3.47ab	10.33ab	4.68a	9.08a	0.88c	4.18a	2.49a	0.20c
		T1	3.96a	9.04abc	3.48bc	4.29b	0.58cd	3.03b	1.62b	0.11c
		T2	1.52d	5.21c	1.24e	2.63b	0.08d	1.48d	0.84c	0.14c
	K326	CK	3.88ab	12.62a	3.82b	9.46a	3.64a	2.51c	0.79c	1.12a
		T1	2.32cd	8.18bc	2.76d	8.97a	2.16b	1.88d	0.90c	1.03a
		T2	2.70bc	8.77abc	2.99cd	5.81ab	3.20a	1.78d	0.54d	0.56b
100	Hongda	CK	2.09bc	9.42ab	2.84a	11.19a	1.04d	3.37a	2.33b	0.24bc
		T1	2.76b	9.67a	3.21b	1.35b	1.20d	3.52a	2.86a	0.08c
		T2	1.39c	4.02c	1.58c	1.22b	0.33e	2.11b	1.12d	0.17bc
	K326	CK	5.14a	9.01ab	4.53b	9.22a	1.91c	2.04b	1.69c	2.30a
		T1	4.73a	7.27abc	3.04b	1.22b	2.69b	1.23c	1.31d	0.46b
		T2	2.99b	4.77bc	1.94c	2.15b	3.01a	1.74b	1.06d	0.49b

Control (CK): no N fertilizer (0 g/plant), medium (T1): 4 g/plant of pure N, and high (T2): 8 g/plant of pure N. Different lowercase letters within a column show the significant difference among treatments according to the least significant difference test (LSD; $p < 0.05$). $N_{in\text{-}SDS}$, SDS-insoluble nitrogen; N_s, SDS-soluble nitrogen; N_w, water-soluble nitrogen; and N_{np}, non-protein nitrogen.

TABLE 4 Allocation ratios of different nitrogen morphologies in stems at different growth stages and under various treatments of tobacco plants.

Days after transplanting	Cultivars	Treatments	2021				2022			
			$N_{in\text{-}SDS}$ (%)	N_w (%)	N_s (%)	N_{np} (%)	$N_{in\text{-}SDS}$ (%)	N_w (%)	N_s (%)	N_{np} (%)
25	Hongda	CK	0.83a	1.66ab	0.73a	0.34c	0.38d	6.24b	4.46b	0.39d
		T1	0.78ab	1.96a	0.94a	0.38c	0.48cd	8.23a	3.46c	0.52d
		T2	0.38c	1.02c	0.30b	1.22b	2.18b	4.55c	5.54a	0.81cd
	K326	CK	0.79ab	1.45bc	0.58ab	2.20a	0.69c	2.65d	1.53e	4.29a
		T1	0.92a	1.66ab	0.63ab	1.13b	0.40d	4.26c	1.42e	3.25b
		T2	0.54bc	1.10c	0.29b	2.29a	2.53a	1.33e	2.85d	1.27c
50	Hongda	CK	2.70a	6.58a	1.86ab	0.68d	1.00c	13.83a	7.18b	4.53b
		T1	1.98ab	6.25a	2.31a	5.36b	0.71c	15.56a	6.92b	3.04b
		T2	0.48c	1.49c	0.34c	7.55a	2.25b	10.88b	11.17a	3.16b
	K326	CK	2.19a	4.37b	1.74ab	3.51c	0.77c	4.83d	3.58c	16.16a
		T1	0.98bc	2.42c	0.83bc	6.45ab	0.40c	9.04bc	3.04c	7.49b
		T2	1.05bc	2.30c	0.87bc	6.23b	5.04a	7.55cd	7.06b	3.53b
75	Hongda	CK	0.71b	6.45a	2.24a	10.62b	5.87a	10.57a	3.44ab	2.80c
		T1	0.47b	3.24bc	1.22b	13.54a	4.86ab	12.71a	5.23a	9.19b
		T2	0.63b	1.39d	0.62cd	4.45c	3.72ab	12.87a	4.58a	14.69ab
	K326	CK	1.21a	4.71b	1.44b	10.42b	2.23b	3.01b	1.42c	18.12a
		T1	0.85b	1.39d	0.48d	14.48a	1.99b	5.87b	2.17bc	13.75ab
		T2	0.58b	2.61cd	0.80c	2.19d	1.66b	6.04b	2.02bc	19.92a
100	Hongda	CK	2.43a	7.69a	3.41a	11.24c	4.13bc	7.90b	4.46b	9.32c
		T1	1.23bc	3.71b	1.44c	13.55bc	6.02a	15.87a	5.54b	3.75d
		T2	0.49c	2.96b	1.02c	15.87ab	4.07bc	15.36a	7.35a	8.70c
	K326	CK	1.93ab	5.87ab	2.48b	16.58ab	2.34d	2.92c	2.27c	18.76a
		T1	0.46c	2.87b	1.03c	17.68a	2.68cd	6.77b	2.62c	15.42ab
		T2	0.56c	3.01b	0.95c	16.13ab	4.20b	9.50b	4.87b	13.09b

Control (CK): no N fertilizer (0 g/plant), medium (T1): 4 g/plant of pure N, and high (T2): 8 g/plant of pure N. Different lowercase letters within a column show the significant difference among treatments according to the least significant difference test (LSD; $p < 0.05$). $N_{in\text{-}SDS}$, SDS-insoluble nitrogen; N_s, SDS-soluble nitrogen; N_w, water-soluble nitrogen; and N_{np}, non-protein nitrogen.

10.3389/fpls.2024.1377364

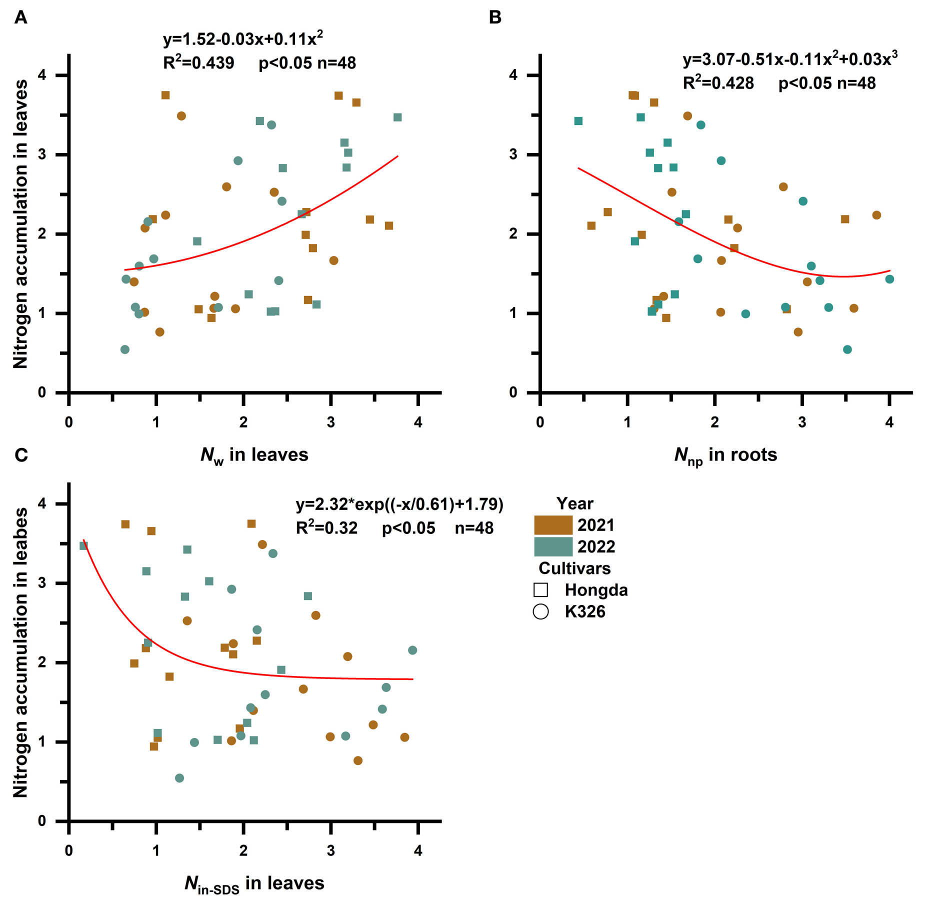

FIGURE 3
Scatterplot with fit curve illustrates the effects of different distributions of nitrogen morphologies on leaf nitrogen accumulation (*Z* score). $N_{in\text{-}SDS}$, SDS-insoluble nitrogen; N_s, SDS-soluble nitrogen; N_w, water-soluble nitrogen; and N_{np}, non-protein nitrogen. **(A–C)** represent the relationship between N_w in leaves, N_{np} in roots, and $N_{in\text{-}SDS}$ in leaves in relation to the nitrogen accumulation of the leaves, respectively.

Despite the fact that extensive studies demonstrated the role of N in plants and its impact on plant growth (Moose and Below, 2009), the specific distribution of N morphologies across different plant organs and their influence on N and biomass accumulation under varying N application levels, growth stages, and cultivars remain poorly understood. Thus, the present study aimed to investigate the effects of various N fertilizer applications on two distinct cultivars, highlighting their varied N and biomass accumulation capabilities at different growth stages over 2 years (2021 and 2022).

Liu et al. (2018) and Ghafoor et al. (2021) emphasized the profound impact of N fertilizer application on N and biomass accumulation in tobacco leaves. Our study revealed that treatments T1 and T2 significantly increased N and biomass accumulation in both cultivars compared to those in plants without N fertilizer treatment (CK). Specifically, compared with the CK, treatments T1 and T2 resulted in notable increases in N accumulation of 58.03% and 118.97%, respectively. Similarly, T1 and T2 significantly enhanced biomass accumulation by 77.59% and 126.86%, respectively, indicating the positive influence of N application on tobacco growth. The findings suggested that the biomass and N accumulation followed the "S model" (Yang et al., 2012). The N and biomass accumulation rate initially increased and then decreased. Under CK, compared with those under T1 and T2, an increasing trend were observed at 50 d after transplanting, possibly due to the inhibition resulting from a high-N environment (Xun et al., 2020; Wang et al., 2022a). However, after 75 d, increased N application

TABLE 5 Curve fitting analysis illustrates the effects of the distributions of different nitrogen morphologies on nitrogen accumulation in leaves ((Z score+2).).

Independent variable	Mode	Relationship	R^2	p	n
N_w in leaves	Quadratic	$y = 1.52 - 0.03x + 0.11x^2$	0.439	$p < 0.05$	48
N_{np} in roots	Cubic	$y = 3.07 - 0.51x - 0.11x^2 + 0.03x^3$	0.428	$p < 0.05$	48
$N_{in\text{-}SDS}$ in leaves	Exponential	$y = 2.32*\exp[(-x/0.61) + 1.79]$	0.320	$p < 0.05$	48

$N_{in\text{-}SDS}$, SDS-insoluble nitrogen; N_w, water-soluble nitrogen; and N_{np}, non-protein nitrogen.

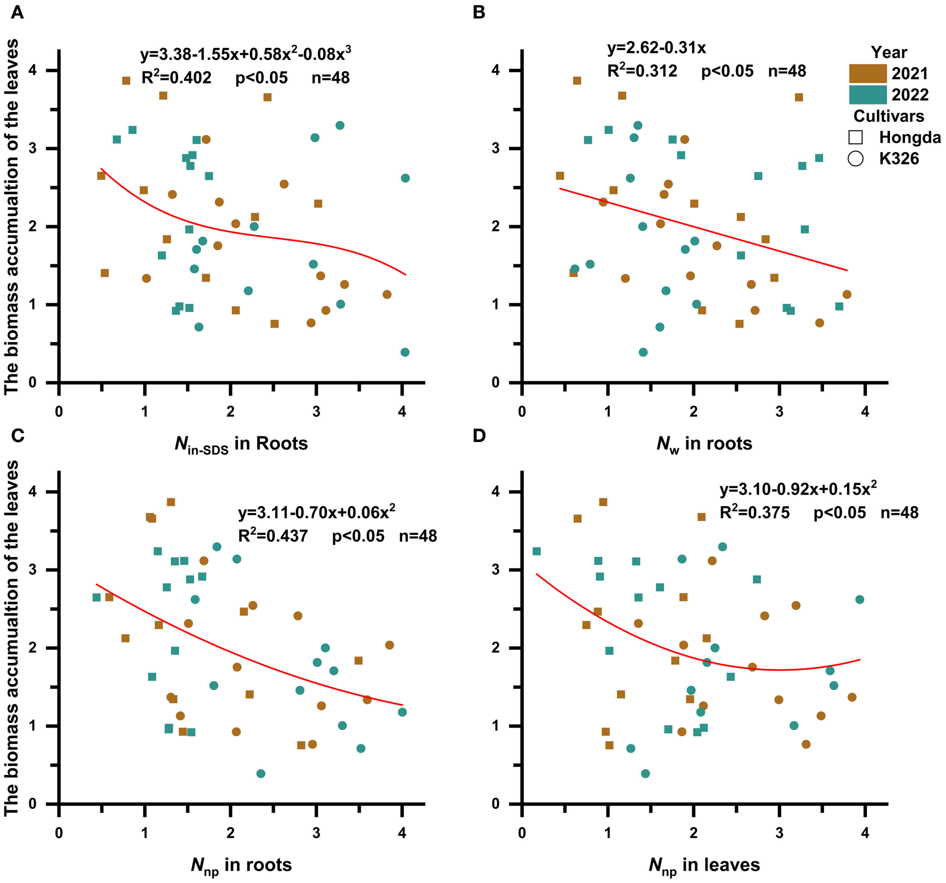

FIGURE 4
Scatterplot with fit curve illustrates the effects of the distributions of different nitrogen morphologies (*Z* score) on leaf biomass accumulation (*Z* score). $N_{in\text{-}SDS}$, SDS-insoluble nitrogen; N_w, water-soluble nitrogen; N_{np}, non-protein nitrogen. **(A–D)** represent the relationship between $N_{in\text{-}SDS}$ in roots, N_w in roots, N_{np} in roots, and N_{np} in leaves in relation to the biomass accumulation of the leaves, respectively.

led to greater N and biomass accumulation rates, ultimately resulting in greater N and biomass accumulation at 125 d after transplanting. Previous studies have emphasized significant differences in NUE among flue-cured tobacco cultivars, which are attributable to variations in their ability to absorb N and accumulate biomass under similar environmental conditions. In earlier studies, Hongda displayed a greater NUE than K326 (Parker, 2008; Liang et al., 2013; Fan et al., 2018). Compared to the K326 cultivar, the Hongda cultivar consistently exhibited enhanced N and biomass accumulation, with increases of 16.18% and 19.83%, respectively, under various treatment conditions. The superior efficiency of Hongda is consistent with earlier research findings. This study monitored the increase in N and biomass in the whole plant and its leaves every 25 d compared to the corresponding periods under CK. Hongda accumulated more biomass and N in the whole plant and leaves 0–50 days after transplanting. Moreover, Hongda plants accumulated more biomass and N under the various N fertilizer treatments at 125 d after transplanting. These results indicate that Hongda possesses greater biomass and N accumulation abilities than K326, which is consistent with previous studies (Parker, 2008; Liang et al., 2013).

In our investigation, N_w (17.5%–32.7% of the total N in the plant) was the predominant morphology in leaves (Supplementary

TABLE 6 Curve fitting analysis illustrates the effects of the distributions of different nitrogen morphologies (Z score+2) on leaf biomass production (Z score+2).

Independent variable	Mode	Relationship	R^2	p	n
$N_{in\text{-}SDS}$ in roots	Cubic	$y = 3.38 - 1.55x + 0.58x^2 - 0.08x^3$	0.402	p < 0.05	48
N_w in roots	Linear	$y = 2.62 - 0.31x$	0.312	p < 0.05	48
N_{np} in roots	Quadratic	$y = 3.11 - 0.70x + 0.06x^2$	0.437	p < 0.05	48
N_{np} in leaves	Quadratic	$y = 3.10 - 0.92x + 0.15x^2$	0.375	p < 0.05	48

$N_{in\text{-}SDS}$, SDS-insoluble nitrogen; N_w, water-soluble nitrogen; and N_{np}, non-protein nitrogen.

Figure 1A), which is consistent with earlier findings (Niinemets and Tenhunen, 1997; Takashima et al., 2004; Liu et al., 2018). N_w was found to be related to plant respiration and carboxylation. Similarly, N_s is associated with electron transport and light capture systems, accounting for 12.9%–19.6% of the total N in the whole plant, a ratio less than that of N_w, which is also in line with earlier studies (Niinemets and Tenhunen, 1997; Takashima et al., 2004; Liu et al., 2018). The proportions of $N_{in\text{-}SDS}$ and N_{np} were lower than those of N_s and N_w, and these morphologies are primarily associated with plant structural and storage functions (Liu et al., 2018). We found that stems exhibited lower N allocation compared to leaves (Supplementary Figure 1B). This distinction can be attributed to the relatively weaker respiration and photosynthetic activity observed in stems than in leaves, as previously suggested (Ávila-Lovera et al., 2017; Tokarz et al., 2021; Salomón et al., 2022). Consequently, noticeable reductions in N_w and N_s levels within the stems were observed. Remarkably, stems contain more N_{np} than other N morphologies, and N_{np} was also recognized for its significant role in plant development (Liu et al., 2018). Moreover, Fritschi et al. (2013) explained that 73%–80% of the N in the roots of soybeans was mobile, which was closely associated with yield. In our study, the mobile N highlighted by Fritschi et al. (2013) may correspond to the N_{np} form of N.

Compared to the N distribution in leaves, a greater proportion of N was allocated to N_w and N_{np} in roots (Supplementary Figure 1C). N_w in roots is mostly associated with root respiration, a critical physiological trait that contributes to root resource acquisition strategies. Similarly, root respiration, a fundamental metabolic process responsible for growth, ion mobilization and uptake, and cell maintenance through ATP production, carbon skeleton production, and redox balancing, is closely related to N absorption and biomass accumulation (Han and Zhu, 2021). Similar to N_{np} in stems, N_{np} in roots also plays a role in remobilizing N, contributing to plant growth (Fritschi et al., 2013; Liu et al., 2018). Among the different treatments, the ratios of N_w, N_s, and N_{np} in the tobacco roots decreased with increasing N application, suggesting a decrease in root respiration and storage functions, resulting in a failure to provide sufficient energy for N uptake and biomass accumulation (Han and Zhu, 2021). N_{np} in stems also decreased with increasing N application, indicating insufficient N sources available for plant growth (Ávila-Lovera et al., 2017). In leaves, $N_{in\text{-}SDS}$ decreased with increasing N application, whereas N_w and N_s increased with increasing N application, indicating that N application can promote respiration and photosynthesis and facilitate N storage for leaf expansion (Liu et al., 2018).

The distribution of N may account for the observed variation in N uptake and biomass accumulation at different growth stages. During the growth of tobacco plants, the proportion of $N_{in\text{-}SDS}$ in leaves decreased, whereas that of N_s and N_{np} increased. Initially, a greater allocation of $N_{in\text{-}SDS}$ to the leaves may facilitate the development of larger leaves, as suggested by Liu et al. (2018). As the plants matured, the increased N_s encouraged robust photosynthesis, whereas elevated N_{np} supported leaf expansion, consistent with prior research indicating rapid early-stage leaf growth, followed by deceleration in later stages (Hernández-Montes et al., 2019; He and Qin, 2020). Concurrently, the proportions of $N_{in\text{-}SDS}$ and N_{np} in the stems decreased as the tobacco plants continued to develop. Initially, a greater $N_{in\text{-}SDS}$ allocation bolstered the growth of sturdy stems, which is beneficial for overall plant development (Guo et al., 2018). Subsequently, the reduced distribution of N_{np} in stems implies a diminished capacity for stem growth, with the utilized N contributing less to storage and promoting plant growth through remobilized N, which is consistent with the findings of Darenova et al. (2020) and Liu et al. (2018). As the tobacco plants developed, the proportion of $N_{in\text{-}SDS}$ in roots decreased. Higher $N_{in\text{-}SDS}$ allocation helped tobacco establish stronger roots in the early stages. Over time, the reduced $N_{in\text{-}SDS}$ distribution in roots indicated a weakened ability of roots to grow and gradually stop, with N being used for respiration, thereby promoting N uptake (Jiang et al., 2023). Plants obtained more vital nutrient absorption abilities in the later stages than in the earlier stages (Khan et al., 2020).

Nitrogen distribution may explain the differences in N uptake and biomass accumulation among different cultivars (Li et al., 2023). The ratio of N_w and N_s in the stems and leaves of the whole plant of Hongda was greater than that in the stems and leaves of the whole plant of K326, suggesting that Hongda had greater respiration and more N sources for stem and leaf growth, contributing to different abilities of N uptake and use (Pan et al., 2016; An et al., 2019). By curve fitting analysis, we determined that $N_{in\text{-}SDS}$, N_w, and N_{np} in roots and N_{np} in leaves were the major factors contributing to biomass accumulation in leaves. N_w in leaves, N_{np} in roots, and $N_{in\text{-}SDS}$ in leaves were the main factors influencing N accumulation, ultimately determining the differences in N uptake and biomass accumulation abilities among different N applications, stages, and cultivars. N_w in leaves, N_{np} in roots, and $N_{in\text{-}SDS}$ in leaves were the primary factors influencing N accumulation. With increasing N fertilizer application, N_w in leaves increases, which enhances carboxylation and respiration and directly provides more energy for N absorption (Khan et al., 2022). The proportion of $N_{in\text{-}SDS}$ in leaves decreased with tobacco growth, promoting N uptake and accelerating N accumulation 75 days after transplanting. Hongda plants had a greater percentage of N_w in their leaves than K326 plants, which improved their photosynthetic ability and promoted N uptake (Balestrini et al., 2020; Su et al., 2020). The distribution of N_w in leaves primarily affected N accumulation at different N fertilizer application levels. In contrast, $N_{in\text{-}SDS}$ in leaves mainly influenced N accumulation in tobacco leaves at different growth stages. Moreover, N_w in leaves primarily affects the N accumulation in different tobacco cultivars. Overall, these N morphologies collectively coordinate N accumulation in tobacco leaves.

Increases in $N_{in\text{-}SDS}$, N_w, and N_{np} in roots and N_{np} in leaves were found to adversely affect biomass accumulation. Although increased N fertilizer application has exhibited adverse effects on the ratio of N_w and N_{np} in roots, inhibiting root respiration and development (Liu et al., 2018), under an abundant N environment, decreased respiration in roots results in decreased organic carbon compound consumption, which can promote biomass accumulation in tobacco leaves (Weitz et al., 2021). In contrast, N_{np} in leaves also increases with increasing N fertilizer application, which decreases the ratio of respiration and photosynthesis abilities and adversely affects leaf development (Niinemets and Tenhunen, 1997; Takashima et al., 2004; Liu et al., 2018). Among the different stages, N_{np} in leaves increased with tobacco growth during the various stages, in contrast to the results of Liu et al. (2018), which might be attributed to the focus on plant growth under low-N environments. In contrast, our study examined N allocation under different N conditions. The ratio of N_{np} in leaves increased at different stages, adversely affecting leaf growth; however, the ratio of $N_{in\text{-}SDS}$ in roots decreased with tobacco growth, promoting leaf biomass accumulation, indicating that N_{np} in leaves is more closely related to leaf biomass accumulation (Liu et al., 2018). Between Hongda and K326, $N_{in\text{-}SDS}$ and N_{np} in roots and N_{np} in leaves were lower in Hongda than in K326, thereby enhancing leaf growth under similar treatment conditions (An et al., 2019). The allocation of N_w in roots and N_{np} in leaves primarily influenced the differences in biomass accumulation among the N application levels. N_{np} in leaves primarily affects the disparities in biomass accumulation at different growth stages. Additionally, $N_{in\text{-}SDS}$ and N_{np} in roots and N_{np} in leaves contributed to determining the differences in biomass accumulation among the varieties.

5 Conclusions

Our study demonstrated significant increases in nitrogen and biomass accumulation in treatments T1 and T2 as compared to control (CK). Across various experimental conditions and growth stages, the Hongda cultivar consistently exhibited greater nitrogen and biomass accumulation than the K326 cultivar. The allocation ratios of nitrogen morphologies profoundly influence vital physiological processes such as photosynthesis and respiration, improve nitrogen absorption, and promote optimal plant growth. In response to diverse nitrogen conditions, tobacco plants adapt to these allocation ratios of nitrogen morphologies to efficiently absorb and utilize nitrogen. Hongda showed superior nitrogen use efficiency to K326, which was credited to its scientific honing strategy of allocating nitrogen. Moreover, these allocation ratios play a pivotal role in aiding nitrogen uptake and utilization and facilitating overall plant development across various growth stages. Future studies should focus on investigating the molecular mechanisms underlying nitrogen partitioning to enhance nitrogen use efficiency and plant productivity.

Data availability statement

The original contributions presented in the study are included in the article/Supplementary Material. Further inquiries can be directed to the corresponding authors.

Author contributions

SL: Conceptualization, Data curation, Investigation, Methodology, Software, Validation, Writing – original draft, Writing – review & editing. WA: Conceptualization, Data curation, Methodology, Software, Writing – original draft, Writing – review & editing. TJ: Data curation, Methodology, Software, Writing – original draft. YY: Writing – original draft, Data curation, Formal analysis. LY: Data curation, Formal analysis, Methodology, Writing – original draft. TZ: Data curation, Investigation, Software, Writing – original draft. FM: Formal analysis, Software, Validation, Writing – original draft. SAA: Writing – original, Writing - review & editing. QS: Conceptualization, Data curation, Methodology, Writing – original draft. CG: Conceptualization, Data curation, Software, Writing – original draft. ZZ: Conceptualization, Funding acquisition, Project administration, Resources, Supervision, Writing – original draft, Writing – review & editing.

Funding

The author(s) declare financial support was received for the research, authorship, and/or publication of this article. This study was financially supported by the National Key Research Plan of China (2022YFD1901504).

Acknowledgments

The authors extend their appreciation to the Researchers Supporting Project Number RSP2025R5, King Saud University, Riyadh, Saudi Arabia.

Conflict of interest

The authors declare that the research was conducted in the absence of any commercial or financial relationships that could be construed as a potential conflict of interest.

Publisher's note

Supplementary material

The Supplementary Material for this article can be found online at: https://www.frontiersin.org/articles/10.3389/fpls.2024.1377364/full#supplementary-material

References

Ahmed, W., Dai, Z., Zhang, J., Li, S., Ahmed, A., Munir, S., et al. (2022). Plant-microbe interaction: mining the impact of native Bacillus amyloliquefaciens WS-10 on tobacco bacterial wilt disease and rhizosphere microbial communities. *Microbiol. Spectr.* 10, e01471–e01422. doi: 10.1128/spectrum.01471-22

An, F., Chen, T., Li, Q. X., Qiao, J., Zhang, Z., Carvalho, L. J., et al. (2019). Protein cross-interactions for efficient photosynthesis in the cassava cultivar SC205 relative to its wild species. *J. Agric. Food Chem.* 67, 8746–8755. doi: 10.1021/acs.jafc.9b00046

Ávila-Lovera, E., Zerpa, A. J., and Santiago, L. S. (2017). Stem photosynthesis and hydraulics are coordinated in desert plant species. *New Phytol.* 216, 1119–1129. doi: 10.1111/nph.14737

Balestrini, R., Brunetti, C., Chitarra, W., and Nerva, L. (2020). Photosynthetic traits and nitrogen uptake in crops: which is the role of arbuscular mycorrhizal fungi? *Plants*. 9, 1105. doi: 10.3390/plants9091105

Cai, Q., Zhou, G., Ahmed, W., Cao, Y., Zhao, M., Li, Z., et al. (2021). Study on the relationship between bacterial wilt and rhizospheric microbial diversity of flue-cured tobacco cultivars. *Eur. J. Plant Pathol.* 160, 265–276. doi: 10.1007/s10658-021-02237-4

Cui, L., Li, D., Wu, Z., Xue, Y., Xiao, F., Gong, P., et al. (2022). Effects of combined nitrification inhibitors on soil nitrification, maize yield and nitrogen use efficiency in three agricultural soils. *PloS One* 17, e0272935. doi: 10.1371/journal.pone.0272935

Cun, Z., Zhang, J.-Y., Wu, H.-M., Zhang, L., and Chen, J.-W. (2021). High nitrogen inhibits photosynthetic performance in a shade-tolerant and N-sensitive species Panax notoginseng. *Photosynth. Res.* 147, 283–300. doi: 10.1007/s11120-021-00823-5

Darenova, E., Horáček, P., Krejza, J., Pokorný, R., and Pavelka, M. (2020). Seasonally varying relationship between stem respiration, increment and carbon allocation of Norway spruce trees. *Tree Physiol.* 40, 943–955. doi: 10.1093/treephys/tpaa039

Evans, J. R., and Seemann, J. R. (1989). The allocation of protein nitrogen in the photosynthetic apparatus: costs, consequences, and control. *Photosynthesis*. 8, 183–205.

Fan, T. F., He, M. J., Li, C. J., Shi, D. X., Yang, C., Chen, Y. Y., et al. (2018). Physiological dissection revealed that both uptake and assimilation are the major components regulating different growth responses of two tobacco cultivars to nitrogen nutrition. *Plant Biol. (Stuttg)* 20, 39–49. doi: 10.1111/plb.12642

Fritschi, F. B., Ray, J. D., Purcell, L. C., King, C. A., Smith, J. R., and Charlson, D. V. (2013). Diversity and implications of soybean stem nitrogen concentration. *J Plant Nutr*. 36, 2111–2131. doi: 10.1080/01904167.2012.748800

Ghafoor, I., Habib-Ur-Rahman, M., Ali, M., Afzal, M., Ahmed, W., Gaiser, T., et al. (2021). Slow-release nitrogen fertilizers enhance growth, yield, NUE in wheat crop and reduce nitrogen losses under an arid environment. *Environ. Sci. pollut. Res. Int.* 28, 43528–43543. doi: 10.1007/s11356-021-13700-4

Guo, Z., Liu, G., Röder, M. S., Reif, J. C., Ganal, M. W., and Schnurbusch, T. (2018). Genome-wide association analyses of plant growth traits during the stem elongation phase in wheat. *Plant Biotechnol. J.* 16, 2042–2052. doi: 10.1111/pbi.12937

Haghighi, H., Daliri, M. S., Mobaser, H. R., and Moosavi, A. A. (2011). Effect of different nitrogen and potassium fertilizer levels on quality and quantity yield of flue-cured tobacco (Coker 347). *World Applied Sci J.* 15, 941–946.

Han, M., and Zhu, B. (2021). Linking root respiration to chemistry and morphology across species. *Glob Chang Biol.* 27, 190–201. doi: 10.1111/gcb.15391

He, J., and Qin, L. (2020). Growth and photosynthetic characteristics of sweet potato (Ipomoea batatas) leaves grown under natural sunlight with supplemental LED lighting in a tropical greenhouse. *J. Plant Physiol.* 252, 153239. doi: 10.1016/j.jplph.2020.153239

Hernández-Montes, E., Tomás, M., Escalona, J. M., Bota, J., and Medrano, H. (2019). Leaf growth rate and nitrogen content determine respiratory costs during leaf expansion in grapevines. *Physiol. Plant* 165, 746–754. doi: 10.1111/ppl.12769

Hu, W., Wei, J., Di, Q., Tao, T., Zhang, J., Liu, J., et al. (2021). Flue-cured tobacco (Nicotiana tabacum L.) leaf quality can be improved by grafting with potassium-efficient rootstock. *Field Crops Res.* 274, 108305. doi: 10.1016/j.fcr.2021.108305

Jiang, Q., Lin, C., Guo, R., Xiong, D., Yao, X., Wang, X., et al. (2023). Root nitrogen uptake capacity of Chinese fir enhanced by warming and nitrogen addition. *Tree Physiol.* 43, 31–46. doi: 10.1093/treephys/tpac103

Khan, S., Amaral Júnior, A. T. D., Ferreira, F. R. A., Kamphorst, S. H., Gonçalves, G. M. B., Simone Mendonça Freitas, M., et al. (2020). Limited nitrogen and plant growth stages discriminate well nitrogen use, uptake and utilization efficiency in popcorn. *Plants* 9 (7), 893. doi: 10.3390/plants9070893

Khan, N. M., Imran, M., Ashraf, M., Arshad, H., and Awan, A. R. (2022). Oxytetracycline and ciprofloxacin antibiotics exhibit contrasting effects on soil microflora, nitrogen uptake, growth, and yield of wheat (Triticum aestivum L.). *J Soil Sci Plant Nutr*. 22, 3788–3797. doi: 10.1007/s42729-022-00927-4

Li, C., Ahmed, W., Li, D., Yu, L., Xu, L., Xu, T., et al. (2022). Biochar suppresses bacterial wilt disease of flue-cured tobacco by improving soil health and functional diversity of rhizosphere microorganisms. *Appl. Soil Ecol.* 171, 104314. doi: 10.1016/j.apsoil.2021.104314

Li, S., Ahmed, W., Zhang, T., Jiang, T., Mei, F., Shan, Q., et al. (2023). Different morphologies and functional nitrogen accumulation results in the different nitrogen use efficiency of tobacco plants. *J Plant Growth Regulation*. 42 (9), 5895–5908. doi: 10.1007/s00344-023-10975-4

Li, Y., Chang, D., Zhang, X., Shi, H., and Yang, H. (2021). RNA-Seq, physiological, and biochemical analysis of burley tobacco response to nitrogen deficiency. *Sci. Rep.* 11, 16802. doi: 10.1038/s41598-021-93363-w

Liang, T., Wang, J., Zhang, Y., Xi, J., Zhou, H., Wang, B., et al. (2013). "Spectral characteristics of tobacco cultivars with different nitrogen efficiency and its relationship with nitrogen use," In Computer and Computing Technologies in Agriculture VII: 7th IFIP WG 5.14 International Conference, CCTA 2013. Revised Selected Papers, Part II 7. (Beijing, China: Springer Berlin Heidelberg). pp. 239–246.

Liu, T., Ren, T., White, P. J., Cong, R., and Lu, J. (2018). Storage nitrogen co-ordinates leaf expansion and photosynthetic capacity in winter oilseed rape. *J. Exp. Bot.* 69, 2995–3007. doi: 10.1093/jxb/ery134

Liu, J., Zhang, K., Bi, J., Yu, X., Luo, L., and Hu, L. (2023). Mesophyll conductance and N allocation co-explained the variation in photosynthesis in two canola genotypes under contrasting nitrogen supply. *Front. Plant Sci.* 14, 1171331. doi: 10.3389/fpls.2023.1171331

Moose, S., and Below, F. E. (2009). Biotechnology approaches to improving maize nitrogen use efficiency. *Mol. Genet. approaches to maize improve*. 63, 65–77. doi: 10.1007/978-3-540-68922-5_6

Niinemets, Ü., and Tenhunen, J. (1997). A model separating leaf structural and physiological effects on carbon gain along light gradients for the shade-tolerant species Acer saccharum. *Plant, Cell Environment*. 20, 845–866. doi: 10.1046/j.1365-3040.1997.d01-133.x

Pan, S., Liu, H., Mo, Z., Patterson, B., Duan, M., Tian, H., et al. (2016). Effects of nitrogen and shading on root morphologies, nutrient accumulation, and photosynthetic parameters in different rice genotypes. *Sci. Rep.* 6, 32148. doi: 10.1038/srep32148

Parker, R. G. (2008). *Evaluation of nitrogen sources and rates on yield and quality of modern flue-cured tobacco cultivars* (North Carolina State University).

Qiang, B., Zhou, W., Zhong, X., Fu, C., Cao, L., Zhang, Y., et al. (2023). Effect of nitrogen application levels on photosynthetic nitrogen distribution and use efficiency in soybean seedling leaves. *J. Plant Physiol.* 287, 154051. doi: 10.1016/j.jplph.2023.154051

Qu, F., Peng, T., Jia, Y., Yang, M., Meng, X., Mao, S., et al. (2022). Adjusting leaf nitrogen allocation could promote photosynthetic capacity, and nitrogen accumulation in cucumis sativus L. *Environmental Experimental Botany*. 198, 104855. doi: 10.1016/j.envexpbot.2022.104855

Salomón, R. L., De Roo, L., Oleksyn, J., and Steppe, K. (2022). Mechanistic drivers of stem respiration: A modelling exercise across species and seasons. *Plant Cell Environ.* 45, 1270–1285. doi: 10.1111/pce.14246

Song, R., Ahmed, W., Tan, Y., and Zhao, Z. (2022). Different levels of nitrogen fertilizer in nursery stage positively affect the activity of defense-related enzymes and resistance of tobacco plant to phytophthora nicotianae. *Chiang Mai J. Sci.* 49, 551–564. doi: 10.12982/CMJS

Su, W., Ahmad, S., Ahmad, I., and Han, Q. J. P. (2020). Nitrogen fertilization affects maize grain yield through regulating nitrogen uptake, radiation and water use efficiency, photosynthesis and root distribution. *PeerJ*. 8. doi: 10.7717/peerj.10291

Sun, H., Sun, X., Wang, H., and Ma, X. (2020). Advances in salt tolerance molecular mechanism in tobacco plants. *Hereditas* 157, 5. doi: 10.1186/s41065-020-00118-0

Takashima, T., Hikosaka, K., and Hirose, T. (2004). Photosynthesis or persistence: nitrogen allocation in leaves of evergreen and deciduous Quercus species. *Plant Cell Environ.* 27, 1047–1054. doi: 10.1111/j.1365-3040.2004.01209.x

Thomas, R., Sheard, R., and Moyer, J. (1967). Comparison of conventional and automated procedures for nitrogen, phosphorus, and potassium analysis of plant material using a single digestion 1. *Agron. J.* 59, 240–243. doi: 10.2134/agronj1967.00021962005900030010x

Tian, G., Qin, H., Liu, C., Xing, Y., Feng, Z., Xu, X., et al. (2023). Magnesium improved fruit quality by regulating photosynthetic nitrogen use efficiency, carbon–nitrogen metabolism, and anthocyanin biosynthesis in 'Red Fuji'apple. *Front. Plant Sci.* 14, 1136179. doi: 10.3389/fpls.2023.1136179

Tokarz, K. M., Wesołowski, W., Tokarz, B., Makowski, W., Wysocka, A., Jędrzejczyk, R. J., et al. (2021). Stem photosynthesis-A key element of grass pea (Lathyrus sativus L.) acclimatisation to salinity. *Int. J. Mol. Sci.* 22 (2), 685. doi: 10.3390/ijms22020685

Viola, S., Roseby, W., Santabarbara, S., Nürnberg, D., Assunção, R., Dau, H., et al. (2022). Impact of energy limitations on function and resilience in long-wavelength Photosystem II. *Elife* 11, e79890. doi: 10.7554/eLife.79890.sa2

Wang, J., Qin, L., Cheng, J., Shang, C., Li, B., Dang, Y., et al. (2022b). Suitable chemical fertilizer reduction mitigates the water footprint of maize production: evidence from Northeast China. *Environ. Sci. pollut. Res. Int.* 29, 22589–22601. doi: 10.1007/s11356-021-17336-2

Wang, F., Wang, Q., Yu, Q., Ye, J., Gao, J., Liu, H., et al. (2022a). Is the NH(4)(+)-induced growth inhibition caused by the NH(4) (+) form of the nitrogen source or by soil acidification? *Front. Plant Sci.* 13, 968707. doi: 10.3389/fpls.2022.968707

Weitz, K. K., Smith, M. L., Hixson, K. K., Hill, E. A., Jansson, J. K., Hofmockel, K. S., et al. (2021). Real-time mass spectrometry measurements of respiration rates in biological systems. *J. Am. Soc. Mass Spectrom* 32, 648–652. doi: 10.1021/jasms.0c00251

Xu, Q., He, H., He, B., Li, T., Liu, Y., Zhu, S., et al. (2022). Nitrogen Allocation Tradeoffs Within-Leaf between Photosynthesis and High-Temperature Adaptation among Different Varieties of Pecan (Carya illinoinensis [Wangenh.] K. Koch). *Plants* 11 (21), 2828. doi: 10.3390/plants11212828

Xun, Z., Guo, X., Li, Y., Wen, X., Wang, C., and Wang, Y. (2020). Quantitative proteomics analysis of tomato growth inhibition by ammonium nitrogen. *Plant Physiol. Biochem.* 154, 129–141. doi: 10.1016/j.plaphy.2020.05.036

Yang, G., Tang, H., Tong, J., Nie, Y., and Zhang, X. (2012). Effect of fertilization frequency on cotton yield and biomass accumulation. *Field Crops Res.* 125, 161–166. doi: 10.1016/j.fcr.2011.08.008

frontiers | Frontiers in Plant Science

TYPE Original Research
PUBLISHED 03 September 2024
DOI 10.3389/fpls.2024.1437631

Check for updates

OPEN ACCESS

EDITED BY
Khurram Shahzad,
Water and Marine Sciences, Pakistan

REVIEWED BY
Xiaohui Chen,
Anhui Agricultural University, China
Shahbaz Khan,
Huazhong Agricultural University, China
Vesna Dragicevic,
Maize Research Institute Zemun Polje, Serbia

*CORRESPONDENCE
Qiuzhu Li
liqz@jlu.edu.cn
Jinhu Cui
cuijinhu@163.com

†These authors share first authorship

RECEIVED 24 May 2024
ACCEPTED 19 August 2024
PUBLISHED 03 September 2024

CITATION
Zhang L, Feng Y, Zhao Z, Cui Z, Baoyin B, Wang H, Li Q and Cui J (2024) Maize/soybean intercropping with nitrogen supply levels increases maize yield and nitrogen uptake by influencing the rhizosphere bacterial diversity of soil. *Front. Plant Sci.* 15:1437631. doi: 10.3389/fpls.2024.1437631

Maize/soybean intercropping with nitrogen supply levels increases maize yield and nitrogen uptake by influencing the rhizosphere bacterial diversity of soil

Liqiang Zhang[1†], Yudi Feng[1†], Zehang Zhao[1], Zhengguo Cui[2], Bate Baoyin[1], Hongyu Wang[1], Qiuzhu Li[1*] and Jinhu Cui[1*]

[1]College of Plant Science, Jilin University, Changchun, China, [2]Soybean Research Institute, Jilin Academy of Agricultural Sciences, Changchun, China

Introduction: Intercropping practices play a crucial role in enhancing and maintaining the biodiversity and resiliency of agroecosystems, as well as promoting stable and high crop yields. Yet the relationships between soil nitrogen, microbes, and yield in maize cultivated under maize/soybean intercropping systems remain unclear.

Methods: To fill that knowledge gap, here we collected maize rhizosphere soil at the staminate stage after 6 consecutive years of maize/soybean intercropping, to investigate how intercropping and nitrogen application rates affected nitrogen utilization by crops and soil microbial community composition and function. We also examined correlations of those responses with yields, to clarify the main ways that yield is enhanced via intercropping and by nitrogenous fertilizer gradient changes generated by different nitrogen application rates.

Results: The amount of applied fertilizer was 240 kg N ha^{-1} was best for obtaining a high maize yield and also led to the greatest nitrogen-use efficiency and bacterial diversity. Under the same N application rate, intercropping increased the maize yield by 31.17% and soil nitrogen (total, ammonium and nitrate nitrogen) by 14.53%, on average, in comparison to monocropping. The enrichment of *Gemmatimonas* and *Bradyrhizobium* significantly increased the soil nitrogen content, and a greater relative abundance of *Sphingomonas* and *Gemmatimonas* increased the maize yield, whereas enrichment of *Candidatus_Udaeobacter* and *Bradyrhizobium* decreased it. The benefits of intercropping mainly arise from augmenting the abundance of beneficial microorganisms and enhancing the efficiency of N use by crop plants.

Discussion: This study's findings are of key importance to bolster the stability of agro-ecosystems, to guide the scientific rational use of nitrogen fertilizers, and to provide a sound theoretical basis for achieving the optimal management of intensive crop-planting patterns and green sustainable development.

KEYWORDS

maize-soybean intercropping, microbial community, nitrogen fertilizer use, soil nitrogen, yield

1 Introduction

As one of the world's staple food crops, maize figures prominently in global agricultural production (Zhou and Butterbach-Bahl, 2014). However, the continuous cultivation of a single crop—i.e., monocropping or a monoculture system—can lead to declining soil quality and its greater susceptibility to pests and diseases (Du et al., 2018). Hence, it is imperative that farmers begin to scientifically and rationally apply maize/soybean intercropping planting techniques to improve their crop yields and economic benefits. Intercropping is a type of ecological agriculture that improves the accumulation of nutrients in soil for uptake by plants, to promote their growth via complementary trait advantages among different crop species (Fan et al., 2023). Proper intercropping patterns can bolster soil structure, alter soil physicochemical properties, and increase soil's nutrient contents and enzymatic activity (Secco et al., 2023). Improved soil conditions then enhance plants' growth, physiology, and nutrient uptake, leading to higher biodiversity overall, which also entails a greater overall yield of intercropping systems (Yang et al., 2020). Intercropping also enriches the diversity of soil microbial communities, improves soil health, and helps to balance beneficial microorganisms vis-à-vis harmful ones, all of which is advantageous for plant growth and development (Guo et al., 2024).

Nitrogen (N) is the most basic element of life, being a key component of proteins, nucleic acids. and other essential substances of living organisms, and thus directly involved in myriad biological processes (Bai et al., 2023). Regarding N uptake and N use in grass-bean intercropping systems, the proven benefits of maize/soybean intercropping are known to include an increased effective N content of soil and fixing of N and its transfer to grasses, thus reducing their demand for chemical N fertilizers and improving the efficiency of water use and other nutrient uses (Lu et al., 2023). In recent years, whether the N fixed by legumes can be transferred to adjacent grass crops in intercropping systems has emerged as a hot research topic (Chen et al., 2023; Liu et al., 2023). Further, intercropping with cereals can reduce the "N-deterrent" effect of chemical N fertilizers on legumes, thereby promoting legume nodulation and increasing the rate of N fixation (Xu et al., 2020). Overall, the two paramount reasons for efficient N use in grass/legume intercropping systems are "N transfer" and "N repression", with both phenomena essentially the outcome of N competition dynamics and complementarity between grass crops and legumes (Zhang et al., 2017).

A healthy soil environment underpins high and stable crop yields and is shaped by land use and land nutrition (Qi et al., 2023). One study showed that rhizosphere soil pH fell markedly in a soybean monoculture, but intercropping was able to mitigate that decline (Zaeem et al., 2019). However, intercropping has a dual effect on the organic matter content of soil. On one hand, intercropping can increase it by enhancing ecological interactions in the soil microenvironment that hasten the decomposition of plant and animal residues (Zhu et al., 2024); on the other hand, plants compete for soil nutrients, which accelerates mineralization, the decomposition of soil organic matter, and nutrient cycling, collectively reducing soil's organic matter content (Roohi et al., 2022).

In intercropping systems, competition and facilitation effects that arise between plant species often enrich the diversity of soil microbial communities and enlarge microbial populations, culminating in mutual benefits and co-promotion achieved under appropriate intercropping modes (Zhang et al., 2023). Previous research has found a substantially increased number of soil bacteria and actinomycetes, but a considerable decrease in the number of fungi under maize/soybean intercropping vis-à-vis maize monocropping (Fu et al., 2019). According to work by Tian et al. (2019), a greater relative abundance of soil beneficial bacteria belonging to dominant taxa, such as Proteobacteria and Acidobacteria, and likewise dominant fungi, namely Ascomycota and Basidiomycota, can help to augment the overall number of beneficial microbes in soil. Recently, Li et al. (2021) showed that the structure of soil microbial populations was altered in intercropped peanut and cereal crops, resulting in less bacteria that are harmful (such as *Spiroplasma*) and more bacteria that are beneficial (such as Streptomycetaceae and *Bacillus*). The above studies uncovered impacts of intercropping for improving soil microbial population types and community structure.

While those studies do provide a good summary of recent progress towards elucidating the effects of intercropping systems upon specific soil environments, the experimental methods employed tend to differ with intercropping patterns varying widely. In recent years, research on maize/soybean intercropping has focused chiefly on the relationship between light energy use and crop yield (Yao et al., 2017; Zheng et al., 2022), leaving far less known about how maize soil N use in combination with changes in the rhizosphere soil microbial community could affect their maize yield. Here we sampled maize soils at the male withdrawal stage in a continuous 6-year maize/soybean intercrop system, then quantified the use of soil nitrogen in its transformation and determined the bacterial community composition via high-throughput sequencing. This study had three objectives: (1) to quantify the effect of maize/soybean intercropping on maize soil nitrogen-use efficiency; (2) to distinguish the influential factors and mechanisms linking the maize-soybean intercropping system to soil microbial changes in the maize rhizosphere; and (3) to clarify the interactions between the soil microenvironment and maize yield under a maize/soybean intercropping system. This study provides a theoretical basis for the implementation of optimal management and environmentally sustainable development of intensive cropping systems.

2 Materials and methods

2.1 Study area

The experiment was run at the Agricultural Experimental Base of Jilin University, Changchun City, Jilin Province (125°14.23’ E, 43°56.60’ N; elevation: 245 m a.s.l). The site has a black soil type, a temperate continental semi-moist monsoon climate, with an average annual precipitation of 600–700 mm and average annual temperature of 4.6°C (max: 40°C and min: –36.5°C). The annual frost-free period lasts 140–150 days and the annual freezing period spans 150–160 days. The soil type in the field is Phaeozems (FAO-WRB classification system, 2014).Prior to the experiment, the pH value in the soil was 5.33, and it had these characteristics: organic carbon (1.37%), total nitrogen (1.41 g·kg^{-1}); total phosphorus (0.48 g·kg^{-1}) and total potassium (21.42 g·kg^{-1}).

2.2 Experimental design

This trial was established as a long-term locational trial, begun 2017. Its fertilizer application rates, and tillage practices remained consistent across all treatments from 2017 through 2023. Likewise, the same field management practices were maintained across the treatments during the fertility period in every year. While the experiment was continued from 2017 to 2023, the samples for analyses were taken in 2023 growing period. This experiment used a two-factor split-plot design, with the nitrogen supply level assigned to the main plots (blocks) and the planting mode to the subplots (strips). The maize variety used for testing was ‘Xianyu 335’ and the soybean variety was ‘Changnong 16’, both supplied by the Jilin Academy of Agricultural Sciences. Their seeds were sown on 26 April 2023, with the maize monoculture (MM) serving as the control group and intercropping of maize and soybean (IM) (maize/soybean, 2:2) set as the experimental group. Each plot was 62.4 m^2 in size and contained 12 rows of maize in the monoculture plot. The maize/soybean intercropping plot consisted of three strips: each strip was planted with two rows of maize and two rows of soybean. The row spacing was 65 cm and the planting density was 90 000 plants ha^{-1} for maize and 180 000 plants ha^{-1} for soybean (Figure 1). Fertilizer application levels were the same for the intercropping and monocropping plots, with maize receiving 0 (N0), 180 (N1), 240

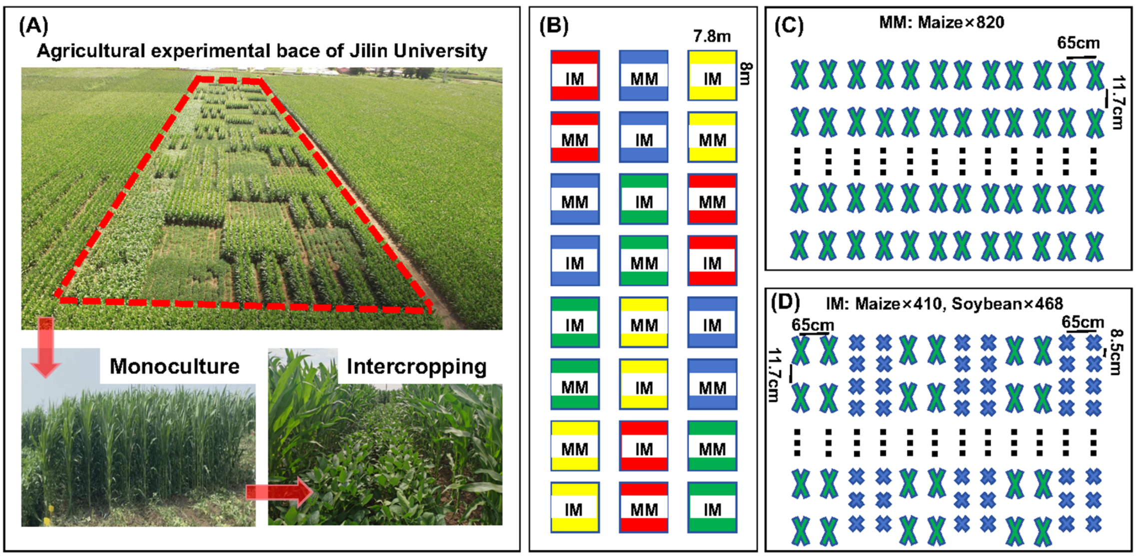

FIGURE 1
Aerial view **(A)** and schematic **(B)** layout of the maize/soybean intercropping experiment under different nitrogen application rates. In (B), red is the N0 level, blue is the N1 level, green is the N2 level, and yellow is the N3 level. **(C)** distribution of maize monoculture (MM) trial plots; **(D)** distribution of maize–soybean intercropping (IM) trial plots. where 820, 468, and 410 are the number of crop plants in the plot; 65 cm refers to the spacing between rows, while 8.5 cm or 11.7 cm is the spacing between plants within a given row.

(N2), or 300 (N3) kg N ha^{-1}. Basal fertilizer rates were 0, 40, 80, and 120 kg N ha^{-1}, with the remainder of the nitrogen fertilizer applied as a top-up fertilizer at the nodulation stage of maize. The phosphorus fertilizer consisted of heavy calcium superphosphate (P_2O_5 46%) applied at 120 kg P_2O_5 ha^{-1}; the potassium fertilizer was potassium sulfate (K_2O 50%), it applied at 100 kg K_2O ha^{-1}. Both phosphorus and potassium fertilizers were applied as basal applications.

2.3 Soil and plant sampling

Surface soil (0–20 cm depth, between adjacent maize on the ridge) and rhizosphere soil samples were collected on 21 July 2023 (at the maize staminate stage). Surface soil was sampled using a soil auger, at five points selected from each plot (in an X formation), with root samples were taken by drilling *in situ* on the ridge using an Eikelkamp root auger (auger diameter 8.0 cm, length 20.0 cm, 75% ethanol disinfection). After air-drying the soil samples indoors and passing them through a 75-mesh sieve, the ensuing fine-grained soil was used for the determination of soil chemical properties. To collect rhizosphere soil, three consecutive plants were excavated from each plot in the field, with their roots and attached soil intact. The top layer of soil was then removed; then, soil loosely bound to the root system was gently shaken and collected, and this mixed it together as a composite sample of rhizosphere soil for later testing (n = 6). All these rhizosphere soil samples were stored in a freezer at –80°C until their microbial diversity analysis. When the maize plants were mature, two rows from each plot were harvested; after threshing all their kernels, the grain weight was measured and converted to hectare yield based on the area harvested. The kernels' moisture content was recorded with a PM8188 moisture meter, for three replicates, and the final yield data then expressed as the seed (grain) weight at 14% moisture. Panicle length, ear diameter, number of grains, 100-seed weight, and barren tip size were recorded as well.

2.4 Soil and plant sampling

2.4.1 Soil nutrients

To determine soil pH and EC (electrical conductivity), a water-to-soil ratio of 5:1 was used, this shaken at 180 r/min for 5 min and allowed to stand for 30 min before taking the respective measurements with a pH meter (pH-100A,100-2000 rpm, LICHEN, Shanghai, China) and a conductivity meter (DDSJ-11A-307, YUEPING, Shanghai, China). Soil ammonium nitrogen ($NH4^+$-N) and nitrate nitrogen (NO_3^-N) fractions were extracted with sodium bicarbonate, shaken at 180 r/min for 2 h, allowed to stand for 30 min, and then filtered through a 0.45-µm PES membrane. For total soil nitrogen (TN), samples were treated with Kjeldahl digestion and filtered through a 0.45-µm PES membrane, and then measured by a continuous flow analyzer (AA3, AutoAnalyzer 3, Technician, Windows/NT) (Wang et al., 2023a). Soil total organic carbon (TOC) fractions were determined by wrapping 10-mg soil samples in aluminum foil and using an elemental analyzer (vario TOC cube, NDIR, 60 000 ppm, 2 ppb, GER) (Zhu et al., 2021).

2.4.2 Nitrogen utilization

Just before the field was harvested, five intact maize plants with uniform and typical growth were selected from each plot, and both parts oven-dried at 105°C for 30 min and then again, at 75°C, to a constant weight. After weighing the dry matter, the samples were crushed, digested with H_2SO_4-H_2O_2, and the nitrogen content of the maize plants and kernels determined using a Seal AA3 flow analyzer. Nitrogen-use efficiency (NUE) (i), nitrogen agronomic efficiency (NAE) (ii), nitrogen partial productivity (NPP) (iii) and nitrogen harvest index (NHI) (iv) were calculated as follows (Bai et al., 2024):

TABLE 1 Information on the sequencing instruments and reagents used in this study.

Types	Instruments/ Reagents	Producers	Specification/ Model/ Lot Number
Amplicon extraction	MoBio PowerSoil DNA Isolation Kit (100)	QIAGEN	100 times
Amplifier amplification	KAPA 2G Robust Hot Start Ready Mix	KAPA	
	ABI 9700 PCR	ABI	
Amplicon purification	Agencourt® AMPure® XP	Beckman Coulter	Dispense 45 mL/ bottle, total 450 mL/bottle
Amplicon building	NEBNext Ultra II DNA Library Prep Kit	NEB	96 reactions
	Agencourt® AMPure® XP	Beckman Coulter	Dispense 45 mL/ bottle, total 450 mL/bottle
	ABI 9700 PCR	ABI	
Library quality control instruments	Bioanalyzer (Agilent 2100)	Agilent	DE13806339
	Biomolecule Analyzer (Labchip GX)	PerkinElmer	
	ABI Qpcr	ABI	Step One Plus
Library quality control reagents	Agilent DNA 1000 Kit	Agilent	300 samples
	HT DNA-Extended Range LabChip	PerkinElmer	
	KAPA Library Quantification Kit	KAPA	500 times
Sequencing equipment	High-throughput second-generation sequencer	Illumina	MiSeq
Sequencing reagents	MiSeq® Reagent Kit v3 (600 cycle) (PE300)	Illumina	
	MiSeq Reagent Kit v2 (500 cycle)	Illumina	

i. NUE (%) = (N accumulation of aboveground plants in the N-applied area – N accumulation of above-ground plants in non-N applied area)/N application × 100.
ii. NAE (kg·kg^{-1}) = (seed yield in the N-applied area – seed yield in non-N applied area)/nitrogen application rate × 100.
iii. NPP (kg·kg^{-1}) = seed yield/applied nitrogen.
iv. NHI (%) = total seed N accumulation/total plant N accumulation.

2.4.3 Diversity of soil bacterial communities

Total DNA was extracted from each soil sample using a DNA kit (MN NudeoSpin 96 Soi) and the DNA concentration was then determined on a NanoDrop 2000 spectrophotometer. The PCR reaction conditions were as follows: pre-denaturation at 94°C for 5 min and then 30 cycles at 94°C for 30 s, 50°C for 30 s and 72°C for 60 s, followed by a stable extension at 72°C for 7 min, and finally stored at 4°C. The extracted genomic DNA was detected by 1% agarose gel electrophoresis. For the bacterial 16S gene, the primer pair of 338F (5'-ACTCCTACGGGAGGCAGCAG-3') and 806R (5'-GGACTACHVGGGTWTCTAAT-3') was used to amplify the V3-V4 region, and the ensuing products were purified, quantified, and standardized. Information about the hardware and software used for sequencing is presented in Table 1.

Library construction went as follows: (1) ligation of the 'Y' junction; (2) removal of junction self-associated fragments by magnetic bead screening; (3) enrichment of the library template via PCR amplification; (4) denaturation by sodium hydroxide to produce single-stranded DNA fragments.

Next, these eight sequencing steps were applied: (1) one end of the DNA fragment that is complementary to the primer base is fixed on the chip; (2) its other end randomly complementary to another primer in the vicinity is also fixed, to form a 'bridge'; (3) PCR amplification is carried out to produce DNA clusters; (4) the DNA amplicon is linearized into a single strand; (5) add the modified DNA polymerase and dNTP with four fluorescent labels, synthesizing only one base per cycle; then (6) scan the surface of the reaction plate with a laser to read the nucleotide species polymerized in the first reaction of each template sequence; (7) chemically cleave the "fluorescent group" and the "termination group" to restore the 3'-end attachment, and continue to polymerize the second nucleotide; and end by (8) counting the fluorescence signals collected in each round to obtain the sequence of the template DNA fragment (Wang et al., 2022b). All obtained sequences were deposited, and expression data uploaded to the NCBI (National Center for Biotechnology Information) (https://www.ncbi.nlm.nih.gov/) (accessed on 13 June 2024), under BioProject ID: PRJNA1132549.

2.5 Soil and plant sampling

Statistical analyses were implemented using SPSS 22.0 software to compare the effects of intercropping upon the soil response variables, using univariate two-way ANOVAs. Pearson correlations were used to evaluate the relationships between relative abundance of dominant genera, soil chemical properties, and maize yield. Beta diversity analysis was done based on the coefficient of variation of the Aitchison distance, and principal component analysis (PCA) used to compare the degree of similarity present between different samples in terms of species community diversity. The visual analysis of microbial ecological networks and derivation of topological indices were carried out in Gephi software (v0.9.6). The following topological indices were used to describe the nodes and connecting lines in the constructed microbial network: (1) the number of connecting lines of a node, which is the sum of all lines linked to each node; (2) the median centrality of a node, which is the node located on the shortest path between two nodes, this calculated according to the Formula 1 below; (3) the topological coefficient of a node, which conveys the proximity of nodes and is expressed by Formula 2 below; (4) the connecting line weight, which reflects the number of connections between a particular OTU (operation taxonomic unit) node and the sample node; (5) the connecting line centrality, a parameter that gauges the importance of each connecting line in the information transfer process of the whole network (Faust, 2021). Structural equation modeling (SEM) of the direct or indirect effects of intercropping and nitrogen application rates on yield pathways was implemented using R v4.3.1 (https://www.r-project.org/).

$$Cb(n) = \sum_{s \neq n \neq t} \left(\frac{\sigma_{st}(n)}{\sigma_{st}} \right) \quad (1)$$

In the above equation, n is the destination node; s and t are nodes in the network other than n; σ_{st} denotes the number of shortest paths from node s to node t, and the term $\sigma_{st}(n)$ denotes the number of shortest paths from node s to node t that must pass through node n.

$$T_n = \frac{avgJ_{(n,m)}}{k_n} \quad (2)$$

Here, $J_{(n,m)}$ is the number of all nodes adjacent to both nodes n and m, where the value of $J_{(n,m)}$ is increased by 1 if n is directly adjacent to m; k_n is the number of all neighbours of that node.

3 Results

3.1 Maize yield

Table 2 presents the effects from the two contrasting modes of cropping and from different nitrogen application rates on the maize yield factors. When their comparing maize yields under the same nitrogen application rates, in all cases IM (intercropping maize) > MM (monoculture maize), with maize yields at N0, N1, N2, and N3 fertilizer levels increased by 45.39%, 25.57%, 25.15% and 28.58%, respectively. From a nitrogen application perspective, the strongest yield effect occurred in going from the N0 to N1 level with an increase of 53.77% and 32.49% in MM and IM, respectively. That increase fell correspondingly to 12.31% and 12.21% at the N2 level; however, when a greater nitrogen application was used, i.e., N3

10.3389/fpls.2024.1437631

TABLE 2 Yields and yield factors of maize in response to two contrasting cropping systems (C) and four nitrogen application rates (N1–4).

Treatment		Panicle length (cm)	Barren tip (cm)	Ear diameter (cm)	Grain number	100-seed weight (g)	Yield (kg·ha^{-1})
MM	N0	14.92 ± 0.86c	2.06 ± 0.22a	4.69 ± 0.04c	405 ± 53.7d	35.24 ± 1.25d	8897 ± 602e
	N1	18.21 ± 0.53b	1.63 ± 0.34ab	4.90 ± 0.03b	575 ± 60.3bc	38.54 ± 1.04bc	13681 ± 716d
	N2	17.94 ± 0.64b	1.60 ± 0.67ab	4.79 ± 0.11bc	596 ± 79.7b	35.46 ± 0.33cd	15365 ± 494c
	N3	17.95 ± 0.43b	1.49 ± 0.49ab	4.91 ± 0.14bc	594 ± 55.9b	36.88 ± 2.20cd	14095 ± 911cd
IM	N0	17.53 ± 0.43b	1.50 ± 0.61ab	4.85 ± 0.06b	547 ± 59.5c	36.13 ± 2.03cd	12935 ± 302d
	N1	19.39 ± 0.15a	0.98 ± 0.26b	4.95 ± 0.26ab	601 ± 39.8b	41.58 ± 2.55ab	17138 ± 794b
	N2	19.97 ± 0.51a	0.86 ± 0.12b	5.13 ± 0.12a	649 ± 62.2a	41.73 ± 2.65a	19230 ± 386a
	N3	19.75 ± 0.27a	0.91 ± 0.58b	5.11 ± 0.58a	637 ± 90.0a	42.52 ± 1.46a	18123 ± 786ab
Two-factor variance analysis (*F*-value)							
	N	**	**	**	**	**	**
	C	**	*	**	**	**	**
	N*C	ns	ns	ns	ns	*	ns

Different lowercase letters (a, b, c) indicate significant differences between treatments (P < 0.05). Asterisks indicate a significant effect on the response variable: * P < 0.05, ** P < 0.01. MM, monoculture; IM, intercropping. ns indicate that there is no significant effect on the response variable.

level, the maize yield decreased by 8.27% and 5.76% relative to that obtained for N2.

The effects on panicle length, ear diameter, grain number, and 100-seed weight were consistent with the maize yield changes, in that all four were higher under IM than MM, but vice versa for barren tip (MM > IM). Most of the yield factors in the MM treatments showed this response, of N1 > N2, with the exception of only a lower grain number and longer barren tip for the N2; hence, the N1 yield under MM was lower than that under N2 mainly due to the effects on grain number and barren tip, while all yield factors in the IM treatment peaked at the N2 level.

The two-factor ANOVAs showed that the nitrogen application rate (N) as well as cropping mode (C) significantly affected all the indicators (P < 0.01), whereas their interaction effect (C*N) was only significant for the 100-seed weight (P < 0.05). Evidently, the N2 treatment was the better level of N application irrespective of planting mode (MM and IM), and IM coupled with N2 resulted in the highest maize yield.

3.2 Soil chemistry and nitrogen content

Soil pH under either monoculture (MM) or intercropping (IM) tended to decrease with an increasing nitrogen application level, being lowest in the N3 treatment for both, under which it was significantly (P < 0.05) reduced by 0.36 and 0.27 vis-à-vis N0 (Figure 2A). However, soil pH was similar under MM and IM at the same level of nitrogen applied. Soil EC values of treatments under MM increased with greater levels of nitrogen application (Figure 2B), significantly rising by 63.48% in N3 over the N0 treatment (P < 0.05). However, soil EC was affected differently under IM, being highest instead at the N1 level, such that with more nitrogen applied, the soil EC values decreased, even falling below that of the N0 treatment. For example, the soil EC value of N3 was reduced by 9.17% in comparison with N0. Under MM and IM, the soil TOC content reached its maximum when the nitrogen application level was increased to N2, but adding more nitrogen led to reductions in the soil TOC content (Figure 2C). In this case, relative to N0, the N2 treatment significantly increased the soil TOC content by 28.24% and 24.09% (P < 0.05) but the soil TOC content did not differ significantly between MM and IM at the same nitrogen level. Overall, different nitrogen application levels emerged as the main factor driving changes in soil pH, EC and TOC, while IM could have led to weakened soil EC.

The effects of different modes of cropping and nitrogen application levels on soil nitrogen content are presented in Figures 2D–F. Evidently, the soil $NH4^+$-N and NO_3^-N contents under MM and IM varied consistently, with both increasing in response to more nitrogen applied and peaking in the N3 treatment, significantly surpassing the N0 treatment by 58.98%–75.83% and 84.38%–93.93%, respectively (P < 0.05). For soil TN content, however, it was maximal at the N2 level and increasing the nitrogen application further reduced it. Notably, there was significant change in the soil TN content with increasing N application between treatments under MM or IM (P > 0.05), and only the N0 treatment under MM differed significantly from the N2 treatment under IM (P < 0.05). By comparing the different cropping systems, the outcome of a higher soil NH_4^+-N and NO_3^-N content was more pronounced under IM, increasing by 20.23% and 16.46% in response to N0 under IM vis-à-vis MM, respectively, while soil TN content increased by only 7.55%.

3.3 Nitrogen-use efficiency

To clarify the effects of different fertilizer application rates and cropping systems on nitrogen fertilizer use, we calculated the

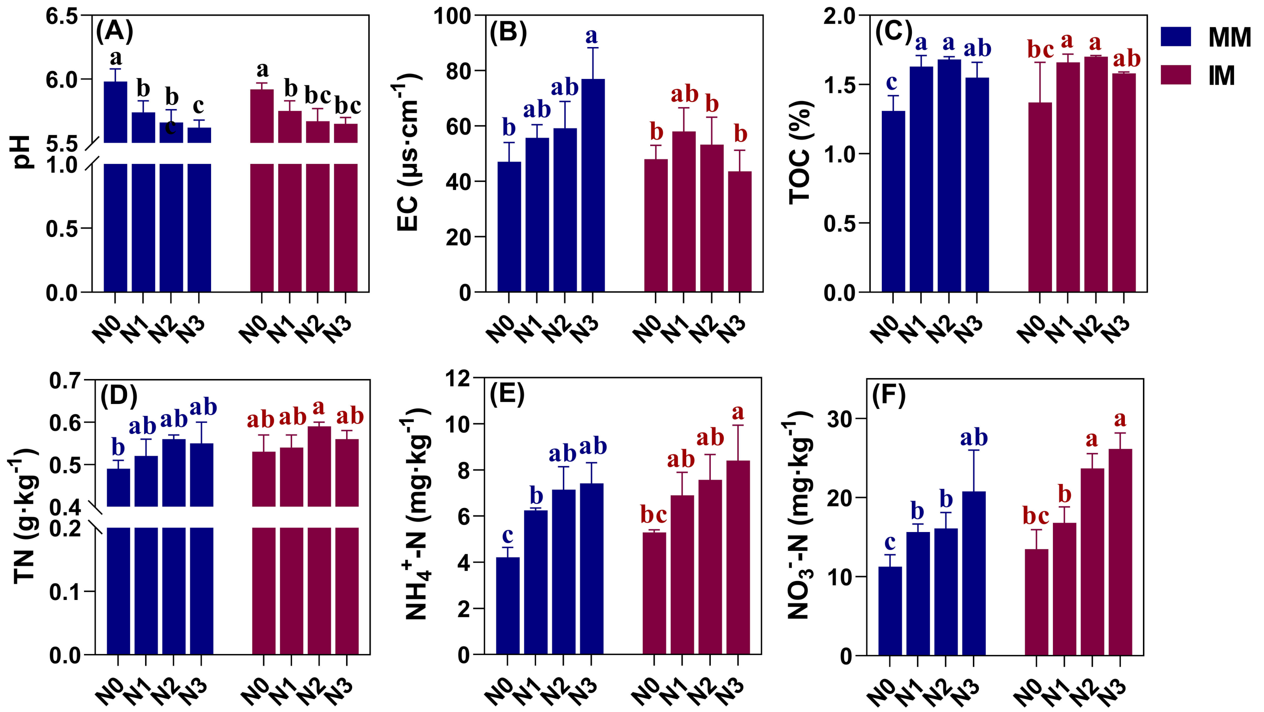

FIGURE 2
Effects of two contrasting cropping systems and nitrogen application rates on soil pH **(A)** and EC **(B)**, and the total organic carbon (TOC) **(C)**, total nitrogen (TN) **(D)**, ammonium nitrogen (NH_4^+-N) **(E)**, and nitrate nitrogen (NO_3^--N) **(F)** in soil. Different lowercase letters (a, b, c) above the bars (mean ± SD, n = 9) indicate significant differences between treatments (P < 0.05). MM, monoculture; IM, intercropping.

nitrogen-use efficiency (NUE), nitrogen agronomic efficiency (NAE), nitrogen partial productivity (NPP), and the nitrogen harvest index (Table 3). This analysis revealed that all indicators except NAE had the response pattern of IM > MM for a given application level, whereas NAE was always similar between the cropping systems. All indicators except NPP reached their maximum values at the N2 level, where NUE and NHI respectively increased significantly (P < 0.05) by 44.56% and 11.20% respectively, and NAE decreased by 2.67% under IM in comparison to MM. The NPP peaked at the N1 level under both IM and MM, after which it decreased significantly (P < 0.05) with more nitrogen applied. Two-way ANOVAs revealed that the application rate was the main factor influencing the nitrogen fertilizer

TABLE 3 Statistics for soil indicators of nitrogen fertilizer use under two contrasting cropping systems (C) and N application rates (N).

Treatment		NUE ($kgatm^{-1}$)	NAE ($kgatm^{-1}$)	NPP ($kgatm^{-1}$)	NHI (%)
MM	N0	–	–	–	77.62 ± 0.41c
	N1	17.11 ± 3.7b	26.58 ± 2.34a	76.01 ± 3.97b	79.11 ± 1.22b
	N2	20.02 ± 3.76b	26.95 ± 1.07a	64.02 ± 2.06c	81.82 ± 1.42b
	N3	17.44 ± 3.22b	17.33 ± 1.04b	46.98 ± 3.04d	80.44 ± 1.11b
IM	N0	–	–	–	86.67 ± 2.28a
	N1	28.55 ± 4.76a	23.35 ± 3.86a	95.21 ± 4.41a	85.29 ± 0.87ab
	N2	28.94 ± 1.38a	26.23 ± 1.07a	80.12 ± 1.61b	88.61 ± 0.95a
	N3	18.37 ± 1.52b	17.3 ± 3.13b	60.41 ± 2.62c	84.12 ± 1.23ab
Two-factor variance analysis (*F*-value)					
	N	**	**	**	*
	C	**	ns	**	*
	N*C	*	ns	ns	*

NUE, nitrogen-use efficiency; NAE, nitrogen agronomic efficiency; NPP, nitrogen partial productivity; NHI, nitrogen harvest index.
Small letters (a, b, c) indicate significant differences between treatments (P < 0.05). Asterisks indicate a significant effect on the response variable: * P < 0.05, ** P < 0.01. MM, monoculture; IM, intercropping. ns indicate that there is no significant effect on the response variable.

TABLE 4 Alpha diversity statistics of bacterial communities under two contrasting cropping systems (C) and four nitrogen application rates (N).

Treatment		Shannon index	Chao1 index	PD_whole_tree	Goods_coverage
MM	N0	15.59 ± 0.13bc	7718 ± 41e	519.9 ± 29.22c	0.96a
	N1	14.64 ± 0.03c	7990 ± 12d	472.0 ± 19.21d	0.96a
	N2	13.62 ± 0.03d	8306 ± 10c	467.6 ± 32.55e	0.96a
	N3	13.40 ± 0.05d	8128 ± 100d	458.9 ± 25.33e	0.96a
IM	N0	17.44 ± 0.01a	8423 ± 168c	576.8 ± 35.67a	0.96a
	N1	16.57 ± 0.01b	8700 ± 280b	546.7 ± 15.34b	0.96a
	N2	15.47 ± 0.06bc	8814 ± 22a	526.6 ± 38.53c	0.96a
	N3	14.36 ± 0.12c	8572 ± 184bc	495.1 ± 6.86cd	0.96a
Two-factor variance analysis (*F*-value)					
	N	**	**	**	ns
	C	**	**	**	ns
	N*C	*	**	**	ns

Small letters (a, b, c) indicate significant differences between treatments ($P < 0.05$). Asterisks indicate a significant effect on the response variable: * $P < 0.05$, ** $P < 0.01$. MM, monoculture; IM, intercropping. ns indicate that there is no significant effect on the response variable.

use. Overall, the N2 level under IM had the greatest nitrogen fertilizer use.

3.4 Changes in soil microbial communities

3.4.1 Alpha diversity of bacterial communities

Upon completing the sequencing in this study, the OTUs were screened for de-low content, after which the non-repetitive sequences (excluding single sequences) were clustered into OTUs based on 97% similarity, with any chimeras removed in the clustering process, to obtain representative sequences of OTUs. The final number of OTUs totaled 3601, resulting in a minimum of 30 566 optimized sequences per sample. To investigate the alpha diversity of individual soil samples, the richness (chao1 index), diversity (Shannon index and PD_whole_tree), and sequence depth (Goods_coverage) of the soil bacterial community were calculated for each cropping system and nitrogen fertilizer treatment. As seen in Table 4, the Goods_coverage for bacteria in all treatments was above 95%. For bacterial community diversity, the Shannon index and PD_whole_tree varied consistently among treatments, being highest at N0 level under both MM and IM modes of cropping; however, increasing the nitrogen application rate led to lower bacterial community diversity, this significantly reduced by 14.05%–17.66% and 11.73%–14.16% in N3 relative to N0 ($P < 0.05$). For the same level of nitrogen application, bacterial community diversity was higher under IM than MM; for example, it significantly increased by 11.86% and 10.94% ($P < 0.05$) under IMN0 than MMN0, but not as much (7.16%–7.88%) when more nitrogen was added up to the N3 level. In terms of bacterial community richness, the Chao1 index had an identical pattern to the diversity index, in that it was higher in IM than MM, rising by 9.13% and IMN0 compared to MMN0. Interestingly, the Chao1 index was likewise disrupted by adding more nitrogen, peaking at the N2 level in both MM and IM, with further increases in the nitrogen application significantly decreasing its value ($P < 0.05$). A two-way ANOVA showed that both the N application level (N) and cropping pattern (C) were highly significantly correlated ($P < 0.01$) with alpha diversity, and overall, intercropping increased the bacterial community's alpha diversity regardless of N application level, with an increasing N application decreasing that diversity.

3.4.2 Community composition for dominant bacterial genera

Altogether, the soil samples could be annotated to 645 bacterial genera. Of these, dominant bacterial genera accounted for 17.48%–20.66% of the total, after selecting the top-50 genera by relative abundance and excluding the seven genera whose abundance was < 1% (Figure 3). At N0 level, the abundance of dominant bacterial genera was 11.49% higher in IM than MM. Across the fertilizer treatment gradient, the total abundance of dominant bacterial genera was lower in IM than in MM at each N application level. This trend was driven by the enrichment of *Bryobacte* in MM at each N application level, whose relative abundance was 32.80%–70.88% higher under N0–N3 than in their counterpart IM treatments. Further comparison of the relative abundance of individual genera showed that the trends of *Sphingomonas* and *Gemmatimonas* under different modes of cropping and nitrogen application levels were consistent: IM > MM. The relative abundance of these two genera responded positively to more nitrogen applied under MM, increasing most at N1, reaching 7.50% and 27.88%, respectively. Under IM, however, their relative abundance peaked at the N2 level.

For *Candidatus_Solibacter*, the relative abundance of this genus changed the most at N0 and N1 levels, increasing by 30.84% IMN0 vis-à-vis MMN0. But in response to N1, its relative abundance

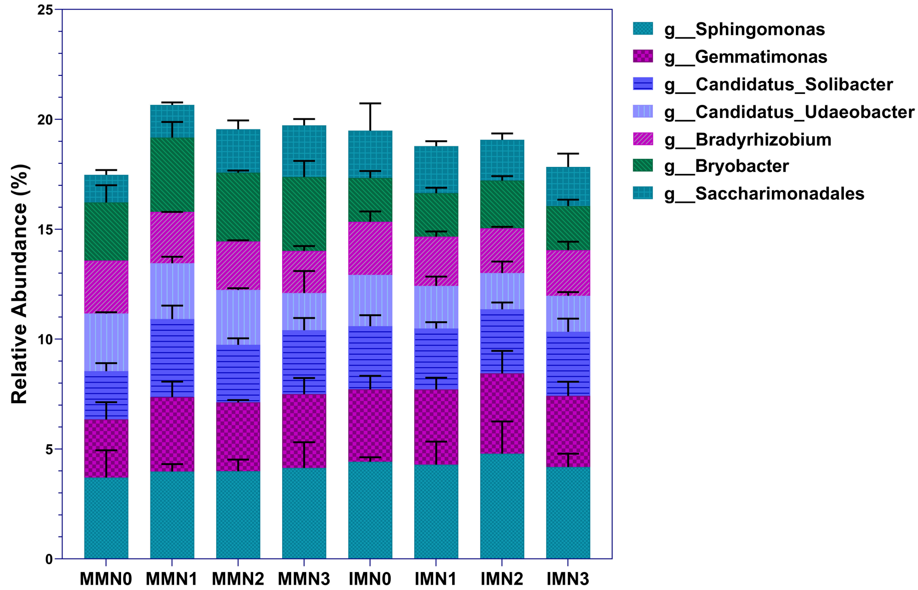

FIGURE 3
Horizontal community composition of bacterial genera in the eight treatment combinations of cropping system (IM, intercropping vs. MM, monoculture) and four levels of nitrogen fertilizer application (N1–4).

increased by 61.53% compared to N0 under MM, now exceeding that of IMN1. The relative abundances of *Candidatus_Udaeobacter* and *Bryobacter* showed the same trend, namely that of MM > IM, regardless of the nitrogen application rate. However, the relative abundance of *Candidatus_Udaeobacter* decreased as the level of nitrogen application increased, with that at N3 being 35.52% and 29.67% lower under MM and IM, respectively, than in the N0 treatment. In stark contrast, *Bryobacter* abundance was maximal in the MMN1 and IMN2 treatment combinations. For *Bradyrhizobium*, its relative abundance was similar under MM and IM, as was its trend across nitrogen application rates: compared with the baseline N0 level, with more nitrogen, *Bradyrhizobium* decreased in abundance by 20.56% and 16.62% in N3 under MM and IM, respectively. The entirely opposite pattern characterized changes in *Saccharimonadales* under MM and IM. With more nitrogen added, its relative abundance under MM tended to increase, being 86.91% in the N3 than N0 treatment; however, under IM showed a decreasing trend in response to fertilization, being 17.47% lower at the N3 than N0 level. To sum up, IM increased the relative abundances of *Sphingomonas*, *Gemmatimonas*, and *Saccharimonadales* yet decreased those of *Candidatus_Udaeobacter* and *Bryobacter*, and different levels of nitrogen application had a greater impact on the enrichment of dominant bacterial genera under the MM cropping system than IM. This pointed to a superior stability of the microbial community under IM than MM.

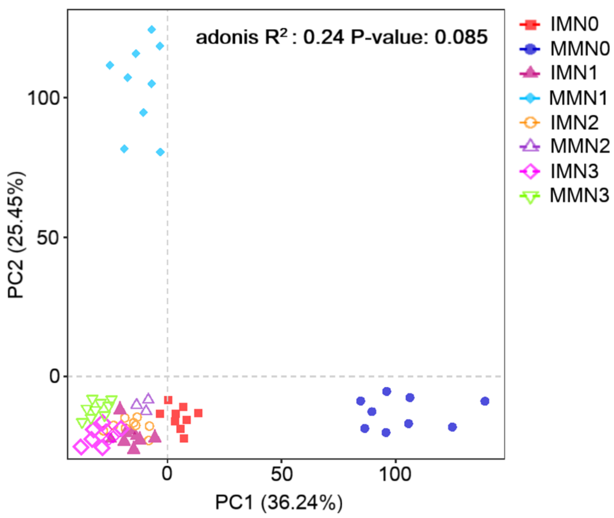

FIGURE 4
Principal component analysis (PCA) of bacterial community structure in the eight treatment combinations of cropping system (IM, intercropping vs. MM, monoculture) and four levels of nitrogen fertilizer application (N1–4).

3.4.3 PCA of the bacterial community

We employed the Aitchison distance for the beta diversity analysis of soil bacterial communities. PCA was used to compare the degree of similarity existing in the diversity of the bacterial community among different samples from the eight treatment combinations (Figure 4). The first (PC1) and second principal component (PC2) of bacterial community structure (97% similarity) explained 36.24% and 25.45% of the total variance, respectively. There was no significant effect of differing nitrogen application rates on bacterial community structure under IM or MM ($P > 0.05$), and most of treatment combinations were clustered in the third quadrant (lower-left) without segregation. Unlike those, the MMN0 and MMN1 treatment combinations separated well

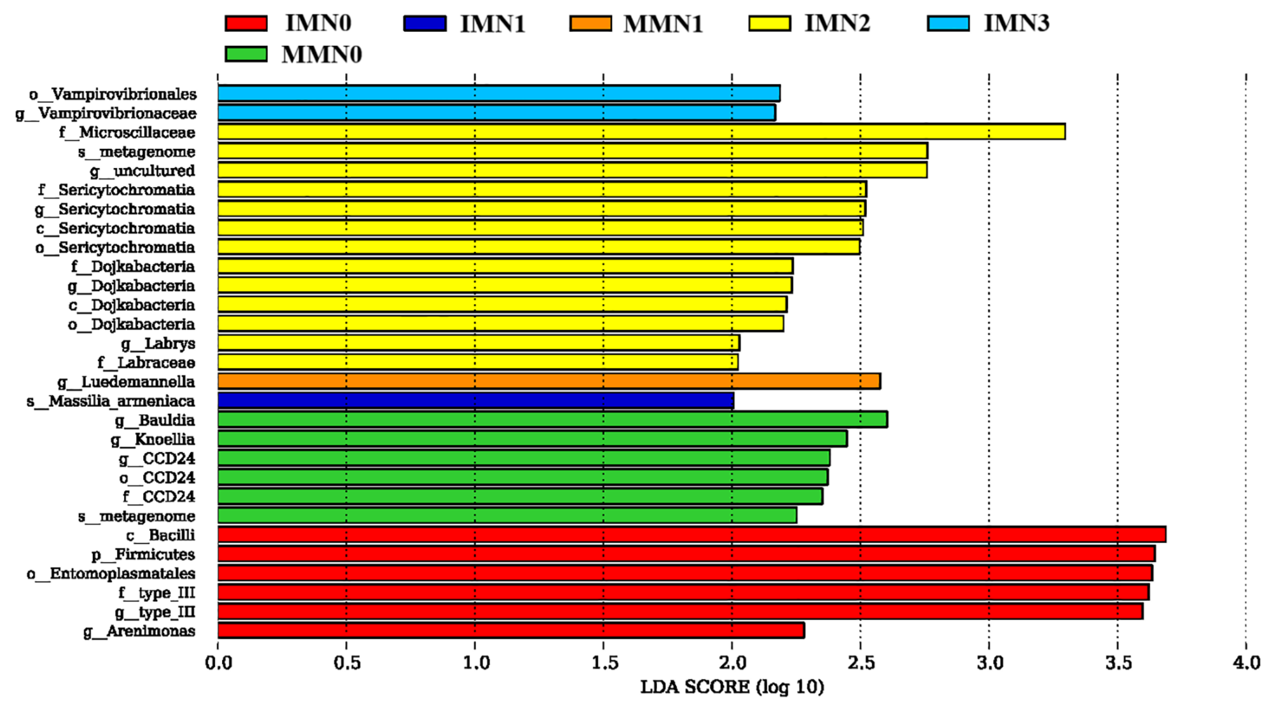

FIGURE 5
Determination of the most significantly different species in soil bacterial communities under contrasting cropping systems (IM, intercropping vs. MM, monoculture) and nitrogen application rates, using linear discriminant analysis (LDA) effect sizes (LEfSe). An LDA score ≥ 2 indicated a differential species, i.e. statistically different biomarkers. The bar length is proportional to the effect size.

along PC1 and PC2, respectively, indicating that their community structure differed substantially from the others ($P < 0.05$). Overall, the IM approach had no significant effect ($P > 0.05$) upon soil bacterial community structure across the nitrogen fertilizer gradient, though the differences under MM for the zero and low nitrogen application rates (N0 and N1, respectively) were significant ($P < 0.05$). Nonetheless, with more nitrogen applied, the soil bacterial community structure of both cropping systems closely resembled each other.

3.4.4 Discrimination of differential bacterial taxa

It is evident that differential species mainly emerged in the IMN2, IMN0, and MMN0 treatment combinations (Figure 5); but not so in either MMN2 or MMN3 (thus not shown). Further analysis indicated that IMN2 harbored the most differential species, with *Microscillaceae* having the highest LDA values followed by 12 others, including *Metagenome*, *Sericytochromatia*, and *Dojkabacteria*. In the IMN0 treatment combination, the differential species consisted mainly of *Bacillus*, *Fiemicutes*, and *Entomoplasmatales* with more similar LDA values. While for MMN0, its differential species were mainly *Bauldia* and *Knoellia*. For IMN1, IMN3 and MMN1 their differential species respectively were *Vampirovibrionaceae*, *Luedemannella*, and *Massilia_armeniaca*. Altogether, the number of differential species decreased as the nitrogen application rate increased under MM, while the IM mode had the greatest number of differential species at the N2 level, indicating that the soil environment responded most to this treatment.

3.4.5 Correlation analysis of dominant bacterial genera with the soil environment and yield

We summarized the dominant bacterial genera in the previous section and tallied their respective relative abundance for correlation tests with the soil environment factors and maize yield factors (Figure 6A). This analysis showed that *Sphingomonas* had a highly significant negative correlation with soil pH ($P < 0.01$) yet a positive correlation with soil TOC and EC ($P < 0.05$). The enrichment of *Gemmatimonas* and *Bradyrhizobium* significantly increased the soil nitrogen content; the positive correlation of *Candidatus_Udaeobacter* with soil EC was highly significant ($P < 0.01$), whereas *Candidatus_Solibacter* had a negative correlation ($P < 0.01$) with both soil TOC and EC, but a significant positive correlation with NO_3^-N ($P < 0.01$). *Bryobacter* was significantly positively correlated with the soil TOC content ($P < 0.05$), while *Saccharimonadales* had a highly significant negative correlation with NO_3^-N ($P < 0.01$).

In terms of yield (Figure 6B), enrichment of both *Sphingomonas* and *Gemmatimonas* significantly reduced the degree of baldness (DOB) ($P < 0.05$) and increased the spike length (SL), number of kernels in the spike (KPS), and 100-seed [grain] weight (100GW) of maize, which in turn significantly increased maize yield ($P < 0.05$). However, *Candidatus_Udaeobacter* and *Bradyrhizobium* had the opposite influence on yield, with enrichment of either increasing the DOB. Still, *Candidatus_Udaeobacter* displayed a greater negative influence on yield, as indicated by its relative abundance being highly significantly negatively correlated with both SL and yield ($P < 0.01$)

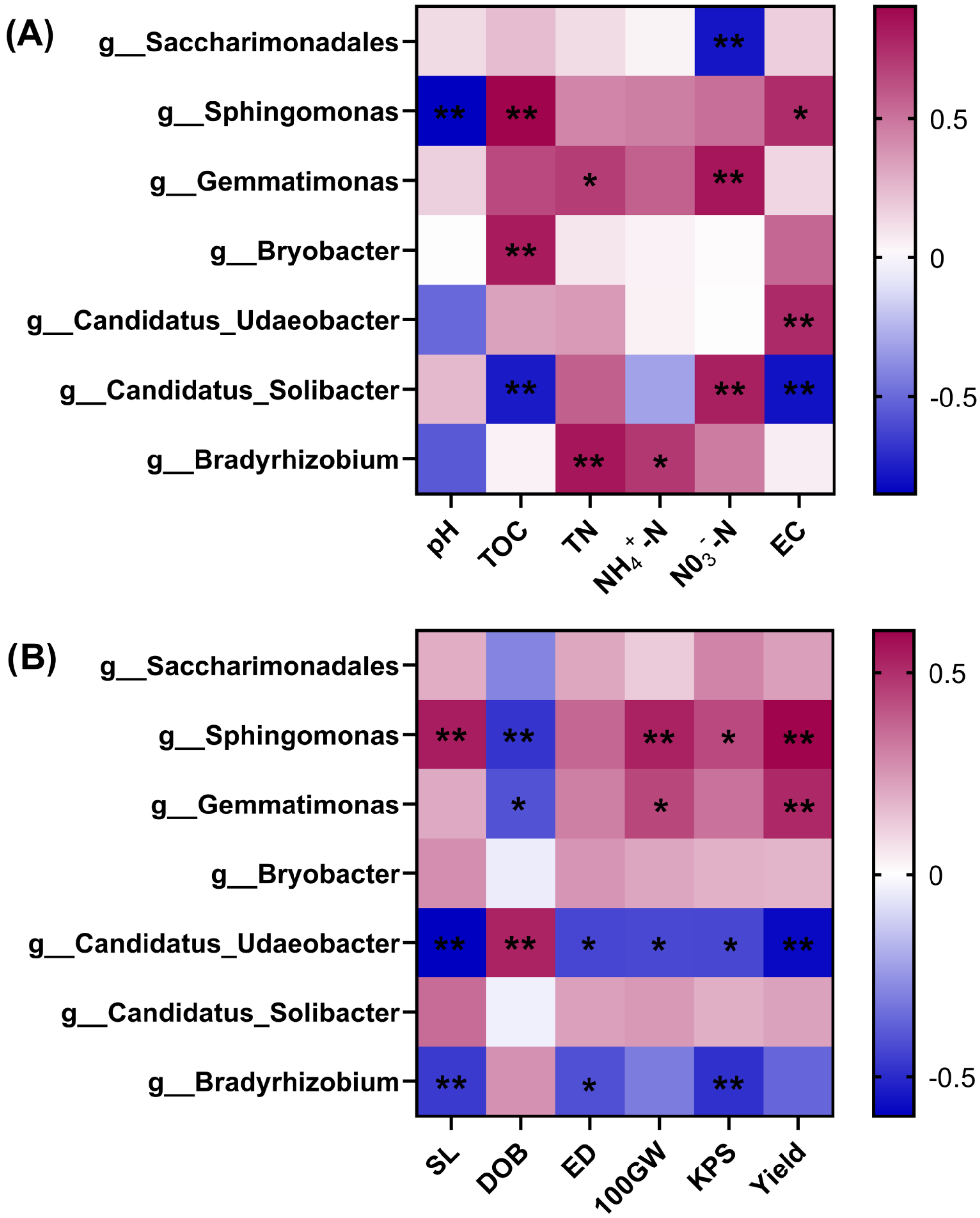

FIGURE 6
Heatmap of Pearson correlations of soil dominant bacterial genera with soil factors **(A)** and yield factors **(B)**. Red coloring indicates a positive correlation, blue coloring indicates a negative correlation; asterisks indicate a significant correlation: *P < 0.05, **P < 0.01.TOC, TN, NH_4^+-N and NO_3^--N denote soil organic carbon, total nitrogen, ammonium nitrogen and nitrate nitrogen, respectively; SL, DOB, ED, 100GW and KPS denote maize panicle length, degree of baldness, ear diameter, 100-seed weight, and kernels in the spike, respectively; UE and CAT denote soil urease and catalase, respectively.

and to a lesser extent with ear thickness (ED), 100GW, and KPS ($P < 0.05$). Finally, a higher relative abundance of *Bradyrhizobium* significantly reduced the maize SL, ED, and KPS ($P < 0.05$).

3.4.6 Co-occurrence network modeling of soil bacterial communities

To clarify the mechanism of synergistic interaction among genera, we built co-occurrence network models of soil bacterial communities at the genus level for the top 200 abundances for different nitrogen application levels (MM and IM fitted by 97% similarity) (Figures 7A–D), and likewise for different cropping modes (N0–N3 fitted by 97% similarity) (Figures 7E, F). We also examined the topology parameters of these network models (Table 5) to compare the interconnections among soil bacterial communities. When compared to the N0 level, the number of soil bacterial community edges decreased by 2.30%–8.74% at the N1–N3 levels, but the proportion of positive correlations increased by 0.66%–5.76%, being highest at the N2 level, with no significant difference detected between the N3 and N0 levels; however, the number of edges and proportion of positive correlations under IM increased by 1.91% and 4.62%, respectively, vis-à-vis MM. In comparing the average degree,

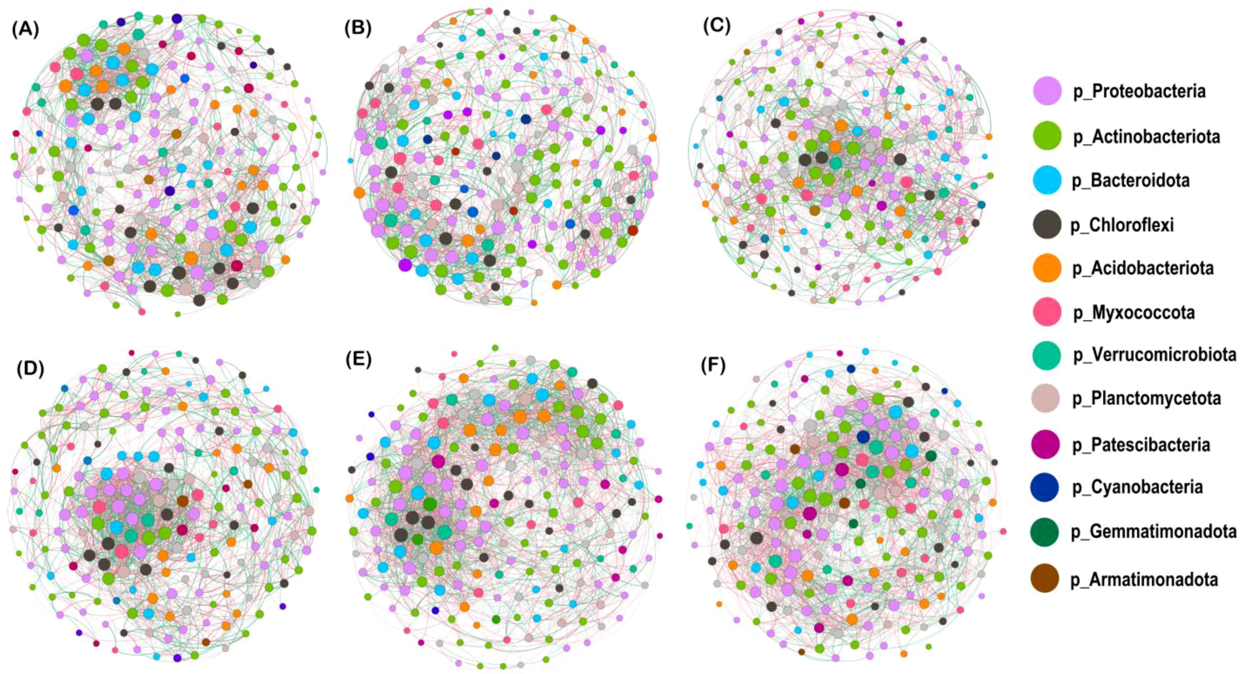

FIGURE 7
Co-occurrence network model of soil bacterial communities under different nitrogen application rates and cropping systems. **(A–D)** Different nitrogen application levels (N0, N1, N2, and N3, respectively) (MS and IS fitted by 97% similarity). **(E)** Maize monocropping and **(F)** intercropping (N0, N1, N2, and N3 fitted by 97% similarity) as contrasting cropping modes. The colored circles are different genus; the size of a circle is used to convey the average abundance of that species; line segments between circles indicate a correlation between two species, whose thickness is proportional to the correlation strengthen between them. Red lines indicate positive correlations, while green lines indicate negative correlations.

average weight, average clustering coefficient, and modularity, we found that all these network topology parameters were lower for the N1–N3 levels than for N0, and always higher under IM than MM. Hence, the degree of connectivity between network nodes in the IM system was likely stronger and the connections between nodes more numerous and complex.

3.4.7 Structural equation modeling analysis of the effects of intercropping and nitrogen application rates on maize yield

The SEM results (Figure 8) showed that both intercropping and nitrogen application could significantly increase the soil nitrogen content and also alter bacterial community composition. Soil nitrogen content and bacterial community composition were in a mutually reinforcing relationship; accordingly, the former's increase and the latter's enrichment could significantly reduce the soil pH, EC, and TOC content generated a synergistic effect in soil, which in turn increased the maize yield. Therefore, intercropping not only bolstered the yield but it also was critical for maintaining soil health and providing a favorable soil environment for crop growth.

4 Discussion

The mechanism underpinning efficient nitrogen uptake in the intercropping system between maize and legume crops has three key aspects. First is interspecific plant competition, where maize outcompetes legume crops for light and nitrogen (and other

TABLE 5 Topological properties of the soil bacterial community co-occurrence networks.

Treatment	Total nodes	Edge	Positive %	Negative%	Average degree	Average weighting	Cluster coefficient	Modularity
N0 (MM,IM)	200	1911	53.06	46.94	19.11	16.89	0.55	0.52
N1 (MM,IM)	200	1744	55.24	44.76	17.44	15.36	0.52	0.51
N2 (MM,IM)	200	1821	58.82	41.18	18.21	16.03	0.51	0.45
N3 (MM,IM)	200	1867	53.72	46.28	18.67	16.52	0.52	0.50
MM (N0-N3)	200	2197	53.71	46.29	21.97	15.55	0.43	0.40
IM (N0-N3)	200	2239	56.19	43.81	22.39	15.69	0.45	0.41

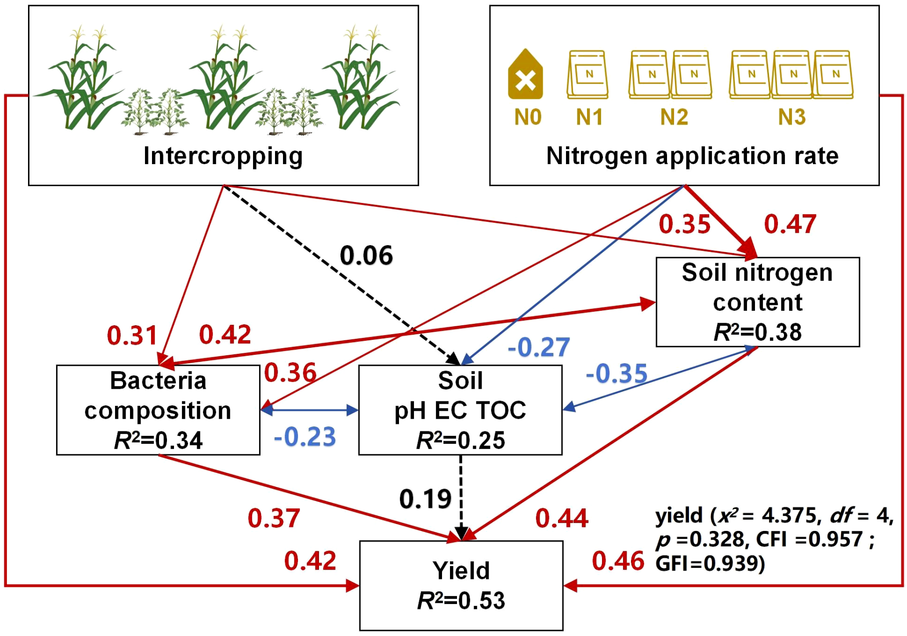

FIGURE 8
Structural equation model (SEM) describing the effects of intercropping and nitrogen application rates on soil chemical properties, bacterial colony composition, and maize yield. Blue arrows indicate negative relationships (correlations); red arrows indicate positive ones.

resources), which promotes the superiority of maize's uptake of nitrogen. Second, the root system's interaction with soil microorganisms promotes the cycling of nutrients and the transfer of nitrogen between plants, such that the nitrogen fixed by legume crops can be absorbed and utilized by maize. Third, legume crops increase tuberculation and their nitrogen-fixing gene expression is enhanced, thereby increasing their own nitrogen-fixing capacity.

4.1 Soil nitrogen and chemical properties

A marked increase in soil pH and salt ion concentrations in soil will lead to the degradation of crop survival/growing environment and soil nutrient deficiencies, which heavily hinders crop growth, development, and yield. In this study, however, our results show that soil pH is negligibly affected in general, being similar at each level of nitrogen application under IM or MM. This suggests intercropping does alter soil pH, whose magnitude is instead mainly influenced by the level of nitrogen application (Wang et al., 2015). Further, we find a lower soil EC in the intercropping system than monoculture (MM) but a higher soil TOC content, which can be largely attributed to the fact that IM could balance the soil nutrient use rate, effectively alleviating the inhibitory effect of soil mono-elements and enhancing soil microbial metabolism. This would have led to a greater TOC content because of the greater decomposition capacity of organic matter (Silva et al., 2022). We also found that, under intercropping, its soil TOC content was consistent with changes in its soil EC. This could be explained by the strong adsorption capacity of soil TOC, which contributes about 20%–70% to soil EC and has a certain buffering effect, delaying the movement of surface salt ions into the deeper soil, thereby augmenting EC (Wang et al., 2023b).

The nitrogen in soil is the main source of this element for plant uptake and use, and is also the primary limiting factor for high-yielding crops, so nitrogen input as fertilizer is a key practice to maintain or improve the soil nitrogen content (Knops et al., 2002). Here, the soil nitrogen supply in IM surpassed that in MM, and the improvement was especially pronounced for the NH_4^+-N and NO_3^--N contents. We attribute this benefit to the maize/soybean intercropping system, whereby the legumes are able to efficiently fix N, which is then utilized by the same crop through various transfer pathways or available in soil to subsequent non-legume crops as residues (Raza et al., 2020).

4.2 Rhizosphere bacterial community of maize

Soil bacteria can influence the metabolic activities of crop roots, as well as soil structure and soil fertility, to varying degrees. When crops are grown in an intercropping system, plant residues and root secretions may come into close contact with each other, directly or indirectly altering the soil bacterial community structure (Duchene et al., 2017). Compared with monocropped maize, we found a more diverse soil bacterial community in the rhizosphere soil of intercropped maize, as well as a greater relative abundance of dominant genera. This result suggests that the composition of bacterial communities in intercropped soils is heavily influenced by changes in agricultural management practices (Lai et al., 2022). However, using too much nitrogen fertilizer disrupts this trend and reduces the number of endemic differential species. This can be explained by the fact that after an excessive nitrogen application, the general plant utilization rate of the fertilizer is only 30%–50%, leaving the rest to get converted to nitrate via nitrification in the soil. That would cause soil acidification and a neutralization reaction with the inorganic carbon (carbonate) in soil, leading to the loss of inorganic carbon and eventually the full deterioration of soil, which inevitably would somehow adversely impact bacterial community diversity. Recent research has shown that increasing plant diversity to ensure the diversity of the soil microbial community can significantly improve soil fertility and reduce the number of pathogenic microorganisms (Jensen et al., 2020). Earlier, Weidner et al. (2015) found that bolstering soil bacterial diversity can improve the nitrogen nutrient supply capacity of soil, thus promoting not only plant growth but also nitrogen use; Trivedi et al. (2012) reported considerably more copies of genes involved in the ecological processes of nitrogen metabolism in healthy soils than diseased soils. This indicates that maize/soybean intercropping promotes the diversity of bacterial communities in surface soil, and thus the availability of nitrogen as well as other nutrients in arable soil. Apart from being useful in maintaining the stability of soil microbial community dynamics, it could probably help to suppress pests and diseases too, collectively promoting the growth and yield increase of intercropped crops. Among dominant bacterial genera compared between modes of cropping, our results reveal that the relative abundances of *Sphingomonas* and *Gemmatimonas* are higher under IM than MM, but this is reversed for *Bryobacter*. Other research found that, under the action of maize root secretion, Ascomycetes came to dominate, for which *Sphingomonas* and *Gemmatimonas* are the main genus members; so it was suggested this phenomenon enables the maize root system to fully utilize inorganic nutrients in soil (Zhang et al., 2018b). Arguably, subsoil intercropping conditions most likely arise through significant changes in the composition of inter-root secretions, leading to dramatic changes in bacterial colonization outcomes and population sizes of dominant bacteria. By constructing a co-occurrence network model, we learned that IM does foster an increase in the number of soil bacterial edges, an increase in the proportion of positive correlations, and an increase in species richness, in tandem with the weakening of competitive relationships between species. This is because intercropping created ecological conditions that improved the survivorship of dominant bacterial genera in surface soil, which in turn led to the enhancement of mutually beneficial relationships and a weakening of their competitive interactions (Wang et al., 2023c). This showed that IM could promote links between the genera and, when used with a reasonable nitrogen application rate (N1 or N2 level), was capable of simplifying the interrelationship between them, presumably weakening the competitive relationship between the genera and enhancing their synergistic ability.

4.3 Soil nutrient–microbe–yield relationships

In recent years, there has been an exponential rise in studies investigating the various effects of agricultural management practices on soil microbial communities (Zhao et al., 2022). Despite that staggering research effort, it is still difficult to elucidate general soil nutrient–microbe–yield relationships and the pathways influencing their dynamics under intercropping systems. Soil microbial community structure and functional diversity are closely tied to restored soil fertility and better soil quality (Yang et al., 2023). It is reasonable to think that plant–microbe interactions between roots are closely related to the growth and yield formation of intercrops.

Here, through a comprehensive soil nutrient–microbe–yield correlation analysis, we find that enrichment of *Gemmatimonas* and *Bradyrhizobium* could drastically increase the soil nitrogen content. Firstly, *Gemmatimonas* is a self-photosynthesizing genus rich in bacterial chlorophyll members; in addition, this genus can reduce N_2O to nitrate in soil (Zou et al., 2023). Secondly, *Bradyrhizobium* bacteria is able to form a nitrogen-fixing symbiosis with *Rhizobium* in soybean's root system, which in turn can increase the soil nitrogen content (Cheng et al., 2023). However, maize is a plant with high fertilizer absorption capacity and high fertilizer requirement. So, in the intercropping system, due to the difference in morphological structure between maize and soybean plants, the reduced absorption of light energy due to their asymmetric competition inhibited the growth and root development of soybean to a certain extent, which indirectly constrained its symbiotic nitrogen-fixing ability (Liu et al., 2018). If so, this would explain rather well why the genus *Bradyrhizobium* was negatively correlated with the maize yield factors in our study. On the contrary, *Saccharimonadales* has a strong negative correlation with soil NO_3^--N, likely because this genus has the function of denitrifying and removing phosphorus, and is mainly involved in the denitrification process leading to soil nitrogen loss (Wang et al., 2022a). We also uncovered a pronounced negative correlation of *Sphingomonas* with soil pH but its positive correlation with soil TOC and yield. The first may be explained by the role of this genus in remediating heavy metal contamination, being vital to restoring soil fertility and promoting plant growth (Liu et al., 2022). The second result can be explained by the ability of *Sphingomonas* to decompose soil carbohydrates (pentoses, hexoses, disaccharides), which produces large amounts of acid during oxidation, which then lowers the soil pH (Cuartero et al., 2022). A greater relative abundance of *Candidatus_Solibacte* was associated with declines in TOC and EC, and an increasing content of soil NO_3^--N. *Candidatus_Solibacte* is known to effectively decompose soil organic matter and reduce soil nitrate and nitrite by consuming the soil carbon sources, which in turn slows or prevents soil acidification (Zhang et al., 2018a). *Candidatus_Udaeobacter* can release antibiotics that cause other microbial cells to lyse and release their nutrients (Guo et al., 2024). We did find a highly significant negative correlation between this genus and maize yield, but although nutrient contents were augmented, the lysis-induced death of other microorganisms may have disrupted the structural composition of soil bacterial communities, which in turn could have affected their functioning.

4.4 Breakthrough areas for future research

This study's results suggest that exploring diversified intercropping patterns that provide reciprocal benefits to different plants, by harnessing inherent differences in their ecological niches, should continue to be the core focus of future research in the intercropping industry. In this study, nitrogen uptake in the intercropping system reached its maximum when 240 kg ha^{-1} of nitrogen fertilizer was applied. Hence, an appropriate application rate of nitrogen fertilizer could effectively improve nitrogen's uptake and accumulation in the general corn–soybean intercropping system.

Currently, most research on intercropping mechanisms tends to focus on plant growth and nutrient uptake and utilization conditions, though some studies have analyzed changes that occur in soil enzymes and their activity. The more intertwined factors, such as the soil–soil enzyme–soil microorganism interactions, under this intercropping pattern have not been studied yet, and the vast majority of published studies are restricted to the soil or soil–soil enzyme level. Therefore, research on intercropping systems should focus on the holistic analysis of each mechanistic link involved, and future studies should also try to investigate the whole intercropping system, from its environmental factors to cultivated plants, down to its soil microorganisms. The more comprehensive the research done, the more conducive its knowledge gained is to the discovery of intercropping mechanisms, and for promoting the development of the intercropping industry. Finally, the use of high-throughput sequencing technology offers a fast and convenient way to analyze intercropping soils and to explore how the soil microbial community influences plant growth/yield changes, leading to a richer, more accurate understanding of intercropping systems and their functioning.

5 Conclusion

This study's results show that under a maize/soybean intercropping pattern, the N2 level (240 kg ha^{-1}) was best suited to achieve a high maize yield, for which the nitrogen-use efficiency was also maximized. We find that the maize crop yield is also correlated with the dominant soil microbial genera and soil nitrogen content. The main ways by which an intercropping mode increases yield, as well as the gradient changes under different N application levels, are also clarified. In the context of research on promoting crop yields and the efficient use of nitrogen fertilizer in intensive agriculture, we believe that intercropping's advantages are more pronounced when an appropriate amount of nitrogen is applied, since using too much can render moot these benefits.

Data availability statement

The original contributions presented in the study are included in the article/supplementary material. Further inquiries can be directed to the corresponding authors.

Author contributions

LZ: Visualization, Writing – original draft, Writing – review & editing. YF: Writing – original draft. ZZ: Investigation, Writing – original draft. ZC: Investigation, Writing – original draft. BB: Investigation, Writing – original draft. HW: Visualization, Writing – review & editing. QL: Supervision, Writing – review & editing. JC: Supervision, Writing – review & editing.

Funding

The author(s) declare financial support was received for the research, authorship, and/or publication of this article. The work was supported by the science and technology development plan of Jilin Province, China (project nos. 20220508095RC and 20230302003NC). National Key Research and Development Project (project nos. 2023YFD1501104).

Acknowledgments

We wish to thank Dr. Wuliang Shi, Dr. Bin Li, Dr. Yubin Zhang, for valuable and encouraging discussions. We appreciate the efforts of the reviewers and the editors' valuable suggestions in earlier versions of this manuscript.

Conflict of interest

The authors declare that the research was conducted in the absence of any commercial or financial relationships that could be construed as a potential conflict of interest.

Publisher's note

References

Bai, F. F., Qi, X. B., Li, P., Du, Z. J., and Guo, W. (2023). Groundwater depth and nitrogen application amount jointly regulate the water and residual soil nitrate accumulation in agricultural soil profile. *Agronomy-Basel* 13, 19. doi: 10.3390/agronomy13041163

Bai, Z. T., Xie, C., Yu, J., Bai, W. Q., Pei, S. Z., Li, Y. X., et al. (2024). Effects of irrigation and nitrogen levels on yield and water-nitrogen-radiation use efficiency of drip-fertigated cotton in south Xinjiang of China. *Field Crops Res.* 308, 13. doi: 10.1016/j.fcr.2024.109280

Chen, G. H., Jiang, F. H., Zhang, S., Zhang, Q., Jiang, G. J., Gao, B. K., et al. (2023). Potential crop yield gains under intensive soybean/maize intercropping in China. *Plant Soil* 16. doi: 10.1007/s11104-023-06423-7

Cheng, Z. Y., Meng, L. B., Yin, T. J., Li, Y., Zhang, Y. H., and Li, S. M. (2023). Changes in soil rhizobia diversity and their effects on the symbiotic efficiency of soybean intercropped with maize. *Agronomy-Basel* 13, 17. doi: 10.3390/agronomy13040997

Cuartero, J., Pascual, J. A., Vivo, J. M., Özbolat, O., Sánchez-Navarro, V., Egea-Cortines, M., et al. (2022). A first-year melon/cowpea intercropping system improves soil nutrients and changes the soil microbial community. *Agric. Ecosyst. Environ.* 328, 8. doi: 10.1016/j.agee.2022.107856

Du, J. B., Han, T. F., Gai, J. Y., Yong, T. W., Sun, X., Wang, X. C., et al. (2018). Maize-soybean strip intercropping: Achieved a balance between high productivity and sustainability. *J. Integr. Agric.* 17, 747–754. doi: 10.1016/S2095-3119(17)61789-1

Duchene, O., Vian, J. F., and Celette, F. (2017). Intercropping with legume for agroecological cropping systems: Complementarity and facilitation processes and the importance of soil microorganisms. A review. *Agric. Ecosyst. Environ.* 240, 148–161. doi: 10.1016/j.agee.2017.02.019

Fan, Z., Deng, M. Z., Lin, Y. R., Liu, P. Z., Wang, X. L., Yang, S. F., et al. (2023). Effects of the border on yield and water use in wheat/maize intercropping in rain-fed areas with different nitrogen levels. *Field Crops Res.* 302, 12. doi: 10.1016/j.fcr.2023.109105

Faust, K. (2021). Open challenges for microbial network construction and analysis. *Isme J.* 15, 3111–3118. doi: 10.1038/s41396-021-01027-4

Fu, Z. D., Zhou, L., Chen, P., Du, Q., Pang, T., Song, C., et al. (2019). Effects of maize-soybean relay intercropping on crop nutrient uptake and soil bacterial community. *J. Integr. Agric.* 18, 2006–2018. doi: 10.1016/S2095-3119(18)62114-8

Guo, T. X., Yao, X. H., Wu, K. L., Guo, A. M., and Yao, Y. H. (2024). Response of the rhizosphere soil microbial diversity to different nitrogen and phosphorus application rates in a hulless barley and pea mixed-cropping system. *Appl. Soil Ecol.* 195, 15. doi: 10.1016/j.apsoil.2023.105262

Jensen, E. S., Carlsson, G., and Hauggaard-Nielsen, H. (2020). Intercropping of grain legumes and cereals improves the use of soil N resources and reduces the requirement for synthetic fertilizer N: A global-scale analysis. *Agron. Sustain. Dev.* 40, 9. doi: 10.1007/s13593-020-0607-x

Knops, J. M. H., Bradley, K. L., and Wedin, D. A. (2002). Mechanisms of plant species impacts on ecosystem nitrogen cycling. *Ecol. Lett.* 5, 454–466. doi: 10.1046/j.1461-0248.2002.00332.x

Lai, H. L., Gao, F. Y., Su, H., Zheng, P., Li, Y. Y., and Yao, H. Y. (2022). Nitrogen distribution and soil microbial community characteristics in a legume-cereal intercropping system: A review. *Agronomy-Basel* 12, 15. doi: 10.3390/agronomy12081900

Li, Q. S., Jia, X. L., Ye, J. H., Li, J. J., Luo, X. M., and Lin, W. X. (2021). Effects of Maize/soybean intercropping on soil microbial community and biochemical properties. *Allelopathy J.* 54, 141–156. doi: 10.26651/AJ

Liu, X., Rahman, T., Song, C., Yang, F., Su, B. Y., Cui, L., et al. (2018). Relationships among light distribution, radiation use efficiency and land equivalent ratio in maize-soybean strip intercropping. *Field Crops Res.* 224, 91–101. doi: 10.1016/j.fcr.2018.05.010

Liu, J., Li, Y., Han, C. Q., Yang, D. L., Yang, J. J., Cade-Menun, B. J., et al. (2022). Maize-soybean intercropping facilitates chemical and microbial transformations of phosphorus fractions in a calcareous soil. *Front. Microbiol.* 13, 12. doi: 10.3389/fmicb.2022.1028969

Liu, X. D., Meng, L. B., Yin, T. J., Wang, X. R., Zhang, S., Cheng, Z. Y., et al. (2023). Maize/soybean intercrop over time has higher yield stability relative to matched monoculture under different nitrogen-application rates. *Field Crops Res.* 301, 10. doi: 10.1016/j.fcr.2023.109015

Lu, M., Zhao, J. X., Lu, Z. R., Li, M. J., Yang, J. F., Fullen, M., et al. (2023). Maize-soybean intercropping increases soil nutrient availability and aggregate stability. *Plant Soil* 16. doi: 10.1007/s11104-023-06282-2

Qi, W. J., Wang, Q., Mak-Mensah, E., Zhu, J. H., Zhang, D. K., Zhou, X. J., et al. (2023). Effects of soil physicochemical properties on maize, wheat, and soybean yields in maize-wheat and maize-soybean intercropping systems in China: a meta-analysis. *J. Soil Sci. Plant Nutr.* 24, 21–29. doi: 10.1007/s42729-023-01556-1

Raza, A., Asghar, M. A., Ahmad, B., Bin, C., Hussain, M. I., Li, W., et al. (2020). Agro-techniques for lodging stress management in maize-soybean intercropping system-A review. *Plants-Basel* 9, 22. doi: 10.3390/plants9111592

Roohi, M., Arif, M. S., Guillaume, T., Yasmeen, T., Riaz, M., Shakoor, A., et al. (2022). Role of fertilization regime on soil carbon sequestration and crop yield in a maize-cowpea intercropping system on low fertility soils. *Geoderma* 428, 11. doi: 10.1016/j.geoderma.2022.116152

Secco, D., Bassegio, D., De Marins, A. C., Chang, P. B., Savioli, M. R., Castro, M. B. S., et al. (2023). Short-term impacts of different intercropping times of maize and ruzigrass on soil physical properties in subtropical Brazil. *Soil Tillage Res.* 234, 9. doi: 10.1016/j.still.2023.105838

Silva, L. S., Laroca, J. V. D., Coelho, A. P., Gonsalves, E. C., Gomes, R. P., Pacheco, L. P., et al. (2022). Does grass-legume intercropping change soil quality and grain yield in integrated crop-livestock systems? *Appl. Soil Ecol.* 170, 10. doi: 10.1016/j.apsoil.2021.104257

Tian, X. L., Wang, C. B., Bao, X. G., Wang, P., Li, X. F., Yang, S. C., et al. (2019). Crop diversity facilitates soil aggregation in relation to soil microbial community composition driven by intercropping. *Plant Soil* 436, 173–192. doi: 10.1007/s11104-018-03924-8

Trivedi, P., He, Z. L., Van Nostrand, J. D., Albrigo, G., Zhou, J. Z., and Wang, N. (2012). Huanglongbing alters the structure and functional diversity of microbial communities associated with citrus rhizosphere. *Isme J.* 6, 363–383. doi: 10.1038/ismej.2011.100

Wang, Z. G., Bao, X. G., Li, X. F., Jin, X., Zhao, J. H., Sun, J. H., et al. (2015). Intercropping maintains soil fertility in terms of chemical properties and enzyme activities on a timescale of one decade. *Plant Soil* 391, 265–282. doi: 10.1007/s11104-015-2428-2

Wang, W. M., Chen, Y., Zhang, F. H., Zhang, W., Liu, J. G., Wang, J. P., et al. (2023a). Cotton-maize intercropping increases rhizosphere soil phosphorus bioavailability by regulating key phosphorus cycling genes in northwest China. *Appl. Soil Ecol.* 182, 10. doi: 10.1016/j.apsoil.2022.104734

Wang, G. W., Jin, Z. X., Wang, X. X., George, T. S., Feng, G., and Zhang, L. (2022a). Simulated root exudates stimulate the abundance of Saccharimonadales to improve the alkaline phosphatase activity in maize rhizosphere. *Appl. Soil Ecol.* 170, 10. doi: 10.1016/j.apsoil.2021.104274

Wang, R. T., Liu, J. X., Jiang, W. Y., Ji, P. S., and Li, Y. G. (2022b). Metabolomics and microbiomics reveal impacts of rhizosphere metabolites on alfalfa continuous cropping. *Front. Microbiol.* 13, 20. doi: 10.3389/fmicb.2022.833968

Wang, W. M., Yin, F. T., Gu, J. C., Wang, Z., Zhang, F. H., Li, L. H., et al. (2023b). Effects of maize/soybean intercropping on rhizosphere soil phosphorus availability and functional genes involved in phosphorus cycling in Northwest China. *Plant Soil* 14. doi: 10.1007/s11104-023-06363-2

Wang, Y. L., Zhang, L. Q., Meng, F. A., Lou, Z. X., An, X. Y., Jiang, X. B., et al. (2023c). Responses of soil microbial communities in soybean-maize rotation to different fertilization treatments. *Agronomy-Basel* 13, 22. doi: 10.3390/agronomy13061590

Weidner, S., Koller, R., Latz, E., Kowalchuk, G., Bonkowski, M., Scheu, S., et al. (2015). Bacterial diversity amplifies nutrient-based plant-soil feedbacks. *Funct. Ecol.* 29, 1341–1349. doi: 10.1111/1365-2435.12445

Xu, Z., Li, C. J., Zhang, C. C., Yu, Y., van der Werf, W., and Zhang, F. S. (2020). Intercropping maize and soybean increases efficiency of land and fertilizer nitrogen use; A meta-analysis. *Field Crops Res.* 246, 10. doi: 10.1016/j.fcr.2019.107661

Yang, X. Q., Wang, Y., Sun, L. Y., Qi, X. N., Song, F. B., and Zhu, X. C. (2020). Impact of maize-mushroom intercropping on the soil bacterial community composition in northeast China. *Agronomy-Basel* 10, 15. doi: 10.3390/agronomy10101526

Yang, Z. Y., Zhang, Y. P., and Luo, G. W. (2023). Regulation of soil C-N-P stoichiometry by intercropping mitigates microbial resource limitations and contributes to maize productivity. *Plant Soil* 498(1-2), 21–38. doi: 10.1007/s11104-023-06251-9

Yao, X. D., Zhou, H. L., Zhu, Q., Li, C. H., Zhang, H. J., Wu, J. J., et al. (2017). Photosynthetic response of soybean leaf to wide light-fluctuation in maize-soybean intercropping system. *Front. Plant Sci.* 8, 10. doi: 10.3389/fpls.2017.01695

Zaeem, M., Nadeem, M., Pham, T. H., Ashiq, W., Ali, W., Gilani, S. S. M., et al. (2019). The potential of corn-soybean intercropping to improve the soil health status and biomass production in cool climate boreal ecosystems. *Sci. Rep.* 9, 17. doi: 10.1038/s41598-019-49558-3

Zhang, L. L., Li, L. J., Pan, X. G., Shi, Z., Feng, X. H., Gong, B., et al. (2018a). Enhanced growth and activities of the dominant functional microbiota of chicken manure composts in the presence of maize straw. *Front. Microbiol.* 9, 11. doi: 10.3389/fmicb.2018.01131

Zhang, M. M., Wang, N., Hu, Y. B., and Sun, G. Y. (2018b). Changes in soil physicochemical properties and soil bacterial community in mulberry (*Morus alba* L.)/alfalfa (*Medicago sativa* L.) intercropping system. *Microbiologyopen* 7, 11. doi: 10.1002/mbo3.555

Zhang, G. Z., Yang, H., Zhang, W. P., Bezemer, T. M., Liang, W. J., Li, Q., et al. (2023). Interspecific interactions between crops influence soil functional groups and networks in a maize/soybean intercropping system. *Agric. Ecosyst. Environ.* 355, 13. doi: 10.1016/j.agee.2023.108595

Zhang, H., Zeng, F. P., Zou, Z. G., Zhang, Z. Q., and Li, Y. Z. (2017). Nitrogen uptake and transfer in a soybean/maize intercropping system in the karst region of southwest China. *Ecol. Evol.* 7, 8419–8426. doi: 10.1002/ece3.3295

Zhao, X. H., Dong, Q. Q., Han, Y., Zhang, K. Z., Shi, X. L., Yang, X., et al. (2022). Maize/peanut intercropping improves nutrient uptake of side-row maize and system microbial community diversity. *BMC Microbiol.* 22, 16. doi: 10.1186/s12866-021-02425-6

Zheng, H. Y., Wang, J. Y., Cui, Y., Guan, Z. Y., Yang, L., Tang, Q. Q., et al. (2022). Effects of row spacing and planting pattern on photosynthesis, chlorophyll fluorescence, and related enzyme activities of maize ear leaf in maize-soybean intercropping. *Agronomy-Basel* 12, 13. doi: 10.3390/agronomy12102503

Zhou, M. H., and Butterbach-Bahl, K. (2014). Assessment of nitrate leaching loss on a yield-scaled basis from maize and wheat cropping systems. *Plant Soil* 374, 977–991. doi: 10.1007/s11104-013-1876-9

Zhu, Q., Liao, K. H., Lai, X. M., and Lv, L. G. (2021). Scale-dependent effects of environmental factors on soil organic carbon, soil nutrients and stoichiometry under two contrasting land-use types. *Soil Use Manage.* 37, 243–256. doi: 10.1111/sum.12695

Zhu, Q. R., Yang, Z. Y., Zhang, Y. P., Wang, Y. Z., Fei, J. C., Rong, X. M., et al. (2024). Intercropping regulates plant- and microbe-derived carbon accumulation by influencing soil physicochemical and microbial physiological properties. *Agric. Ecosyst. Environ.* 364, 12. doi: 10.1016/j.agee.2023.108880

Zou, X. X., Liu, Y., Huang, M. M., Li, F., Si, T., Wang, Y. F., et al. (2023). Rotational strip intercropping of maize and peanut enhances productivity by improving crop photosynthetic production and optimizing soil nutrients and bacterial communities. *Field Crops Res.* 291, 13. doi: 10.1016/j.fcr.2022.108770

TYPE Original Research
PUBLISHED 18 October 2024
DOI 10.3389/fpls.2024.1400261

Carbon and nitrogen stoichiometry across plant–soil system accounts for the degradation of multi-year alfalfa grassland

Wei Wang[1,2‡], Tao Tian[2‡], Meng-Ying Li[2], Bao-Zhong Wang[2], Fu-Jian Mei[2], Ji-Yuan Li[2], Ning Wang[2], Yu-Miao Yang[2], Qiang Zhang[1], Hong-Yan Tao[2], Li Zhu[2,3*†] and You-Cai Xiong[2,3*†]

[1]Key Laboratory of Soil Environment and Nutrient Resources in Shanxi Province, Shanxi Agricultural University, Taiyuan, China, [2]State Key Laboratory of Herbage Improvement and Grassland Agro-ecosystems, College of Ecology, Lanzhou University, Lanzhou, China, [3]College of Biology and Agricultural Resources, Huanggang Normal University, Huanggang, China

Alfalfa (*Medicago sativa* L.) grassland is prone to degradation following multi-year maintenance. Yet, its mechanism regarding the stoichiometry of carbon (C) and nitrogen (N) across plant–soil system is still unclear. To address this issue, the method of space-for-time sampling was employed to investigate alfalfa grasslands with five planting years (5-, 8-, 10-, 15-, and 20-year periods) in the semiarid Loess Plateau. The results showed that the alfalfa above- and underground biomass decreased steadily decrease after the fifth to eighth years, showing a degradation tendency with the extension of planting duration. The mean weight diameter of aggregate registered an increase with planting years. However, the C and N stocks decreased with planting years in five soil aggregate fractions. Specifically, they were the highest in the fifth year and then started to gradually decrease along the 8th, 10th, 15th, and 20th year. Redundancy and correlation analysis confirmed that the C and N stocks of soil aggregates were closely positively associated with those of plant. Overall, the highest stability of soil physical structure was found during the period from the fifth to eighth year, and, afterward, the stability declined. In conclusion, alfalfa plantation improved soil structure stability but aggravated soil C and N stocks, and biomass and soil aggregate indicators accounted for alfalfa field degradation after a certain year of plantation.

KEYWORDS

alfalfa field, soil aggregates, carbon and nitrogen stoichiometry, degradation, semiarid region

OPEN ACCESS

EDITED BY
Khurram Shahzad,
Lasbela University of Agriculture, Water and Marine Sciences, Pakistan

REVIEWED BY
Muhammad Qayyum,
Bahauddin Zakariya University, Pakistan
Qamar Sarfaraz,
Lasbela University of Agriculture, Water and Marine Sciences, Pakistan
Muhammad Baqir Hussain,
MNS University of Agriculture, Multan, Pakistan

*CORRESPONDENCE
You-Cai Xiong
xiongyc@lzu.edu.cn
Li Zhu
zhuli@hgnu.edu.cn

†PRESENT ADDRESS
You-Cai Xiong,
State Key Laboratory of Herbage Improvement and Grassland Agro-Ecosystems, College of Ecology, Lanzhou University, Lanzhou, China
Li Zhu,
State Key Laboratory of Herbage Improvement and Grassland Agro-Ecosystems, College of Ecology, Lanzhou University, Lanzhou, China

‡These authors have contributed equally to this work

RECEIVED 13 March 2024
ACCEPTED 26 August 2024
PUBLISHED 18 October 2024

CITATION
Wang W, Tian T, Li M-Y, Wang B-Z, Mei F-J, Li J-Y, Wang N, Yang Y-M, Zhang Q, Tao H-Y, Zhu L and Xiong Y-C (2024) Carbon and nitrogen stoichiometry across plant–soil system accounts for the degradation of multi-year alfalfa grassland. *Front. Plant Sci.* 15:1400261. doi: 10.3389/fpls.2024.1400261

Highlights

- There exists a steady degradation with planting years in perennial alfalfa field.
- Field productivity and soil aggregate quality declined after 5- to 8-year planting.
- C and N stocks in aggregate fractions were the highest at the fifth year and then declined.
- C and N stocks of soil aggregates were positively linked with that of alfalfa ($p < 0.05$).
- Steady deterioration of C and N stocks from soil to plant explains system degradation.

1 Introduction

The Loess Plateau is one of the most seriously degraded soil regions, which is located in northern China (Li et al., 2021; Yuan et al., 2024). Soil degradation is related to the climatic, environmental, and geological features of this region (Gong et al., 2020); it is also strongly tied to unreasonable land-use management (Fan et al., 2016). To restrain soil degradation, alfalfa (*Medicago sativa* L.) was extensively planted until the 1960s in the Loess Plateau due to the characteristics of the nutrient-rich forage crop with high biological yield potential, high resistance ability, and wide adaptability in extreme environments (Zhang X. L. et al., 2021; Song et al., 2024). Alfalfa has the potential to enhance nitrogen (N) input into soil ecosystems while promoting soil carbon (C) and N accumulation (Vitousek et al., 2013). However, alfalfa forage biomass is gradually reduced with the duration of planting years, and continuous planting for many years will degrade the alfalfa biomass and soil quality (Gu et al., 2018; Fang et al., 2021; Qi et al., 2023). Therefore, it is essential to study the optimum cultivation period and the degradation mechanism of alfalfa grasslands.

Ecological stoichiometry was used to explore the degradation mechanism for plant responses to environmental change (Austin and Vitousek, 2012). The ecological stoichiometry of C and N across ecosystem components can provide a new strategy for elucidating the nutrient cycle process (Du and Gao, 2021; Tang et al., 2022). Carbon is an essential energy source for above- and underground ecosystem biogeochemical processes (Wang et al., 2021b), whereas N is an essential plant nutrient as a key limiting factor determining primary production in ecosystems (Wang et al., 2021a). The C and N stoichiometry of plants and their interaction with the soil significantly affect ecosystem functions (Yang et al., 2019; Xu et al., 2024). Soil C and N availability affects plant nutrient absorption and assimilation (Zhang et al., 2019); In turn, plant litter and root exudates will provide substrates to enhance soil C and N cycling processes (Zhou et al., 2019; Dan et al., 2023). Overall, the variation in C and N cycles in ecosystems can change the stoichiometry of plants and soils (Wang et al., 2021a). C and N stoichiometric flexibility might affect terrestrial ecosystem biogeochemical cycling, a changing the ecosystem productivity and terrestrial degradation (Sardans et al., 2017; Li et al., 2023). Therefore, it is necessary to determine the C and N stoichiometry in plants and soil to explore the degradation mechanism of perennial alfalfa grasslands.

Soil aggregates are composed of granular or small clumped structures, and soil aggregate stability is a key index for characterizing soil degradation (Zhu et al., 2018; Tan et al., 2024). Soil aggregates are affected by many factors, such as the soil physical and chemical properties, soil microbes, plant root distribution, and artificial cultivation (Bodner et al., 2014; Shen et al., 2024). Based on soil size, aggregates are classified into three parts: macroaggregates (>0.25 mm), microaggregates (0.053–0.25 mm), and the silt-clay fraction (<0.053 mm) (Lu et al., 2021). The soil aggregate size distribution often influences soil aeration, corrosion resistance, and water permeability (Bissonnais and Arrouays, 1997). Soil aggregation is a process driven the biotic and abiotic factors that plant-derived organic matter input, microorganisms, and soil conditions combination (Liu et al., 2023). Increasing plant cover to prevent the surface erosion and to protect soil physical disturbance promotes the plant-derived organic matter input and contributes soil aggregation formation (Wang et al., 2022). In addition, more plant residue input also promotes the microbial grower, regulate microbial activity, and microbial-derived C and ultimately affects the formation of soil aggregate (Zhao et al., 2024). Higher C concentrations and mineralization rates are often found to be associated with macroaggregates (Wang et al., 2018; Araujo et al., 2024). This is because macroaggregates are easily disintegrated and broken by external interference, whereas microaggregates may be more physically protected and are, therefore, more biochemically recalcitrant to C mineralization (Kubar et al., 2021). Previous studies have investigated the soil aggregates in various land-use types, including forests, cultivated lands, grazing lands, and woodlands. In fact, most of above investigations on soil aggregates are mainly aimed at the stability and C and N characteristics (Wang et al., 2018; Bhatt et al., 2023), and few studies have focused on the relationship between alfalfa aggregates and plant C and N stoichiometry. Therefore, knowledge of C and N stoichiometry is crucial for understanding the biochemical mechanisms of plant and soil aggregates.

Plant–soil interactions via both positive and negative feedbacks can constrain or promote plants development in the novel environment, and plant–soil interaction is strongly influenced by the rhizosphere microbiota (Lustenhouwer et al., 2024). Plant–soil interaction plays an important role in global C and N biogeochemical cycles, and previous study found that rhizobacteria symbiotic with legumes can drive positive effect, and promote nutrient uptake and plant growth (Yahui et al., 2023). However, there is still controversy about how multi-year alfalfa planting affects the C and N in soil aggregates and plant organs in the semiarid regions. We hypothesized that the dynamics of C and N sequestration might be key indicators to explain soil degradation following continuous alfalfa plantation. To clarify this issue, the method of space for time was employed to investigate 5-year succession of alfalfa grasslands in the semiarid region. The purposes of this study were 1) to determine the changes in the production of alfalfa with planting years, 2) to identify the stocks dynamics of C and N in soil aggregate distribution with planting years, 3) to reveal the changes C and N across plant–soil system in the multi-year alfalfa grassland, and 4) to explore the degradation mechanisms of perennial alfalfa. The findings will help formulate an appropriate management strategy for ecological restoration and sustainable soil development.

2 Materials and methods

2.1 Description of the study site

The study area is located in Yuzhong County, Gansu Province, China (36°02′N, 104°25′E, 2,400 m) (Figure 1). The average annual temperature is 6.5°C, and the monthly average maximum and minimum temperatures are 19.0°C and −8.0°C, respectively. The mean annual precipitation from 2000 to 2018 was 323.5 mm, the maximum year was 2018 (458.8 mm), and the minimum precipitation occurred in 2004 (202.0 mm). The average annual water evaporation is approximately 1,450 mm. The local soil type is Calcic Kastanozems (Siltic) or rusty dark loess soil with a pH of 8.2 (Guo et al., 2010). The rainfall data were derived from the perennial positioning automatic meteorological recording instrument (Figure 1).

2.2 Experimental design

We selected five alfalfa grasslands in October 2018 and formed a time series of 5, 8, 10, 15, and 20 years, which represented successional series with similar topographic conditions. Where fields planted with alfalfa were recorded in 2013, 2010, 2008, 2003, and 1998, respectively. Abandoned farmland was chosen as the control group (CK; abandoning 15 years). The aspect and slope of each selected alfalfa field remained relatively consistent (Figure 1). In all the selected plots, the alfalfa variety *Algonquin* was planted, each plot was sown with alfalfa seeds of 35 kg ha^{-1}, the depth was approximately 2 cm, and each row was almost 20 cm. There was no irrigation throughout the growing season. Fertilization was only applied in the first year of planting (N, 185.6 kg ha^{-1}; P, 48 kg ha^{-1}), and no fertilization was conducted afterward. There was no grazing treatment for the alfalfa grassland, which was harvested in June and October of each year (weeds were

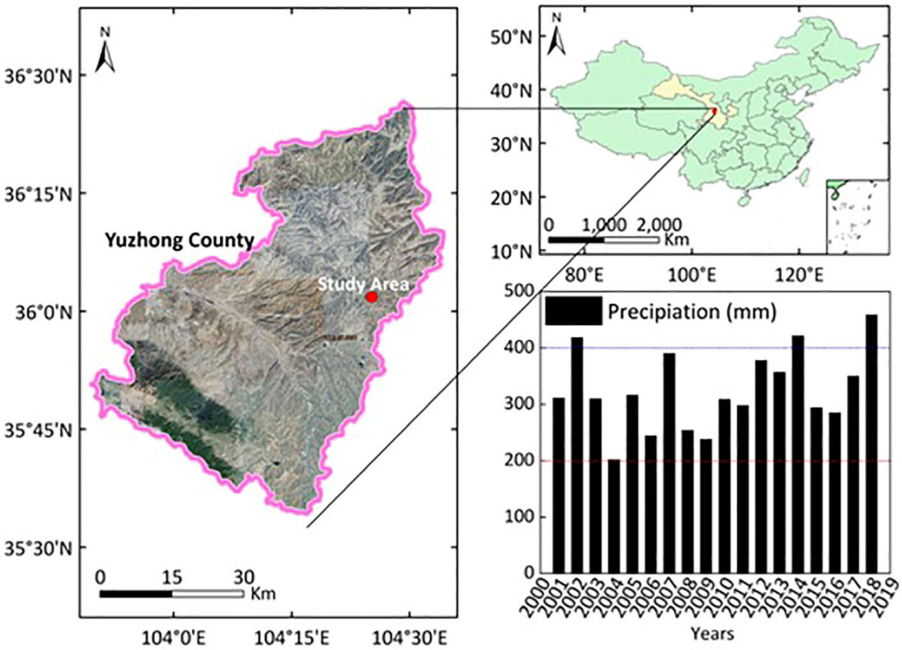

Tre.	Latitude	longitude	Altitude	Main weeds
CK	36°1′59″ N	104°25′05″ E	2321.42 m	*Artemisia frigida* Willd.,
5-Y	36°1′47″ N	104°24′48″ E	2347.36 m	*Leymus secalinus* (Georgi) Tzvel.,
8-Y	36°1′59″ N	104°25′01″ E	2344.95 m	*Poa annua* L.,
10-Y	36°1′45″ N	104°24′45″ E	2354.13 m	*Aster altaicus* Willd.,
15-Y	36°1′59″ N	104°25′03″ E	2340.55 m	*Stipa capillata* L.
20-Y	36°1′59″ N	104°25′04″ E	2330.98 m	*Agropyron cristatum* (L.) Gaertn

FIGURE 1
Location of study area and its precipitation and biodiversity background. CK, abandoned farmland. 5-Y, 8-Y, 10-Y, 15-Y, and 20-Y planting indicate the variations across 5, 8, 10, 15, and 20 years, respectively.

also mowed at the same time). The control group had no fertilization and mowing treatment. The only difference in the selected alfalfa grassland was in planting years. In the alfalfa grassland, weed biomass increased with prolonged plantation years. The dominant vegetation species are *Artemisia frigida Willd.*, *Leymus secalinus (Georgi) Tzvel.*, *Poa annua* L., *Aster altaicus Willd.*, *Stipa capillata* L., and *Agropyron cristatum* L. *Gaertn*. The weeds were periodically cleared by hand when needed to avoid interspecific disturbance.

2.3 Sampling

In October 2018, 15 plots of 1 m × 1 m of each field were randomly selected and marked to measure the biomass of each field. Soil samples of 0-cm to 20-cm depth were randomly collected from the field using a soil auger (diameter of 5 cm) with five replicates for each planting period, and each alfalfa field was mixed in three samples. Before air-drying, the soil was sieved through 2.0-mm screens for available nutrient analyses, and, after drying, it was sieved through 0.15-mm screens for total nutrient analyses. The soil aggregate sample was collected with a hard Polyvinyl Chloride (PVC) pipe with a diameter of 10 cm and a height of 20 cm. After sampling, the aggregate sample was divided into small clods a diameter of 1 cm for air-drying.

2.4 Physical and chemical analysis

Soil bulk density (SBD) was determined using cutting ring (0–20 cm). Soil water storage (SWC) was measured gravimetrically (0–20 cm, 20–40 cm, 40–60 cm, 60–80 cm, and 80–100 cm). The soil aggregate-size fraction was measured using a dry- and wet-sieving method (Su et al., 2009). For the dry sieving method, we used 100 g of air-dried soil samples in a stainless-steel vibrating sieve divided into five sizes: >2 mm, 2–1 mm, 1–0.5 mm, 0.5–0.25 mm, and <0.25 mm. The wet sieving method used 50 g of air-dried soil, which was weighed according to dry sieving and moistened for 10 min with distilled water. The apparatus specifications were an oscillation of 10 min at a frequency of 30 cycle min^{-1}. Aggregates retained in the sieve were air dried at 65°C, weighed, and stored for C and N content measurements. The soil aggregate distribution is calculated with Equation 1. The mean weight diameter (MWD) and percentage of aggregate destruction (PAD) are calculated using Equations 2 and 3, respectively.

$$AD = ADi/TO \times 100\,\% \quad (1)$$

$$MWD = [\sum_{i=1}^{n}(\overline{Xi}\ ADi)]/\sum_{i=1}^{n} ADi \quad (2)$$

$$PAD = (ADd - ADw)/ADd \quad (3)$$

where AD is the aggregate distribution of each fraction (%), ADi is the i size aggregate weight (g), and TO is the total weight of the soil (g). Xi is the mean diameter of the aggregate, and ADd and ADw are the proportions of dry and water stable aggregates (>0.25 mm), respectively.

The SOC content and C of aggregate fractions are determined by Puget et al. (2000). The soil total nitrogen (TN) content and TN of the aggregate fractions were measured by Bremner (1997). The above- and underground biomass of alfalfa and weeds (soil depth up to 40 cm) were collected from a 1 m × 1 m area of each plot (collected twice in late June and early October). The above- and underground biomass were dried at 105°C for 30 min and then at 65°C to constant weight (Wilson et al., 2009). The C and N contents of alfalfa plants were measured following Yu et al. (2021); aggregate C and N stocks were measured according to Equation 4 (Zhang L. Q. et al., 2015).

$$C(N)stock = ADi \times M \times SOCi(TNi) \times 0.001$$

$$M = SBD \times H \times 0.01 \times 10000 \quad (4)$$

where C and N stocks are stocks of soil carbon and nitrogen [Mg ha^{-1}; where M is soil quality per unit area (Mg ha^{-1})], SOCi and TNi are different size aggregates of soil carbon and nitrogen content (g kg^{-1}), SBD is the soil bulk density (g cm^{-3}), and H is 20 cm.

2.5 Statistical analysis

All statistical data were tested for normality and homogeneity of variance before further analysis. One-way ANOVA was used to compare the differences among the six treatments. The difference was tested by Tukey's honestly significant difference (HSD) to check the statistical significance of the treatments between different planting years. Mean comparisons were performed using the least significant difference at a probability level of 0.05. Redundancy analysis (RDA) and correlation analysis were used to evaluate the relationship between aggregate C and N stocks, plant biomass, and the C and N concentrations of alfalfa plants. RDA was plotted using Canoco 5.0. Graphs were prepared using ArcGis 10.0 and Origin 2021.

3 Results

3.1 Dynamics of aboveground and belowground biomass with planting years

Above- and underground biomass varied significantly among alfalfa cultivation years (Table 1). Throughout various planting for alfalfa, a significant change in above- and underground biomass was occurred. In the aboveground biomass, alfalfa yields reached the highest after approximately 5 years, whereas those of the remaining years declined approximately 20 years after alfalfa planting. Conversely, underground biomass was at a maximum value after alfalfa planting for 8 years but then decreased with the duration years. Therefore, the above- and underground biomass of alfalfa grassland declined with the number of years of planting.

TABLE 1 Variations of above- and belowground biomass and the C and N stocks in alfalfa along varying planting durations.

Years	Aboveground				Underground			
	Biomass (kg ha^{-1})	C content (g kg^{-1})	N content (g kg^{-1})	C-N ratio	Biomass (kg ha^{-1})	C content (g kg^{-1})	N content (g kg^{-1})	C-N ratio
CK	2,349.3 ± 23.1e	522.8 ± 1.2a	6.42 ± 0.0e	81.5 ± 0.0a	1,866.3 ± 11.5f	413.3 ± 1.1f	4.11 ± 0.1e	100.9 ± 2.6a
5-Y	3,985.6 ± 11.5a	506.1 ± 1.1b	16.4 ± 0.1bc	30.8 ± 0.1b	3,906.3 ± 23.1e	588.4 ± 1.1a	9.83 ± 0.1c	59.8 ± 0.6b
8-Y	3,788.3 ± 11.5b	475.2 ± 1.2c	16.9 ± 0.2a	28.5 ± 0.1c	5,757.3 ± 11.5a	520.6 ± 1.2b	9.26 ± 0.2d	56.2 ± 0.8c
10-Y	3,516.0 ± 11.4c	463.5 ± 1.2d	16.7 ± 0.1ab	27.7 ± 0.1d	5,542.6 ± 11.5b	513.9 ± 1.1c	11.8 ± 0.1b	43.8 ± 0.3d
15-Y	2,743.9 ± 11.7d	451.2 ± 0.6e	16.3 ± 0.1c	27.7 ± 0.2d	5,259.3 ± 11.5c	456.0 ± 1.1d	12.2 ± 0.2a	37.6 ± 0.3e
20-Y	1,925.4 ± 23.1f	432.1 ± 1.2f	15.8 ± 0.2d	27.3 ± 0.1e	4,856.4 ± 5.8d	440.2 ± 1.2e	12.1 ± 0.2a	36.4 ± 0.2e

Different lowercase letters indicate significant differences among the same parameter at $p < 0.05$ according to Tukey HSD tests. CK, abandoned farmland. 5-Y, 8-Y, 10-Y, 15-Y, and 20-Y represent planting variations for 5, 8, 10, 15, and 20 years, respectively.

3.2 Dynamics of the organic carbon and total nitrogen concentrations of plants with planting years

The C and N contents and C-N ratio of alfalfa varied with planting years (Table 1). The C contents of alfalfa above- and underground decreased after continuous planting 5 years. The N content of the aboveground also showed significant change; however, the N content of underground significantly increased with planting years. Similarly, the C-N ratio of alfalfa above- and underground also declined under cultivated 5 years.

3.3 The responses of soil water content and soil bulk density to planting years

As the depth of the soil layer increases, the SWC of the 0-cm to 100-cm soil layer decreases significantly, and the soil moisture content of alfalfa grassland is significantly lower than that of the control (Figure 2A). At different planting times, the SWC was the highest after

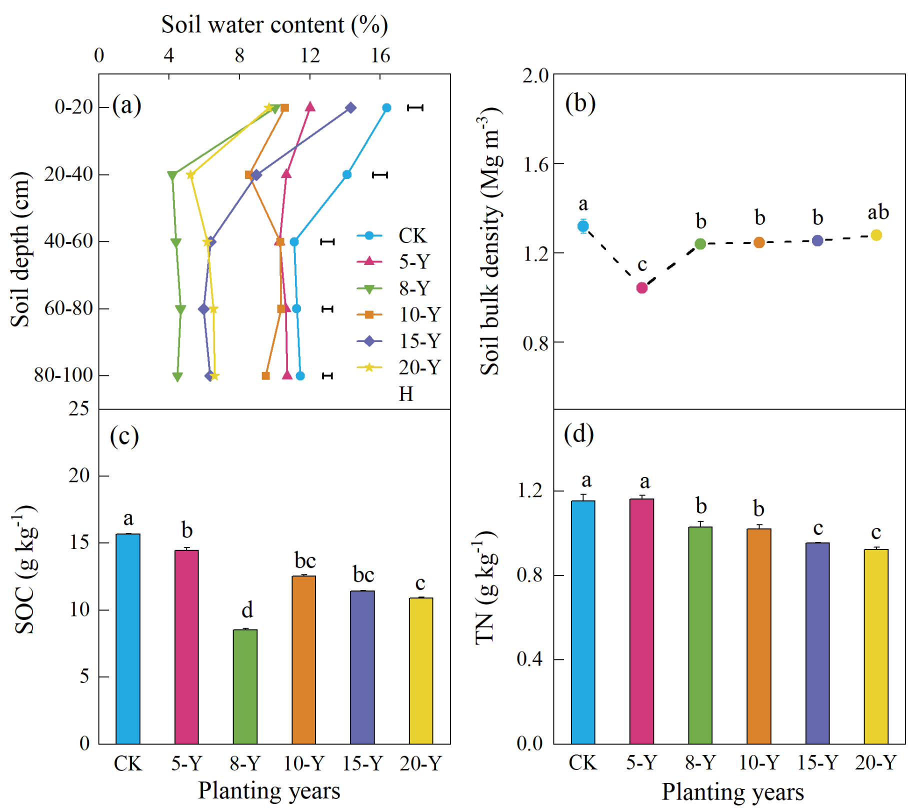

FIGURE 2
Dynamics of soil water content (SWC; 0–100 cm) **(A)**, soil bulk density **(B)**, SOC content **(C)**, and TN content **(D)** at 0-cm to 20-cm soil depth in response to different durations of alfalfa planting. Different letters indicate significant differences in planting duration ($p < 0.05$). The values are mean + SE (error bar). CK, abandoned farmland. 5-Y, 8-Y, 10-Y, 15-Ym and 20-Y represent planting variations for 5, 8, 10, 15, and 20 years, respectively.

10 years of planting and the lowest after 8 years of planting. The SBD of alfalfa grassland ranged from 1.04 g cm^{-3} to 1.28 g cm^{-3}, and there was a significantly variable trend in 5 years, and there is less change after cultivated 8 to 20 years (Figure 2B). The change in SBD after 8, 15, and 20 years of planting was significantly higher than that after 5 years of planting, followed by 10 years of planting.

3.4 The dynamics of soil organic carbon and nitrogen contents under different planting years

The soil organic carbon (SOC) content of artificial alfalfa grassland at 0-cm to 20-cm soil depth showed a V-shaped trend with increasing alfalfa planting duration. The highest value of planting for 5 years was 14.4 g kg^{-1}, and the lowest value of planting for 8 years was 8.54 g kg^{-1} (Figure 2C). The soil TN content was between 0.89 g kg^{-1} and 1.02 g kg^{-1}, and the planting years had a significant effect on soil TN content, which showed a decreasing trend with increasing planting years (Figure 2D).

3.5 The dynamics of soil aggregate distribution with planting years

In general, the distribution of soil aggregates in size ranged considerably among various years of cultivation (Table 2). The proportion of aggregates with sizes > 2 mm and < 0.25 mm is significantly higher than that of aggregates with other sizes. After 8 years of planting, the proportion of aggregates > 2-mm size was higher than that for other planting durations, the proportions of aggregates of 1.0–2.0 mm, 0.5–1.0 mm, and 0.25–0.5 mm after 5 years of planting were higher than those for other planting durations (except for the 1.0–2.0 mm). The proportion of <0.25-mm aggregates after 20 years of planting was higher than that for other periods of cultivation.

In addition, both the mechanical and water-stable aggregates, soil aggregate, $R_{0.25}$ and MWD showed a declining trend with increase planting years. The mechanical and water-stable aggregates $R_{0.25}$ ranged from 62.9% to 43.7% and from 23.7% to 14.2% accordingly. The mechanical and water-stable aggregates MWD change from 1.16 mm to 0.90 mm and from 0.46 mm to 0.35 mm, respectively. In contrast, PAD presented an increasing trend and ranged from 62.2% for planting for 5 years to 67.4% for planting for 20 years.

3.6 The soil organic carbon and total nitrogen contents of different aggregates in response to planting years

The soil organic carbon (SOC), TN, and C-N ratios in different aggregates of alfalfa grassland showed a variable trend in planting years. The SOC and TN contents of each size were the highest at 5 years of planting, but the lowest was at 8 years of planting. The C-N ratio in all five sizes showed that the highest value was in the 10-year plantation, and the lowest was in the 5-year plantation (except for the 1–2 mm) (Figure 3).

TABLE 2 Responses of soil mechanical and water-stable aggregate compositions to varying planting years in alfalfa field.

Years	Composition of soil mechanical stable aggregate (%)					$R_{0.25}$ (%)	MWD (mm)	
	< 0.25 mm	0.25–0.5 mm	0.5–1.0 mm	1.0–2.0 mm	> 2.0 mm			
CK	45.4 ± 1.14BCa	3.96 ± 0.38Ab	3.86 ± 0.27Ab	5.05 ± 0.24Ab	41.7 ± 0.51Ca	54.6 ± 1.14BC	1.01 ± 0.01C	
5-Y	37.1 ± 2.04Db	3.70 ± 0.04Ac	4.86 ± 0.42Ac	3.88 ± 0.22Bc	50.5 ± 2.30Aa	62.9 ± 2.04A	1.16 ± 0.04A	
8-Y	40.4 ± 0.99CDb	3.49 ± 0.14ABc	2.02 ± 0.25Bc	2.41 ± 0.25Cc	51.7 ± 0.93Aa	59.6 ± 0.99AB	1.15 ± 0.02AB	
10-Y	46.8 ± 1.06Ba	2.72 ± 0.04BCb	1.52 ± 0.21Bb	1.67 ± 0.25CDb	47.3 ± 1.05ABa	53.2 ± 1.06C	1.05 ± 0.02BC	
15-Y	53.0 ± 0.55Aa	1.84 ± 0.25CDc	1.46 ± 0.12Bc	1.63 ± 0.14CDc	42.1 ± 0.23BCb	47.0 ± 0.55D	0.95 ± 0.01CD	
20-Y	56.3 ± 0.73Aa	1.50 ± 0.04Dc	1.21 ± 0.03Bc	1.32 ± 0.03Dc	39.6 ± 0.72Cb	43.7 ± 0.73D	0.90 ± 0.01D	
Years	Composition of soil water stable aggregate (%)					$R_{0.25}$ (%)	MWD (mm)	PAD (%)
	< 0.25 mm	0.25–0.5 mm	0.5–1.0 mm	1.0–2.0 mm	> 2.0 mm			
CK	81.0 ± 0.94CDa	3.36 ± 0.32Ac	2.61 ± 0.19Bc	1.40 ± 0.16Ac	11.6 ± 0.50Bb	19.0 ± 0.94B	0.39 ± 0.01B	65.3 ± 1.27A
5-Y	76.3 ± 0.69Ea	3.14 ± 0.04Ac	3.80 ± 0.03Ac	1.44 ± 0.08Ac	15.3 ± 0.58Ab	23.7 ± 0.69A	0.46 ± 0.01A	62.2 ± 2.30A
8-Y	78.2 ± 0.85DEa	2.63 ± 0.22ABc	2.38 ± 0.13Bc	1.45 ± 0.29Ac	15.3 ± 0.35Ab	22.1 ± 0.57A	0.45 ± 0.01A	62.9 ± 1.40A
10-Y	82.5 ± 0.49BCa	2.30 ± 0.03BCc	1.74 ± 0.10Cc	1.33 ± 0.11Ac	12.1 ± 0.48Bb	17.5 ± 0.49BC	0.39 ± 0.01B	67.1 ± 0.29A
15-Y	85.0 ± 0.65ABa	1.61 ± 0.07Cc	1.31 ± 0.05CDc	0.86 ± 0.03Ac	11.2 ± 0.58Bb	15.0 ± 0.65CD	0.36 ± 0.01B	68.1 ± 1.32A
20-Y	85.8 ± 0.36Aa	1.55 ± 0.01Cc	1.16 ± 0.03Dc	0.83 ± 0.03Ac	10.7 ± 0.32Bb	14.2 ± 0.36D	0.35 ± 0.01B	67.4 ± 1.27A

Different capital letters indicate significant differences among different planting durations in the same-sized aggregate at the 0.05 level, and different small letters indicate significant differences among different-sized aggregates in the same planting durations at the 0.05 level. The values are mean + SE. $R_{0.25}$, aggregates of diameter >0.25 mm; MWD, mean weight diameter; PAD, percentage of aggregate destruction; CK, abandoned farmland. 5-Y, 8-Y, 10-Y, 15-Y, and 20-Y represent planting variations for 5, 8, 10, 15, and 20 years, respectively.

In addition, the SOC and TN contents and C-N ratio of different size aggregates in the same planting years also showed a significant difference (Figure 3). In general, the SOC and TN contents of macroaggregates in the alfalfa grassland were higher than those in other particle sizes, and the < 0.25-mm particle size was the lowest. In the alfalfa grassland field, the C-N ratio of >2 mm, 0.25–0.5 mm, and <0.25 mm in 8 years was the lowest than that in the other years. After planting for 8 years, the ratios of the five size aggregates increased in all five sizes.

3.7 The dynamics of carbon and nitrogen stocks with planting years

The variation in the C and N stocks of the alfalfa succession series with different planting years is shown in Figure 4. In general, the C and N stocks of aggregates > 2 mm were the highest in each planting year (except for <0.25 mm). Among different planting years, the stock of C after 5 years of planting was the highest, and, after 8 years, it was declined. Similarly, in each planting year, the N stocks of aggregates > 2 mm were the largest. The N stocks after 5 years were the highest among the five planting years. Overall, the C and N stocks slightly decreased with prolonged planting.

3.8 Relationships of aggregate carbon and nitrogen stocks with alfalfa plants

The RDA showed that the CK treatment was concentrated in the first quadrant, and alfalfa grasslands were distributed in the other three quadrants (Figure 5). The first and second axes accounted for 84.63% (a) and 84.62% (b) of the variability explained. Aboveground biomass was negatively correlated with SBD and planting years, whereas underground biomass was positively correlated with planting years. At the same time, we found that aggregate C and N stocks were closely related to the C-N ratio of alfalfa above- and underground plants.

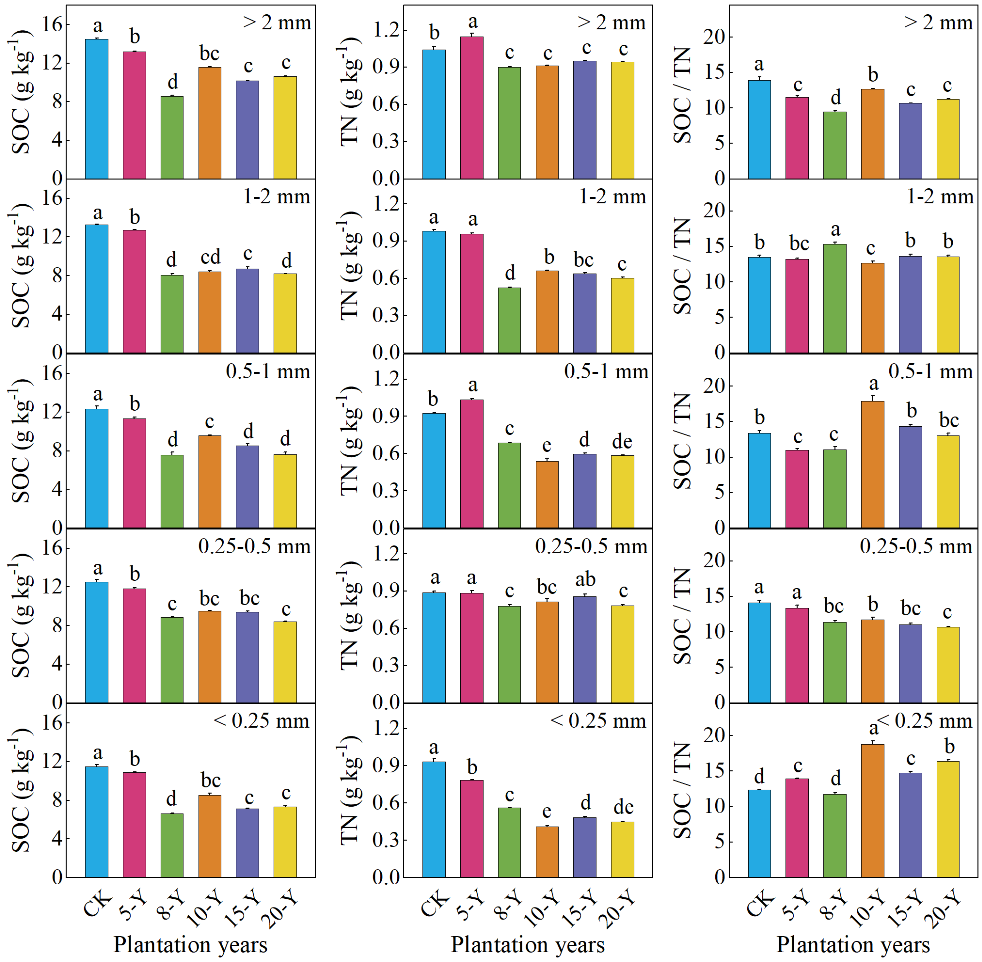

FIGURE 3
SOC, TN contents, and SOC/TN of different-sized aggregates at 0-cm to 20-cm soil depth in alfalfa plantations with different planting durations. Different letters indicate significant differences among different planting durations for the same-sized aggregate at the 0.05 level. The values are mean + SE (error bar). CK, abandoned farmland. 5-Y, 8-Y, 10-Y, 15-Y, and 20-Y represent planting variations for 5, 8, 10, 15, and 20 years, respectively.

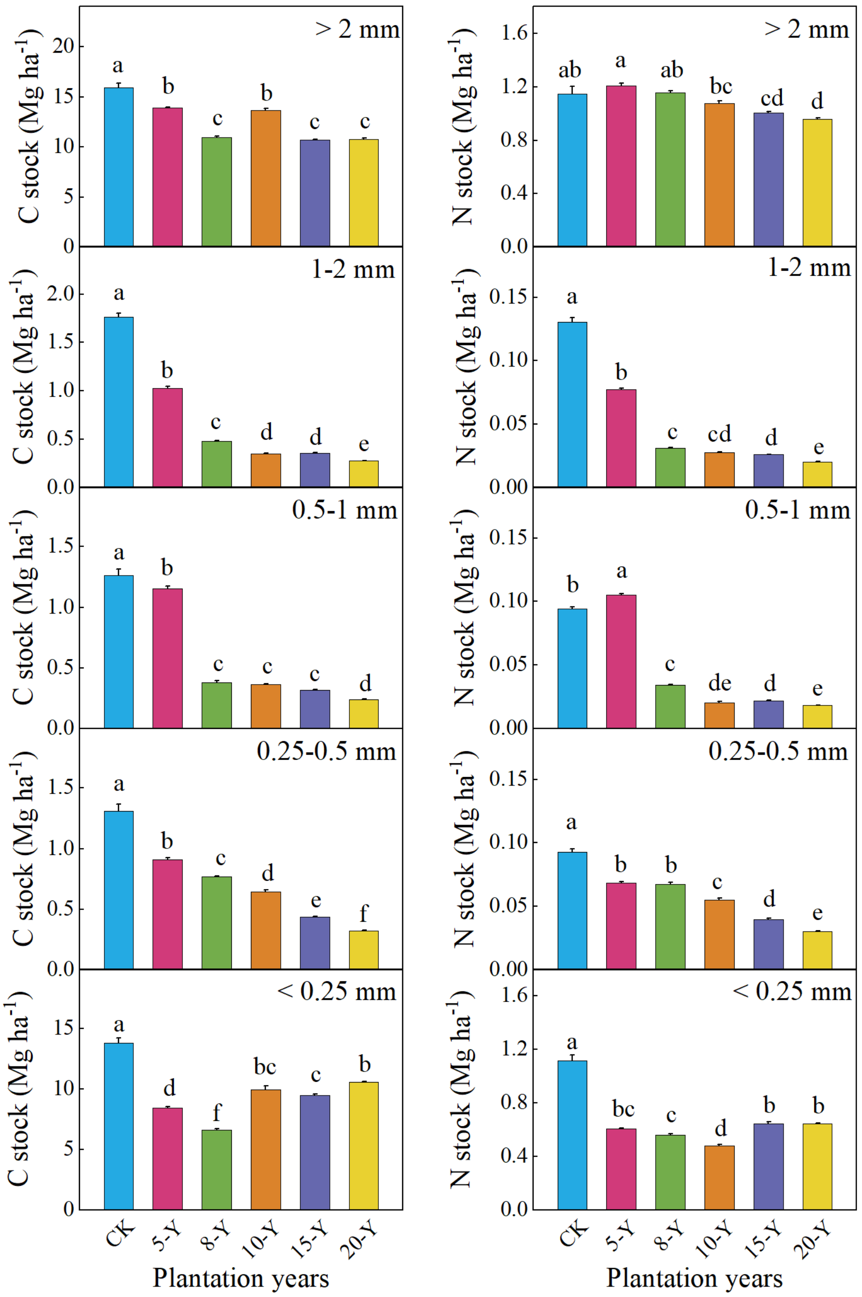

FIGURE 4
C and N stocks of different-sized aggregates at 0- to 20-cm soil depth in alfalfa plantations with different planting durations. Different letters indicate significant differences among different planting durations for the same-sized aggregate at the 0.05 level. The values are mean + SE (error bar). CK, abandoned farmland. 5-Y, 8-Y, 10-Y, 15-Y, and 20-Y represent planting variations for 5, 8, 10, 15, and 20 years, respectively.

The correlation analysis indicated that aggregate MWD was positively correlated with alfalfa aboveground biomass and the above- and underground C content (Figure 6). The aggregate C stock was markedly positively correlated with the SWC, the C and N content of aggregates, the C content of alfalfa aboveground, and the C-N ratio of above- and underground. Similarly, the aggregate N stock was markedly positively correlated with the SWC, C and N content of the soil surface and each aggregate size, the aboveground C content of alfalfa, and the aboveground C-N ratio. The C and N stocks of aggregates were negatively correlated with underground biomass and the above- and underground N content. In addition, the aboveground C content of alfalfa was positively correlated with SWC and MWD. The above- and underground N content was negatively correlated with the SWC and aboveground C content.

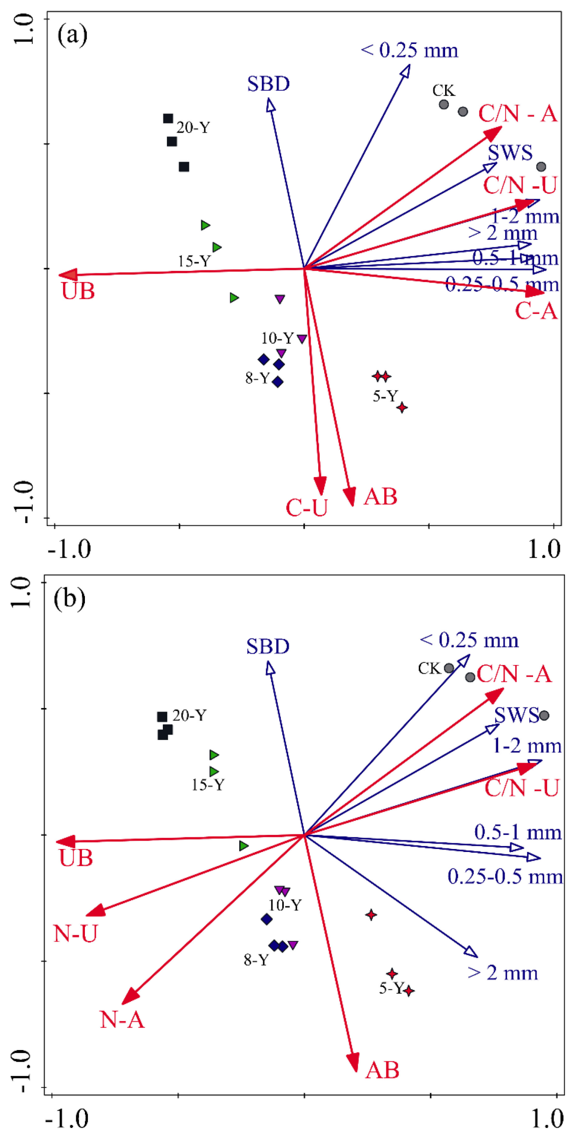

FIGURE 5
RDA biplot based on biomass and C and N concentrations of alfalfa plant variables in all treatments under different size aggregates C **(A)** and N **(B)** stocks. CK, abandoned farmland. 5-Y, 8-Y, 10-Y, 15-Y, and 20-Y represent planting variations for 5, 8, 10, 15, and 20 years, respectively, AB, aboveground biomass; UB, underground biomass; C-A, carbon concentration of alfalfa aboveground plant; C-U, carbon concentration of alfalfa underground plant; N-A, nitrogen concentration of alfalfa aboveground plant; N-U, carbon concentration of alfalfa underground plant; C/N-A, carbon-nitrogen ratio of alfalfa aboveground plant; C/N-U, carbon-nitrogen ratio of alfalfa underground plant; SBD, soil bulk density; SWS, soil water storage.

4 Discussion

4.1 The dynamic of alfalfa productivity under cultivation years

The productivity of alfalfa is affected by soil fertility, soil physical conditions, and other ecological factors (Feng et al., 2022). Soil moisture will affect the growth of roots, and excessive or limited water supply will change the distribution of crop roots, thereby affecting yields (Jia et al., 2009; Fan and Schutze, 2024). The results of this study showed that the largest aboveground biomass was found after 5 years in a cultivated field (Table 1), which is related to the precipitation in previous and subsequent years (Figure 1). Water is the main limiting factor restricting vegetation restoration and reconstruction, and it determines the water–soil ecological relationship of grassland on the Loess Plateau (Jiang et al., 2006). Soil moisture is affected by many factors, such as soil characteristics, land-use structure, topography, vegetation types, and weather, resulting in complex dynamic changes (Fan et al., 2016). In this paper, compared to the control, the soil water content of alfalfa with different planting years has a greater decrease (Figure 2A), which indicates that the soil water deficit is obvious. Because the local soil is loess soil, it is beneficial for rainwater to penetrate the soil and restore the water content. On the other hand, we found that the root biomass was negatively correlated with SWC (Figure 6), which may be because the root system of alfalfa is relatively wide, and the proliferation of the root system in the soil increases the porosity of the soil (Jia et al., 2009; Heinze, 2020). In addition, as the planting time increases, the distribution of root systems becomes wider and deeper, which often leads to more consumption and utilization of shallow soil water (Li and Huang, 2008). Moreover, as the planting time increases, the soil moisture gradually decreases, which is directly related to the root biomass. The accumulation of root biomass requires sufficient soil moisture, which leads to water depletion in the soil profile. In addition, alfalfa productivity was also affected by local rainfall (Zhang X. L. et al., 2021). In our study, we found that planting alfalfa for 5 years had the highest aboveground biomass, which may be related to the increasing rainfall from 2010 to 2013, and, after 2013 years, alfalfa biomass showed a declining trend due to the relative decreasing precipitation (Figure 1).

4.2 The driving factors of soil aggregate distribution in alfalfa grasslands

Soil aggregates are closely connected with soil physical, chemical, and biological properties (Plaza et al., 2013; Li et al., 2019). In this experiment, the particle size distribution of soil aggregates in different years of alfalfa cultivation and abandoned land showed a "V"-shaped trend, and soil aggregate size distributions of >2 mm and <0.25 mm were dominant (Table 2). This can be further explained by the fact that the stability of loess soil is generally low. Therefore, macroaggregates will decompose into microaggregates or smaller soil particles after being immersed in water (Lu et al., 2021). In addition, alfalfa planting for numerous years significantly increased the macroaggregate content in certain years, which is directly related to the proliferation of alfalfa roots. Because the root biomass can be increased by producing thick roots or multiple thin roots (Heinze, 2020), the increase in planting time will lead to more accumulation of root biomass, and this extensively proliferating root system helps to consolidate broad soil particles from smaller ones (Tisdall and Oades, 1982). However, due to the reduced physical and mechanical disturbance, the surface herbs,

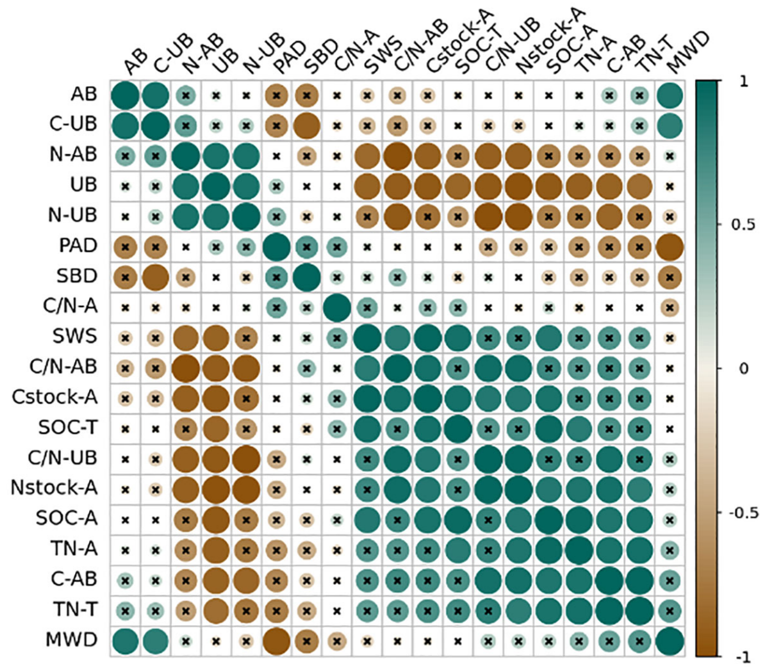

FIGURE 6
Correlation matrix of the study variables. Color and the size of the circles are proportional to the correlation coefficients between the variables. SWS is soil water storage, SBD is soil bulk density, SOC-T is surface soil organic carbon content of 0-cm to 20-cm depth, TN-T is surface soil total nitrogen content of 0-cm to 20-cm depth, MWD is the mean weight diameter, PAD is the percentage of aggregate destruction, SOC-A is the average SOC content of five size aggregates, TN-A is the average TN content of five size aggregates, Cstock-A is the sum of SOC stock in the five size aggregates, Nstock-A is the sum of TN stock in the five size aggregates, AB is the aboveground biomass, UB is the underground biomass, C-AB is the SOC content of aboveground plant, C-UB is the SOC content of root, N-AB is the TN content of aboveground plant, N-UB is the TN content of root, C/N-AB is the C/N content of aboveground plant, C/N-UB is the C/N content of root. The values in the figure represent correlation coefficients.

litter, and root biomass increase in natural-restored grassland, resulting in increased soil organic carbon, which is beneficial for aggregate formation (Xiao et al., 2019). Similar outcomes have been reported by Song et al. (2024) who found that the plant residue accelerates the soil aggregates turnover, promoting the soil macroaggregate formation. In addition, we found that dissolved organic matter that, as a substrate for microorganism, contributes to the increase in microbial activity may contribute to macroaggregate formation and stability (Sonsri and Watanabe, 2023).

4.3 The driving factors of plant–soil C and N stoichiometry of alfalfa grasslands

Plant–soil C and N concentrations and their ratios are essential in the restoration process of grasslands, not only for a better understanding of the C and N cycles but also for management practices (Du and Gao, 2021). We evaluated alfalfa above- and underground plant C and N contents and their ratios during the multiyear growing season. Our results showed that multiple planting durations decreased aboveground plant C and N concentrations and the C-N ratio (Table 1). These findings are supported by years of continuous planting, soil nutrient deficiency, gradual alfalfa grassland degradation, and plant biomass decrease due to self-toxic and self-thinning effects, which eventually results in less photosynthetic function and a lack of C assimilates in alfalfa grasslands (Zhang et al., 2017). At the same time, the results of Table 1 indicated that the N concentration of alfalfa roots increased with increasing planting years, which is similar to the findings of other studies (Cao et al., 2020). The higher N concentrations of roots in plantations than those in natural-restored grassland can be explained by the N_2 fixation of leguminous forage (Song et al., 2021). Additionally, in our paper, we found that alfalfa planting duration resulted in soil C and N decreases in the topsoil layer compared to the control (Figure 2). These results were mainly attributed to decreased plant inputs due to yearly plant removal, a decrease in outside litter input, and increased decomposition rates (Zhang J. H. et al., 2015). Moreover, the degree of C and N decrease depends on many factors, such as basic soil SOC and TN contents, climate conditions, and surface erosion status (Yang et al., 2019).

The SOC content of soil aggregates is a microscopic expression of SOC balance and mineralization rate, which is of great significance to soil fertility and soil carbon sequestration, and the TN content of soil is one of the main indicators of soil fertility (Lu et al., 2021). In this experiment, alfalfa grassland planted for 5 years had higher SOC and TN contents, and the largest SOC and TN storage were found in particles >2 mm and <0.25 mm, whereas the lowest SOC and TN contents were found in particles of 0.25–2.00 mm (Figure 3). This is mainly because macroaggregates are made up of many microaggregates and because of the formation of microaggregates through the combination of organic molecules with clay and cations and not by aggregated particles (Devine et al., 2014). Therefore, soil macroaggregates and microaggregate are rich in organic matter, and soil macroaggregates have a faster turnover time than middle aggregates (Puget et al., 2000). The microaggregates and the surrounding small particles combine to form large aggregates; when the large soil aggregates decompose into microaggregates, the particulate organic matter decomposes, resulting in a greatly reduced SOC content of the microaggregates (Bissonnais and Arrouays, 1997). At the same time, the binding and bonding effects of macroaggregates also reduces the SOC of microaggregates (Tisdall and Oades, 1982). Previous studies have shown that the SOC content of aggregates mainly exists in the particle size of <0.25 mm, which is a combination of smaller organic and inorganic colloids. The smaller aggregates have a larger specific surface area after being combined, resulting in more adsorbed organic matter (He et al., 2011).

Considering the aggregate size distribution and the SOC and TN of specific aggregates, the aggregate size distribution not only represents the contribution rate of aggregates to SOC and TN, but it might also completely depict the interaction of different planting durations to the soil C and N pools (Xu et al., 2012). In different numbers of alfalfa planting years, the stocks of SOC and TN in different proportions of aggregates were mainly restricted by aggregates > 2 mm, which were significantly higher than those of aggregates of other sizes (Figure 4). After 5 years of planting, the SOC and TN reserves of the soil aggregates were the highest. This is because, after 5 years of planting, the soil formed a stable plant community, increased the biomass of underground roots, and accumulated more SOC in the soil. At the same time, alfalfa is a leguminous crop with strong nitrogen fixation ability. The roots fix atmospheric nitrogen, which is conducive to the accumulation of soil nitrogen (Liu et al., 2005; Thomas et al., 2009). In our study, the soil C and N stocks decreased after alfalfa planting duration, which may be caused by the very low C and N inputs from plants and soil. Aminiyan et al. (2015) reported higher aggregate-related SOC content in larger aggregate fractions (> 2 mm). In short, large aggregates > 2 mm are the main contributors to the SOC and TN contents in soil aggregates. This may be due to the increase in the strength or stability of the aggregates due to the humidification of crop residues, thereby increasing the SOC concentration of the large aggregates (Kushwaha et al., 2001). Therefore, increasing the number of aggregates with a particle size greater than 2 mm can enhance soil carbon and nitrogen fixation. These findings may be limited by the method of observing spatial and temporal changes used in this article. However, we will focus on research on long-term positioning to overcome these shortcomings in the future.

4.4 The degradation mechanism of perennial alfalfa grasslands

Obtaining sustainable high biomass and suitable soil nutrient management is crucial for cultivate alfalfa grassland (Fang et al., 2021); however, degraded continuous alfalfa grasslands are frequently characterized by substantially reduced of biomass output and potential losses in soil nutrient (Gu et al., 2018). In the Loess Plateau of China, the low precipitation and high evapotranspiration of alfalfa field will limit its sustainable development (Ren et al., 2010). The lack of soil water content is the mainly parameter caused the perennial alfalfa grassland degradation (Wang et al., 2019). Alfalfa is a deep root plant that gives it access to water deeper in the soil than annual pastures and crops (Cheng et al., 2005). Alfalfa used soil water from deeper soil profile than other crops and extracted more water and thus creates a large soil water deficit (Huang et al., 2018). Previous study showed that the length of the alfalfa cropping phase in the short term (2–4 years) depends on soil water replenishment, and alfalfa continuously, for 6 years, reduces a relatively desiccation layer in the soil with 2-m to 10-m depth (Li, 1983). Li and Chao (1992) also found that the biomass output of continuous alfalfa markedly decreased after 7 or 8 years due to the declined of soil water. Jia et al. (2009) reported that the alfalfa average yield reached a peak after continuous 9 years planting and, more than 11 years, cultivated had higher soil water use efficiency. In our results, we also found that the soil water content was quickly declined after continuous cultivated alfalfa for 8 years (Figure 2A), the dynamic of underground biomass (the underground biomass reached the higher value in 8 year) (Table 1), because the longer the growing years of alfalfa, the deeper its root distribution, which intensified the high water consumption at deep soil (there was no rainfall when we collected soil moisture samples during the first half of the month). On the contrary, the soil water content increased from 10 to 20 years; this was probably because the alfalfa plants' low transpiration and low productivity made less water consumption. The above results were coincided with the found by Li and Huang (2008) and Ren et al. (2010) and Li et al. (2018). Therefore, the long alfalfa stand duration may deplete available soil water, which would negatively impact production (Li and Huang, 2008) and thus caused the alfalfa grassland degradation.

On the other hand, the deficiency of soil nutrient also limits the alfalfa grassland sustainable development, and eventually leading to alfalfa grassland degradation and, conversely, enhancing the fertilizer application in perennial alfalfa can boost biomass output and prolong the alfalfa degradation timeline (Hakl et al., 2016; Gu et al., 2018; Fang et al., 2021). The decrease of soil nutrients, especially soil nitrogen, limits the perennial alfalfa growth, which, in turn, becomes a crucial restricting factor for the alfalfa cultivation (Yuan, 2017; Fang et al., 2021). In our results, we found that the soil C concentration decreased in the eight year and then increased after the 10th year of alfalfa cultivation (Figure 2). The soil C dynamical dramatically declined mainly because the fertilizer was applied in early planting alfalfa, and the carbon source in the soil is increased. With the continuous cultivated, a large amount of aboveground biomass was removed from alfalfa grassland, and the less carbon source will add to soil. In addition, the root biomass litters were not converted to carbon source by microbe decomposition. However, after cultivation alfalfa for the 10th to 20th years, the soil C storage increased, especially in the microaggregate, and this agrees with the findings from other researchers (Li and Huang, 2008). It seems that soil C storage rose through enhancing the aggregate stability with the increased in cultivation years. However, in this study, TN content continues decreased compared to the fifth year of alfalfa cultivation (Figure 2), mainly because the N that was derived from symbiotic fixation by perennial alfalfa over 20th years does not reach the N value of farmland, and artificial nitrogenous fertilizer losses were larger than N fixation by perennial alfalfa. However, the TN storage in the microaggregate presented less declined and finally increased after continuous cultivation on the 15th to 20th years (Figure 4). This was probably because this growing stage reached an imbalance between TN fixation and loss and reduced the consumption of TN on account of decreased alfalfa plant. Similar results were reported by Ji et al. (2020), who found that the highest values of SOC and TN content were observed in the begin stage of alfalfa grassland, and, with the cultivated prolong, the above contents declined, and the decline soil nutrients restricted alfalfa growth and biomass output.

5 Conclusion

We first found the ecological indicator of C and N stoichiometry from plant to soil aggregate fractions affecting soil degradation. Alfalfa plantations can improve soil structure and promote the number of macroaggregates within a certain year. Different planting periods display different effects on the SOC and TN distribution of aggregates. In the present study, the inputs of organic C compounds via root exudates provide a material base for the rapid turnover of C and N stocks. Both low-quality resources (high C/N) and high-quality material supply (low C/N) exert their effects on sustaining soil nutrients. Thus, alfalfa production can promote larger aggregates and accordingly improve soil C and N in large aggregates. This process would help improve the soil structure under the condition of continuous alfalfa planting. However, after 5–8 years of planting, alfalfa grassland productivity and soil quality began to degrade gradually. In conclusion, a certain period of alfalfa planting strengthened the stability of the soil physical structure, yet it resulted in a steady deterioration of the C and N stocks from soil to plant. Our findings provide novel insight into perennial alfalfa grassland degradation and, therefore, help explore a potentially sustainable solution in semiarid rainfed agricultural areas.

Data availability statement

The original contributions presented in the study are included in the article/supplementary material. Further inquiries can be directed to the corresponding authors.

Author contributions

WW: Conceptualization, Data curation, Formal analysis, Funding acquisition, Investigation, Methodology, Project administration, Resources, Software, Supervision, Validation, Visualization, Writing – original draft, Writing – review & editing. TT: Conceptualization, Data curation, Formal analysis, Investigation, Methodology, Project administration, Resources, Software, Supervision, Writing – original draft, Writing – review & editing. M-YL: Conceptualization, Data curation, Formal analysis, Investigation, Methodology, Validation, Writing – original draft, Writing – review & editing. B-ZW: Conceptualization, Data curation, Formal analysis, Investigation, Methodology, Software, Writing – original draft, Writing – review & editing. QZ: Conceptualization, Data curation, Formal analysis, Resources, Software, Validation, Writing – original draft, Writing – review & editing. F-JM: Data curation, Formal analysis, Investigation, Software, Writing – original draft, Writing – review & editing. J-YL: Data curation, Investigation, Methodology, Software, Writing – original draft, Writing – review & editing. NW: Data curation, Investigation, Methodology, Software, Writing – original draft, Writing – review & editing. Y-MY: Data curation, Investigation, Methodology, Software, Writing – original draft, Writing – review & editing. H-YT: Investigation, Writing – original draft, Writing – review & editing. LZ: Conceptualization, Data curation, Formal analysis, Funding acquisition, Investigation, Methodology, Project administration, Resources, Software, Supervision, Validation, Visualization, Writing – original draft, Writing – review & editing. Y-CX: Conceptualization, Data curation, Formal analysis, Funding acquisition, Investigation, Methodology, Project administration, Resources, Software, Supervision, Validation, Visualization, Writing – original draft, Writing – review & editing.

Funding

The author(s) declare financial support was received for the research, authorship, and/or publication of this article. This research was supported by the Research Start-up Project of Shanxi Agricultural University for Recruited Talents (2023BQ120), Promotive Scientific Research Fund for New PhD Graduates working in Shanxi Province (SXBYKY2023038), Youth Science and Technology Research Program of Shanxi Province Basic Research Program (202303021222077 and 202303021212104), National Natural Science Foundation of China (32161143012), Key Research and Development Program of Gansu Province (20YF8WA083), and "111" Program (BP0719040).

Conflict of interest

The authors declare that the research was conducted in the absence of any commercial or financial relationships that could be construed as a potential conflict of interest.

Publisher's note

All claims expressed in this article are solely those of the authors and do not necessarily represent those of their affiliated organizations, or those of the publisher, the editors and the reviewers. Any product that may be evaluated in this article, or claim that may be made by its manufacturer, is not guaranteed or endorsed by the publisher.

References

Aminiyan, M. M., Sinegani, A. A. S., and Sheklabadi, M. (2015). Assessment of changes in different fractions of the organic carbon in a soil amended by nanozeolite and some plant residues: incubation study. *Int. J. Recycl. Organ. Waste Agric.* 4, 239–247. doi: 10.1007/s40093-015-0110-6

Araujo, R. A., Gamarodrigues, E. F., Gamarodrigues, A. C., and M. Vieira, R. A. (2024). Carbon mineralization in soil aggregate classes under Leguminous tree planting in north Fluminense, Brazil. *Floresta Ambient.* 31, e20230033. doi: 10.1590/2179-8087-FLORAM-2023-0033

Austin, A. T., and Vitousek, P. M. (2012). Introduction to a virtual special issue on ecological stoichiometry and global change. *New Phytol.* 196, 649–651. Available at: https://www.jstor.org/stable/newphytologist.196.3.649.

Bhatt, R., Singh, P., and Sharma, S. (2023). Changes in soil organic pool and carbon preservation capacity of macro- and micro-aggregates in response to land-use change in north-western India. *J. Soil Sci. Plant Nutt.* 23, 2849–2867. doi: 10.1007/s42729-023-01239-x

Bissonnais, Y. L. E., and Arrouays, D. (1997). Aggregate stability and assessment of soil crustability and erodibility: II. Application to humic loamy soils with various organic carbon contents. *Eur. J. Soil Sci.* 48, 39–48. doi: 10.1111/j.1365-2389.1997.tb00183.x

Bodner, G., Leitner, D., and Kaul, H. P. (2014). Coarse and fine root plants affect pore size distributions differently. *Plant Soil* 380, 133–151. doi: 10.1007/s11104-014-2079-8

Bremner, J. M. (1997). "Nitrogen-total," in *Part3. Chemical methods*. Ed. D. L. Sparks (ASA and SSSA, Madison, WI), 1085–1121.

Cao, Y., Li, Y. N., Zhang, G. Q., Zhang, J., and Chen, M. (2020). Fine root C:N:P stoichiometry and its driving factors across forest ecosystems in northwestern China. *Sci. Total Environ.* 737, 140299. doi: 10.1016/j.scitotenv.2020.140299

Cheng, J. M., Wan, H. E., and Wang, J. (2005). Alfalfa growth and its relation with soil water status in loess hilly and gully region. *(In Chinese) Chin. J. Appl. Ecol.* 3, 435–438.

Dan, X., He, M., Meng, L., He, X., Wang, X., Chen, S., et al. (2023). Strong rhizosphere priming effects on N dynamics in soils with higher soil N supply capacity: The 'Matthew effect' in plant-soil system. *Soil Biol. Biochem.* 178, 108949. doi: 10.1016/j.soilbio.2023.108949

Devine, S., Markewitz, D., Hendrix, P., and Coleman, D. (2014). Soil aggregates and associated organic matter under conventional tillage, no-tillage, and forest succession after three decades. *PloS One* 9, 1–12. doi: 10.1371/journal.pone.0084988

Du, C. J., and Gao, Y. H. (2021). Grazing exclusion alters ecological stoichiometry of plant and soil in degraded alpine grassland. *Agric. Ecosyst. Environ.* 308, 107256. doi: 10.1016/j.agee.2020.107256

Fan, J. W., Du, Y. L., Wang, B. R., Turner, N. C., Wang, T., Abbott, L. K., et al. (2016). Forage yield, soil water depletion, shoot nitrogen and phosphorus uptake and concentration, of young and old stands of alfalfa in response to nitrogen and phosphorus fertilisation in a semiarid environment. *Field Crops Res.* 198, 247–257. doi: 10.1016/j.fcr.2016.08.014

Fan, X. Y., and Schutze, N. (2024). Assessing crop yield and water balance in crop rotation irrigation systems: Exploring sensitivity to soil hydraulic characteristics and initial moisture conditions in the North China Plain. *Agri Water Mange.* 300, 108897. doi: 10.1016/j.agwat.2024.108897

Fang, Y., Huang, Z., Cui, Z., He, H. H., and Liu, Y. (2021). Trade-offs between forage crop productivity and soil nutrients for different ages of alfalfa grassland. *Land Degrad. Dev.* 32, 374–386. doi: 10.1002/ldr.3686

Feng, Y. P., Shi, Y., Zhao, M. Y., Shen, H. H., Xu, L. C., Luo, Y. K., et al. (2022). Yield and quality properties of alfalfa (Medicago sativa L.) and their influencing factors in China. *Eur. J. Agron.* 141, 126637. doi: 10.1016/j.eja.2022.126637

Gong, Y. H., Zhao, D. M., Ke, W. B., Fang, C., Pei, J. Y., and Sun, G. J. (2020). Legacy effects of precipitation amount and frequency on the aboveground plant biomass of a semi-arid grassland. *Sci. Total Environ.* 705, 135899. doi: 10.1016/j.scitotenv.2019.135899

Gu, Y. J., Han, C. L., Fan, J. W., Shi, X. P., Kong, M., Shi, X. Y., et al. (2018). Alfalfa forage yield, soil water and P availability in response to plastic film mulch and P fertilization in a semiarid environment. *Field Crops Res.* 215, 94–103. doi: 10.1016/j.fcr.2017.10.010

Guo, Z. B., Yan, G. J., Zhang, R. H., Li, F. M., Zeng, Z. X., and Liu, H. (2010). Improvement of soil physical properties and aggregate-associated C, N, and P after cropland was converted to grassland in semiarid Loess Plateau. *Soil Sci.* 175, 99–104. doi: 10.1097/ss.0b013e3181cda54a

Hakl, J., Kunzova, E., and Konecna, J. (2016). Impact of long-term organic and mineral fertilization on lucerne forage yield over an 8-year period. *Plant Soil Env.* 62, 36–41. doi: 10.17221/660/2015-pse

He, S. Q., Zheng, Z. C., and Gong, Y. B. (2011). Distribution characteristics and soil organic carbon of soil water-stable aggregates with different de-farming patterns. *J. Soil Water Conserv.* 25, 229–233. doi: 10.13870/j.cnki.stbcxb.2011.05.045

Heinze, J. (2020). Herbivory by aboveground insects impacts plant root morphological traits. *Plant Ecol.* 221, 725–732. doi: 10.1007/s11258-020-01045-w

Huang, Z., Liu, Y., Cui, Z., Fang, Y., He, H. H., Liu, B. R., et al. (2018). Soil water storage deficit of alfalfa (Medicago sativa) grasslands along ages in arid area (China). *Field Crops Res.* 221, 1–6. doi: 10.1016/j.fcr.2018.02.013

Ji, B., Wang, Z., Pan, Z., Xu, H., Han, X. S., and Xie, Y. Z. (2020). Soil carbon storage characteristics of alfalfa (Medicago sativa) artificial grasslands in the semi-arid hilly gully region of the loess plateau, China. *Russ J. Ecol.* 51, 466–476. doi: 10.1134/S1067413620050045

Jia, Y., Li, F. M., Zhang, Z. H., Wang, X. L., Guo, R. Y., and Siddique, K. H. M. (2009). Productivity and water use of alfalfa and subsequent crops in the semiarid Loess Plateau with different stand ages of alfalfa and crop sequences. *Field Crops Res.* 114, 58–65. doi: 10.1016/j.fcr.2009.07.004

Jiang, H. M., Jiang, J. P., Jia, Y., Li, F. M., and Xu, J. Z. (2006). Soil carbon pool and effects of soil fertility in seeded alfalfa fields on the semi-arid Loess Plateau in China. *Soil Biol. Biochem.* 38, 2350–2358. doi: 10.1016/j.soilbio.2006.02.008

Kubar, K. A., Huang, L., Xue, B., Li, X. K., and Lu, J. W. (2021). Straw management stabilizes the chemical composition of soil organic carbon (SOC): the relationship with aggregate-associated C in a rice-rape cropping system. *Land Degrad. Dev.* 32, 851–866. doi: 10.1002/ldr.3727

Kushwaha, C., Tripathi, S., and Singh, K. (2001). Soil organic matter and water-stable aggregates under different tillage and residue conditions in a tropical dryland agroecosystem. *Appl. Soil Ecol.* 16, 229–241. doi: 10.1016/S0929-1393(00)00121-9

Li, Y. (1983). The properties of water cycle in soil and their effect on water cycle for land in the Loess Plateau. *Acta Ecol. Sin.* 3, 91–101.

Li, Q., and Chao, Z. (1992). Survey and analysis to development of alfalfa in the Loess Plateau. *Chin. Pasture Sci.* 9, 7–11.

Li, J., Deng, L., Peuelas, J., Wu, J., Shangguan, Z., Sardans, J., et al. (2023). C:N:P stoichiometry of plants, soils, and microorganisms: Response to altered precipitation. *Global Change Biol.* 29, 7051–7071. doi: 10.1111/gcb.16959

Li, Y. S., and Huang, M. B. (2008). Pasture yield and soil water depletion of continuous growing alfalfa in the Loess Plateau of China. *Agric. Ecosyst. Environ.* 124, 24–32. doi: 10.1016/j.agee.2007.08.007

Li, F. Q., Qiu, P. F., Shen, B., and Shen, Q. R. (2019). Soil aggregate size modi fi es the impacts of fertilization on microbial communities. *Geoderma* 343, 205–214. doi: 10.1016/j.geoderma.2019.02.039

Li, J. P., Xie, Y. Z., Deng, L., Wang, K. B., and Li, X. W. (2018). Soil physico-chemical property dynamics when continually growing alfalfa (Medicago sativa) in the loess plateau of China. *Nat. Environ. pollut. Technol.* 17, 11–20.

Li, Y., Zhang, X., Cao, Z., Liu, Z., Lu, Z., and Liu, Y. (2021). Towards the progress of ecological restoration and economic development in China's Loess Plateau and strategy for more sustainable development. *Sci. Total. Environ.* 756, 143676. doi: 10.1016/j.scitotenv.2020.143676

Liu, J. X., Price, D. T., and Chen, J. M. (2005). Nitrogen controls on ecosystem carbon sequestration: a model implementation and application to Saskatchewan, Canada. *Ecol. Modell* 186, 178–195. doi: 10.1016/j.ecolmodel.2005.01.036

Liu, Y. L., Zhang, M., Xiong, H., Li, Y., Zhang, Y. R., Huang, X. C., et al. (2023). Influence of long-term fertilization on soil aggregates stability and organic carbon occurrence characteristics in karst yellow soil of Southwest China. *Front. Plant Sci.* 14. doi: 10.3389/fpls.2023.1126150

Lu, X. F., Hou, E. Q., Guo, J. Y., Gilliam, F. S., Li, J. L., Tang, S. B., et al. (2021). Nitrogen addition stimulates soil aggregation and enhances carbon storage in terrestrial ecosystems of China: A meta-analysis. *Glob. Change Biol.* 27, 2780–2792. doi: 10.1111/gcb.15604

Lustenhouwer, N., Chanbet, T. M. R., Melen, M. K., Putten, W. H. V. D., and Parker, I. M. (2024). Plant–soil interactions during the native and exotic range expansion of an annual plant. *J. J. Evolution Biol.* 37, 653–664. doi: 10.1093/jeb/voae040

Plaza, C., Courtier-murias, D., Fernández, J. M., Polo, A., and Simpson, A. J. (2013). Physical, chemical, and biochemical mechanisms of soil organic matter stabilization under conservation tillage systems: A central role for microbes and microbial by-products in C sequestration. *Soil Biol. Biochem.* 57, 124–134. doi: 10.1016/j.soilbio.2012.07.026

Puget, P., Chenu, C., and Balesdent, J. (2000). Dynamics of soil organic matter associated with particle-size fractions of water-stable aggregates. *Eur. J. Soil Sci.* 51, 595–605. doi: 10.1111/j.1365-2389.2000.00353.x

Qi, J. J., Fu, D. Q., Wang, X. Z., Zhang, F. F., and Ma, C. H. (2023). The effect of alfalfa cultivation on improving physicochemical properties soil microorganisms community structure of grey desert soil. *Sci. Rep.* 13, 13747. doi: 10.1038/s41598-023-41005-8

Ren, X. L., Jia, Z. K., Wan, S. M., and Chen, X. L. (2010). Soil water distribution on different number of growing years of alfalfa pasture in the Loess Plateau of Northwest China. *Afr. J. Biotechnol.* 9, 5686–5693. doi: 10.5897/AJB10.245

Sardans, J., Grau, O., Chen, H., Janssens, I. A., Ciais, P., Piao, S., et al. (2017). Changes in nutrient concentrations of leaves and roots in response to global change factors. *Glob. Change Biol.* 23, 3849–3856. doi: 10.1111/gcb.13721

Shen, Y., Zhang, R., Yang, Q., Liu, Z., Li, G., Han, H., et al. (2024). Long-term subsoiling and tillage rotation increase carbon storage in soil aggregates and the abundance of autotrophs. *Appl. Soil Ecol.* 200, 105444. doi: 10.1016/j.apsoil.2024.105444

Song, X., Fang, C., Yuan, Z. Q., and Li, F. M. (2021). Long-term growth of alfalfa increased soil organic matter accumulation and nutrient mineralization in a semi-arid environment. *Front. Env. Sci.* 9. doi: 10.3389/fenvs.2021.649346

Song, X., Yuan, Z. Q., Fang, C., Hu, Z. H., Li, F. M., Sardans, J., et al. (2024). The formation of humic acid and micro-aggregates facilitated long-time soil organic carbon sequestration after *Medicago sativa* L. introduction on abandoned farmlands. *Geoderma* 445, 116889. doi: 10.1016/j.geoderma.2024.116889

Sonsri, K., and Watanabe, A. (2023). Insights into the formation and stability of soil aggregates in relation to the structural properties of dissolved organic matter from various organic amendments. *Soil Till. Res.* 232, 105774. doi: 10.1016/j.still.2023.105774

Su, Y. Z., Liu, W. J., Yang, R., and Chang, X. X. (2009). Changes in soil aggregate, carbon, and nitrogen storages following the conversion of cropland to alfalfa forage land in the Marginal Oasis of northwest China. *Environ. Manage.* 43, 1061–1070. doi: 10.1007/s00267-009-9284-x

Tan, M., Li, W., Zong, R., Li, X., Han, Y., Luo, P., et al. (2024). Long-term mulched drip irrigation enhances the stability of soil aggregates by increasing organic carbon stock and reducing salinity. *Soil Till. Res.* 240, 106069. doi: 10.1016/j.still.2024.106069

Tang, X., Qiu, J. C., Xu, Y. Q., Li, J. H., Chen, J. H., Li, B., et al. (2022). Responses of soil aggregate stability to organic C and total N as controlled by land-use type in a region of south China affected by sheet erosion. *Catena* 218, 106543. doi: 10.1016/j.catena.2022.106543

Thomas, R. Q., Canham, C. D., Weathers, K. C., and Goodale, C. L. (2009). Increased tree carbon storage in response to nitrogen deposition in the US. *Nat. Geosci.* 3, 13–17. doi: 10.1038/ngeo721

Tisdall, J. M., and Oades, J. M. (1982). Organic matter and water-stable aggregates in soils. *J. Soil Sci.* 33, 141–163. doi: 10.1111/j.1365-2389.1982.tb01755.x

Vitousek, P. M., Menge, D. N. L., Reed, S. C., and Cleveland, C. C. (2013). Biological nitrogen fixation: rates, patterns and ecological controls in terrestrial ecosystems. *Philos. Trans. R. Soc B-Biol. Sci.* 368, 20130119. doi: 10.1098/rstb.2013.0119

Wang, M., Gong, Y., Lafleur, P., and Wu, Y. (2021b). Patterns and drivers of carbon, nitrogen and phosphorus stoichiometry in southern China's grasslands. *Sci. Total Environ.* 785, 147201. doi: 10.1016/j.scitotenv.2021.147201

Wang, S. Q., Li, T. X., and Zheng, Z. C. (2018). Tea plantation age effects on soil aggregate-associated carbon and nitrogen in the hilly region of western Sichuan, China. *Soil Till. Res.* 180, 91–98. doi: 10.1016/j.still.2018.02.016

Wang, C. T., Sun, Y., Chen, H. Y., and Ruan, H. H. (2021a). Effects of elevated CO2 on the C:N stoichiometry of plants, soils, and microorganisms in terrestrial ecosystems. *Catena* 201, 105229. doi: 10.1016/j.catena.2021.105219

Wang, Z. T., Yang, L., Li, G., Chai, C. S., Zhang, Y. D., Chen, R., et al. (2019). Effects of alfalfa (Medicago sativa L.) degradation on herbage distribution and diversity in the semi-arid Loess Plateau. *Acta Ecol. Sin.* 39, 3720–3729. doi: 10.5846/stxb201805181099

Wang, W., Zhou, R., Wang, B. Z., Zhao, L., Zhao, Z. Y., Sheteiwy, M. S., et al. (2022). Biocrust as a nature-based strategy (NbS) to restore the functionality of degraded soils in semiarid rainfed alfalfa (Medicago sativa L.) field. *J. Clean. Prod.* 336, 130378. doi: 10.1016/j.jclepro.2022.130378

Wilson, G. W. T., Rice, C. W., Rillig, M. C., Springer, A., and Hartnett, D. C. (2009). Soil aggregation and carbon sequestration are tightly correlated with the abundance of arbuscular mycorrhizal fungi: results from long-term field experiments. *Ecol. Lett.* 12, 452–461. doi: 10.1111/j.1461-0248.2009.01303.x

Xiao, L., Zhang, Y., Li, P., Xu, G. C., Shi, P., and Zhang, Y. (2019). Effects of freeze-thaw cycles on aggregate-associated organic carbon and glomalin-related soil protein in natural-succession grassland and Chinese pine forest on the Loess Plateau. *Geoderma* 334, 1–8. doi: 10.1016/j.geoderma.2018.07.043

Xu, H., Wang, M., You, C., Tan, B., Xu, L., Li, H., et al. (2024). Warming effects on C:N:P stoichiometry and nutrient limitation in terrestrial ecosystems. *Soil Till. Res.* 235, 105896. doi: 10.1016/j.still.2023.105896

Xu, M. X., Wang, Z., Zhang, J., and Liu, G. B. (2012). Response of soil organic carbon sequestration to the "Grain for Green Project" in the hilly Loess Plateau region. *Acta Ecologica Sin.* 32, 5405–5415. doi: 10.5846/stxb201112312027

Yahui, J., Le, Y., Xuesong, C., Feiran, C., Jing, L., Jiangshan, Z., et al. (2023). Carbon dots promoted soybean photosynthesis and amino acid biosynthesis under drought stress: reactive oxygen species scavenging and nitrogen metabolism. *Sci. Total Environ.* 856, 159125–159125. doi: 10.1016/j.scitotenv.2022.159125

Yang, D., Song, L., and Jin, G. (2019). The soil C:N:P stoichiometry is more sensitive than the leaf C:N:P stoichiometry to nitrogen addition: a four-year nitrogen addition experiment in a Pinus koraiensis plantation. *Plant Soil* 442, 183–198. doi: 10.1007/s11104-019-04165-z

Yu, H., Gao, R. Y., Yang, W. J., Yang, L. S., Li, S. Y., Lin, Y. M., et al. (2021). Contents and relationships of C, N, P of leaf, root and soil in dominant herbs in dry-hot valley. *Chin. J. Appl. Environ. Biol.* 28 (3), 727–735. doi: 10.19675/j.cnki.1006-687x.2021.01008

Yuan, Z. Q. (2017). Factors affecting lucerne-rich vegetation under revegetation in a semi-arid environment. *Ecol. Eng.* 108, 249–254. doi: 10.1016/j.ecoleng.2017.08.030

Yuan, S., Xu, Q., Zhao, K., Zhou, Q., Wang, X., Zhang, X., et al. (2024). Dynamic analyses of soil erosion and improved potential combining topography and socio-economic factors on the Loess Plateau. *Ecol. Indic.* 160, 111814. doi: 10.1016/j.ecolind.2024.111814

Zhang, Y., Li, C., and Wang, M. (2019). Linkages of C: N: P stoichiometry between soil and leaf and their response to climatic factors along altitudinal gradients. *J. Soils Sediments* 19, 1820–1829. doi: 10.1007/s11368-018-2173-2

Zhang, J. H., Wang, Y., and Li, F. C. (2015). Soil organic carbon and nitrogen losses due to soil erosion and cropping in a sloping terrace landscape. *Soil Res.* 53, 87–56. doi: 10.1071/SR14151

Zhang, L. Q., Wei, X. R., Hao, M. D., and Zhang, M. (2015). Changes in aggregate-associated organic carbon and nitrogen after 27 years of fertilization in a dryland alfalfa grassland on the Loess Plateau of China. *J. Arid Land* 7, 429–437. doi: 10.1007/s40333-015-0003-6

Zhang, G. Q., Zhang, P., Peng, S. Z., Chen, Y. M., and Cao, Y. (2017). The coupling of leaf, litter, and soil nutrients in warm temperate forests in northwestern China. *Sci. Rep.* 7, 11754. doi: 10.1038/S41598-017-12199-5

Zhang, X. L., Zhao, Y. Y., Gao, W. J., Song, X., Zhang, X. T., Shi, X. Y., et al. (2021). Converting alfalfa pasture into annual cropland achieved high productivity and kept soil organic carbon in a semiarid area. *Land Degrad. Dev.* 32, 1478–1486. doi: 10.1002/ldr.3808

Zhao, R. N., Kuzyakov, Y., Zhang, H. Y., Wang, Z. R., Li, T. P., Shao, L. Y., et al. (2024). Labile carbon inputs offset nitrogen-induced soil aggregate destabilization via enhanced growth of saprophytic fungi in a meadow steppe. *Geoderma* 443, 116841. doi: 10.1016/j.geoderma.2024.116841

Zhou, G., Xu, S., Ciais, P., Manzoni, S., Fang, J., Yu, G., et al. (2019). Climate and litter C/N ratio constrain soil organic carbon accumulation. *Nati. Sci. Rev.* 6, 746–757. doi: 10.1093/nsr/nwz045

Zhu, G., Deng, L., and Shangguan, Z. (2018). Effects of soil aggregate stability on soil N following land use changes under erodible environment. *Agric. Ecosyst. Environ.* 262, 18–28. doi: 10.1016/j.agee.2018.04.012

frontiers | Frontiers in Plant Science

TYPE Original Research
PUBLISHED 11 November 2024
DOI 10.3389/fpls.2024.1478162

Check for updates

OPEN ACCESS

EDITED BY
Khurram Shahzad,
Lasbela University of Agriculture, Water and Marine Sciences, Pakistan

REVIEWED BY
Wajid Nasim,
The Islamia University of Bahawalpur, Pakistan
Kai Zhou,
Nanjing Forestry University, China

*CORRESPONDENCE
Jiumao Cai
caijiumao@163.com

†These authors have contributed equally to this work and share first authorship

RECEIVED 09 August 2024
ACCEPTED 14 October 2024
PUBLISHED 11 November 2024

CITATION
Wang M, Zhao B, Jiang N, Li H and Cai J (2024) Advancing nitrogen nutrition index estimation in summer maize using continuous wavelet transform.
Front. Plant Sci. 15:1478162.
doi: 10.3389/fpls.2024.1478162

Advancing nitrogen nutrition index estimation in summer maize using continuous wavelet transform

Mingxia Wang[1†], Ben Zhao[2†], Nan Jiang[1], Huan Li[1] and Jiumao Cai[3*]

[1]School of Hydraulic Engineering, Yellow River Conservancy Technical Institute, Kaifeng, China, [2]College of Tobacco Science, Henan Agricultural University, Zhengzhou, China, [3]Farmland Irrigation Research Institute, Chinese Academy of Agricultural Sciences, Xinxiang, Henan, China

Rapid and non-destructive diagnosis of plant nitrogen (N) status is crucial to optimize N management during the growth of summer maize. This study aimed to evaluate the effectiveness of continuous wavelet analysis (CWA) in estimating the nitrogen nutrition index (NNI), to determine the most suitable wavelet analysis method, and to identify the most sensitive wavelet features across the visible to near-infrared spectrum (325–1,025 nm) for accurate NNI estimation. Field experiments were conducted across two sites (Kaifeng and Weishi) during the 2022 and 2023 growing seasons using four summer maize cultivars (XD20, ZD958, DH661, and DH605) under varying N application rates (0, 80, 160, 240, and 320 kg N ha^{-1}). Canopy reflectance spectra and plant samples were collected from the V6 to V12 growth stages. The wavelet features for each spectral band were calculated across different scales using the CWA method, and their relationships with NNI, plant dry matter (PDM), and plant N concentration (PNC) were analyzed using four regression models. The results showed that NNI varied from 0.61 to 1.19 across different N treatments during the V6 to V12 stages, and the Mexican Hat wavelet was identified as the most suitable mother wavelet, achieving an R^2 value of 0.73 for NNI assessment. The wavelet features derived from the Mexican Hat wavelet were effective in estimating NNI, PDM, and PNC under varying N treatments, with the most sensitive wavelet features identified as 745 nm at scale 7 for NNI, 819 nm at scale 5 for PDM, and 581 nm at scale 6 for PNC using linear regression models. The direct and indirect methods for NNI estimation were compared using independent field data sets. Both methods proved valid to predict NNI in summer maize, with relative root mean square errors of 10.8% for the direct method and 13.4% for the indirect method. The wavelet feature at 745 nm, scale 7, from the direct method (NNI = 0.14 WF (745 nm, 7) + 0.3) was found to be simpler and more accurate for NNI calculation. These findings provide new insights into the application of the CWA method for precise spectral estimation of plant N status in summer maize.

KEYWORDS

maize, critical nitrogen concentration, nitrogen nutrition index, wavelet feature, Mexican Hat

1 Introduction

Nitrogen nutrition index (NNI) is a well-known tool that can diagnose crop nitrogen (N) status accurately and has shown potential for estimating crop yield and quality, plant N uptake and partition, photosynthesis capacity, and so on (Ata-Ul-Karim et al., 2016, 2017; Dordas, 2017; Hu et al., 2014). Its calculation is the ratio between actual plant N concentration (PNC) and plant critical N concentration (N_c) based on the same plant dry matter (PDM) (Lemaire et al., 2008). The NNI provides a quantitative measure of the N status of crops, which is essential to optimize N fertilizer use in improving crop yield and quality. The NNI is increasingly used to assess and manage crop N requirements more accurately. However, the current methods to determine NNI have certain limitations, such as reliance on labor-intensive field sampling and variability in measurements due to environmental factors (Ziadi et al., 2010). In order to reduce the determination time of NNI, previous studies have reported some rapid and non-destructive methods to assess NNI based on chlorophyll meter and remote sensing (Zhao et al., 2018).

The assessment of plant N status is an important application of remote sensing in the agriculture sector; its application is based on the analysis of canopy spectral reflectance on crops (Li et al., 2014). Many spectral indices have been developed to estimate crop growth indices (PDM, PNC, leaf area index, and chlorophyll and pigment content) to monitor and diagnose crop N status (Schlemmer et al., 2013; Gnyp et al., 2014; Jay et al., 2016). However, these growth indices are difficult to use in estimating the extent of plant N deficit qualitatively and quantitatively due to the lack of a critical value during crop growth. NNI is better to use than a single growth index (PDM, PNC, and so on) to estimate plant N status qualitatively and quantitatively since it contains two growth indices (PDM and PNC) and is based on the theory of N_c dilution (Lemaire et al., 2008). At present, a few studies have developed some empirical models to estimate NNI value using canopy spectral reflectance; the estimation method was classified into two types: direct method and indirect method. The two methods with traditional spectral indices are indeed mentioned, but to fully understand their impact on practical applications, it is important to delve deeper into the specific reasons for their instability in different environments. Traditional spectral indices often suffer from sensitivity to variations in soil background, atmospheric conditions, and sensor angles, which can lead to inconsistencies in the data and unreliable results.

The direct method is such that spectral indices construct the relationship with NNI directly. Mistele and Schmidhalter (2008) utilized the red edge inflection point (REIP) to directly estimate the NNI of winter wheat. The indirect method involves estimating PDM and PNC using canopy sensing technologies to calculate NNI. Cao et al. (2013) demonstrated that while PDM could be reliably estimated using spectral indices, the performance of PNC estimation using Crop Circle ACS-470 was less satisfactory due to a lower R^2 value. Previous studies have shown that the accuracy of NNI estimation varies across different crops and environmental conditions. The spectral indices used in these studies are typically designed to estimate specific growth parameters, such as PDM, PNC, or leaf area index, rather than being exclusively tailored for NNI assessment. Additionally, the structure of some spectral indices is quite complex, requiring reflectance measurements at multiple points along the spectral curve. A simple and exclusive spectral index is needed to estimate NNI.

Recently, continuous wavelet analysis (CWA) is considered as an emerging spectroscopy tool for the quantitative analysis of biochemical constituent concentrations from leaf and canopy spectral reflectance (Cheng et al., 2011, 2014a). CWA decomposes the reflectance spectra into a series of scale components, and every component has the same length as reflectance spectrum and is composed of wavelet features as a function of wavelength and scale (Li et al., 2018). This analysis has shown the potential to estimate water content (Cheng et al., 2011; Cheng et al., 2014a; Ullah et al., 2012), chlorophyll content (Liao et al., 2013; Li et al., 2017; He et al., 2018), and nitrogen content (Li et al., 2018) from leaf and canopy reflectance spectra. The CWA method can offer greater stability and accuracy by reducing sensitivity to such environmental factors. By focusing on the specific spectral features of the target parameter, CWA can provide more consistent and reliable measurements, even under varying conditions. This robustness in diverse environments underscores the practical benefits of adopting the CWA method in modern agricultural applications.

Unlike traditional spectral indices, which often struggle with the complexity and volume of hyperspectral data, CWA excels in decomposing and analyzing these data sets. It allows for the extraction of meaningful features across multiple scales, leading to more accurate and nuanced interpretations of the data (Kaewpijit et al., 2003). To date, there is no attempt to analyze systematically the relationship between the wavelet feature of reflectance spectrum from visible light to near infrared and NNI using CWA method. The hypothesis of this study was that CWA could be used to assess the N status of summer maize. Therefore, the objectives of this study are to compare different mother wavelets in CWA method to determine the most suitable mother wavelet, to develop wavelet features based on a mother wavelet across a series of scales and wavelengths (visible light to near infrared), to identify the most accurate of the wavelet features to estimate NNI based on comprehensive analysis, to construct optimum regression models between wavelet features and NNI using the direct and indirect methods during the V6 to V12 growth stages of summer maize, and to validate the developed regression models of the direct and indirect methods to establish the most appropriate way for NNI estimation. This study will provide a new technical support to diagnose plant N status based on CWA method to analyze the canopy reflectance spectra of summer maize.

2 Materials and methods

2.1 Experiment design

During the 2022 and 2023 seasons, field experiments of summer maize were carried out at Kaifeng and Weishi in China, respectively. These experiments included four cultivars of summer maize and five N application treatments. Detailed information about the series

10.3389/fpls.2024.1478162

of field experiments is shown in Table 1. The 0–20-cm soil samples were sampled before the planting of summer maize and then air-dried, and sieved to measure total N, Olsen-P, NH_4OAc-K^+, and organic matter (Nelson and Sommers, 1982; Bremner and Mulvancy, 1982; Olsen et al., 1954; van Reeuwijk, 1992). Weather information of the season of summer maize is shown in Figure 1. Randomized complete block design was used in every experiment with three replicates. The size of each plot was 60 m^2 (6 m × 10 m) in every field experiment. The total N fertilizer was divided into base fertilizer (50%) and top-dressing fertilizer (50%), which were applied before sowing and at the V6 stage, respectively. Adequate amounts of phosphate fertilizer (triple superphosphate) and potash fertilizer (potassium chloride) were applied into the soil before sowing. The planting density for all the experiments was 60,000 plants ha^{-1}, with a row spacing of 60 cm. Moreover, 40 mm was irrigated into the field to ensure the emergence of summer maize. During the growth progress of summer maize, the irrigation amount ranged from 250 to 350 mm, and the fertilization timings were in mid-August during the 2022 and 2023 growth seasons. Additional crop management was consistent with local agriculture production. There was no obvious water, disease, and pest stress during growth season of summer maize. The amount of N input was the only limiting factor during the process of the field experiments.

2.2 Field sampling and measurement

To obtain a representative plant sample, six plants were destructively sampled at the V6, V9, and V12 stages by randomly cutting in the middle of each plot. All of these samples were oven-dried at 80°C to a constant weight and then weighed and ground for chemical analysis later. PNC was determined using the traditional Kjeldahl method (Bremner and Mulvancy, 1982). Canopy spectral reflectance was measured using a portable spectrometer (FieldSpec Handheld 2; Analytical Spectral Devices (ASD), USA) at 10 A.M. and 14 P.M. local time under cloudless conditions. The canopy reflectance was calculated through the calibration of measurements of dark current and a white spectrum on the reference panel with known reflectance properties. The spectrometer covers the 325–1,075-nm (visible light to near-infrared) spectral range, with 1.4-nm sampling interval and 25°field of view. The data of spectral reflectance was re-sampled to 1-nm bandwidth using a self-driven interpolation method of this machine and then saved. Each measurement was taken randomly at five sites in each plot at a height of 50 cm above the plant canopy; scans of 10 times were collected in each site and then calculated as an average curve to represent the canopy reflectance spectra of each plot. The calibration of the spectrometer was taken every 15 min to correct potential effects caused by changes in the external environment.

TABLE 1 Characteristics of the six experiments in this study.

Experiment No.	Cultivar	Soil characteristics	N(kg N ha^{-1})	Sampling stage
Experiment 1	Xundan20	Type: sandy soil	0 (N0)	V6
(2022 Kaifeng)	(XD20)	Organic matter: 9.3 g kg^{-1}	80 (N1)	V9
		Total N: 0.62 g kg^{-1}	160 (N2)	V12
		Olsen-P: 10.5 mg kg^{-1}	240 (N3)	
		NH_4oAc-K^+: 72.5 mg kg^{-1}	320 (N4)	
Experiment 2	Zhengdan958	Type: light loam soil	0 (N0)	V6
(2022 Weishi)	(ZD958)	Organic matter: 11.73 g kg^{-1}	75 (N1)	V9
		Total N: 0.58 g kg^{-1}	150 (N2)	V12
		Olsen-P: 34.52 mg kg^{-1}	225 (N3)	
		NH_4oAc-K^+: 75 mg kg^{-1}	300 (N4)	
Experiment 3	Denghai661	Type: sandy soil	0 (N0)	V6
(2023Kaifeng)	(DH661)	Organic matter: 8.4g kg^{-1}	75 (N1)	V9
		Total N: 0.52 g kg^{-1}	150 (N2)	V12
		Olsen-P: 11.3 mg kg^{-1}	225 (N3)	
		NH_4oAc-K^+: 71.5 mg kg^{-1}	300 (N4)	
Experiment 4	Denghai605	Type: light loam soil	0 (N0)	V6
(2023Weishi)	(DH605)	Organic matter: 11.2 g kg^{-1}	90 (N1)	V9
		Total N: 0.48 g kg^{-1}	180 (N2)	V12
		Olsen-P: 21.52 mg kg^{-1}	270 (N3)	
		NH_4oAc-K^+: 54.23 mg kg^{-1}		

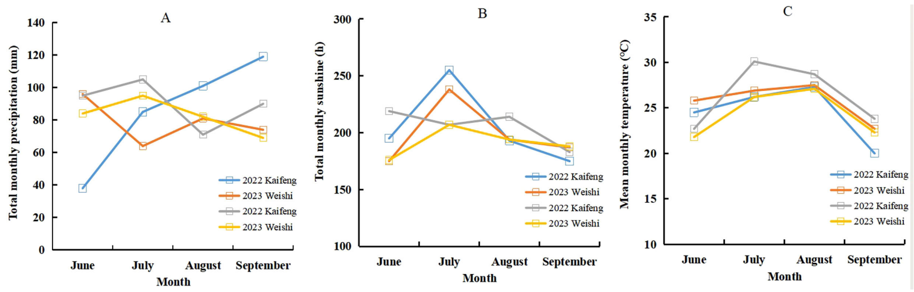

FIGURE 1
Total monthly precipitation (**A**, mm), total monthly sunshine (**B**, h) and mean monthly temperature (**C**, ℃) during 2022 and 2023 seasons of summer maize.

Due to machine noise and the external environment, the spectral value varied irregularly at the 906- to 1,075-nm region. In this study, 325–905 nm was used to develop the relationships between spectral value and NNI. Canopy reflectance was collected at the V6, V9, and V12 stages of summer maize. These stages are the critical time windows for top-dressing N fertilizers on summer maize.

2.3 Calculation of nitrogen nutrition index

NNI is calculated based on the N_c dilution curve of summer maize. This curve has been developed by Plénet and Lemaire (2000) and shown in (Equation 1). The calculation of NNI is listed in (Equation 2).

$$N_c = 3.4PDM^{-0.37} \quad (1)$$

$$NNI = \frac{N_a}{N_c} \quad (2)$$

where PDM is plant dry matter (t ha^{-1}), N_c is plant critical N concentration (%), and N_a is plant actual N concentration (%).

2.4 Wavelet analysis

Wavelet analysis is an efficient signal processing tool that can decompose the original signal into multiple scales, which has been successfully applied to hyperspectral data for dimensionality reduction (Bruce et al., 2001). Wavelet transform is a very important step to analyze hyperspectral data in wavelet analysis. Wavelet transform includes two variations: discrete wavelet transform (DWT) and continuous wavelet transform (CWT) (Cheng et al., 2014a). Cheng et al. (2011) recommended the CWT method to analyze the relationships between hyperspectral data and agronomy variables.

Continuous wavelet transform is a linear operation that transforms the convolution of reflectance spectra f(λ) with a scaled and shifted mother wavelet. The mother wavelet is expressed as shown below (Equation 3):

$$\varphi_{a,b}(\lambda) = \frac{1}{\sqrt{a}}\varphi(\frac{\lambda - b}{a}) \quad (3)$$

where ϕ(λ) is the mother wavelet function, *a* is the scaling factor representing the width of the mother wavelet, which can be comparable with the width of an absorption feature, and *b* is the shifting factor determining the position, which denotes the band position (325 to 905 nm) of the hyperspectral curve. The result of CWT is calculated as shown below (Mallat, 1991) (Equation 4):

$$W_f(a, b) = \langle f, \varphi_{a,b} \rangle = \int_{-\infty}^{+\infty} f(\lambda)\varphi_{a,b}(\lambda)d\lambda \quad (4)$$

where $W_f(a,b)$ is the wavelet feature (coefficient) that is the inner product of wavelets and spectrum reflectance. In this study, Mexican Hat, Gaussian Hat, Morlet Hat, and Haar Hat are used as the mother wavelet bases. Figure 2 shows the shape of the four mother wavelets, which was used to compare which mother wavelet can best represent the relationship with NNI (Ngui et al., 2013). All CWT procedures are completed by means of the wavelet toolbox of MATLAB 7.

The selection method of the sensitive wavelet feature is divided by four main steps. At the first step, the average R^2 values were used to compare the difference between NNI and wavelet features under different mother wavelet conditions. At the second step, the spectral curve of each treatment is imported into the continuous wavelet 1-D function of the wavelet toolbox in MATLAB 7. The wavelet coefficient of every reflectance spectra was calculated as a function of wavelength (325 to 905 nm) and scale (Power 2 Mode; power coefficient is 10). A scalogram of wavelet power with dimensions of power, wavelength, and scale is shown using the analysis system of continuous wavelet 1-D function. At the third step, the wavelet coefficient of the scalogram was read progressively within the range of 325–905-nm wavelength and 2^1 to 2^{10} scale; every wavelet coefficient is regressed with NNI, including linear, power, and logarithmic and exponential types. The contour map of determination coefficients (R^2) is plotted according to the change of R^2 values. This step is completed with a self-programmed software by using MATLAB 7. At the fourth step, the most sensitive region and wavelet coefficient (wavelength in nanometers, scale) were determined by the maximum R^2 value based on the scalogram plot. The specific technical flowchart is shown in Figure 3. The regression figure between the optimum wavelet coefficient and NNI was plotted using Microsoft Excel (Microsoft Corporation, Redmond, WA, USA).

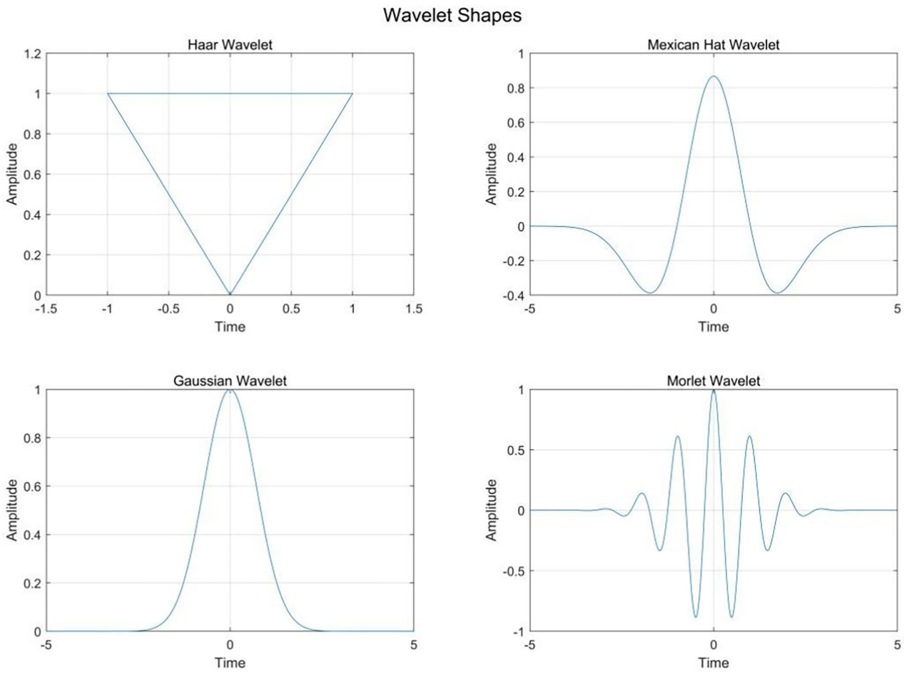

FIGURE 2
The shape of four different mother wavelets.

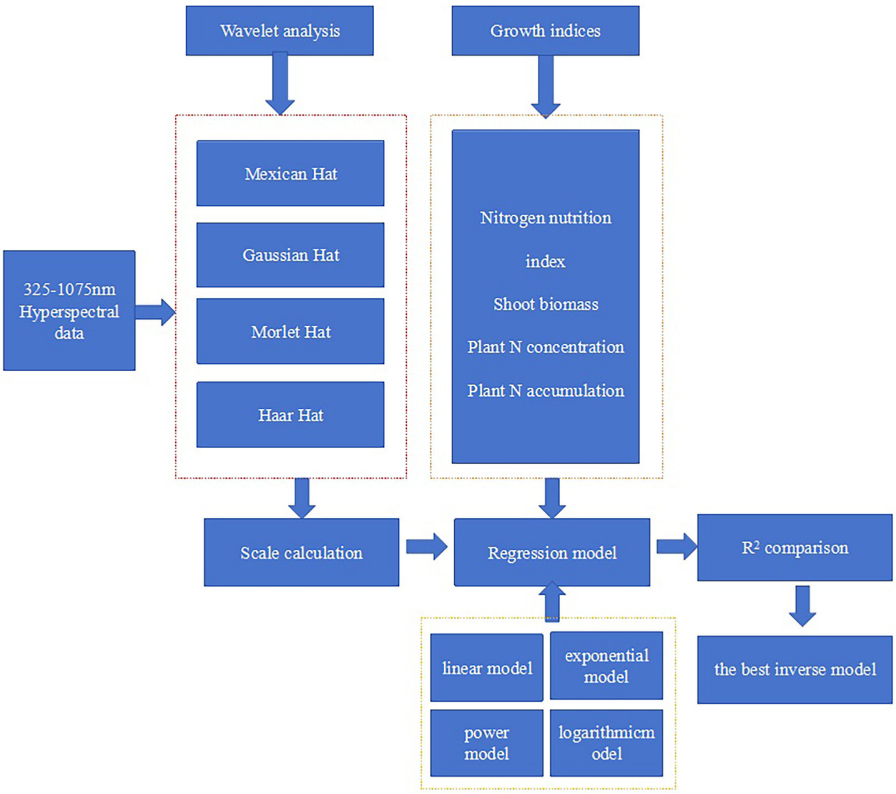

FIGURE 3
Flowchart for constructing a nitrogen nutrition index inversion model based on wavelet analysis.

2.5 Statistical analysis

Univariate multivariate analysis of variance is used to analyze the difference of PNC, plant nitrogen uptake, PDM, and NNI using SPSS v.13 software package (SPSS Inc., Chicago, IL, USA). The fix factors are season, cultivar, and N treatment in the analysis process. The significance level was preset as P <0.05, P <0.01, and P <0.001 for all hypothesis testing. The calibration data sets from experiments 1 and 3 are used to develop the relationships between NNI and wavelet feature, and the validation data sets from experiments 2 and 4 are used to validate these developed relationships. The statistical parameters coefficient of determination (R^2), root mean square error of calibration (RMSEC), and relative error of calibration (REC) are used to evaluate goodness of fit, and the other statistical parameters relative root mean square root (RRMSE), root mean square error of prediction (RMSEP), and relative error of prediction (REP) were used to assess prediction abilities and stability. Microsoft Excel (Microsoft Corporation, Redmond, WA, USA) was used to calculate the parameters. The calculation equations of R^2, RMSEC, REC, RMSEP, RRSME, and REP are shown as follows (Equations 6–11):

$$R^2 = 1 - \frac{\sum_{i=1}^{n}(O_i - P_i)^2}{\sum_{i=1}^{n}(O_i - \bar{O})^2} \quad (5)$$

$$RMSEC = \sqrt{\frac{\sum_{i=1}^{n}(O_i - O_i^{'})^2}{n}} \quad (6)$$

$$RMSEP = \sqrt{\frac{\sum_{i=1}^{n}(O_i - P_i)^2}{n}} \quad (7)$$

$$RRMSE = \frac{RMSEP}{\bar{O}} \times 100\,\% \quad (8)$$

$$REC = \frac{\sum_{i=1}^{n}\left|O_i - O_i^{'}\right|}{n \times \bar{O}} \times 100\,\% \quad (9)$$

$$REP = \frac{\sum_{i=1}^{n}\left|O_i - P_i\right|}{n \times \bar{O}} \times 100\,\% \quad (10)$$

where P_i is the estimated value from the regression model, O_i is the observed value, Ō is the average value of all observed values, O' is the calculation value of the regression model, and n is the number of samples. The higher R^2 value and the lower values of RMSEC and REC are considered as a higher goodness of fit between wavelet feature and NNI, and the lower values of RMSEP, REP, and RRMSE are considered as a higher predicted accuracy of the developed models.

2.6 Spectral indices

Some spectral indices have been used to estimate the NNI values of different crops. In this study, three commonly used spectral indices (Table 2) were chosen to test their usefulness to estimate the NNI of summer maize. Red edge inflection point (REIP-LI) was used by Mistele and Schmidhalter (2008) to assess the NNI of winter wheat. MTCI was proposed by Chen (2015) to relate canopy reflectance with the NNI of winter wheat. Modified red edge simple ratio index (mSR_{705}) was recommended by Liu et al. (2018) to estimate the NNI of winter oilseed rape.

3 Results

3.1 Variance analysis of plant nitrogen concentration, plant biomass, plant nitrogen uptake, and nitrogen nutrition index

In this study, there was no significant difference of plant N concentration, plant N uptake, plant biomass, and NNI across cultivars (XD20 and DH661) and seasons (2022 and 2023). PNC, PDM, NNI, and plant N uptake differed significantly by N application rate at the P <0.001 level (Table 3). The effect on PNC, PDM, NNI, and plant N uptake was shown non-significantly under the interaction of season × cultivar condition; however, the effects on PDM and plant N uptake (P < 0.001) and PNC and NNI (P < 0.01) were observed significantly under the interaction of season × N treatment and cultivar × N treatment condition. There was a significant effect (P < 0.05) on PNC, NNI, PDM, and plant N uptake (P < 0.01) under the season × cultivar × N treatment condition. These parameters have shown a large variability under different N conditions, which made a good data set to develop the relationship between NNI and reflectance spectra.

TABLE 2 Spectral indices for predicting nitrogen nutrition index.

Index	Name	Formula	Developed by
REIP-LI	Red edge inflection point	$700 + 40\frac{(R_{670} + R_{780})/2 - R_{700}}{R_{740} - R_{700}}$	Mistele and Schmidhalter, (2008)
MTCI	MERIS Terrestrial Chlorophyll Index	$\frac{R_{750} - R_{710}}{R_{710} - R_{680}}$	Chen (2015)
mSR_{705}	Modified Red Edge Simple Ratio Index	$\frac{R_{750} - R_{445}}{R_{705} + R_{445}}$	Liu et al. (2018)

TABLE 3 Variance analysis of plant nitrogen concentration, plant dry matter, plant nitrogen uptake and nitrogen nutrition index affected by season, cultivar, nitrogen treatments and their interactions.

Source	PNC (%)	Plant N uptake (kg ha^{-1})	PDM (t ha^{-1})	NNI
Cultivar(C)	NS	NS	NS	NS
Season(S)	NS	NS	NS	NS
N treatment (N)	***	***	***	***
S×C	NS	NS	NS	NS
S×N	***	**	***	**
C×N	***	**	***	**
S×C×N	**	*	**	*

NS represents no significant at 0.05 probability level.* Represents significant at 0.05 probability level.** Represents significant at 0.01 probability level.*** Represents significant at 0.001 probability level.

3.2 Change of nitrogen nutrition index across different nitrogen treatments and growth stages

There was significant difference of nitrogen nutrition index (NNI) under different N treatments (Figure 4). NNI increased with the application of N fertilizer, NNI values of XD20 ranged from 0.68 to 1.15 (Figure 4A), and NNI values of DH661 ranged from 0.69 to 1.14 (Figure 4B). The NNI values of the two cultivars were lower than those at the N0, N1, and N2 treatments, and the NNI values were nearly equal to those at the N3 treatments and were higher than those at the N4 treatments. The NNI values decreased gradually from the V6 to V12 stages of summer maize at the N0, N1, and N2 treatments; however, the NNI values increased gradually at the same stages of summer maize at the N3 and N4 treatments.

3.3 Change of canopy spectral reflectance across different N treatments and growth stages

In this study, the canopy spectral reflectance of summer maize increased with the growth process in the near-infrared bands, but the reflectance was not significantly different across the V6 to V12 stages in the visible bands (Figure 5A). N application had a significant influence on the change of canopy spectral reflectance (Figure 5B); the trend was similar to the growth stage. The main difference of the reflectance also existed in the near-infrared bands. The near-infrared bands could better show the effect of growth stages and N application to the canopy spectral reflectance of summer maize. The change of canopy spectral curves across different growth stages and N applications provided a basic support to analyze and develop empirical relationships between NNI and the canopy reflectance spectra of summer maize.

3.4 Performance of four mother wavelets with nitrogen nutrition index, shoot biomass, plant N concentration, and plant N accumulation

The relationships between four mother wavelets and nitrogen nutrition index, shoot biomass, plant N concentration, and plant N accumulation were developed across different average spectral values. The performance of the four mother wavelets is shown in Figure 6. The result indicated that the values of the determination

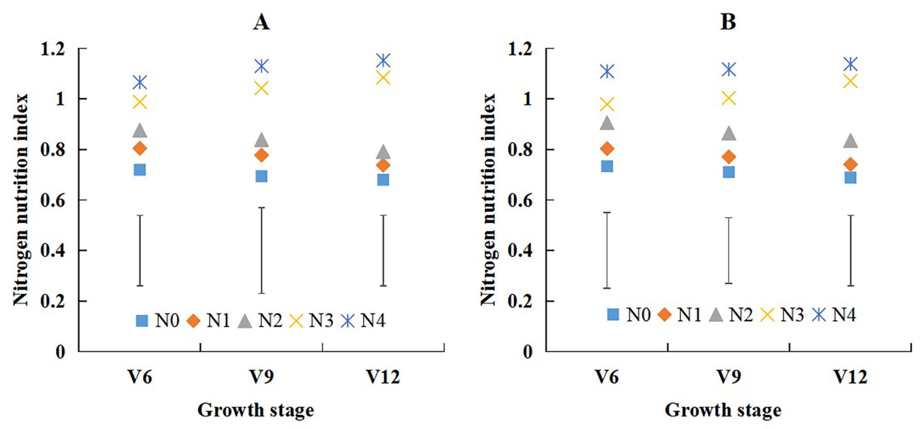

FIGURE 4
The change of nitrogen nutrition index across different nitrogen treatments from V6 to V12 growth stages of summer maize during 2022 and 2023 seasons ((**A**): 2022 XD20; (**B**): 2023 DH661).Vertical bars represent the value of least significant difference (P<0.05) for each growth stage.

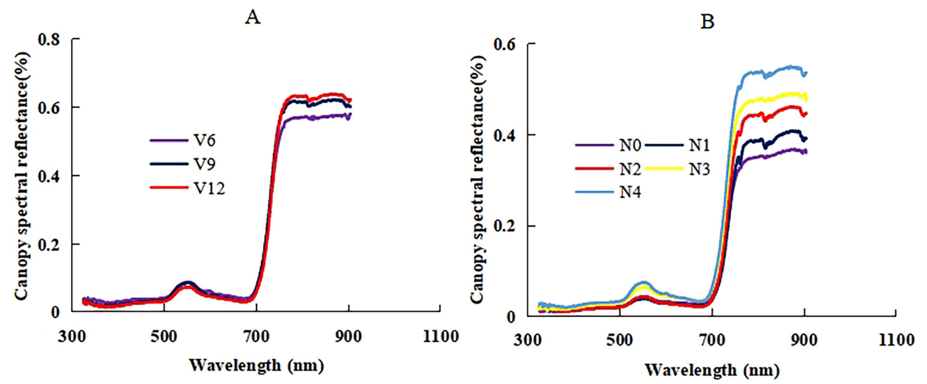

FIGURE 5
The change of canopy reflectance spectra across V6 to V12 growth stages (**(A)**: XD20 N3 treatment of 2022 season) and N0 to N4 nitrogen treatments (**(B)**: DH661 V6 stage of 2023 season) of summer maize.

coefficient (R^2) of NNI, shoot biomass, plant N concentration, and plant N accumulation with Mexican Hat were significantly higher than those of the three other mother wavelets across 1 to 10 scales. The R^2 values from Mexican Hat ranged from 0.5 to 0.7 about NNI, from 0.35 to 0.75 about shoot biomass, from 0.32 to 0.82 about plant N concentration, and from 0.28 to 0.78 about plant N accumulation across 1 to 10 scales, which was, on average, 30% to 50% higher than those of the three other methods (Figure 6). Therefore, the Mexican Hat could be considered as the best mother wavelet to assess NNI and growth indices in summer maize.

3.5 Estimation model of nitrogen nutrition index using the direct method

The correlation analysis between NNI and wavelet feature was developed to select the best wavelet feature to assess NNI using linear, exponential, power, and logarithmic regression models through a direct method. All of the bands were used to construct the empirical relationships between NNI and wavelet feature, from the visible light to NIR bands (325 to 905 nm), based on continuous wavelet analysis. The results indicated that the R^2 values were higher than 0.8 at the NIR region compared with the four regression types. The R^2 values of the linear and exponential regression models were greater than those of the power and logarithmic regression models at the NIR region (Figures 7A, B). The R^2 values of the power and logarithmic regression models were equal to 0 at the lower scale region of the wavelet feature, which could not be used to develop the relationship between NNI and wavelet feature (Figures 7C, D). The higher scale of wavelet feature was more suitable to assess the NNI of summer maize from the V6 to V12 growth stages using the linear and exponential regression models. The strongest relationship between NNI and wavelet feature was observed for feature (745 nm, 7) based on the linear regression and feature (784 nm, 7) based on the exponential regression. The feature (745 nm, 7) was located among the red edge region, and the feature (784 nm, 7) occurred on

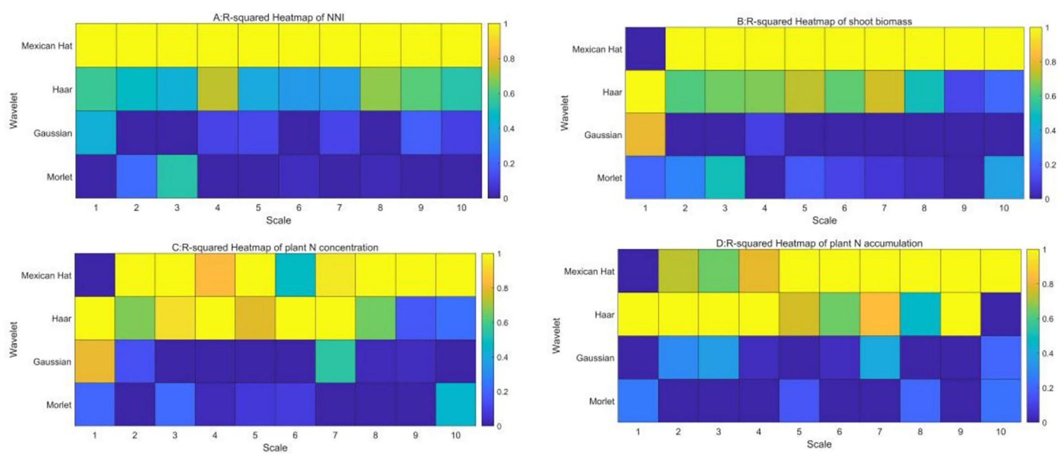

FIGURE 6
The determination coefficient of four mother wavelets with nitrogen nutrition index **(A)**, shoot biomass **(B)**, plant N accumulation **(C)** and plant N concentration **(D)**.

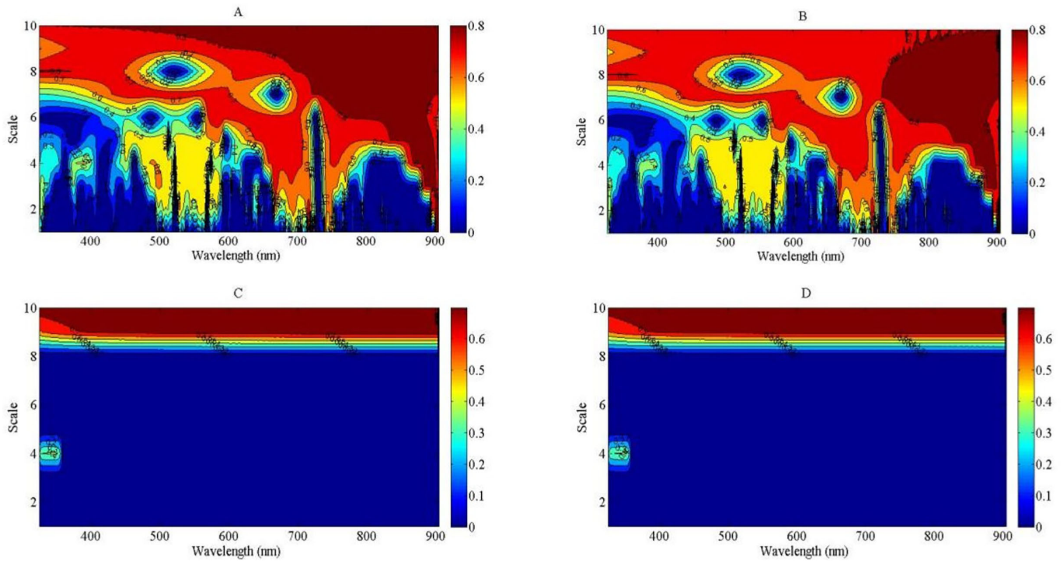

FIGURE 7
The contour maps of determination coefficient for the linear, exponential, power and logarithmic regression types between nitrogen nutrition index (NNI) and wavelet feature from 325 to 905 nm. **(A)**: R^2 between NNI and wavelet feature using linear model; **(B)**: R^2 between NNI and wavelet feature using exponential model; **(C)**: R^2 between NNI and wavelet feature using power model; **(D)**: R^2 between NNI and wavelet feature using logarithmic model.

the right shoulder of the red edge region. The relationships between NNI and the features (745 nm, 7) and (784 nm, 7) are shown in Supplementary Figure S1, respectively.

3.6 Estimation model of nitrogen nutrition index using the indirect method

In the indirect method, PDM was estimated using continuous wavelet analysis to calculate the NNI. The R^2 values of the regression models between PDM and wavelet feature are shown in Figure 8. The regression type was based on linear, exponential, power, and logarithmic regression types (Figure 9), respectively. The result indicated that the power and logarithmic regression types were not suitable to estimate PDM, and the R^2 value was equal to 0 at the lower scale of the wavelet feature and lower than 0.5 at the higher scale of the wavelet feature. The linear and exponential regression types were more suitable to develop the relationship between PDM and wavelet feature, and the R^2 values based on linear and exponential regression types were higher than those based on

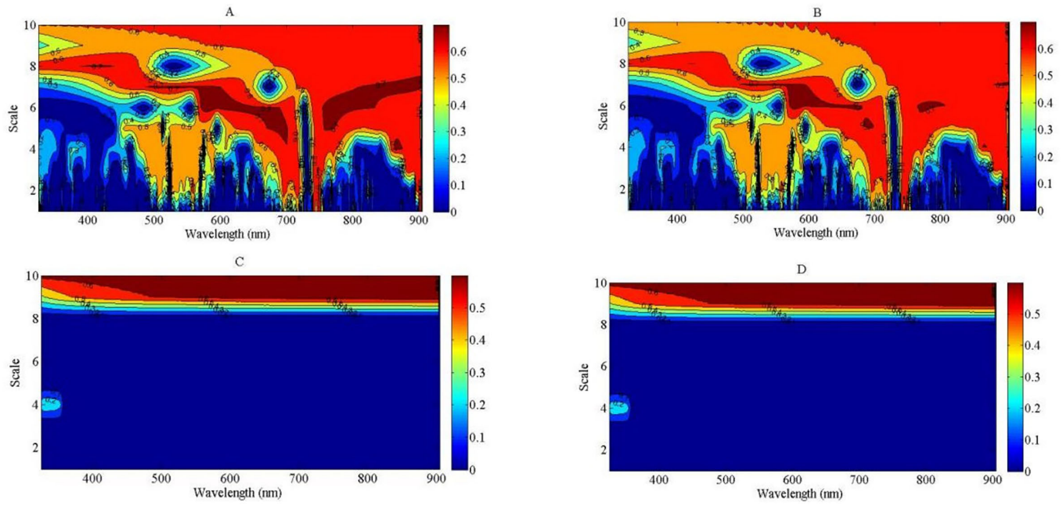

FIGURE 8
The contour maps of determination coefficient (R^2) for the linear, exponential, power and logarithmic regression types between plant dry matter (PDM) and wavelet feature from 325 to 905 nm. **(A)**: R^2 between PDM and wavelet feature using linear model; **(B)**: R^2 between PDM and wavelet feature using exponential model; **(C)**: R^2 between PDM and wavelet feature using power model; **(D)**: R^2 between PDM and wavelet feature using logarithmic model.

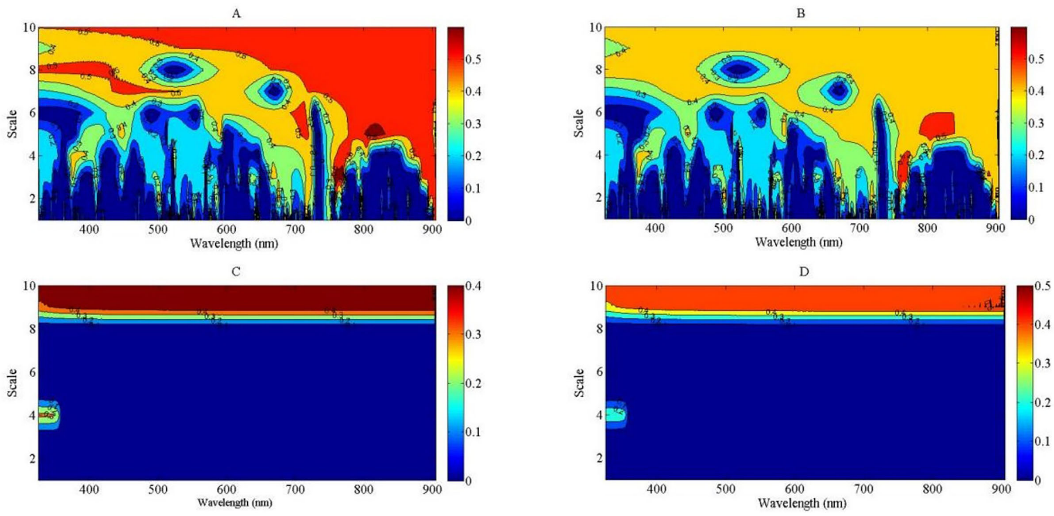

FIGURE 9
The contour maps of determination coefficient for the linear, exponential, power and logarithmic regression types between plant nitrogen concentration (PNC) and wavelet feature from 325 to 905 nm. **(A)**: R^2 between PNC and wavelet feature using linear model; **(B)**: R^2 between PNC and wavelet feature using exponential model; **(C)**: R^2 between PNC and wavelet feature using power model; **(D)**: R^2 between PNC and wavelet feature using logarithmic model.

power and logarithmic regression types across different scales of the wavelet feature. The strongest relationship between PDM and wavelet feature was observed for feature (819 nm, 5) based on the linear regression and feature (782 nm, 3) based on the exponential regression. The features (819 nm, 5) and (782 nm, 3) were located at the near-infrared region. The relationships between PDM and the features (819 nm, 5) and (782 nm, 3) are shown in Supplementary Figure S2, respectively.

Another estimated variable was PNC to calculate NNI in the indirect method. The four regression types (linear, exponential, power, and logarithmic) were used to develop the relationship between PNC and wavelet feature based on continuous wavelet analysis. The regression performance of power and logarithmic types between PNC and wavelet feature was similar with that between PDM and wavelet feature (Figures 8C, D). The R^2 value was lower at the low-scale region of the wavelet feature than at the high-scale region of the wavelet feature across the two regression types, which was equal to 0 at the low scale. The regression performance of the linear and exponential types was better than that of the power and logarithmic types. The R^2 value was higher than 0.7 from the visible light to the NIR bands under the linear and exponential regression types (Figures 8A, B). The sensitive region between PNC and wavelet feature was greater under the linear regression type than under the exponential regression type. The optimal relationship between PNC and wavelet feature was observed for feature (581 nm, 6) under the linear regression type and feature (573 nm, 6) under the exponential regression type (Supplementary Figure S3). The optimal WP mainly existed at the higher region of scale. The R^2 value was slightly higher based on linear regression than exponential regression. Therefore, the PDM estimation model of feature (819 nm, 5) and the PNC estimation model of feature (581 nm, 6) were used to assess the NNI value in the indirect method. The integrated model of NNI was expressed as follows:

$$NNI = \frac{-3.38WP(581nm, 6) + 2.1}{3.4(6.59WP(819nm, 5) + 0.03)^{-0.37}} \quad (11)$$

3.7 Validation of the estimation linear model of nitrogen nutrition index based on wavelet features

The calibration result showed that the goodness of fit of the linear model was better than that of the exponential model, so this study chose the linear model to validate the feasibility of wavelet analysis for assessing NNI. The independent experiment data sets (experiments 3 and 4) were used to validate the newly developed regression models based on wavelet features (Figure 10). The result indicated that the performances of the new models were acceptable using the direct and indirect methods. In the direct method, the wavelet feature (745 nm, 7) produced an accurate prediction of NNI values, with RMSEP, RRMSE, and REP values of 0.09, 10.8%, and 9.88%, respectively. In the indirect method, (Equation 11), which included wavelet feature (581 nm, 6) and (819 nm, 5), predicted NNI values with RMSEP, RRMSE, and REP values of 0.12, 13.4%, and 10.68%, respectively. The validation result of the direct method was better than that of the indirect method. The two new models provided enhanced accuracy and stability in estimating the NNI of summer maize with a simplified and applicable formulation.

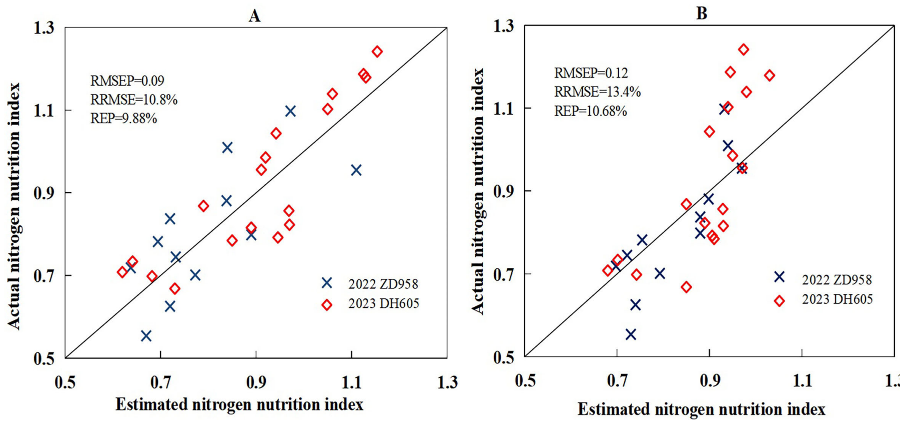

FIGURE 10
The validation result between estimated nitrogen nutrition index based on the direct method (**A**, linear) and indirect method (**B**, linear) and actual nitrogen nutrition index using the validation data set acquired from experiments 3 and 4.0

4 Discussion

4.1 Theoretical analysis of plant nitrogen diagnosis based on nitrogen nutrition index

Nitrogen plays a crucial role in the growth and development of crops (Ata-Ul-Karim et al., 2016). As a key component of chlorophyll, nitrogen was essential for photosynthesis, the process by which plants convert light energy into chemical energy. It is also a major constituent of amino acids, the building blocks of proteins, which are vital for cell growth and function. An adequate nitrogen supply promotes vigorous vegetative growth, leading to a larger leaf area, enhanced root development, and overall improved plant health. Conversely, nitrogen deficiency could result in stunted growth, yellowing of leaves (chlorosis), and reduced crop yields. Thus, N treatments had a significant effect on specific parameters (such as PNC and PDM).

The responses of plant DM accumulation and N uptake varied under different N application conditions. Under low N application, both DM accumulation and N uptake were jointly influenced by the plant's growth potential and the soil's N supply capacity. As N application increased, both DM accumulation and N uptake also increased (Justes et al., 1994), showing significant differences as shown in Table 3. However, under optimal or excessive N application, plant N uptake was primarily determined by soil N availability, independent of the plant's growth potential. Conversely, under these conditions, DM accumulation was dictated by the plant's growth potential and was independent of soil N availability (Plénet and Lemaire, 2000). As a result, while plant N concentration (PNC) continued to increase with higher N application, DM accumulation did not significantly increase once N application reached a critical level (Zhao et al., 2017). Based on the behavior of DM accumulation and PNC under varying N conditions, Lemaire and Salette (1984) introduced the concept of N_c dilution concentration, which refers to the minimum N concentration required for maximum crop growth. Plénet and Lemaire (2000) further developed the first N_c dilution curve for maize, which has since been widely adopted to diagnose the N status of maize globally.

Nitrogen nutrition index was developed based on N_c dilution curve (Equation 1). A statistical significance existed between different N treatments, which is due to the difference of plant DM and PNC. When NNI was equal to or higher than 1, plant N status was considered optimal or excessive, and when NNI was lower than 1, plant N status was considered insufficient. The lower plant DM and PNC were from the low N treatments, which can contribute to the low NNI value. Due to the characteristic of the N_c curve, even if the plant DM accumulation of maize was not significantly different under excessive N condition, NNI could still recognize a plant's excessive N status by comparing PNC with plant N_c concentration (Ziadi et al., 2008; Ata-Ul-Karim et al., 2017).

4.2 Wavelet features for the estimation of nitrogen nutrition index

The Mexican Hat wavelet may have performed better due to its strong localization in both the time and frequency domains, which makes it particularly effective at detecting subtle variations in crop reflectance at certain scales. In contrast, other wavelets like the Haar or Morlet wavelet may have struggled with capturing these variations due to their different frequency responses or poorer localization properties (Cheng et al., 2011). Including this type of comparative analysis in the "Results" section would not only clarify why the Mexican Hat wavelet was superior but also provide valuable insights into the suitability of different wavelets for agricultural spectral analysis (Ngui et al., 2013).

Nitrogen nutrition index was estimated using four regression types—linear, exponential, power, and logarithmic—in this study. The linear models offer simplicity and ease of interpretation but may not capture complex, non-linear relationships as effectively as exponential models could provide valuable context. Conversely, exponential models might better fit certain data patterns, especially when there are diminishing returns in response to increasing nitrogen levels, but they can be more challenging to interpret and apply. In this study, the regression types of power and logarithmic could not be used to fit the relationship between NNI and wavelet feature (Figures 7C, D). This is because there was a negative value appearing in the lower scale of the wavelet feature; the fitting result of power and logarithmic types was invalid between NNI and wavelet feature. The R^2 value is shown as 0 in Figures 7C, D under the lower scale conditions. Cheng et al. (2011) considered that more than 2^{10} scale ought to be discarded because the decomposed components at higher scales do now carry meaningful spectral information. The linear and exponential regression types were fit to develop the relationships between NNI and wavelet feature (Figures 7A, B). The R^2 value of wavelet power (745 nm, 7) deduced from the linear regression was slightly better than that of wavelet power (784 nm, 7) based on exponential regression. The wavelet feature (745 nm, 7) was close to the leading red edge position. Many studies reported that the red edge was very sensitive to the change of PDM and PNC, which can reflect plant N stress (Yao et al., 2010; Pellissier et al., 2015; Li et al., 2017). The feature (745 nm, 7) carried information of reflectance spectra across the red edge and near-infrared region (715 to 775 nm) that is mainly controlled by crop N stress and biophysical parameters (PDM) centered at 740 nm (Thenkabail et al., 2004; Chan and Paelinckx, 2008).

High-scale wavelet features are particularly adept at capturing large-scale patterns in the spectral reflectance data, which are often influenced by the overall structure of the crop, such as leaf area, canopy density, and plant height. These structural characteristics can significantly impact how light interacts with the crop, affecting the absorption and reflection of different wavelengths. Cheng et al. (2011) explained that low-scale components are suitable for capturing the characteristics of narrow absorption features, while high-scale components are better suited for defining the overall spectral shape of the canopy spectra. Since NNI reflects the canopy structure throughout the crop growth process, the higher-scale wavelet features in this study were found to be particularly effective in establishing a relationship with NNI. These high-scale features can capture the impact of crop structure on the amplitude of reflectance spectra and partially reduce the influence of the biochemical absorption characteristics (Li, 2016). Consequently, using high-scale wavelet features helps maintain more stable NNI estimations.

In this indirect method, the wavelet features (819 nm, 5) for PDM and (581 nm, 6) for PNC were determined to develop the relationships between wavelet feature and NNI. The power and logarithmic regression types could not be used to fit the relationships between PDM, PNC, and wavelet feature (Figures 9C, D, 8C, D). The wavelet feature (819 nm, 5) was located at the near-infrared region (814 to 824 nm) of the reflectance spectra and was close to the sensitive region of the wavelet feature based on NNI. There was a significantly positive relationship between leaf area index and PDM during the V6 to V12 stages of summer maize. The amplitude of the reflectance spectra was also affected by PDM, which made the sensitive wavelet feature to PDM influenced by other biophysical parameters (leaf area index). The sensitive wavelet feature (581 nm, 6) to PNC was located at the green light region (567 to 587 nm) of the reflectance spectra and was close to the strong reflected peak (550 nm) of chlorophyll, which has been identified as a sensitive wavelength for N estimation in previous studies (Huang et al., 2004). During the vegetative growth stage of crops, plants invest a higher proportion of photosynthate in the structural compartment (low N concentration), and more absorbed N was transported into the upper leaves due to plant light distribution (Lemaire et al., 2008). Therefore, PNC decreased gradually with plant growth. Due to the capture capacity of the high scale of wavelet feature to the information of reflectance amplitude, the estimation of PNC was more suitable using a higher scale based on continuous wavelet transform method.

4.3 Comparison with the traditional method and existing wavelet feature

The change of spectral reflectance from visible to near-infrared region could represent the change of plant N status. In the visible region, changes in reflectance are often linked to chlorophyll content, which directly correlates with nitrogen status. A decrease in nitrogen can lead to chlorosis, reducing chlorophyll and thereby increasing reflectance in the green and red bands. In the near-infrared region, reflectance is largely influenced by the internal structure of plant leaves, including cell density and water content. N deficiency can alter these structural properties, leading to changes in near-infrared reflectance.

In this study, the three existing spectral indices were used to estimate NNI of summer maize using the calibration data set (Table 2). The result confirmed that these indices could represent the change of NNI, but the performance was not unsatisfactory (Supplementary Figure S4). The strongest relationship was found between MTCI and NNI. The R^2 value was 0.61, which was lower than 0.7. The performance of the developed wavelet feature (R^2 value higher than 0.8) was better than the existing spectral indices (Figure 7). The first reason was that the traditional spectral indices were not specifically designed to estimate NNI; they were originally developed to assess parameters like PNC or PDM across different crops (Mistele and Schmidhalter, 2008; Chen, 2015; Liu et al., 2018). The second reason was that these traditional indices typically rely on two or three independent spectral bands to evaluate crop growth status. This approach was highly susceptible to external environmental factors and cultivar characteristics, leading to inconsistent and unstable predictive performance of the spectral indices. The CWA method was particularly effective because it could isolate and capture relevant features at different scales, allowing it to account for variations in crop structure and minimize the influence of noise or irrelevant spectral information. This led to more consistent and reliable NNI predictions across varying conditions. The contained spectral information of the single spectral band was very limited, and the reflectance of the neighboring spectral bands might be different with the determined spectral band, which led to substantial decreases in the predictive performance to the same objective (Cheng et al., 2014a).

In the indirect method, PDM and PNC were estimated using wavelet features based on continuous wavelet transform, respectively. The wavelet feature (581 nm, 6) was the most sensitive feature to PNC. The wavelet features based on the green light region have been reported as a sensitive feature to estimate N or chlorophyll content by many studies (Liao et al., 2013; Wang et al., 2016, 2017). All R^2 values between wavelet features and PDM were lower than 0.7 (Figures 9A, B), and their performance was also weaker than the two other indices estimated (NNI and PNC), which indicated that the better wavelet feature to estimate PDM might be located at the longer wavelengths (shortwave infrared region) of the reflectance spectra. The decomposition scale (5) of this study was similar with that (4 or 5) determined by Cheng et al. (2014b). The correlation between dry matter and wavelet feature was better for scale 5 than for a higher scale. The most sensitive wavelet feature (819 nm, 4) that integrated reflectance information from the spectral segment (814–824 nm) characterized the change of dry matter in spectral shape more efficiently than the traditional spectral indices (Supplementary Figure S5). This could eliminate the effect of canopy structure on spectral segment and therefore was highly promising for canopy-level applications.

Through the calibration and validation of the relationships between NNI and wavelet feature using field data set, each of the direct and indirect methods could assess the NNI of summer maize, but the performance of the direct method was better than that of the indirect method. External environmental factors such as variations in weather conditions, soil heterogeneity, and unexpected pest or disease outbreaks could introduce variability that impacts the predictive accuracy of the developed models in this study. Additionally, errors during data collection, such as inaccuracies in sensor readings or sampling inconsistencies, could further contribute to discrepancies between the predicted and observed outcomes. These sources of error could lead to overestimation or underestimation of certain variables, thereby affecting the model's overall reliability. These factors would not only highlight the limitations of the current model but also suggest areas for improvement, such as refining data collection methods or incorporating additional environmental variables into the model. Addressing these potential errors is crucial to enhance the model's predictive ability and ensure its robustness in different scenarios.

The combination structure and calculation method for the newly developed wavelet feature (745 nm, 7) were simpler than those of the two wavelet features (581 nm, 6) and (819 nm, 5), which could reduce the risk of NNI prediction. This new wavelet feature will be useful to design an exclusive index to diagnose the plant N status of summer maize. However, due to the limitation of the experiment data and spectral band, future work is required to test the adaptation and reliability of the newly developed wavelet feature under diverse external environments.

5 Conclusion

This study confirmed the effectiveness of using wavelet features to predict the nitrogen nutrition index (NNI) in summer maize through the continuous wavelet analysis (CWA) method, with the Mexican Hat wavelet identified as the most suitable mother wavelet. In the direct method, the most sensitive wavelet feature (745 nm, scale 7) was identified to assess NNI, and the linear regression model established was NNI = 0.14 WF (745 nm, 7) + 0.3. In the indirect method, wavelet features (819 nm, scale 5) to predict PDM and (581 nm, scale 6) for PNC were used to construct the calculation model for NNI. The two methods of NNI estimation were compared by using independent data sets. The result indicated that the performances of the direct and indirect estimation methods were accurate and stable. Compared with the established spectral indices, Mexican Hat is shown to have a more effective capacity in collecting meaningful spectral information that relates to NNI, PDM, and PNC. By decomposing the reflectance spectra into various scales, the high scale features could capture the information of the reflectance amplitude based on the shape of the spectral curve, and the low scale features could capture the absorption characteristics of the objective index (PNC and PDM). The result of this study revealed that the wavelet feature of NNI successfully differentiated the different plant N status of summer maize. The CWA method was extended to the field of plant N diagnosis and enlarged its application range. Further research could focus on optimizing the wavelet analysis method by exploring different wavelet functions or scales to enhance its predictive accuracy. Moreover, validating the method across a broader range of crops and environmental conditions would help establish its generalizability and practical applicability in diverse agricultural settings.

Data availability statement

The original contributions presented in the study are included in the article/Supplementary Material. Further inquiries can be directed to the corresponding author.

Author contributions

MW: Conceptualization, Formal analysis, Investigation, Project administration, Writing – original draft. BZ: Conceptualization, Data curation, Formal analysis, Writing – original draft, Writing – review & editing. NJ: Formal analysis, Investigation, Methodology, Project administration, Software, Writing – original draft. HL: Investigation, Methodology, Project administration, Software, Validation, Writing – original draft. JC: Conceptualization, Data curation, Formal analysis, Investigation, Writing – review & editing, Writing – original draft.

Funding

The author(s) declare financial support was received for the research, authorship, and/or publication of this article. The research was funded from the key scientific and technological project of Henan Province (232102111004).

Conflict of interest

The authors declare that the research was conducted in the absence of any commercial or financial relationships that could be construed as a potential conflict of interest.

Publisher's note

All claims expressed in this article are solely those of the authors and do not necessarily represent those of their affiliated organizations, or those of the publisher, the editors and the reviewers. Any product that may be evaluated in this article, or claim that may be made by its manufacturer, is not guaranteed or endorsed by the publisher.

Supplementary material

The Supplementary Material for this article can be found online at: https://www.frontiersin.org/articles/10.3389/fpls.2024.1478162/full#supplementary-material

References

Ata-Ul-Karim, S. T., Cao, Q., Zhu, Y., Tang, L., Rehmani, M. I. A., and Cao, W. (2016). Non-destructive assessment of plant nitrogen parameters using leaf chlorophyll measurements in rice. *Front. Plant Sci.* 7, 1829. doi: 10.3389/fpls.2016.01829

Ata-Ul-Karim, S. T., Zhu, Y., Lu, X. J., Cao, Q., Tian, Y. C., and Cao, W. (2017). Estimation of nitrogen fertilizer requirement for rice crop using critical nitrogen dilution curve. *Field Crops Res.* 201, 32–40. doi: 10.1016/j.fcr.2016.10.009

Bremner, J. M., and Mulvancy, C. S. (1982). "Nitrogen-total," in *Methods of Soil Analysis, Part 2*. Ed. A. L. Page (American Society of Agronomy, Madison, WI), 595–624.

Bruce, L. M., Morgan, C., and Larsen, S. (2001). Automated detection of subpixel hyperspectral targets with continuous and discrete wavelet transforms. *IEEE Trans. Geosci. Remote Sens.* 39, 2217–2226. doi: 10.1109/36.957284

Cao, Q., Miao, Y., Wang, H., Huang, S., Cheng, S., Khosla, R., et al. (2013). Non-destructive estimation of rice plant nitrogen status with Crop Circle multispectral active canopy sensor. *Field Crops Res.* 154, 133–144. doi: 10.1016/j.fcr.2013.08.005

Chan, J. C. W., and Paelinckx, D. (2008). Evaluation of Random Forest and Adaboost tree-based ensemble classification and spectral band selection for ecotope mapping using airborne hyperspectral imagery. *Remote Sens. Environ.* 112, 2999–3011. doi: 10.1016/j.rse.2008.02.011

Chen, P. F. (2015). A comparison of two approaches for estimating the wheat nitrogen nutrition index using remote sensing. *Remote Sens.* 7, 4527–4548. doi: 10.3390/rs70404527

Cheng, T., Riaño, D., and Ustin, S. L. (2014a). Detecting diurnal and seasonal variation in canopy water content of nut tree orchards from airborne imaging spectroscopy data using continuous wavelet analysis. *Remote Sens. Environ.* 143, 39–53. doi: 10.1016/j.rse.2013.11.018

Cheng, T., Rivard, B., and Sánchez-Azofeifa, G. A. (2011). Spectroscopic determination of leaf water content using continuous wavelet analysis. *Remote Sens. Environ.* 115, 659–670. doi: 10.1016/j.rse.2010.11.001

Cheng, T., Rivard, B., Sánchez-Azofeifa, G. A., Féret, J. B., Jacquemoud, S., and Ustin, S. L. (2014b). Deriving leaf mass per area (LMA) from foliar reflectance across a variety of plant species using continuous wavelet analysis. *ISPRS J. Photogramm.* 87, 28–38. doi: 10.1016/j.isprsjprs.2013.10.009

Dordas, C. A. (2017). Chlorophyll meter readings, N leaf concentration and their relationship with N use efficiency in oregano. *J. Plant Nutt.* 40, 391–403. doi: 10.1080/01904167.2016.1240200

Gnyp, M. L., Miao, Y., Yuan, F., Ustin, S. L., Yu, K., Yao, Y., et al. (2014). Hyperspectral canopy sensing of paddy rice aboveground biomass at different growth stages. *Field Crops Res.* 155, 42–55. doi: 10.1016/j.fcr.2013.09.023

He, R., Li, H., Qiao, X., and Jiang, J. (2018). Using wavelet analysis of hyperspectral remote-sensing data to estimate canopy chlorophyll content of winter wheat under stripe rust stress. *Int. J. Remote Sens.* 39, 4059–4076. doi: 10.1080/01431161.2018.1454620

Hu, D., Sun., Z., Li., T., Yan., H., and Zhang., H. (2014). Nitrogen nutrition index and its relationship with N use efficiency, tuber yield, radiation use efficiency, and leaf parameters in potatoes. *J. Int. Agric.* 13, 1008–1016. doi: 10.1016/S2095-3119(13)60408-6

Huang, Z., Turner, B. J., Dury, S. J., Wallis, I. R., and Foley, W. J. (2004). Estimating foliage nitrogen concentration from HYMAP data using continuum removal analysis. *Remote Sens. Environ.* 93, 18–29. doi: 10.1016/j.rse.2004.06.008

Jay, S., Bendoula, R., Hadoux, X., Féret, J.-B., and Gorretta, N. (2016). A physically-based model for retrieving foliar biochemistry and leaf orientation using close-range imaging spectroscopy. *Remote Sens. Environ.* 177, 220–236. doi: 10.1016/j.rse.2016.02.029

Justes, E., Mary, B., and Machet, J. M. (1994). Determination of a critical nitrogen dilution curve for winter wheat crops. *Ann. Bot.* 74, 397–407. doi: 10.1006/anbo.1994.1133

Kaewpijit, S., Moigne, J. L., and El-Ghazawi, T. (2003). Automatic reduction of hyperspectral imagery using wavelet spectral analysis. *IEEE Trans. Geosci.* 41, 863–871. doi: 10.1109/TGRS.2003.810712

Lemaire, G., Marie-Helene, J., and Grancois, F. (2008). Diagnosis tool for plant and crop N status in vegetative stage: Theory and practices for crop N management. *Eur. J. Agron.* 28, 614–624. doi: 10.1016/j.eja.2008.01.005

Lemaire, G., and Salette, J. (1984). Relation entre dynamique de croissance et dynamique de prél evement dazote pour un peuplement de graminées fourragéres. I Etude de leffet du milieu. *Agronomie* 4, 423–430. doi: 10.1051/agro:19840503

Li, D. (2016). *Application of continuous wavelet analysis to reflectance spectra for the spectroscopic estimation of wheat* (Nanjing, China: Ph. D. Dissertation, Nanjing Agricultural University).

Li, D., Cheng, T., Zhou, K., Zheng, H., Yao, X., Tian, Y., et al. (2017). WREP: A wavelet-based technique for extracting the red edge position from reflectance spectra for estimating leaf and canopy chlorophyll contents of cereal crops. *ISPRS J. Photogramm.* 129, 103–117. doi: 10.1016/j.isprsjprs.2017.04.024

Li, D., Wang, X., Zheng, H., Zhou, K., Yao, X., Tian, Y., et al. (2018). Estimation of area- and mass-based leaf nitrogen contents of wheat and rice crops from water-removed spectra using continuous wavelet analysis. *Plant Methods* 14, 76. doi: 10.1186/s13007-018-0344-1

Li, F., Miao, Y., Feng, G., Yuan, F., Yue, S., Gao, X., et al. (2014). Improving estimation of summer maize nitrogen status with red edge-based spectral vegetation indices. *Field Crops Res.* 157, 111–123. doi: 10.1016/j.fcr.2013.12.018

Liao, Q. H., Wang, J. H., Yang, G. J., Zhang, D. Y., Li, H. L., and Fu, Y. Y. (2013). Comparison of spectral indices and wavelet transform for estimating chlorophyll content of maize from hyperspectral reflectance. *J.Appl. Remote Sens.* 7, 073575. doi: 10.1117/1.JRS.7.073575

Liu, S., Li, L., Gao, W., Zhang, Y., Liu, Y., Wang, S., et al. (2018). Diagnosis of nitrogen status in winter oilseed rape (*Brassica napus* L.) using *in-situ* hyperspectral data and unmanned aerial vehicle (UAV) multispectral images. *Comput. Electron. Agr.* 151, 185–195. doi: 10.1016/j.compag.2018.05.026

Mallat, S. (1991). Zero-crossings of a wavelet transform. *IEEE T. Inform. Theory.* 37, 1019–1033. doi: 10.1109/18.86995

Mistele, B., and Schmidhalter, U. (2008). Estimating the nitrogen nutrition index using spectral canopy reflectance measurements. *Eur. J. Agron.* 29, 184–190. doi: 10.1016/j.eja.2008.05.007

Nelson, E. W., and Sommers, L. E. (1982). "Total carbon, organic carbon, and organic matter," in *Methods of Soil Analysis. Part 2, 2nd ed*, vol. 9 . Ed. A. L. Page (ASA and SSSA, Madison), 539–579.

Ngui, W. K., Leong, M. S., Hee, L. M., and Abdelrhman, A. M. (2013). Wavelet analysis: Mother wavelet selection methods. *Appl. Mech. Mater.* 393, 953–958. doi: 10.4028/www.scientific.net/AMM

Olsen, S. R., Cole, C. V., Watanabe, F. S., and Dean, L. A. (1954). *Estimation of Available Phosphorus in Soils by Extraction with Sodium Bicarbonate USDA Circ. 939* (Washington, D.C: U.S.Government Printing Office).

Pellissier, P. A., Ollinger, S. V., Lepine, L. C., Palace, M. W., and Mcdowell, W. H. (2015). Remote sensing of foliar nitrogen in cultivated grasslands of human dominated landscapes. *Remote Sens. Environ.* 167, 88–97. doi: 10.1016/j.rse.2015.06.009

Plénet, D., and Lemaire, G. (2000). Relationships between dynamics of nitrogen uptake and dry matter accumulation in maize crops. *Plant Soil* 216, 65–82. doi: 10.1023/A:1004783431055

Schlemmer, M., Gitelson, A., Schepers, J., Ferguson, R., Peng, Y., Shanahan, J., et al. (2013). Remote estimation of nitrogen and chlorophyll contents in maize at leaf and canopy levels. *Int. J. Appl. Earth Obs. Geoinf.* 25, 47–54. doi: 10.1016/j.jag.2013.04.003

Thenkabail, P. S., Enclona, E. A., Ashton, M. S., and van der Meer, B. (2004). Accuracy assessments of hyperspectral waveband performance for vegetation analysis applications. *Remote Sens. Environ.* 91, 354–376. doi: 10.1016/j.rse.2004.03.013

Ullah, S., Skidmore, A. K., Naeem, M., and Schlerf, M. (2012). An accurate retrieval of leaf water content from mid to thermal infrared spectra using continuous wavelet analysis. *Sci. Total Environ.* 437, 145–152. doi: 10.1016/j.scitotenv.2012.08.025

van Reeuwijk, L. P. (1992). *Procedures for Soil Analysis. 3rd edition* (Wageningen, the Netherlands: ISRIC).

Wang, H., Huo, Z., Zhou, G., Liao, Q., Feng, H., and Wu, L. (2016). Estimating leaf SPAD values of freeze-damaged winter wheat using continuous wavelet analysis. *Plant Physiol. Bioch.* 98, 39–45. doi: 10.1016/j.plaphy.2015.10.032

Wang, Z., Skidmore, A. K., Wang, T., Darvishzadeh, R., Heiden, U., Heurich, M., et al. (2017). Canopy foliar nitrogen retrieved from airborne hyperspectral imagery by correcting for canopy structure effects. *Int. J. Appl. Earth Obs.* 54, 84–94. doi: 10.1016/j.jag.2016.09.008

Yao, X., Zhu, Y., Tian, Y. C., Feng, W., and Cao, W. X. (2010). Exploring hyperspectral bands and estimation indices for leaf nitrogen accumulation in wheat. *Int. J. Appl. Earth Obs. Geoinf.* 12, 89–100. doi: 10.1016/j.jag.2009.11.008

Zhao, B., Ata-Ul-Karim, S. T., Liu, Z. D., Ning, D. F., Xiao, J. X., Liu, Z. G., et al. (2017). Development of a critical nitrogen dilution curve based on leaf dry matter for summer maize. *Field Crops Res.* 208, 60–68. doi: 10.1016/j.fcr.2017.03.010

Zhao, B., Ata-Ul-Karim, S. T., Liu, Z., Zhang, J., Xiao, J., Liu, Z., et al. (2018). Simple assessment of nitrogen nutrition index in summer maize by using chlorophyll meter readings. *Front. Plant Sci.* 9, 11. doi: 10.3389/fpls.2018.00011

Ziadi, N., Brassard, M., Bélanger, G., Cambouris, A. N., Tremblay, N., Nolin, M. C., et al. (2008). Critical nitrogen curve and nitrogen nutrition index for corn in eastern Canada. *Agron. J.* 100, 271–276. doi: 10.2134/agronj2007.0059

Ziadi, N., Bélanger, G., Claessens, A., Lefebvre, L., Tremblay, N., Cambouris, A. N., et al. (2010). Plant-based diagnostic tools for evaluating wheat nitrogen status. *Crop Sci.* 50, 2580–2590. doi: 10.2135/cropsci2010.01.0032

frontiers | Frontiers in Plant Science

TYPE Original Research
PUBLISHED 13 November 2024
DOI 10.3389/fpls.2024.1439523

Check for updates

OPEN ACCESS

EDITED BY
Henry Yabbey Sintim,
The University of Georgia, Tifton Campus, United States

REVIEWED BY
Sudip Sengupta,
Swami Vivekananda University, India
Sri Nuryani Hidayah Utami,
Gadjah Mada University, Indonesia

*CORRESPONDENCE
R. Krishna Murthy
stcruasbangalore@gmail.com

RECEIVED 28 May 2024
ACCEPTED 15 October 2024
PUBLISHED 13 November 2024

CITATION
Murthy RK, Nagaraju B, Govinda K, Uday Kumar SN, Basavaraja PK, Saqeebulla HM, Gangamrutha GV, Srivastava S and Dey P (2024) Soil test crop response nutrient prescription equations for improving soil health and yield sustainability—a long-term study under Alfisols of southern India. *Front. Plant Sci.* 15:1439523. doi: 10.3389/fpls.2024.1439523

Soil test crop response nutrient prescription equations for improving soil health and yield sustainability—a long-term study under Alfisols of southern India

R. Krishna Murthy[1*], Bhavya Nagaraju[1], K. Govinda[1], S. N. Uday Kumar[1], P. K. Basavaraja[1], H. M. Saqeebulla[1], G. V. Gangamrutha[1], Sanjay Srivastava[2] and Pradip Dey[3]

[1]All India Coordinated Research Project on Soil Test Crop Response, University of Agricultural Sciences, Bangalore, India, [2]All India Coordinated Research Project on Soil Test Crop Response, Indian Council of Agricultural Research (ICAR)-Indian Institute of Soil Science, Bhopal, India, [3]Soil Science, Indian Council of Agricultural Research-Agricultural Technology Application Research Institute, Kolkata, India

Introduction: Enhancing soil health and nutrient levels through fertilizers boosts agricultural productivity and global food security. However, careful fertilizer use is essential to prevent environmental damage and improve crop yields. The soil test crop response (STCR) is a scientific approach to fertilizer recommendation that ensures efficient use, supporting higher crop production while protecting the environment and preserving resources.

Methodology: A long-term field experiment on the STCR approach was initiated in 2017 at the Zonal Agriculture Research Station, University of Agricultural Sciences, Bangalore, India. The experiment aimed to study the impact of STCR-based nutrient prescription along with farmyard manure (FYM) for a targeted yield of soybean (*Glycine max*), sunflower (*Helianthus annuus*), dry chili (*Capsicum annuum*), aerobic rice (*Oryza sativa* L.), foxtail millet (*Setaria italica*), okra (*Abelmoschus esculentus*), and kodo millet (*Paspalum scrobiculatum*) on yield and changes in soil health in comparison with other approaches of fertilizer recommendation.

Results: The results showed a significant and positive impact of the integrated use of fertilizer with FYM based on the STCR approach on the productivity of all the crops and soil fertility. Significantly higher yields of soybean (23.91 q ha^{-1}), sunflower (27.13 q ha^{-1}), dry chili (16.67 q ha^{-1}), aerobic rice (65.46 q ha^{-1}), foxtail millet (14.07 q ha^{-1}), okra (26.82 t ha^{-1}), and kodo millet (17.10 q ha^{-1}) were observed in the STCR NPK + FYM approach at yield level 1 compared to the general recommended dose and soil fertility rating approach. This approach outperformed the standard recommendations, enhancing nutrient uptake and efficiency across various crops. Utilizing the principal component analysis, the soil quality index effectively reflected the impact of nutrient management on soil properties, with the STCR NPK + FYM treatment at yield level 1 showing the highest correlation with improved soil physical and chemical parameters.

Discussion: The STCR approach led to improved yield, nutrient uptake, utilization efficiency, and soil health, thanks to a balanced fertilization strategy. This strategy was informed by soil tests and included factors like crop-induced nutrient depletion, baseline soil fertility, the efficiency of inherent and added nutrients through fertilizers and farmyard manure, and the success of yield-targeting techniques in meeting the nutritional needs of crops.

KEYWORDS

STCR, yield, nutrient use efficiency, soil quality, principle component analysis

1 Introduction

India's quest for agricultural abundance in the 21st century hinges on its ability to sustainably satisfy the escalating demands for food, feed, fiber, and fuel amid its burgeoning population (Gulati et al., 2023). The nation has witnessed a dramatic escalation in chemical fertilizer usage, skyrocketing from a mere 69.8 thousand tons in 1950–1951 to a staggering 29.796 million tons in 2021–2022, propelling food grain production from 50.85 to 305.6 million tons (FAI, 2022). However, this reliance on chemical fertilizers, accounting for half of the food grain yield boost (Shukla et al., 2022), has precipitated a cascade of ecological quandaries—from nitrate contamination and soil acidification to eutrophication and greenhouse gas emissions—threatening the very fabric of India's agricultural sustainability (Kumar et al., 2022).

In the dynamic arena of soil science, the strategic application of plant nutrients emerges as a cornerstone for the enduring yield of crops. Precision in nutrient delivery, tailored to the soil's inherent nutrient profile and expected crop uptake, is paramount. Yet, the relentless use of potent fertilizers has led to the depletion of essential micro and secondary nutrients, undermining crop yields across various regions (Singh, 2010). The plateau in India's crop production is largely attributed to outdated fertilizer practices, suboptimal utilization, and disproportionate fertilizer application. A methodical assessment of fertilizer quantities can be instrumental in bolstering yields while concurrently elevating nutrient efficiency. This challenge is met by adopting an integrated nutrient management approach, combining organic, biological, and synthetic fertilizers. It is acknowledged that neither organic manures nor chemical fertilizers alone can fulfill the quest for food and nutritional security (Paramesh et al., 2023). The habitual incorporation of organic matter not only invigorates soil life and diversity but also ameliorates its physical structure (Kumar and Tripathi, 2009). Thus, the synergistic merger of inorganic and organic inputs is pivotal in perpetuating crop productivity and augmenting soil vitality, as evidenced by their mutual benefits (Antil et al., 2011).

On the other hand, the art of balanced fertilization involves the precise deployment of vital plant nutrients, tailored in perfect harmony and quantity to meet the unique demands of each crop scenario. The innovative approach of calibrating nutrient recommendations through the soil test crop response (STCR) for targeted yield using developed fertilizer adjustment equations offers a superior strategy for the judicious application of nutrients (Sharma et al., 2016). Such meticulous fertilizer guidance is rendered with prudence, taking into account yield dynamics and desired agronomic efficiencies while also acknowledging the nutrient contributions from both external sources, such as chemical and organic fertilizers, and internal, indigenous soil reserves (Haokip et al., 2023). The STCR approach is used to determine the optimal fertilizer recommendations for crops based on soil test values. This approach helps in achieving the yield target of a crop while maintaining soil fertility and minimizing environmental impact. Set against this scientific canvas, a pioneering study was embarked upon to evaluate the long-term effects of strategic nutrient management, grounded in soil testing and crop response, on the enduring productivity and vitality of soil within a *Typic Haplustalf* setting.

2 Materials and methods

2.1 Experimental site

A field experiment has been conducted since 2017 at the Zonal Agricultural Research Station, University of Agricultural Sciences, Bangalore, Karnataka, India. This site is characterized by a dry tropical savanna climate, with hot summers and cool winters, located at 13°04′55.2′′N, 77°34′10.0′′E, and an elevation of 930 m. The well-drained red soil in the study location belonged to the taxonomically defined large group, Typic *Kandic Paleustalfs* belonging to the fine mixed *Isohyperthermic* family. Prior to the experiment, soil samples were taken from the top 15 cm, shade-dried, and analyzed for their physical, chemical, and biological properties. Measurements included a bulk density of 1.39 g/cm^3, 35.98% porosity, and 30.10% maximum water holding capacity. Soil chemistry revealed a pH of 5.49, electrical conductivity of 0.09 dS m^{-1}, organic carbon content of 0.28%, and levels of available nitrogen, phosphorus, and potassium at 230.50 kg ha^{-1}, 58.66 kg ha^{-1}, and

120.00 kg ha^{-1}, respectively. Biological assessments showed microbial biomass carbon at 115.56 mg kg^{-1}, microbial biomass nitrogen at 13.48 mg kg^{-1}, and enzyme activities of dehydrogenase, alkaline phosphatase, and acid phosphatase at 35.42 µg TPF g^{-1} 24 h^{-1}, 2.01 µg PNP g^{-1} h^{-1}, and 5.31 µg PNP g^{-1} h^{-1}, respectively.

Figure 1 encapsulates a dataset of weather parameters recorded over 6 years, from 2017 to 2022. The data indicate both the highest and average precipitation levels (in millimeters) and temperatures (in degrees Celsius) for each year. From June to September, the weather data reveal distinct patterns in rainfall and temperature. During the crop growth period, rainfall levels in June were moderate, showing a noticeable increase compared to May. July experiences peak rainfall, with the highest levels observed across all years. In August, rainfall remains high but slightly lower than in July, and by September, it starts to decrease, marking the end of the monsoon season. The highest temperatures were recorded in the warmer months, particularly May, with a slight fluctuation but generally close to 35°C. The average temperatures remained relatively stable, with a slight decrease, hovering approximately 20°C to 25°C. The year-to-year variations show some differences in the exact timing and intensity of these peaks, but the overall trend remains consistent.

2.2 Experimental design and treatments

The soil test crop response-targeted yield nutrient prescription equations for sunflower, dry chili, aerobic rice, foxtail millet, okra, and

FIGURE 1
Variation in rainfall and temperature (maximum and minimum) during the experimental period from 2017 to 2023.

kodo millet were developed after developing fertility gradient for each crop by following the guidelines given by Ramamoorthy et al. (1967) in 2016, 2017, 2018, 2019, 2020, 2021, and 2022, respectively, and the STCR-targeted yield nutrient prescription equations for each crop are detailed in Supplementary Material S1. Validation of the developed nutrient prescription equations for different crops was conducted in the permanent plot during 2017, 2018, 2019, 2020, 2021, 2022, and 2023. The study was first initiated in 2017, focusing on a soybean crop, and continued annually with different crops. A randomized complete block design was employed, featuring six fertilization treatments plus an absolute control, each replicated thrice. Sequentially, sunflower, dry chili, aerobic rice, foxtail millet, okra, and kodo millet were cultivated from 2018 to 2023. The treatments included T_1: STCR NPK for yield level 1, T_2: STCR NPK with farmyard manure (FYM) for yield level 1, T_3: STCR NPK for yield level 2, T_4: STCR NPK with FYM for yield level 2, T_5: general recommended dose, T_6: soil fertility rating, and T_7: absolute control. The targeted yield levels 1 and 2 were identified based on the ±20% of the genetic potential yield of the crops. Soil samples from 0 to 15 cm depth were collected before sowing and after the harvest of each crop and analyzed for available N, P, and K. Nitrogen, phosphorus, and potassium sources were urea, single superphosphate, and muriate of potash, respectively. The initial soil test readings and the amount of fertilizer added for each crop are presented in Supplementary Table S2. FYM was applied 15 days before sowing; half the nitrogen and full amounts of phosphorus and potassium were applied as basal. For all the crops, standard agronomic practices under irrigated conditions were followed for crop cultivation, and plants were harvested at peak maturity. The economics in terms of value cost ratio (VCR) were computed by using the standard formulae as shown below (Ramamoorthy et al., 1967).

$$\text{VCR} = \frac{[\text{Yield in treated plot (kg ha}^{-1}) - \textit{Yield in treated plot}\ (\text{kg ha}^{-1})]}{\text{Cost of fertelizers and FYM applied to treated plot}} \times \textit{Cost kg}^{-1}$$

2.3 Analysis of soil and plant samples

The initial and post-harvest soil samples collected from the experimental plot at 0–20 cm depth as per the layout of the experiment after each crop were air-dried under a shade and ground to pass through a 2-mm sieve. Bulk density was determined in the experimental field by using rings of known volume (5 cm inner diameter and 5 cm height). Soil cores were dried at 105°C in an oven for 48 h. Bulk density was calculated by dividing the weight of dried soil by the volume of the core used (Veihmeyer and Hendrickson, 1948). The soil pH was measured in a 1:2.5 soil:water suspension after stirring for 30 min by the potentiometric method using a glass electrode, and electrical conductivity was measured in a supernatant liquid of soil:water (1:2.5) suspension with the help of a conductivity meter as described by Jackson (1973). The organic carbon in soil samples was determined using $K_2Cr_2O_7$ as an oxidizing agent (1 N) and back titrating with 0.5 N FAS method as suggested by Walkley and Black (1934). The available N was estimated by the alkaline $KMnO_4$ method where organic matter present in the soil was oxidized with a hot alkaline $KMnO_4$ solution in the presence of NaOH. The ammonia (NH_3) that evolved during oxidation was distilled and trapped in a boric acid mixed indicator solution. The amount of ammonia trapped was estimated by titrating with standard acid (Subbiah and Asija, 1956), and the available P was extracted with Bray's extractant (i.e., 0.025 M of HCl and 0.03 M of NH_4F) and was determined colorimetrically by the ascorbic acid method. The intensity of the blue color was read at 660 nm using a spectrophotometer (Bray and Kurtz, 1945), and the available K was extracted with 1 N of ammonium acetate (pH 7.0) and fed directly to a flame photometer (Page et al., 1982).

Plant samples were collected at the harvesting stage. Five plants from each plot which were randomly selected and labeled were collected by pulling out the entire plant carefully. All the plant samples were washed first with tap water and then with distilled water to remove the adhering soil and dusts. Then, they were air-dried and later dried in a hot air oven at 65°C. The plant samples were ground in a willey mill. The N content in the plant samples was determined by the micro Kjeldahl method using a digestion mixture consisting of copper sulfate, potassium sulfate, and selenium catalytic mixture. Plant samples weighing 1 g were digested in digestion flasks in a macro Kjeldahl unit using sulfuric acid and the digestion mixture. After complete digestion, the digested materials were distilled in an alkaline medium, and the liberated ammonia was trapped in a 4% boric acid solution containing a mixed indicator. The trapped ammonia was titrated against standard sulfuric acid (Piper, 1966). Di-acid extract was prepared as per the method outlined by Jackson (1973). It was carried out using a 9:4 mixture of HNO_3:$HClO_4$. The predigestion of the sample was done by using 10 mL of HNO_3 g^{-1} sample. This di-acid extract was used to determine P and K content in the plant samples. Phosphorus content in the digested plant sample was estimated by the vanadomolybdophosphoric yellow color method in nitric acid medium, and the color intensity was measured at 460 nm wavelength as described by Jackson (1973) from the di-acid extract. Potassium was estimated from the di-acid extract by atomizing the diluted acid extract in a flame photometer (Jackson, 1973). From the chemical analytical data, the uptake of each nutrient was calculated.

$$\text{Nutrient uptake (kg ha}^{-1}) = \text{Nutrient control (\%)} \times \text{dry weight in kg ha}^{-1}/100$$

2.4 Microbial analysis of the soil

The soil microbial properties, viz., microbial biomass carbon (MBC), microbial biomass nitrogen (MBN), and soil enzymatic activities, were analyzed to know the long-term effect of the integrated use of NPK and FYM under STCR approaches on soil biological properties under a validation trial. The fresh soil samples were immediately transported to the laboratory and stored in a freezer for the assessment of biological parameters. The microbial biomass carbon in the soil was estimated using the chloroform fumigation extraction method using the formula Bc = Fc/Kc, where Bc represents biomass carbon, Fc represents the difference in the amount of carbon that can be extracted from fumigated and non-fumigated soil, and Kc represents the efficiency factor, which is 0.45 (Vance et al., 1987). The soil extract obtained after fumigation extraction for microbial biomass carbon was digested and examined for total nitrogen in order to estimate the amount of microbial biomass nitrogen (Nelson and Sommers, 1982). Dehydrogenase activity was estimated by adopting the methodology given by Casida et al. (1964). It is based on the principle that 2,3,5-triphenyl tetrazolium chloride (TTC), which is used as an electron acceptor, is reduced to triphenyl formazan (TPF), which imparts color. The quantity of TPF in terms of the color intensity formed was measured using a spectrophotometer at 485 nm wavelength. The acid and alkaline phosphatase activity was carried out by adopting the methodology outlined by Tabatabai and Bremer (1969). It is based on the incubation of soil samples mixed with a buffer solution of p-nitrophenylphosphate at 37°C for 1 h. The released p-nitrophenol is stained and measured spectrophotometrically at 400 nm.

2.5 Nutrient use efficiency

The nutrient (N, P, and K) use efficiency parameters, viz., apparent recovery efficiency (RE), agronomic nutrient use efficiency (AE), partial nutrient budget (PNB), utilization efficacy (UE), and partial factor productivity (PFP), were calculated using the following formulae, as per Singh et al. (2021) to know the crop response to the added fertilizers and to compare the use efficiency of added nutrients and economics under different approaches of fertilizer recommendation.

$$ARE(kg\ \ kg^{-1}) = \frac{[\text{Total nutrient uptake in treated plot (kg ha}^{-1}) - \text{Total nutrient uptake in control plot (kg ha}^{-1})]}{\text{Fertilizer nutrient applied (kg ha}^{-1})}$$

$$AE(kg\ \ kg^{-1}) = \frac{[\text{Yield in treated plot (kg ha}^{-1}) - \text{Yield in control plot (kg ha}^{-1})]}{\text{Fertilizer nutrient applied (kg ha}^{-1})}$$

$$PNB(kg\ \ kg^{-1}) = \frac{\text{Nutrient uptake (kg ha}^{-1})}{\text{Fertilizer nutrient applied (kg ha}^{-1})}$$

$$UE(kg\ \ kg^{-1}) = \frac{\text{Nutrient uptake by economic part (kg ha}^{-1})}{\text{Economic Yield (kg ha}^{-1})}$$

$$PFP(q\ \ kg^{-1}) = \frac{\text{Yield (q ha}^{-1})}{\text{Fertilizer nutrient added (kg ha}^{-1})}$$

2.6 Soil quality index

The tool in question was crafted through a tripartite methodology, initiating with the selection of the minimal dataset (MDS) and culminating in the amalgamation of indicator scores into a soil quality index, as delineated by Andrews et al. (2021). A univariate statistical analysis alongside a correlation matrix of indicators distilled the dataset to its MDS core. Noteworthy variables from different soil parameters, demonstrating significance ($p < 0.05$), were incorporated into the MDS and subjected to principal component analysis (PCA). Utilizing the SPSS software and varimax rotation, PCA was conducted on each pivotal indicator to categorize them into principal component (PC) factors for relational assessment. PCs, boasting an eigenvalue exceeding 1, as per Brejda et al. (2000), and accounting for a minimum of 5% variance in data, were earmarked for indicator selection. Within each PC, the indicator with the most substantial factor loading, be it positive or negative, was scored. To curtail data overlap, multivariate correlation was employed for factors consolidated under a single PC. Variables with a high correlation (>0.60), deemed redundant by Legaz et al. (2017), were narrowed down to a singular representative for the MDS, while the remainder were excised from the dataset. Conversely, uncorrelated yet heavily weighted variables were retained, underscoring their significance to the MDS.

For the computation of the soil quality index (SQI), the top 15 cm of soil underwent analysis for its physical, chemical, and biological characteristics. The selection criteria for the MDS included indicators within 10% of the highest weighted loading for each principal component. Legaz et al. (2017) assessed the influence of each variable in a multifaceted principal component analysis, retaining those with a correlation coefficient of less than 0.60. Each observation of the MDS indicators was standardized. This standardized value is termed the "indicator score" (S). Indicators are assessed using a linear scoring approach and are classified into three categories: "more is better," "less is better," and "optimum is better." In the case of "more is better," an observation is divided by the maximum observed value, assigning a score of 1 to the highest observation and less than 1 to all others. Conversely, for "less is better," the minimum observed value is divided by each observation, giving the lowest value indicator a score of 1 and less than 1 to the remaining, until the threshold level is reached. Beyond this point, the scoring for "optimum is better" switches from "more is better" to "less is better."

$$L\ (Y) = X/Xmax \quad \text{“More is better” approach} \tag{1}$$

$$L\ (Y) = Xmin/X \quad \text{“Less is better” approach} \tag{2}$$

Where,
L(Y) is the linear score varying from 0 to 1,
X is the soil indicator value,
Xmax is the maximum value of each soil indicator, and
Xmin is the minimum value of each soil indicator.

The SQI is computed by integrating the score and weight factor of each indicator. This can be explained by the following equation:

$$SQI = \sum_{i=1}^{n} WiSi$$

Where,
Si = score for subscripted variable, and
Wi = weighing factor derived from the PCA.

2.7 Statistical analysis

The data were subjected to analysis of variance (ANOVA) technique of randomized block design as per the procedure outlined by Gomez and Gomez (1984). Online statistical program OPSTAT was used for the data analysis and least significance difference (LSD) values at α = 0.05 were used to compare treatment means. Pearson's correlation coefficients were used as a measure of the strength of linear dependence between studied parameters at $p \leq 0.05$ and $p \leq 0.01$. The SPSS 29.0 software also performed the MDS through PCA for SQI selection. PCA was applied to the correlation matrix of the soil variables in order to obtain a few new components explaining most of the variation of the original variables. The principal components (PCs) that explained cumulatively a high percentage of the total variance and had an eigenvalue greater than one (Kaiser criterion) were retained. Together with the eigenvalue, the percentage of variation explained by the single component was taken into account, considering the threshold of 5% suggested by Wander and Bollero (1999). Variable loadings were examined. Within each PC, only highly weighted loadings, defined as having absolute values within 10% of the highest loading (Sharma et al., 2005), were considered and signs were examined to investigate relationships among selected variables.

3 Results

3.1 Crop yield

Table 1 provides a comparative analysis of agricultural yields for various crops under different treatments over the period 2017 to 2022. The STCR NPK + FYM–yield level 1 treatment consistently achieved higher yield increases compared to the general recommended dose, with increases of 8.88% for soybean, 25.85% for sunflower, 16.65% for dry chili, 24.53% for aerobic rice, 22.35% for foxtail millet, 28.70% for okra, and 24.33% for kodo millet. Similarly, the STCR NPK + FYM approach registered higher yields at both yield levels compared to the sole NPK application. The absolute control treatment, which represents the baseline yield without any fertilization, had the lowest yield across all crops, emphasizing the importance of fertilization in crop yield enhancement.

3.2 Nutrient uptake

The data on nutrient uptake as influenced by different approaches of fertilizer recommendation are depicted in Table 2. Significantly higher uptake of NPK among all the crops, viz., soybean (95.78, 28.95, and 69.67 kg NPK ha^{-1}), sunflower (65.50, 43.95, and 79.67 kg NPK ha^{-1}), dry chili (72.38, 7.17, and 56.30 kg NPK ha^{-1}), aerobic rice (84.00, 13.82, and 124.25 kg NPK ha^{-1}), foxtail millet (54.33, 22.17, and 68.32 kg NPK ha^{-1}), okra (150.93, 54.62, and 160.396 kg NPK ha^{-1}), and kodo millet (22.61, 7.6, and 71.71 kg NPK ha^{-1}) was recorded with the application of fertilizer

TABLE 1 Effect of soil test crop response alongside various fertilization strategies on the yield and value cost ratio of diverse crops.

Treatments	Soybean (2017)		Sunflower (2018)		Dry chili (2019)		Aerobic rice (2020)		Foxtail millet (2021)		Okra (2022)		Kodo millet (2023)	
	Yield (t ha^{-1})	VCR	Yield (t ha^{-1})	VCR	Yield (t ha^{-1})	VCR	Yield (t ha^{-1})	VCR	Yield (t ha^{-1})	VCR	Yield (t ha^{-1})	VCR	Yield (t ha^{-1})	VCR
STCR NPK–yield level 1	2.18	10.32	2.518	14.91	1.695	12.40	6.761	8.88	1.547	4.05	25.95	32.06	1.67	15.03
STCR NPK + FYM–yield level 1	2.39	5.62	2.713	3.88	1.667	3.40	6.546	10.10	1.407	3.00	26.82	16.25	1.71	4.06
STCR NPK–yield level 2	1.83	9.51	2.426	13.30	1.359	17.84	6.002	9.78	1.371	3.70	22.29	27.36	1.407	14.96
STCR NPK + FYM–yield level 2	2.01	4.30	2.494	6.74	1.447	2.83	5.759	10.99	1.296	2.67	22.84	12.05	1.36	3.02
General recommended dose	2.20	3.31	2.155	2.30	1.429	2.43	5.256	1.57	1.15	0.96	20.84	8.87	1.377	2.78
Soil fertility rating	2.16	3.07	2.299	2.40	1.582	2.97	5.011	1.34	1.226	2.06	21.51	9.27	1.394	2.83
Absolute control	1.47		1.052		0.56		2.068		0.985		13.89		0.527	
SEm±	**0.068**		**0.066**		**0.066**		**0.20**		**0.096**		**0.074**		**0.300**	
CD @ 5%	**0.193**		**0.187**		**0.188**		**0.562**		**0.272**		**0.211**		**0.086**	

SEm, Standard error of Mean; CD, Critical Difference.

TABLE 2 Effect of soil test crop response alongside various fertilization strategies on the NPK uptake in different crops.

Treatments	Soybean			Sunflower			Dry chili			Aerobic rice			Foxtail millet			Okra			Kodo millet		
	N	P	K	N	P	K	N	P	K	N	P	K	N	P	K	N	P	K	N	P	K
	kg ha^{-1}																				
STCR NPK–yield level 1	92.62	27.25	60.05	54.97	42.25	70.05	74.93	7.11	50.25	89.38	14.85	110.95	58.19	23.40	70.15	137.70	50.19	150.13	21.32	6.82	69.79
STCR NPK + FYM–yield level 1	95.78	28.95	69.67	62.50	43.95	79.67	72.38	7.17	56.30	84.00	13.82	124.25	54.33	22.17	68.32	150.93	54.62	160.39	22.61	7.61	71.71
STCR NPK–yield level 2	78.23	26.24	53.43	49.03	41.24	63.43	63.35	5.83	38.58	82.02	13.74	102.67	53.12	21.33	67.12	113.16	37.56	120.73	21.61	5.21	60.17
STCR NPK + FYM–yield level 2	82.90	26.22	56.16	52.92	41.22	66.16	62.74	6.27	46.06	77.27	13.26	117.22	50.70	19.91	63.90	124.41	43.78	131.37	18.87	4.72	59.86
General recommended dose	83.93	23.09	49.63	53.20	38.09	59.63	62.45	5.49	38.48	70.41	11.88	105.89	44.58	16.64	56.94	111.56	39.08	107.40	19.20	6.44	57.89
Soil fertility rating	82.26	23.71	50.42	51.99	38.71	60.42	62.27	5.52	35.97	62.37	11.07	95.65	47.77	17.99	57.38	125.43	54.05	122.75	21.18	6.10	62.03
Absolute control	62.57	11.25	29.10	20.05	26.25	39.10	23.13	2.54	15.92	25.48	4.91	36.96	35.97	12.89	44.18	94.32	32.41	84.84	6.44	2.15	21.36
SEm±	**4.02**	**2.18**	**3.12**	**1.42**	**2.20**	**3.12**	**5.50**	**0.72**	**6.16**	**6.22**	**0.74**	**9.50**	**2.54**	**1.81**	**4.18**	**1.43**	**1.84**	**2.37**	**0.60**	**0.43**	**3.04**
CD @ 5%	**11.45**	**6.20**	**8.88**	**4.06**	**6.60**	**8.88**	**15.67**	**2.04**	**17.55**	**17.73**	**2.11**	**27.07**	**7.83**	**2.56**	**12.88**	**4.48**	**5.75**	**7.39**	**1.70**	**1.24**	**8.66**

SEm, Standard error of Mean; CD, Critical Difference.

based on the STCR approach along with FYM at yield level 1 compared to the other treatments. The treatment with absolute control invariably resulted in minimal absorption of nutrients among all the crops tested.

3.3 Nutrient use efficiency

The highest apparent recovery efficiency of nitrogen and potassium was observed in STCR NPK + FYM at yield level 2 with absorption rates of 0.73 and 4.98 kg kg^{-1} (Table 3). Similarly, the recovery efficiency of phosphorus was higher in STCR NPK + FYM at yield level 1. However, minimal apparent recovery efficiency (ARE) for nitrogen was observed in the soil fertility rating approach, registering at 0.34 kg kg^{-1}. Regarding phosphorus (P), the STCR NPK–YIELD Level 2 treatment exhibits the least ARE at 0.17 kg per kg. For potassium (K), both the general recommended dose and soil fertility rating treatments show the lowest ARE, with values of 0.90 and 0.86 kg kg^{-1}, respectively. The agronomic nutrient use efficiency (ANUE) for nitrogen, phosphorus, and potassium in STCR NPK + FYM at yield levels 2 and 1 shows significant increases over the general recommended doses. The ANUE of N increased by 125%, P by 51.54%, and K by 187.17%, under STCR NPK + FYM at yield level 1 compared to the general recommended dose, indicating a substantial improvement in nutrient utilization with the STCR NPK + FYM approach.

The study reveals that combining STCR NPK + FYM at yield levels 1 and 2 improved PNB for NPK. The most notable increase was seen in nitrogen at yield level 1 (2.79), and phosphorus and potassium were higher at yield level 2 (0.54 and 8.59, respectively). On the other hand, UE was higher under the general recommended dose and soil fertility rating approach. However, the values were comparable with the STCR approach of fertilizer recommendation. Similarly, the partial factor productivity was higher for nitrogen in the treatment STCR NPK + FYM at yield level 1 (87.11 kg q^{-1}), and the PFP for phosphorus (77.25 kg q^{-1}) and potassium (210.82 kg q^{-1}) was the highest in STCR NPK + FYM at yield level 2.

3.4 Soil properties

The soil fertility rating treatment exhibited the highest pH value at 5.89, marking a 4.25% increase over the absolute control baseline of 5.65 (Table 4). Conversely, the absolute control also recorded the lowest electrical conductivity (EC) at 0.09 dS m^{-1}, which is a significant 57.14% lower than the highest EC observed in STCR NPK–yield level 1 at 0.21 dS m^{-1}. Additionally, the STCR NPK + FYM–yield level 1 treatment showed the highest levels of organic carbon (OC), nitrogen (N), and potassium (K), at 0.5%, 288.58 kg ha^{-1}, and 156.72 kg ha^{-1}, respectively. These figures represent increases of 1.34-fold for OC, 1.27-fold for N, and 1.55-fold for K when compared to the absolute control values of 0.35% OC, 120.56 kg N ha^{-1}, and 96.28 kg K ha^{-1}. However, the general recommended dose has the highest available phosphorous content at 150.28 kg ha^{-1}.

TABLE 3 Effect of soil test crop response alongside various fertilization strategies on nutrient use efficiency.

Treatments	ARE			ANUE			PNB			UE			PFP		
	N	P	K	N	P	K	N	P	K	N	P	K	N	P	K
	kg kg^{-1}										kg q^{-1}				
STCR NPK–yield level 1	0.42	0.19	1.51	27.50	33.01	45.12	1.13	0.36	2.38	0.41	1.79	0.32	42.26	49.48	68.11
STCR NPK + FYM–yield level 1	0.67	0.26	3.91	60.93	45.66	102.98	2.79	0.49	5.94	0.41	1.85	0.30	87.11	67.45	151.81
STCR NPK–yield level 2	0.42	0.17	1.34	29.52	33.28	43.80	1.32	0.39	2.52	0.39	1.86	0.32	45.87	53.47	70.65
STCR NPK + FYM–yield level 2	0.73	0.24	4.98	54.35	48.60	130.16	2.59	0.54	8.59	0.41	1.94	0.31	81.10	77.25	210.82
General recommended dose	0.43	0.18	0.90	27.00	30.13	35.86	1.22	0.38	1.74	0.43	1.82	0.36	46.64	50.33	61.26
Soil fertility rating	0.34	0.25	0.86	23.28	41.16	35.35	0.99	0.51	1.55	0.45	1.95	0.39	39.40	66.80	58.65
Absolute control	–	–	–	–	–	–	–	–	–	0.41	1.58	0.31	–	–	–

ARE, apparent recovery efficiency; ANUE, agronomic nutrient use efficiency; PNB, partial nutrient budget; UE, utilization efficiency; PFP, partial factor productivity.

3.5 Principal component analysis

Significant correlations ($p < 0.05$) among most soil properties led to their inclusion in the PCA for MDS development (Table 5). Only principal components with eigenvalues greater than 1 were considered, as depicted in Figure 2. The PCA revealed that the first two components accounted for 86.57% of the data variance, with PC1 and PC2 individually explaining 72.15% and 14.42%, respectively (Table 6; Figure 2). Factors such as dehydrogenase activity, organic carbon, electrical conductivity, nitrogen, potassium, acid phosphatase, microbial biomass carbon, and nitrogen received the highest loadings in PC1 and were highly intercorrelated, leading to the selection of dehydrogenase activity for the MDS. Bulk density, which had a higher loading in PC2 as shown in Table 7, was also included. Indicators were normalized on a 0 to 1 scale using a linear scoring function, with weighted factors of 0.83 for PC1 and 0.17 for PC2, culminating in the formulation of the SQI equation.

$$\text{SQI} = 0.83 \times \text{DHA score} + 0.17 \times \text{bulk density score} \quad (2)$$

The STCR NPK + FYM plots under yield level 1 registered a high DHA and low bulk density. The nutrient management options clearly manifested their effect on these two soil parameters, making these apt SQI indicators. The SQI was significantly higher under the STCR NPK + FYM–yield level 1 (0.98) treatment as compared to the other treatments (Table 8). Furthermore, the hierarchy of fertilizer recommendation approaches on SQI was as follows: STCR NPK + FYM–yield level 1 > STCR NPK + FYM–yield level 1 > STCR NPK–yield level 1 > STCR NPK–yield level 1 > soil fertility rating > general recommendation dose > absolute control.

In the study, plots treated with STCR NPK + FYM at yield levels 1 and 2 exhibited SQI values that were 13.95% and 12.79% greater, respectively, than those treated with the general recommendation dose, as shown in Table 8. The established SQI was corroborated by the mean yield of seven different crops, as depicted in Figure 3, which presented a scattered plot and a linear trend line with an R^2 value of 0.85.

TABLE 4 Effect of soil test crop response alongside various fertilization strategies on the soil properties.

Treatments	pH	Electrical conductivity	Organic carbon	Avail. N	Avail. P_2O_5	Avail. K_2O
	(1:2.5)	dS m^{-1}	%	kg ha^{-1}		
STCR NPK–yield level 1	5.66	0.21	0.43	281.56	121.25	145.56
STCR NPK + FYM–yield level 1	5.81	0.20	0.50	288.58	130.56	156.72
STCR NPK–yield level 2	5.73	0.19	0.4	230.58	114.58	125.58
STCR NPK + FYM–yield level 2	5.79	0.2	0.46	245.49	129.56	141.58
General recommended dose	5.68	0.18	0.45	254.56	150.28	115.25
Soil fertility rating	5.89	0.17	0.41	270.56	95.68	119.71
Absolute control	5.65	0.09	0.35	120.56	55.69	96.28
SEm±	**0.09**	**0.01**	**0.01**	**6.5**	**12.49**	**8.62**
CD @ 5%	**0.26**	**0.02**	**0.02**	**18.53**	**35.6**	**24.57**

SEm, Standard error of Mean; CD, Critical Difference.

TABLE 5 Pearson correlation coefficient values (*r*) between various soil quality attributes of 0–15 cm soil layer.

p\Group	BD	MWHC	Porosity	Ph	EC	OC	N	P	K	MBC	MBN	DHA	AP	ALP
BD	1													
MWHC	−0.55	1												
Porosity	−0.53	1	1											
pH	−0.12	0.41	0.41	1										
EC	−0.15	0.82	0.83	0.033	1									
OC	−0.35	0.8	0.8	0.12	0.84	1								
N	−0.12	0.81	0.82	0.23	0.95	0.91	1							
P	−0.14	0.74	0.75	−0.12	0.95	0.71	0.83	1						
K	0.086	0.59	0.6	−0.056	0.87	0.8	0.88	0.73	1					
MBC	0.037	0.67	0.68	−0.064	0.93	0.76	0.87	0.83	0.97	1				
MBN	0.036	0.67	0.68	−0.064	0.93	0.76	0.87	0.83	0.97	1	1			
DHA	0.04	0.71	0.72	0.014	0.93	0.77	0.89	0.83	0.96	0.99	0.99	1		
AP	0.1	0.62	0.64	−0.13	0.91	0.76	0.85	0.83	0.96	0.99	0.99	0.99	1	
ALP	0.083	0.65	0.66	0.28	0.73	0.74	0.8	0.54	0.88	0.86	0.86	0.89	0.86	1

MWHC, Minimum water holding capacity; EC, Electrical Conductivity; OC, Organic Carbon; N, Nitrogen; P, Phosphorus; K, Potassium; MBC, Microbial Biomass Carbon; MBN, Microbial Biomass Nitrogen; DHA, Dehydrogenase; AP, Acid Phosphatase; ALP, Alkaline Phosphatase.

10.3389/fpls.2024.1439523

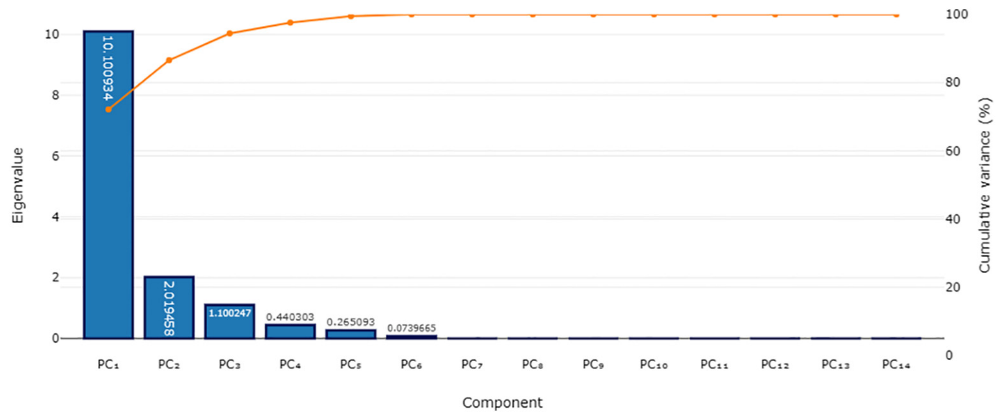

FIGURE 2
Scree plot explaining the relationship of the eigenvalues and the principal components.

TABLE 6 Eigenvalues from principal component analysis (PCA) of soil quality parameters.

Principal component	Initial eigenvalues			Weightage factor
	Total	% Variance	Cumulative %	
1	10.10	72.15	72.15	0.83
2	2.02	14.42	86.57	0.17
			Total	1.00

TABLE 7 Principal component analysis of soil quality parameters.

Component matrix		
	PC1	PC2
Dehydrogenase activity	**<u>0.972</u>**	0.197
Electrical conductivity	**0.971**	−0.004
Microbial biomass carbon	**0.961**	0.242
Microbial biomass nitrogen	**0.961**	0.242
Nitrogen	**0.955**	−0.083
Acid phosphatase	**0.944**	0.312
Available potassium	**0.929**	0.289
Organic carbon	**0.881**	−0.206
Available phosphorus	0.871	0.026
Alkaline phosphatase	0.862	0.102
Porosity	0.839	−0.526
Maximum water holding capacity	0.830	−0.541
Bulk density	−0.139	**<u>0.812</u>**
pH	0.100	−0.627
10%HF	**0.097201**	**0.081248**
	0.875	**0.731**

Boldface eigenvalues correspond to the PCs examined for the index. Boldface factor loadings are considered highly weighed; Bold-underlined factors correspond to the indicators included in the index. PC, principal component.

4 Discussion

The integration of FYM with NPK fertilization based on the STCR approach appears to be beneficial for most crops at yield level 1, with some exceptions at yield level 2, particularly for aerobic rice and foxtail millet where the sole use of NPK seemed more effective. The data suggest that the combined use of organic and inorganic fertilizers can enhance crop yields, aligning with sustainable agricultural practices which might be due to enhanced microbial activity and conversion of unavailable nutrients into available forms and also due to improved physical, chemical, and biological properties (Katkar et al., 2011) that lead to increased productivity. Similarly, the higher yield under the STCR NPK + FYM approach might be due to the balanced application of nutrients which is based on soil analysis and considers the amount of nutrients removed by the crops, the initial levels of soil fertility, the efficiency of nutrients present in the soil, manure added through the fertilizers (Krishna Murthy et al., 2023a), and the ability of targeted yield approaches to satisfy the nutrient demand of crop more efficiently. These factors might have provided the optimum nutrients at the optimum time for better uptake and ultimately resulted in higher dry matter and yield (Krishna Murthy et al., 2023b).

The STCR NPK + FYM treatment generally resulted in higher nutrient uptake (NPK) across most crops and other fertilizer recommendation approaches, except dry chili (N) and aerobic rice (N, P), where STCR NPK alone had higher uptake (Table 2). This suggests that the combined use of organic and inorganic fertilizers can enhance nutrient absorption by crops, which is

TABLE 8 Score, weight, and soil quality index values of selected minimum dataset variables under STCR alongside various fertilization strategies in different crops.

Treatments	Dehydrogenase activity			Bulk density			SQI
	S	W	T	S	W	T	
STCR NPK–yield level 1	0.93	0.83	**0.78**	0.925	0.17	**0.16**	0.94
STCR NPK + FYM–yield level 1	0.98	0.83	**0.83**	0.890	0.17	**0.15**	0.98
STCR NPK–yield level 2	0.92	0.83	**0.77**	0.932	0.17	**0.16**	0.93
STCR NPK + FYM–yield level 2	1.00	0.83	**0.82**	0.897	0.17	**0.15**	0.97
General recommended dose	0.8	0.83	**0.70**	0.932	0.17	**0.16**	0.86
Soil fertility rating	0.88	0.83	**0.74**	0.937	0.17	**0.16**	0.90
Absolute control	0.65	0.83	**0.55**	1.000	0.17	**0.17**	0.72

W, weightage factor; S, score value; T, total; SQI, soil quality index.

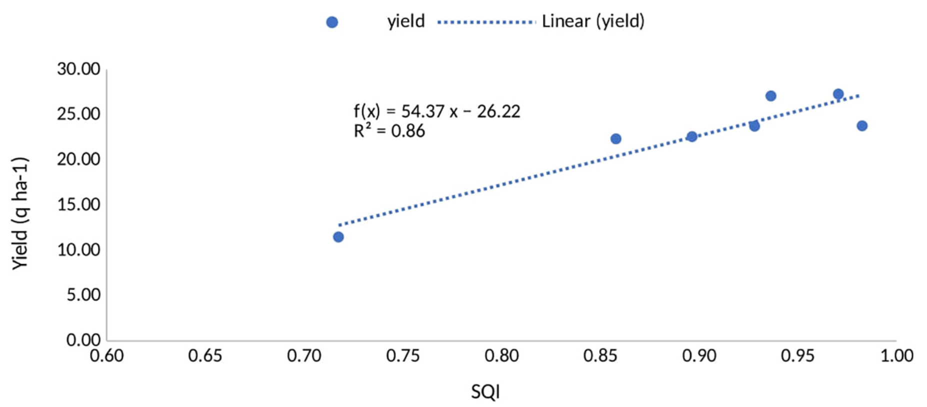

FIGURE 3
Relationship between soil quality index with crop yield under different fertilizer recommendation approaches.

beneficial for crop growth and yield. Specifically, dry chili demonstrated the least assimilation of phosphorus and potassium across the majority of treatments, suggesting that a specialized fertilization approach may be necessary for this particular crop (Singh et al., 2021).

The data indicated in Table 3 show that the treatment STCR NPK + FYM–yield level 1 generally had the highest nutrient use efficiency, suggesting that it may be the most effective treatment among those listed. Combining STCR with FYM seems to boost nutrient recovery. FYM improves soil quality and nutrient availability, enhancing the absorption of nutrients by crops thereby increasing crop productivity (Abid et al., 2020). Conversely, the general recommended dose and soil fertility rating treatments tend to show the lowest values, indicating they may be less effective compared to the other treatments due to the soil's inherent limitations in providing nitrogen without supplemental fertilization (Barłóg et al., 2022). The least recovery of phosphorus in the soil fertility rating approach was potentially due to the ineffectiveness of the nutrient management approach that excludes FYM in rendering phosphorus accessible to plants. Similarly, lower potassium recovery in the general recommended dose and soil fertility rating indicates that standard guidelines and soil fertility assessments may fall short in ensuring adequate potassium uptake, likely a consequence of potassium's reduced solubility under these conditions (Andrews et al., 2021). These findings highlight the importance of integrating organic amendments like FYM with tailored nutrient management strategies to maximize nutrient recovery efficiency, particularly for potassium and nitrogen.

The most notable improvements of ANUE were observed at yield level 1 for nitrogen and yield level 2 for phosphorus and potassium, suggesting that FYM may improve soil fertility and structure (Meena et al., 2018). In contrast, the general recommended doses showed lower ANUE, implying that customized STCR NPK + FYM treatments could be more effective for nutrient utilization (Rao et al., 2021). The balance of nutrients available to the crop can affect the uptake of N, P, and K, as they can interact synergistically or antagonistically (Xie et al., 2021). These findings are essential for understanding how to optimize nutrient use for maximum crop production while ensuring environmental sustainability. By analyzing PFP, farmers and agronomists can make informed decisions about fertilizer application rates and methods (Huang and Karimanzira, 2018).

Based on the data, adding FYM to STCR NPK significantly increases the organic carbon content and the availability of nitrogen and potassium (Moharana et al., 2017). The application of STCR NPK + FYM in yield level 1 plots resulted in elevated DHA and reduced bulk density, establishing them as suitable indicators of soil quality (Sharma et al., 2019). These indicators, reflecting the soil's physical and chemical attributes, showed a strong correlation with other soil parameters across physical, chemical, and biological spectrums (Parihar et al., 2020). The findings indicated that the STCR NPK + FYM treatment markedly improved soil quality indicators, with yield level 1 plots exhibiting an SQI that was 13.95% greater than that achieved with the general recommendation dose. STCR-based treatments reported higher SQI when compared with RDF due to judicious, balanced, and profitable fertilization along with the use of organic manure in a definite proportion based on nutrient status of the soil and as required by the crops (Sharma et al., 2016). Application of fertilizers and manures based on the STCR approach not only helps in achieving the target yield but also maintains overall soil health (Sharma et al. 2019). Among the STCR-based treatments, the combined application of inorganic fertilizers and FYM resulted in better soil quality when compared with the use of inorganic fertilizers alone (Huang et al., 2010). The synergistic approach of combining organic and inorganic nutrients, along with strategic management, not only bolstered soil physical health but also maximized nutrient efficiency, which in turn was linked to an increase in biomass production, corroborated by studies from Sapkota et al. (2014) and Parihar et al. (2017).

5 Conclusion

The findings of this study suggest that the STCR NPK + FYM approach could be a viable strategy for improving soil health and achieving yield sustainability in Alfisols of southern India. The percent achievement of the targeted yield was within ±10% variance at both targets, demonstrating the validity of the equations for prescribing integrated fertilizer doses. The increased crop yields, improved nutrient uptake, and enhanced soil quality indicators provide a strong foundation for recommending this balanced fertilization method as a cornerstone for sustainable agricultural practices. Continuous research and development activities to refine STCR models for different crops and regions will ensure accuracy and effectiveness. Also, integrating STCR with advanced technologies like GPS, GIS, and remote sensing can enhance precision in fertilizer application.

Data availability statement

The datasets presented in this study can be found in online repositories. The names of the repository/repositories and accession number(s) can be found in the article/Supplementary Material.

Author contributions

RK: Writing – review & editing, Validation, Supervision, Methodology, Investigation, Formal analysis, Data curation, Conceptualization. BN: Writing – review & editing, Writing – original draft, Data curation. KG: Writing – review & editing, Writing – original draft. US: Writing – review & editing, Data curation. PB: Writing – review & editing, Methodology. HS: Writing – review & editing, Formal analysis, Data curation. GG: Writing – review & editing, Data curation. SS: Writing – review & editing, Project administration, Methodology. PD: Writing – review & editing, Project administration, Methodology.

Funding

The author(s) declare financial support was received for the research, authorship, and/or publication of this article. This study was funded by the Indian Council of Agricultural Research (Grant number: CRP-18).

Conflict of interest

The authors declare that the research was conducted in the absence of any commercial or financial relationships that could be construed as a potential conflict of interest.

The reviewer SS declared a past collaboration with the author PD to the handling editor.

Publisher's note

All claims expressed in this article are solely those of the authors and do not necessarily represent those of their affiliated organizations, or those of the publisher, the editors and the reviewers. Any product that may be evaluated in this article, or claim that may be made by its manufacturer, is not guaranteed or endorsed by the publisher.

Supplementary material

The Supplementary Material for this article can be found online at: https://www.frontiersin.org/articles/10.3389/fpls.2024.1439523/full#supplementary-material

References

Abid, M., Batool, T., Siddique, G., Ali, S., Binyamin, R., Shahid, M. J., et al. (2020). Integrated nutrient management enhances soil quality and crop productivity in maize-based cropping system. *Sustain* 12, 102–104. doi: 10.3390/su122310214

Andrews, E. M., Kassama, S., Smith, E. E., Brown, P. H., and Khalsa, S. D. S. (2021). A review of potassium-rich crop residues used as organic matter amendments in tree crop agroecosystems. *Agriculture* 11, 580. doi: 10.3390/agriculture11070580

Antil, R. S., Narwal, R. P., Singh, B., and Singh, J. P. (2011). Long-term effects of FYM and N application on soil health and productivity under pearl millet–wheat cropping system. *Indian J. Fert* 7, 14–32.

Barłóg, P., Grzebisz, W., and Łukowiak, R. (2022). Fertilizers and fertilization strategies mitigating soil factors constraining efficiency of nitrogen in plant production. *Plants* 11, 18–55. doi: 10.3390/plants11141855

Bray, R. H., and Kurtz, L. T. (1945). Determination of total, organic and available phosphorus in soil. *Soil Sci.* 9, 39–46. doi: 10.1097/00010694-194501000-00006

Brejda, J. I., Moorman, T. B., Karlen, D. L., and Dao, T. H. (2000). Identification of regional soil quality factors and indicators of central and southern high plains. *Soil Sci. Soc. America J.* 64, 2115–2124. doi: 10.2136/sssaj2000.6462115x

Casida, L. E.Jr., Klein, D. A., and Santoro, T. (1964). Soil dehydrogenase activity. *Soil Sci.* 98, 371–376. doi: 10.1097/00010694-196412000-00004

Gomez, K. A., and Gomez, A. A. (1984). *Statistical procedures for agricultural research* (New York: John Wiley & Sons).

Gulati, A., Paroda, R., Puri, S., Narain, D., and Ghanwat, A. (2023). Food system in India: Challenges, performance and promise. *Sci. Innov. Food Syst. Transform.*, 813–828.

Haokip, I. C., Devi, M. H., BH, S., Srivastava, S., and Santhi, R. (2023). Impacts of long-term nutrient management based on soil test and crop response on soil health and yield sustainability in typic haplustalf. *Int. J. Plant Soil Sci.* 35, 342–348. doi: 10.9734/ijpss/2023/v35i244365

Huang, Z., and Karimanzira, T. T. P. (2018). Investigating key factors influencing farming decisions based on soil testing and fertilizer recommendation facilities (STFRF)—a case study on rural Bangladesh. *Sustain* 10, 43–31.

Huang, S., Zhang, W., Yu, X., and Huang., Q. (2010). Effects of long-term fertilization on corn productivity and its sustainability in an *Ultisols* of southern China. *Agric. Ecosyst. Environ.* 138, 44–50. doi: 10.1016/j.agee.2010.03.015

Jackson, M. L. (1973). *Soil Chemical Analysis* (Englewood Cliffs, New Jersey, USA: Prentice Hall. Inc.).

Katkar, R. N., Sonune, B. A., and Kadu, P. R. (2011). Long-term effect of fertilization on soil chemical and biological characteristics and productivity under sorghum (Sorghum bicolor)-wheat (*Triticum aestivum*) system in Vertisol. *Indian J. Agric. Sci.* 81, 734.

Krishna Murthy, R., Basavaraja, P. K., Bhavya, N., Dey, P., Mohamed Saqueebulla, H., Gangamurtha, G. V., et al. (2023a). Development and validation of soil test based fertilizer prescription equations for enhancing yield, uptake and nutrient use efficiency of foxtail millet (*Setaria italica*) under dryland condition. *J. Plant Nutr.* 46, 3082–3100. doi: 10.1080/01904167.2023.2188065

Krishna Murthy, R., Bhavya, N., Govinda, K., Uday Kumar, S. N., Basavaraja, P. K., Mohamed Saqeebulla, H. S., et al. (2023b). Modelling soil, plant and fertilizer relationship to optimize nutrient management for chilli (*Capsicum annuum* L) under Alfisols of Southern India. *Arch. Agron. Soil Sci.* 69, 3570–3586. doi: 10.1080/03650340.2023.2264210

Kumar, D., Sinha, N. K., Haokip, I. C., Kumar, J., Wanjari, R. H., Verma, S., et al. (2022). Impact of fertilizer consumption on soil health and environmental quality in India. *Indian J. Fertil.* 18, 992–1005.

Kumar, A., and Tripathi, R. P. (2009). Effect of continuous use of manures and fertilizers on physical properties of soil under paddy-wheat-cowpea system. *Crop Res.* 3, 7–13.

Legaz, B. V., De, S., Maia, D., Teixeira, R. F. M., Anton, A., Putman, B., et al. (2017). Soil quality, properties, and functions in life cycle assessment: An evaluation of models. *J. Clean. Produc* 140, 502–515. doi: 10.1016/j.jclepro.2016.05.077

Meena, K. B., Alam, M. S., Singh, H., Bhat, M. A., Singh, A. K., Mishra, A. K., et al. (2018). Influence of farmyard manure and fertilizers on soil properties and yield and nutrient uptake of wheat. *Int. J. Chem. Stud.* 6, 386–390.

Moharana, P. C., Sharma, B. M., and Biswas, D. R. (2017). Changes in the soil properties and availability of micronutrients after six-year application of organic and chemical fertilizers using STCR-based targeted yield equations under pearl millet-wheat cropping system. *J. Plant Nutr.* 40, 165–176. doi: 10.1080/01904167.2016.1201504

Nelson, D. E., and Sommers, L. E. (1982). Total carbon, organic carbon, and organic matter. *Methods of Soil Analysis. 2nd Ed./Amer. Soc. Agron.* (Madison, United States).

Page, A. L., Miller, R. H., and Keeny, D. R. (1982). *Methods of soil and plant analysis* (Madison: American Society of Agronomy).

Paramesh, V., Kumar, R. M., Rajanna, G. A., Gowda, S., Nath, A. J., Madival, Y., et al. (2023). Integrated nutrient management for improving crop yields, soil properties, and reducing greenhouse gas emissions. *Front. Sustain. Food Syst.* 7. doi: 10.3389/fsufs.2023.1173258

Parihar, C. M., Jat, S. L., Singh, A. K., Majumdar, K., Jat, M. L., Saharawat, Y. S., et al. (2017). Bio-energy, water-use efficiency and economics of maize-wheat-mungbean system under precision-conservation agriculture in semi-arid agro-ecosystem. *Energy* 119, 245–256. doi: 10.1016/j.energy.2016.12.068

Parihar, C. M., Singh, A. K., Jat, S. L., Dey, A., Nayak, H. S., Mandal, B. N., et al. (2020). Soil quality and carbon sequestration under conservation agriculture with balanced nutrition in intensive cereal-based system. *Soil Tillage Res.* 202, 104–653. doi: 10.1016/j.still.2020.104653

Piper, C. S. (1966). *Soil and Plant Analysis* (Bombay: Hans Publishers), 137–153.

Ramamoorthy, B., Narasimham, R. L., and Dinesh., R. S. (1967). Fertilizer application for specific yield targets on Sonora 64 (wheat). *Indian Farm.* 17, 43–45.

Rao, D. L. N., Dey, P., and Reddy, K. S. (2021). Plant demand adapted fertilization in organic and precision farming. *Soil Recycling Manage. Anthrop. Era*, 137–166.

Sapkota, T. B., Majumdar, K., Jat, M. L., Kumar, A., Bishnoi, D. K., McDonald, A. J., et al. (2014). Precision nutrient management in conservation agriculture-based wheat production of Northwest India: Profitability, nutrient use efficiency and environmental footprint. *Field Crops Res.* 155, 233–244. doi: 10.1016/j.fcr.2013.09.001

Sharma, K. L., Chary, G. R., Reddy, K. S., Singh, A. P., Abrol, V., Sharma, A., et al. (2019). Effect of integrated nutrient management on soil quality indicators and soil quality indices in hill and mountainous Inceptisol soils in Northern India under maize (*Zea mays*)-black gram (*Vigna mungo*) system. *Indian J. Dryland Agric. Res. Dev.* 34, 01–08. doi: 10.5958/2231-6701.2019.00001.0

Sharma, K. L., Mandal, U. K., Srinivas, K., Vittal, K. P. R., Mandal, B., Grace, J. K., et al. (2005). Long-term soil management effects on crop yields and soil quality in a dryland Alfisol. *Soil Tillage Res.* 83, 246–259. doi: 10.1016/j.still.2004.08.002

Sharma, V. K., Pandey, R. N., and Sharma, B. M. (2016). Studies on long term impact of STCR based integrated fertilizer use on pearl millet (*Pennisetum glaucum*)-wheat (*Triticum aestivum*) cropping system in semi arid condition of India. *J. Environ. Biol.* 36, 241.

Shukla, A. K., Behera, S. K., Chaudhari, S. K., and Singh, G. (2022). Fertilizer use in Indian agriculture and its impact on human health and environment. *Indian J. Fertil* 18, 218–237.

Singh, M. (2010). The 12th Dr. NS Randhawa Memorial Lecture-Nutrient management: A key to soil health and long-term sustainability. *J. Indian Soc Soil Sci.* 58, S47.

Singh, V. K., Gautam, P., Nanda, G., Dhaliwal, S. S., Pramanick, B., Meena, S. S., et al. (2021). Soil test based fertilizer application improves productivity, profitability and nutrient use efficiency of rice (Oryza sativa L.) under direct seeded condition. *Agronomy* 11, 17–56. doi: 10.3390/agronomy11091756

Subbiah, B. V., and Asija, G. L. (1956). A rapid procedure for the determination of available nitrogen in soils. *Curr. Sci.* 25, 259–260.

Tabatabai, M. A., and Bremer, J. M. (1969). Use of p-nitro-phenyl phosphate for assay of soil phosphatase activity. *Soil Biol. Biochem.* 4, 479–487.

The Fertilizers Association of India (2022). *Fertilizers Statistics 2021-22.* The Fertilizers Association of India (2022). (New Delhi: The Fertilizers Association of India).

Vance, E. D., Brookes, P. C., and Jenkinson, D. S. (1987). An extraction method for measuring soil microbial biomass C. *Soil Biol. Biochem.* 19, 703–707. doi: 10.1016/0038-0717(87)90052-6

Veihmeyer, F. J., and Hendrickson, A. (1948). Soil density and root penetration. *Soil Sci.* 65, 487–494. doi: 10.1097/00010694-194806000-00006

Walkley, A. J., and Black, I. A. (1934). Estimation of soil organic carbon by the chromic acid titration method. *Soil Sci.* 37, 29–38. doi: 10.1097/00010694-193401000-00003

Wander, M. M., and Bollero, G. A. (1999). Soil quality assessment of tillage impacts in Illinois. *Soil Sci. Soc Am. J.* 63, 961–971. doi: 10.2136/sssaj1999.634961x

Xie, K., Cakmak, I., Wang, S., Zhang, F., and Guo, S. (2021). Synergistic and antagonistic interactions between potassium and magnesium in higher plants. *Crop J.* 9, 249–256. doi: 10.1016/j.cj.2020.10.005

TYPE Original Research
PUBLISHED 19 December 2024
DOI 10.3389/fpls.2024.1501400

Check for updates

OPEN ACCESS

EDITED BY
Khurram Shahzad,
Water and Marine Sciences, Pakistan

REVIEWED BY
Muhammad Imran,
Ayub Agriculture Research Institute, Pakistan
Muhammad Mazhar Iqbal,
University of Sargodha, Pakistan

*CORRESPONDENCE
Yong Xie
yongx_km@163.com

†These authors have contributed equally to this work and share first authorship

RECEIVED 25 September 2024
ACCEPTED 29 November 2024
PUBLISHED 19 December 2024

CITATION
Zou Q, Zhao L, Guan L, Chen P, Zhao J, Zhao Y, Du Y and Xie Y (2024) The synergistic interaction effect between biochar and plant growth-promoting rhizobacteria on beneficial microbial communities in soil.
Front. Plant Sci. 15:1501400.
doi: 10.3389/fpls.2024.1501400

The synergistic interaction effect between biochar and plant growth-promoting rhizobacteria on beneficial microbial communities in soil

Qianmei Zou[1†], Longyuan Zhao[1†], Lirong Guan[2], Ping Chen[1], Jie Zhao[1], Yueying Zhao[1], Yunlong Du[1,3] and Yong Xie[1,3*]

[1]College of Plant Protection, Yunnan Agricultural University, Kunming, China, [2]College of Chemical Engineering, Yunnan Open University, Kunming, China, [3]State Key Laboratory for Conservation and Utilization of Bio-Resources in Yunnan, Yunnan Agricultural University, Kunming, China

Excessive use of chemical fertilizers and extensive farming can degrade soil properties so that leading to decline in crop yields. Combining plant growth-promoting rhizobacteria (PGPR) with biochar (BC) may be an alternative way to mitigate this situation. However, the proportion of PGPR and BC at which crop yield can be improved, as well as the improvement effect extent on different eco-geographic region and crops, remain unclear. This research used cabbage [*Brassica pekinensis* (Lour.) Rupr.] as the target crop and established as treatment conventional fertilization as a control and a 50% reduction in nitrogen fertilizer at the Yunnan-Guizhou Plateau of China, adding BC or PGPR to evaluate the effects of different treatments on cabbage yield and the soil physicochemical properties. Specifically, high-throughput sequencing probed beneficial soil microbial communities and investigated the impact of BC and PGPR on cabbage yield and soil properties. The results revealed that the soil alkaline hydrolyzable nitrogen (AH-N), available phosphorus (AP), and available potassium (AK) contents were higher in the BC application than in control. The BC application or mixed with PGPR significantly increased the soil organic matter (OM) content ($P<0.05$), with a maximum of 42.59 g/kg. Further, applying BC or PGPR significantly increased the abundance of beneficial soil microorganisms in the whole growth period of cabbage ($P<0.05$), such as *Streptomyces*, *Lysobacter*, and *Bacillus*. Meanwhile, the co-application of BC and PGPR increased the abundance of *Pseudomonas*, and also significantly enhanced the Shannon index and Simpson index of bacterial community ($P<0.05$). Combined or not with PGPR, the BC application significantly enhanced cabbage yield ($P<0.05$), with the highest yield reached 1.41 fold of the control. Our research indicated that BC is an suitable and promising carrier of PGPR for soil improvement, combining BC and PGPR can effectively ameliorate the diversity of bacterial community even in acid red soil rhizosphere, and the most direct reflection is to improve soil fertility and cabbage yield.

KEYWORDS

beneficial microbial communities, biological agents, rhizosphere microorganisms, soil improvement, soil physicochemical properties

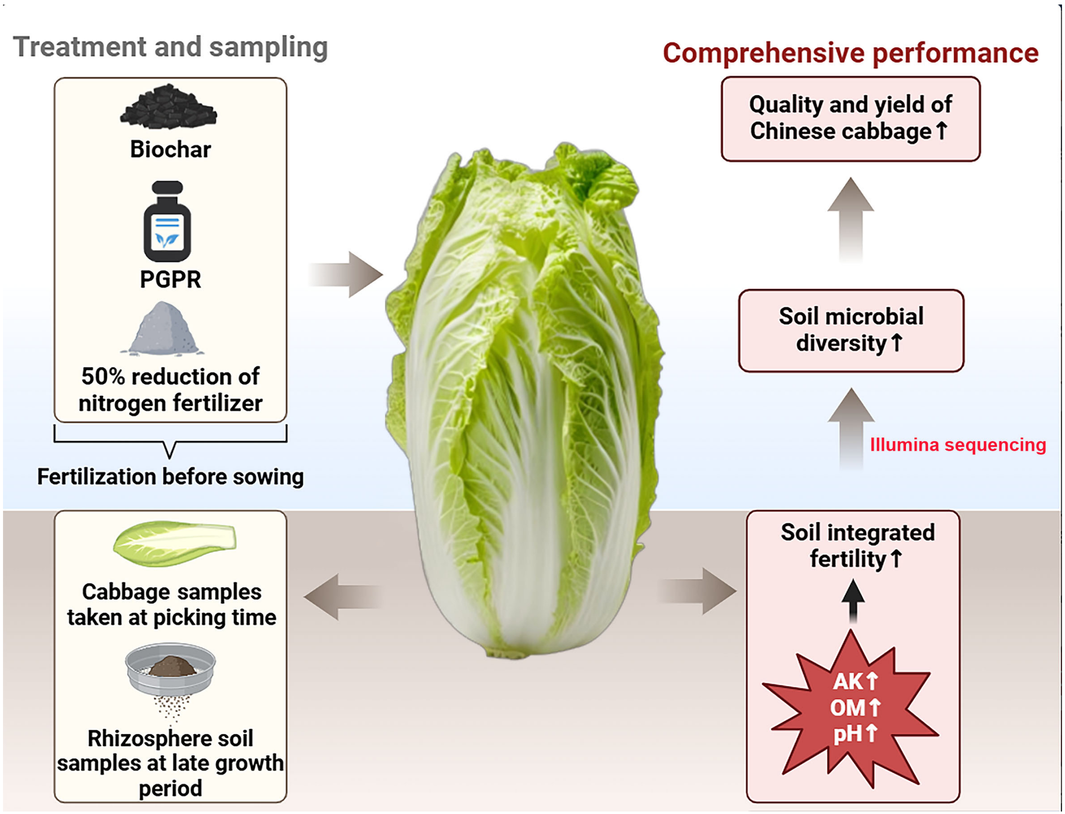

GRAPHICAL ABSTRACT

1 Introduction

The invention and application of chemical fertilizers are paramount in addressing human food security and ensuring an adequate supply of horticultural products, serving as the material foundation for high-quality and high-yield vegetables. However, due to lack of access to optimizing cultivation techniques and over-pursuing high yield, producers are prone to overusing chemical fertilizers in the vegetable production. Such excessive fertilizer application results in low fertilizer efficiency and poor production benefits, resource waste and product quality declines, and other environmental concern, which adversely impacting the sustainability in agriculture (Lyu et al., 2023). As a result, microbial fertilizers that figuring with improving soil nutrient content, fertilizer utilization and restore soil health have emerged.

Microbial fertilizers contain active microorganisms that can yield specific fertilization effects in agricultural production. Active microorganisms are crucial in generating these effects (Liu et al., 2022). The availability and broad spectrum of plant growth-promoting rhizobacteria (PGPR) are particularly prominent among potential soil microorganisms used for preparing microbial fertilizers. Recently, the application of PGPR in agriculture has steadily increased and is expected to replace chemical fertilizers, pesticides, and other growth regulators, serving as a significant nutritional source for crop growth. Plant growth-promoting rhizobacteria (PGPR) are bacteria that inhabit the rhizosphere of plants and enhance plant growth when inoculated onto seeds, root systems, root tubers, rhizomes, or soil. The mechanism of action of PGPR includes phytohormone production (Park et al., 2017), nitrogen fixation and phosphorus solubilization (Bargaz et al., 2018), inter-organismal signal production (Smith et al., 2015), antibiotic release as biocontrol agents and so on (Ogran et al., 2019). Therefore, research on utilizing PGPR for biological control has become a hot topic (De La Torre-Ruiz et al., 2016). However, studies have also indicated that PGPR may negatively affect plant growth, as cyanides produced by bacteria could adversely impact development (Agbodjato and Babalola, 2024). Moreover, directly incorporating liquid inoculants into the soil may lead to complex exogenous bacteria adhering to soil particles, significantly reducing their vertical mobility and capacity to colonize the rhizosphere (Ahmed et al., 2023). Therefore, adding carriers can enhance the colonization capacity and effectiveness of microorganisms during plant growth and development (Ehinmitan et al., 2024). Thus, exploring colonization carriers or supporting technologies that favor beneficial microbial has become a direction for further promoting microbial fertilizers.

Biochar (BC) is a pyrolytic product derived from organic matter under high-temperature and oxygen-limited conditions. BC possesses an excellent porous structure, and it can improve soil physicochemical properties and enhance soil fertility (Sui et al., 2021). This high-temperature carbon adsorbs non-polar or weakly polar organic solutes, particularly those containing aromatic structures, including enzymes and other substances essential for microbial processes in soil. Research indicates that BC can alter the composition and abundance of soil microorganism communities, suggesting that it is beneficial for the growth of indigenous soil microorganisms (Tan et al., 2022). Besides, BC significantly influences microorganism-mediated soil nutrient transformations, affecting soil structure or nutrient cycling, directly or indirectly impacting plant growth. For instance, BC-based rhizobial inoculants can remarkably enhance the symbiotic relationship between legumes and rhizobia, reducing nitrogen fertilizer requirements and promoting crop growth (Egamberdieva et al., 2016).

Furthermore, studies have shown that the use of BC as a carrier material for microorganism inoculation can provide survival niches and nutrients for microorganism proliferation, safeguarding microorganism from various external stressors, such as desiccation, high temperatures, and toxic elements (Bolan et al., 2023). Biochar exhibits stable properties and has a long residence time in the soil, making its use as a soil amendment a tripartite win strategy influencing crop yield, soil carbon-nitrogen transformation, and global warming potential (Hossain et al., 2020). Thus, we hypothesized that utilizing BC can improve the survival rate of inoculants after entering the soil as a carrier for PGPR and enhance soil properties.

Plant growth-promoting rhizobacteria acted as alive agent, its effects, especially the BC and PGPR synergistic interaction output may varies on different geographic and crop conditions. Currently, research on the co-application of BC and PGPR primarily focuses on drought resistance and productivity effects in food crops such as wheat (*Triticum aestivum* L.) and peanuts (*Arachis hypogaea* L.) (Alam et al., 2024; Noureen et al., 2024), with few of studies focusing on vegetable, especially foliage vegetable (e.g cabbage [*Brassica pekinensis* (Lour.) Rupr.]) which characterizing short-period growth and high multiple cropping index pattern. As a result, excessive use of fertilizers has become a conventional measurement in the production of such horticulture crops. Reasonably, it is sound that reducing fertilizer application is a instant and effective strategy to mitigate adverse consequences. However, this approach may lead to challenges such as nutrient deficiency in the soil and decreased crop yields. Therefore, the purpose of the present research is to elucidate whether the co-application of BC and PGPR can effectively compensate for the adverse effects of fertilizer reduction in the specific environment as the Yunnan-Guizhou Plateau. Specifically, we attempt to shed light on whether the combination can effectively enrich beneficial microorganisms in the soil to improve soil health condition, and whether they have synergistic effects in improving vegetable production. Thus, we employed a nitrogen fertilizer reduction approach to improve soil in conjunction with BC and microbial formulation applications. The effectiveness of BC and PGPR in enhancing soil microorganism communities was determined by comparing soil physicochemical properties, the structure of soil microorganism communities, and crop yields under different treatments. The present study aims to provide a theoretical basis for the effective application of PGPR in agricultural/horticultural production.

2 Materials and methods

2.1 Overview of the experimental area

The experimental area was set at Taixing Agricultural Technology Co., Ltd. Vegetable Production Base, Dali City, Xiangyun County, Yunnan Province (25°12’05” N,100°25’22” E). The experimental area is located in northwest central Yunnan Province. The area has a northern subtropical monsoon climate of the plateau, with an average annual temperature of 14.7°C, a frost-free period of 228 days, an annual rainfall of 810 mm, and an annual sunshine duration of 2,624 h. Initially, an analysis of soil physicochemical properties was conducted, the relevant index are as follows: the contents of soil pH (pH), organic matter (OM), alkaline hydrolyzable nitrogen (AH-N), available phosphorus (AP), and available potassium (AK) are 7.60, 26.59 mg/kg, 90.30 mg/kg, 27.97 mg/kg, respectively.

2.2 Materials

The tested crop was cabbage [*Brassica pekinensis* (Lour.) Rupr.], and the seeds were supplied by the Taixing Agricultural Technology Co., Ltd. The fertilizers applied, sources and their nutrient content are summarized in Supplementary Table 1. The BC treatment was formulated using a 3:2 mass ratio of BC to lignite, and the biological agents were granular PGPR (Supplementary Table 2).

2.3 Experimental design

Six treatments and one control were designed in this experiment (Table 1). A completely randomized experimental design was adopted, repeated three times, with a plot area of 14 m^2, totaling 21 residential areas. The planted density of Chinese cabbage was 25 cm × 25 cm, totaling eight rows (28 plants per row) and 28 lines (eight plants per line).

Two-season cabbage was planted to avoid the influence of temperature and light conditions across different seasons. Biochar, lignite, and PGPR were sprayed and plowed evenly before planting cabbage. The fertilization schemes for each treatment are detailed in Supplementary Table 3. The control and conventional fertilization amounts of nitrogen, phosphorus, and potassium were 347.70 kg/hm^2, 86.25 kg/hm^2, 123.00 kg/hm^2. The nitrogen, phosphorus, and potassium amounts in the nitrogen reduction treatment were 174.75 kg/hm^2, 79.20 kg/hm^2, 173.10 kg/hm^2. All treatments used a water fertilization mixture, and the reduction ratios were respectively 50%, 8%, and -41%.

2.4 Methods

2.4.1 Sample collection

Before the two-season cabbage planting, soil samples before planting cabbage (CK) and soil samples adding microbial agents to

TABLE 1 Field trails design and treatments in this research.

Treatment	Experimental design			
	BC(kg/hm$^{2)}$	Lignite (kg/hm^2)	PGPR (kg/hm^2)	Reduction in nitrogen fertilizer (%)
A	0	0	0	0
B	9.00×10^3	6.00×10^3	0	0
C	0	0	1.50×10^2	0
D	9.00×10^3	6.00×10^3	1.50×10^2	0
E	9.00×10^3	6.00×10^3	0	50
F	0	0	1.50×10^2	50
G	9.00×10^3	6.00×10^3	1.50×10^2	50

the soil before planting cabbage (CK-0) were collected using the five-point sampling method as blank controls for measuring the soil microbial community structure. Soil samples of 0–20 cm depth were collected each time. These samples were collected from each plot repeatedly three times and were mixed. A total of six rhizosphere samples were collected each season. Five cabbage plants with the same growth vigor were determined using an "S"-shaped point arrangement in the middle and late growth periods of the two seasons of cabbage. Next, the weeds and dead leaves around the cabbages were cleaned. Later, the cabbage plants were uprooted, and after shaking off the larger pieces of soil from the root system, small pieces of soil or soil particles attached to the root surface (about 2–3 mm) were collected as rhizosphere soil samples (Lu et al., 2015), soil samples in the same plot were evenly mixed as a mixed sample, and 21 rhizosphere samples were collected in each period. A total of 42 rhizosphere samples were collected in each season. Some mixed soil samples were air dried and stored to determine soil physicochemical properties. In contrast, others were stored in a refrigerator at −80°C to extract the total deoxyribonucleic acid (DNA) of microorganisms for high-throughput sequencing.

Five additional plants collected in each plot were weighed during the late growth of the two-season cabbage. The number of missing and variant plants in the plot was investigated. The actual final harvested plants in the plot were determined, and the entire harvest was obtained as the yield.

2.4.2 Cabbage yield

The actual yield during the harvesting of Chinese cabbage was measured for each plot and converted to yield per unit area using the equation below:

$$Y_p(kg/hm^2) = \frac{A_y(kg)}{A_p(m^2)} \times 10^3$$

(Y_p represents the yield per unit area; A_y represents the actual yield per plot; A_p represents the area per plot).

2.4.3 Soil physicochemical properties

The available nutrient content in the soil was determined after drying the sampled soil using the following methods: Soil pH was determined at a 1:5 (w/v) soil/distilled water ratio using a pH meter (Mettler Toledo Delta 320). Soil OM was determined using the potassium dichromate external heating method. Soil AH-N was measured using the alkaline hydrolysis diffusion method. Soil AP was measured using molybdenum antimony colorimetry. Soil AK was measured using the flame photometry method (Klotz et al., 2023).

2.4.4 High-throughput sequencing of soil bacteria

The Illumina sequencing technology was used for high-throughput sequencing. Soil DNA was extracted using a DNA extraction solution. The DNA concentration was detected using agarose gel electrophoresis and NanoDrop2000 (Thermo Scientific, Wilmington, USA). The V4 region of bacterial 16S ribosomal ribonucleic acid (rRNA) genes was amplified using the primers 515F (5'-GTGYCAGCMGCCGCGGTAA-3') and 806R(5'-GGACTACHVGGGTWTCTAAT -3') with genomic DNA as a template. The PCR products were quantified using Qubit 2.0 Fluorometer (Thermo Scientific, Wilmington, USA) based on the preliminary results from electrophoresis. Then, according to the sequencing requirements of each sample, the corresponding proportions were mixed. Using the PE250 sequencing method, the raw offline data obtained from sequencing were concatenated and filtered to obtain high-quality target sequences for subsequent analysis.

2.5 Statistical analysis of data

Field experiment and laboratory test data were preliminarily organized and drawn using Excel 2013. Using SPSS 19.0, conducted variance analysis and significance tests on soil physicochemical properties and cabbage yield. GraphPad Prism 8.0.2 and R software were used for beta diversity analyses and graphic analysis.

Based on the Usearch software (http://drive5.com/uparse/), the UPARSE algorithm was utilized for OTU clustering at a consistency level of 97%. The sequence with the highest frequency within each OTU was selected as the representative sequence. Taxonomic annotation analysis was conducted using the UCLUST classification method in conjunction with the SILVA database

(Release_123 http://www.arb-silva.de/). Representative sequences underwent multiple sequence alignment via PyNAST. Additionally, a phylogenetic tree was constructed using FastTree. Use R language for various data conversions and use ggplot2 package for bacterial community composition analysis.

Alpha diversity analysis was performed using R language. Wilcoxon rank sum test and Kruskal-Wallis rank sum test were performed, and multiple comparisons were also performed. Beta diversity analysis was performed using R language. The Unifrac distance, Bray-Curtis and Jaccard distances were calculated. PCA analysis was performed using vegan package.

3 Results

3.1 Effect of different fertilization treatments on soil physicochemical properties

Adding BC and PGPR increased the AH-N content. The BC application in the E treatment significantly increased the AP content at 160 days, reaching 19.49 mg/kg. In contrast, the improvement effect was not significant among the other treatments. Treatments D, B, and F increased pH that reached 7.78, indicating that BC and PGPR have an upward-regulating effect on pH. The F treatment reached the highest AK content at 60 days (389.95 mg/kg). The F and G treatments reached the highest content after 160 days. This result indicated that the PGPR application or a combination of BC and PGPR enhanced the AK content. Treatment D reached the highest content at 115 days, and treatment G had the highest content at 160 days, reaching 42.59 g/kg. The results showed that BC and PGPR applications could increase OM content. Still, the effect of applying PGPR alone was smaller than that of applying BC alone or BC in combination with PGPR (Table 2).

In conclusion, adding BC and PGPR positively impacted soil physicochemical properties, improving soil health and fertility.

3.2 Effect of different fertilization treatments on soil microbial community diversity

3.2.1 Analysis of the sequencing structure of rhizosphere soil

A total of 3,183,060 sequences were obtained during the experiment. The final number of tag sequences used for subsequent analysis was 2,849,972 after filtering for chimeras. These tag sequences had an average sequence length of 288 bp. The dilution curves for each soil sample tended to slow gradually, indicating that the sequencing depth contained most bacterial types in the samples (Supplementary Figure 1). This result suggests that the sequencing adequacy was appropriate and could be utilized to analyze the community structure of bacteria.

3.2.2 Structure of soil bacterial phylum-level communities

The bacterial operational taxonomic units (OTUs) obtained from sequencing soil samples were classified into 45 phyla, 117 classes, 310 orders, 547 families, and 1167 genera. *Proteobacteria*, *Acidobacteria*, *Chloroflexi*, *Firmicutes*, *Gemmatimonadete*, *Bacteroidetes*, *Actinobacteria*, *Planctomycetes*, *Verrucomicrobia*, and *Thaumarchaeota* were the dominant soil bacteria, and their average relative abundance was greater than 0.70% (Figure 1). The relative abundance of *Proteobacteria*, *Gemmatimonadetes*, *Actinobacteria*, *Bacteroidetes*, and *Firmicutes* significantly increased after the cultivation of cabbage compared to the control, whereas *Chloroflexi* and *Thaumarchaeota* decreased.

3.2.3 Structure of soil bacterial genus-level communities

Figure 2A illustrated the relative abundance and correlations of bacteria among the nine samples collected during the mid-growth period of cabbage in the summer season. There were significant differences between B1 and G1 and among CK, CK-0, and A1. Significant differences in community structure among C1, F1, E1, and D1 and CK, CK-0, and A1 were also detected. Therefore, the BC or PGPR application altered the soil bacterial community structure (Figure 2A). We compared the 50 high-ranking species with high abundance rankings between treatments based on the community abundance data from the samples. At the genus level, the BC and PGPR applications significantly increased the relative abundance of beneficial microorganisms in the soil, including *Nitrosospira* and *Lysobacter*, which have biocontrol functions. *Thermomonas* and *Luteimonas* are associated with antibacterial effects, and *Bacteroides* is related to nutrient cycling. Furthermore, the BC and PGPR applications also significantly reduced the relative abundance of organic pollutant-degrading bacteria *Reyranella*, *Nitrosospira*, and *Nitrobacter*, which are associated with the nitrogen cycling process. Besides, the reduction of nitrogen fertilizer application did not decrease the relative abundance of beneficial bacteria, which is feasible (Figure 2B; Supplementary Table 4).

Figure 2C illustrated the relative abundance and correlations of bacteria among nine samples collected during the late growth period of cabbage in the summer. There were significant differences between the treatments (CK and CK-0 and others) and significant differences in community structure among B2 and G2, D2 and F2, and A2. Applying BC, PGPR, or both combined with reduced nitrogen fertilizer altered the soil community structure. At the genus level of bacteria, applying BC and PGPR significantly increased the relative abundance of *Bacillus*, *Lysobacter*, and *Bradyrhizobium*, all were biocontrol agents that enhanced plant growth and inhibited the growth of pathogenic microorganisms. The abundance of these three microorganisms constituted 0.77% of the total microbial population in the samples, indicating that the application of BC and PGPR can promote plant growth and development and inhibit the occurrence of diseases (Figure 2D; Supplementary Table 5).

TABLE 2 Changes in the physicochemical properties of soil under different treatments at the same time.

Physicochemical property	Time/ Day	A	B	C	D	E	F	G
AH-N (mg/kg)	30d	138.60 ± 3.21a	139.30 ± 6.10a	105.00 ± 17.94bc	117.60 ± 2.10ab	102.90 ± 3.64bc	107.80 ± 9.72bc	86.10 ± 5.56c
	60d	120.40 ± 19.03a	102.90 ± 29.40a	101.50 ± 6.89a	90.30 ± 12.77a	100.80 ± 16.31a	97.30 ± 3.05a	94.50 ± 9.15a
	115d	128.80 ± 2.52a	128.10 ± 13.66a	149.10 ± 29.87a	133.00 ± 7.41a	128.11 ± 25.66a	155.40 ± 18.35a	112.70 ± 7.41a
	160d	129.50 ± 20.91a	102.90 ± 10.50ab	116.20 ± 1.85ab	121.10 ± 6.89ab	125.30 ± 7.89a	88.90 ± 9.10b	132.30 ± 8.49a
AP (mg/kg)	30d	44.04 ± 9.66a	34.60 ± 8.31a	38.49 ± 15.10a	23.12 ± 5.29a	27.78 ± 6.02a	44.74 ± 0.40a	20.40 ± 6.11a
	60d	9.57 ± 1.80a	8.88 ± 1.48a	8.01 ± 0.81a	9.49 ± 1.59a	10.10 ± 2.23a	8.22 ± 0.50a	8.28 ± 1.78a
	115d	8.94 ± 0.47a	9.46 ± 1.02a	6.93 ± 1.47b	10.10 ± 2.44a	11.77 ± 1.17a	9.46 ± 0.70a	9.59 ± 0.35a
	160d	18.18 ± 3.17ab	18.11 ± 4.67ab	12.26 ± 0.38b	13.08 ± 0.77ab	19.49 ± 2.91a	14.10 ± 4.47ab	14.07 ± 0.41ab
AK (mg/kg)	30d	345.29 ± 22.52a	346.34 ± 15.10a	308.73 ± 19.98a	357.44 ± 2.74a	346.86 ± 20.68a	342.16 ± 22.46a	374.02 ± 22.49a
	60d	305.47 ± 28.99ab	286.93 ± 25.79b	351.56 ± 40.74ab	309.90 ± 26.57ab	345.69 ± 24.74ab	389.95 ± 8.51a	382.64 ± 15.16a
	115d	319.18 ± 21.78a	302.60 ± 9.42a	367.49 ± 36.87a	308.86 ± 18.19a	320.22 ± 15.49a	339.03 ± 14.69a	334.85 ± 11.99a
	160d	264.73 ± 35.42b	289.15 ± 39.04ab	307.43 ± 4.31ab	334.33 ± 34.32ab	344.25 ± 29.81ab	373.24 ± 3.41a	364.10 ± 6.77a
OM (g/kg)	30d	27.89 ± 4.29bc	34.75 ± 3.86abc	25.80 ± 0.96bc	41.69 ± 5.89ab	43.42 ± 3.39a	26.81 ± 6.84bc	34.79 ± 5.17abc
	60d	29.08 ± 3.60a	39.90 ± 0.51a	23.66 ± 4.03a	41.36 ± 4.41a	35.72 ± 7.03a	24.71 ± 5.31a	32.86 ± 8.89a
	115d	35.86 ± 2.90c	71.74 ± 4.63b	45.25 ± 12.90c	102.05 ± 2.42a	80.53 ± 2.45b	34.61 ± 4.34c	72.80 ± 6.69b
	160d	34.34 ± 6.10a	31.98 ± 6.79a	28.32 ± 4.96a	39.25 ± 7.44a	41.02 ± 9.85a	24.47 ± 8.20a	42.59 ± 10.12a
pH	30d	7.42 ± 0.09ab	7.22 ± 0.02b	7.36 ± 0.06b	7.62 ± 0.18a	7.58 ± 0.09a	7.44 ± 0.09ab	7.58 ± 0.01a
	60d	7.63 ± 0.14a	7.66 ± 0.01a	7.49 ± 0.07a	7.78 ± 0.14a	7.66 ± 0.02a	7.60 ± 0.03a	7.76 ± 0.03a
	115d	7.57 ± 0.01a	7.58 ± 0.03a	7.55 ± 0.05a	7.51 ± 0.04a	7.47 ± 0.04a	7.45 ± 0.05a	7.56 ± 0.09a
	160d	7.40 ± 0.03b	7.41 ± 0.05b	7.46 ± 0.02ab	7.41 ± 0.03b	7.38 ± 0.06b	7.61 ± 0.06a	7.45 ± 0.06b

The data in the table is the mean ± standard error of 3 replicates. Different lowercase letters in the same row indicate significant differences between treatments ($p<0.05$), the same as below.

Figure 3A illustrated the relative abundance and correlations of bacteria among the nine samples collected during the mid-growth period of cabbage in the winter season. There were significant differences between the treatments (CK, CK-0) and others, and significant differences in community structure between B3, D3, E3, or G3 and A2. This indicated that A3–G3 treatments resulted in substantial changes in the community structure compared to the control. At the genus level, the BC and PGPR application significantly increased the relative abundance of beneficial microorganisms in the soil. For instance, the abundance of *Lactobacillus, Bacillus*, and *Pseudomonas*, which have biocontrol functions, increased, along with that of *Pseudoxanthomonas* and *Streptomyces*, which have antibiotic properties and facilitate rhizosphere colonization. The abundance of *Chthoniobacter* and *Luteolibacter*, which have plant growth-promoting functions, and *Bacteroides* and *Bradyrhizobium*, which participate in the nitrogen cycle and have the nitrogen-fixing capabilities of the genera, also increased (Figure 3B; Supplementary Table 6). In summary, applying BC and PGPR effectively suppressed diseases, promoted plant growth and development, and enhanced soil quality.

Figure 3C illustrated the relative abundance and correlations of bacteria among the nine samples collected during the late growth period of cabbage in winter. There were significant differences between treatments (CK and CK-0). The A4–G4 treatments resulted in substantial alterations in the community structure compared to the control treatment. At the genus level, the BC and PGPR application or their combination with reduced nitrogen fertilization, significantly increased the relative abundance of beneficial microorganisms in the soil. These microorganisms included *Bacillus*, *Pseudomonas*, and *Lactobacillus*, which have biocontrol functions, *Pseudoxanthomonas* and *Streptomyces*, which have antibiotic properties and facilitate rhizosphere colonization, *Chthoniobacter* and *Luteolibacter*, which have a plant growth-promoting function, *Nitrobacter*, *Bacteroides*, and *Bradyrhizobium*, which participate in the nitrogen cycle and have the nitrogen-fixing capabilities of the genera (Figure 3D; Supplementary Table 7). The BC and PGPR applications or their combination with reduced nitrogen fertilization enhanced soil health and fertility.

3.2.4 Alpha diversity analyses

The Simpson index for the E treatment was lower than the control at 30 days. In contrast, the indexes in other treatments increased compared to control. The indexes across various treatments were not significant difference at 60 days. However, the indexes were the highest for the E treatment at 115 and 160 days

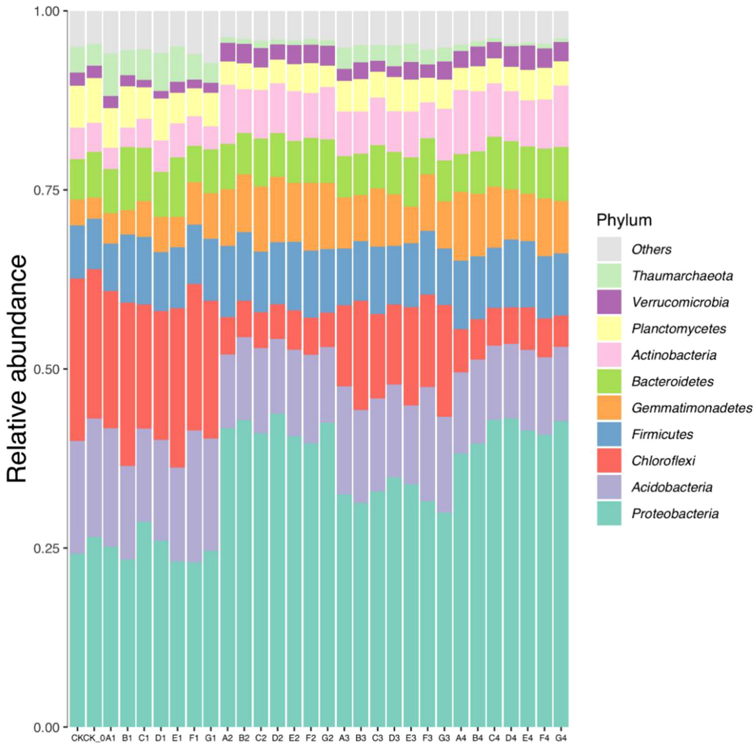

FIGURE 1
The relative abundance of dominant groups of bacteria at the phylum level in soil samples.

(Table 3). In summary, the application of BC and PGPR significantly enhanced the richness and diversity of soil microorganisms, with nitrogen reduction combined with BC having a better effect. According to Supplementary Table 8, the species richness and community diversity of the treatments increased with the advancement of the growth period of the cabbage. Regarding species dominance, there were no significant differences across various periods under G treatment, indicating that species dominance remained unchanged. Still, other treatments increased with the growth stages of the cabbage (Supplementary Table 8).

3.2.5 Beta diversity analyses

A PCA was conducted to compare the CK and CK-0 treatments with other fertilization treatments and to examine the alterations in bacterial community structure during the growth period of the summer season cabbage. The PC1 contribution rate more than PC2 (Figures 4A, B). The analysis of the Figure 4A revealed that the CK, CK-0, A1, B1, and G1 treatments were separated from the C1–F1 treatment on PC1, and the differences were considerable. The C1–F1 treatments altered the bacterial community structure in the soil. The analysis of the Figure 4B revealed that the CK and CK-0 treatments were distinctly separated from the A2–G2 treatments on PC1. The observed differences were consistent with the bacterial relative abundance heat map analysis. The A2–G2 treatments altered the bacterial community structure in the soil. In summary, the BC and PGPR application or their combined reduction of nitrogen fertilizers can change the structure of soil bacterial communities.

PCA was conducted to compare CK and CK-0 with other fertilization treatments, examining the alterations in bacterial community structure during the growth period of the winter season cabbage, indicating PC1 contributes more significantly than PC2 (Figures 4C, D). The CK, CK-0, E3, F3, and G3 treatments were distinctly separated from the A3–D3 treatments on PC1. The differences were considerable, showing that the A3–D3 treatments altered the bacterial community structure in the soil (Figure 4C). The CK and CK-0 treatments were distinctly separated from the A4–G4 treatments on PC1, and the differences were considerable and consistent with the heatmap analysis of bacterial relative abundance. The A4–G4 treatments altered the bacterial community structure in the soil (Figure 4D). In summary, the BC and PGPR applications or their combined reduction of nitrogen fertilizers altered the structure of soil bacterial communities, but the enhancement effect of PGPR is significantly strong.

3.3 Effect of different fertilization treatments on Chinese cabbage yield

The yield of cabbage planted in winter was higher than that grown in summer due to climate differences. During the summer, the yield of all treatments increased compared to control A, with D

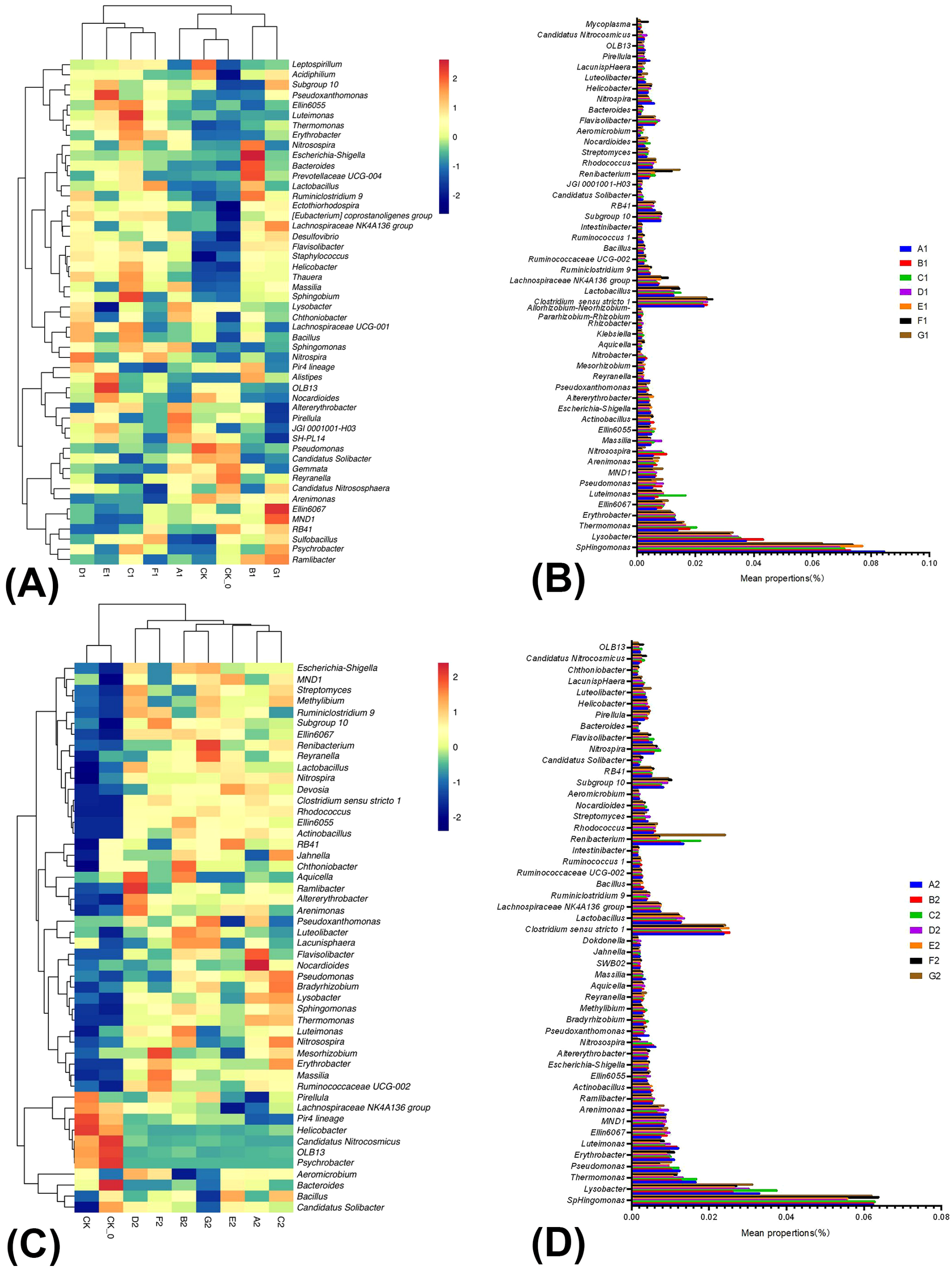

FIGURE 2
The relative abundance and similarity of bacterial genus level in soil under different treatments in summer season Chinese cabbage and the classification. The panel **(A)** is the relative abundance and similarity of bacterial genus level in soil under different treatments in the mid-growth of summer season Chinese cabbage; The panel **(B)** is the classification of bacteria in the mid-growth of summer season Chinese cabbage; The panel **(C)** is the relative abundance and similarity of bacterial genus-level in soil under different treatments at the late growth of summer season Chinese cabbage; The panel **(D)** is the classification of bacteria in the late growth of summer season Chinese cabbage.

exhibiting the significantly highest yield. The B, C, and G treatments followed in order of yield. Still, there were no significant differences among the three treatments. The yield of the E and F treatments was the lowest, with no significant difference between them. During the winter, the D treatment reached the highest yield compared to control A, and the E treatment reached the lowest yield during winter (Figure 5). The combined BC and PGPR applications significantly enhanced the yield of Chinese cabbage. At the same time, such a combined application reduced the application of nitrogen fertilizer without decreasing the yield.

10.3389/fpls.2024.1501400

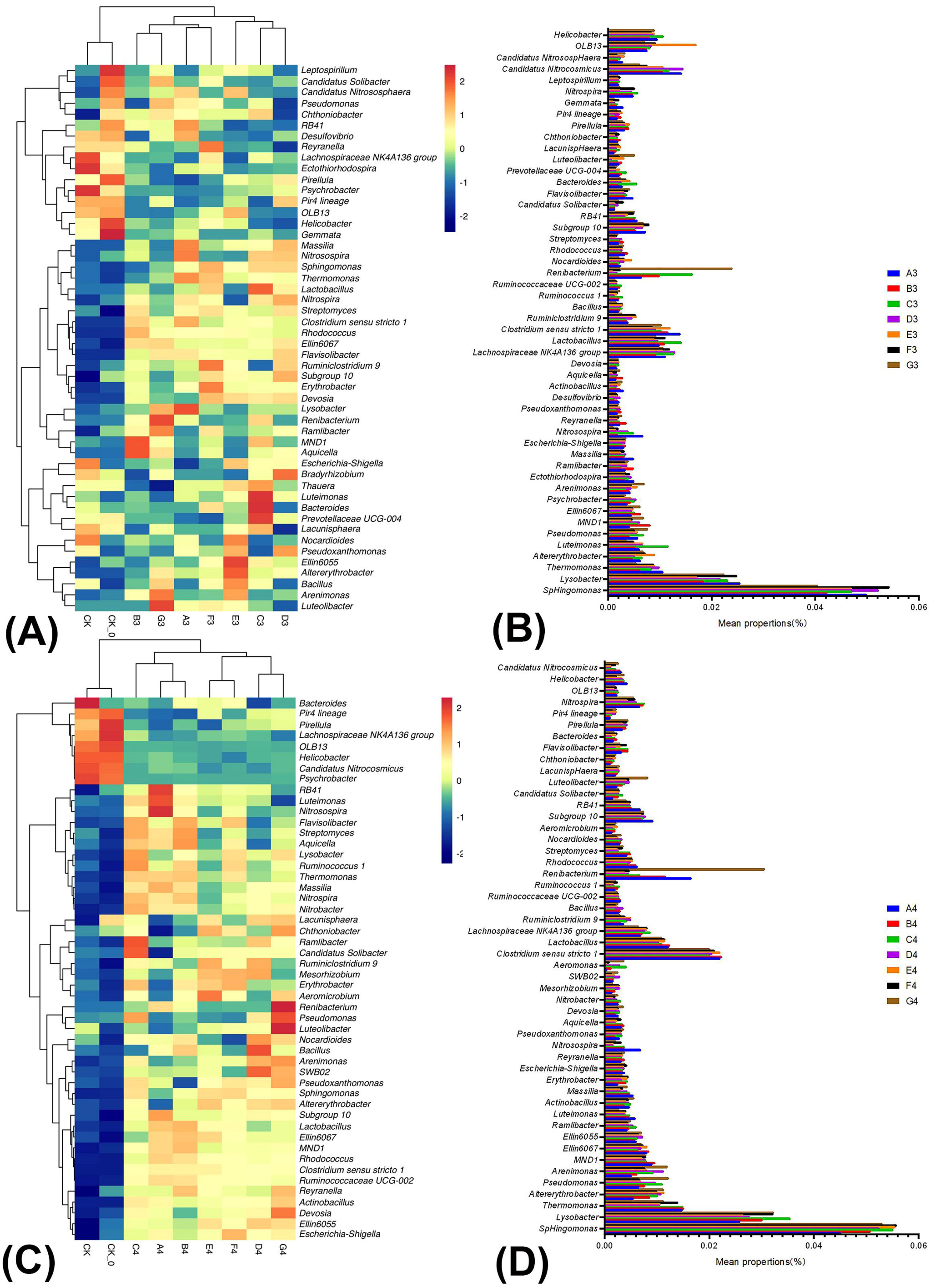

FIGURE 3
The relative abundance and similarity of bacterial genus level in soil under different treatments in winter season Chinese cabbage and the classification. The panel **(A)** is the relative abundance and similarity of bacterial genus level in soil under different treatments at the mid-growth of winter season Chinese cabbage; The panel **(B)** is the classification of bacteria in the mid-growth of winter season Chinese cabbage; The panel **(C)** is the relative abundance and similarity of bacterial genus-level in soil under different treatments at the late growth of winter season Chinese cabbage; The panel **(D)** is the classification of bacteria in the late growth of winter season Chinese cabbage.

TABLE 3 Bacterial diversity index comparison of different treatments at the same time.

Time	Treatments	Observed	Chao1	Shannon	Simpson
30d	A	943.33 d	1971.46 b	6.22 c	0.9954 de
	B	1034.33 a	2363.63 a	6.41 a	0.9965 ab
	C	986.33 bc	2162.81 ab	6.30 b	0.9960 bc
	D	967.33 cd	2143.18 ab	6.27 bc	0.9958 cd
	E	975.00 bcd	2021.41 ab	6.25 bc	0.9949 e
	F	941.00 d	2006.25 ab	6.24 c	0.9956 cd
	G	1006.67 ab	2274.97 ab	6.39 a	0.9966 a
60d	A	1035.00 a	2456.52 a	6.42 a	0.9967 a
	B	1029.67 a	2370.26 a	6.40 a	0.9966 a
	C	1034.00 a	2447.25 a	6.40 a	0.9966 a
	D	1020.33 a	2155.77 a	6.41 a	0.9968 a
	E	1066.33 a	2408.25 a	6.49 a	0.9970 a
	F	1018.00 a	2100.30 a	6.44 a	0.9969 a
	G	1014.00 a	2278.52 a	6.41 a	0.9968 a
115d	A	1102.33 a	2612.89 a	6.52 bc	0.9971 bc
	B	1131.33 a	2511.65 a	6.60 ab	0.9975 a
	C	1103.00 a	2730.49 a	6.52 bc	0.9971 bc
	D	1094.00 a	2387.58 a	6.54 bc	0.9973 ab
	E	1167.00 a	2745.82 a	6.65 a	0.9976 a
	F	946.00 b	1731.75 b	6.39 d	0.9969 c
	G	1094.33 a	2404.12 a	6.53 bc	0.9969 c
160d	A	1070.33 c	2417.82 a	6.50 c	0.9970 c
	B	1123.00 ab	2662.78 a	6.57 ab	0.9973 b
	C	1106.33 abc	2583.75 a	6.56 b	0.9974 ab
	D	1114.00 abc	2522.94 a	6.57 ab	0.9975 a
	E	1127.00 ab	2672.02 a	6.60 ab	0.9975 a
	F	1146.67 a	2727.46 a	6.62 a	0.9975 a
	G	1093.67 bc	2556.51 a	6.50 c	0.9967 d

Different lowercase letters in the same row indicate significant differences between treatments ($p<0.05$).

4 Discussion

4.1 Effect of fertilization level on soil physicochemical properties

The physicochemical properties are the evaluation index of soil quality. Wei et al. (2023) found that the soil pH of the BC application treatment was 7.0% higher than that of the control. This result was also observed here (Table 2). The BC application and the reduction of nitrogen fertilizer with PGPR in this study significantly increased soil pH. The mechanism of BC induce soil pH change depends on the alkaline ions and surface functional groups of it. Additionally, the increase in pH can constrain the mobility of heavy metals, thereby ensuring soil health (Pan et al., 2021). The BC application with reduced nitrogen fertilizer, the sole PGPR application, and the combined BC and PGPR application significantly increased the soil OM content (Table 2). This result is consistent with the research results found by Urooj et al. (2022). Such an increase in OM content occurs because BC is rich in organic carbon. Biochar application adds exogenous organic carbon to the soil, increasing the carbon pool and OM content and affecting soil fertility.

Alkaline hydrolyzable nitrogen can reflect the nitrogen supply capacity of the soil for the current or recent season. Alkaline hydrolyzable nitrogen is a crucial indicator of soil fertility and is

10.3389/fpls.2024.1501400

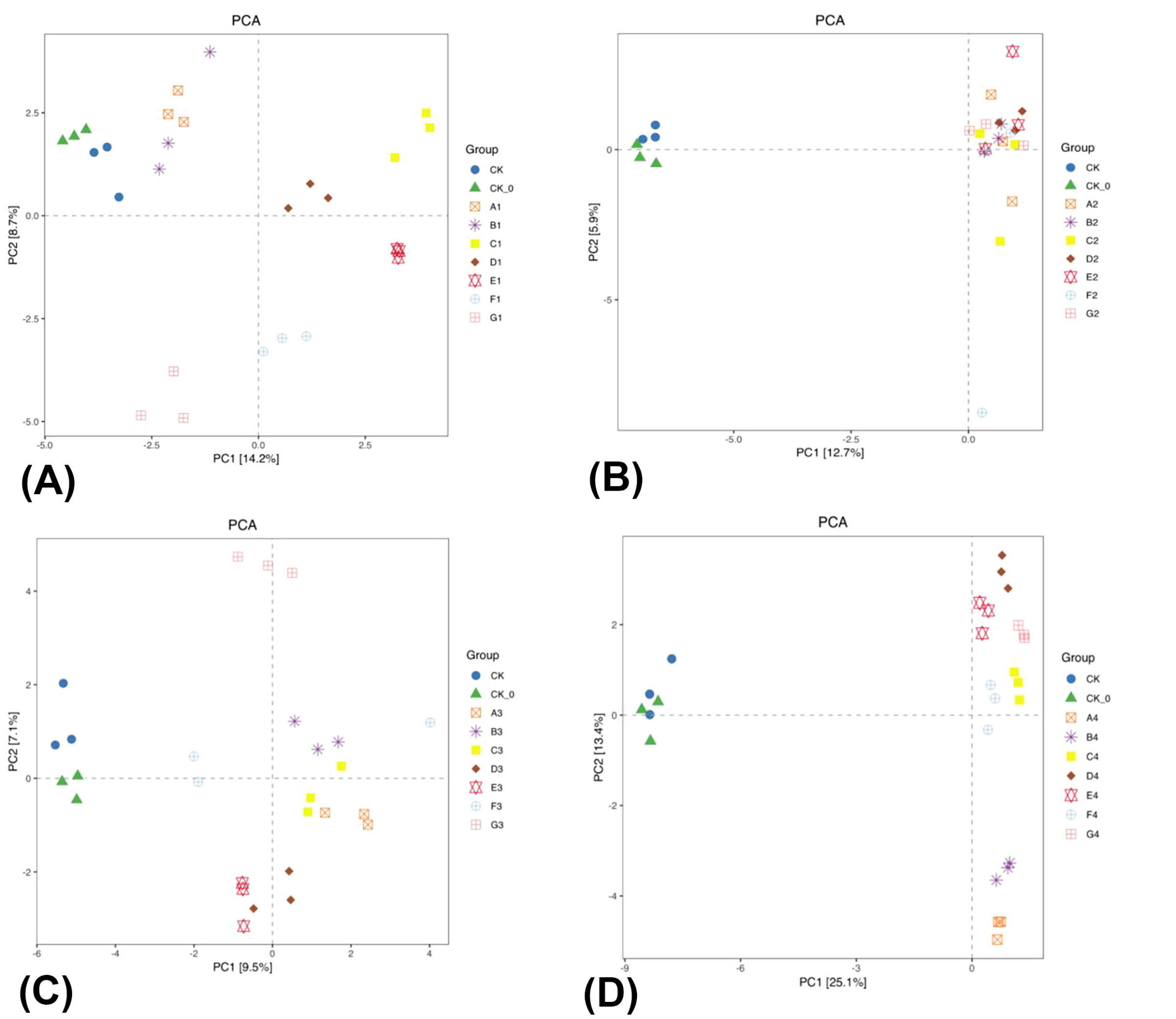

FIGURE 4
Principal component analysis (PCA) two-dimensional diagram of bacterial β-diversity in rhizosphere soil of the two season Chinese cabbage. The panel **(A)** is the PCA analysis map of the mid-growth period of the summer season of Chinese cabbage; The panel **(B)** is the PCA analysis map of the late growth period of the summer season Chinese cabbage; The panel **(C)** is the PCA analysis map of the mid-growth period of the winter season of Chinese cabbage; The panel **(D)** is the PCA analysis map of the late growth period of the winter season of Chinese cabbage.

critical for balancing fertilization and effectively controlling agricultural non-point source pollution. Both BC and PGPR enhanced the AH-N content in the soil (Table 2). This result is consistent with the research results of Lalay et al. (2022). This result may be attributed to BC enhancing the biological nitrogen fixation capacity and reducing soil N_2O emissions (Harter et al., 2014). Moreover, PGPR can achieve nitrogen fixation, phosphorus solubilization, potassium release, and other functions by producing nitrogenase, phosphatase, nuclease, or organic acids through metabolism, thereby improving the AH-N, AP, and AK contents and soil fertility. The combination of nitrogen fertilizer reduction and PGPR and their combined use with BC significantly increased the AK content in the soil (Table 2). This result may be because the PGPR used in this experiment is a growth-promoting strain with the ability to dissolve phosphorus and potassium, which is conducive to activating potassium in the soil, promoting plant absorption, and thus increasing the content of AK in the soil (Olaniyan et al., 2022). Sui et al. (2022) have noted that adding BC and reducing nitrogen fertilizer application with BC can enhance the AP content in the soil. This result is consistent with this study (Table 2), possibly because BC can directly interact with the applied chemical fertilizers, adsorbing phosphate within its porous structure, resulting in a slow loss of effective phosphorus from the soil (Yang et al., 2021).

4.2 Effect of fertilization level on soil microbial community diversity

The changes of microorganisms in soil can impact plant growth, and the development of plants may also influence the variations in soil microorganisms (Singh et al., 2022). This study utilized Illumina sequencing technology to demonstrate that different fertilizer treatments significantly impacted the structure of rhizosphere microbial communities in cabbage. The distribution characteristics of the dominant bacteria at the phyla and genera

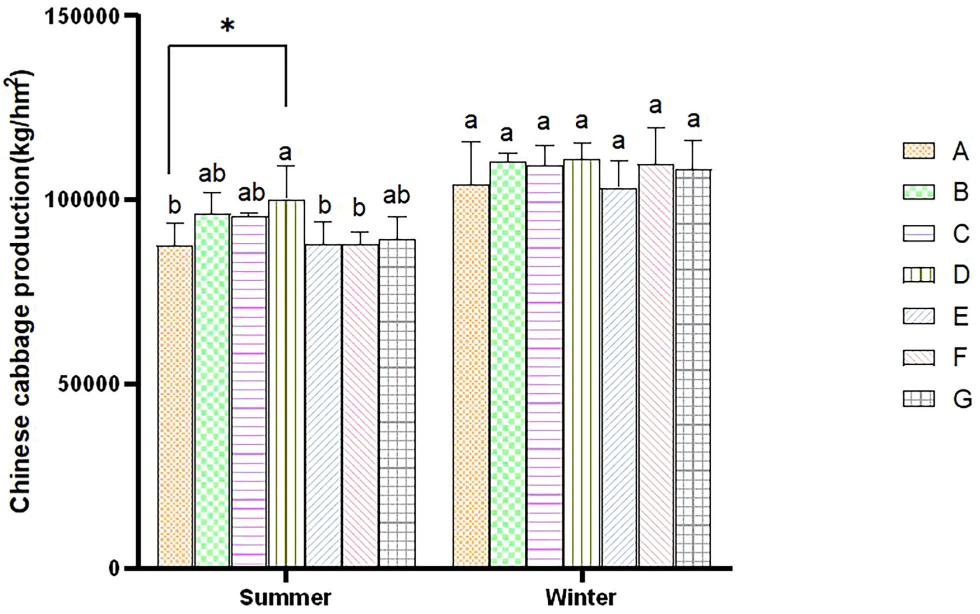

FIGURE 5
Comparative analysis of cabbage yield within the same season. Error bars refer to the average value ± SD from three biological replicates. Different letters above the columns indicate significant differences (P<0.05). * indicates significance differences at the P<0.05 level.

levels in the soil samples in this experiment were analyzed. *Proteobacteria*, *Chloroflexi*, *Firmicutes*, *Bacteroidetes*, and *Actinobacteria* were the dominant abundant bacteria in each treatment (Figure 1). These microflora organisms have also been identified as dominant populations in several other studies (Jin et al., 2022; Yin et al., 2022). This result indicated that the soil rhizosphere of the different treatments in this experiment had a common composition of dominant soil microbial communities, but the proportions were different.

Research has shown that *Proteobacteria* are primarily facultative or obligate anaerobes and heterotrophic microorganisms, and that *Sphingomonas* can remove refractory pollutants (Wang et al., 2024), *Bradyrhizobium* has a bioremediation function on soil (Harter et al., 2017). The relative abundance of *Proteobacteria* in the BC and PGPR combined applications was the highest in this study (Figures 2, 3). This result indicated that beneficial microbial communities in the rhizosphere soil were greater than in the other treatments. The ability to remove soil pollutants and repair soil was also the strongest, and environmental friendliness was also the highest (Saeed et al., 2022). *Actinomycetes* can decompose cellulose and lignin, and abundant *Actinomycetes* are beneficial to decomposing plant organic residues in soil (Zhang et al., 2021). In this study, the relative abundance of *Actinomycetes* in the combined BC and PGPR application was the highest (Figures 2, 3), indicating that the OM content in the rhizosphere soil was high, and the soil fertility was the strongest under this treatment condition. This confirmed that the addition of BC and PGPR can indeed improve soil fertility. In addition, some *Firmicutes* can repair their environments, degrade or transform pollutants, and reduce the impact of soil pollution on the ecological environment. *Bacillus* in *Firmicutes* are a widely used biocontrol bacteria with long survival periods and strong resistance. Many strains of these genera have attracted widespread attention from researchers due to their nitrogen-fixing ability, resistance to pathogenic bacteria, and growth-promoting effects on plants (Li et al., 2020; Sun et al., 2022). The relative abundance of *Firmicutes* in the single PGPR application in this study was the highest, followed by the combined BC and PGPR application with reduced nitrogen fertilizer application (Figures 2, 3). This result indicated that both treatments have high environmental friendliness, strong resistance to pathogens, and nitrogen-fixing capability. *Bacteroidetes* participate in the nitrogen cycling process in soil, influencing the content of mineralized nitrogen through its activities. The abundance of *Bacteroidetes* is also high in environments with a high OM content in the soil. In addition, the microbial *Bacteroidetes* community may help enhance plant defense capabilities and reduce disease occurrence (Pan et al., 2023). The relative abundance of *Bacteroidetes* in this study was highest in the single BC or PGPR application (Figures 2, 3), indicating that the two treatments had strong nitrogen-fixing ability and increased soil OM content and disease resistance. In summary, the application of BC and PGPR can effectively increase the relative abundance of beneficial microbial communities in soil, especially biocontrol bacteria. They are direct indicators of root diseases in Chinese cabbage. For example, cabbage clubroot disease caused by *Plasmodiophora brassicae* (Javed et al., 2023). It implied that the application of BC and PGPR could reduce the occurrence of root diseases in Chinese cabbage, but more evidence is needed.

The alpha and beta diversity analyses showed differences in the richness and diversity of rhizosphere soil bacterial communities under different treatments (Table 3; Supplementary Table 8; Figure 4). Compared to conventional fertilization, the application of single BC, single PGPR, and a combination of BC and PGPR significantly increased both the Shannon and Simpson indices of bacteria in the soil (Table 3), indicating that the microbial diversity and species dominance of these three treatments were significantly increased, which was consistent with the results of previous studies (Gulnaz et al., 2017; Di Salvo et al., 2018). The differences in the microbial community structure may be attributed to significant differences in environmental factors, as soil physicochemical properties have significant impacts on the microbial community structure. For example, Wang et al. (2021) found that soil physicochemical properties were determinant factors driving changes in the number of soil microorganisms of Gastrodia elata. Another reason may be that different fertilizations lead to different degrees of enrichment of microbial communities. The above showed that soil physicochemical properties and fertilizers were the key factors that produce differences in the microbial community structures.

4.3 Effect of fertilization level on Chinese cabbage yield

Dry matter is the final form of crop photosynthetic products, and it guarantees an increased crop yield. Dry matter accumulation is closely related to nitrogen supply at different growth stages. The application of nitrogen fertilizer is irreplaceable in crop production and yield enhancement. The cabbage yield in the three treatments with a 50% nitrogen reduction did not significantly decrease compared to the control (Figure 5). This result is consistent with previous research results. Fan et al. (2024) showed that reducing nitrogen between 54% and 80% will not significantly impact the yield of vegetables grown in Southwest China. Therefore, optimizing nitrogen fertilizer application strategies and technologies can maintain or increase vegetable yield, significantly improve nitrogen use efficiency (NUE), and reduce crop nitrogen loss. Our research also showed that BC addition could increase the yield of Chinese cabbage (Figure 5), consistent with the results of Tang et al. (2022). At the same time, PGPR has been proven to promote plant growth (Vejan et al., 2016). In this experiment, the application of PGPR also promoted increased cabbage yield, consistent with previous research findings (Gul et al., 2023).

Our study confirmed that a co-application of BC and PGPR can positively affect the Chinese cabbage yield, and even a 50% nitrogen reduction did not lower the Chinese cabbage output. Therefore, more extensive exploration of the optimal application scheme of BC and PGPR at different scenarios and crops needs to be further studied.

5 Conclusion

The BC application combined with PGPR significantly increased the yield of cabbage, enhanced soil fertility, optimized the microbial community structure, and increased the bacterial community diversity and relative abundance of potential growth-promoting bacteria (e.g., *Sphingomonas*, *Bradyrhizobium*, *Bacillus*, and *Pseudomonas*). A 50% nitrogen reduction did not significantly impact the above indicators.

In summary, BC can improve the colonization ability and effectiveness of PGPR in plant growth and development and may be an appropriate carrier for PGPR. Combining BC and PGPR could synergistically affect crop yield, soil fertility amelioration, and microbial community optimization. Our research provides a practical case for efficient fertilizer application and chemical fertilizer pollution reduction in crop production.

Data availability statement

The data presented in the study are deposited in the Figshare repository, accession number 10.6084/m9.figshare.27932247.

Author contributions

QZ: Data curation, Methodology, Validation, Visualization, Writing – original draft, Writing – review & editing. LZ: Conceptualization, Resources, Writing – review & editing. LG: Investigation, Writing – original draft. PC: Visualization, Writing – review & editing. JZ: Data curation, Software, Writing – review & editing. YZ: Software, Writing – original draft. YD: Funding acquisition, Visualization, Writing – review & editing. YX: Funding acquisition, Project administration, Supervision, Writing – review & editing.

Funding

The author(s) declare financial support was received for the research, authorship, and/or publication of this article. This work was supported by the Yunnan Academician Expert Workstation (202405AF140070), the National Natural Science Foundation of China (31260415, 31760500) and the Key Project of Yunnan Provincial Department of Science and Technology (202301AS070082).

Conflict of interest

The authors declare that the research was conducted in the absence of any commercial or financial relationships that could be construed as a potential conflict of interest.

Publisher's note

Supplementary material

The Supplementary Material for this article can be found online at: https://www.frontiersin.org/articles/10.3389/fpls.2024.1501400/full#supplementary-material

References

Agbodjato, N. A., and Babalola, O. O. (2024). Promoting sustainable agriculture by exploiting plant growth-promoting rhizobacteria (PGPR) to improve maize and cowpea crops. *PeerJ* 12, e16836. doi: 10.7717/peerj.16836

Ahmed, T., Noman, M., Qi, Y., Shahid, M., Hussain, S., Masood, H. A., et al. (2023). Fertilization of microbial composts: A technology for improving stress resilience in plants. *Plants (Basel).* 12, 3550. doi: 10.3390/plants12203550

Alam, T., Bibi, F., Fatima, H., Munir, F., Gul, A., Haider, G., et al. (2024). Biochar and PGPR: A winning combination for peanut growth and nodulation under dry spell. *J. Soil Sci. Plant Nutr.* 2024. doi: 10.1007/s42729-024-02067-3

Bargaz, A., Lyamlouli, K., Chtouki, M., Zeroual, Y., and Dhiba, D. (2018). Soil microbial resources for improving fertilizers efficiency in an integrated plant nutrient management system. *Front. Microbiol.* 9. doi: 10.3389/fmicb.2018.01606

Bolan, S., Hou, D., Wang, L., Hale, L., Egamberdieva, D., Tammeorg, P., et al. (2023). The potential of biochar as a microbial carrier for agricultural and environmental applications. *Sci. Total Environ.* 886, 163968. doi: 10.1016/j.scitotenv.2023.163968

De La Torre-Ruiz, N., Ruiz-Valdiviezo, V. M., Rincón-Molina, C. I., Rodríguez-Mendiola, M., Arias-Castro, C., Gutiérrez-Miceli, F. A., et al. (2016). Effect of plant growth-promoting bacteria on the growth and fructan production of Agave americana L. *Braz. J. Microbiol.* 47, 587–596. doi: 10.1016/j.bjm.2016.04.010

Di Salvo, L. P., Cellucci, G. C., Carlino, M. E., and García de Salamone, I. E. (2018). Plant growth-promoting rhizobacteria inoculation and nitrogen fertilization increase maize (Zea mays, L.) grain yield and modified rhizosphere microbial communities. *Appl. Soil Ecol.* 126, 113–120. doi: 10.1016/j.apsoil.2018.02.010

Egamberdieva, D., Wirth, S., Behrendt, U., Abd Allah, E. F., and Berg, G. (2016). Biochar treatment resulted in a combined effect on soybean growth promotion and a shift in plant growth promoting rhizobacteria. *Front. Microbiol.* 7. doi: 10.3389/fmicb.2016.00209

Ehinmitan, E., Losenge, T., Mamati, E., Ngumi, V., Juma, P., and Siamalube, B. (2024). BioSolutions for green agriculture: unveiling the diverse roles of plant growth-promoting Rhizobacteria. *Int. J. Microbiol.* 2024, 6181491. doi: 10.1155/2024/6181491

Fan, Y., Feng, Q., Huang, Y., Yang, N., Fan, H., Li, B., et al. (2024). Determining optimal range of reduction rates for nitrogen fertilization based on responses of vegetable yield and nitrogen losses to reduced nitrogen fertilizer application. *Sci. Total Environ.* 924, 171523. doi: 10.1016/j.scitotenv.2024.171523

Gul, F., Khan, I. U., Rutherford, S., Dai, Z. C., Li, G., and Du, D. L. (2023). Plant growth promoting rhizobacteria and biochar production from Parthenium hysterophorus enhance seed germination and productivity in barley under drought stress. *Front. Plant Sci.* 14. doi: 10.3389/fpls.2023.1175097

Gulnaz, Y., Kulmitra, A. K., Ghosh, A., and Thejesha, A. G. (2017). Effect of PGPR and PSB on soil chemical properties, nutrient status and microbial population changes after harvest of irrigated maize under varying levels of phosphorus. *Int. J. Curr. Microbiol. Appl. Sci.* 6, 1707–1712. doi: 10.20546/IJCMAS.2017.610.206

Harter, J., El-Hadidi, M., Huson, D. H., Kappler, A., and Behrens, S. (2017). Soil biochar amendment affects the diversity of nosZ transcripts: implications for N_2O formation. *Sci. Rep.* 7, 3338. doi: 10.1038/s41598-017-03282-y

Harter, J., Krause, H. M., Schuettler, S., Ruser, R., Fromme, M., Scholten, T., et al. (2014). Linking N_2O emissions from biochar-amended soil to the structure and function of the N-cycling microbial community. *ISME J.* 8, 660–674. doi: 10.1038/ismej.2013.160

Hossain, M. Z., Bahar, M. M., Sarkar, B., Donne, S. W., Ok, Y. S., Palansooriya, K. N., et al. (2020). Biochar and its importance on nutrient dynamics in soil and plant. *Biochar.* 2, 379–420. doi: 10.1007/s42773-020-00065-z

Javed, M. A., Schwelm, A., Zamani-Noor, N., Salih, R., Silvestre Vañó, M., Wu, J., et al. (2023). The clubroot pathogen Plasmodiophora brassicae: A profile update. *Mol. Plant Pathol.* 24, 89–106. doi: 10.1111/mpp.13283

Jin, N., Jin, L., Wang, S., Li, J., Liu, F., Liu, Z., et al. (2022). Reduced chemical fertilizer combined with bio-organic fertilizer affects the soil microbial community and yield and quality of lettuce. *Front. Microbiol.* 13. doi: 10.3389/fmicb.2022.863325

Klotz, M., Schaller, J., and Engelbrecht, B. M. J. (2023). Effects of plant-available soil silicon on seedling growth and foliar nutrient status across tropical tree species. *Oikos* 2023, e10030. doi: 10.1111/oik.10030

Lalay, G., Ullah, S., and Ahmed, I. (2022). Physiological and biochemical responses of Brassica napus L. @ to drought-induced stress by the application of biochar and Plant Growth Promoting Rhizobacteria. *Microsc Res. Tech.* 85, 1267–1281. doi: 10.1002/jemt.23993

Li, W., Lee, S. Y., Cho, Y. J., Ghim, S. Y., and Jung, H. Y. (2020). Mediation of induced systemic resistance by the plant growth-promoting rhizobacteria Bacillus pumilus S2-3-2. *Mol. Biol. Rep.* 47, 8429–8438. doi: 10.1007/s11033-020-05883-9

Liu, H., Li, S., Qiang, R., Lu, E., Li, C., Zhang, J., et al. (2022). Response of soil microbial community structure to phosphate fertilizer reduction and combinations of microbial fertilizer. *Front. Environ. Sci.* 10. doi: 10.3389/fenvs.2022.899727

Lu, H., Lashari, M. S., Liu, X., Ji, H., Li, L., Zheng, J., et al. (2015). Changes in soil microbial community structure and enzyme activity with amendment of biocharmanure compost and pyroligneous solution in a saline soil from Central China. *Eur. J. Soil Biol.* 70, 67–76. doi: 10.1016/j.ejsobi.2015.07.005

Lyu, D., Backer, R., Berrué, F., Martinez-Farina, C., Hui, J. P. M., and Smith, D. L. (2023). Plant growth-promoting rhizobacteria (PGPR) with microbial growth broth improve biomass and secondary metabolite accumulation of *Cannabis sativa* L. *J. Agric. Food Chem.* 71, 7268–7277. doi: 10.1021/acs.jafc.2c06961

Noureen, S., Iqbal, A., and Muqeet, H. A. (2024). Potential of drought tolerant Rhizobacteria amended with biochar on growth promotion in wheat. *Plants (Basel)* 13, 1183. doi: 10.3390/plants13091183

Ogran, A., Yardeni, E. H., Keren-Paz, A., Bucher, T., Jain, R., Gilhar, O., et al. (2019). The plant host induces antibiotic production to select the most-beneficial colonizers. *Appl. Environ. Microbiol.* 85, e00512–e00519. doi: 10.1128/AEM.00512-19

Olaniyan, F. T., Alori, E. T., Adekiya, A. O., Ayorinde, B. B., Daramola, F. Y., Osemwegie, O. O., et al. (2022). The use of soil microbial potassium solubilizers in potassium nutrient availability in soil and its dynamics. *Ann. Microbiol.* 72, 45. doi: 10.1186/s13213-022-01701-8

Pan, H., Yang, X., Chen, H., Sarkar, B., Bolan, N., Shaheen, S. M., et al. (2021). Pristine and iron-engineered animal- and plant-derived biochars enhanced bacterial abundance and immobilized arsenic and lead in a contaminated soil. *Sci. Total Environ.* 763, 144218. doi: 10.1016/j.scitotenv.2020.144218

Pan, X., Raaijmakers, J. M., and Carrión, V. J. (2023). Importance of Bacteroidetes in host-microbe interactions and ecosystem functioning. *Trends Microbiol.* 31, 959–971. doi: 10.1016/j.tim.2023.03.018

Park, Y. G., Mun, B. G., Kang, S. M., Hussain, A., Shahzad, R., Seo, C. W., et al. (2017). Bacillus aryabhattai SRB02 tolerates oxidative and nitrosative stress and promotes the growth of soybean by modulating the production of phytohormones. *PloS One* 12, e0173203. doi: 10.1371/journal.pone.0173203

Saeed, M., Ilyas, N., Jayachandran, K., Shabir, S., Akhtar, N., Shahzad, A., et al. (2022). Advances in Biochar and PGPR engineering system for hydrocarbon degradation: a promising strategy for environmental remediation. *Environ. pollut.* 305, 119282. doi: 10.1016/j.envpol.2022.119282

Singh, R. P., Pandey, D. M., Jha, P. N., and Ma, Y. (2022). ACC deaminase producing rhizobacterium Enterobacter cloacae ZNP-4 enhance abiotic stress tolerance in wheat plant. *PloS One* 17, 267127. doi: 10.1371/journal.pone.0267127

Smith, D. L., Praslickova, D., and Ilangumaran, G. (2015). Inter-organismal signaling and management of the phytomicrobiome. *Front. Plant Sci.* 6. doi: 10.3389/fpls.2015.00722

Sui, L., Tang, C., Cheng, K., and Yang, F. (2022). Biochar addition regulates soil phosphorus fractions and improves release of available phosphorus under freezing-thawing cycles. *Sci. Total Environ.* 848, 157748. doi: 10.1016/j.scitotenv.2022.157748

Sui, L., Tang, C., Du, Q., Zhao, Y., Cheng, K., and Yang, F. (2021). Preparation and characterization of boron-doped corn straw biochar: Fe (II). *J. Environ. Sci.* 106, 116–123. doi: 10.1016/j.jes.2021.01.001

Sun, C., Li, Q., Han, L., Chen, X., and Zhang, F. (2022). The effects of allelochemicals from root exudates of Flaveria bidentis on two Bacillus species. *Front. Plant Sci.* 13. doi: 10.3389/fpls.2022.1001208

Tan, C. L., Liu, Y., Huang, X. G., Zhang, J. Y., and Luo, W. H. (2022). Effect of biochar on soil microbial metabolic activities. *Chin. J. Eco-Agriculture.* 30, 333–342. doi: 10.12357/cjea.20210542

Tang, Z., Zhang, L., He, N., Liu, Z., Ma, Z., Fu, L., et al. (2022). Influence of planting methods and organic amendments on rice yield and bacterial communities in the rhizosphere soil. *Front. Microbiol.* 13. doi: 10.3389/fmicb.2022.918986

Urooj, N., Bano, A., and Riaz, A. (2022). Role of PGPR on the physiology of sunflower irrigated with produced water containing high total dissolved solids (TDS) and its residual effects on soil fertility. *Int. J. Phytoremediation.* 24, 567–579. doi: 10.1080/15226514.2021.1957771

Vejan, P., Abdullah, R., Khadiran, T., Ismail, S., and Nasrulhaq Boyce, A. (2016). Role of plant growth promoting rhizobacteria in agricultural sustainability-a review. *Molecules* 21, 573. doi: 10.3390/molecules21050573

Wang, L., Liu, H., Wang, F., Wang, Y., Xiang, Y., Chen, Y., et al. (2024). The different effects of molybdate on Hg(II) bio-methylation in aerobic and anaerobic bacteria. *Front. Microbiol.* 15. doi: 10.3389/fmicb.2024.1376844

Wang, P., Meng, G. Y., Mao, R. Z., Yang, K., Su, Z. H., Wang, Z. Q., et al. (2021). Soil physical and chemical properties, microorganisms and metabolites in different culture environments of Gastrodia elata. *Chin. J. Exp. Traditional Med. Formulae.* 14, 164–174. doi: 10.13422/j.cnki.syfjx.20210915

Wei, B., Peng, Y., Jeyakumar, P., Lin, L., Zhang, D., Yang, M., et al. (2023). Soil pH restricts the ability of biochar to passivate cadmium: A meta-analysis. *Environ. Res.* 219, 115110. doi: 10.1016/j.envres.2022.115110

Yang, L., Wu, Y., Wang, Y., An, W., Jin, J., Sun, K., et al. (2021). Effects of biochar addition on the abundance, speciation, availability, and leaching loss of soil phosphorus. *Sci. Total Environ.* 758, 143657. doi: 10.1016/j.scitotenv.2020.143657

Yin, S., Suo, F., Zheng, Y., You, X., Li, H., Wang, J., et al. (2022). Biochar-compost amendment enhanced sorghum growth and yield by improving soil physicochemical properties and shifting soil bacterial community in a coastal soil. *Front. Environ. Sci.* 10. doi: 10.3389/fenvs.2022.1036837

Zhang, X., Zhu, Y., Li, J., Zhu, P., and Liang, B. (2021). Exploring dynamics and associations of dominant lignocellulose degraders in tomato stalk composting. *J. Environ. Manage.* 294, 113162. doi: 10.1016/j.jenvman.2021.113162

frontiers | Frontiers in Plant Science

TYPE Original Research
PUBLISHED 20 December 2024
DOI 10.3389/fpls.2024.1500544

Check for updates

OPEN ACCESS

EDITED BY
Henry Yabbey Sintim,
The University of Georgia, United States

REVIEWED BY
Wenqing Zhao,
Nanjing Agricultural University, China
Nana Kusi,
South Carolina State University, United States

*CORRESPONDENCE
Ziting Wang
zitingwang@gxu.edu.cn

RECEIVED 23 September 2024
ACCEPTED 29 November 2024
PUBLISHED 20 December 2024

CITATION
Zhu R, He S, Ling H, Liang Y, Wei B, Yuan X, Cheng W, Peng B, Xiao J, Wei J, He Y, Xiao H and Wang Z (2024) Optimizing tobacco quality and yield through the scientific application of organic-inorganic fertilizer in China: a meta-analysis.
Front. Plant Sci. 15:1500544.
doi: 10.3389/fpls.2024.1500544

Optimizing tobacco quality and yield through the scientific application of organic-inorganic fertilizer in China: a meta-analysis

Ruixuan Zhu[1], Shijie He[1], Huarong Ling[1], Yongjin Liang[2], Beilei Wei[1], Xiaomai Yuan[1], Wuyang Cheng[2], Bo Peng[2], Jinglin Xiao[2], Jianyu Wei[2], Yi He[3], Heyou Xiao[4] and Ziting Wang[1,5]*

[1]College of Agriculture, University of Guangxi, Nanning, China, [2]Guangxi China Tobacco Industry Co., Ltd., Nanning, China, [3]Hunan China Tobacco Industry Co., Ltd., Changsha, China, [4]Hunan Shaoyang Tobacco Co., Ltd., Shaoyang, China, [5]China Key Lab for Conservation and Utilization of Subtropical Agri-Biological Resources, University of Guangxi, Nanning, China

China is the largest producer and consumer of tobacco (*Nicotiana tabacum* L.) in the world, and the cultivation and production of tobacco have extremely high economic value and social influence. Applying organic-inorganic fertilizer is a key strategy for boosting tobacco yield and quality. This meta-analysis examines 632 observations from 169 articles to determine the precise influence of organic-inorganic fertilizer on tobacco. It evaluates the effects of different tobacco types and fertilizer compositions on yield and quality after fertilizer application. The application of organic-inorganic fertilizer significantly increased the yield (3.4%), but it mainly improved the balance of chemical composition and enhance the quality of tobacco (high-grade tobacco, 10.3%; reducing sugar content, 5.5%; nicotine content, −5.6%). The Y85 and Y87 varieties showed the most positive response to fertilization, with yield increases of 5.59% and 5.82%, respectively, and high-grade tobacco leaf rates increased by 14.92% and 11.04%, respectively. Fertilizers with a low organic nitrogen ratio (15%-30%) are more effective for increasing yield, while those with a medium to high ratio (50%-60%) improve tobacco's chemical quality. The application of organic-inorganic fertilizer balanced the nutrient distribution within the tobacco plants, leading to simultaneous increases in both yield and quality. This study quantitatively assessed the effects of organic-inorganic fertilizer on the yield and quality of tobacco and provides a solid theoretical foundation for the scientific and high-quality application of organic-inorganic fertilizer in various tobacco cultivation areas.

KEYWORDS

tobacco, organic-inorganic fertilizer, meta-analysis, yield, quality

1 Introduction

Tobacco is one of the most important cash crops in China, and according to the World Health Organization (WHO), China is also the world's largest producer and consumer of tobacco (https://www.who.int/china/health-topics/tobacco). The cultivation area of tobacco in China had reached 1,000,520 ha by the end of 2022 (National Bureau of Statistics data, https://data.stats.gov.cn/). Meanwhile, India and Brazil, ranking second and third respectively, had cultivation areas of 450,000 ha (India Brand Equity Foundation, https://www.ibef.org) and 261,740 ha (Associação Brasileira dos Produtores de Tabaco, https://afubra.com.br). Therefore, improving the yield and quality of tobacco can create enormous economic benefits in China. Fertilizer is the material basis for increasing tobacco yield, and the rational application of fertilizer is an important measure for improving tobacco yield and quality (Wang et al., 2020). Modern agriculture is characterized by high input, high yield, and high efficiency (Xi et al., 2004), and high crop yields can be achieved with limited arable land and minimal manpower. Continuous and uncontrolled application of fertilizer has become a basic means to increase yield (Guo and Wang, 2021). However, excessive fertilizer use damages land resources, wastes fertilizer, and causes a chemical imbalance in tobacco leaves (Paramesh et al., 2023). The purpose of rational fertilization is not only to increase tobacco yield but also to improve the quality of tobacco leaves.

Organic fertilizer contains a large amount of organic material derived from organic waste, such as animal and plant remain after composting. Compared with inorganic fertilizer, organic fertilizer contains more trace elements and has the ability to regulate the soil structure and improve soil water conservation, fertility, and permeability (Lu et al., 2024; Shang et al., 2020), thereby promoting enzyme and microbial activity in soil. Moreover, the long-term application of organic fertilizer causes less damage to the environment compared with that of inorganic fertilizer (Ouyang et al., 2018). However, the application of organic fertilizers alone leads to a series of problems, such as slower fertilizer release, and in certain regions, higher costs compared to inorganic fertilizer (Panday et al., 2024). It also affects the normal growth and nutrient accumulation of tobacco plants. Therefore, the use of organic-inorganic fertilizer has shown a significant development trend (Yang et al., 2023). Studies have shown that organic-inorganic fertilizer can combine the advantages of organic and inorganic fertilizers thereby improving the yield and quality of tobacco (Bilalis et al., 2010). The correlation between yield increase and quality improvement in tobacco has not been fully established, which may be influenced by numerous factors, including the fertilizer type, chemical composition, and tobacco variety. Gaining a deeper understanding of the relationship between yield increase and quality improvement under the application of organic-inorganic fertilizer is conducive to the continuous and stable increase in the yield, quality, and economic benefits of tobacco crops.

The organic-nitrogen ratio in organic-inorganic fertilizer significantly impacts the fertilization effects on tobacco. A nutrient release rate corresponding to a 25% organic-nitrogen ratio in the fertilizer aligns with the tobacco plant's growth and development requirements. This alignment is beneficial for enhancing the agronomic indicators, yield, and quality of tobacco, as well as for coordinating the chemical composition within tobacco leaves. However, if the organic nitrogen ratio is too high, the organic-inorganic fertilizer may negatively affect the yield and quality of tobacco. The variety of tobacco is also an important factor that affects the yield of tobacco, and some varieties may show higher yield potential in specific environments because of their genetic characteristics (Tan et al., 2012). Additionally, the variety also affects the chemical composition of tobacco, such as nicotine content, total nitrogen content, reducing sugar, K content, among others (Ma et al., 2018), which directly determine the quality and taste of tobacco (Abubakar et al., 2000; Chen et al., 2017). China has a vast territory, and different planting areas plant different varieties according to their climate and environmental conditions (Sun et al., 2016). Therefore, establishing the quantitative relationship between varieties and changes in tobacco yield and chemical quality after the application of organic-inorganic fertilizer will help tobacco farmers choose the correct organic-inorganic fertilizer to suit their needs.

Several basic field experiments have been carried out in different tobacco planting areas in China to study the different effects of organic-inorganic fertilizer on tobacco. The experiment results of Li et al. (2015) reported that the use of organic-inorganic fertilizer increased the yield (11.4%), output value (18.3%), and high-grade tobacco rate (11%) of the Y97 variety compared with the application of inorganic fertilizer alone, and the authors suggested that the application of organic-inorganic fertilizer with organic-nitrogen ratio of 25-50% was more conducive to the growth and development of tobacco and improved the yield and quality. Ma et al. (2013) found that the application of organic-inorganic fertilizer significantly increased the total sugar content (27.86%), the reducing sugar content (23.00%), sugar-to-nicotine ratio (72.60%), nitrogen-nicotine ratio (22.66%), and K content (6.21%) in tobacco leaves but reduced the total nitrogen content (5.29%) and nicotine (-27.21%), thus leading to a more balanced chemical composition. However, owing to the great differences in climatic conditions, soil physicochemical properties and field management measures in different regions, the experimental results obtained from different studies are inconsistent. To achieve production goals, a suitable organic-inorganic fertilizer ratio scheme should be formulated according to the chemical composition requirements, tobacco varieties, and other factors before planting and fertilization.

Therefore, our study performed a meta-analysis of 169 peer-reviewed studies to (1) identify the specific effects of organic-inorganic fertilizer on tobacco yield and chemical components in tobacco leaves; (2) determine how different tobacco varieties and fertilizer components alter the effects of organic-inorganic fertilizer on tobacco; and (3) reveal the impact of applying organic-inorganic fertilizer on the balance between tobacco yield and quality. This

Abbreviations: PS, Planting Site; AAP, Annual Average Precipitation; AAT, Annual Average Temperature; AAS, Annual Average Sunshine; PD, Planting Density; TV, Tobacco Variety; AP, Available Phosphorus; AN, Available Nitrogen; OMC, Organic Matter Content; AK, Available Potassium; Cl, Chloride; K, Potassium; K326, Y85, Y87, Y97: Tobacco Varieties.

study provides a scientific theoretical reference for improving the fertilization regime of tobacco.

2 Materials and methods

2.1 Data collection

We searched relevant articles published between 1990-2023 from the China National Knowledge Infrastructure and Web of Science. The search keyword included "flue-cured tobacco" or "tobacco" and "organic fertilizer" or "inorganic fertilizer" and "yield" or "quality" or "chemical composition". According to the data requirements of the meta-analysis and the purpose of this study, articles were screened using the following criteria: (1) tests in the article should include the application of inorganic fertilizer alone and organic-inorganic fertilizer for comparison; (2) the test materials and environmental background of the test sites should be described (the test sites are located in China); (3) the test results should include the mean and standard deviation of indicators, as these parameters are essential for meta-analysis. (4) the fertilizer treatment section should include the organic-nitrogen ratio; and (5) only one article from the same study can be selected. After screening and evaluation, 169 articles were finally obtained for follow-up analysis.

2.2 Data categorization and treatment

For each study, we extracted the mean, standard deviation and sample size of tobacco yield, high-grade tobacco rate, output value, total nitrogen content, nicotine content, reducing sugar content, K content and Cl content (the chemical compositions come from the middle leaves of tobacco). These tobacco indicators are the primary subjects of study in Chinese research, reflecting the key aspects of tobacco yield and quality. Extract the mean and standard deviation directly from the article's tables; use Origin 2023 to extract them from figures; and if only the mean is provided, calculate the standard deviation based on other parameters reported. The following relevant information was collected for analysis: climate conditions (planting site,average annual precipitation, average annual temperature, and average annual sunshine), soil conditions (pH, organic matter content, available nitrogen content, available phosphorus content, and available potassium content), field management measures (planting density, type of organic fertilizer, and organic-nitrogen ratio in mixed fertilizer), and tobacco varieties (K326, Y85, Y87, Y97, and others). A total of 632 sets of observations were selected from drawings and graphs in the 169 articles (Supplementary Figure S4). Rosenthal's fail-safe number was calculated to test publication bias in the studies, if its coefficient >5n + 10 (n is the sample size), then the variable had no publication bias (Supplementary Table S1). The location distribution of each experiment in the meta-analysis is shown in Figure 1.

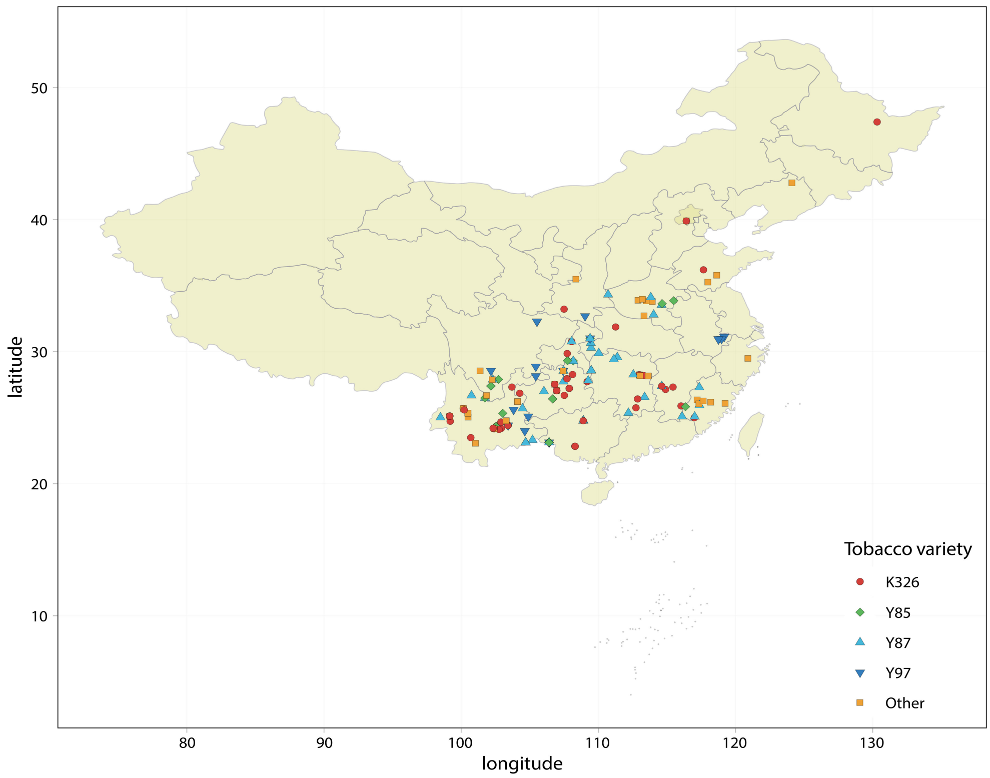

FIGURE 1
Geographical distribution in China of the tests collected in the meta-analysis.

2.3 Data analysis

Meta-analysis is a quantitative analysis method that summarizes the results of several relatively independent similar studies and draws conclusions (Nakagawa et al., 2023). To better study the effects of organic-inorganic fertilizer on the yield and chemical composition of tobacco and determine the different influences of other factors on the fertilizer's effects, we performed a meta-analysis of the data in the database and used the log response ratio (lnRR) as the statistical effect value indicator (Gurevitch et al., 2018). Individual lnRRs for each observation were calculated using Equation 1:

$$\ln RR = \ln \frac{Y_e}{Y_c} \quad (1)$$

where Ye and Yc represent the mean values of the treatment and control groups, respectively.

Owing to the large spatiotemporal span of the data in this study and the great differences in planting methods, climate conditions, soil physical-chemical properties in different regions, random effect model (REM) was selected for calculation. The meta-analysis weighted the log response ratio of each observation to obtain the variance (V), weighted factor (Wi), weighted log response ratio (lnRR++), and standard deviation of the weighted log response ratio (SD). They can be calculated using Equations 2–5:

$$V = \frac{SD_e^2}{N_e Y_e^2} + \frac{SD_c^2}{N_c Y_c^2} \quad (2)$$

where N_e nd N_c represent the sample sizes of the treatment and control groups, respectively; and SDe and SDc represent standard deviation for the treatment and control groups, respectively.

$$W_i = 1/\,(V + \tau^2) \quad (3)$$

$$\ln RR_{++} = \frac{\sum_{i=1}^{k} W_i \ln RR}{\sum_{i=1}^{k} W_i} \quad (4)$$

$$SD = \left(\frac{1}{\sum_{i=1}^{k} W_i} \right)^{1/2} \quad (5)$$

where i represent the i-th treatment, and k represent the number of observations. τ^2 represent the variance between studies due to different studies. Positive values of $\ln RR_{++}$indicated that the variable increased after the application of organic-inorganic fertilizer, and vice versa.

Equation (6) was used to calculate the 95% confidence interval (CI) of $\ln RR_{++}$. If the 95% CI did not contain 0, then the application of organic-inorganic fertilizer has a significant impact on this indicators (Du et al., 2020).

$$95\,\%\,CI = \ln RR_{++} \quad 1.96 * SD \quad (6)$$

To perceive the rate of change more clearly, $\ln RR_{++}$ and its 95% CI were transformed back to the percentage change, as shown in Equation 7.

$$E = \exp(\ln RR_{++}) * 100\,\% - 1 \quad (7)$$

Data processing and statistical analysis for the meta-analysis were performed using R version 4.3.1 by package "metafor" (Viechtbauer, 2010). Random forest analysis was carried out using the "rfPermute" package in R software, and all images were drawn using the "ggplot2" package in R software. Correlation analysis was performed to examine the pairwise relationships between the $\ln RR_{++}$ of the indicators. Optimal model regression analysis was performed to explain the influence of fertilizer composition on the effect of organic-inorganic fertilizer and the relationship between yield and quality of tobacco. The omnibus test (Qm-test) was used to compare the response of indicators to application of organic-inorganic fertilizer among different subgroups. If the p-value of Qm< 0.05, it suggested a significant effect of this factor on the overall effect (Supplementary Table S2).

3 Result

3.1 Overall effect of organic-inorganic fertilizer on tobacco

After performing an overall analysis of the 632 sets of data from all 169 studies, we found that the application of organic-inorganic fertilizer significantly increased the yield of tobacco leaves (3.4%), output value (10.1%), high-grade tobacco rate (10.3%), K content (3.76%), and reducing sugar content (5.5%) and significantly decreased the nicotine content (-5.6%) compared with inorganic fertilizer alone (Figure 2). However, significant changes were not observed in the Cl or total nitrogen content in tobacco leaves. From the network correlation analysis of indicator $\ln RR_{++}$, the output value (R=0.796, p<0.01), high-grade tobacco rate (R=0.234, p<0.01), total nitrogen content (R=0.177, p<0.01) and K content (R=0.168, p<0.01) in tobacco leaves was strongly positively correlated with yield. Notably, total nitrogen content and reducing sugar content had significant negative correlations (R=-0.214, p<0.01).

3.2 Effect of fertilizer composition on the application of organic-inorganic fertilizer

We collected the organic-nitrogen ratio and the amount of total nitrogen in fertilizers used in different experiments and performed regression analysis of the optimal model with indicators lnRR. As shown in Supplementary Figure S1 within the range of total nitrogen collected in the study (0-116 kg/hm^2), the high-grade tobacco rate (p=0.013) and reducing sugar content (p=0.030) in tobacco leaves increased regardless of the total nitrogen, whereas the nicotine content (p=0.087) decreased. The tobacco yield (p<0.001) and output value (p<0.001) only when the amount of total nitrogen exceeded 30 kg/hm^2. In particular, when the amount of total nitrogen was 50-60 kg/hm^2, the application of organic-inorganic fertilizer effectively improved the yield, output value and high-grade tobacco rate of tobacco, reduced the nicotine content and increased the content of some chemical components.

For the yield (p<0.001) and output value (p<0.001) of tobacco, within the range of organic-nitrogen ratio collected in the study (7-100%), their lnRR decreased as the organic-nitrogen ratio increased compared with inorganic nitrogen application alone, and the change of Cl content (p=0.003) was similar to yield (Figure 3). Notably, the tobacco yield decreased when the organic-nitrogen ratio exceeded 50%. Regarding the chemical indicators in tobacco leaves, we found that nicotine content (p=0.043) and total nitrogen content (p=0.023) decreased as the organic-nitrogen ratio increased. The reducing sugar (p=0.015) and K content (p=0.089) increased regardless of the organic-nitrogen ratio. When the organic-nitrogen ratio in fertilizer was in the range of 50-60%, the reducing sugar and K content showed the greatest increase, and the nicotine content also decreased significantly after fertilization.

3.3 Influence significance of subgroups on the application of organic-inorganic fertilizer

We analyzed the influence significance of various factors on the application of organic-inorganic fertilizer, including climatic conditions (planting site, annual average precipitation, annual average temperature, and annual average sunshine), soil conditions (pH, organic matter content, available nitrogen content, available phosphorus content, and available potassium content), planting density and tobacco varieties (Supplementary Figure S2). Contrary to our initial expectations, climatic factors had a relatively low impact on the effectiveness of organic-inorganic fertilizer; they were not the primary determinants. In contrast, soil factors showed a more pronounced influence on the application of organic-inorganic fertilizer, with significant differences observed in tobacco yield, high-grade tobacco rate, nicotine content, and total nitrogen content under varying soil conditions. Notably, among the various factors assessed, planting density and tobacco varieties exerted the most significant influence on the application effects of organic-inorganic fertilizer.

3.4 Effects of varieties on the application of organic-inorganic fertilizer

Four main tobacco varieties (K326, Y85, Y87 and Y97) that have been frequently studied and cultivated in China were selected and analyzed in this study. The yield and quality of K326 tobacco showed a weak in response to organic-inorganic substances, only K content was significantly increased (6.67%, p<0.001). Y85 and Y87 were closely related, their yield (5.59%, p<0.001; 5.82%, p<0.001), high-grade tobacco rate (14.92%, p<0.001; 11.04%, p<0.001), output value (11.94%, p<0.001; 10.78%, p<0.001) and reducing sugar content (4.25%, p<0.05; 5.82%, p<0.001) were significantly increased after applying organic-inorganic fertilizer. For Y97 tobacco, yield (4.03%, p<0.05), high-grade tobacco rate (5.94%, p<0.001), output value (5.71%, p<0.01), K content (5.46%, p<0.05) and total nitrogen content (6.06%, p<0.01) were all significantly increased after applying organic-inorganic fertilizer (Figure 4).

Regression curves were constructed for the organic nitrogen ratio and indicators lnRR for the four main varieties. For K326, the results showed that organic-inorganic fertilizer with an organic nitrogen ratio below 50% slightly increased the yield (p<0.001), value (p<0.001), and the rate of high-grade tobacco leaves (p=0.013) of K326 tobacco. When the organic nitrogen was about 50%, the K content significantly increased (p=0.083, Figure 5). For Y85, yield (p<0.001) and output value (p<0.001) were increased when the organic-nitrogen ratio was less than 80%. Moreover, nicotine content (p<0.001) and total nitrogen content (p<0.001) in Y85 tobacco were significantly affected by the organic-nitrogen ratio.

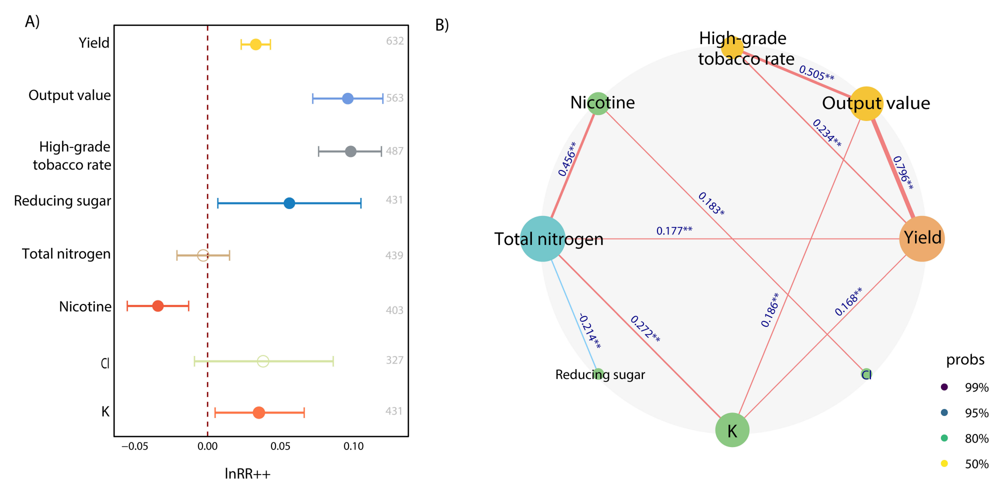

FIGURE 2
(A) Overall effect of organic-inorganic fertilizer on yield and quality of tobacco. The x-axis represents the $lnRR_{++}$ of the indicators. Error bars represent the 95% confidence intervals. Solid circles represent significant effects and hollow circles indicate insignificant. The Arabic numerals on the right indicate the sample size of an indicator. **(B)** Network correlation analysis of indicator $lnRR_{++}$. The numbers on the horizontal axis represent the correlation coefficient. Significant levels at *p< 0.05 and **p< 0.01.

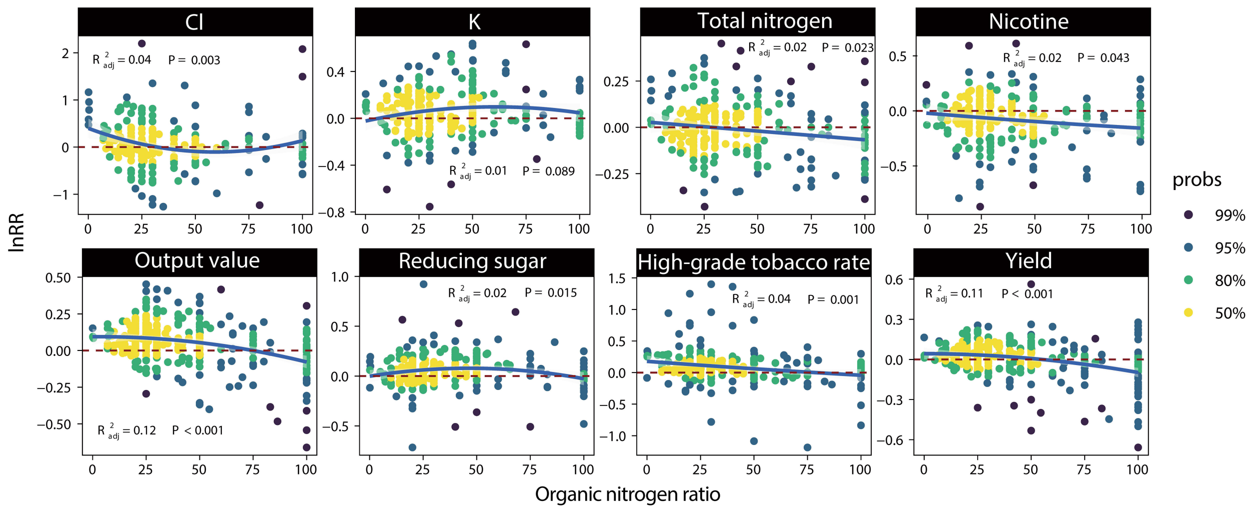

FIGURE 3
Regression curve of indicators lnRR and organic-nitrogen ratio in fertilizer. Different colored points represent the density of the observed distribution. R^2_{adj} represent the fitting precision of this regression curve, and p represent the significance of the curve.

The higher the organic-nitrogen ratio, the greater the reduction in nicotine and total nitrogen (Figure 5).

3.5 Relationship between yield and quality of different tobacco varieties after applying organic-inorganic fertilizer

As shown in Figure 6, among the four varieties, K326 and Y87 showed strong correlations with each indicator while Y85 showed the weakest correlations. The output value of all varieties was positively correlated with the yield (p<0.01), high-grade tobacco rate (p<0.01), and the total nitrogen content was positively correlated with the nicotine content (p<0.01). Reducing sugar content was positively correlated with yield (R=0.166, p<0.05), output value (R=0.095, p<0.05), and high-grade tobacco rate (R=0.071, p<0.05) in K326 tobacco.

The yield of Y85 was positively correlated with the K content (R=0.319, p<0.05), and the K content was positively correlated with the reducing sugar content (R=0.333, p<0.05). In Y87, increase in the K content significantly increased the high-grade tobacco rate (R=0.309, p<0.01).

Figure 7; Supplementary Figure S3 show the regression relationship between yield and other indicators of four varieties after applying organic-inorganic fertilizer. With an increase of yield, the

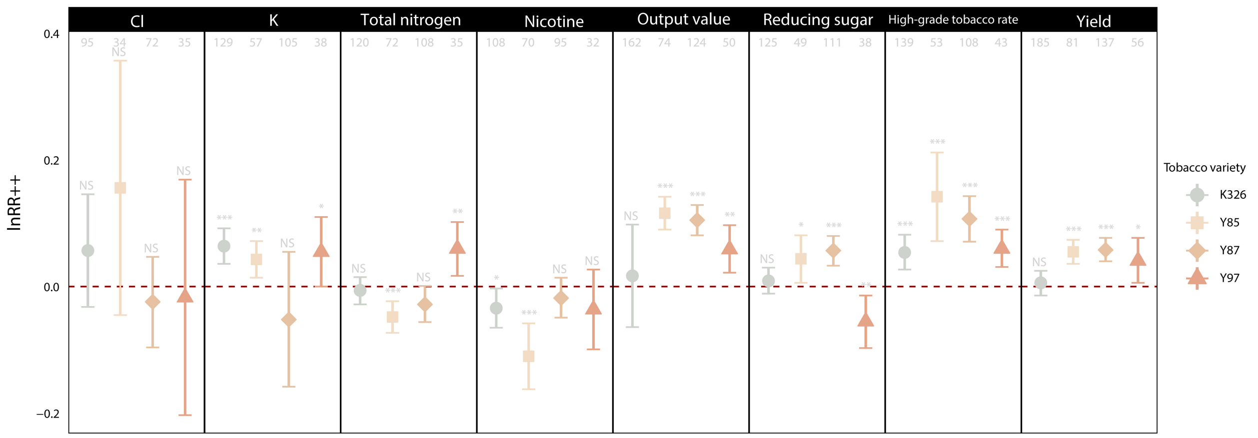

FIGURE 4
Overall effect of organic-inorganic fertilizer on yield and quality of different varieties tobacco. The y-axis represents the $lnRR_{++}$ of the indicators. Error bars represent the 95% confidence intervals. Significant levels at NS p>0.05, *p< 0.05, **p< 0.01 and ***p< 0.001.The Arabic numerals on the top indicate the sample size of an indicator.

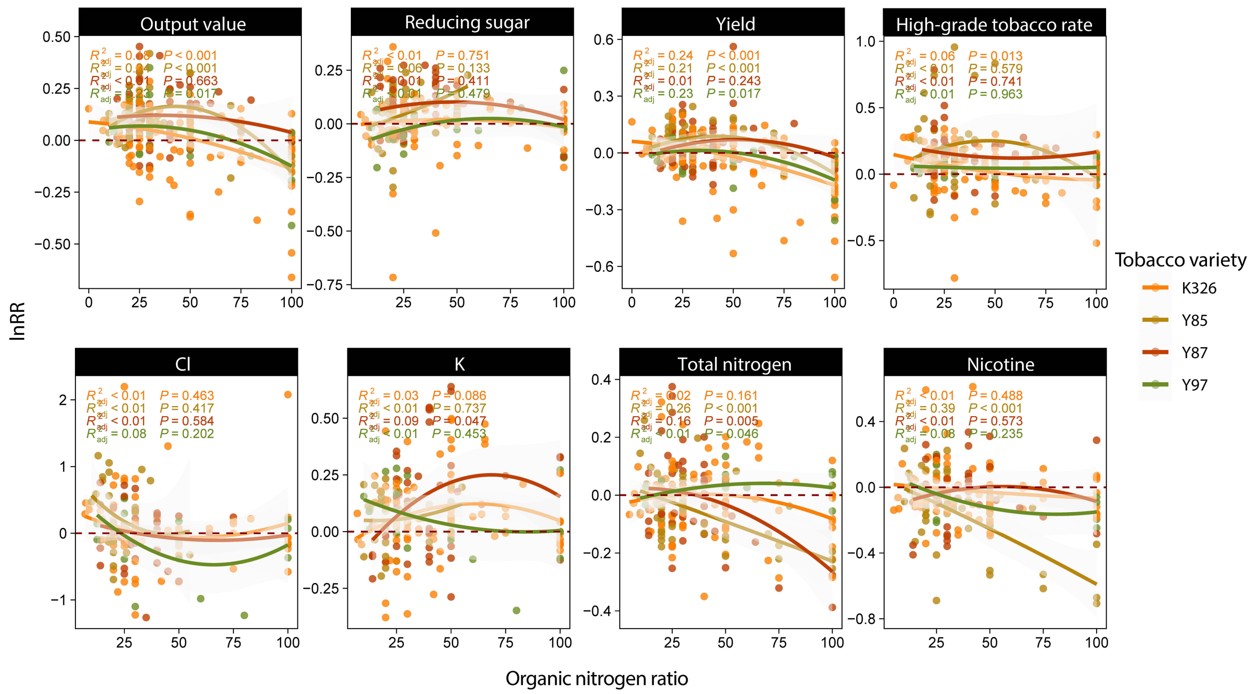

FIGURE 5
Regression curve of indicators lnRR and organic-nitrogen ratio of different varieties tobacco. The points and curves of different colors represent tobacco varieties. R^2_{adj} represent the fitting precision of this regression curve, and p represent the significance of the curve.

high-grade tobacco rate (p<0.001, p=0.038, p=0.005, p=0.047) and output value (p<0.001, p<0.001, p<0.001, p<0.001) of the four varieties increased. Organic-inorganic fertilizer application can simultaneously improve yield and quality. However, except for K326, the curve between the high-grade tobacco rate and yield of the other three varieties is similar to a parabola, which means that the increase in the high-grade tobacco rate become declined when the yield increased to a certain extent and even had a negative effect. In Y85, K content (p=0.010) and reducing sugar content (p=0.045) increased while the total nitrogen (p=0.045) and nicotine (p<0.001) content significantly decreased as the yield increased (Supplementary Figure S3).

4 Discussion

4.1 Effects of application of organic-inorganic fertilizer on tobacco yield and quality

We found that the yield, output value and high-grade tobacco rate of tobacco were significantly increased after applying organic-inorganic fertilizer, and the increase in yield also affected the increase in output value and high-grade tobacco rate (Figure 2A). Tobacco has strict nitrogen requirements at different growth stages (Rosa et al., 2006). In the early growth stage, sufficient nitrogen is required to maintain the full growth of tobacco until flowering, and a high nitrogen supply is not subsequently required. The application of inorganic fertilizer alone provided nutrients required by tobacco in the early stage. Compared with inorganic fertilizer, the release of nutrients in organic fertilizer is slower (Peng et al., 2014). Therefore, the application of organic-inorganic fertilizer can provide tobacco with an appropriate nutrient supply during the entire growth and development period, thereby ensuring the nutrient absorption and growth of tobacco. Moreover, organic fertilizer can improve the plant root environment, enrich the types of soil microorganisms, enhance the activity of soil extracellular enzymes (Jiang et al., 2022), and improve the content of nutrient element in the soil, which contributes to an increase in the tobacco yield and high-grade tobacco rate. However, compared with the increase of output value and high-grade tobacco rate, the increase of yield was small, indicating that the main effect of the application of organic-inorganic fertilizer on tobacco was not to increase yield but to improve the quality of tobacco (Figure 2A).

Superior quality tobacco exhibits a balance and coordination between carbohydrates and nitrogen compounds (Banožić et al., 2020). Compared with inorganic fertilizer alone, the application of organic-inorganic fertilizer significantly increased the reducing sugar content in tobacco (Figure 2A). Organic -inorganic fertilizer can improve soil invertase activity (Song et al., 2022), and the invertase in the rhizosphere soil of tobacco can split disaccharides, increase the available carbon content in the soil, and promote the tobacco to absorb and use carbon to synthesize carbohydrates. Meanwhile, the application of organic fertilizer brought a large amount of humic acid to the soil (Li et al., 2008). Humic acid can affect the physiological metabolism of tobacco by promoting root growth and nutrient absorption, thereby increasing the accumulation of reducing sugar content (Ampong et al., 2022). Organic-inorganic fertilizer also reduced nicotine content in

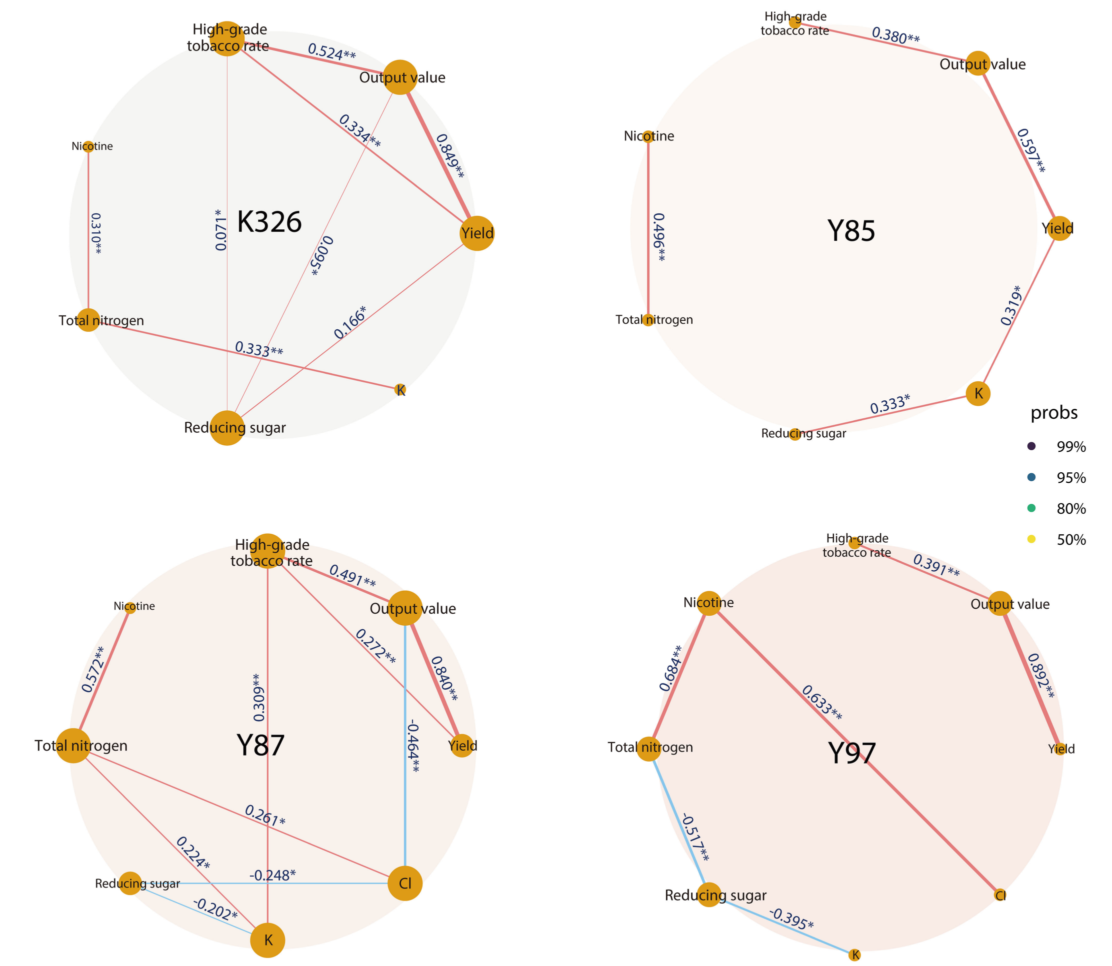

FIGURE 6
Network correlation analysis of $lnRR_{++}$ of indicators of different tobacco varieties. The numbers on the horizontal axis represent the correlation coefficient. Significant levels at *p< 0.05, **p< 0.01 and ***p< 0.001.

tobacco (Figure 2A), and increased the sugar-to-nicotine ratio, which shifted the sugar-to-nicotine ratio to the high-quality range. The application of organic-inorganic fertilizer improved the situation of excessive N supply from inorganic fertilizer and slow N supply from organic fertilizer, making the N supply from fertilizer more stable and lasting. Nicotine and total nitrogen were positively correlated in the tobacco plants (Figure 2B), thereby, adjusting the nitrogen was also conducive

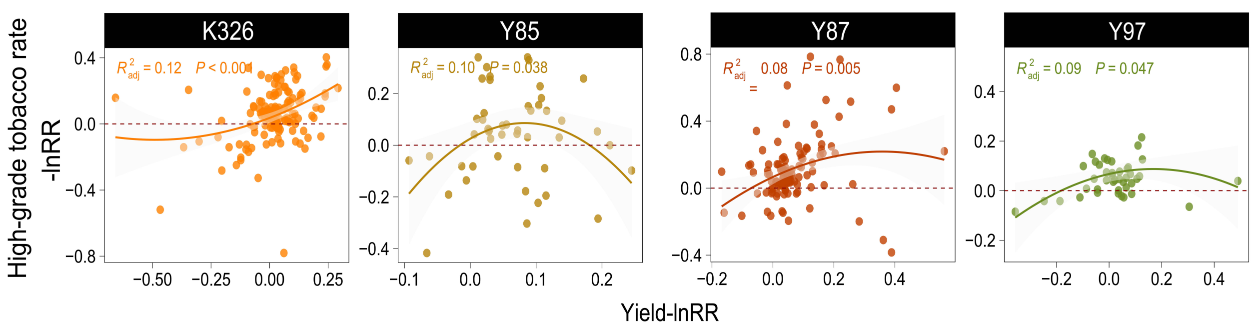

FIGURE 7
Regression curve between yield of lnRR different varieties and high-grade tobacco rate lnRR. The points and curves of different colors represent tobacco varieties. R^2_{adj} represent the fitting precision of this regression curve, and p represent the significance of the curve.

to the decrease of nicotine content (Liu et al., 2020; Fu et al., 2016). In general, organic-inorganic fertilizer has been found to harmonize the carbon-nitrogen relationship in tobacco and enhance tobacco quality.

4.2 Effect of fertilizer composition on yield and quality of tobacco

As mentioned above, the absorption of organic and inorganic fertilizers by tobacco is related to different growth periods. Therefore, if the organic-nitrogen ratio in organic-inorganic fertilizer is unbalanced, the content of available nitrogen in the soil during the early stages will be lower and the yield will be reduced (Suchoff et al., 2020; Xi et al., 2005). we found that organic-inorganic fertilizer with low organic-nitrogen ratio could increase tobacco yield, and when the organic-nitrogen ratio exceeded 50%, organic-inorganic fertilizer would reduce tobacco yield (Figure 3). The organic-nitrogen ratio can affect tobacco yield by controlling the synthesis and degradation of chlorophyll in leaves. Organic-inorganic fertilizer with 15%-30% organic nitrogen increases the chlorophyll content of tobacco leaves in the early growth stage, ensuring the normal degradation of chlorophyll in the later stage, and show normal yellowing maturation, which enhances the photosynthetic rate and promote the accumulation of tobacco dry matter, thereby helping to increase the yield of tobacco leaves. Whereas when organic nitrogen is more than 45%, the chlorophyll cannot be degraded normally at maturity, thus causing late ripening of tobacco and reducing the yield (Zhou et al., 2009). The yield and output value required the amount of total nitrogen to exceed 30 kg/hm^2 to increase in Supplementary Figure S1, which also confirms our thesis.

When the ratio of organic nitrogen was within the range of 50-60% and the amount of total nitrogen was controlled within 50-60 kg/hm^2, organic-inorganic fertilizer had the best effect on coordinating the chemical composition (Supplementary Figures S1, 3). At this ratio, organic-inorganic fertilizer can enhance the C metabolism in the sugar accumulation period and effectively regulate the N metabolism of tobacco (Tang et al., 2010), which is conducive to the coordinated development of carbon and nitrogen and the improvement of quality of tobacco. Liu et al. (2018) also found that when the organic nitrogen substitution ratio was 50%, the abundance of beneficial bacteria in soil could be maximized. These beneficial bacteria not only participate in the decomposition of soil organic matter and also accelerate the soil nitrogen cycle (Meng et al., 2022), but also directly carry out biological nitrogen fixation, carbon fixation, oxygen increase and perform other physiological activities to improve soil fertility (Álvarez et al., 2023). Beneficial bacteria help tobacco roots to better absorb and utilize nutrients and coordinate the chemical composition of tobacco leaves. In summary, we believe that the ratio of organic nitrogen applicable to increasing yield and coordinating chemical composition of tobacco is different. Only a small ratio of organic nitrogen can achieve a good yield-increasing effect, whereas a higher ratio of organic nitrogen is required to improve the chemical composition. This finding may play a guiding role in the scientific fertilization of tobacco and improving its economic benefits.

4.3 Effects of application of organic-inorganic fertilizer on yield and quality of different tobacco varieties

Different tobacco varieties responded differently to the application of organic-inorganic fertilizer. The effect was the best in Y85 and Y87 varieties, followed by Y97, and was least effective in K326 (Figures 4, 5, 7). This variation is mainly attributed to differences in growth habits, genetic characteristics, root distribution, and nutrient requirements. K326 is widely planted in various regions of China (Figure 1). Observations of the microstructure of the tobacco leaf tissues and stomata showed that K326 had a balanced leaf thickness, tissue, and stomatal structure and good ecological adaptability, making it suitable for planting in most environments. Our study suggests that K326 can absorb sufficient nutrients for normal growth and development even with less effective fertilizers because of its good adaptation and resilience (Zhou, 2005; Pandey et al., 2021). Therefore, the yield and most chemical components of this variety did not change significantly after the application of organic-inorganic fertilizer, while only the K content in tobacco leaves increased significantly. Organic-inorganic fertilizer can promote the synthesis of more K in tobacco. The K content of K326 was approximately 2%, higher than that of the other varieties. More nutrients related to K synthesis need to be absorbed during growth and development (Luo et al., 2014). Consequently, the K content of K326 increased significantly after the application of organic-inorganic fertilizer, with an organic-nitrogen ratio of approximately 50% being particularly beneficial for enhancing K content in K326 (Figure 7). The yield and output value of Y85 and Y87 responded positively to organic-inorganic fertilizer (Figure 4). Chen et al., 2024 found that the leaf growth and dry matter accumulation rate of Y87 and Y85 were slower than those of K326 and other varieties. Thus, the application of organic-inorganic fertilizer is particularly beneficial for accelerating yield formation in these varieties. Compared with Y87, total nitrogen content and nicotine content in Y85 were more affected by organic-inorganic fertilizer (Figure 4). Total nitrogen and nicotine contents decreased significantly and continued to decline with an increasing proportion of organic nitrogen. Nicotine content in roasted tobacco leaves can neutralize the acidic substances produced by the burning of carbohydrates, which is conducive to the formation of a good taste (Sun et al., 2012), but when its content exceeds a certain range, it will have a certain negative impact on the taste (Wu and Wang, 2010). The nicotine content in Y85 tobacco leaves was higher compared to other varieties (Wu et al., 2010). The application of organic-inorganic fertilizer can reduce the nicotine content to a certain extent, which is helpful to improve the sensory quality of this variety. In conclusion, the application of organic-inorganic fertilizer significantly increased the K content of K326, improved the yield and quality of Y87 and Y85, effectively reduced the total nitrogen content and nicotine content of Y85 tobacco leaves, and coordinated the chemical composition of Y85 better.

4.4 Relationship between yield and quality of tobacco after applying organic-inorganic fertilizer

Due to the limited nutrients within crop, increasing crop yield and improving crop quality are two aspects that are closely related but contradictory. The high-grade tobacco rate is the ratio of tobacco leaves rated as superior relative to the total number of tobacco leaves. This parameter comprehensively considers the agronomic indicators, chemical quality, and sensory quality of tobacco, and its level directly reflects the quality of the tobacco. We found that after the application of organic-inorganic fertilizer, the yield and high-grade tobacco rate of the four tobacco varieties increased to different degrees (Figure 4). However, the high-grade tobacco rate does not continue to increase with an increase in yield, and when the yield increase reaches a certain value, the increase in high-grade tobacco rate begins to decline. When the yield is too high, plants use more energy and nutrients for the growth of stems and leaves, thus ignoring the formation of tobacco quality substances (Raza et al., 2017). Wang et al. (2009) also found that the relationship between tobacco yield and quality was similar to a parabola. When the yield ranged from 2040 kg/hm^2 to 2 775 kg/hm^2, the quality of tobacco increased; however, after the yield exceeded 2775 kg/hm^2, the quality of tobacco leaves began to deteriorate.

The K and reducing sugar content in Y85 were positively correlated with the yield (Figure 6), and they both increased with an increase in yield (Supplementary Figure S3). This is consistent with our expectations, because the essence of the increase in tobacco yield is that the leaves become larger and thicker, and the leaf area increases, which is more conducive to the photosynthesis. Photosynthesis is the main method of accumulating carbohydrates in plants, and an increase in photosynthesis increase the reducing sugar content (Muhie, 2022). K participates in the movement of leaves and stomata and is an important cation that promotes the synthesis and transportation of photosynthetic and assimilation products. K deficiency will enhance stomatal and mesophyll resistance, and reduce the absorption of CO^2 at the leaf surface (Hafsi et al., 2014; Ho et al., 2020; Lu et al., 2019). Therefore, an increase in yield must be accompanied by an increase in photosynthesis, K content and reducing sugar content in Y85 tobacco leaves. Bilalis et al. (2015) found that plants need more nutrients to be transported to the leaves when the tobacco yield increases, which leads to the redistribution of some nutrients and the removal of some alkaloid substances from the roots. Total nitrogen and nicotine in the tobacco leaves may be reduced or transferred to other parts of the tobacco plant. This is consistent with the results of the present study, in where we found that an increase in yield led to a significant decrease in total nitrogen in Y85 tobacco leaves and a decrease in nicotine content (Supplementary Figure S3). In conclusion, organic-inorganic fertilizer has the potential to coordinate the distribution of nutrients within tobacco plants and simultaneously improve yield and quality. However, further research is needed to achieve this goal.

5 Conclusions

Our meta-analysis results showed that although the application of organic-inorganic fertilizer improved the yield of tobacco, the main effect was to improve the balance of the chemical composition and improve the quality of tobacco. Second, by analyzing the effects of organic-inorganic fertilizer components on the application effect, we concluded that organic-inorganic fertilizer with a low ratio of organic nitrogen (15–30%) was more beneficial for increasing tobacco yield while fertilizer with a medium and high ratio of organic nitrogen (50–60%) had a better effect on improving tobacco chemical quality. Application of organic-inorganic fertilizer had the best effect on Y85 and Y87 and improved the yield and quality, and it also effectively reduced the total nitrogen and nicotine content of Y85 tobacco leaves. It had the worst effect on K326, which only showed an increase in the K content. This study also concluded that organic-inorganic fertilizer simultaneously increased the yield and high-grade tobacco rate of the four main varieties under certain conditions. Moreover, organic-inorganic fertilizer also increased the reducing sugar and K content, reduced the nicotine content in Y85 while increasing the yield.

Data availability statement

The raw data supporting the conclusions of this article will be made available by the authors, without undue reservation.

Author contributions

RZ: Writing – original draft, Writing – review & editing. SH: Writing – original draft, Writing – review & editing. HL: Writing – original draft, Writing – review & editing. YL: Writing – original draft. BW: Writing – original draft, Writing – review & editing. XY: Writing – original draft, Writing – review & editing. WC: Funding acquisition, Writing – original draft. BP: Funding acquisition, Writing – original draft. JX: Funding acquisition, Writing – original draft. YH: Funding acquisition, Writing – original draft. HX: Funding acquisition, Writing – original draft. JW: Funding acquisition, Writing – original draft, Writing – review & editing. ZW: Writing – original draft, Writing – review & editing.

Funding

The author(s) declare financial support was received for the research, authorship, and/or publication of this article. This work was supported by the Guangxi China Tobacco Industry Co., LTD. Industry-university-research cooperation project (GXZYCX2023B005).

Acknowledgments

We appreciate all of the researchers whose data were used in this meta-analysis. This work was supported by the National Natural Science Foundation of China (32260546).

Conflict of interest

Authors YL, WC, BP, JX, and JW were employed by Guangxi China Tobacco Industry Co., Ltd. Author YH was employed by Hunan China Tobacco Industry Co., Ltd. Author HX was employed by Hunan Shaoyang Tobacco Co., Ltd.

The remaining authors declare that the research was conducted in the absence of any commercial or financial relationships that could be construed as a potential conflict of interest.

Publisher's note

All claims expressed in this article are solely those of the authors and do not necessarily represent those of their affiliated organizations, or those of the publisher, the editors and the reviewers. Any product that may be evaluated in this article, or claim that may be made by its manufacturer, is not guaranteed or endorsed by the publisher.

Supplementary material

The Supplementary Material for this article can be found online at: https://www.frontiersin.org/articles/10.3389/fpls.2024.1500544/full#supplementary-material

References

Abubakar, Y., Young, J. H., Johnson, W. H., and Weeks, W. W. (2000). Changes in moisture and chemical composition of flue-cured tobacco during curing. *Tob Sci.* 44, 51–58. doi: 10.3381/0082-4623-44.1.51

Álvarez, C., Jiménez-Ríos, L., Iniesta-Pallarés, M., Jurado-Flores, A., Molina-Heredia, F. P., Ng, C. K. Y., et al. (2023). Symbiosis between cyanobacteria and plants: from molecular studies to agronomic applications. *J. Exp. Bot.* 74, 6145–6157. doi: 10.1093/jxb/erad261

Ampong, K., Thilakaranthna, M. S., and Gorim, L. Y. (2022). Understanding the role of humic acids on crop performance and soilHealth. *Front. Agron.* 4. doi: 10.3389/fagro.2022.848621

Banožić, M., Jokić, S., Ačkar, D., Blažić, M., and Šubarić, D. (2020). Carbohydrates—key players in tobacco aroma formation and quality determination. *Molecules* 25, 1734. doi: 10.3390/molecules25071734

Bilalis, D., Karkanis, A., Triantafyllidis, V., Ladavos, A., Bizos, D., Patsiali, S., et al. (2010). Effects of organic and inorganic fertilization on growth, yield and nicotine content of flue-cured and oriental tobacco (Nicotiana tabacum L.) seedlings grown in organic and conventional float system. *J. Food Agric. Environ.* 8, 585–589.

Bilalis, D. J., Travlos, I. S., Portugal, J., Tsioros, S., Papastylianou, Y., Papatheohari, Y., et al. (2015). Narrow row spacing increased yield and decreased nicotine content in sun-cured tobacco (Nicotiana tabacum L.). *Ind. Crops Prod.* 75, 212–217. doi: 10.1016/j.indcrop.2015.05.057

Chen, Z., Ren, Z. G., Fan, Y. K., Zhao, H., Chen, G. Q., Zhao, P. P., et al. (2017). Research progress on quality evaluation of chemical components in tobacco leaf based on grey incidence analysis. *J. Agric. Sci. Technol.* 05), 129–137. doi: 10.13304/j.nykjdb.2016.352

Chen, K. L., Wang, D. Q., Zhang, J. L., Yang, M. F., Dong, X. W., Wang, D. H., et al. (2024). Study on growth characteristics and differences of upper leaves of main flue-cured tobacco varieties in China. *Jiangsu Agric. Sci.* 52, 76–82. doi: 10.15889/j.issn.1002-1302.2024.01.011

Du, Y. D., Cui, B. J., Zhang, Q., Wang, Z., Sun, J., and Niu, W. Q. (2020). Effects of manure fertilizer on crop yield and soil properties in China: A meta-analysis. *Catena* 193, 104617. doi: 10.1016/j.catena.2020.104617

Fu, X. H., Tu, N. M., Zhang, Q. Z., Hou, F. Z., and Yang, X. C. (2016). Research progress of influencing factors on nicotine content in tobacco. *Crop Res.* 30, 100–104. doi: 10.16848/j.cnki.issn.1001-5280.2016.01.026

Guo, Y. Z., and Wang, J. Y. (2021). Spatiotemporal changes of chemical fertilizer application and its environmental risks in China from 2000 to 2019. *Int. J. Environ. Res. Public Health* 18, 11911. doi: 10.3390/ijerph182211911

Gurevitch, J., Koricheva, J., Nakagawa, S., and Stewart, G. (2018). Meta-analysis and the science of research synthesis. *Nature* 555, 175–182. doi: 10.1038/nature25753

Hafsi, C., Debez, A., and Abdelly, C. (2014). Potassium deficiency in plants: effects and signaling cascades. *Acta Physiol. Plant* 36, 1055–1070. doi: 10.1007/s11738-014-1491-2

Ho, L. H., Rode, R., Siegel, M., Reinhardt, F., and Pommerrenig, B. (2020). Potassium application boosts photosynthesis and sorbitol biosynthesis and accelerates cold acclimation of common plantain (Plantago major L.). *Plants* 9, 1259. doi: 10.3390/plants9101259

Jiang, Y. L., Zhang, R. Q., Zhang, C. P., Su, J. E., Cong, W. F., and Deng, X. P. (2022). Long-term organic fertilizer additions elevate soil extracellular enzyme activities and tobacco quality in a tobacco-maize rotation. *Front. Plant Sci.* 13. doi: 10.3389/fpls.2022.973639

Li, H. L., Li, J. P., Fu, Y. L., Lu, Q. H., Yang, X. L., Jiang, M., et al. (2015). Effect of different fertilizer formula on the growth and quality of tobacco. *J. Yunnan Agric. Univ. Sci.* 30(02), 271–276. doi: 10.16211/j.issn.1004-390X(n).2015.02.017

Li, J., Zhao, B. Q., and Li, X. Y. (2008). Effects of long-term combined application of organic and mineral fertilizers on soil microbiological properties and soil fertility. *Sci. Agric. Sin.* 41(1), 144–152. doi: 10.3864/j.issn.0578-1752.2008.01.019

Liu, C., Huang, Y., Chen, X., Yu, Q. W., Xia, Z. W., Xiong, J., et al. (2018). Effects of proportion of organic and inorganic fertilizers on tobacco-planting soil bacteria composition, yield and quality of flue-cured tobacco. *J. Henan Agric. Sci.* 47, 52–58. doi: 10.15933/j.cnki.1004-3268.2018.06.010

Liu, L. Y., Li, C. Z., Zhu, S. H., Xu, Y., Li, H. Y., Zheng, X. Q., et al. (2020). Combined application of organic and inorganic nitrogen fertilizers affects soil prokaryotic communities compositions. *Agronomy* 10, 132. doi: 10.3390/agronomy10010132

Lu, W. D., Hao, Z. Q., Ma, X. L., Gao, J. L., Fan, X. Q., Guo, J. F., et al. (2024). Effects of different proportions of organic fertilizer replacing chemical fertilizer on soil nutrients and fertilizer utilization in gray desert soil. *Agronomy* 14, 228. doi: 10.3390/agronomy14010228

Lu, Z. F., Hu, W. S., Ren, T., Zhu, C., Li, X. K., Cong, R. H., et al. (2019). Impact of K deficiency on leaves and siliques photosynthesis via metabolomics in Brassica napus. *Environ. Exp. Bot.* 158, 89–98. doi: 10.1016/j.envexpbot.2018.11.008

Luo, Y. L., Zhao, H. J., Su, X. K., Wang, F., and University, G. (2014). Analysis on tobacco leaf quality of K326 in different ecological zones of neutral flavor type. *Guangdong Agric. Sci.* 41 (19), 13–17 + 22. doi: 10.3969/j.issn.1004-874X.2014.19.004

Ma, E. D., li, J. Y., Ma, J. H., Li, X. Y., and J, Y. (2013). Effects of different organic fertilizers on chemical quality of flue-cured tobacco leaf. *Southwest China J. Agric. Sci.* 26(05), 1935–1940. doi: 10.16213/j.cnki.scjas.2013.05.048

Ma, W. G., Zhou, Y. H., Liu, X. F., and Zhang, Y. X. (2018). Current status and outlook of flue-cured tobacco variety development in China. *Acta Tabacaria Sin.* 24, 116–122. doi: 10.16472/j.Chinatobacco.2017.303

Meng, D. Y., Cheng, H. X., Shao, Y., Luo, M., Xu, D. D., Liu, Z. M., et al. (2022). Progress on the effect of nitrogen on transformation of soil organic carbon. *Processes* 10, 2425. doi: 10.3390/pr10112425

Muhie, S. H. (2022). Optimization of photosynthesis for sustainable crop production. *CABI Agric. Biosci.* 3, 50. doi: 10.1186/s43170-022-00117-3

Nakagawa, S., Yang, Y., Macartney, E. L., Spake, R., and Lagisz, M. (2023). Quantitative evidence synthesis: a practical guide on meta-analysis, meta-regression, and publication bias tests for environmental sciences. *Environ. Evid.* 12, 8. doi: 10.1186/s13750-023-00301-6

Ouyang, Y., Reeve, J. R., and Norton, J. M. (2018). Soil enzyme activities and abundance of microbial functional genes involved in nitrogen transformations in an organic farming system. *Biol. Fertil. Soils* 54, 437–450. doi: 10.1007/s00374-018-1272-y

Panday, D., Bhusal, N., Das, S., and Ghalehgolabbehbahani, A. (2024). Rooted in nature: the rise, challenges, and potential of organic farming and fertilizers in agroecosystems. *Sustainability* 16, 1530. doi: 10.3390/su16041530

Pandey, R., Vengavasi, K., and Hawkesford, M. J. (2021). Plant adaptation to nutrient stress. *Plant Physiol. Rep.* 26, 583–586. doi: 10.1007/s40502-021-00636-7

Paramesh, V., Mohan Kumar, R., Rajanna, G. A., Gowda, S., Nath, A. J., Madival, Y., et al. (2023). Integrated nutrient management for improving crop yields, soil properties, and reducing greenhouse gas emissions. *Front. Sustain. Food Syst.* 7. doi: 10.3389/fsufs.2023.1173258

Peng, Y., Zhang, Y. G., Li, Z. H., Liu, L. Q., Jiang, W., Feng, Y., et al. (2014). Effect of combined application of organic-inorganic fertilizer on biomass accumulation, nitrogen uptake and distribution in flue-cured tobacco on yellow soils. *Soil Fertil. Sci. China* 16, 54–58. doi: 10.11838/sfsc.20140311

Raza, M., Zhang, P., and Shen, H. L. (2017). Influence of nitrogen and phosphorous on the growth and root morphology of Acer mono. *PloS One* 12, e0171321. doi: 10.1371/journal.pone.0171321

Rosa, M., Fabio, C., and Renato, C. (2006). Nitrogen requirements for flue-cured tobacco. *Agron. J.* 98, 666–674. doi: 10.2134/agronj2005.0105

Shang, L. R., Wan, L. Q., Zhou, X. X., Li, S., and Li, X. L. (2020). Effects of organic fertilizer on soil nutrient status, enzyme activity, and bacterial community diversity in Leymus chinensis steppe in Inner Mongolia, China. *PloS One* 15, e0240559. doi: 10.1371/journal.pone.0240559

Song, Y., Zhao, Q., Guo, X. Z., Ali, I., Li, F. Y., Lin, S. S., et al. (2022). Effects of biochar and organic-inorganic fertilizer on pomelo orchard soil properties, enzymes activities, and microbial community structure. *Front. Microbiol.* 13. doi: 10.3389/fmicb.2022.980241

Suchoff, D. H., Vann, M. C., McGinnis, M., Mason, J. H., and Fisher, L. (2020). Nitrogen fertilizer programs for organic flue-cured tobacco (Nicotiana tabacum L.) seedling production. *Tob Sci.* 57, 1–9. doi: 10.3381/tobsci-d-22-00001

Sun, J. P., Wu, Z. H., Li, X. J., Sun, H., Ding, Y. F., Ping, W. L., et al. (2016). Analysis of regional variation and major varieties of flue-cured tobacco planted in China in the twenty-first century. *Chin. Tob Sci.* 37, 86–92. doi: 10.13496/j.issn.1007-5119.2016.03.015

Sun, W. F., Zhou, Z. L., Li, Y., Xu, Z. Q., Xia, W. S., and Zhong, F. (2012). Differentiation of flue-cured tobacco leaves in different positions based on neutral volatiles with principal component analysis (PCA). *Eur. Food Res. Technol.* 235, 745–752. doi: 10.1007/s00217-012-1799-3

Tan, Z. D., Guo, H. Y., Chen, J. J., Lv, Y. H., Li, M. J., Zhong, J. Z., et al. (2012). Effects of sowing date on tobacco yield and quality. *Chin. J. Eco-Agric.* 20, 556–560. doi: 10.3724/SP.J.1011.2012.00556

Tang, L. N., Zhang, Q. F., and Zhang, S. H. (2010). Effects of appling organic manures combined with chemical-fertilizers on diversity of PLFAs biomarkers of microbial community in tobacco-growing soil and its consequences on flue-cured tobacco leaf quality. *Acta Tabacaria Sin.* 16, 36–40. doi: 10.3724/SP.J.1011.2010.01385

Viechtbauer, W. (2010). Conducting meta-analyses in R with the metafor package. *J. Stat. Software* 36, 1–48. doi: 10.18637/jss.v036.i03

Wang, S. N., Cheng, J. K., and Liao, Y. C. (2020). Fertilization model for flue-cured tobacco (nicotiana tabacum l.) in southwest China. *Appl. Ecol. Environ. Res.* 18, 7853–7863. doi: 10.15666/aeer/1806_78537863

Wang, G. P., Xiang, P. H., and Xiao, Y. (2009). Relationship between the yield and the chemistry quality of hengyang leaf tobacco. *Hunan Agric. Sci.* 2, 22–24. doi: 10.16498/j.cnki.hnnykx.2009.02.018

Wu, Y. P., Deng, J. H., Wen, D. R., Zhao, L. H., and Chen, P. (2010). Difference of nicotine content in flue-cured tobacco of different varieties and producing areas in Yunnan. *Tobacco Sci. Tech.* 9, 40–42 + 50. doi: 10.3969/j.issn.1002-0861.2010.09.009

Wu, C., and Wang, Z. H. (2010). Correlation and path analysis between smoking quality and main chemical components in flue-cured tobacco. *Guizhou Agric. Sci.* 38, 63–66.

Xi, X. Y., Li, C. J., and Zhang, F. S. (2005). Nitrogen supply after removing the shoot apex increases the nicotine concentration and nitrogen content of tobacco plants. *Ann. Bot.* 96, 793–797. doi: 10.1093/aob/mci229

Xi, Z. B., Wang, Y. Q., and Yang, P. Z. (2004). The issue on organic manure in developing modern agriculture in China. *Sci. Agric. Sin.* 12), 1874–1878. doi: 10.1088/0004-637X/807/1/89

Yang, J. H., Mattoo, A. K., Liu, Y., Zvomuya, F., and He, H. L. (2023). Trade-offs of organic and organic-inorganic fertilizer combinations in tomato quality and yield: A global meta-analysis, (1992–2021). *Eur. J. Agron.* 151, 126985. doi: 10.1016/j.eja.2023.126985

Zhou, J. X. (2005). Yield and quality changes of tobacco varieties in different ecological zones. *Tob Sci. Technol.* 9, 32–35. doi: 10.3969/j.issn.1002-0861.2005.09.011

Zhou, X., Zhu, X., Kan, H. W., Wei, J. Y., Zeng, X. N., and Gu, M. H. (2009). Effects of combined application with different ratios of organic fertilizers on photosynthesis, yield and quality of flue-cured tobacco. *Guangxi Agric. Sci.* 40, 517–520. doi: 10.3969/j.issn.2095-1191.2009.05.017

frontiers | Frontiers in Plant Science

TYPE Systematic Review
PUBLISHED 07 January 2025
DOI 10.3389/fpls.2024.1485237

Check for updates

OPEN ACCESS

EDITED BY
Henry Yabbey Sintim,
The University of Georgia, United States

REVIEWED BY
Meng Xu,
Chinese Academy of Agricultural Sciences, China
Samuel Kwakye,
Sand County Foundation, United States

*CORRESPONDENCE
Guangping Qi
qigp@gsau.edu.cn
Minhua Yin
yinmh@gsau.edu.cn

RECEIVED 23 August 2024
ACCEPTED 12 December 2024
PUBLISHED 07 January 2025

CITATION
Jiang Y, Li H, Ma W, Yu W, Chen J, Gao Y, Qi G, Yin M, Kang Y, Ma Y, Wang J and Xu L (2025) A meta-analysis of the effects of nitrogen fertilizer application on maize (*Zea mays* L.) yield in Northwest China.
Front. Plant Sci. 15:1485237.
doi: 10.3389/fpls.2024.1485237

A meta-analysis of the effects of nitrogen fertilizer application on maize (*Zea mays* L.) yield in Northwest China

Yuanbo Jiang, Haiyan Li, Wenqiong Ma, Wenjing Yu, Junxian Chen, Yalin Gao, Guangping Qi*, Minhua Yin*, Yanxia Kang, Yanlin Ma, Jinghai Wang and Liting Xu

College of Water Conservancy and Hydropower Engineering, Gansu Agricultural University, Lanzhou, China

Nitrogen fertilizer application is an important method for the production of high-quality maize. However, nitrogen fertilizer addition patterns vary according to regional climate, field management practices, and soil conditions. In this study, a meta-analysis was used to quantify the yield effects of nitrogen addition on maize, and meta-regression analysis and a random forest model were used to study the main factors affecting the yield effects of nitrogen addition on maize. The results showed that nitrogen addition significantly increased maize yield by 50.26%–55.72%, and a fluctuating increasing trend was observed with the advancement of the experimental year. The increase in maize yield upon nitrogen addition was the highest in Gansu Province, and showed a decreasing trend with the rise in average annual temperature, but did not change significantly with the average annual precipitation. Among the field management factors, the increase in maize yield was better with the variety Qiangsheng 51, topdressing at the jointing and tasseling stages (JS, TS), nitrogen application rate of 175–225 $kg \cdot ha^{-1}$, and controlled release of nitrogen fertilizer and urea (CRNFU) or the application of a combination of organic and inorganic nitrogen (OIF). Moreover, the positive effects of nitrogen fertilizer application on maize yield improved with soil pH, organic matter, available potassium, available phosphorus, and total nitrogen content; decreased with soil carbon and nitrogen ratio and available nitrogen (AN) content; and were enhanced in chestnut soil, clay, and at a bulk density of 1.2–1.4 $g \cdot cm^{-3}$. Random forest model and multifactorial optimization revealed that the effects of nitrogen addition on maize yield in Northwest China were primarily influenced by experimental year, variety, soil type, AN, and soil pH.

KEYWORDS

nitrogen fertilizer, maize yield, meta-analysis, Northwest China, influencing factor

1 Introduction

Maize (Zea mays L.) is a rich source of various nutrients such as starch, protein, and fat. Mainly grown in countries such as the United States, China, Brazil, and Argentina, it is an economically important food, feed, and industrial raw-material crop worldwide (Yan et al., 2015; Li et al., 2020). China ranks second in global maize production, with an annual output of 260 million tonnes. However, in recent years, maize imports have surged due to rising domestic demand and low production. In 2021, maize imports in China reached 28.4 million tonnes, which accounted for approximately 10% of the total demand (Luo et al., 2023). Northwest China is the core region in the Belt and Road Strategy of China, the Western Development, and the high-quality development of the Yellow River Basin (Wu et al., 2023), covering 33.1% China's total land area. With 10% of the national water resources, the western region is responsible for 12% of China's food production, which plays an important role in guaranteeing national food security (Shan et al., 2021). Nonetheless, because of the limited possibility for expansion of maize acreage, China must increase its maize production (output per unit area) if it needs to achieve self-sufficiency. Fertilizer application is an effective measure to achieve an increase in maize yields, and in Northwest China, high fertilizer inputs have provided a significant yield advantage to growing maize (Wu et al., 2022), with maize yields reaching 8.9 t·ha^{-1} in 2018, far exceeding the national average of 6.1 t·ha^{-1} (Qiao et al., 2022). However, the large input of fertilizers not only puts the environment constantly under pressure but also contradicts the national strategic plan to discontinue the use of chemical fertilizers and pesticides by 2030 (Sainju et al., 2003; Wang et al., 2016a, 2022). Therefore, promoting the use of highly efficient fertilizers and realizing the organic combination of production and ecology in maize production is of great significance for sustainable agriculture development in Northwest China.

Maize growth and development are influenced by both environmental and genetic factors (Jiang et al., 2022). Among various environmental factors, fertilizers play a crucial role in enhancing maize yield, wherein nitrogen, as an essential mineral nutrient and the basis of vital substances, is directly involved in the synthesis of a wide range of plant organic matter (Li, 2015). Nitrogen fertilizer application is the most direct and effective way to increase the content of available nitrogen in the soils of maize-growing areas. However, studies suggest that although nitrogen fertilizers are the most produced and used fertilizers in China, their utilization efficiency is approximately 30% (Li, 2015). Excessive application of nitrogen fertilizers causes soil acidification, nitrogen redundancy, leaching, and nitrogen deposition while significantly reducing maize yield and nitrogen-use efficiency (Cassman et al., 2002; Lv et al., 2007; Guo et al., 2010; Liu et al., 2023). Furthermore, variations in factors such as regional climate, field management practices, and soil conditions influence how nitrogen addition affects maize yield. The effects of nitrogen addition on maize yield vary in different ecological zones in Jilin Province, China, with the highest yield increase notes in the eastern region, followed by the central region, and a significantly lower yield increase in the western region (Wang et al., 2016c). In India and northern Florida, USA, optimum maize yields of 4.5–4.6 t·ha^{-1} and 12.2 t·ha^{-1} were achieved at recommended nitrogen application rates (NARs) of 150 kg·ha^{-1} and 264 kg·ha^{-1}, respectively (Zamora-Re et al., 2020; Kumar et al., 2021). Dirks and Bolton (1981) showed that more than 80% of maize yield could be explained by the temperature of Brookston clay soils in Canada. Frequent low-intensity precipitation and high-temperature environments can promote crop response to nitrogen fertilizers by reducing leaching and volatile losses and enhancing adsorption (Xie et al., 2013). Bacon et al. (2016) found that in Timor-Leste, high temperatures and no nitrogen fertilizer application increased maize yields in colder, high-altitude areas and reduced yields in warmer coastal areas. They also noted that increasing temperatures after nitrogen application resulted in a decreasing trend in maize yields in all regions.

Among the field management factors, the frequency and period of nitrogen application exhibited significant effects on maize yield. Adriaanse and Human (1993) showed that maize yield was lower when nitrogen fertilizer was applied two or three times compared to a single application under dry cropping conditions. Additionally, maize yield was not altered upon delaying nitrogen application to the 10th (V10) or 11th leaf nutritive growth period, but it showed a decreasing trend upon delaying nitrogen application to the tasseling or silking stage (Scharf et al., 2002; Da Silva et al., 2005; Walsh et al., 2012). However, Lv et al. (2012) found that nitrogen application at the jointing stage, V10, and 10 days after anthesis increased maize yield. In addition, the location of nitrogen application and type of nitrogen fertilizer largely influenced maize yield. Sepahvand et al. (2014) found that strip- and spread-applied nitrogen fertilizers increased maize kernel yield by 91.4% and 3.9%, respectively, compared to no nitrogen fertilizer application. The combination of organic and inorganic nitrogen can significantly improve soil nitrogen supply capacity, promote biological nitrogen fixation, reduce nitrogen loss, and increase nitrogen-use efficiency (Han et al., 2014). Chinese farmers typically apply around 209 kg·ha^{-1} of nitrogen fertilizers to maize fields (Wang, 2007), which exceeds the recommended 150–180 kg·ha^{-1} (Li, 1998). The increase in nitrogen fertilizer application does not mean a simultaneous increase in yield and nitrogen-use efficiency; when nitrogen fertilizer application was < 60 kg·ha^{-1}, the maize yield was 6.21 t·ha^{-1} and the nitrogen fertilizer-utilization rate was 40.2%; and when nitrogen fertilizer application was > 240 kg·ha^{-1}, maize yield dropped to 5.52 t·ha^{-1} and the nitrogen fertilizer-utilization rate dropped sharply to 14.4% (Zhang et al., 2008). However, Wang et al. (2018) found that maize yield and nitrogen-recycling efficiency under mulch drip irrigation in Inner Mongolia, China, first showed an increasing and then a decreasing trend with the increase in nitrogen fertilizer application, and the optimal range of nitrogen application to ensure high maize yield was 240–253 kg·ha^{-1}. In addition to the report on how to ensure rational field management, in terms of soil environmental factors, few scholars have found that coarse-grained soils usually ensure higher yields than fine-grained soils in humid environments, while clay soils (high water-holding properties) are more capable of providing higher crop yields under arid conditions (Tremblay et al., 2012). A single application of chemical fertilizers can also increase maize yield by increasing the content of soil organic matter (OM), but when nitrogen application is > 360 kg·ha^{-1}, the content of soil OM increases slowly, which affects the increase in maize yield (Liu et al., 2021). Studies showed that maize yield was negatively correlated with soil bulk density and pH, and positively correlated with soil quick-acting nutrients, such as alkaline dissolved nitrogen and available phosphorus (Cheng et al., 2024). Overall, the yield characteristics of maize fertilized using nitrogen fertilizers are affected by the complex effects of regional climate, field management practices, and soil conditions.

While several studies have examined the impact of nitrogen addition on maize yield, most were conducted at fixed locations, complicating the interpretation of these effects and their determinants over broader regions. Additionally, there are fewer studies on the effects of integrating the regional climate, field management practices, and soil environmental factors on the yield of maize fertilized using nitrogen fertilizers. In addition, the following questions remain unanswered: Are there specific environmental conditions that ensure the positive effects of nitrogen addition on maize yield, and if so, do they influence the strength of the positive effects? What are the most important environmental factors affecting nitrogen-fertilized maize field management? In this regard, meta-analysis—a statistical method for comparing and integrating the results of multiple studies—can reveal the potential factors affecting the target on a regional or global scale through comprehensive quantitative analysis of existing experimental data (Wang et al., 2019; Zhang et al., 2022b). The results of a meta-analysis can be supplemented by meta-regression analysis, which elucidates the main factors affecting the dependent variable and the magnitude and direction of the effect (Benitez-Lopez et al., 2017), and the random forest model, which is an efficient combinatorial classification method to rank the importance of factors affecting the dependent variable (Terrer et al., 2021). Thus, this study explored the effects of nitrogen addition on maize yield in Northwest China using a meta-analysis based on published data, and screened the main factors affecting the changes in maize yield upon nitrogen addition using meta-regression analysis and the random forest model, with the aim of (1) quantifying the effects of nitrogen addition on maize yield in Northwest China; (2) analyzing how this effect varies with environmental conditions and farmland management practices; and (3) providing a reference for further improvement of maize yield and sustainable agriculture development in nitrogen application environments.

2 Materials and methods

2.1 Data sources and collection criteria

In this study, we identified peer-reviewed studies focusing on the effects of nitrogen fertilizer application on maize yield in the China National Knowledge Infrastructure (CNKI, http://www.cnki.net/) and the Web of Science (https://www.webofscience.com/) in December 2022, using the keywords corn/maize, nitrogen application, yield, Northwest China, Gansu, Inner Mongolia, Ningxia, Qinghai, Xinjiang, and Shaanxi. To minimize data impact, papers were strictly screened based on the following criteria: (1) the trial must be a field trial and the trial site is located in Northwest China (Figure 1); (2) the trial must have a nitrogen application treatment and no nitrogen application treatment, with the same experimental conditions except for the nitrogen application factor; (3) the yield data of the two treatments are

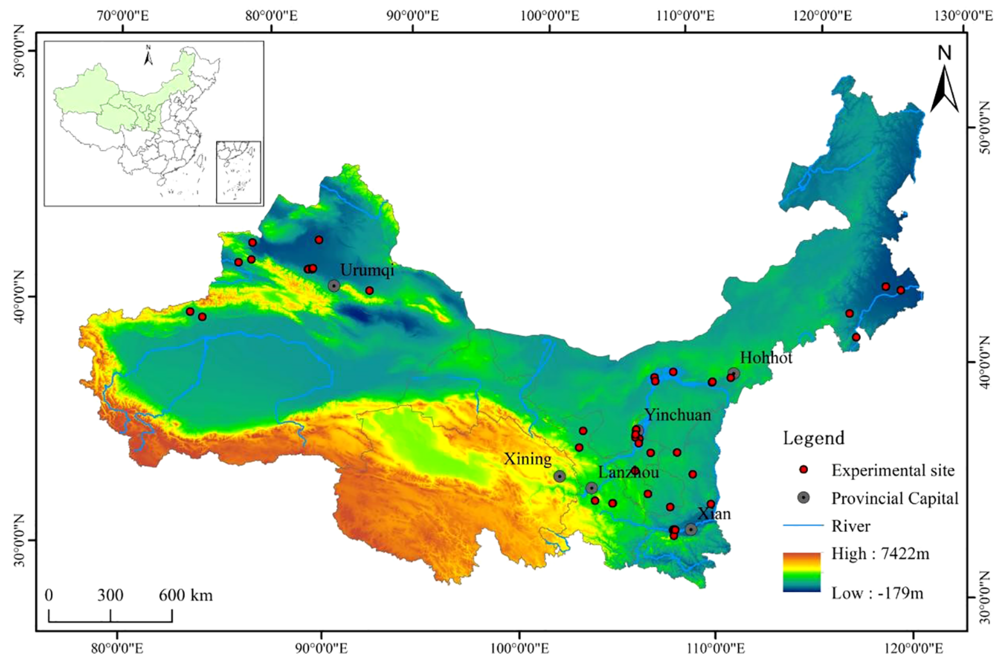

FIGURE 1
Location distribution of cases in this meta-analysis.

explicitly mentioned and their averages and standard deviations are given or can be obtained by computation; and (4) the type of nitrogen application, amount, period, and data on temperature, precipitation, irrigation, test year, soil, etc. can be obtained for one or more of these. Based on the above criteria, a total of 53 papers (containing 496 pairs of yield data) were obtained, and the data were derived from tables or figures in these papers (obtained using Web Plot Digitizer software).

2.2 Data classification and processing

2.2.1 Data classification

As the effects of nitrogen fertilizer application on maize yield are directly or indirectly affected by the external environment and genetic characteristics, a subgroup analysis of each factor was used to examine its effect on maize yield. The classification criteria for each factor were as follows: (1) five provinces of Northwest China [Gansu, Inner Mongolia, Ningxia, Xinjiang, and Shaanxi (no data were retrieved for Qinghai)]; (2) nitrogen fertilizer types [controlled release of nitrogen fertilizer (CRNF), controlled release of nitrogen fertilizer and urea (CRNFU), urea, urea and ammonium nitrate (UAN), organic and inorganic nitrogen fertilizer (OIF), and fertilizer for maize drip irrigation (FMDI)]; (3) NAR (< 125, 125–175, 175–225, 225–275, 275–325, 325–375, 375–425, and ≥ 425 kg·ha^{-1}); (4) topdressing (yes or no); (5) application stage [jointing stage (JS), tasseling stage (TS), grain filling stage (GS), JS + TS, JS + GS, and JS + TS + GS]; (6) average annual precipitation (AAP; < 200, 200–400, and ≥ 400 mm); (7) average annual temperature (AAT; < 4, 4–8, 8–12, and ≥ 12 °C); (8) cropping systems (maize succession cropping and winter wheat–summer maize rotation); (9) planting density (< 5×10^4, 5–8×10^4, 8–11×10^4, and ≥ 11×10^4 plants·ha^{-1}); (10) maize varieties with the largest sample sizes (Xianyu 335, Zhengdan 958, LuoDan 9, Qiangsheng 51, ShanDan 609, and Xianfeng 335); (11) soil types according to the China Soil Classification and Codes 2009 (GB/T 17296-2009, 2009) [meadow soil (MeS), moisture soil (MS), irrigated desert soil (IDS), anthropogenic-alluvial soil (AS), cinnamon soil (CiS), heilu soil (HS), loessal soil (LS), sierozem (Si), desert gray soil (DGS), chestnut soil (CS), and new sediment soil (NSS)]; (12) soil texture [clay (C), loam (L), sandy soil (SS), sandy loam soil (SLS), and silty clay loam (SCL)]; (13) soil bulk density (BD; < 1.2, 1.2–1.4, 1.4–1.6, and ≥ 1.6 g·cm^{-3}); (14) soil pH (< 7.5, 7.5–8.5, and ≥ 8.5); (15) soil OM (< 10, 10–15, 15–20, and ≥ 20 g·kg^{-1}); (16) soil carbon–nitrogen ratio (C/N; < 9, 9–11, and ≥ 11); (17) soil total nitrogen (TN; < 0.6, 0.6–1.0, and ≥ 1.0 g·kg^{-1}); (18) soil available nitrogen (AN; < 20, 20–35, and ≥ 35 mg·kg^{-1}); (19) soil available phosphorus (AP; < 15, 15–30, 15–30, and ≥ 30 mg·kg^{-1}); (20) soil available potassium (AK; < 100, 100–170, and ≥ 170 mg·kg^{-1}); (21) irrigation (yes or no); and (22) irrigation method [drip irrigation (DI), flood irrigation (FI), and border irrigation (BI)].

2.2.2 Data Processing

1. Partial factor productivity of nitrogen (PFP_N, kg·kg^{-1}) was calculated using the following formula:

$$PFP_N = Y/N \quad (1)$$

where Y is the yield (kg·ha^{-1}), and N is the NAR (kg·ha^{-1}).

2. Soil C/N was determined as follows:

$$SOC = 0.58 \times SOM \quad (2)$$

$$C/N = SOC/TN \quad (3)$$

where SOC is the soil organic carbon content (g·kg^{-1}), SOM is the soil organic matter content (g·kg^{-1}), 0.58 is the conversion coefficient, and TN is the soil total nitrogen content (g·kg^{-1}).

2.3 Meta-analysis

2.3.1 Calculation of effect size and weight for individual cases

In this study, logarithmic response ratio (ln$R$) was used to characterize the effects of nitrogen addition on maize yield, with the advantage that data dimensions can be eliminated, and the range can extended from negative infinity to positive infinity (Hedges and Gurevitch, 1999):

$$\ln R = \ln (X_a/X_c) \quad (4)$$

where R is the response ratio, X_a is the average yield of maize upon nitrogen addition (kg·ha^{-1}), and X_c is the average yield of maize without nitrogen addition (kg·ha^{-1}).

The variance within the case (v_i) was calculated as follows:

$$v_i = \frac{S_a^2}{N_a X_a^2} + \frac{S_c^2}{N_c X_c^2} \quad (5)$$

where v_i is the within-case variance for a single case; S_a and S_c are the standard deviations of maize yield with and without nitrogen application, respectively; and when the standard deviation was missing in the study, it was calculated using the methodology described by Gattinger et al. (2012). N_a and N_c are the numbers of replicated trials for maize yield with and without nitrogen application, respectively.

The weight of the ith study (w_i) was calculated as follows:

$$w_i = 1/(v_i + \tau^2) \quad (6)$$

where τ^2 is the between-case variance.

2.3.2 Calculation of cumulative effect size

In this study, external factors, such as regional climate, field management practices, and soil properties, affected the results, which were considered heterogeneous. Hence, the random-effects model was used to calculate the cumulative effect size ($\bar{y}$).

$$\bar{y} = \sum_{i=1}^{k} w_i y_i / \sum_{i=1}^{k} w_i \quad (7)$$

$$SE = \sqrt{\frac{1}{\sum_{i=1}^{k} w_i}} \quad (8)$$

$$95\,\%\, CI = \bar{y} \pm 1.96SE \quad (9)$$

where 95% *CI* is the 95% confidence interval, and *SE* is the overall standard error.

To directly represent maize yield increase upon nitrogen application in response to each factor, ln*R* was converted to the rate of yield improvement (*Z*) over the control treatment (Hedges and Gurevitch, 1999).

$$Z = [exp(\ln R) - 1] \times 100 \quad (10)$$

2.3.3 Analysis of influencing factors

If the heterogeneity test found that Q_t did not obey the chi-squared distribution ($P < 0.05$), we introduced explanatory variables, subgroup analysis, or meta-regression analysis (Buhmann et al., 2015; R Core Team, 2018). Additionally, significant heterogeneity (Q_M) caused by a variable ($P < 0.05$) indicated that the factor exhibited significant effects on maize yield upon nitrogen application.

2.3.4 Model test

In this study, publication favoritism of the model was tested using the coefficient of insecurity. If the coefficient of insecurity was > 5k+10, the results of the study were not affected by publication favoritism and were highly credible (Xiang et al., 2017).

2.4 Data analyses

The "metafor" package of R software (4.3.0) was used for meta-analysis, the "randomForest" package for random forest analysis, the "glmulti" package for multivariate optimization, Microsoft Excel 2016 for data preparation, and Origin 2021 for plotting.

3 Results

3.1 Data distribution and overview

Influenced by factors, such as regional climate, field management practices, and soil conditions, maize yield exhibited large variability with and without nitrogen addition and showed normal distribution (Figure 2). Maize yield upon nitrogen addition ranged from 2.8×10^3 kg·ha^{-1} to 21.6×10^3 (average: 12.2×10^3 kg·ha^{-1}), and that without nitrogen addition ranged from 2.2×10^3 kg·ha^{-1} to 16.0×10^3 kg·ha^{-1} (average: 8.3×10^3 kg·ha^{-1}). As shown in Figure 3, the median maize yields in the five provinces with and without nitrogen addition were 10.2×10^3–17.2×10^3 kg·ha^{-1} and 5.3×10^3–12.4×10^3 kg·ha^{-1}, respectively. This study on the relationship between NAR and partial factor productivity of nitrogen found that the two were negatively correlated in a power function type, with a fitting curve of $y = 3934x^{-0.796}$ and R^2 of 0.628, indicating that maize yield per unit of nitrogen application gradually decreased with the amount of nitrogen applied.

3.2 Bias testing

In this study, the collected yield data pairs were tested for bias by fitting the yield effect value distribution to a Gaussian function (Figure 4). The Kolmogorov-Smirnov test showed that the frequency distribution of the yield effect value under different fertilization conditions did not obey normal distribution ($P < 0.01$). Therefore, lnR and 95% CI generated by the non-parametric estimation method (bootstrap resampling; 1000 times) were used for data analyses (Wang et al., 2019).

3.3 Cumulative effect size of nitrogen application on yield response of maize and test for publication preference

Table 1, Figure 5 demonstrate that the cumulative effect size of nitrogen addition on maize yield was 0.4255 (95% CI, 0.4072–0.4429), that is, compared to no nitrogen addition, under 95% CI, nitrogen addition increased maize yield by 50.26%–55.72% (average: 53.04%). In addition, the variance between cases accounted for 99.6% of the total variance of the model I^2, and the random-effects model indicated highly heterogeneous data (Q_t =

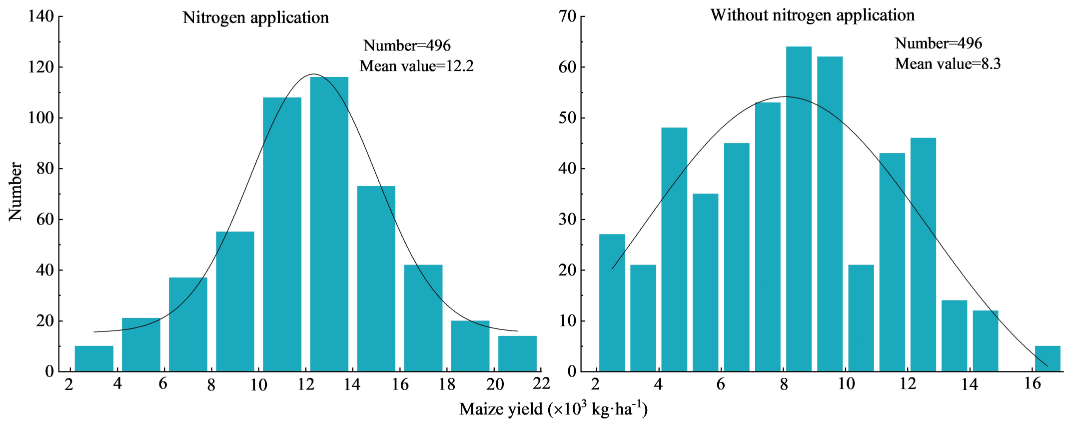

FIGURE 2
Frequency distribution of maize yield with and without added nitrogen conditions.

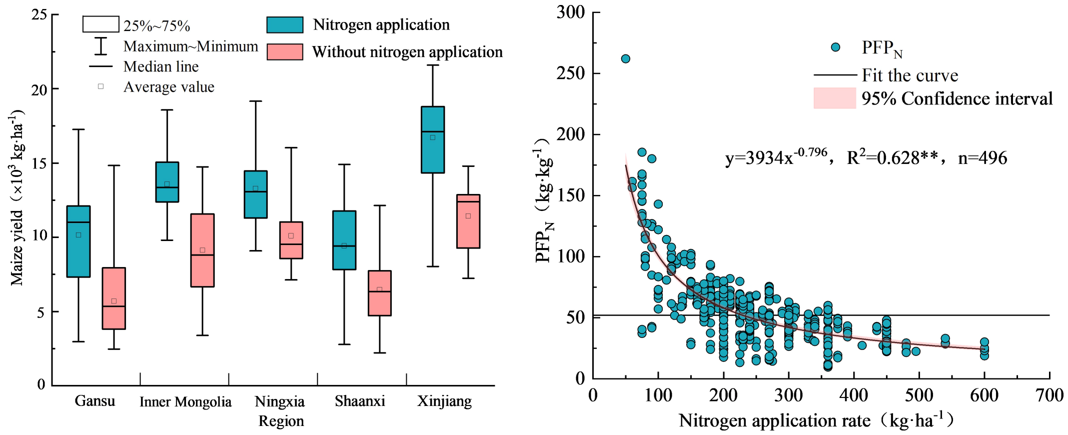

FIGURE 3
Regional distribution of maize yield and the relationship between nitrogen application and PFP_N. ** in the figure represents significant correlation at the P<0.01 level.

44580.2262, $P_Q < 0.0001$). Therefore, it was necessary to introduce explanatory variables to study the factors affecting maize yield on nitrogen. The failure safety factor of 5657075 was much larger than that of 5k + 10 (n is the sample size), indicating that the test results were not affected by publication bias, and the results exhibited high credibility.

3.4 Analysis of the influence factors of nitrogen addition on maize yield change

3.4.1 Regional climate factors

As can be seen from Figure 6, regional climate factors significantly influenced the yield effects of nitrogen addition on maize. The difference between the yield-increasing effects of AAP was not significant, with a maximum maize yield increase of 59.27% (95% CI, 54.47%–63.89%) at AAP < 200 mm, and the yield-increasing effect of AAP of ≥ 400 mm being the second highest. The yield-increasing effects of AAT increased with rising temperatures, but the yield-increasing effects of nitrogen application with AAT < 12°C were not significant, and the minimum increase in maize yield was noted at AAT > 12°C, which was 29.64% (95% CI, 24.16%–34.97%). The effects of nitrogen application on maize yield increase in Gansu was 81.59% (95% CI, 73.24%–90.77%), followed by Inner Mongolia, Shaanxi, and Xinjiang, and the lowest in Ningxia. The increase in maize yield upon nitrogen application showed a fluctuating, increasing trend as the year progressed, and the maize yield increase in 2020 was 183.60% (95% CI, 148.93%–224.14%). Overall, the years closer to the present, lower AAP and AAT were conducive to increased maize yield upon nitrogen application.

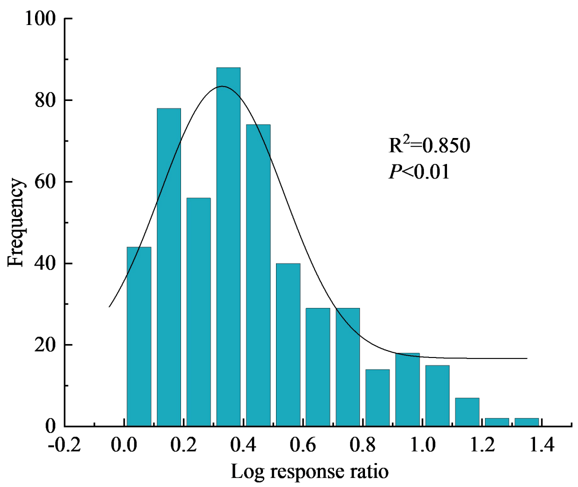

FIGURE 4
Frequency distribution of maize yield effect size in response to nitrogen application.

3.4.2 Field management factors

The Q_m value (P < 0.05) of each field management factor (Table 2) suggested that the field management factors significantly affected the yield effect of nitrogen addition on maize. Among the field management factors (Figure 7), topdressing significantly increased the yield-increasing effect of nitrogen application by 56.74% (95% CI, 53.56%–60.06%) compared to basal nitrogen application. Moreover, with an increase in NAR, the yield-increasing effects first increased and then decreased gradually. When NAR was 175–225 kg·ha^{-1}, the yield-increasing effect was the highest (67.74%; 95% CI, 59.27%–76.17%). However, when the NAR was 375–425 kg·ha^{-1}, the yield-increasing effect of nitrogen application began to decrease significantly. Concerning nitrogen application, the yield-increasing effects of urea, UAN, OIF, and CRNFU, followed by CRNF, on maize were high, but not significantly different. Nonetheless, the yield-increasing effect of DI was minimal, and the order for fertilization period was JS + TS > GS > JS + TS + GS > JS > JS + GS > TS, among which the yield-increasing effect at JS + TS was up to 69.67% (95% CI, 59.79%–80.16%). Furthermore, the variety with the highest yield-increasing effect [95.52% (95% CI, 82.08%–109.78%)] was Qiangsheng 51, followed by Xianfeng

TABLE 1 Cumulative effect size analysis of nitrogen application on maize yield.

$\bar{y}$	k	*P* value	95% LCI	95% UCI	I^2(%)	heterogeneity test		K	5k+10
						Q_t	P_Q		
0.4255	496	<0.0001	0.4072	0.4429	99.69	44580.2262	<0.0001	5657075	2490

k is the sample size, 95% LCI is lower limit of 95% confidence interval, 95% UCI is upper 95% confidence interval. I^2 represents the between-case variance as a percentage of the total model variance. K is the coefficient of insecurity.

335. When the planting density was more than 5×10^4 plants·ha^{-1}, the yield-increasing effects of nitrogen application was significantly high, but later, the effects of increase in planting density was not significant. Compared to winter wheat–summer maize rotation, maize succession cropping exhibited a higher yield-increasing effect [58.84% (95% CI, 55.46%–62.34%). The yield-increasing effect of nitrogen application without irrigation was higher than that with irrigation, and it followed this order: FI > DI > BI.

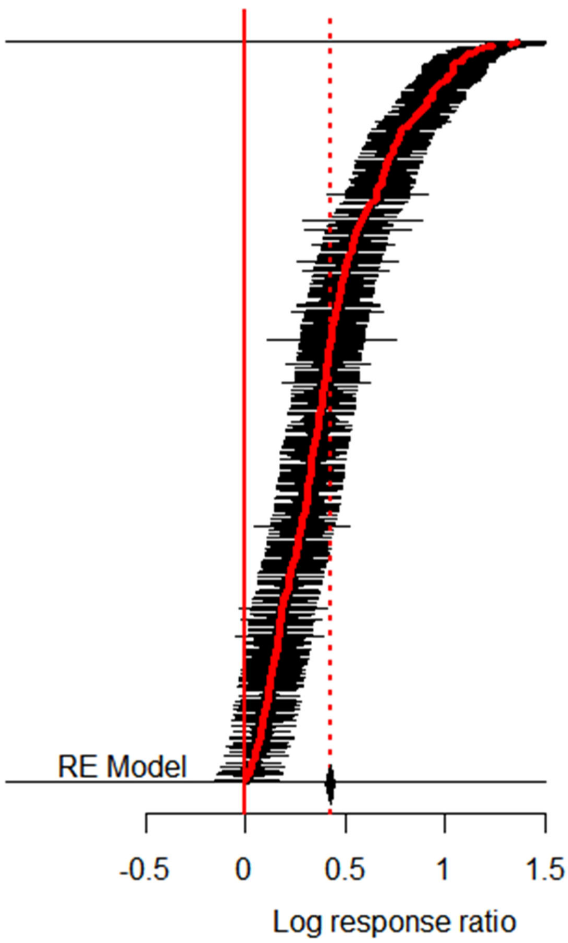

FIGURE 5
Distribution of individual effect sizes and their cumulative effect size of nitrogen application on maize yield response cases. The black diamonds in the figure represent the cumulative effect size of nitrogen application on the yield response of maize, and the black shading represents the distribution of effect size for individual cases.

3.4.3 Soil environment

Figure 8 illustrates that different soil conditions significantly affected the increase in maize yield upon nitrogen addition. With the increase in soil pH, the yield-increasing effects of nitrogen fertilization improved gradually, with the maximum value at pH ≥ 8.5, which was 70.93% (95% CI, 64.03%–79.00%). From the perspective of soil texture, maize showed the highest yield increase of 95.52% (95% CI, 82.45% –109.53%) in C, followed by SL, SS, and SCL, and finally L. In addition, the most significant increase in maize yield upon nitrogen application [98.91% (95% CI, 88.49%–108.57%)] was observed in CS, followed by HS [69.45% (95% CI, 60.87%–78.71%)], and the weakest increase in maize yield was observed in NSS. The yield-increasing effects of nitrogen application on maize gradually decreased with increasing soil AN content, with the highest yield-increasing effect of 106.27% (95% CI, 96.34%–117.19%) at AN content < 20 mg·kg^{-1}. A yield-increasing effect of 54.23% (95% CI, 50.35%–58.57%) was observed in maize at 0.6–1 g·kg^{-1} of soil TN. However, with an increase in soil C/N, the yield-increasing effects of nitrogen application decreased gradually, but there was no significant difference in yield increase between soils with different C/N. The yield-increasing effects of nitrogen application increased gradually with increasing soil OM content, with the highest yield-increasing effect of 58.01% (95% CI, 41.30%–75.91%) when the soil OM content was ≥ 20 g·kg^{-1}. Furthermore, with the increase in soil BD, the yield-increasing effects of nitrogen application showed an increasing and then a decreasing trend, and the maximum value was recorded at soil BD of 1.2–1.4 g·cm^{-3}, which was 72.19% (95% CI, 66.05%–78.57%). With increasing soil AK content, the yield-increasing effects of nitrogen application showed an increasing trend, and the maximum yield-increasing effect [53.50% (95% CI, 47.09%–60.35%)] was noted at ≥ 170 mg·kg^{-1}. Moreover, with an increase in soil AP content, the yield-increasing effects of nitrogen application gradually increased, and the maximum yield-increasing effect of maize was 62.53% (95% CI, 54.64%–70.74%) when the soil AP content was ≥ 30 mg·kg^{-1}.

3.4.4 Meta-regression analysis

To further understand the effects of the experimental year, meteorological factors, planting density, and soil physicochemical properties on maize yield changes upon nitrogen addition, a single-factor meta-regression analysis was performed. As shown in Figure 9, the experimental year, AAT, planting density, soil OM, pH, AN, AK, and BD exhibited a significant effect (P < 0.05) on maize yield increase upon nitrogen addition. In contrast, AAP, C/N, and AP did not exhibit a significant effect (P > 0.05). Additionally, the experimental year, soil OM, pH, AK and TN positively influenced the yield-increasing effects of nitrogen application on

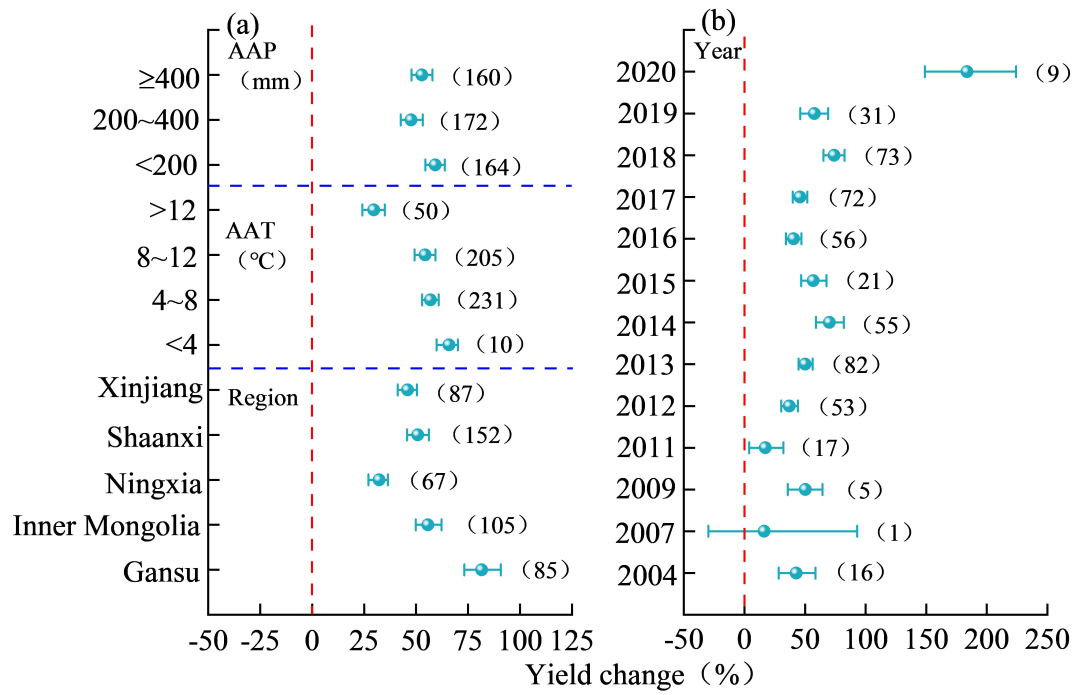

FIGURE 6
Influence of regional climatic factors on yield changes in nitrogen-applied maize. In **(A)** AAP stands for average annual precipitation, AAT stands for average annual temperature and Region stands for different provinces in China. In **(B)** Year stands for the year of the experiment.

maize, suggesting a synergistic effect of soil nutrients on maize yield enhancement through nitrogen application. In contrast, AAT, planting density, AN, and BD exhibited a negative effect on the yield-increasing effects of nitrogen application on maize.

3.5 Different factors influencing the importance of maize yield effects

Figure 10 shows the order of importance of the factors influencing maize yield changes upon nitrogen addition based on the random forest model. The Q_m value and significance of the heterogeneity test of each influencing factor indicated in Table 2, Figure 9 suggested that the soil AK, AP, C/N, TN, and AAP did not significantly affect the changes in maize yield. Hence, they were excluded, and the remaining 18 factors were included in the random forest model to determine the importance of the variables. The model explained 83.7% of the variance, where the experimental year exhibited the highest relative importance (41.95%), followed by maize variety (35.61%), soil AN (34.02%), type (22.64%), pH (20.21%), BD (17.99%), soil texture (17.35%), and nitrogen application (14.34%); the remaining factors exhibited weak relative importance (Figure 10).

TABLE 2 Heterogeneity analysis of each influencing factor.

Factor	Q_M	*P* value	Factor	Q_M	*P* value
NAT	20.47	0.0010	Maize variety	317.81	<0.0001
NAR	29.48	0.0001	STy	75.35	<0.0002
Topdressing or not	21.51	<0.0001	STe	95.61	<0.0003
FT	17.81	0.0032	Irrigstion or not	40.52	<0.0004
Region	58.75	0.0001	IM	24.47	<0.0005
CS	36.23	0.0001			

NAT represents Nitrogen application type; NAR represents nitrogen application rate; FT represents fertilizing time; CS represents cropping system; STy represents soil type; STe represents soil texture; IM represents irrigation method.

3.6 Identification of the optimal model using multi-factor analysis

In this study, multi-factor model optimization was performed for the top 6 factors after random forest model prediction. The model in Table 3 shows the lowest AICc value and is the optimal model. The weight of this model in the optimal model set was 0.7851, and it considered 85.45% of the heterogeneity sources. A factor importance of > 0.8 suggested that the factor was important (Figure 11). Using the model, we noted that soil AN, maize variety, experimental year, soil type, and pH were the important factors affecting maize yield upon nitrogen application.

4 Discussion

In this study, we synthesized research cases on the effect of nitrogen addition on maize yield in Northwest China and

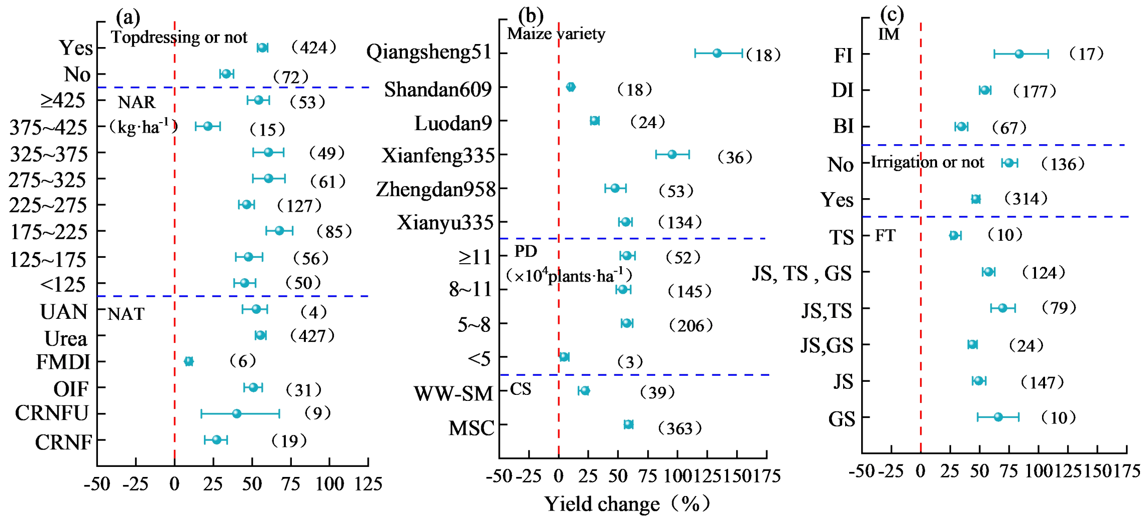

FIGURE 7
Effect of field management on yield changes in nitrogen-applied maize. In **(A)** NAR stands for nitrogen application rate, NAT stands for nitrogen application type, UAN stands for urea and ammonium nitrate, FMDI stands for fertilizer for maize drip irrigation, OIF for organic and inorganic fertilization, CRNFU for controlled release nitrogen fertilizer and urea, CRNF for controlled release nitrogen fertilizer. In **(B)** PD stands for planting density, CS stands for cropping system, WW-SM stands for winter wheat-summer maize, and MSC stands for maize succession cropping. In **(C)** IM stands for irrigation method, FT for fertilization time, FI for flood irrigation, DI for drip irrigation, BI for border irrigation, TS for tasseling stage, JS for jointing stage, GS for grain filling stage.

systematically analyzed the effect of nitrogen addition on maize yield in Northwest China, and concluded that nitrogen addition was able to increase maize yield by 50.26% to 55.72% compared with no nitrogen addition. However, the yield increase effect of nitrogen addition on maize is largely influenced by regional climate, field management and soil environment.

4.1 Effects of regional climatic factors on maize yield

Providing adequate nutrients to crops through nitrogen fertilizer application is important to maintain high and stable yields and ensure national food security (Kong et al., 2022). Owing to

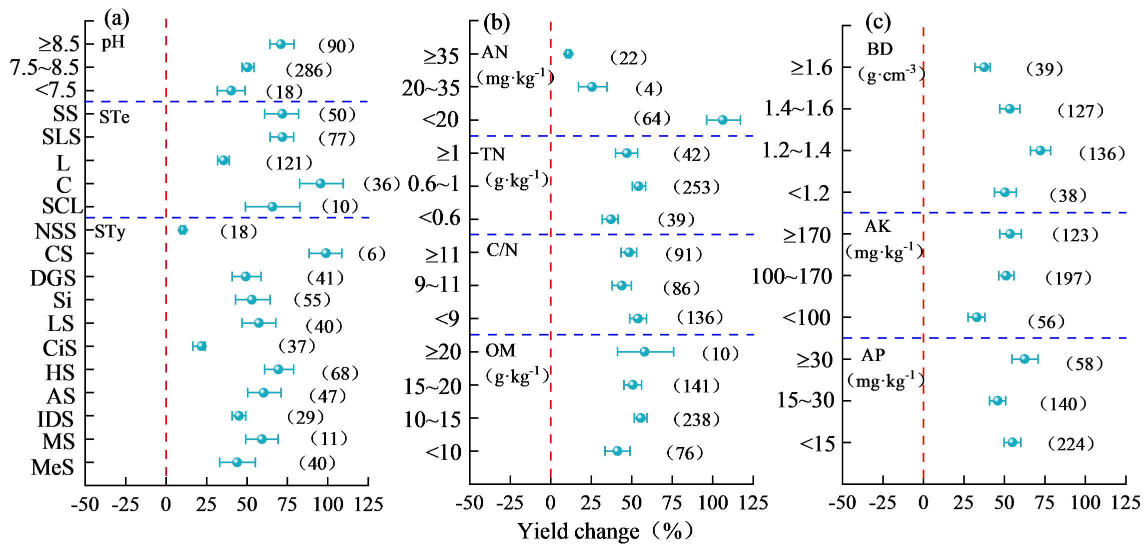

FIGURE 8
Influence of soil environment on yield changes in nitrogen-applied maize. In **(A)**, STe stands for soil texture, STy stands for soil type, SS stands for sandy soil, SLS stands for sandy loam soil, L stands for loam, C stands for clay, SCL stands for silty clay loam, NSS stands for new sediment soil, CS for chestnut soil, DGS for desert gray soil, Si for sierozem, LS for loessal soil, CiS for cinnamon soil, HS for heilu soil, AS for anthropogenic-alluvial soil, IDS for irrigated desert soil, MS for moisture soil, and MeS for meadow soil. In **(B)** AN stands for available nitrogen, TN for total nitrogen, and OM for organic matter, and in **(C)** BD stands for bulk density, AK stands for available potassium, and AP stands for available phosphorus.

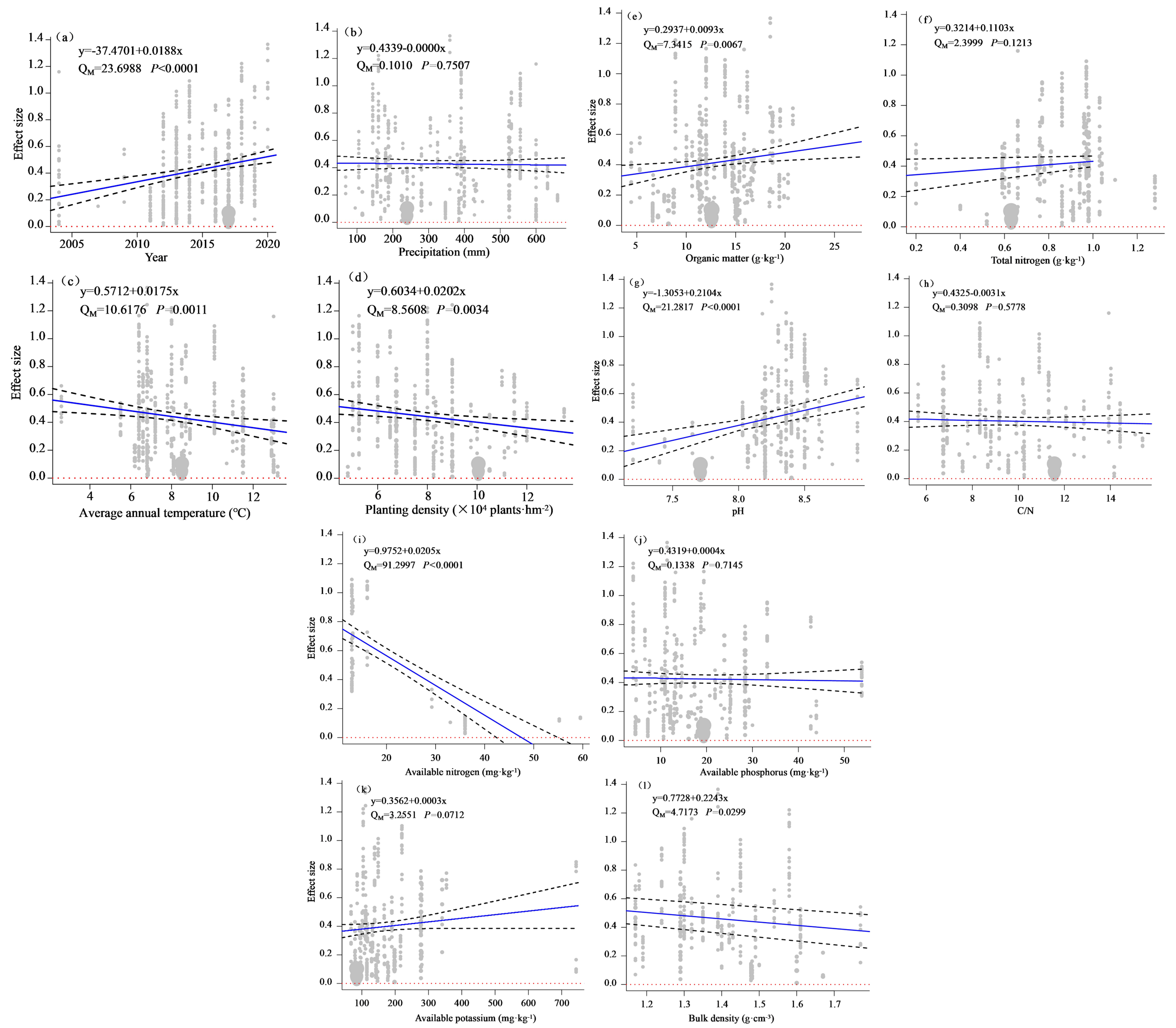

FIGURE 9
Meta regression analysis of yield effect size with each influencing factor i.e. year **(A)**, average annual precipitation **(B)**, average annual temperature **(C)**, planting density **(D)**, soil organic matter **(E)**, soil total nitrogen **(F)**, pH **(G)**, the ratio of soil organic carbon content to soil total nitrogen content **(H)**, available nitrogen **(I)**, available phosphorus **(J)**, available potassium **(K)**, and bulk density **(L)** respectively. Q_M is the heterogeneity caused by a variable, and *P* represents the level of significance.

different climatic characteristics, soil conditions, and field management practices, the increase in maize yield varies greatly among regions. In this study, we found the highest increase in maize yield upon nitrogen application in Gansu province, probably because the crop matured once a year, and plant growth was largely dependent on the local climatic conditions. Gansu province has an arid and semi-arid climate with relatively infertile soils. However, soil fertility was significantly improved upon nitrogen application, and hence, it exhibited the most notable effect on maize yields in the region. Anwar et al. (2009) pointed out that plant growth is highly sensitive to temporal (precipitation and temperature) and spatial (soil) factors. The combination of these factors controls the effectiveness of irrigation and fertilizer application, as well as nitrogen mineralization, during the growing season (Kay et al., 2006). In this study, we found that the highest increase in maize yield upon nitrogen addition was found in the area with an AAP < 200 mm, probably due to the fact that in areas with low precipitation, nitrogen application can alleviate the limitation of maize growth by precipitation to some extent, and at the same time, soil nutrients are relatively scarce in this environment, and maize yields are lowest without nitrogen application, and the most sensitive response to nitrogen addition. In contrast, the increase in maize yield decreased in the area with an AAP of 200–400 mm, and increased in the area with an AAP of ≥ 400 mm. This trend can be explained by the coupling effect of water and nitrogen, and the complex relationship between precipitation and temperature, as suggested by Yamoah et al. (1998), who found that nitrogen fertilizer application was more effective in wet years than in dry years. The regression analysis of precipitation on yield effect size was not significant in this study, which may be attributed to the fact that all the regions were located in Northwest China, which is characterized by relatively low precipitation. Meng et al. (2023) pointed out that when the

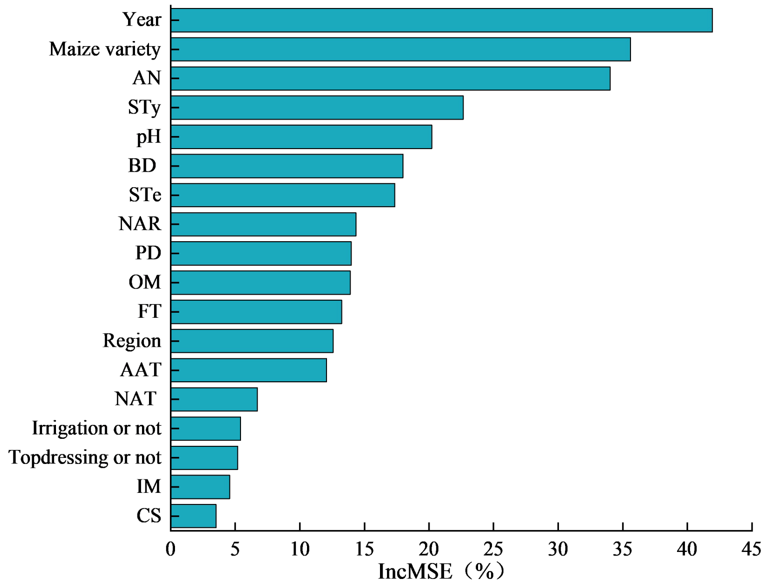

FIGURE 10
Order of importance of variables. IncMSE is increase in mean squared error, which is determined by randomly assigning a value to each predictor, and if the predictor is more important, the larger the model prediction error is when its value is replaced. Therefore, the larger the value, the higher the importance of the variable. AN stands for Available nitrogen, STy stands for soil type, BD stands for bulk density, STe stands for soil texture, NAR stands for Nitrogen application rate, PD stands for planting density, OM stands for Organic Matter, FT stands for fertilization time, AAT stands for Average annual temperature, NAT stands for Nitrogen application type, IM stands for Irrigation method, and CS stands for Cropping system.

temperature is 5–10°C, the nitrogen content in the soil is an important limiting factor for maize yield increase, and the increased application of nitrogen fertiliser can significantly promote maize yield. Too high or too low temperature will reduce the enzyme activity in the soil, limit the mineralisation of soil organic nitrogen, and reduce the nitrogen uptake efficiency of maize. Tremblay et al. (2012) found that high temperatures were beneficial in enhancing the response of maize to nitrogen fertilizers, and high average temperatures enhanced microbial activity, which accelerated the rate of nitrogen mineralization. However, high temperatures can also cause excessive nitrogen volatilization losses from the soil, as well as early plant senescence and reduced nutrient accumulation, resulting in reduced yields. Our study indicated that as AAT increased, the positive impact of nitrogen application on maize yield diminished, likely due to the combined effects of high temperatures and low soil moisture, which decreased nitrogen use efficiency. Consequently, this resulted in a decline in maize production. This study also revealed that the increase in maize yield in Northwest China exhibited a fluctuating, rising trend with year progression. This can be explained by the fact that the application of chemical fertilizers has been maintained at a high rate since the latest reforms in China. Some studies have shown that in 2018, the application of chemical fertilizers in China was still as high as 340.77 kg·ha^{-1}, and the application of nitrogen fertilizer reached 124.50 kg·ha^{-1} (Zhang et al., 2022c), which improved nutrient availability in the infertile soils of Northwest China, and promoted the improvement of maize yields. Moreover, in recent years, new high-yield maize varieties have been vigorously promoted in China, and the related updates in production technology are inseparable.

TABLE 3 Multi-factor optimization model.

Item	parameters
Optimal model	yi~1+Year+Maize variety+STy +AN+pH
Aicc	-385.9291
weights	0.7851
Percentage of heterogeneity considered R^2	85.45%

AN represents available nitrogen; STy represents soil type.

4.2 Effects of field management on maize yield

Appropriate field management measures create favorable environmental conditions for the growth of maize plants and promote stable and high maize production (Zhang et al., 2022a). Studies have shown that under proper soil moisture conditions, nitrogen recovery and yield are the highest when nitrogen is applied 4–8 weeks after maize planting (Adriaanse and Human, 1993). Zhang et al. (2024) found that maize yield increased with increasing frequency of nitrogen application. In this study, we also concluded that the increase in maize yield was higher with the supplementary fertilizer during the maize-growing period than with the one-time basal fertilizer application, and both of them exhibited similar conclusions. Single-application fertilization during growth stages results in a mismatch between the critical period of crop fertilizer requirement and nitrogen supply, leading to unbalanced nitrogen

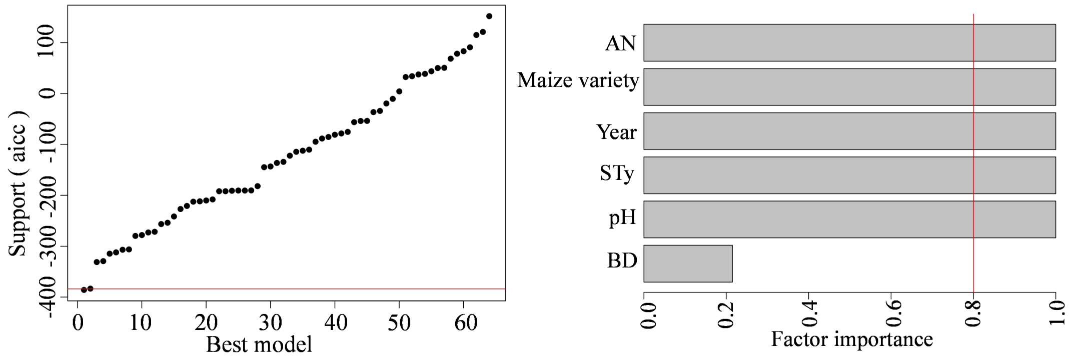

FIGURE 11
Multi-factor model optimization results and importance of optimal model factors. AN stands for available nitrogen, STy stands for soil type, and BD stands for bulk density.

and nutrient loss during crop growth stages (Xu et al., 2022). Moreover, ample nitrogen supply during the critical growth period after split fertilization can increase the duration of high photosynthetic values and align photosynthetic characteristics with the accumulation of dry matter and nutrients, thereby boosting crop yields (Ma et al., 2007). Overman and Scholtz (1999) found that the nitrogen demand of most crops exhibits an S-shaped curve, and most crops require increased nitrogen application during the middle stage of rapid growth, particularly from the small tassel stage to the tasseling stage in maize. Liu et al. (2023) showed that nitrogen fertilizer application at the JS + anthesis or JS + large tassel + anthesis stage under DI significantly increased maize yield compared to one-time nitrogen fertilizer application at the JS under conventional BI. This finding was consistent with the findings of this study, which suggested that the increase in maize yield upon nitrogen application at the JS + TS or JS + GS, or JS + TS + GS was significantly higher than that at the JS and that the increase in maize yield upon DI was higher than that upon BI. In addition, this study concluded that the highest yield-increasing effect was observed under FI with nitrogen application, probably because under no nitrogen application, maize yield upon FI was significantly lower than that upon other irrigation methods such as DI and BI. In contrast, maize yield under FI was significantly higher after nitrogen application, which resulted in a significant improvement in yield change.

The type and amount of nitrogen fertilizer likewise affects the yield-enhancing effect of maize. Unreasonable nitrogen application is easy to cause nitrogen leaching and volatilization, especially in the maize growing season when precipitation is more concentrated and high temperature (Liu et al., 2022). This study showed that with the increase of nitrogen application, the yield increase effect of maize showed a trend of increasing and then decreasing, and the highest value of the yield increase effect appeared in the nitrogen application of 175–225 kg·ha^{-1}. This is consistent with the findings of Li et al. (2021), who found that the yield-enhancing effect of nitrogen application to summer maize increased and then decreased with the increase of nitrogen application, and Wang et al. (2016b), who showed that nitrogen application significantly enhanced the yield of maize, but that there was a decrease in yield when nitrogen fertilizer exceeded 225 kg·ha^{-1}. Different types of nitrogen fertilizers have different fertilizer efficacy due to their different mechanisms of nutrient release. Ordinary urea, as the most commonly used quick-acting nitrogen fertilizer, can rapidly increase soil nitrate nitrogen content after two weeks of soil application, but it is easy to pollute the environment if it is applied in excess or in an improper way (Ren et al., 2012). Controlled-release urea can better synchronize the nitrogen demand during the growing season, promote crop growth and yield accumulation, and avoid early plant failure (Ye et al., 2013). Organic and inorganic fertilization meets the requirements of sustainable development of modern agriculture, improves soil granular structure, promotes soil microbial vitality and thus increases soil nutrient content, and also reduces the amount of chemical fertilizers (Akiyama et al., 2010). Zhang et al. (2024) concluded that the application of slow-release fertilizer was more beneficial to increase maize yield compared to urea because it was able to maintain the match between nitrogen supply and plant uptake throughout the reproductive period, which differed from the results of this study where the maize yield-increasing effect of urea application was higher than that of controlled-release nitrogen fertilizer, probably because this study was located in northwestern China, where soils are generally infertile, and the fertilizer release after slow-release fertilizer were applied was slower, and could not meet the nutrient demand of the plant quickly, thus the yield-increasing effect was lower. This study found that although the maize yield increase effect of applying urea, urea + ammonium nitrate, organic and inorganic fertilization, controlled-release nitrogen fertilizer + urea was higher and there was no significant difference between them, but based on the requirements of sustainable development of green modern agriculture, the nitrogen application methods of organic and inorganic fertilization, controlled-release nitrogen fertilizer + urea are recommended to achieve the increase in maize yield.

In addition, this study concluded that Qiangsheng 51 maize has the highest yield increase, because the planting area is Gansu, the climate is arid, and this maize variety has the advantages of drought resistance, high yield and disease resistance, high seed yield, better adapted to the local environmental conditions, so that the effect of yield increase is significant. The improvement of crop yield is often inseparable from the level of group production, and increasing planting density is an important measure (Zhao et al., 1997). Ma et al. (2008) showed that the optimal planting density for high yield of maize through the coupling of planting density and nitrogen fertilizer was 6.17–6.62×10^4 plants·ha^{-1}, and the appropriate pure nitrogen application was 309.88–569.02 kg·ha^{-1}. In this study, it was concluded that when maize was planted with a density of > 5×10^4 plants·ha^{-1}, the maize yield increase effect was significantly enhanced, but thereafter, increasing the planting density, the maize yield increasing effect increased insignificantly. The possible reason for this is that water and fertilizer resources are limited in Northwest China, and at too high planting densities, individual competition for water and nutrients is more intense, producing irreversible damage, increasing the rate of empty stalks, decreasing the number of grains in the ears and the resistance of the crop stalks to topple, which would reduce the rate of yield increase. In this study, the yield increase of maize with nitrogen application in rainfed conditions was higher than that in irrigated conditions, probably due to the generally infertile soil environment in the rainfed areas of the Northwest compared to the irrigated areas, where maize yields without nitrogen application were significantly lower than those in the irrigated areas, and where the application of nitrogen significantly improved the soil nutrient conditions, coupled with the effect of precipitation, which resulted in significantly higher yields of maize. In this study, it was found that the yield-gaining effect of the winter wheat-summer maize rotation system was lower than that of the continuous maize crop. Although the gain of additional winter wheat yield is obtained in the winter wheat-summer maize crop rotation system, this crop rotation system in the case of this study is basically located in high latitude areas such as Shaanxi, which is an arid and semi-arid region with limited total precipitation, and the planting of winter wheat will result in the competition for water, nutrients, and other resources with summer maize, which will result in the reduction of the yield of summer maize. Zhang et al. (2016) concluded that in high-latitude areas, cover crops can be planted in the summer when precipitation and temperature are high, and winter wheat can be planted afterward to solve the contradiction of resource competition.

4.3 Effects of soil environment on maize yield

The goal of nitrogen fertilizer management is to ensure an adequate supply of effective mineral nitrogen in the soil throughout the growth period of the crop (Adriaanse and Human, 1993). Thus, crop yield is closely associated with soil nitrogen effectiveness and soil characteristics (water-holding capacity, texture, and fertility) (Armstrong et al., 2009). Kyveryga et al. (2009) found that the response of maize to nitrogen application was slightly affected by soil texture, with inter-annual variability having a greater impact than spatial soil differences. Tremblay et al. (2012) demonstrated that soil texture largely determined soil response to nitrogen, with fine-textured soils (C and SC) responding to nitrogen addition more than medium-textured soils (L and SL). This was consistent with the findings of this study, which indicated that the highest increase in maize yield upon nitrogen application was found in clay soils, which may be attributed to the fact that clay soils are denser than sandy and loamy soils in arid environments, exhibit improved water-locking properties, and are less susceptible to nutrient loss, thereby exhibiting the best yield increase. Different soil textures and types significantly affect nitrogen mineralization capacity and crop yield accumulation, with black soils exhibiting significantly higher nitrogen mineralization than red loam and tidal soils (Wang et al., 2004; Wang and Sun, 2011). Feng et al. (2017) studied continuous spring maize in Jilin Province and found that maize yield in black soil averaged 8623 kg·ha^{-1}, significantly higher than that in wind-sand soil. The present study showed that the yield-increasing effects were the most significant in the CS. This was probably because when the experimental area was located in the arid CS-rich area, the higher soil calcium carbonate content reduced the risk of soil acidification by chemical fertilizers, which promoted microbial activation and the increase in soil nutrient content, leading to a significant rise in yield change (Gao et al., 2023). Wang et al. (2004) revealed that the higher the soil OM content, the greater the amount of soil nitrogen mineralization. The present study also noted that the yield-increasing effects of nitrogen application gradually increased with the increase in soil OM content.

Changes in soil bulk density can lead to changes in water, fertilizer, air and heat in the soil, which in turn affects the formation of crop yields (Chen et al., 2019; Minhas et al., 2023), and it was found that the range of soil bulk density suitable for crop growth is 1.2–1.3 g·cm^{-3} (Suuster et al., 2011). This is similar to the present study which found that the highest soil bulk density for yield increasing effect of nitrogen added maize was 1.2–1.4 g·cm^{-3}. In addition, in our study, when the soil bulk density exceeded 1.4 g·cm^{-3}, the yield-increasing effects of N application on maize began to decline significantly, which is consistent with Cui et al. (2024) finding that increasing soil bulk density had a negative effect on maize yield, probably because soils with higher bulk densities tended to be more compact, which impeded the growth of the plant's root system, and at the same time, high bulk density soils were unfavourable to the root system's uptake of water and nutrients, which led to the crop's yield reduction. Soil pH is one of the important factors affecting soil nitrification and has a regulatory effect on soil microbial community and soil nutrient transformation. In this study, it was concluded that the yield-enhancing effect of nitrogen application to maize increased gradually with increasing soil pH. Within a certain range, elevated soil pH increases the solubility of soil organic matter, providing a large amount of material rich in carbon and nitrogen groups for microbial activity, thus promoting nitrogen mineralization, and thus increasing maize yield. Use of nitrogen fertilizer in soils with too high a pH can lead to increased volatilization of soil NH_3, resulting in nitrogen losses affecting crop nutrient uptake and reducing yields (Laegreid, 1999; Zhang et al., 2022a). Soil C/N ratio is an indicator for evaluating soil nitrogen mineralization capacity, low C/N ratio accelerates nitrogen mineralization rate and soil microbial decomposition, while high carbon to nitrogen ratio produces inhibitory effects (Ge et al., 2013). In this study, we found that the yield increasing effect of N application to maize in Northwest China was higher at low carbon to nitrogen ratio. If the soil C/N ratio increases, it will lead to increased competition for nitrogen between the crop and the microorganisms in the soil (Gunther and Holger, 2003), and this increased competition will limit the amount of nitrogen released from the soil, which will further lead to a decrease in the nitrogen content of the crop leaves, a decrease in the rate of photosynthesis, and a decrease in yield (Gao et al., 2021). In addition, this study found that the highest yield increasing effect of N application to maize was found at the time when the soil quick-acting N content was low. At the time of low soil fertility, the soil demand for nitrogen fertilizer is high, when the appropriate amount of nitrogen fertilizer supply will instead make the yield increase effect higher. Phosphorus and potassium elements are large amounts of essential elements for crop growth and development, and play an important role in plant yield and quality formation (Qian et al., 2023). Shi et al. (2020) concluded that low soil potassium content would reduce the plant photosynthetic rate, thus affecting yield accumulation. Chen et al. (2020) found that appropriate phosphorus application would significantly enhance seed yield of wheat. This is in agreement with the present study which found that the yield-increasing effects of N application in maize were higher in areas with higher soil available phosphorus and available potassium. In our study, soil organic matter, pH, available potassium and total nitrogen all showed positive effects on the yield-increasing effects of N application on maize, reflecting a complex interaction effect between soil nutrients on maize growth, which is similar to Zhang et al. (2024) conclusion that high nutrient soil conditions (organic matter >15 $g \cdot kg^{-1}$; total nitrogen >1.5 $g \cdot kg^{-1}$) are the least restrictive to crop growth and development.

5 Conclusions

In this study, a meta-analysis was used to quantitatively investigate the effects of nitrogen addition on maize yield and its primary determinants in Northwest China. We found that nitrogen addition significantly increased maize yield by 53.04% in Northwest China, and the appropriate range of nitrogen application was 175–225 $kg \cdot ha^{-1}$. The analyzed data was highly heterogeneous (Q_t = 44580.2262, P_Q < 0.0001). After introducing explanatory variables using the random forest and multivariate optimality-seeking models, the effect of nitrogen addition on maize yield was mainly attributed to experimental year, maize variety, soil type, AN, and pH. Thus, we concluded that nitrogen must be added to maize cultivated in Northwest China and similar ecological zones to achieve sustainable, high yields while considering climatic conditions, field management practices, and soil environmental factors. Future research could investigate optimal nitrogen application strategies for various environmental conditions and evaluate how precision agriculture techniques enhance nitrogen fertilizer efficiency while minimizing environmental harm. Research should also focus on the effects of climate change on maize production potential in Northwest China and the formulation and assessment of adaptive management practices.

Data availability statement

The original contributions presented in the study are included in the article/supplementary material. Further inquiries can be directed to the corresponding authors.

Author contributions

YJ: Conceptualization, Data curation, Formal analysis, Investigation, Methodology, Writing – original draft, Writing – review & editing. HL: Data curation, Writing – review & editing. WM: Formal analysis, Writing – review & editing. WY: Formal analysis, Writing – review & editing. JC: Investigation, Writing – review & editing. YG: Investigation, Writing – review & editing. GQ: Conceptualization, Funding acquisition, Project administration, Supervision, Writing – review & editing. MY: Conceptualization, Project administration, Supervision, Writing – review & editing. YK: Funding acquisition, Project administration, Writing – review & editing. YM: Funding acquisition, Writing – review & editing. JW: Funding acquisition, Writing – review & editing. LX: Methodology, Writing – review & editing.

Funding

The author(s) declare financial support was received for the research, authorship, and/or publication of this article. This work was supported by the National Natural Science Foundation Project, China (52069001 and 51969003), the Industry Support Projects in Gansu Province Department of Education (2021CYZC-20); Key Research and Development Project of Gansu Province (22YF7NA110), Key science and technology projects of Gansu Province (23YFFA0020); the Innovation Fund for Universities in Gansu Province, China (2023A-054), the Science and Technology Program of Lanzhou City (2022-2-60), Gansu Agricultural University "Northwest arid region Collaborative Utilization of water and soil resources innovation team" discipline team construction project (Grant No. GAU-XKTD-2022-09), Gansu Agricultural University Youth Mentor Support Fund Project (GAU-QDFC-2022-22 and GAU-QDFC-2023-12).

Acknowledgments

We thank all the researchers whose data were used in this meta-analysis. We also gratefully acknowledge the editors and reviewers who put forward constructive comments on this article.

Conflict of interest

The authors declare that the research was conducted in the absence of any commercial or financial relationships that could be construed as a potential conflict of interest.

Publisher's note

References

Adriaanse, F. G., and Human, J. J. (1993). Effect of time of application and nitrate: ammonium ratio on maize grain yield, grain N concentration and soil mineral N concentration in a semi-arid region. *Field Crop Res.* 34, 57–70. doi: 10.1016/0378-4290(93)90111-Y

Akiyama, H., Yan, X., and Yagi, K. (2010). Evaluation of effectiveness of enhanced-efficiency fertilizers as mitigation options for N_2O and NO emissions from agricultural soils: meta-analysis. *Global Change Biol.* 16, 1837–1846. doi: 10.1111/j.1365-2486.2009.02031.x

Anwar, M. R., O'Leary, G. J., Rab, M. A., Fisher, P. D., and Armstrong, R. D. (2009). Advances in precision agriculture in south-eastern Australia. V. Effect of seasonal conditions on wheat and barley yield response to applied nitrogen across management zones. *Crop Pasture Sci.* 60, 901–911. doi: 10.1071/CP08351

Armstrong, R. D., Fitzpatrick, J., Rab, M. A., Abuzar, M., Fisher, P. D., and O'Leary, G. J. (2009). Advances in precision agriculture in south-eastern Australia: III. Interactions between soil properties and water use help explain spatial variability of crop production in the Victorian Mallee. *Crop Pasture Sci.* 60, 870–884. doi: 10.1071/CP08349

Bacon, S. A., Mau, R., Neto, F. M., Williams, R. L., and Turner, N. C. (2016). Effect of climate warming on maize production in Timor-Leste: interaction with nitrogen supply. *Crop Pasture Sci.* 67, 156–166. doi: 10.1071/CP15078

Benitez-Lopez, A., Alkemade, R., Schipper, A. M., Ingram, D. J., Verweij, P. A., Eikelboom, J. A. J., et al. (2017). The impact of hunting on tropical mammal and bird populations. *Science* 356, 180–183. doi: 10.1126/science.aaj1891

Buhmann, A. K., Waller, U., Wecker, B., and Papenbrock, J. (2015). Optimization of culturing conditions and selection of species for the use of halophytes as biofilter for nutrient-rich saline water. *Agr. Water Manage.* 149, 102–114. doi: 10.1016/j.agwat.2014.11.001

Cassman, K. G., Dobermann, A., and Walters, D. T. (2002). Agroecosystems, nitrogen-use efficiency, and nitrogen management. *Ambio* 31, 132–140. doi: 10.1579/0044-7447-31.2.132

Chen, C. X., Zhang, Y. Q., Xue, L. H., Lei, J. J., Chen, X. W., Liu, Y. X., et al. (2019). A comparison of physical properties of castanozem in rain-fed wheat fields with different yields in the Ili river valley. *Chin. J. Soil Sci.* 50, 304–309. doi: 10.19336/j.cnki.trtb.2019.02.08

Chen, Y. L., Zhang, P. P., Wang, L. F., Ma, G., Li, Z., and Wang, C. Y. (2020). Interaction of nitrogen and phosphorus on wheat yield, N use efficiency and soil nitrate nitrogen distribution in the North China plain. *Int. J. Plant Prod.* 14, 415–426. doi: 10.1007/s42106-020-00093-6

Cheng, Y. G., Jin, H., Zheng, P. S., Sun, C. F., Jiang, H. J., Jin, J., et al. (2024). Impact of intercropping green manure on saline-alkali soil characteristics and silage maize yield. *J. Agric. Resour. Environ.* 41, 1100–1110. doi: 10.13254/j.jare.2023.0618

Cui, J. J., Mak-Mensah, E., Wang, J. W., Li, Q., Huang, L., Song, S., et al. (2024). Interactive effects of drip irrigation and nitrogen fertilization on wheat and maize yield: a meta-analysis. *J. Soil Sci. Plant Nutr.* 24, 1547–1559. doi: 10.1007/s42729-024-01650-y

Da Silva, P. R. F., Strieder, M. L., Da Silva, C. R. P., Rambo., L., Sangoi, L., Argenta, G., et al. (2005). Grain yield and kernel crude protein content increases of maize hybrids with late nitrogen side-dressing. *Sci. Agr.* 62, 487–492. doi: 10.1590/S0103-90162005000500014

Dirks, V. A., and Bolton, E. F. (1981). Climatic factors contributing to year-to-year variation in grain yield of corn on Brookston clay. *Can. J. Plant Sci.* 61, 293–305. doi: 10.4141/cjps81-042

Feng, G. Z., Wang, Y., Yan, L., Mi, G. H., and Gao, Q. (2017). Effect of soil type and nitrogen application rate on yield of monocropping spring maize and nitrogen balance in crop field. *Acta Pedol. Sin.* 54, 444–455. doi: 10.11766/trxb201603230053

Gao, Y., Shao, G., Yang, Z., Zhang, K., Lu, J., Wang, Z., et al. (2021). Influences of soil and biochar properties and amount of biochar and fertilizer on the performance of biochar in improving plant photosynthetic rate: A meta-analysis. *Eur. J. Agron.* 130, 126345. doi: 10.1016/j.eja.2021.126345

Gao, R. P., Zhao, P. Y., Liu, X. Y., Zhang, J., Li, H. C., Huang, J., et al. (2023). Effects of long-term fertilization on soil physicochemical and biological properties of chestnut calcareous soil in agro-pastoral ecotone. *Chin. J. Ecol.* 42, 552–560. doi: 10.13292/j.1000-4890.202303.019

Gattinger, A., Muller, A., Haeni, M., Skinner, C., Fliessbach, A., Buchmann, N., et al. (2012). Enhanced top soil carbon stocks under organic farming. *PNAS* 109, 18226–18231. doi: 10.1073/pnas.1209429109

GB/T 17296-2009. (2009). *Chinese soil classification and code (National Standard of the People's Republic of China)*. Beijing: The Standardization Administration of China.

Ge, S. F., Zhou, L., Li, H. N., Men, Y. G., Wei, S. C., and Jiang, Y. M. (2013). Effect of soil C/N ratio on nitrogen utilization and growth of apple. *Chin. J. Eco-Agriculture.* 21, 795–800. doi: 10.3724/SP.J.1011.2013.00795

Gunther, S., and Holger, K. (2003). Bulk soil C to N ratio as a simple measure of net N mineralization from stabilized soil organic matter in sandy arable soils. *Soil Biol. Biochem.* 35, 629–632. doi: 10.1016/S0038-0717(03)00052-X

Guo, J. H., Liu, X. J., Zhang, Y., Shen, J. L., Han, W. X., Zhang, W. F., et al. (2010). Significant acidification in major Chinese croplands. *Science* 327, 1008–1010. doi: 10.1126/science.1182570

Han, S. X., Wang, S., Gao, Z. L., and Wang, D. W. (2014). Impact of N application on the yield of alfalfa, N accumulation and nitrogen use efficiency. *Acta Agric. Boreali Sin.* 29, 220–225. doi: 10.7668/hbnxb.2014.06.037

Hedges, L. V., and Gurevitch, J. (1999). The meta-analysis of response ratios in experimental ecology. *Ecology* 80, 150–1156. doi: 10.1890/0012-9658(1999)080

Jiang, Y. B., Qi, G. P., Yin, M. H., Kang, Y. X., Ma, Y. L., Wang, J. H., et al. (2022). Effects of water regulation and planting patterns on soil moisture, yield and quality in artificial grassland. *J. Soil Water Conserv.* 36, 260–270. doi: 10.13870/j.cnki.stbcxb.2022.06.032

Kay, B. D., Mahboubi, A. A., Beauchamp, E. G., and Dharmakeerthi, R. S. (2006). Integrating soil and weather data to describe variability in plant available nitrogen. *Soil Sci. Soc Am. J.* 70, 1210–1221. doi: 10.2136/sssaj2005.0039

Kong, F. L., Wu, Y. W., Cui, S. L., Wang, X. L., Wei, G., Liu, Q. L., et al. (2022). Effect of chemical fertilizer application on maize production in China over the past 15 years: a meta-analysis. *Agron. J.* 12, 1563–1572. doi: 10.3390/agronomy12123005

Kumar, D., Patel, R. A., Ramani, V. P., and Rathod, S. V. (2021). Evaluating precision nitrogen management practices in terms of yield, nitrogen use efciency and nitrogen loss reduction in maize crop under Indian conditions. *Int. J. Plant Prod.* 15, 243–260. doi: 10.1007/s42106-021-00133-9

Kyveryga, P. M., Blackmer, A. M., and Zhang, J. (2009). Characterizing and classifying variability in corn yield response to nitrogen fertilization on subfield and field scales. *Agron. J.* 101, 269–277. doi: 10.2134/agronj2008.0168

Laegreid, M. (1999). *Agriculture, fertilizers and the environment* Vol. 1 (New York: CABI Publishing in Association with Norsk Hydro ASA).

Li, Q. K. (1998). *Fertilizer problem in the sustainable development of Chinese agriculture* (Nanchang: Jiangxi Science and Technology Press), 38–51.

Li, Z. J. (2015). *Evaluating nitrogen loss and water and nitrogen use efficiencies in a double cropping system under different integrated managements in the North China Plain* (China Agricultural University: Beijing).

Li, M. Y., Hu, T. T., Cui, X. L., Luo, L. H., and Chen, S. M. (2021). Study on fertilization effect on winter wheat-summer corn yield in Guanzhong Plain based on Meta analysis. *Soil Fert. Sci.* 6, 300–311. doi: 10.11838/sfsc.1673-6257.20413

Li, G. H., Zhao, B., Dong, S. T., Zhang, J. W., Liu, P., and Lu, W. P. (2020). Controlled-release urea combining with optimal irrigation improved grain yield, nitrogen uptake, and growth of maize. *Agr. Water Manage.* 227, 105834. doi: 10.1016/j.agwat.2019.105834

Liu, R. L., Wang, Y., Hong, Y., Wang, F., Mao, X. P., and Yi, J. (2023). Controlled-release urea application and optimized nitrogen applied strategy reduced nitrogen leaching and maintained grain yield of paddy fields in Northwest China. *Front. Plant Sci.* 14. doi: 10.3389/fpls.2023.1033506

Liu, S., Xu, Y. F., Jia, J., Meng, F. G., Zhu, Z. X., Zhang, Y. L., et al. (2023). Effects of nitrogen application rate and topdressing stage on dry matter accumulation and nitrogen utilization of summer maize under drip irrigation. *Agr. Res. Arid Areas.* 41, 122–129. doi: 10.7606/j.issn.1000-7601.2023.02.14

Liu, X. T., Zheng, C. L., Cao, W., Dang, H. K., Cao, C. Y., Li, X. S., et al. (2021). Effects of long-term located fertilization on soil organic matter, nitrogen forms and crop yields. *Crops* 4, 130–135. doi: 10.16035/j.issn.1001-7283.2021.04.020

Liu, J., Zhu, G. L., Shi, G. F., Yi, W. P., and Xiao, Q. (2022). Assessment of yield and nitrogen utilization of the mixed CRU and urea in wheat-maize production in a 5-year field trial. *Sustainability* 14, 14943. doi: 10.3390/su142214943

Luo, N., Meng, Q. F., Feng, P. Y., Qu, Z. R., Yu, Y. D., Liu, D. L., et al. (2023). China can be self-sufficient in maize production by 2030 with optimal crop management. *Nat. Commun.* 14, 2637. doi: 10.1038/s41467-023-38355-2

Lv, C. Q., Tian, H. Q., and Huang, Y. (2007). Ecological effects of increased nitrogen deposition in terrestrial ecosystems. *J. Plant Ecol.* 31, 205–218. doi: 10.17521/cjpe.2007.0025

Lv, P., Zhang, J. W., Jin, L. B., Liu, W., and Liu, P. (2012). Effects of nitrogen application stage on grain yield and nitrogen use efficiency of high-yield summer maize. *Plant Soil Environ.* 58, 211–216. doi: 10.1016/j.fcr.2012.02.029

Ma, J. Y., Li, K. J., Cao, C. Y., and Zheng, C. L. (2007). Effect of long-term located organic-inorganic fertilizer application on Fluvo-aquic soil fertility and crop yield. *J. Plant Nutr. Fertil.* 13, 236–241. doi: 10.3321/j.issn:1008-505X.2007.02.009

Ma, G. S., Xue, J. Q., Lu, H. D., Zhang, R. H., Tai, S. J., and Ren, J. H. (2008). Effects of planting density and nitrogen fertilization on population physiological indexes of summer maize (*Zea mays* L.) in Guanzhong irrigated zone. *Acta Ecol. Sin.* 28, 661–668. doi: 10.3321/j.issn:1000-0933.2008.02.026

Meng, Y. X., Ma, W., Yao, X. H., Sun, Y. Q., Zhong, X., Huang, S., et al. (2023). Study on the response factors of maize yield to nitrogen fertilizer. *J. Agric. Sci. Technol.* 25, 153–160. doi: 10.13304/j.nykjdb.2021.1032

Minhas, W. A., Mumtaz, N., Ur-Rehman, H., Farooq, S., Farooq, M., and Ali, H. M. (2023). Weed infestation and productivity of wheat crop sown in various cropping systems under conventional and conservation tillage. *Front. Plant Sci.* 14. doi: 10.3389/fpls.2023.1176738

Overman, A. R., and Scholtz, R. V. (1999). Model for accumulation of dry matter and plant nutrients by corn. *Commun. Soil Sci. Plan.* 30, 15–16. doi: 10.1080/00103629909370355

Qian, C. C., Chen, L., Ma, Q., Li, C. Y., Zhu, M., Zhu, X. K., et al. (2023). Effects of phosphorus and potassium fertilizer on grain yield, nutrient uptake and utilization in low-gluten wheat. *J. Plant Nutr. Fertil.* 29, 287–299. doi: 10.11674/zwyf.2022314

Qiao, Y., Yang, H., Luo, J. L., Wang, S. X., Liang, L. Y., Chen, X. P., et al. (2022). Inputs and ecological environment risks assessment of maize production in Northwest China. *Sci. Agric. Sin.* 55, 962–976. doi: 10.3864/j.issn.0578-1752.2022.05.010

R Core Team. (2018). *R: A Language and Environment for Statistical Computing* (Vienna, Austria: R Foundation for Statistical Computing). Available online at: https://www.R-project.org/ (Accessed 2 June 2019).

Ren, C. L., Ma, Y. L., Dong, X. X., Zhang, L. J., and Ji, Y. Z. (2012). Effects of applying controlled-release urea on the yield, nitrogen use efficiency and soil NO_3^--N of summer maize. *J. Hebei Agric. Univ.* 35, 12–17. doi: CNKI:SUN:CULT.0.2012-02-004

Sainju, U. M., Whitehead, W. F., and Singh, B. P. (2003). Agricultural management practices to sustain crop yields and improve soil and environmental qualities. *Sci. World J.* 3, 768–789. doi: 10.1100/tsw.2003.62

Scharf, P., Wiebold, W., and Lory, J. (2002). Corn yield response to nitrogen fertilizer timing and deficiency level. *Agron. J.* 94, 435–441. doi: 10.2134/agronj2002.0435

Sepahvand, P., Sajedi, N., Mousavi, S. K., and Ghiasvand, M. (2014). Effects of nitrogen application method and weed control on corn yield and yield components. *Pak. J. Biol. Sci.* 17, 497–503. doi: 10.3923/pjbs.2014.497.503

Shan, L., Wu, P. T., and Shangguan, Z. P. (2021). *Research on sustainable development strategy of food security in Northwest China* (Beijing: Science press).

Shi, X. X., Zhang, J. Q., Zhang, Y. M., Wang, N., Ma, J. R., and Xiao, K. (2020). Functional characterization on the wheat potassium channel gene *TaPC*/in mediating plant adaptation to potassium deprivation. *J. Plant Nutr. Fertil.* 26, 840–849. doi: 10.11674/zwyf.19381

Suuster, E., Ritz, C., Roostalu, H., Reintam, E., Kolli, R., and Astover, A. (2011). Soil bulk density pedotransfer functions of the humus horizon in arable soils. *Geoderma* 163, 74–82. doi: 10.1016/j.geoderma.2011.04.005

Terrer, C., Phillips, R. P., Hungate, B. A., Rosende, J., and Jackson, R. B. (2021). A trade-off between plant and soil carbon storage under elevated CO_2. *Nature* 591, 599–603. doi: 10.1038/s41586-021-03306-8

Tremblay, N., Bouroubi, Y. M., Belec, C., Mullen, R. W., Kitchen, N. R., Thomason, W. E., et al. (2012). Corn response to nitrogen is influenced by soil texture and weather. *Agron. J.* 104, 1658. doi: 10.2134/agronj2012.0184

Walsh, O., Raun, W., Klatt, A., and Solie, J. (2012). Effect of delayed nitrogen fertilization on maize (*Zea mays* L.) grain yields and nitrogen use efficiency. *J. Plant Nutr.* 35, 538–555. doi: 10.1080/01904167.2012.644373

Wang, J. Q. (2007). *Analysis and evaluation of yield increase effect and nutrient use efficiency of main grain crops in China* (China Agricultural University: Beijing).

Wang, L., Coulter, J. A., Palta, J. A., Xie, J., and Deng, X. (2019). Mulching-induced changes in tuber yield and nitrogen use efficiency in potato in China: a meta-analysis. *Agron. J.* 9, 1–15. doi: 10.3390/agronomy9120793

Wang, Y., Guo, D., Gao, Q., Yan, L., Song, L. X., and Liu, Z. G. (2016c). Differences in yield response and N use efficiency of maize crops in different ecological zones of Jilin province. *Acta Pedol. Sin.* 53, 1464–1475. doi: 10.11766/txb201603230019

Wang, D., Li, G. Y., Mo, Y., Cai, M. K., and Bian, X. Y. (2018). Evaluation of optimal nitrogen rate for corn production under mulched drip fertigation and economic benefits - ScienceDirect. *Field Crop Res.* 216, 225–233. doi: 10.1016/j.fcr.2017.10.002

Wang, S. J., Luo, S. S., Li, X. S., Yue, S. C., Shen, Y. F., and Li, S. Q. (2016a). Effect of split application of nitrogen on nitrous oxide emissions from plastic mulching maize in the semiarid Loess Plateau. *Agr. Ecosyst. Environ.* 220, 21–27. doi: 10.1016/j.agee.2015.12.030

Wang, A. X., Ma, Y. L., Qi, G. P., Kang, Y. X., Yin, M. H., Wang, J. H., et al. (2022). Water and nitrogen regulation patterns for productivity improvement of *Bromus inermis* and *Alfalfa* mixed grassland. *J. Soil Water Conserv.* 36, 322–330. doi: 10.13870/j.cnki.stbcxb.2022.02.041

Wang, S. L., Qi, H., Wang, Y., Zhang, Q., Feng, G. Y., Lin, Y. Z., et al. (2016b). Effects of fertilization of N P K on maize yield, nutrients uptake and using efficiency. *J. Shanxi Agric. Univ. (Nat. Sci. Ed.)* 36, 768–773. doi: 10.13842/j.cnki.issn1671-8151.2016.11.002

Wang, L. L., and Sun, B. (2011). Effects of temperature and soil type on nitrogen mineralization. *J. Plant Nutr. Fertil.* 17, 583–591. doi: 10.11674/zwyf.2011.0445

Wang, C. H., Xing, X. R., and Han, X. G. (2004). Advances in study of factors affecting soil N mineralization in grassland ecosystems. *Chin. J. Appl. Ecol.* 15, 2184–2188. doi: 10.13287/j.1001-9332.2004.0451

Wu, P. X., Jiang, J. Y., Fang, Y., and Shangguan, Z. P. (2023). High-quality developmental methods for dryland farming in Northwest China. *Agr. Res. Arid Areas.* 41, 21–24 + 95. doi: 10.7606/j.issn.1000-7601.2023.03.04

Wu, X. Y., Tong, L., Kang, D. K., Wang, L., Ma, D. Q., Yang, Q. K., et al. (2022). Effects of regulated deficit irrigation on water consumption and yield of maize under different planting densities in Northwest China. *Trans. CSAE.* 38, 59–67. doi: 10.11975/j.issn.1002-6819.2022.z.007

Xiang, Y. Z., Deng, Q., Duan, H. L., and Guo, Y. (2017). Effects of biochar application on root traits: a meta-analysis. *Glob. Change Biol. Bioenergy* 9, 1563–1572. doi: 10.1111/gcbb.12449

Xie, M., Tremblay, N., Tremblay, G., Bourgeois, G., Bouroubi, M. Y., and Wei, Z. (2013). Weather effects on corn response to in-season nitrogen rates. *Can. J. Plant Sci.* 93, 407–417. doi: 10.4141/cjps2012-145

Xu, R. Z., Wu, X. J., and Yang, H. M. (2022). Effect of topdressing after cutting on alfalfa growth and production. *Acta Prataculturae Sin.* 31, 195–204. doi: 10.11686/cyxb2021265

Yamoah, C. F., Francis, C. A., Varvel, G. E., and Waltman, W. J. (1998). Weather and management impact on crop yield variability in rotations. *J. Prod Agric.* 11, 219. doi: 10.2134/jpa1998.0219

Yan, P., Zhang, Q., Shuai, X. F., Pan, J. X., Zhang, W. J., Shi, J. F., et al. (2015). Interaction between plant density and nitrogen management strategy in improving maize grain yield and nitrogen use efficiency on the North China Plain. *J. Agric. Sci.* 154, 978–988. doi: 10.1017/S0021859615000854

Ye, Y. S., Liang, X. Q., Chen, Y. X., Liu, J., Gu, J. T., Guo, R., et al. (2013). Alternate wetting and drying irrigation and controlled-release nitrogen fertilizer in late-season rice. Effects on dry matter accumulation, yield, water and nitrogen use. *Field Crop Res.* 144, 212–224. doi: 10.1016/j.fcr.2012.12.003

Zamora-Re, M. I., Dukes, M. D., Hensley, D., Rowland, D., and Graham, W. (2020). The effect of irrigation strategies and nitrogen fertilizer rates on maize growth and grain yield. *Irrigation Sci.* 38, 461–478. doi: 10.1007/s00271-020-00687-y

Zhang, L. C., Meng, F. C., Zhang, X. Y., Gao, Q., and Yan, L. (2024). Optimum management strategy for improving maize water productivity and partial factor productivity for nitrogen in China: A meta-analysis. *Agr. Water Manage.* 303, 109043. doi: 10.1016/j.agwat.2024.109043

Zhang, Z. J., Shi, X., and Ling, T. (2022c). Influencing factors and empirical test of spatial variation of fertilizer application intensity in China. *Shanxi Agric. Univ* 21, 10–19. doi: 10.13842/j.cnki.issn1671-816X.2022.03.002

Zhang, L. G., Shi, X. Y., Wang, Y. B., Yang, X. R., Yu, F., Jiang, T., et al. (2022b). Meta-analysis for the impacts of straw return on the diseases of major grain crops in China. *Trans. CSAE.* 38, 93–100. doi: 10.11975/j.issn.1002-6819.2022.21.012

Zhang, F. S., Wang, J. Q., Zhang, W. F., Cui, Z. L., Ma, W. Q., Chen, X. P., et al. (2008). Nutrient use efficiencies of major cereal crops in China and measures for improvement. *Acta Pedol. Sin.* 45, 915–924. doi: 10.3321/j.issn:0564-3929.2008.05.018

Zhang, D. B., Yao, P. W., Na, Z., Cao, W. D., Zhang, S. Q., Li, Y. Y., et al. (2016). Soil water balance and water use efficiency of dryland wheat in different precipitation years in response to green manure approach. *Sci. Rep-UK* 6, 26856. doi: 10.1038/srep26856

Zhang, L. C., Zhang, X. Y., Gao, Q., and Yan, L. (2022a). Study on the effect of nitrogen fertilizer application on maize yield in North China based on meta-analysis. *J. Sichuan Agric. Univ.* 40, 550–557. doi: 10.16036/j.issn.1000-2650.202202084

Zhao, S. L., Li, F. M., Zhang, D. Y., and Duan, S. S. (1997). Crop production is a population process. *Acta Ecol. Sin.* 17, 102–106. doi: CNKI:SUN:STXB.0.1997-01-014

frontiers | Frontiers in Plant Science

TYPE Original Research
PUBLISHED 07 January 2025
DOI 10.3389/fpls.2024.1504083

OPEN ACCESS

EDITED BY
Khurram Shahzad,
Lasbela University of Agriculture, Water and Marine Sciences, Pakistan

REVIEWED BY
Yunshan Yang,
Shihezi University, China
Hassan Karim,
Department of Agricultural and Forest Sciences and Engineering, University of Lleida, Spain
Abu Zar Ghafoor,
Warsaw University of Life Sciences, Poland

*CORRESPONDENCE
Dong Wang
wangd@nwafu.edu.cn
Xiang Lin
sdslinxiang@163.com

RECEIVED 30 September 2024
ACCEPTED 29 November 2024
PUBLISHED 07 January 2025

CITATION
Ali MF, Han R, Lin X and Wang D (2025) Controlled-release nitrogen combined with ordinary nitrogen fertilizer improved nitrogen uptake and productivity of winter wheat. *Front. Plant Sci.* 15:1504083.
doi: 10.3389/fpls.2024.1504083

Controlled-release nitrogen combined with ordinary nitrogen fertilizer improved nitrogen uptake and productivity of winter wheat

Muhammad Fraz Ali, Ruifeng Han, Xiang Lin* and Dong Wang*

State Key Laboratory for Crop Stress Resistance and High-Efficiency Production, College of Agronomy, Northwest A & F University, Yangling, Shaanxi, China

Background: Blending controlled-release nitrogen fertilizer (CRNF) with ordinary nitrogen fertilizer (ONF) is a strategic approach to improve winter wheat nutrient management. This blend provides nitrogen (N) to winter wheat in a balanced and consistent manner, ensuring long-term growth, reducing nutrient loss due to leaching or volatilization, and increasing N use efficiency (NUE).

Aims: CRNF aims to enhance N application suitability, optimizes soil nutrient dynamics, and its widespread use can boost crop NUE and yield. The study investigates how different CRNF and ONF blending ratios affect soil N content, winter wheat growth, and yield.

Methods: The experiment used two N application rates of 192(N_1) and 240(N_2) kg ha^{-1} of ONF, with five different blending ratios CRNF. The proportions of CRNF were 0%(F_1), 30%(F_2), 50%(F_3), 70%(F_4), and 100%(F_5), respectively. The effects of changes in soil nitrate concentration, dry matter accumulation, N uptake, and transportation at various growth stages and yield were analyzed.

Results: CRNF at the jointing and anthesis stages helps maintain nitrate N levels throughout the growth cycle. Compared to full CRNF application at different N rates, this method also reduces nitrate N leaching in the soil. The 0-60 cm soil layer was primarily influenced by increasing the proportion of CRNF, especially from jointing to maturity. CRNF promotes a higher plant population during the turning green and jointing stages by increasing soil N content, thereby establishing a strong yield foundation for winter wheat. It increases winter wheat N accumulation and correlates positively with soil N content during key growth stages.

Conclusion: Winter wheat grain yield has increased, with significant yield increases observed at 70% blending with a higher amount of N at 240 kg ha^{-1} and achieved a 2.8% increase in NUE and a 3.0%-15.3% increase in grain yield. In order to improved winter wheat yields through effective N utilization, N2 application (240 kg ha^{-1}) with the combination of (F_4) 30% ONF + 70% CRNF would be recommended for northwest region of Shaanxi province in China. By increasing the amount of N accumulation at the anthesis stage, N transport is significantly increased after anthesis, and N accumulation and distribution ratio in grains are significantly increased at maturity.

KEYWORDS

controlled released nitrogen fertilizer, grain yield, nitrogen accumulation, soil nitrogen supply, winter wheat

Highlights

- Increasing CRNF increased soil nitrate N content and reduced leaching across winter wheat growth.
- Combination of CRNF and ONF increased DM accumulation from jointing to maturity in winter wheat.
- CRNF at 70% combined with ONF increased N accumulation, N uptake and N use efficiency of winter wheat.
- Using 70% CRNF combined with ONF at 240 kg ha^{-1} overcame the bottleneck of increasing the yield and NUE.

1 Introduction

Farmers were using fertilizers from the ancient time itself, but the long-term use of fertilizers had affected the soil fertility which led to pollution of water, air, and soil. Nitrogen (N), particularly in the form of urea, is an essential nutrient fertilizer, which has been critical for increasing plant growth and yield and is widely used to maintain soil fertility (Dimkpa et al., 2020). China is the largest user of urea, which has been used to increase crop production and address food security challenges (Snapp et al., 2023; Gu, 2023). According to statistics, synthetic N input to field crops in China has increased by 215% since 1980 (Zhang et al., 2022a). However, crop N uptake has only increased by 109% in the last 30 years, resulting in lower N fertilizer recovery efficiency (Yan et al., 2014). When urea is applied to farmland, nutrients are rapidly released, and a significant portion is lost due to ammonia volatilization and nitrate N leaching, which are the primary causes of low N utilization efficiency (NUE) (Hussain et al., 2022; Xiao et al., 2019). Furthermore, applying more N than the crop requirement may disturb groundwater, surface water, and atmosphere via N leaching, runoff, and volatilization (Ntinyari et al., 2022), resulting in a waste of resources and energy, as well as an increase in environmental pollution and production costs (Hussain et al., 2023b). Additionally, low NUEs lead to lower economic returns for growers from their fertilizer investments (Snapp et al., 2023).

Global reliance on winter wheat as a primary food source is increasing, with demand expected to double in the 21st century, exceeding current production requirements (Wu et al., 2023; Erenstein et al., 2022). Wheat production is reducing due to numerous factors such as environmental stresses, late sowing, lack of high-quality seeds, climate variability, and insect pests. Fertilizer use must be optimized to address environmental concerns while ensuring global food security (Anderson et al., 2020). The Chinese Ministry of Agriculture introduced the 'Zero Increase Action Plan' a strategy to boost crop yields and mitigate environmental issues without increasing fertilizer usage (Liu et al., 2016). This policy proposed several management practices for optimal N fertilizer application, one of which is the development of a controlled-release N fertilizer (CRNF), which provides a new theoretical method for simple and efficient fertilization technology for field crops (Vejan et al., 2021).

Controlled-release urea (CRU) is a new type of urea fertilizer with a physical coating that ensures controlled N release into the soil over time to ensure a continuous supply of N, thereby improving crop N demand and supply coordination (Zhang et al., 2022; Vejan et al., 2021). It is frequently used as a basal fertilizer because it saves labor costs for split application compared to regular urea and improves the synchronization of N supply to soil (Geng et al., 2015; Ma et al., 2021). Various studies have confirmed that the application of CRU significantly increased the NUE and yield of winter wheat (Yang et al., 2011; Zhang et al., 2022; Ma et al., 2021; Zheng et al., 2016; Zhu et al., 2020). For example, Zhou et al. (2023) proposed CRU optimization and stated that CRU proportion was more critical than CRU longevity, reporting that under N treatments of 157.5, 180, and 225 kg ha^{-1}, the optimal ranges of CRU proportion were 41~64%, 38~64%, and 24~40% for wheat yield, respectively. In another study, Li et al. (2020) reported that irrigation management and CRU significantly impacted maize growth and development, enhancing plant dry matter (DM) accumulation and N uptake. Similarly, Zheng et al. (2016) reported in a 5-year study of CRU in a wheat-maize cropping system that the application of CRU as a basal fertilizer outperformed normal urea (NU) applied as split fertilization with the same quantity of N application.

Abbreviations: N, Nitrogen; NUE, Nitrogen utilization efficiency; CRNF, controlled-release nitrogen fertilizer; CRU, controlled-release urea; DM, dry matter; NU, normal urea; ONF, ordinary nitrogen fertilizer; NUpE, nitrogen uptake efficiency; NFPP, nitrogen fertilizer partial productivity.

Winter wheat has a more extended growing season and requires more labor, which is becoming expensive, so it is vital to promote the use of CRU in wheat cultivation and save labor costs. The CRU application is sub-optimal, so the combination of CRU and NU can make soil N supply more consistent with winter wheat N demand, increase N absorption, and affect wheat grain quality characteristics (Zhang et al., 2018; Zhou et al., 2019). A combination of CRU and NU should be used as a base fertilizer for winter wheat for winter wheat balances N supply, overcoming initial slow release and ensuring long-term availability (Zhang et al., 2022; Li et al., 2018). As a result, this combination is a potential N fertilizer management strategy for increasing wheat grain yield and protein content, and its mechanism should be thoroughly investigated.

Previous research has primarily focused on the release timing of CRNF related to crop N uptake and the resulting yield benefits. However, more research is needed to understand how CRNF responds to variations in soil N availability and N supply capacity. We hypothesized that combining CRNF and ONF would make the soil N supply more consistent with the N demand of winter wheat, increase N absorption in winter wheat, and possibly affect grain yield. Based on this, the current experiment used different blending ratios of CRNF and ONF to explore the soil N supply situation during the entire growth period of winter wheat. The current study aims to investigate winter wheat growth under different soil N supply conditions and to analyze how different blending ratios of CRNF and ONF can affect soil nutrient dynamics and winter wheat productivity. The regulatory pathways and mechanisms of different CRNF and ONF mixing ratios on N accumulation and transport, and the physical properties of winter wheat will be investigated, in order to develop high-quality, appropriate, and effective fertilization solutions.

2 Materials and methods

2.1 Experimental site and materials

The experiment was conducted during two wheat growing seasons from 2020 to 2022 at the an experimental demonstration site of Northwest A&F University, in Liangma Village, Wugong County, Xianyang City, Shaanxi Province (34°21'N, 108°02'E). The experimental site has an altitude of 443 m, with an average annual rainfall of 504.6 mm and a temperature of 14.37°C. The cropping system of the experimental site was summer maize-winter wheat rotation. All maize residue was crushed during the experiment and returned to the field after harvest. The average daily temperature and rainfall in the two-winter wheat cropping season (2020-2022) are shown in Figure 1. The physical and chemical properties of the soil (0-20 cm) in the soil layer before sowing for the two years are shown in Table 1.

This study used the winter wheat cultivar 'Xinong 20', which is widely grown locally. The N fertilizers included in this study were resin-coated urea (CRNF 44%, N) and ordinary urea (ONF 46.4% N). The controlled-release period was 90 days, and it was supplied by Weituoer Company, Yangling District, Shaanxi Province. Potassium chloride (K_2O 60%) and heavy superphosphate fertilizer (P_2O_5 46%) were utilized as potassium and phosphate fertilizer, respectively.

2.2 Experimental design

The experiment used a randomized complete block design with two factors and three replications. The factors include two N application rates (N_1, 192 kg ha^{-1}; N_2 240 kg ha^{-1}) of ONF and different blending ratios of CRNF and ONF are set under two N application rates, which were 100% ONF (F_1), 70% ONF + 30% CRNF (F_2), and 50% ONF + 50% CRNF (F_3), 30% ONF + 70% CRNF (F_4), and 100% CRNF (F_5). The N_2 (240 kg ha^{-1}) is the local conventional N application amount while N_1 (192 kg ha^{-1}) is a 20% reduction in N. The application rate of phosphorus and potassium fertilizers in all treatments was the same, 120 kg ha^{-1}. Nitrogen, phosphorus, and potassium fertilizers were applied as basal fertilizers in every treatment. The area of the test plots was 10 m length × 2 m width (20 m^2). The winter wheat for 2020-2021 was planted on October 26 and harvested on June 11, while the winter wheat for 2021-2022 was planted on

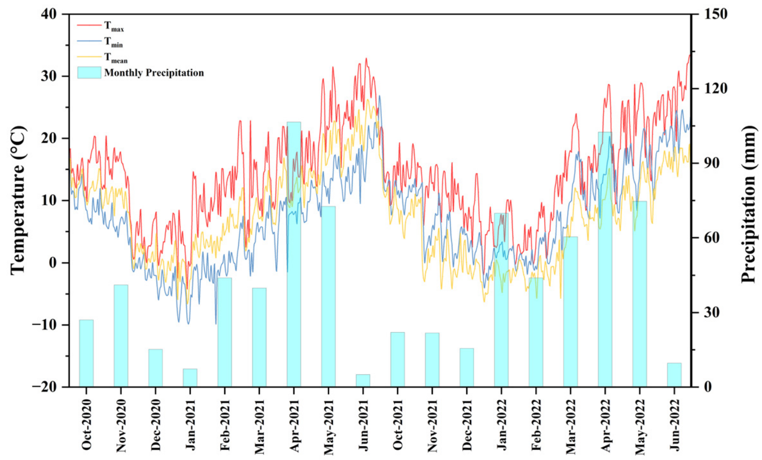

FIGURE 1
Daily precipitation and temperature during the winter wheat growing season from 2020-2022.

TABLE 1 Soil physical and chemical properties of 0-20 cm soil layer before sowing.

Year	Organic matter (g kg^{-1})	Total nitrogen (g kg^{-1})	Hydrolysable nitrogen (mg kg^{-1})	Available phosphorus (mg kg^{-1})	Available potassium (mg kg^{-1})
2020-2021	1.5	0.97	64.1	10.4	220.2
2021-2022	1.6	0.93	54.5	20.7	231.5

October 17 and harvested on June 9. Irrigation, weeding, and other management practices during the growth period of winter wheat are the same as those of local farmers.

2.3 Sampling and measurements

2.3.1 Soil nitrogen dynamics

Two core soil samples were collected from the 0-10, 10-20, 20-30 and 30-40 cm soil layers using an auger having an inner diameter of 4.0 cm. Soil samples were collected and stored in a labeled plastic bag from each plot during the overwintering, greening, jointing, and anthesis stages of winter wheat. Soil samples were collected from the 0-200 cm soil layer at maturity stage. After air drying, the soil sample was sieved and weighed 5.0 g (accurate to 0.001), were extracted with 50 mL of 1 mol L^{-1} KCl, shaken for 30 minutes, then filtered, and the soil nitrate N and ammonium N content were measured using the continuous flow analyzer (Model AA3-A001-02E, Bran-Luebbe, Germany) in the laboratory (Markus et al., 1985).

2.3.2 Dry matter accumulation and distribution

Plant samples were taken during the overwintering, greening, jointing, anthesis, and maturity stages to determine the aboveground DM accumulation and distribution. Stem, leaves, and spike were sampled at overwintering, greening, jointing, and anthesis stages, while stem, leaves, rachis+glume, and grain were sampled at the maturity stage. The separated plants were placed in an oven at 105°C for 30 minutes and dried at 70°C to a constant weight. The samples were then weighed separately. The calculation formulas for each indicator are as follows:

$$DM\ distribution\ to\ grains\ at\ maturity\ stage(\%) = \frac{Distribution\ of\ dry\ matter\ in\ grains\ at\ maturity\ stage}{Accumulation\ above\ ground\ dry\ matter\ at\ maturity\ stage} \times 100 \quad (1)$$

$$Contribution\ rate\ of\ assimilates\ stored\ in\ vegetative\ organs\ before\ anthesis\ to\ grain(\%) = \frac{assimilates\ transported\ in\ vegetative\ organs\ stored\ before\ anthesis}{dry\ weight\ of\ grains\ at\ maturity} \times 100 \quad (2)$$

$$Contribution\ rate\ of\ assimilates\ to\ grains\ after\ anthesis\ (\%) = \frac{allocation\ amount\ of\ assimilates\ in\ grains\ after\ anthesis}{dry\ weight\ of\ grains\ at\ maturity} \times 100 \quad (3)$$

$$Storage\ and\ assimilation\ of\ vegetative\ organs\ before\ anthesis(kg\ ha^{-1}) = dry\ matter\ at\ anthesis - dry\ matter\ at\ maturity \quad (4)$$

$$Distribution\ of\ assimilates\ in\ grains\ after\ anthesis\ (kg\ ha^{-1}) = dry\ weight\ of\ grains\ at\ maturity - assimilates\ transported\ in\ vegetative\ organ\ storage\ before\ anthesis \quad (5)$$

2.3.3 Nitrogen accumulation and transport in plants

The N content of dried plant samples was determined using the semi-micro Kjeldahl N determination method after they were crushed with a plant crusher and passed through a 100-mesh sieve. The following were the calculation formula for the related indicators of N absorption, accumulation, distribution, and utilization of winter wheat:

$$N\ accumulation\ (kg\ ha^{-1}) = N\ content\ \times Dry\ matter\ accumulation \quad (6)$$

$$N\ transport\ before\ anthesis\ (kg\ ha^{-1}) = N\ accumulation\ in\ vegetative\ organs\ during\ anthesis - N\ accumulation\ in\ vegetative\ organs\ during\ maturity \quad (7)$$

$$N\ transport\ efficiency\ before\ anthesis\ (\%) = \frac{N\ transport\ amount\ before\ anthesis}{N\ accumulation\ during\ anthesis\ period} \quad (8)$$

$$Contribution\ rate\ of\ before\ anthesis\ N\ to\ grain\ N\ (\%) = \frac{Before\ anthesis\ N\ transport\ amount}{Grain\ N\ accumulation\ amount} \quad (9)$$

$$N\ accumulation\ after\ anthesis\ (kg\ ha^{-1}) = N\ accumulation\ in\ grains - N\ trasnport\ before\ anthesis \quad (10)$$

$$Contribution\ rate\ of\ post\ anthesis\ N\ to\ grain\ N\ (\%) = \frac{Post\ anthesis\ N\ accumulation}{Grain\ N\ accumulation} \quad (11)$$

The calculation formula for NUE related indicators is as follows:

$$N\ absorption\ efficeincy\ (NUpE,\ kg\ kg^{-1}) = \frac{Plant\ N\ accumulation}{N\ application\ rate} \quad (12)$$

$$N\ use\ efficeincy\ (NUE,\ kg\ kg^{-1}) = \frac{Grain\ Yield}{Aboveground\ N\ accumulation} \quad (13)$$

$$N\ fertilizer\ partial\ productivity\ (PFP,\ kg\ kg^{-1}) = \frac{Grain\ yield}{N\ application\ rate} \quad (14)$$

2.3.4 Yield and its components

Plants were harvested at the maturity stage from a 2.0 m^2 area from each plot. After threshing, impurities were removed, and the grains were air-dried, and adjusted standard moisture content (12%) to calculate the grain yield per hectare. In each plot, a sample of 1.0 m^2 area is used for calculating number of spikes per unit area and grains number per spike. The 1000-grain weight was calculated from 1000 grains of the yield measurement samples taken for each plot to measure the yield components.

2.4 Statistical analysis

The data were recorded, analyzed and plotted using Microsoft Excel 2016, IBM SPSS 16.0 ((https://www.ibm.com/products/spss-statistics) and Origin 2023b (https://www.originlab.com/index.aspx?go=PRODUCTS/Origin), respectively. Duncan's test was used for multiple comparisons ($P < 0.05$). The structural equation (SEM) model is an extension of factor analysis used to test entity theory from empirical data. It is an advanced and robust multivariate statistical method for testing complex path relationship networks. This study assumes that CRNF and ONF application directly or indirectly affect yield components; it was conducted using the 'plspm' package of R software, version 3.5.1. model, and report the standardization coefficient of each path in each component model. Significance tests were conducted based on the path coefficients between latent variables.

3 Results

3.1 Soil nitrogen dynamics

3.1.1 Nitrate nitrogen

Nitrate N is essential for amino acid synthesis, protein production, and promotes tillering in winter wheat. The CRNF fertilizer treatments significantly increased soil N availability. Compared to N_1, the N_2 application rate for soil nitrate N was significantly higher at the greening, jointing, and anthesis stages in the 0-20 cm soil layer. During the wintering period, under various CRNF treatments, the F_1 and F_2 treatments had significantly higher nitrate N content in the 0-40 cm soil layer (Figure 2). At the anthesis and maturity stages, the F_1, F_2, and F_3 treatments were significantly lower than the F_4 and F_5 treatments. In 2021-2022, there were no significant differences in the nitrate N content in the 0-40 cm soil layer between treatments (Figure 2). Notably, the proportion of CRNF with F_4 provides a more sustained supply of soil nitrate N from the regreening stage to the anthesis stage of winter wheat compared to the sole application of ONF.

3.1.2 Ammonium nitrogen

Ammonium N promotes and stimulates root growth and development, enhancing water and nutrient uptake. The soil ammonium N content in the 0-40 cm soil layer was lower in 2020-2021 than in 2021-2022 (Figure 3). There was no significant difference in ammonium N content between the two N application rates at the wintering, regreening, and jointing stages. When the proportion of CRNF was increased to 70%, higher ammonium N content was observed at the regreening and jointing stages in the 0-20 cm soil layer among different CRNF treatments (Figure 3). At jointing stage, the performance of ammonium N in soil was ranked as follow: $F_4 > F_3$, $F_5 > F_1$, F_2. The results show that the ammonium N content in 0-40 cm soil is generally lower than the nitrate N content, as the proportion of CRNF increases in the winter wheat regreening and jointing stages.

3.1.3 Soil nitrate nitrogen at maturity stage

The soil nitrate N content at 0-100 cm during the winter wheat maturity period in 2021-2022 was generally higher than in 2020-2021 (Figure 4). The nitrate N accumulation in the 100-200 cm soil layer was significantly higher in the N_2 application of N rates, when the proportion of CRNF is 0%, 30%, and 50%. The nitrate N accumulation in the 100-200 cm soil layer showed no significant difference between N_1 and N_2 application rates when the proportion of CRNF is 70% and 100% (Figure 4). Overall, nitrate levels are relatively low, but notable increases are observed between 80-120 cm depth, likely originating from previous seasons' excessive rainfall and irrigation. The results showed that increasing the amount of ONF applied promotes downward leaching of soil nitrate N, which is detrimental to winter wheat absorption and utilization. CRNF leaches less soil nitrate N and can provide more soil N supply than ONF due to its slower release rate in the early stage. The amount of CRNF applied should be increased appropriately.

3.2 Dry matter accumulation and transport

3.2.1 Dry matter accumulation dynamics

Dry matter (DM) accumulation and transport play pivotal roles in winter wheat development and yield, progressively increasing throughout the growth period. The DM accumulation in 2021-2022 was overall higher than that in 2020-2021. Under the two ONF application rates, the N_2 nitrogen application rate was significantly more significant than the N_1 nitrogen application rate during the

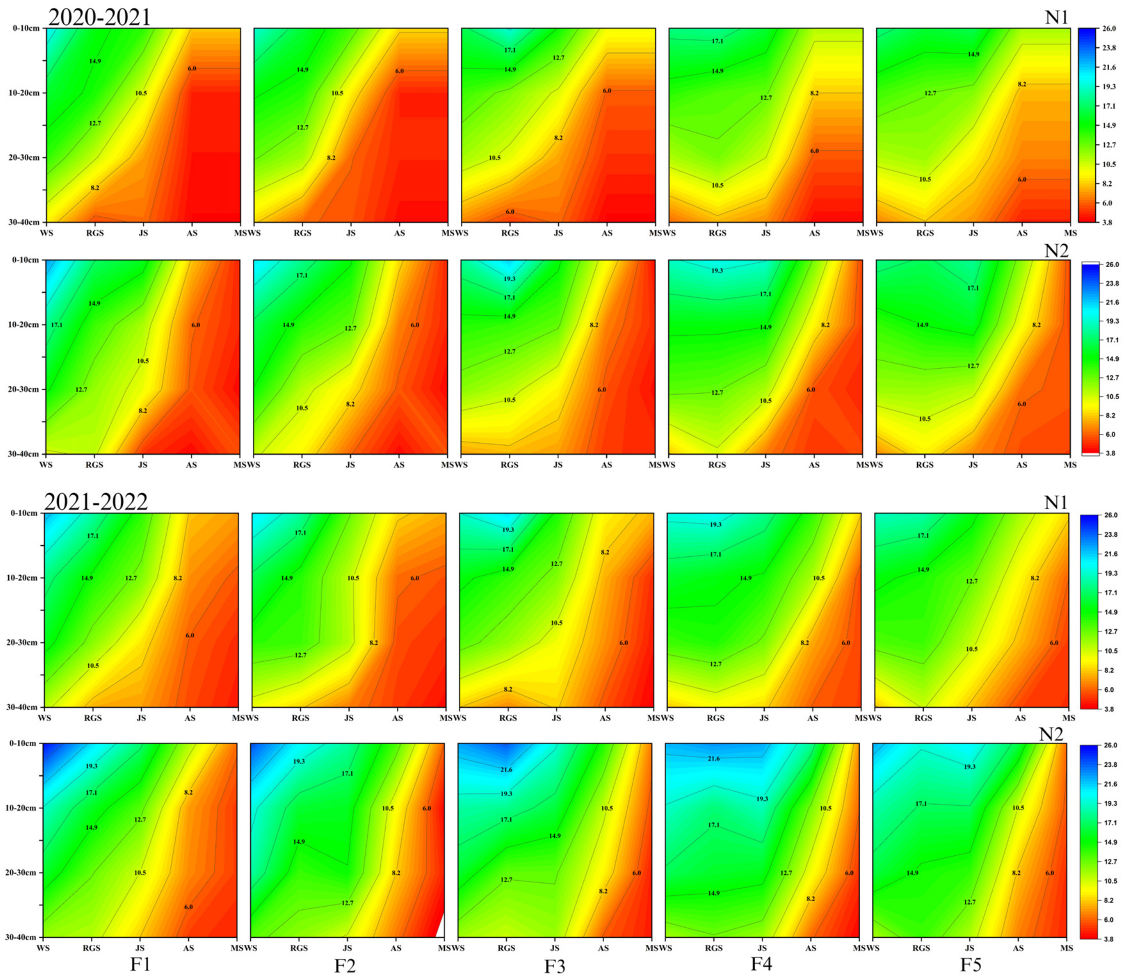

FIGURE 2
Dynamics of soil nitrate nitrogen (NO_3^-N) concentrations in the 0-40 cm soil layer under various combinations of ONF and CRNF treatments at before wintering stage (WS), regreening stage (RGS), jointing stage (JS), anthesis stage (AS) and maturity stage (MS) for the winter wheat planted a) 2020-2021 and b) (2021-2022) growing season. CRNF and ONF are set under two N application rates N_1 (192 kg ha^{-1}) N_2 (240 kg ha^{-1}) of ONF (F_1) 100% ONF, (F_2) 70% ONF + 30% CRNF, (F_3) 50% ONF + 50% CRNF, (F_4) 30% ONF + 70% CRNF, and (F_5) 100% CRNF.

entire growth stages of winter wheat (Figure 5). For the proportions of CRNF, there was no significant difference between the blending ratio treatments at the wintering and greening stage; the DM accumulation of winter wheat was higher in the F_2 and F_3 treatments than in the other treatments. At the jointing stage, the N_1 ONF application rate and the F_4 and F_5 treatments were significantly higher than others. Under the N_2 ONF application rate, the F_4 treatment was significantly higher than the other treatments. At the anthesis and maturity stages, the differences in DM accumulation between different treatments were consistent with the dynamics of the winter wheat population. As the proportion of CRNF increases, the DM accumulation of winter wheat at the anthesis and maturity stages increases. It shows that ONF treatment has obvious advantages before the jointing stage. In contrast, applying CRNF has increased DM accumulation at the anthesis and maturity stages.

3.2.2 Dry matter distribution in various organs

The ranking of DM accumulation and distribution ratio among different organs at maturity for both years was as follows: grain > stem and sheath > spike axis and glume > leaf (Figure 6A). When comparing the F_4 treatment of CRNF to the other treatments, the DM accumulation of grains at the maturity stage was significantly higher in the F_4 treatment. The DM content in the stem + leaf sheath, spike axis + glume, and leaves was significantly higher in the F_4 treatment (Figure 6). It suggests that increasing the amount of N application can significantly increase the DM distribution of each organ during the maturity stage without significant changes in the distribution ratio (Figure 6B). A high proportion of CRNF is beneficial for increasing DM accumulation in each organ during the maturity stage, which is helpful for winter wheat.

The translocation amount, transport efficiency, and contribution rate of assimilates stored in vegetative organs before

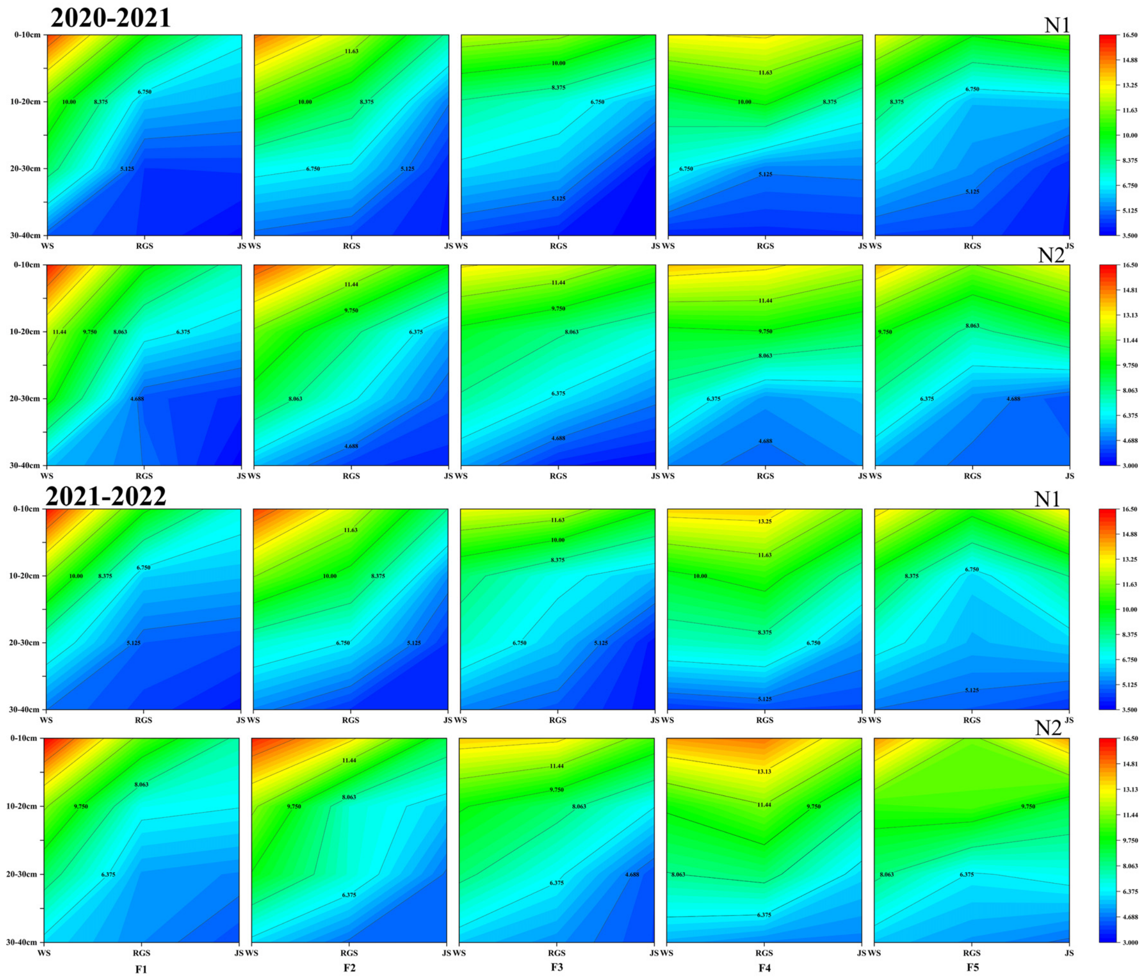

FIGURE 3
Dynamics of soil ammonium N (NH_4^+-N) concentration in 0-40 cm soil layer under various combinations of ONF and CRNF treatments at before wintering stage (WS), regreening stage (RGS) and jointing stage (JS) for the winter wheat planted a) 2020-2021 and b) (2021-2022) growing season. CRNF and ONF are set under two N application rates N_1 (192 kg ha^{-1}) N_2 (240 kg ha^{-1}) of ONF (F_1) 100% ONF, (F_2) 70% ONF + 30% CRNF, (F_3) 50% ONF + 50% CRNF, (F_4) 30% ONF + 70% CRNF, and (F_5) 100% CRNF.

anthesis of winter wheat in 2021-2022 are significantly higher than in 2020-2021, while post-anthesis assimilates in the grains and their contribution rate to the grains was significantly lower in 2020-2021 (Table 2). The results show that increasing the amount of N can increase the distribution of assimilates in the grains after anthesis; appropriately increasing the proportion of CRNF can increase the assimilates amount stored in the vegetative organs before anthesis and the distribution of assimilates in the grains after anthesis. There is no significant difference in the contribution rate of DM to grains before and after anthesis. Among CRNF treatments, the transfer amount of assimilates stored in vegetative organs before anthesis was significantly higher in the F_4 and F_5 treatments than in other treatments; the distribution amount of assimilates in the grains after anthesis was significantly higher in the F4 treatment.

3.3 Nitrogen accumulation and transport

3.3.1 Nitrogen accumulation dynamics

Under different N application rates, N accumulation at different growth stages in 2021-2022 was significantly higher than in 2020-2021. During winter wheat's anthesis and maturity stages, the treatment N_2 accumulated more N than N_1 (Figure 7). There was no significant difference between treatments with different proportions of CRNF at the wintering, regreening, and jointing stages (Figure 7). At the anthesis and maturity stages, the F_4 treatment was significantly higher than other treatments, and the overall performance was F_4>F_5, F_3>F_2, and F_1, with significant differences between treatments. The rules for each treatment's blending ratio were consistent with the anthesis stage. The results

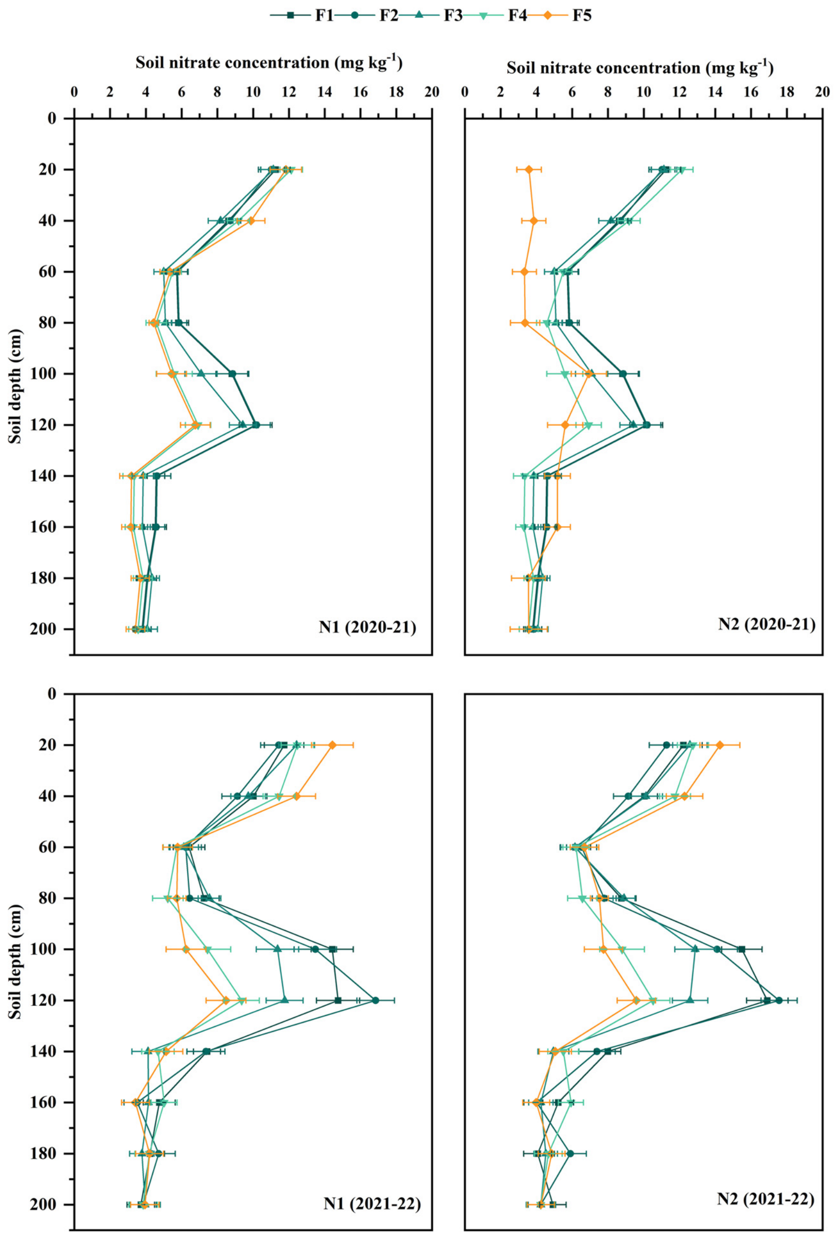

FIGURE 4
Nitrate N concentration in 0-200 cm soil layer at maturity stages under various combinations of ONF and CRNF treatments for the winter wheat planted (2020-2022) growing season. CRNF and ONF are set under two N application rates N_1 (192 kg ha^{-1}) N_2 (240 kg ha^{-1}) of ONF (F_1) 100% ONF, (F_2) 70% ONF + 30% CRNF, (F_3) 50% ONF + 50% CRNF, (F_4) 30% ONF + 70% CRNF, and (F_5) 100% CRNF.

showed that increasing the amount of N applied can increase the N accumulation in winter wheat at the anthesis and maturity stages.

3.3.2 Nitrogen distribution in various organs

The N accumulation in mature winter wheat grains did not differ significantly between the two years; however, the N distribution amount and distribution ratio of the stem + sheath, rachis + glume, and leaves were significantly higher in 2021-2022 (Figure 8A). The amount of N distributed in the grains at maturity was significantly higher in the F4 treatment of CRNF. The overall performance was F_4>F_5>F_3>F_2>F_1, with significant differences between treatments (Figure 8). The results showed that appropriately increasing the amount of N can increase the amount of N distributed and the distribution ratio in winter wheat grains during the maturity stage while decreasing the amount of N distributed and the distribution ratio in leaves (Figure 8B). Increasing the proportion of CRNF improves the N distribution of vegetative organs. The grain N accumulation and distribution ratio reaches its maximum when the proportion of CRNF is at 70%.

3.3.3 Nitrogen redistribution

The contribution rate of post-anthesis N to grain N, the transport efficiency of pre-anthesis N in winter wheat, and the

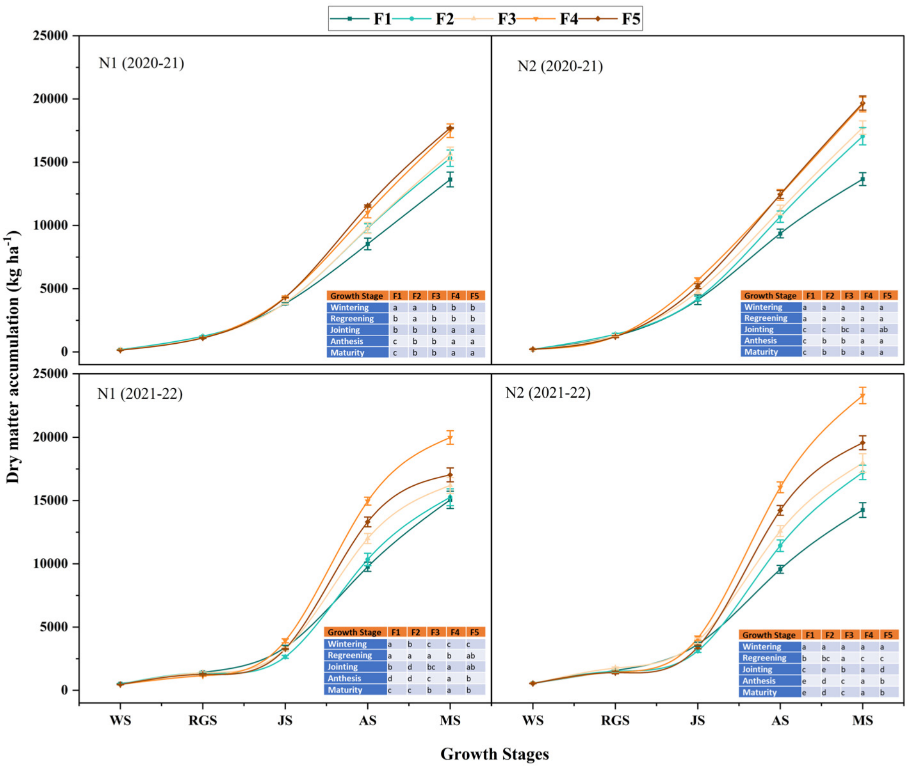

FIGURE 5
Dynamic changes of dry matter accumulation amounts of winter wheat under various combinations of ONF and CRNF treatments at before wintering stage (WS), regreening stage (RGS) and jointing stage (JS) for the winter wheat planted a) 2020-2021 and b) (2021-2022) growing season. Small letters indicate a significant level of 5% difference. CRNF and ONF are set under two N application rates N_1 (192 kg ha^{-1}) N_2 (240 kg ha^{-1}) of ONF (F_1) 100% ONF, (F_2) 70% ONF + 30% CRNF, (F_3) 50% ONF + 50% CRNF, (F_4) 30% ONF + 70% CRNF, and (F_5) 100% CRNF.

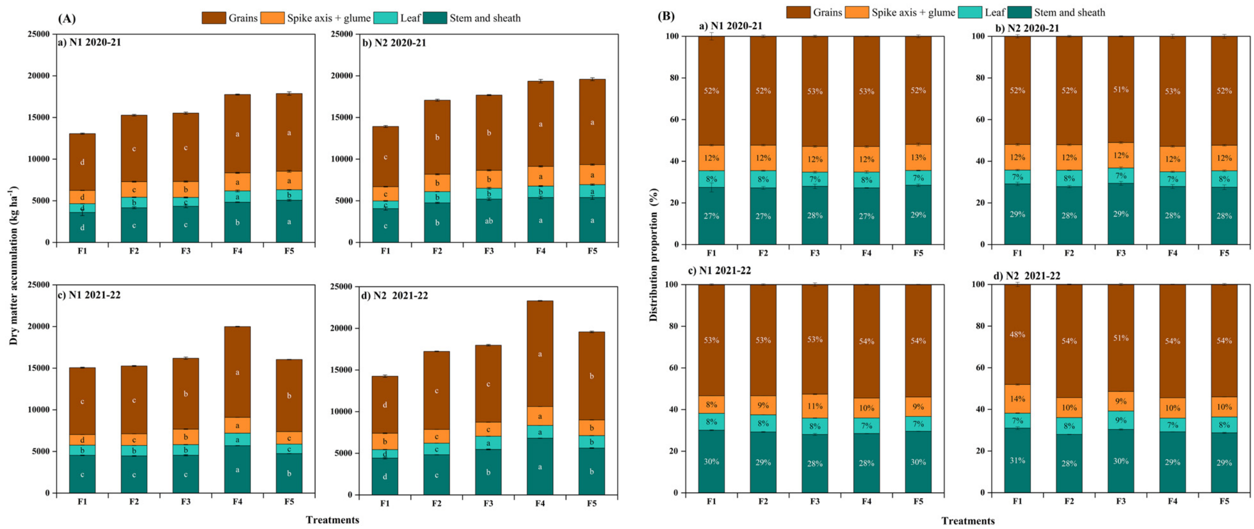

FIGURE 6
Plant dry matter accumulation **(A)** and distribution proportion **(B)** in different organs of winter wheat under various combinations of ONF and CRNF treatments at anthesis stage for the winter wheat planted in 2020-2021 and 2021-2022 growing seasons. Small letters indicate a significant level of 5% difference; CRNF and ONF are set under two N application rates N_1 (192 kg ha^{-1}) N_2 (240 kg ha^{-1}) of ONF (F_1) 100% ONF, (F_2) 70% ONF + 30% CRNF, (F_3) 50% ONF + 50% CRNF, (F_4) 30% ONF + 70% CRNF, and (F_5) 100% CRNF.

 10.3389/fpls.2024.1504083

TABLE 2 Dry matter assimilation and its contribution to grain of winter wheat after anthesis under different treatments.

Treatment	Pre-anthesis			Post anthesis	
	Translocation Amount (kg ha^{-1})	Translocation (%)	Contribution (%)	Translocation Amount (kg ha^{-1})	Contribution (%)
2020-2021	2710.8b	25.38b	31.23b	6024.4a	68.77a
2021-2022	4234.0a	33.37a	45.10a	5060.3b	54.90b
N_1	3502.7a	30.61a	40.28a	5094.4b	59.72a
N_2	3442.1a	28.13a	36.05a	5990.4a	63.95a
F_1	2470.2b	26.43b	34.18a	4761.9c	65.82a
F_2	2947.5b	27.71ab	34.28a	5648.3b	65.72a
F_3	3313.2b	28.72ab	37.91a	5434.4bc	62.09a
F_4	4313.3a	30.93ab	39.30a	6486.9a	60.70a
F_5	4317.9a	33.07a	45.15a	5380.5bc	54.85a
N	ns	ns	ns	**	ns
F	**	ns	ns	**	ns
N×F	ns	ns	ns	ns	ns

CRNF and ONF are set under two N application rates N_1 (192 kg ha^{-1}) N_2 (240 kg ha^{-1}) of ONF (F_1) 100% ONF, (F_2) 70% ONF + 30% CRNF, (F_3) 50% ONF + 50% CRNF, (F_4) 30% ONF + 70% CRNF, and (F_5) 100% CRNF. Different letters indicate the significance within the same year at 5% level by LSD test. ns: not significant, ($p > 0.05$); **: Significant at $p < 0.01$.

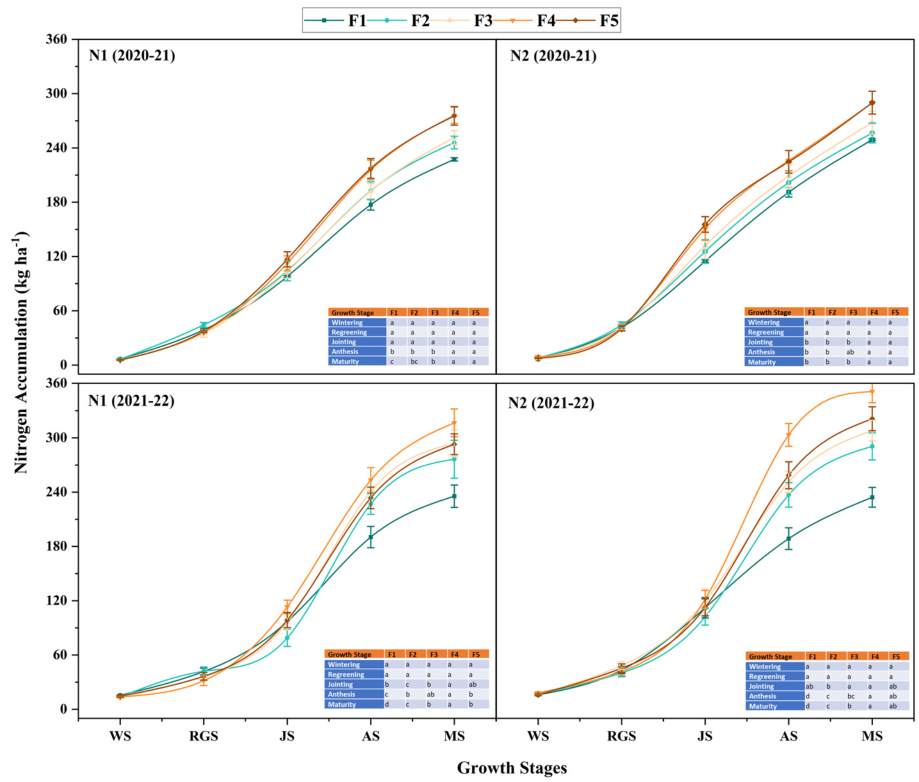

FIGURE 7
Dynamic changes of nitrogen accumulation amount of winter wheat under various combinations of ONF and CRNF treatments at before wintering stage (WS), regreening stage (RGS) and jointing stage (JS) for the winter wheat planted a) 2020-2021 and b) (2021-2022) growing season. Small letters indicate a significant level of 5% difference; CRNF and ONF are set under two N application rates N_1 (192 kg ha^{-1}) N_2 (240 kg ha^{-1}) of ONF (F_1) 100% ONF, (F_2) 70% ONF + 30% CRNF, (F_3) 50% ONF + 50% CRNF, (F_4) 30% ONF + 70% CRNF, and (F_5) 100% CRNF.

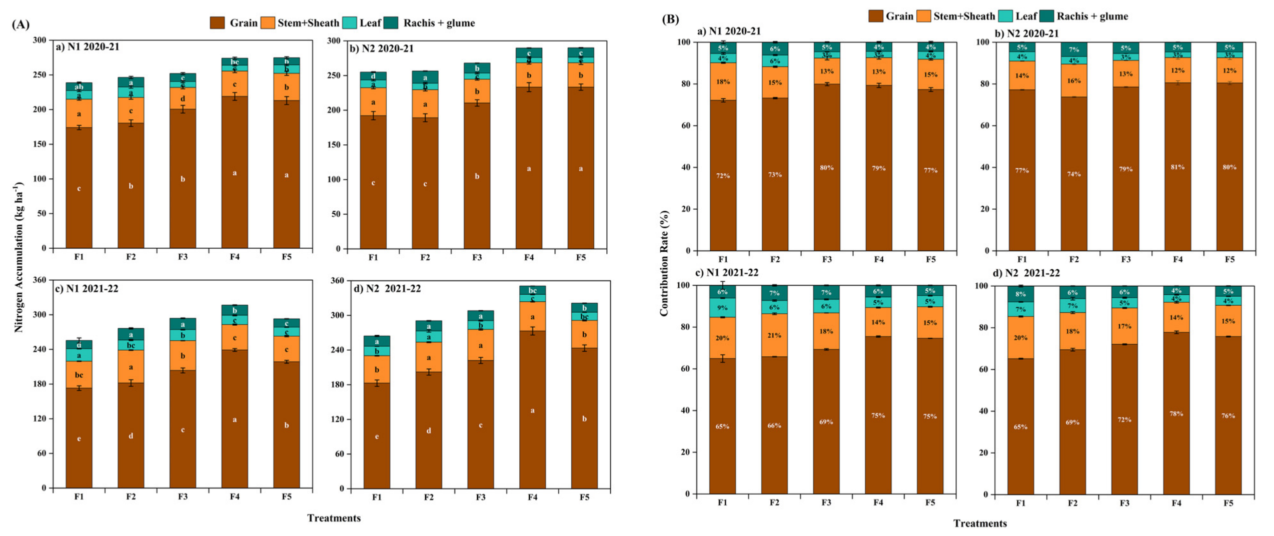

FIGURE 8
Nitrogen accumulation **(A)** and distribution proportion **(B)** in different organs of winter wheat under various combinations of ONF and CRNF treatments at anthesis stage for the winter wheat planted in 2020-2021 and 2021-2022 growing season. Note: Small letters indicate a significant level of 5% difference; CRNF and ONF are set under two N application rates N_1 (192 kg ha^{-1}) N_2 (240 kg ha^{-1}) of ONF (F_1) 100% ONF, (F_2) 70% ONF + 30% CRNF, (F_3) 50% ONF + 50% CRNF, (F_4) 30% ONF + 70% CRNF, and (F_5) 100% CRNF.

contribution of pre-anthesis N to grain N were given in Table 3. The pre-anthesis N transfer amount and post-anthesis N accumulation amount of N application N_2 were significantly higher than those of N application N_1. The amount of pre-anthesis N transport in the F_4 treatment of CRNF was significantly higher than others. The overall performance was F_4>F_5>F_3>F_2>F_1, and have significant differences between treatments (Table 3). The contribution rate of pre-anthesis N to grain N was significantly lower in the F_1 treatment. The F_1 treatment has the lowest post-anthesis N accumulation, and the F_1 treatment has a significantly higher post-anthesis N contribution rate to the grains. The results show that increasing the N application rate can increase the N accumulation in winter wheat grains during maturity by increasing pre-anthesis N transport and post-anthesis N accumulation. Increasing the grain accumulation of winter wheat at maturity relied on enhancing both the amount and efficiency of N transport before anthesis.

3.4 Nitrogen utilization efficiency

The N use efficiency (NUE), N uptake efficiency (NUpE), and N fertilizer partial productivity (NFPP) in 2021-2022 are significantly higher than that in 2020-2021. The NUE revealed no significant difference in N_1 and N_2 application amounts of ONF when the proportion of CRNF was F_4 (70%) and F_5 (100%) (Figure 9). For both years, the CRNF treatment F_4 combined with ONF at N_2 had the highest NUpE and NFPP, significantly higher than the other treatments. There was no significant difference in NUE between N_1 and N_2 of ONF for the CRNF for F_4 treatment, although when the N application amount increased, the NUE did not change significantly. Appropriately increasing the proportion of CRNF can improve winter wheat's NUE, NUpE, and NFPP in comparison to the F_1 of CRNF; the NUE of the F_4 treatment increased by an average of 2.14% under the N_2 application of ONF in both years.

TABLE 3 Effects of different ONF and CRNF treatments on nitrogen redistribution in winter wheat plants.

	Pre-anthesis			Post anthesis	
	NRA (kg ha^{-1})	NRR (%)	NRCT (%)	NAG (kg ha^{-1})	NACT (%)
2020-2021	145.34a	70.76a	71.32b	58.16a	28.68a
2021-2022	152.89a	64.42b	72.99a	56.01a	27.01b
N_1	145.34b	66.35a	71.93a	55.12b	28.07a
N_2	152.89a	68.83a	72.38a	59.05a	27.62a
F_1	115.74e	61.94c	69.97b	49.73c	30.03a
F_2	135.45d	63.32c	71.89a	52.88b	28.11b
F_3	152.22c	68.61b	72.75a	56.92ab	27.25b
F_4	176.42a	73.06a	73.15a	64.63a	26.85b
F_5	165.75b	71.03ab	73.00a	61.27ab	27.00b
N	**	**	ns	ns	ns
F	**	**	ns	ns	ns
N×F	ns	**	ns	ns	ns

NRA, N remobilization amount in vegetative organs; NRR, N remobilization ratio in vegetative organs; NRCT, total contribution rate of N remobilization pre-anthesis to grain N; NAG, N uptake amount after anthesis; NACT, total contribution rate of N accumulated post-anthesis to the grain N. CRNF and ONF are set under two N application rates N_1 (192 kg ha^{-1}) N2 (240 kg ha^{-1}) of ONF (F_1) 100% ONF, (F_2) 70% ONF + 30% CRNF, (F_3) 50% ONF + 50% CRNF, (F_4) 30% ONF + 70% CRNF, and (F_5) 100% CRNF. Different alphabets indicate the significance within the same year at 5% level by LSD test. ns: not significant, ($p > 0.05$); **: Significant at $p < 0.01$.

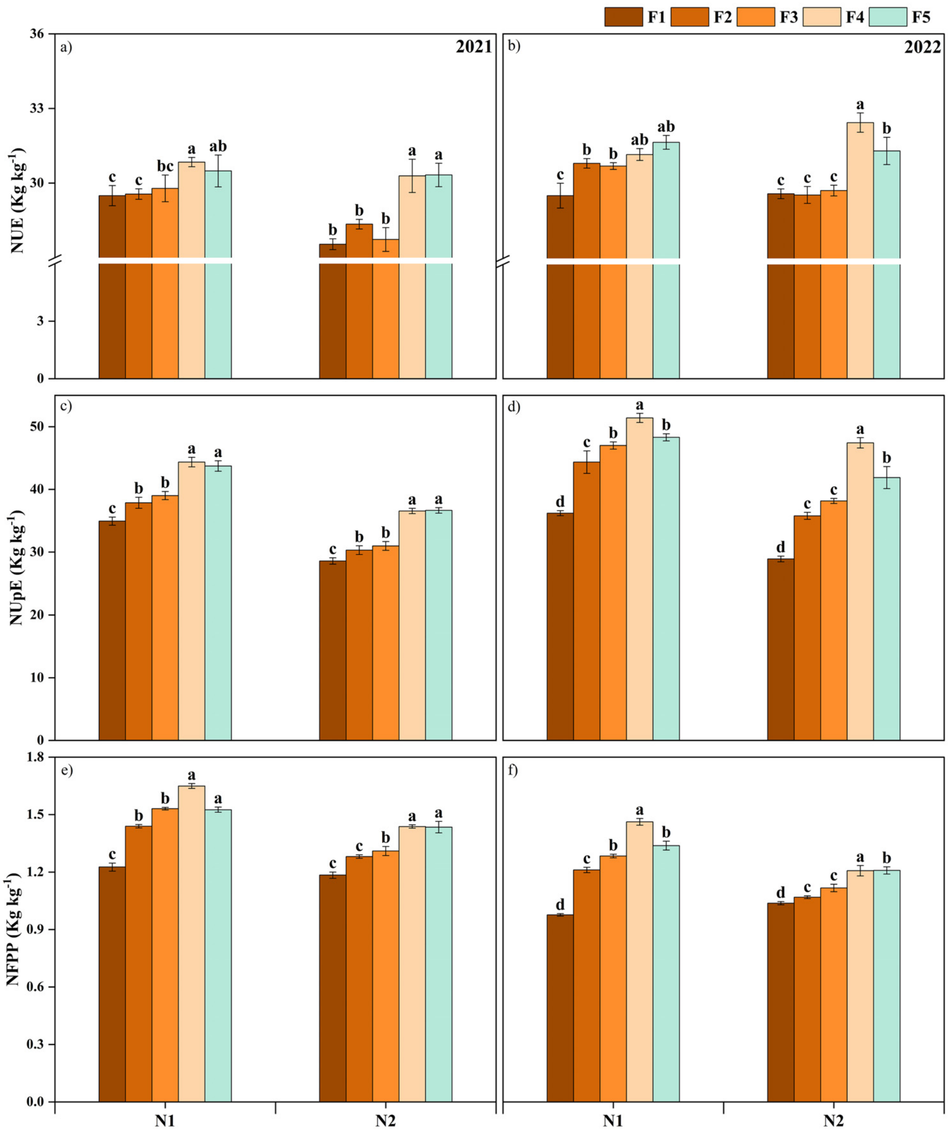

FIGURE 9
Nitrogen use efficiency (a, b) nitrogen uptake efficiency (c, d) nitrogen fertilizer partial productivity (e, f); winter wheat under various combinations of ordinary nitrogen fertilizer and controlled released nitrogen fertilizer treatments for the winter wheat planted 2020-2022 growing season. CRNF and ONF are set under two N application rates N1 (192 kg ha-1) N2 (240 kg ha-1) of ONF (F1) 100% ONF, (F2) 70% ONF + 30% CRNF, (F3) 50% ONF + 50% CRNF, (F4) 30% ONF + 70% CRNF, and (F5) 100% CRNF. Vertical bars are means ± standard deviation. Different letters mean that the difference of the means between treatments was significant (LSD test, P < 0.05).

3.5 Yield and its components

Winter wheat yield and its components were significantly enhanced by the combination of CRNF with ONF for both years ($p < 0.05$). Compared to 2020-2021, the number of spikes, grains per spike, and grain yield in 2021-2022 were significantly higher, while the 1000-grain weight was higher in 2020-2021 than in 2021-2022 (Table 4). Winter wheat yield gradually increased in all blended treatments of CRNF. There was no significant difference in the number of grains per spike or 1000-grain weight between the two N application rates when the proportion of CRNF was 0%, 30%, or 50%. The results showed that appropriately increasing the amount of applied N can increase grain yield by increasing the number of spikes. Compared to other fertilizer applications, the maximum number of spikes, grains per spike, and grain yield were observed with treatment of CRNF 70% combined with N_2 of ONF.

3.6 Relationship between nitrogen fertilizer dynamics to yield and its components

The linear relationship between ordinary N fertilizer (ONF), controlled released N fertilizers (CRNF), N use efficiency (NUE), uptake efficiency (NUpE), partial fertilizer productivity (NPFP) with yield and its components (Grain Number, 1000 Grain Weight, Spikes Number) combined for both the 2020–2022 growing seasons was fitted using structural equation modelling as illustrated in Figures 10A,B. The results showed that CRNF has a

TABLE 4 Winter wheat grain yield and its components under various treatments of ONF combined with CRNF.

Treatment		Number of spikes (× 10^4 ha^{-1})	2020-2021		Grain yield (kg ha^{-1})	Number of spikes (× 10^4 ha^{-1})	2021-2022		Grain yield (kg ha^{-1})
			Grains per spike	1000-Grain weight (g)			Grains per spike	1000-Grain weight (g)	
N_1	F_1	431.33 ± 21.36c	34.60 ± 0.58a	49.7 ± 0.30ab	6705.97 ± 71.77c	473.98 ± 3.54d	35.93 ± 2.35b	48.02 ± 0.45a	6950.50 ± 44.49d
	F_2	469.33 ± 4.25b	36.90 ± 1.02a	49.1 ± 0.30b	7268.17 ± 97.45b	543.32 ± 4.22c	37.13 ± 0.67ab	46.64 ± 0.76a	8547.33 ± 198.76c
	F_3	475.33 ± 4.37b	36.56 ± 1.82a	50.1 ± 0.48ab	7489.17 ± 72.19b	553.74 ± 9.03bc	39.06 ± 1.14ab	46.44 ± 0.13a	8989.77 ± 62.85b
	F_4	506.00 ± 7.54ab	35.70 ± 1.12a	50.6 ± 0.60a	8513.90 ± 84.32a	599.60 ± 2.07a	39.76 ± 0.90a	47.08 ± 1.52a	9867.83 ± 80.69a
	F_5	515.66 ± 2.33a	36.40 ± 0.75a	49.7 ± 0.55ab	8395.03 ± 92.20a	566.95 ± 1.67b	39.73 ± 0.40a	47.83 ± 0.76a	9271.81 ± 62.58b
N_2	F_1	446.33 ± 8.29c	36.36 ± 1.47a	48.5 ± 0.29a	6857.30 ± 69.49c	463.69 ± 9.95e	37.83 ± 1.38a	46.17 ± 0.20a	6934.97 ± 62.48d
	F_2	500.00 ± 1.00b	34.13 ± 0.73a	48.8 ± 0.08a	7271.83 ± 97.65b	546.52 ± 2.32d	37.56 ± 0.61a	47.72 ± 0.20a	8800.20 ± 77.12c
	F_3	504.00 ± 1.73b	34.50 ± 0.43a	49.4 ± 0.05a	7432.00 ± 97.04b	583.20 ± 5.55c	39.43 ± 0.68a	46.46 ± 0.94a	8940.87 ± 55.17c
	F_4	536.66 ± 5.69a	34.83 ± 0.98a	49.7 ± 0.41a	8770.87 ± 58.81a	639.20 ± 1.83a	39.86 ± 0.41a	45.98 ± 0.07a	11381.80 ± 114.38a
	F_5	541.00 ± 2.88a	35.63 ± 0.49a	49.6 ± 0.46a	8793.57 ± 61.41a	605.70 ± 5.27b	40.00 ± 1.56a	46.65 ± 0.27a	10051.63 ± 243.67b
N		*	ns	ns	ns	*	ns	ns	ns
F		**	ns	ns	**	**	ns	ns	**
N×F		ns	ns	ns	ns	ns	ns	ns	ns

CRNF and ONF are set under two N application rates N_1 (192 kg ha^{-1}) N_2 (240 kg ha^{-1}) of ONF (F_1) 100% ONF, (F_2) 70% ONF + 30% CRNF, (F_3) 50% ONF + 50% CRNF, (F_4) 30% ONF + 70% CRNF, and (F_5) 100% CRNF. Different alphabets indicate the significance within the same year at 5% level by LSD test. ns: not significant, ($p > 0.05$); *: Significant at $p < 0.05$; **: Significant at $p < 0.01$.

positive impact on NUE, NUpE, and NPFP with path coefficients (λ) of 0.704, 0.897, 0.891 respectively and indirectly increased winter wheat yield by increasing the number of grains in spikes (Figure 10). While, ONF directly affected winter wheat and increased yield (λ: 0.774), while CRNF positively impacted yield (λ: -0.064). The N application also indirectly increased yield by increasing spike number (λ: 0.686). The three N-related indexes have a direct positive effect on winter wheat yield was mainly due to the significant increase in spikes number.

4 Discussion

4.1 Impact of CRNF on soil nitrogen supply and dry matter accumulation

Nitrogen is essential for plant growth and development, so its availability is critical for crop productivity and applying ONF combined with CRNF offers a simple and efficient framework to improve fertilizer utilization efficiency. Slowly releasing nutrients from the CRNF over time can effectively prevent N accumulation in the soil quickly, reduce nutrient loss to the environment, and thus increase nutrient availability for crops (Vejan et al., 2021; Ma et al., 2021). The results showed that the soil nitrate N and ammonium N content in the jointing and anthesis stages were higher in the CRNF treatments by 70% when combined with the N2 application of ONF. A high amount of CRNF can provide a sufficient supply of soil N in the late growth period of winter wheat. Because the N-release characteristics of CRNF are greatly affected by soil moisture content and temperature, the early nutrient release of CRNF will be too slow, and a one-time basal application will result in insufficient soil nutrient supply in the early stages of winter wheat growth (Geng et al., 2015; Ma et al., 2021). When the proportion of CRNF is 70% and ONF at N2, it can not only ensure the soil nitrate N and ammonium N content in the early growth period of winter wheat but also significantly increase the soil nitrate N and ammonium N content in the jointing stage. In this way, one-time fertilization of CRNF can meet the N demand of crops throughout the growth stages, thereby increasing grain yield and NUE, minimizing N leaching and volatilization losses, and reducing the impact on the environment (Azeem et al., 2014).

In the current study, compared to the application of ONF, the application of CRNF increases the nitrate N accumulation in the 0-40 cm soil layer of winter wheat during the maturity period, and

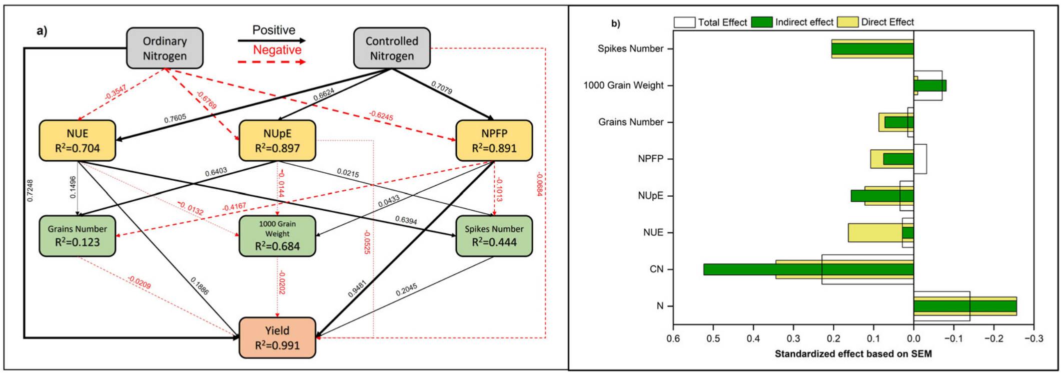

FIGURE 10
Relationship between ONF and CRNG and yield components of winter wheat. **(A)** The structural equational model (SEM) framework describing ONF and CRNF, NUE, NUpE, NPFP, grain number, 1000 grain weight, spike number, and grain yield. The red dotted lines and black solid lines are indirect and direct effects. Numbers above/below the arrow line indicate correlation. The interpretation variance (R2) ratio appears next to each indicator in the model. **(B)** The direct, indirect, and total effects of different potential variables on winter wheat yield are based on SEM data. N, Ordinary nitrogen; CN, Controlled nitrogen; NUE, Nitrogen use efficiency; NUpE, Nitrogen uptake efficiency; and NPFP, Nitrogen fertilizer partial productivity.

when the proportion of CRNF is 70%, it can reduce nitrate N content in the 60-100 cm soil layer and reducing N leaching. Our study shows no significant difference in the nitrate N content in the 0-40 cm soil layer during the winter wheat maturity stage, while the nitrate N content in the 1-2 m soil layer is significantly higher than that of other treatments (Figure 4). The lowest N-releasing proportions were CRNF at 70% and 100%, and there was no significant difference in nitrate N accumulation in the 1-2 m soil layer with ONF N2 application, indicating that winter wheat requires more N in the late growth period. The soil N release in the later growth period of winter wheat is more consistent with the N uptake of winter wheat when the proportion of CRNF is 70%, thereby increasing the N accumulation during the maturity period of winter wheat while reducing N leaching risk.

Nitrogen fertilizer significantly impacts the number of tillers in the early growth stage of winter wheat. Stem and tiller dynamics are essential for regulating winter wheat population dynamics and achieving the maximum yield. Nutrient release is too slow in the early growth stage, but increasing the dosage of CRNF can increase soil nutrients before and after the jointing stage of winter wheat, significantly increasing the number of spikes at maturity (Ma et al., 2021, Ma et al., 2022a, Ma et al., 2022b). The application of CRNF at 70% combined with ONF can significantly increase the DM accumulation of winter wheat from regreening to anthesis stages compared with the other proportions of CRNF. Nishimura et al. (2022) reported a similar finding that CRNF can regulate the population size of winter wheat and increase the number of spikes per plant to varying degrees, thus increasing the number of spikes at maturity. The application of CRNF maintains a higher tiller number in the late growth stage, laying the foundation for increased yield.

Winter wheat yield formation depends on DM accumulation, particularly post-anthesis DM accumulation, which can significantly improve harvest index and grain yield (Ercoli et al., 2008; Lijuan et al., 2023). In this study, CRNF combined with ONF has increased the DM accumulation from the greening to the maturity stages by increasing the population number. The amount of stored assimilates transported by vegetative organs before anthesis increased when the CRNF (70%) was combined with ONF (N2). However, the distribution of DM in the grains following anthesis was significantly reduced (Table 2). The distribution amount was significantly higher than that of other treatments. However, there was no significant difference among the blending ratio treatments in the contribution rate of assimilates stored in vegetative organs before anthesis and assimilates after anthesis to grains. It shows that the soil nutrient supply in the treatment with CRNF (70%) is more consistent with the nutrient absorption of winter wheat. The DM accumulation increased to varying degrees during the vegetative and reproductive growth stages, thereby increasing the grain yield of winter wheat. The results are consistent with the findings of Cui et al. (2022).

4.2 Impact of CRNF on nitrogen accumulation and transport

Understanding the dynamics of nutrient accumulation in crops is essential to obtain optimum yield. The ability of a crop to accumulate nutrients varies according to the nutrients used. The translocation of pre-anthesis N to the grain is essential for winter wheat to get maximum yield (Xu et al., 2005). Our results showed that the N accumulation of CRNF (100%) combined with ONF (N2) at the greening stage of winter wheat is low. In contrast, the N accumulation increases rapidly after the jointing stage. The N accumulation of winter wheat has been significantly increased at winter wheat's anthesis and maturity stages by improving the soil N supply at later growth stages. The N accumulation in grains includes the transfer of N from vegetative organs to the grain and N accumulation in grains after anthesis (Kong et al., 2016). Our results align with the previous findings of Abid et al. (2016), which show that increasing soil N during the early growth period increases the N content of vegetative organs. Increasing soil N in the late growth period can improve the distribution of N in grains after anthesis, resulting in higher grain N content (Chen et al., 2015). The N uptake during the maturity stage was significantly lower in combination with CRNF and ONF. As ONF releases fertilizer efficiency quickly, one-time basal fertilization of ONF cannot meet the N requirement in the later crop growth stages (Zhang et al., 2022a). The amount of N released in the early stage of CRNF is small, making N absorption by vegetative organs difficult, which is not conducive to the transport of N to the grain (Ma et al., 2023). Our findings showed that CRNF (70%) combined with ONF (N2) not only ensured the soil N supply during the greening and jointing stages of winter wheat, but also significantly increased the soil N content at the anthesis stage.

In winter wheat, the N uptake by grains has been affected by N accumulation during anthesis. When N accumulation is increased during anthesis, it can promote the transfer of N from pre-anthesis vegetative organs to the grain and inhibit post-anthesis N absorption (Wu et al., 2021). Our results showed that when the N accumulation during the anthesis period is 272.8 kg ha-1, the contribution rate of pre-anthesis N to grain N reaches the maximum. When it is lower than 272.8 kg ha-1, increasing N accumulation during the anthesis period increased the contribution rate of pre-anthesis N to grain N. The treatment with CRNF (70%) combined with ONF (N2) has increased N accumulation during the anthesis stage of winter wheat and significantly increased the transfer of N from vegetative organs to the grain, resulting in higher grain N content during the maturity stage. Although the input of assimilated N into grains after anthesis showed an increasing trend, the contribution rate of post-anthesis N to grain N showed a decreasing trend. It showed that CRNF at 70% combined with ONF (N2) can provide a good supply of soil nutrients during the reproductive growth stage of winter wheat; because winter wheat accumulates more N during the vegetative growth stage, the N in the grain is transported from the vegetative organs.

4.3 Impact of CRNF on yield and nitrogen use efficiency

Nitrogen fertilizer application is critical to the growth of winter wheat, and its management is the key to improving crop yields (Duan et al., 2019; Hussain et al., 2023a). Our results showed that increasing soil N supply after the greening stage with CRNF (70%) increased plant populations at the jointing and anthesis stages, significantly increasing wheat spikes at maturity and hence increasing the yield. Our experiment also found that when the proportion of CRNF was 0%, 30%, and 50%, there was no significant difference in yield between ONF 192 kg ha^{-1} and 240 kg ha^{-1}. However, when the proportion of CRNF (70%) was combined with ONF (N2), the yield was significantly improved. Our results are in line with Yang et al. (2011) for the winter wheat yield. Compared to the sole ONF, the CRNF treatment has increased the grain yield with an average of 6.64% for both years. CRNF was applied twice (at the sowing and re-greening stage) and synchronized with the N demand of winter wheat, which has several advantages, such as significantly improved grain yield and NUE. It shows that appropriately increasing the proportion of CRNF can further unleash the potential of N fertilizer input to increase production and efficiency and break the bottleneck of increasing N without increasing production to a certain extent.

The judicious application of fertilizers ensures the supply of nutrients required for crop growth and development, reduces fertilizer losses and improves fertilizer use efficiencies (Dimkpa et al., 2020). Because the application cost of CRNF is higher than ONF's, the cost can be reduced by combining CRNF with ONF, and the benefits of CRNF can be enhanced. In our experiment, CRNF at 70% combined with ONF (N2) application rates significantly improved N accumulation in the aboveground portion, thus improving grain yield and NUE during the maturity period. The effects of combining CRNF and ONF on NUE were variable and may be related to essential soil fertility and N fertilizer type. The results of our experiments show that a 70% CRNF combined with ONF (N2) outperforms a 20% improvement in NUE. For the improvement of NUE, our results are those of (Ma et al, 2021; Ma et al., 2022a) and Duan et al. (2019).

Our findings support the initial hypothesis, as discussed in the results and discussion sections, a combination of CRNF and ONF has numerous advantages, including 1) can provide a sufficient supply of soil N in the late growth period of winter wheat; 2) can significantly increase the dry matter accumulation of winter wheat from regreening to anthesis stages 3) synchronized the N demand of winter wheat and improved the NUE and grain yield; 4) improved the soil nutrient structure and effectively promote crop yield. Our results indicate that a combination of CRNF and ONF in different soils may be adjusted to meet crop demand for nutrients according to crop type. However, soil type and climate differences among cropping regions must be considered when changing the combination of ONF and CRNF application. Furthermore, special attention should be given to differences in types of available CRNF among crop species. This necessitates the development of predictive models that integrate climate, soil, and crop factors to optimize CRNF application and ensure maximum efficacy. Furthermore, investigating potential synergies between CRNF and other sustainable agricultural practices, such as conservation tillage and integrated pest management, can unlock new opportunities for environmentally conscious and productive farming systems.

5 Conclusion

This study examined the combinations of ONF and CRNF to investigate the soil N supply, winter wheat growth and productivity over two consecutive growing seasons. It has been found that increased CRNF application provides adequate soil N for winter wheat throughout its late growth period. When the N application rate is 240 kg ha^{-1}, a combination of (CRNF: ONF =70:30), have increased soil N supply after the regreening stage, improved plant populations in the jointing and anthesis stages, and significantly increase the number of spikes, thereby increasing yield. This combination of CRNF with ONF have increased N accumulation during the anthesis stage, the transfer of N to the grain prior to anthesis is significantly increased, as is the grain N content and distribution ratio. It has been concluded that a controlled-release mixed N fertilizer application plan strategy is beneficial for improving grain characteristics is used to achieve high winter wheat yield and efficient N utilization.

Data availability statement

The raw data supporting the conclusions of this article will be made available by the authors, on request.

Author contributions

MA: Conceptualization, Data curation, Formal analysis, Investigation, Visualization, Writing – original draft, Writing – review & editing. RH: Data curation, Formal analysis, Investigation, Visualization, Writing – original draft, Writing – review & editing. XL: Data curation, Formal analysis, Investigation, Methodology, Supervision, Writing – review & editing. DW: Conceptualization, Funding acquisition, Methodology, Project administration, Resources, Supervision, Writing – original draft, Writing – review & editing.

Funding

The author(s) declare financial support was received for the research, authorship, and/or publication of this article. This work was supported by the Key Research and Development Technology Projects in Shaanxi Province (2023-ZDLNY-01), the Xi'an Science and Technology Plan Projects (23NYGG0001), the Key Research and Development Technology Projects in Shandong Province (2022LZGCQY002), the National Key Research and Development Program of China (2022YFD2300802).

Conflict of interest

The authors declare that the research was conducted in the absence of any commercial or financial relationships that could be construed as a potential conflict of interest.

Publisher's note

All claims expressed in this article are solely those of the authors and do not necessarily represent those of their affiliated organizations, or those of the publisher, the editors and the reviewers. Any product that may be evaluated in this article, or claim that may be made by its manufacturer, is not guaranteed or endorsed by the publisher.

References

Abid, M., Tian, Z., Ata-Ul-Karim, S. T., Cui, Y., Liu, Y., Zahoor, R., et al. (2016). Nitrogen nutrition improves the potential of wheat (Triticum aestivum L.) to alleviate the effects of drought stress during vegetative growth periods. *Front. Plant Sci.* 7, 981. doi: 10.3389/fpls.2016.00981

Anderson, R., Bayer, P. E., and Edwards, D. (2020). Climate change and the need for agricultural adaptation. *Curr. Opin. Plant Biol.* 56, 197–202. doi: 10.1016/j.pbi.2019.12.006

Azeem, B., KuShaari, K., Man, Z. B., Basit, A., and Thanh, T. H. (2014). Review on materials & methods to produce controlled release coated urea fertilizer. *J. Controlled release* 181, 11–21. doi: 10.1016/j.jconrel.2014.02.020

Chen, Y., Xiao, C., Wu, D., Xia, T., Chen, Q., Chen, F., et al. (2015). Effects of nitrogen application rate on grain yield and grain nitrogen concentration in two maize hybrids with contrasting nitrogen remobilization efficiency. *Eur. J. Agron.* 62, 79–89. doi: 10.1016/j.eja.2014.09.008

Cui, P., Chen, Z., Ning, Q., Wei, H., Zhang, H., Lu, H., et al. (2022). One-time nitrogen fertilizer application using controlled-release urea ensured the yield, nitrogen use efficiencies, and profits of winter wheat. *Agronomy* 12, 1792. doi: 10.3390/agronomy12081792

Dimkpa, C. O., Fugice, J., Singh, U., and Lewis, T. D. (2020). Development of fertilizers for enhanced nitrogen use efficiency–Trends and perspectives. *Sci. Total Environ.* 731, 139113. doi: 10.1016/j.scitotenv.2020.139113

Duan, J., Shao, Y., He, L., Li, X., Hou, G., Li, S., et al. (2019). Optimizing nitrogen management to achieve high yield, high nitrogen efficiency and low nitrogen emission in winter wheat. *Sci. Total Environ.* 697, 134088. doi: 10.1016/j.scitotenv.2019.134088

Ercoli, L., Lulli, L., Mariotti, M., Masoni, A., and Arduini, I. (2008). Post-anthesis dry matter and nitrogen dynamics in durum wheat as affected by nitrogen supply and soil water availability. *Eur. J. Agron.* 28, 138–147. doi: 10.1016/j.eja.2007.06.002

Erenstein, O., Jaleta, M., Mottaleb, K. A., Sonder, K., Donovan, J., and Braun, H. J. (2022). "Global trends in wheat production, consumption and trade," in *Wheat improvement: food security in a changing climate* (Springer International Publishing, Cham), 47–66.

Geng, J., Ma, Q., Zhang, M., Li, C., Liu, Z., Lyu, X., et al. (2015). Synchronized relationships between nitrogen release of controlled release nitrogen fertilizers and nitrogen requirements of cotton. *Field Crops Res.* 184, 9–16. doi: 10.1016/j.fcr.2015.09.001

Gu, J. (2023). Optimizing irrigation and nitrogen regimes in rice plants can contribute to achieving sustainable rice productivity. *Agronomy* 13, 2495. doi: 10.3390/agronomy13102495

Hussain, T., Gollany, H. T., Hussain, N., Ahmed, M., Tahir, M., and Duangpan, S. (2022). Synchronizing nitrogen fertilization and planting date to improve resource use efficiency, productivity, and profitability of upland rice. *Front. Plant Sci.* 13. doi: 10.3389/fpls.2022.895811

Hussain, T., Gollany, H. T., Mulla, D. J., Ben, Z., Tahir, M., Ata-Ul-Karim, S. T., et al. (2023a). Assessment and application of EPIC in simulating upland rice productivity, soil water, and nitrogen dynamics under different nitrogen applications and planting windows. *Agronomy* 13, 2379. doi: 10.3390/agronomy13092379

Hussain, T., Mulla, D. J., Hussain, N., Qin, R., Tahir, M., Liu, K., et al. (2023b). Optimizing nitrogen fertilization to enhance productivity and profitability of upland rice using CSM–CERES–rice. *Plants* 12, 3685. doi: 10.3390/plants12213685

Kong, L., Xie, Y., Hu, L., Feng, B., and Li, S. (2016). Remobilization of vegetative nitrogen to developing grain in wheat (Triticum aestivum L.). *Field Crops Res.* 196, 134–144. doi: 10.1016/j.fcr.2016.06.015

Li, G., Zhao, B., Dong, S., Zhang, J., Liu, P., and Lu, W. (2020). Controlled-release urea combining with optimal irrigation improved grain yield, nitrogen uptake, and growth of maize. *Agric. Water Manage.* 227, 105834. doi: 10.1016/j.agwat.2019.105834

Li, J., Wan, Y., Wang, B., Waqas, M. A., Cai, W., Guo, C., et al. (2018). Combination of modified nitrogen fertilizers and water saving irrigation can reduce greenhouse gas emissions and increase rice yield. *Geoderma* 315, 1–10. doi: 10.1016/j.geoderma.2017.11.033

Lijuan, M., Ali, M. F., Xiaohu, H., Zili, P., Zulfiqar, U., and Rui, W. (2023). Changes in nitrogen-related performance attributes of winter wheat varieties released between 1950 and 2020 in dryland region of China. *J Soil Sci Plant Nutr.* 23, 5404–5418. doi: 10.1007/s42729-023-01410-4

Liu, X., Vitousek, P., Chang, Y., Zhang, W., Matson, P., and Zhang, F. (2016). Evidence for a historic change occurring in China. *Environmental Science & Technology*, 50, 505–506. doi: 10.1021/acs.est.5b05972

Ma, Q., Qian, Y., Yu, Q., Cao, Y., Tao, R., Zhu, M., et al. (2023). Controlled-release Nitrogen fertilizer application mitigated N losses and modified microbial community while improving wheat yield and N use efficiency. *Agriculture Ecosyst. Environ.* 349, 108445. doi: 10.1016/j.agee.2023.108445

Ma, Q., Sun, Q., Zhang, X., Li, F., Ding, Y., Tao, R., et al. (2022a). Controlled-release nitrogen fertilizer management influences grain yield in winter wheat by regulating flag leaf senescence post-anthesis and grain filling. *Food Energy Secur.* 11, e361. doi: 10.1002/fes3.v11.2

Ma, Q., Tao, R., Ding, Y., Zhang, X., Li, F., Zhu, M., et al. (2022b). Can split application of slow-release fertilizer improve wheat yield, nitrogen efficiency and their stability in different ecological regions? *Agronomy* 12, 407. doi: 10.3390/agronomy12020407

Ma, Q., Wang, M., Zheng, G., Yao, Y., Tao, R., Zhu, M., et al. (2021). Twice-split application of controlled-release Nitrogen fertilizer met the nitrogen demand of winter wheat. *Field Crops Research. 267* 108163, 1–9. doi: 10.1016/j.fcr.2021.108163

Markus, D. K., McKinnon, J. P., and Buccafuri, A. F. (1985). Automated analysis of nitrite, nitrate, and ammonium nitrogen in soils. *Soil Sci. Soc. America J.* 49, 1208–1215. doi: 10.2136/sssaj1985.03615995004900050028x

Nishimura, S., Yoshimura, M., Yamane, T., and Oka, N. (2022). Effects of coated slow-release fertilizers on nitrous oxide emission from winter wheat field in a cool-temperate region in Japan. *Soil Sci. Plant Nutr.* 68, 305–316. doi: 10.1080/00380768.2022.2038521

Ntinyari, W., Giweta, M., Mutegi, J., Masso, C., and Gweyi-Onyango, J. P. (2022). "Managing agricultural nitrogen losses in crop production and mitigation of climate change effects," in *Agriculture, livestock production and aquaculture: advances for smallholder farming systems*, vol. Volume 1. (Springer International Publishing, Cham), 21–41.

Snapp, S., Sapkota, T. B., Chamberlin, J., Cox, C. M., Gameda, S., Jat, M. L., et al. (2023). Spatially differentiated nitrogen supply is key in a global food–fertilizer price crisis. *Nat Sustain* 6, 1268–1278. doi: 10.1038/s41893-023-01166-w

Vejan, P., Khadiran, T., Abdullah, R., and Ahmad, N. (2021). Controlled release fertilizer: A review on developments, applications and potential in agriculture. *J. Controlled Release* 339, 321–334. doi: 10.1016/j.jconrel.2021.10.003

Wu, B., Lin, X., Ali, M. F., and Wang, D. (2023). Development of an irrigation regime for winter wheat to save water resources by avoiding irrigation at anthesis stage. *J. Agron. Crop Sci.* 209, 188–203. doi: 10.1111/jac.v209.1

Wu, B., Shang, Y., Wang, S., Hu, X., Zhang, R., Zhang, B., et al. (2021). Response of nitrogen redistribution to irrigation at jointing in winter wheat. *Agron. J.* 113, 381–396. doi: 10.1002/agj2.v113.1

Xiao, Y., Peng, F., Zhang, Y., Wang, J., Zhuge, Y., Zhang, S., et al. (2019). Effect of bag-controlled release fertilizer on nitrogen loss, greenhouse gas emissions, and nitrogen applied amount in peach production. *J. cleaner production* 234, 258–274. doi: 10.1016/j.jclepro.2019.06.219

Xu, Z. Z., Yu, Z. W., Wang, D., and Zhang, Y. L. (2005). Nitrogen accumulation and translocation for winter wheat under different irrigation regimes. *J. Agron. Crop Sci.* 191, 439–449. doi: 10.1111/j.1439-037X.2005.00178.x

Yan, X., Ti, C., Vitousek, P., Chen, D., Leip, A., Cai, Z., et al. (2014). Fertilizer nitrogen recovery efficiencies in crop production systems of China with and without consideration of the residual effect of nitrogen. *Environ. Res. Lett.* 9, 095002. doi: 10.1088/1748-9326/9/9/095002

Yang, Y. C., Zhang, M., Zheng, L., Cheng, D. D., Liu, M., and Geng, Y. Q. (2011). Controlled release urea improved nitrogen use efficiency, yield, and quality of wheat. *Agron. J.* 103, 479–485. doi: 10.2134/agronj2010.0343

Zhang, G., Liu, S., Dong, Y., Liao, Y., and Han, J. (2022). A nitrogen fertilizer strategy for simultaneously increasing wheat grain yield and protein content: Mixed application of controlled-release urea and normal urea. *Field Crops Res.* 277, 108405. doi: 10.1016/j.fcr.2021.108405

Zhang, S., Shen, T., Yang, Y., Li, Y. C., Wan, Y., Zhang, M., et al. (2018). Controlled-release urea reduced nitrogen leaching and improved nitrogen use efficiency and yield of direct-seeded rice. *J. Environ. Manage.* 220, 191–197. doi: 10.1016/j.jenvman.2018.05.010

Zheng, W., Zhang, M., Liu, Z., Zhou, H., Lu, H., Zhang, W., et al. (2016). Combining controlled-release urea and normal urea to improve the nitrogen use efficiency and yield under wheat-maize double cropping system. *Field Crops Res.* 197, 52–62. doi: 10.1016/j.fcr.2016.08.004

Zhou, H., Zhang, M., Liu, Z., Zheng, W., Zhu, Q., and Wan, Y. (2019). Maize yield and economic return with controlled-release urea. *Nutrient Cycling Agroecosystems* 115, 427–440. doi: 10.1007/s10705-019-10020-5

Zhou, X., Yang, X., Feng, S., Zhang, J., Wu, J., Liu, J., et al. (2023). Optimization of controlled-release urea application based on the winter wheat yield. *Eur. J. Agron.* 151, 126987. doi: 10.1016/j.eja.2023.126987

Zhu, S., Liu, L., Xu, Y., Yang, Y., and Shi, R. (2020). Application of controlled release urea improved grain yield and nitrogen use efficiency: A meta-analysis. *PloS One* 15, e0241481. doi: 10.1371/journal.pone.0241481

frontiers | Frontiers in Plant Science

TYPE Original Research
PUBLISHED 28 January 2025
DOI 10.3389/fpls.2024.1481882

Check for updates

OPEN ACCESS

EDITED BY
Khurram Shahzad,
Lasbela University of Agriculture, Water and Marine Sciences, Pakistan

REVIEWED BY
Gunasekhar Nachimuthu,
NSW Government, Australia
Sudip Sengupta,
Swami Vivekananda University, India
Deepu Pandita,
Government Department of School Education, India

*CORRESPONDENCE
Kuppayevalasu Malayappagounder Sellamuthu
kmsellamuthu@tnau.ac.in

RECEIVED 16 August 2024
ACCEPTED 20 December 2024
PUBLISHED 28 January 2025

CITATION
Arulmani R, Sellamuthu KM, Maragatham S, Senthil A, Thamaraiselvi SP, Malathi P and Sridevi G (2025) Development and validation of soil test crop response model for beetroot (*Beta vulgaris*) grown in ultisols of India.
Front. Plant Sci. 15:1481882.
doi: 10.3389/fpls.2024.1481882

Development and validation of soil test crop response model for beetroot (*Beta vulgaris*) grown in ultisols of India

Ramasamy Arulmani[1,2], Kuppayevalasu Malayappagounder Sellamuthu[1,2*], Subramaniam Maragatham[1,2], Alargarsamy Senthil[1,3], Seenapuram Palaniswami Thamaraiselvi[1,4], Palaniappan Malathi[1,2] and Govindaraja Sridevi[1,2]

[1]Tamil Nadu Agricultural University, Coimbatore, India, [2]Department of Soil Science and Agricultural Chemistry, Coimbatore, India, [3]Department of Crop Physiology, Coimbatore, India, [4]Department of Floriculture and Landscape Architecture, Coimbatore, India

Soil Test Crop Response (STCR), a combined plant nutrient management system that enables to develop fertilizer prescription equations for balanced crop nutrition, higher yield, profitability, and better nutrient efficiency. Field trial was carried out on Typic Haplohmult soil of Nilgiris, Tamil Nadu during 2023-2024 by Implementing an Inductive combined with a targeted yield model. Field trial includes a gradient experiment with a green viz., *Chenopodium album*; a test crop experiment with beetroot (Hybrid Improved Crystal) and a validation experiment with beetroot. First, the fertility gradient was ensured by the biomass yield and soil fertility. Then, test crop experiment with beet root were conducted in the same field to derive the basic parameters viz., Nutrient Requirement (NR), contribution of nutrients from fertilizers (C_f), contribution of nutrients from soil (C_s) and contribution of nutrients from the Farm Yard manure (C_{fym}). Using the basic parameters, fertilizer prescription equations were developed based on Integrated Plant Nutrition System and validated. We found that 0.38, 0.29, and 0.46 kg of N, P_2O5, and K_2O, respectively, were required for producing one quintal of beetroot tuber under the integrated approach. Readily customized of fertilizer nutrient doses was developed for varying soil test values and desired yield targets of beetroot, for both inorganic (NPK) alone and NPK + Farm Yard Manure (FYM). The model was validated in the same soil series with the achievement of 40 and 45 tonnes of beetroot ha^{-1} with 100.9% and 96.9% of yield achievement, respectively. The Soil analysis crop response - combined Plant Nutrition System model proved that beetroot yield can be increased by 34.74%, in relation to the generally recommended dose This inductive method could save 37, 26 and 34 kg of Nitrogen, Phosphorus and Potassium, respectively when Nitrogen, Phosphorus, Potassium fertilizers are combined with 12.5 t ha^{-1} FYM as per soil test and targeted yield of beetroot.

KEYWORDS

beetroot, fertilizer prescription, STCR-IPNS, targeted yield model, NPK uptake, BCR

10.3389/fpls.2024.1481882

1 Introduction

Precision agriculture plays a vital role in fertilizer economy, plant yield productivity and soil health. Fertilizers are crucial for boosting agricultural production. Though fertilizer consumption over the years is increasing, achieving the fertilizer use efficiency at farm level is still in question due to variety of reasons. Continuous escalation of expense of fertilizers and limited quantity of organic manures left the farmers mainly rely on chemical fertilizers. The current blanket fertilizer recommendation in developing countries fails to ensure efficient and economical fertilizer use due to its oversight of fertility variations, leading to imbalanced utilization of fertilizer nutrients. Constant use of straight fertilizers resulted in deficiency of micronutrients in crops. The scientific community realized depending solely of chemical fertilizer or organic manure cannot sustain the crop productivity and soil health. Considering the fragmented small and marginal farms, soil test based fertilizer application found the most suited fertilizer recommendation model for country like India. Fertilizer recommendations based on soil test result in effective fertilizer use and sustain of soil fertility. Among the different techniques of fertilizer recommendation, the approach based on yield aimed stands out for its uniqueness, as it not only provides soil analysis based fertilizer doses but also predicts the achievable yield(production) level through appropriate crop management practices. The aimed yield methods also establishes a scientific foundation for equitable fertilization, ensuring equilibrium not only between nourishment from external input but also with those present in the soil.

The STCR method aids farmers in lowering fertilizer consumption and minimizing environmental contamination by supplying crops with precisely the nutrients they require. It also boosts crop productivity and profitability by optimizing nutrient application and preventing nutrient shortages or surpluses. One of the precision agriculture techniques that relies on soil fertility information combined with plant nutrient requirements to maximize nutrient management and crop yields is the Soil Test Crop Response approach. The utilization of this information concerning soil fertility and the plant requirements may help alleviate over-fertilization by minimizing the quantities needed and reduce environmental pollution. It can also enhance crop yields and profitability in the light of optimizing nutrient management and limiting the deficiencies or excesses of nutrient. Further, precision agriculture technologies like variable rate application can make nutrient management even more accurate and efficient.

Beta vulgaris L. (Beetroot) belong to Chenopodiaceae family, an crucial root vegetable which contain minerals like magnesium, manganese, sodium, potassium, iron, and copper. Beetroot has a various therapeutic characteristics that can help prevent heart disease and certain malignancies. Beetroot has many beneficial compounds, including glycine, betaine, saponins, betacyanin, carotenoids, folates, betanins, polyphenols, and flavonoids. Beetroot, a significant root vegetable crop cultivated in 2164 hectares, 36260 tonnes and 16.75 t ha^{-1} of productivity in India. The study area is Nilgiris, which covers 507 hectares and produces 11,915 tonnes, resulting in a productivity of 23.50 t h^{-1} (Kadam et al., 2018). Given that beetroot productivity is below the global average, it is imperative to boost productivity through improved technologies. A unique inductive cum targeted yield approach proposed by Ramamoorthy et al. (1967) that considers soil nutrient availability and economic yield target of crops with an inclusive fertilizer and manure combination suits the present situation for India. Santhi et al. (2011) developed the fertilizer prescription equation for beetroot grown in Alfisols distributed in plains of Tamil Nadu while there is no comprehensive fertilizer prescription equation for beetroot grown in Ulitsols (hilly soils) of Tamil Nadu. Hence, the present experiment was carried out in red non calcareous soils of Typic Haplohmult of Nilgiris (Ooty), Tamil Nadu (TN), India aimed to formulate a balanced fertilizer schedule to enhance both productivity and sustaining soil health with fertilizer economy in hill beetroot cultivation system.

2 Materials and methods

2.1 Details of the experimental field

Field trial were conducted in Typic Haplohmult soil series at Horticultural Research Station (HRS), a constituent research farm of Tamil Nadu Agricultural University (TNAU), in Nilgiris (11° 25' N Latitude, 76° 43' E Longitude), Tamil Nadu, India during 2023-2024. Surface (0-5.90 inch deep) soil sample was collected as per the standard procedure and analyzed for physical and chemical properties (Jackson, 1973). The fixing capacities of phosphorus were assessed using an equilibrium method with monocalcium phosphate, according to the procedure outlined by Waugh and Fitts (1966). Using an equilibrium technique using potassium chloride, the potassium fixation capacities were assessed in accordance with the protocol described by (Waugh and Fitts, 1966). The soil was red non calcareous, deep, well drained, clay loam in texture, acidic (pH 4.56), non-saline (EC 0.34 dSm^{-1}) and medium in CEC (17 cmol (p+) kg^{-1}). Initial soil fertility status indicated that the soil organic carbon, $KMnO_4$-available nitrogen (N), Bray available phosphorus (P), NH_4OAc- available potassium (K) were found to be 31.47 g kg^{-1}, 450 kg ha^{-1}, 185 kg ha^{-1}, and 510 kg ha^{-1}, respectively. The phosphorus and potassium fixing capacities of the initial soil were 250 and 100 kg ha^{-1}, respectively. Available micronutrients (DTPA extractable- mg kg^{-1}) viz., iron (42.14), Manganese (10.34), Zine(1.24) and Copper (1.82) were in sufficient ranges (Figure 1). Figure 1 shows the overall protocol followed in the development STCR-IPNS model.

The field trial was carried out in three phase: Phase I: Fertility gradient field trial using a green, *Chenopodium album* from April to June 2023; Phase II: Test crop field trial with beetroot from September to December 2023; Phase III: Validation field trial with beetroot from January to April 2024 to confirm the accuracy of the developed targeted yield equation.

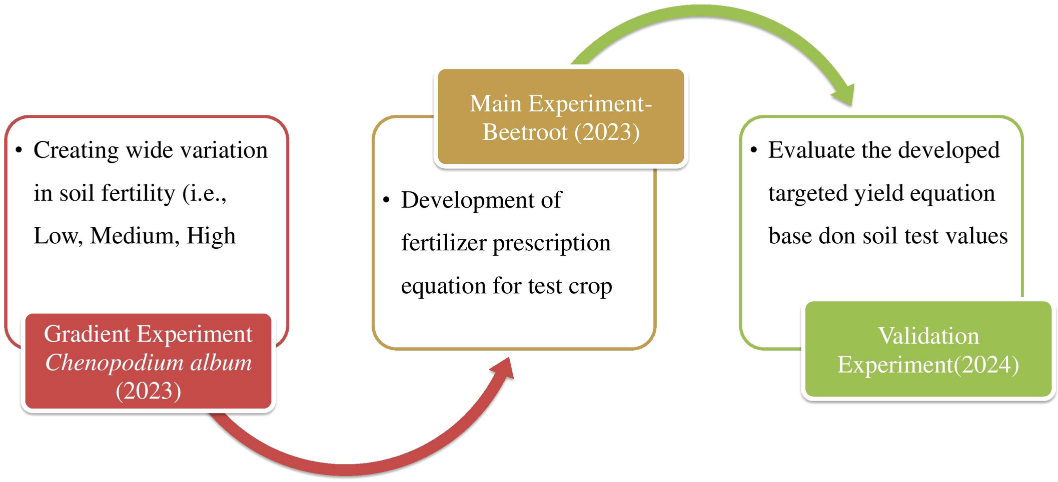

FIGURE 1
Graphical representation of experiment for development of fertilizer prescription equation.

2.2 Fertility gradient field trial (phase I)

First, a gradient experiment was conducted with a green, *Chenopodium album* var. Ooty 1. According to the inductive methodology proposed by Ramamoorthy et al. (1967), the fertility variation developed artificially. The experimental field trial was divided into three equal rectangular strips and applied with varying amounts of N, P_2O_5, and K_2O fertilizers ($N_0P_0K_0$; $N_1P_1K_1$; $N_2P_2K_2$). Strip I remained untreated nutrient (control), Strip II received the general recommendation of N recommended for *Chenopodium album*, while P_2O_5 and K_2O were applied based on soil fixing capacities of 250 and 100 kg ha^{-1}, respectively. Strip III received a double the dose of fertilizers compared to Strip II. Fertilizers were calculated, applied and ploughed which establishes a uniform mixing of fertilizers in each strip. After the ensuring mixing of fertilizers, *Chenopodium album* var. Ooty 1 was sown and irrigated. The intensive cultivation of *Chenopodium album* var. Ooty 1 led to alterations in the soil fertility. After 65 days of sowing, the crop was harvested in each fertility strip, and the yield of green biomass was recorded. Twenty four soil samples from each strip was collected and analyzed before and after the harvest of gradient crop for $KMnO_4$ -nitrogen (N), Bray phosphorus (P) and ammonium acetate (NH_4OAc) potassium (K). Based on the dry matter production, uptake of N, P and K, post harvest $KMnO_4$-nitrogen (N), Bray phosphorus (P) and ammonium acetate (NH_4OAc) potassium (K), the development of fertility gradient was ensured (Figure 2). Figure 2 shows the layout of the gradient experiment and levels of nutrients added to each Strip.

2.3 Test crop field trail (phase II)

Second, a test crop experiment was planned with beet root (hybrid-Improved crystal). After the verification of gradient establishment, the principal experiment commenced with beetroot as the test crop. After the harvest of gradient crop, each strip was divided into 24 plots and soil samples from each plot was collected and analyzed for available potassium permanganate ($KMnO_4$) nitrogen (N) (Subbiah and Asija, 1956), Bray phosphorus (P) (Bray and Kurtz, 1945), ammonium acetate (NH_4OAc) potassium (K) (Stanford and English, 1949). The test crop experiment was laid out in a fractional factorial randomized block design comprising 24 treatments with four levels of N (0, 60, 120, and 180 kg ha^{-1}), four levels of P_2O_5 (0, 80, 160, and 240 kg ha^{-1}), four levels of K_2O (0, 50, 100, and 150 kg ha^{-1}) and three levels of FYM @ 0, 6.25, and 12.5 t ha^{-1}. Within the field trial, each strip was subdivided into three sub-strips to apply three levels of FYM across the fertility gradient. The layout of the field trial is illustrated in Figure 3 which

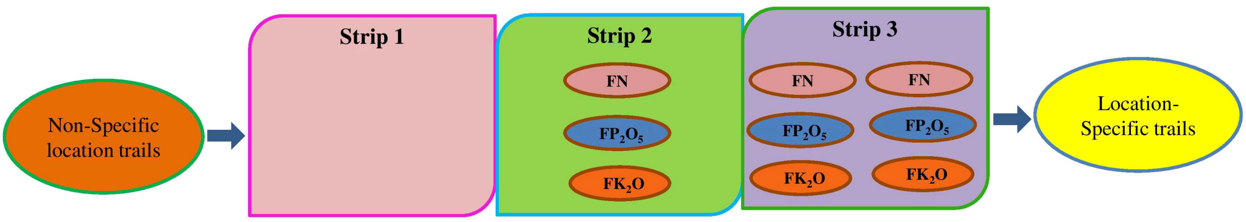

FIGURE 2
Illustration of the fertility gradient experiment.

shows the major nutrient combination for each treatment and superimposition of level of manure in each Strip main experiment. The test crop was cultivated using 24 treatment combinations by applying 21 selected treatment combinations, along with three control treatments as outlined in Table 1. Care was taken to super impose the IPNS treatments viz., NPK (inorganic) alone, NPK + FYM (integrated) at 6.25 t ha^{-1}, and NPK + FYM (integrated) at 12.5 t ha^{-1}) across the strips. Attention was ensured to randomize the 21 fertilizer treatments and three control treatments in such a way that all the 24 treatments present in all the three strips in either direction of the plots. All the nutrient management and plant protection packages were done as per the Crop Production Guide prescribed by Tamil Nadu Agricultural University and Government of Tamil Nadu. The fertilizer P_2O_5, K_2O, and FYM were applied basally while fertilizer nitrogen (N) was applied during basal and 30 days after sowing. The crop was grown to maturity, fresh roots were harvested and the root yield was recorded. From each plot, plant and root samples were collected, processed, and analyzed for total N (Humphries, 1956), P, and K contents (Jackson, 1973), and the NPK uptake by beetroot was computed based on dry matter yield and NPK nutrient content.

The SPAD (Soil-Plant Analysis Development) meter value, which serves as an indirect measure of chlorophyll content in the leaf, was recorded at 30, 60, and 90 days after sowing (DAS) and utilized to calculate the chlorophyll concentration. This measurement acts as a diagnostic tool for assessing the nitrogen status of crops.

2.3.1 Principal component analysis

Principal component analysis (PCA), as described by Wold et al. (1987), was employed to evaluate the potential impact of available soil nutrients, NPK fertilizers, and farmyard manures (FYM) on beetroot yield.

2.3.2 Computation of basic parameters

Making use of the data on root yield, nutrient uptake, presowing soil available nutrients, and applied fertilizer doses, the basic parameters viz., nutrient requirement (NR) and contributions of nutrients from soil (C_s) and contributions of nutrients from fertilizers (C_f) were calculated as outlined by (Ramamoorthy et al., 1967; Velayutham et al., 1985; Krishna Murthy et al., 2023; Rao and Srivastava, 2000) and contributions of nutrients from Farm Yard Manure (C_{fym}) were estimated as described by (Santhi et al., 1999). The nutrient requirement, soil, fertilizer, and farmyard manure efficiencies were derived as discussed by (MaruthiSankar, 1986). The basic parameters, NR expressed in kg per quintal while, C_s, C_f, and C_{fym}, expressed as a percentage.

TABLE 1 Treatment structure for test crop experiment (Beetroot).

S. No	Treatment combination			Levels of nutrients ($kgha^{-1}$)		
	N	P	K	N	P_2O_5	K_2O
1	0	0	0	0	0	0
2	0	0	0	0	0	0
3	0	0	0	0	0	0
4	0	2	2	0	160	100
5	1	1	1	60	80	50
6	1	2	1	60	160	50
7	1	1	2	60	80	100
8	1	2	2	60	160	100
9	2	1	1	120	80	50
10	2	0	2	120	0	100
11	2	1	2	120	80	100
12	2	2	2	120	160	100
13	2	2	1	120	160	50
14	2	2	0	120	160	0
15	2	2	3	120	160	150
16	2	3	2	120	240	100
17	2	3	3	120	240	150
18	3	1	1	180	80	50
19	3	2	1	180	160	50
20	3	2	2	180	160	100
21	3	3	1	180	240	50
22	3	3	2	180	240	100
23	3	2	3	180	160	150
24	3	3	3	180	240	150

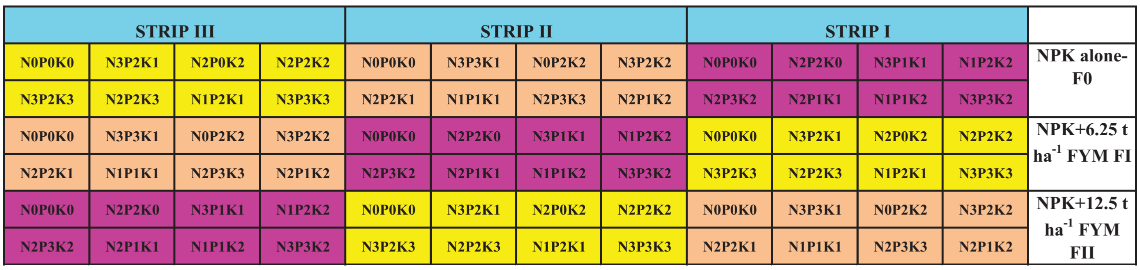

FIGURE 3
Layout plan of test crop experiment with Beetroot.

$$F = \frac{NR}{Cf}Y - \frac{Cs}{Cf}S - \frac{CYFM}{Cf}FYM$$

where F is fertilizer (kg ha^{-1}), NR is nutrient requirement of N or P_2O_5 or K_2O kg q^{-1} produce, Cs is percent contribution from soil, $C_f$is percent contribution from fertilizer, C_{FYM} is percent contribution from FYM, S is soil-test value for available N, P, or K (kg ha^{-1}), Y is yield target (q ha^{-1}), and FYM is farmyard manure (t ha^{-1}).

The relationship among soil test values, crop yield, and fertilizer dosage was determined using standard regression techniques, as outlined by (Draper and Smith, 1998). The current research investigates the fluctuation in beetroot yield resulting from the use of various fertilizer dosages, with other factors of soil and crop management practices are kept steady.

2.4 Validation experiment (phase III)

Third, a validation field trial was carried out in farmer's land in same soil series, using beetroot (Hybrid: Improved Crystal) to verify the STCR-IPNS model. Based on the survey of the potential yield of the hybrid in Nilgiris, three beet root yield targets were taken (35.00 t ha^{-1}, 40.00 t ha^{-1} and 45.00 t ha^{-1}). This validation includes assessing the percentage achievement from the fixed target, beetroot yield, response ratio (RR), and economic comparisons with other fertilizer recommendation approaches such as the general fertilizer recommended dose, all within a RBD - randomized block design with three replication. Treatment consisted of T_1-General fertilizer recommended dose (100% GFRD alone), T_2-General fertilizer recommended dose (100% GFRD) + FYM @ 12.5 t ha^{-1}, T_3-STCR-Inorganic-TY_1 35.00 $_t$ ha^{-1}, T_4-STCR-Inorganic-TY_2 40.00 $_t$ ha^{-1}, T_5 - STCR-Inorganic-TY_3 45.00 $_t$ ha^{-1}, T_6-STCR-Integrated-TY_1 35.00 $_t$ ha^{-1}, T_7-STCR-Integrated-TY_2 40.00 $_t$ ha^{-1} T_8-STCR-Inorganic-TY_3 45.00 $_t$ ha^{-1},T_9- Farmer's fertilizer Practice (FFP), T_{10}-Absolute control (untreated nutrients). Composite soil samples were taken from each plot at a depth of 0-5.90inch before initiating the experiment, following the layout plan. Fertilizer application for STCR treatments (T_3 to T_8) was determined using STCR equations. The crop was cultivated according to standard crop production guide procedure, harvested at full maturity, and beetroot yields were computed based on the net plot area, expressed in tons per hectare (kg ha^{-1}).

2.4.1 Per cent achievement

$$\text{Per cent achievement} = \frac{\text{Yield obtained in the STCR treatment (kg or q ha}^{-1})}{\text{Yield targeted (kg or q ha}^{-1})} \times 100$$

2.4.2 Response ratio

$$\text{Response ratio} = \frac{\text{Response (kg h}a^{-1})}{\text{Quantities of fertiliser N, } P_2O_5 \text{and } K_2O \text{ applied (kg ha}^{-1})}$$

3 Results

3.1 Fertility gradient field trial

A fertility gradient field trial was carried out to introduce variation in soil available NPK status across the trial field. Table 2 illustrates the mean and range soil analysis values (STVs) for N, P_2O_5, and K_2O, demonstrating the variation across fertility strips. Strip III exhibited the highest nutrient levels (467kg N, 213kg P_2O_5, and 620 kg K_2O ha^{-1} respectively) due to the use of maximum fertilizers, compared to strip I (409 kg N, 178kg P_2O_5, and 509 kg K_2O ha^{-1} respectively), and strip II (432 kg N, 194 kg phosphorus pentoxide (P_2O_5), and 550 kg potassium oxide (K_2O) ha^{-1} respectively). Biomass yield of gradient crop (*Chenopodium album)* was also highest in strip III with 27.69 t ha^{-1}, compared to strip II (24.00 t ha^{-1}) and strip I (12.00 t ha^{-1}).

3.2 Fertility strip variations influenced soil nutrient availability, beetroot yield, and nutrient uptake

The mean and range values of soil analysis results, nutrient uptake and beetroot yield for each strip is given in Table 3. The pre-sowing soil analysis values for beetroot indicated that the mean $KMnO_4$- available nitrogen (N) was found to be 416, 435, and 475 kg ha^{-1} in strips I, II, and III, respectively. Similarly, the average pre-sowing soil analysis values for Bray-P were 184, 197, and 209 kg ha^{-1} in strips I, II, and III, respectively. Pre-sowing soil analysis values for NH_4OAc-K were 515, 552, and 620 kg ha^{-1} in strips I, II, and III, respectively. The average values of $KMnO_4$- available nitrogen (N), Bray-Phosphorus (P), and NH_4OAc-available potassium (K) in inorganic treated plots were 442, 196, and 562 kg ha^{-1}, respectively. In control plots, the average values of $KMnO_4$- available nitrogen (N), Bray-Phosphorus (P), and NH_4OAc-available potassium (K) were 438, 196, and 566 kg ha^{-1}, respectively.

In strip I, the beetroot yield varied from 10,040 to 50,835 kg ha^{-1}, with a mean (average) of 33,500 kg ha^{-1}; in strip II, it ranged from 15,545 to 58,045 kg ha^{-1}, with average of 38,950 kg ha^{-1}; and in strip III, it ranged from 18,311 to 61,800 kg ha^{-1}, with average of 44,833 kg ha^{-1}. The average beetroot yield in inorganic treated plots and untreated nutrient plots were 41,951 kg ha^{-1} and 19,099 kg ha^{-1}, respectively, representing a percentage increase of 119.65% over the control. The nutrient uptake data indicated variations in N uptake ranged from 64.5 to 210.1 kg ha^{-1}, P uptake from 12.9 to 85.1 kg ha^{-1}, and K uptake from 99.5 to 220.2 kg ha^{-1} across strips I, II, and III, respectively. The overall average values of nitrogen (N), phosphorus (P), and potassium (K) uptake in inorganic treated plots were 156.0, 52.4, and 155.4 kg ha^{-1}, respectively. Within the control plots, the overall mean values for nitrogen (N), phosphorus (P), and potassium (K) uptake were 97.4, 23.1, and 120.5 kg ha^{-1}, respectively.

3.3 Potential of available nutrients, Nitrogen, Phosphorus, Potassium fertilizers, FYM in beetroot yield production

Principal component analysis (PCA) was conducted for each strip to analyze the relationship between beetroot yield production and various factors, including available soil nutrients, N,P,K uptake, applied NPK chemical fertilizers, and FYM. Figure 4A presents the PCA plot illustrating the variables and observations for all strips. The PCA explained an average cumulative variability of 60.80% in beetroot production across all strips. This variability was attributed

TABLE 2 Descriptive statistics of Green biomass yield available soil nutrients (0-15 cm), after the soil fertility gradient experiment.

Strips		Soil available nutrients (kg ha^{-1})			Green Biomass yield (t ha^{-1})
		Nitrogen	Phosphorus	Potassium	
I	Range	395.00-424.00	170.40-184.94	487.62-532.46	11.82-12.36
	Mean ± SD	409 ± 11.10	178 ± 4.94	509 ± 4.60	12 ± 0.05
	(CV %)	2.70	2.77	2.56	1.33
	Median	412.50	178.63	509.99	11.99
II	Range	423.36-449.28	186.03-199.48	544.00-559.24	23.44-25.10
	Mean ± SD	432 ± 8.71	194 ± 4.29	550 ± 1.48	24 ± 0.17
	(CV %)	2.01	2.20	0.76	0.41
	Median	429.54	195.37	549.96	23.94
III	Range	445.00-482.00	209.00-224.00	610.08-639.84	27.35-29.28
	Mean ± SD	467 ± 11.10	213 ± 4.62	620 ± 3.18	28 ± 0.27
	(CV %)	2.37	2.16	1.45	0.64
	Median	469.50	213.00	619.00	27.69

SD, standard deviation; CV (%), coefficient of variation (%).
Strip I, Untreated nutrient (control); Strip II, General recommendation of N recommended for *Chenopodium album*, while P_2O_5 and K_2O were applied based on soil fixing capacities of 250 and 100 kg ha^{-1}, respectively; Strip III, Double the dose of fertilizers compared to Strip II.

to 24 distinct combinations of NPK and FYM treatments under varying soil fertility variation. PCA analysis showed that among the variables assessed, application of NPK mineral fertilizer, NPK nutrient uptake, and organic manure (FYM) were consistently located orthogonally in the positive (+) quadrant (PC1 and PC2) across all strips. This positioning indicates that these variables made a significant positive (+) contribution to beetroot yield production.

PCA showed that PC1 of strip 1 comprised for 46.5% of the total cumulative variability. PCA analysis indicated that all evaluated variables were located orthogonally in the positive (+) quadrant (PC1 and PC2) (Figure 4B). Likewise, in strip 2 [available soil potassium (K)] and Strip 3 [available soil nitrogen (N) and potassium (K)], these variables were found in the negative (-) quadrant. This positioning may indicate lower nutrient contributions from the higher gradient soil towards beetroot yield.

In relation to those plots, the optimal sets of potential treatments were located in the "high" (+,+) quadrant and "moderate" (+,-) quadrants of the PCA plot (Figures 4C, D). Conversely, the treatment that exhibited lower potential in beetroot production revealed negative (-) correlation with the variables and was positioned in the "low" (-,-) and (-,+) quadrants.

Multiple regression equations were derived using variable as an independent variable (UN,UP,UK,SN,SP,SK,FN,FP_2O_5,FK_2O, FYM) and the dependent variable yield was derived for each strip separately and as a whole. The relationship between yield and the variables was determined as follows:

TABLE 3 Initial soil available NPK, as well as the yield and NPK uptake by beetroot, were recorded in various strips of the test crop experiment (kg ha^{-1}).

Parameters (kg ha^{-1})	Strip I		Strip II		Strip III		Overall			
							NPK treated		Control (NPK)	
	Range	Mean	Range	Mean	Range	Mean	Range	Mean	Range	Mean
$KMnO_4$-N	411-421	416	431-441	435	471-481	475	411-481	442.33	411-473	438.89
Bray-P	182.3-186.2	184.3	195.2-200.0	197.4	207.1-211.5	209.4	182.3-211.5	197.0	182.2-210.0	196.3
NH_4OAc-K	510-519	515	547-557	552	615-625	620	510-625	562.00	517-625	566.00
Tuber Yield	10040-50835	33500	15545-58045	38950	18311-61800	44833	18481-61800	41951	10040-28072	19099
N uptake	64.5-191.0	135.7	89.3-205.1	145.9	93.3-210.1	164.5	83.15-210.19	156.08	64.5-112.6	97.4
P uptake	12.9-69.9	41.0	21.3-83.1	49.3	23.5-85.1	55.9	22.94-85.04	52.45	12.9-28.5	23.1
K uptake	99.5-161.0	135.5	123.5-175.2	149.4	125.4-220.2	168.1	108.03-220.22	155.43	99.5-138.4	120.54

Strip I: Untreated nutrient (control); Strip II: General recommendation of N recommended for *Chenopodium album*, while P_2O_5 and K_2O were applied based on soil fixing capacities of 250 and 100 kg ha^{-1}, respectively; Strip III: Double the dose of fertilizers compared to Strip II.

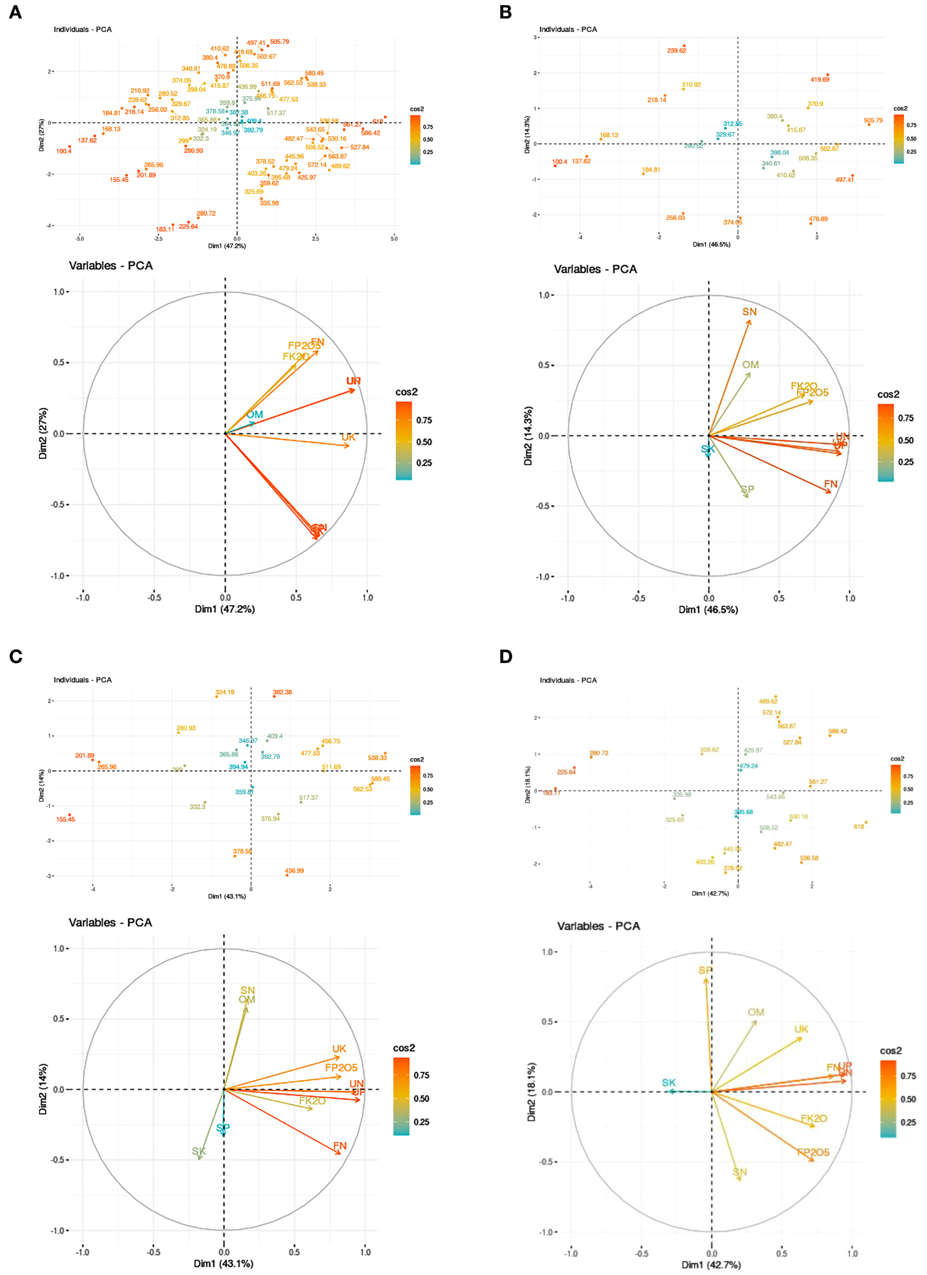

FIGURE 4
(A) Principle component analysis plots of overall relating the beetroot yield and the active variables. (i) Scoring plot showing the positions of each treatment. (ii) Loading plot showing the orthogonal positions of variable (Soil available nutrient (kg ha^{-1}), NPK fertilizer (kg ha^{-1}), FYM application (t ha^{-1}), and NPK uptake by plant (kg ha^{-1}). **(B)** Principle component analysis plots of strip 1 relating the beetroot yield and the active variables. (i) Scoring plot showing the positions of each treatment. (ii) Loading plot showing the orthogonal positions of variable [Soil available nutrient (kg ha^{-1}), NPK fertilizer (kg ha^{-1}), FYM application (t ha^{-1}), and NPK uptake by plant (kg ha^{-1})]. **(C)** Principle component analysis plots of strip 2 relating the beetroot yield and the active variables. (i) Scoring plot showing the positions of each treatment. (ii) Loading plot showing the orthogonal positions of variable [Soil available nutrient (kg ha^{-1}), NPK fertilizer (kg ha^{-1}), FYM application (t ha^{-1}), and NPK uptake by plant (kg ha^{-1})]. **(D)** Principle component analysis plots of strip 3 relating the beetroot yield and the active variables. (i) Scoring plot showing the positions of each treatment. (ii) Loading plot showing the orthogonal positions of variable [Soil available nutrient (kg ha^{-1}), NPK fertilizer (kg ha^{-1}), FYM application (t ha^{-1}), and NPK uptake by plant (kg ha^{-1})].

$$\textbf{Yield in stripI} = -1264.03 + (0.687 \times UN) + (0.47 \times UP) + (1.046 \times UK) - (1.084 \times SN) + (3.135 \times SP) + (2.056 \times SK) + (0.881 \times FN) + (0.169 \times FP_2O_5) + (0.133 \times FK_2O) + (4.825 \times FYM) \quad (1)$$

Yield in strip II

$$= -799.56 + (0.794 \times UN) + (0.968 \times UP) + (0.642 \times UK) + (2.014 \times SN) - (9.11 \times SP) + (3.081 \times SK) + (0.772 \times FN) + (0.060 \times FP_2O_5) + (0.398 \times FK_2O) + (4.499 \times FYM) \quad (2)$$

Yield in strip III

$$= 622.634 + (0.509 \times UN) + (2.605 \times UP) + (0.111 \times UK) - (0.336 \times SN) + (1.603 \times SP)(1.155 \times SK) + (0.683 \times FN) + (0.141 \times FP_2O_5) + (0.176 \times FK_2O) + (1.851 \times FYM) \quad (3)$$

Yield in overall strips

$$= -211.45 + (0.932 \times UN) + (1.171 \times UP) + (0.643 \times UK) - (0.892 \times SN) + (0.582 \times SP) + (0.816 \times SK) + (0.679 \times FN) + (0.183 \times FP_2O_5) + (0.168 \times FK_2O) + (3.026 \times FYM) \quad (4)$$

The coefficient of determination (R^2) values were ≥0.97 for each strip, as well as for the overall strip collectively. The results from multiple regression equations served as corroborating data for the PCA analysis.

3.4 Chlorophyll content

The SPAD meter data ranged from 14.5 to 42.6 at 30 DAS, 24.0 to 55.9 at 60 DAS, and 29.6 to 61.9 at 90 DAS. The data indicated a gradual upward trend in chlorophyll content, with the mean values rising from 27.73 at 30 DAS to 45.51 at 90 DAS (Figures 5A-C).

3.5 Basic parameters

In the targeted yield model, the basic parameters were computed using data on beetroot yield, initial soil analysis values, NPK uptake and the amounts of applied N, P_2O_5, and K_2O. The basic parameters for developing fertilizer prescription equations for beetroot are (i) nutrient requirement in kg per quintal of beetroot (NR) and percentage contributions from soil-available nutrients (C_s), fertilizer nutrients (C_f), and Farm yard manure (C_{fym}) are given in Table 4.

3.6 Nutrient requirement

The nutrient requirement (NR) is defined as the amount of nutrient needed to produce a single unit of economic yield. To produce 100 kg of beetroot yield, the required amounts of nutrients were found to be 0.38 kg of N, 0.29 kg of P_2O_5, and 0.46 kg of K_2O (Figure 6).

3.7 Percentage contributions of nutrients from soil, fertilizers, and farm yard manure to total uptake

The soil's available nutrient contribution (Cs) was reported as 20.25% for N, 11.02% for P_2O_5, and 19.67% for K_2O. The percentage contribution of N, P_2O_5, and K_2O from fertilizers (C_f) was 55.16, 46.62, and 56.62, respectively, following the order of $K_2O > N > P_2O_5$. The organic manure (FYM) contribution (C_{fym}) was recorded as 34.40% for N, 17.46% for P_2O_5 and 29.65% for K_2O, respectively (Table 4).

3.8 Fertilizer prescription equations

The beetroot yield target model was developed based on basic parameters.

STCR-Inorganic equation

$$FN = 0.69\,T - 0.37\,SN\,(KMnO_4 - N) \quad (5)$$

$$FP_2O_5 = 0.61\,T - 0.54\,SP\,(Bray - P_2O_5) \quad (6)$$

$$FK_2O = 0.82\,T - 0.42\,SK\,(Am.\,Ace. - K_2O) \quad (7)$$

STCR-IPNS equation

$$FN = 0.69\,T - 0.37\,SN(KMnO_4 - N) - 0.62\,ON \quad (8)$$

$$FP_2O_5 = 0.61\,T - 0.54\,SP(Bray - P_2O_5) - 0.86\,OP \quad (9)$$

$$FK_2O = 0.82\,T - 0.42\,SK(Am.\,Ace. - K_2O) - 0.63\,OK \quad (10)$$

where FN, FP_2O_5, and FK_2O are fertilizer N, P_2O_5, and K_2O in kg ha^{-1}, respectively; T is the yield target in q ha^{-1}; SN, SP, and SK are available soil nutrients as $KMnO_4$-N, Bray's-P_2O_5, and NH_4OAc-K_2O in kg ha^{-1}, respectively, and ON, OP, and OK are the quantities of Nitrogen, Phosphorus, and Potassium supplied through farmyard manure in kg ha^{-1}

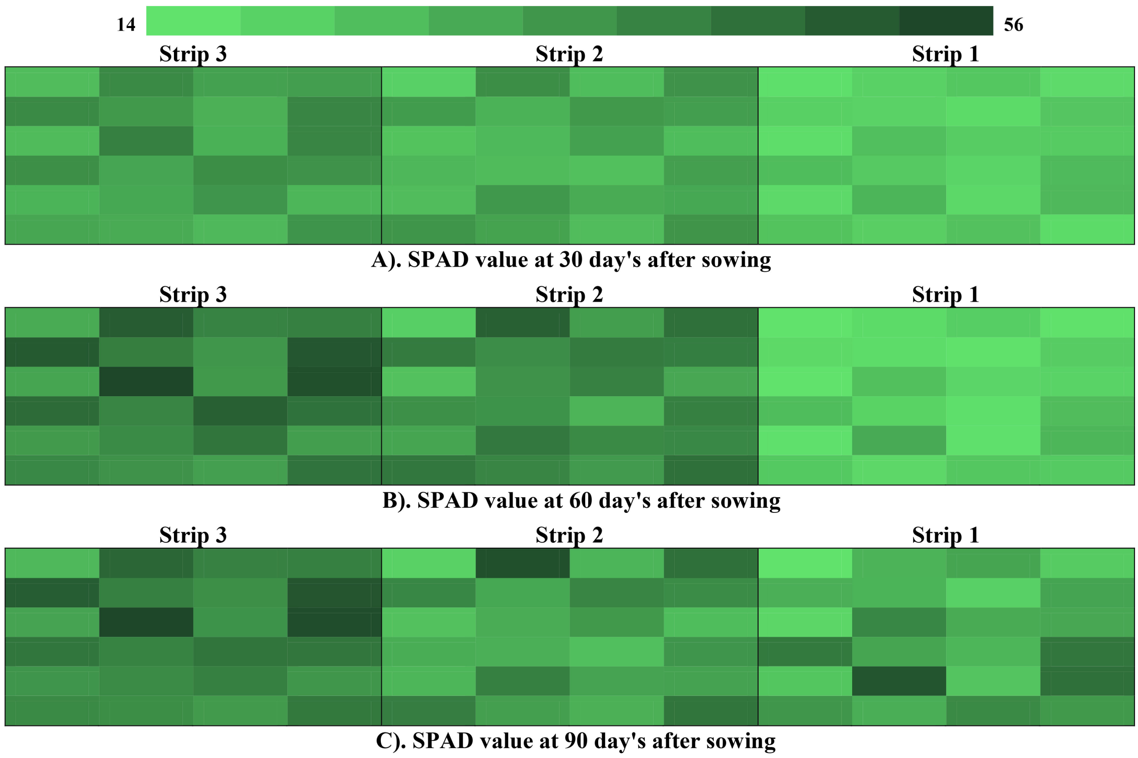

FIGURE 5
(A) SPAD value at 30 day's after sowing. **(B)** SPAD value at 60 day's after sowing. **(C)** SPAD value at 90 day's after sowing.

3.9 Fertilizer prescription under integrated for desired yield target of beetroot

A readily available table was developed according to these equations for diverse soil test values and a yield target of 400 q ha^{-1} (Table 5). The findings clearly revealed that the fertilizer requirements for N, P_2O_5, and K_2O decreased as soil analysis values increased.To attain a yield goal of 400 q ha^{-1} of beetroot with soil analysis values of 400 kg ha^{-1} for $KMnO_4$-N, 180 kg ha^{-1} for Bray P, and 520 kg $ha^{-1}$for NH_4OAc-K, the required fertilizer doses were 128 kg $ha^{-1}$of N, 147 kg $ha^{-1}$of P_2O_5, and 110 kg $ha^{-1}$of K_2O, respectively. When farmyard manure (containing 26% moisture and 0.56%, 0.23%, and 0.47% of N, P, and K, respectively) was applied at a rate of 12.5 t ha^{-1}, along with NPK, the required fertilizer doses were 91 kg ha^{-1} of N, 121 kg $ha^{-1}$of P_2O_5, and 76 kg $ha^{-1}$of K_2O, respectively. Under IPNS, the savings in fertilizer were 18 kg $ha^{-1}$of N, 13 kg $ha^{-1}$of P_2O_5, and 17 kg $ha^{-1}$of K_2O when using NPK plus FYM at 6.25 t ha^{-1}, and 37 kg $ha^{-1}$of N, 26 kg $ha^{-1}$of P_2O_5, and 34 kg $ha^{-1}$of K_2O when using NPK plus farmyard manure at 12 t ha^{-1}, respectively.

TABLE 4 Nutrient requirement and contributions of nutrients from soil, fertilizer, and FYM for beetroot.

Parameters	Nutrients		
	N	P_2O_5	K_2O
Nutrient requirement (kg q^{-1})	0.38	0.29	0.46
Per cent contribution from soil (C_s) (%)	20.25	11.02	19.67
Per cent contribution from fertilizers (C_f) (%)	55.16	46.62	56.62
Per cent contribution from FYM (C_{fym}) (%)	34.40	17.46	29.65

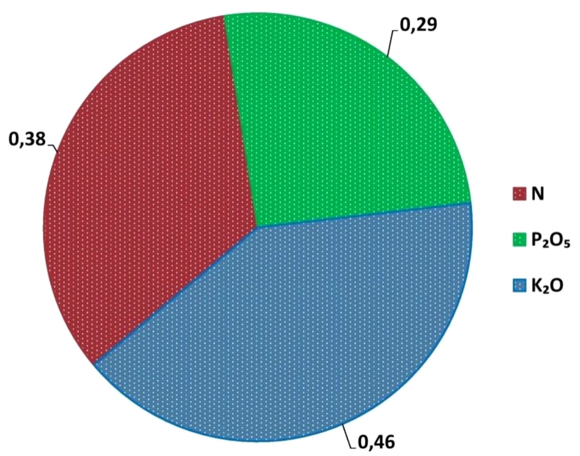

FIGURE 6
Nutrient requirement (kg q^{-1}) of N, P_2O_5 and K_2O for Beetroot.

TABLE 5 Reduction of inorganic fertilizers when soil-test-based fertilizer prescription under integrated (IPNS) for 400 q ha^{-1} target yield of beetroot (kg ha^{-1}).

Parameter	NPK alone (kg ha^{-1})	NPK+FYM @6.25 t ha^{-1}	Reduction over NPK alone (%)	NPK+FYM @12.5 t ha^{-1}	Reduction over NPK alone (%)
$KMnO_4$-N (kg ha^{-1})					
400	128	110	14.1	91	28.9
420	121	102	15.7	84	30.6
440	113	95	15.9	77	31.9
460	106	88	17.0	69	34.9
480	98	80	18.4	62	36.7
500	91	73	19.8	60*	34.1
Bray-P (kg ha^{-1})					
180	147	134	8.8	121	17.7
190	141	128	9.2	115	18.4
200	136	123	9.6	110	19.1
210	131	118	9.9	104	20.6
220	125	112	10.4	99	20.8
230	120	107	18.8	94	21.7
NH_4OAc-K (kg ha^{-1})					
520	110	93	15.5	76	30.9
540	101	84	16.8	68	32.7
560	93	76	18.3	59	36.6
580	84	68	19.0	51	39.3
600	76	59	22.4	50*	34.2
620	68	51	25.0	50*	26.5

3.10 Validation experiment

3.10.1 Beetroot yield

In our research, notable variation in beetroot yield was recorded across various treatments, lowest yield being 24.96 t ha^{-1} in the absolute control (untreated nutrient) to 43.60t ha^{-1}, the highest yield, achieved by the STCR- integrated (IPNS)-45.00 t ha^{-1} treatment, as outlined in Table 6, exceeding all other treatments.

3.10.2 Per cent achievement

The effectiveness of fertilizer recommendation calculations relies on the percentage attainment falling within the ±10% range scope of the yield target. In this context, the percentage achievement varied from 96.5% in STCR-inorganiconly at 45 t ha^{-1} to 103.5% in STCR-integrated at 35 t ha^{-1}, indicating the applicability of the inductive model for beetroot across all three yield target tiers within both the STCR-inorganic only and integrated categories. In the STCR- integrated category, the higher yield target attainment was recorded in STCR-integrated-35 t ha^{-1} (103.5%), followed by STCR-inorganic alone 35 t ha^{-1} (101.3%) and STCR- integrated 40 t ha^{-1} (100.9%). Conversely, in the case of STCR- inorganiconly, the percentage achievement for yield targets of 35, 40, and 45 t ha^{-1} was 103.5%, 100.9%, and 96.9%, respectively (Table 6).

3.10.3 Response ratio and B:C ratio

The response ratio observed for different treatments varied from 4.86 kg kg^{-1} in farmer's fertilizer practice to 44.16 kg kg^{-1} in STCR-integrated-35 t ha^{-1}, followed by STCR-integrated-40 t ha^{-1} (39.37), STCR-integrated-45 t ha^{-1} (35.24 kg kg^{-1}), and STCR-inorganiconly 45 t ha^{-1} (32.39 kg kg^{-1}) (Table 6). Among the STCR treatments, STCR-integrated consistently showed highest response ratios compared to their respective STCR-inorganic only treatments. The general fertilizer recommended dose (100% GFRD alone), and the general fertilizer recommended dose (100% GFRD) + FYM @ 12.5 t ha^{-1} recorded response ratios of 9.19 and 11.85 kg kg^{-1}, respectively, which were comparatively lower than all STCR treatments. According to the BCR data, STCR- integrated-45 t ha^{-1} (02.66) exhibited the highest value, followed by STCR-inorganic alone - 45 t ha^{-1} (2.63).

TABLE 6 Influence of different approaches of nutrient recommendations on yield, per cent achievement, Response Ratio (RR) and Benefit Cost ratio of beetroot crop.

S.No	Treatments	FYM (t ha^{-1})	Fertilizer doses (kg ha^{-1})			Beetroot Yield (t ha^{-1})	Per cent achievement	RR (kg kg^{-1})	BCR
			FN	FP$_2$O$_5$	FK$_2$O				
1	T_1	–	120	160	100	28.45	–	9.19	2.35
2	T_2	12.5	120	160	100	29.46	–	11.85	2.41
3	T_3	–	123	141	89	35.45	101.3	29.72	2.42
4	T_4	–	172	201	128	39.40	98.5	28.81	2.53
5	T_5	–	180**	240**	150**	43.42	96.5	32.39	2.63
6	T_6	12.5	91	114	50*	36.22	103.5	44.16	2.44
7	T_7	12.5	140	174	77	40.36	100.9	39.37	2.55
8	T_8	12.5	180**	233	116	43.60	96.9	35.24	2.66
9	T_9	–	100	120	80	26.42	–	4.86	1.74
10	T_{10}	–	0	0	0	24.96	–	–	1.38

*Maintenance dose **maximum dose.
T_1-General fertilizer recommended dose (100% GFRD alone), T_2-General fertilizer recommended dose (100% GFRD) + FYM @ 12.5 t ha^{-1}, T_3-STCR-Inorganic-TY_1 35.00 $_t$ ha^{-1}, T_4-STCR-Inorganic-TY_2 40.00 $_t$ ha^{-1}, T_5 - STCR-Inorganic-TY_3 45.00 $_t$ ha^{-1}, T_6-STCR-Integrated-TY_1 35.00 $_t$ ha^{-1}, T_7-STCR-Integrated-TY_2 40.00 $_t$ ha^{-1} T_8- STCR-Inorganic-TY_3 45.00 $_t$ ha^{-1},T_9- Farmer's fertilizer Practice (FFP), T_{10}-Absolute control (untreated nutrients).

4 Discussion

The statistical evaluation revealed that every strip differs significantly from the others, and the use of varying levels of NPK fertilizers led to a notable rise in the soil's available N, P, and K content, demonstrating the establishment of soil fertility variations in the field trial. Therefore, the establishment of soil fertility variation was verified by the soil analytical data for all three essential nutrients. The statistical analysis of post-harvest soil test data highlighted that significant difference in soil fertility status were present among the three strips (Udayakumar and Santhi, 2017; Singh et al., 2020; Vamshi et al., 2023). Using a graded level of fertilizer on gradient crops of rice, researchers found that grain and straw yields were higher. This could be because of the increased availability of nutrients in the soil with the increased levels of N, P, and K fertilizers, as well as the positive effects of these nutrients on fodder crops (Verma et al., 2014).

The experimental data clearly indicated significant variations in soil analysis value before sowing, nutrient uptake, and beetroot yield among the fertility strips and between NPK treated and control plots (untreated nutrient). These variations are crucial for establishing soil fertility gradients and are necessary for computing basic parameters and formulating fertilizer recommendation equations. These results align with the previous findings of (Umadevi, 2005; Singh, 2021) for carrot and Smitha John, 2004) for cabbage. The PCA results indicated that all variables were located in the positive quadrant, indicating their high importance for beetroot yield production. This finding aligns with the conclusions of a study by (Abishek et al., 2023).

SPAD value(chlorophyll content) increase may be due to the readily available micro and macronutrients, especially nitrogen, provided by farm yard manure (FYM), which is a crucial component of chlorophyll. These results are consistent with the findings of (Dhakal et al., 2009) in spinach beet. The application of farm yard manure (FYM) may have enhanced microbial activity in the root zone of the beetroot plant, facilitating nutrient transformation. These findings are consistent with the experiments conducted by (Tovihoudji et al., 2015: Singh et al., 2017; Dhakal et al., 2016; Nagar et al., 2016). Chlorophyll exhibited a positive (+) correlation with beetroot yield Figure 7, with r values of strip 1 (0.93), strip 2 (0.96), and strip 3 (0.92). Similar results were reported in beetroot (Mounika et al., 2022; Kumar et al., 2023).

The nutrient requirements data indicated that the hierarchy of nutrient requirements was K_2O >N > P_2O_5(descending order). Similar findings were observed by (Santhi et al., 2011 in beetroot; Kaushik et al., 2015 in radish; Dibyendu et al., 2010 in potato; KasthuriThilagam and Natesan, 2009 in cauliflower). Among the three essential nutrients, the soil's contribution is highest for N, followed by K_2O, and then P_2O_5. These findings closely align with those reported by (Gayathri et al., 2009) for Potato on Ultisols.

The data indicated that the ranking of nutrient requirements was K_2O > N > P_2O_5. The results are also consistent with the findings of (Santhi et al., 2011; Basavaraja et al., 2011; Polara et al., 2012; Sellamuthu et al., 2015; ParvathiSugumari et al., 2021; Bhavya et al., 2023) who observed a similar trend of relatively higher nutrient contribution of K_2O compared to N and P_2O_5 from fertilizer. The organic manure (FYM) contributes more towards N (Figure 8). These results are consistent with the findings of (Gayathri et al., 2009; Anil et al., 2008; Singh et al., 2019). The basic parameters were computed based on the pre sowing soil test values, nutrient uptake and crop yield by beetroot. Using these basic parameters, fertilizer prescription equations were developed for beetroot on Ultisol to achieve precise beetroot yield targets.

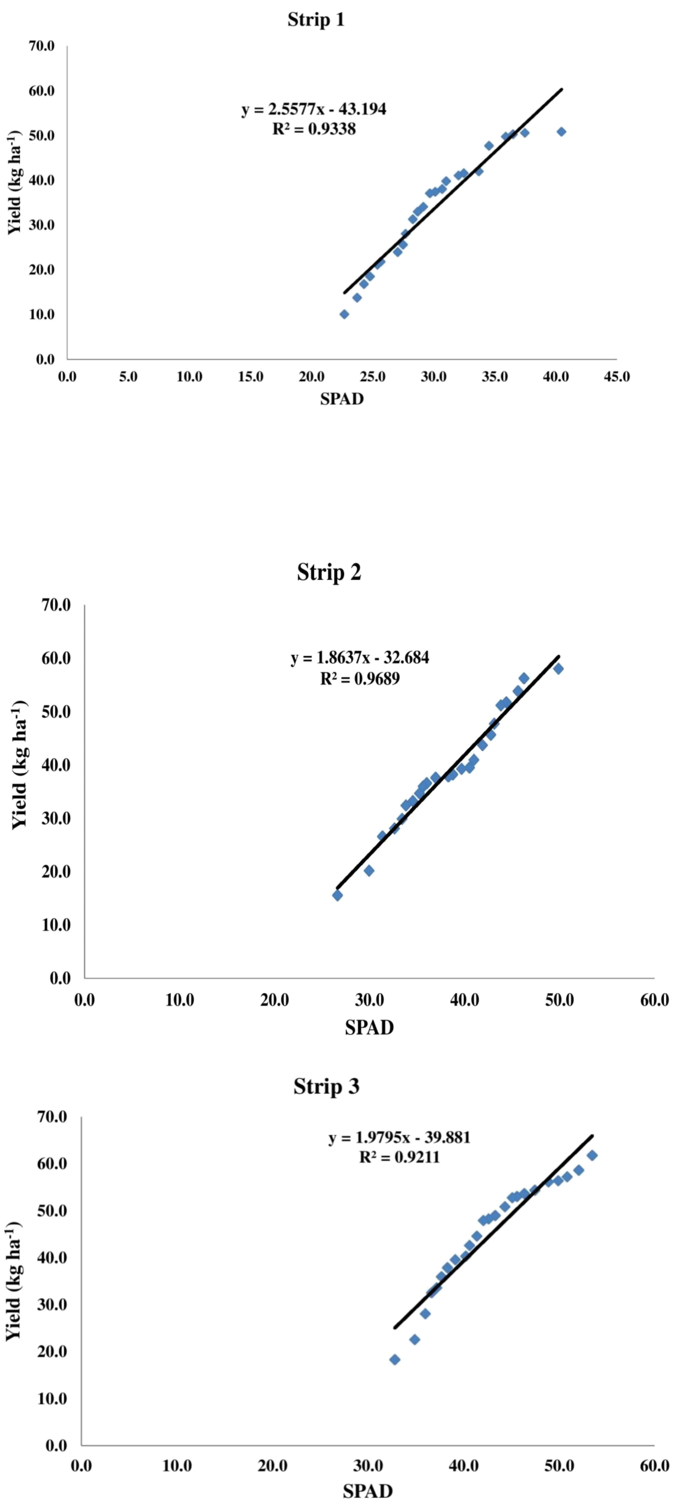

FIGURE 7
Linear regression of yield and chlorophyll content.

Santhi and her colleague formulated fertilizer prescription equations and recorded them for various crops such as rice (Santhi et al., 1999), beetroot (Santhi et al., 2011), aggregatum onion (Santhi et al., 2005), and sunflower across different regions of Tamil Nadu.

The nutrient amounts can be subtracted from the recommended fertilizer quantity based on specific soil analysis values and yield targets. Kaushik et al. (2015) also reported that applying 12.5 t ha^{-1} of farmyard manure along with chemical

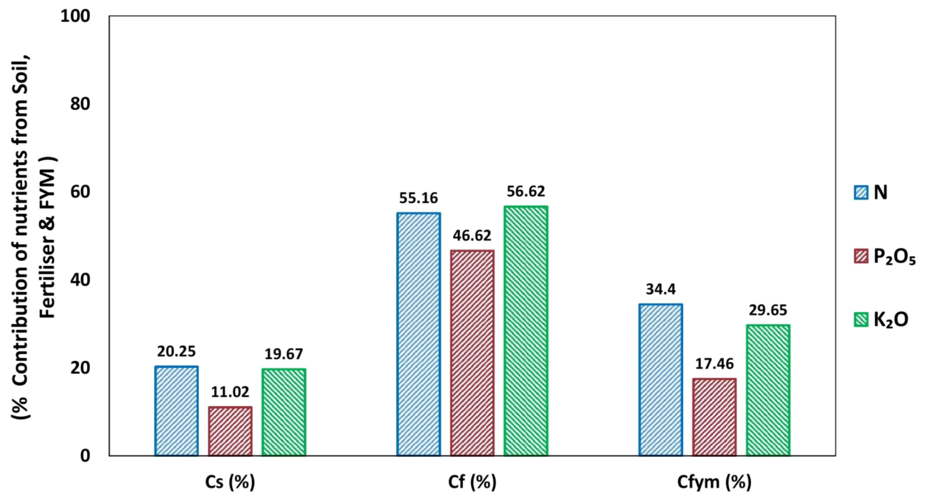

FIGURE 8
Contribution of Nutrient from Soil, Fertilizer and FYM(%).

fertilizer resulted in savings of 15 kg ha^{-1}of N, 1.8 kg ha^{-1}of P_2O_5, and 5 kg ha^{-1}of K_2O in radish. Comparatively, when inorganic fertilizer was applied alongside FYM, there was a significant reduction in fertilizer amounts compared to applying inorganic fertilizer alone, owing to the nutrient supplementation provided by FYM. There was an increasing percentage reduction in fertilizers when applied alongside FYM, with a corresponding increase in soil test values. Similar findings were reported by (Singh et al., 2018). Sellamuthu et al. (2019) also found that using 12.5 t ha^{-1} of farmyard manure in combination with chemical fertilizers saved 40 kg ha^{-1}of N, 20 kg ha^{-1}of P_2O_5, and 33 kg ha^{-1}of K_2O in big onion.

In contrast to STCR-NPK alone treatments with corresponding yield targets, STCR-IPNS treatments consistently exhibited higher yields, highlighting the beneficial synergy of combining inorganic fertilizers with organic manures. This combination demonstrated its superiority in enhancing crop productivity. The slow release of nutrient from FYM hindered its ability to sufficiently meet the essential nutrient needs during the crucial growth stages of the crop. The utilization of farmyard manure (FYM) in this context probably strengthened the nitrogen provision, thereby boosting beetroot production. Similar findings were reported by (Laharia et al., 2020; Zannat et al., 2020; Mohamed et al., 2023 and Anasuyamma et al., 2022).

Per cent achievement results suggest that utilizing IPNS for yield targeting consistently attained a greater percent of the desired target compared to employing inorganic alone treatments. This observation resonates with findings from a study conducted by (Dey and Bhogal, 2016; Santhi et al., 2017; Udayakumar and Santhi, 2016 for pearl millet; Abishek et al., 2022 on castor; Mohamed, 2023 for finger millet).

Benefit-Cost Ratio (BCR) of STCR- integrated (IPNS)was significantly greater than that of STCR-inorganic alone. The BCRs for the general fertilizer recommended dose (100% GFRD alone) and farmer's fertilizer practice were 2.35 and 1.74, respectively, which were lower than all soil analysis crop response treatments. The fluctuations in benefit-cost ratios (BCRs) were mainly attributed to differences in crop yields and varying expenses associated with the use of farm farmyard manure (FYM). It is evident that the prudent utilization of organic inputs, like on FYM, alongside synthetic fertilizers, results in a more profitable outcome. Similar results were reported by (Lakum et al., 2011; Choudhary et al., 2014; Sipai et al., 2014; Singh and Chauhan, 2016; Meena et al., 2017; Raghav et al., 2019).

5 Conclusions

Blanket recommendation of fertilizers to crops leads to either overuse or under use of fertilizers. Soil test and yield targeting based STCR-IPNS approach by inductive methodology demonstrated that the fertilizer prescription to beetroot, enhances the beetroot yield. It has been clarified that STCR- Integrated (IPNS)provides a well-proportioned supply, accounting contribution from farmyard manure, soil and fertilizer, to achieve desired yield aimed of beetroot. When a farmer applying 12.5 t ha^{-1} of FYM, they can reduce 37, 26 and 34 kg of Nitrogen (N), Phosphorus (P) and Potassium (K), respectively from the prescribed dose of inorganic fertilizers. Under conventional recommendation, along with FYM, mineral fertilizers are applied without considering other sources. Findings from these experiments revealed that there is a significant response by beetroot to N, P and K fertilizers. Nutrient prescription using STCR-IPNS approach is able to achieve 100.9% and 96.9% yield targets of 40 t ha^{-1} (40.36 t ha^{-1}) and 45 t ha^{-1} (43.60 t ha^{-1}) respectively. The percentage attainment of the desired yield was within a ±10% deviation at yield target, confirming the accuracy of the fertilizer prescription model for recommending combined fertilizer (inorganic, organic) doses for beetroot. Though availability of the FYM is reducing day by day, explicit adoption of STCR-IPNS model will encourage the farmers to produce FYM at farm level and use it for sustaining soil health with higher economic returns.

Data availability statement

The raw data supporting the conclusions of this article will be made available by the authors, without undue reservation.

Author contributions

AR: Writing – original draft. SK: Writing – review & editing. MS: Conceptualization, Writing – original draft. SA: Writing – review & editing. TS: Formal analysis, Writing – review & editing. MP: Investigation, Writing – review & editing. SG: Conceptualization, Writing – review & editing.

Funding

The author(s) declare financial support was received for the research, authorship, and/or publication of this article. The research was supported by ICAR-All India Co-ordinated Research Project on STCR.

Acknowledgments

The authors wish to thank Tamil Nadu Agricultural University for providing necessary support and facilities to perform this work.

Conflict of interest

The authors declare that the research was conducted in the absence of any commercial or financial relationships that could be construed as a potential conflict of interest.

Publisher's note

References

Abishek, R., Santhi, R., Maragatham, S., Gopalakrishnan, M., Venkatachalam, S., Uma, D., et al. (2022). Soil test crop response based integrated plant nutrition system for hybrid castor on an Alfisol. *Agric. Sci. Dig.* 44, 1–6. doi: 10.18805/ag.D-5635

Abishek, R., Santhi, R., S. Maragatham, S., Venkatachalam, S. R., Uma, D., and Lakshmanan, A. (2023). Response of hybrid castor under different fertility gradient: Correlation between castor yield and normalized difference vegetation index (NDVI) under inductive cum targeted yield model on an alfisol. *Commun. Soil Sci. Plan.* 54, 1816–1831. doi: 10.1080/00103624.2023.2211099

Anasuyamma, B., Singh, S., Asirinaidu, B., and Abhigna, K. (2022). Effect of organic manures and Inorganic fertilisers on the growth and yield of Blackgram (*Vignamungo* L.). *J. Pharm. Innov.* 11, 1214–1218.

Anil, K. S., Sobaran, S., Ajaya, S., and Poonam, G. (2008). Yield target approach under integrated nutrient management for assessing fertilizer requirements of onion in Mollisols of Uttarakhand. *Indian J. Hortic.* 65, 302–306.

Basavaraja, P. K., Narasimhareddy, P. N., Rajesh, N. L., and Apoorva, K. B. (2011). Development of fertilizer prescription targeted yield-equation for carrot crop based on soil test vales. *J. Hortic. Sci.* 6, 33–36. doi: 10.24154/jhs.v6i1.438

Bhavya, N., Krishna Murthy, R., Govinda, K., Uday Kumar, S. N., Basavaraj, P. K., Mohamed Saqeebulla, H., et al. (2023). Fertilizer prescription model through soil test crop response approach for carrot (*Daucuscarota*) on an Alisols of Southern India. *Theor. Biol. Forum* 12, 93–100.

Bray, R. H., and Kurtz, L. T. (1945). Determination of total organic and available forms of phosphorus in soils. *Soil Sci.* 59, 39–45. doi: 10.1097/00010694-194501000-00006

Choudhary, R., Yadav, L., Shivran, A., and Parihar, S. (2014). Effect of vermicompost and fertility levels on the growth, yield, nutrient uptake and net returns in pearl millet (Pennisetumglaucum). *Indian J. Agric. Sci.* 84, 1428–1430.

Dey, P., and Bhogal, H. (2016). *Progress Report, (2013-16) of the All India Coordinated research Project for Investigation on Soil Test Crop Response Correlation* (Bhopal: Indian Institute of Soil Science), 1–224.

Dhakal, D. D., Paneru, R. B., and Subedi, S. (2009). Effect of organic manure on growth, yield, and quality of spinach beet (Beta vulgaris l.). *J. Agric. Food Environ.* 10, 33–42.

Dhakal, Y., Meena, R. S., and Kumar, S. (2016). Effect of INM on nodulation, yield, quality and available nutrient balance in soil after harvest of green gram. *Legume Res.* 39, 590–594.

Dibyendu, C., Ajaya, S., and Singh, R. K. (2010). Fertilizer recommendations based on targeted yield concept involving integrated nutrient management for potato (*Solanumtuberosum*) in tarai belt of Uttarakhand. *Indian J. Agric. Sci.* 80, 38–43.

Draper, N. R., and Smith, H. (1998). *Applied Regression Analysis* (New York: Willy).

Gayathri, A., Vadivel, A., Santhi, R., MurugesaBoopathi, P., and Natesan, R. (2009). Soil test based fertilizer recommendation under integrated plant nutrient system for potato (*SolanumTuberosum.L*) in hilly tracts of Nilgiris District. *Indian J. Agric. Res.* 43, 52–56.

Humphries, E. C. (1956). Mineral components and ash analysis.Modern methods of plant analysis. *Springer-Verlag Berlin* 1, 468–562.

Jackson, M. L. (1973). *Soil chemical analysis* (New Delhi, India: Prentice Hall of India).

Kadam, V. D., Shinde, S. J., and Satav, D. C. (2018). Effect of different spacing and fertilizer levels on yield and economics of beetroot (Beta vulgaris l.). *J. Pharmacogn Phytochem.* 7 (6), 31–35.

KasthuriThilagam, V., and Natesan, R. (2009). Fertilizer prescription equations for desired yield targets of cauliflower under integrated plant nutrient system based on targeted yield model. *Agric. Sci. Dig.* 29, 250–253.

Kaushik, B., Dibyendu., S., and Biswapati, M. (2015). Fertilizer-prescription equations for targeted yield in radish under integrated nutrient management system. *J. Hortic. Sci.* 10, 18–23. doi: 10.24154/jhs.v10i1.148

Krishna Murthy, R., Basavaraja, P. K., Bhavya, N., Dey, P., Saqueebulla, H. M., Gangamurtha, G. V., et al. (2023). Development and validation of soil test based fertilizer prescription equations for enhancing yield, uptake and nutrient use efficiency of foxtail millet (Setariaitalica) under dryland condition. *J. Plant Nutr.* 7, 1–9.

Kumar, S., Baksh, H., Singh, R., Prajapati, N. K., and Kumar, A. (2023). Effect of integrated nutrient management on growth and yield of beetroot (Beta vulgaris l.) cv. ruby queen. *Int. J. Plant Soil Sci.* 35 (19), 816–824.

Laharia, G., Kadam, Y., Age, A. A., Jadhao, S., Mali, D., and Rakhonde, O. (2020). Interactive effect of biochar, fym and nitrogen on soil properties and yield of blackgram grown in vertisol. *J. Pharmacogn. Phytochem.* 9, 249–253.

Lakum, Y., Patel, S., and Mehta, P. (2011). Reducing fertilizer requirement with the use of bio-fertilizers in summer pearl millet [*Pennisetumglaucum* (L.). *Asian J. Soil Sci.* 6, 50–53.

MaruthiSankar, G. R. (1986). On screening of regression models for selection of optimal variable subsets. *J. Indian Soc. Agric. Stat* 38, 161–168.

Meena, R., Maurya, S., and Meena, R. (2017). Productivity, soil properties and economics of rainfed pearl millet as influenced by mulching and organic sources of nutrients.*Int. J. Curr. Microbiol. Appl. Sci.* 6, 566–574. doi: 10.20546/ijcmas.2017.602.064

Mohamed, A. B. (2023). Fertiliser prescription for finger millet through integrated plant nutrition system based on inductive cum targeted yield concept on alfisol. Ph.D. (Ag.) Thesis submitted to TNAU Coimbatore.

Mohamed, B. A., Santhi, R., Maragatham, S., Ravikesavan, R., Geetha, P., Gopalakrishnan, M., et al. (2023). Impact of soil fertility characteristics on artificial fertility gradient approach developed using sorghum (Sorghum bicolor) in Alfisols. *J. Appl. Nat. Sci.* 15, 793–801.

Mounika, V., Lakshminarayana, D., Srinivas, J., Sathish, G., and Gouthami, P. (2022). Influence of Integrated Nutrient Management in Beet Root (*Beta vulgaris* L.) Cv. Crimson Globe for Growth and Yield under Alkaline conditions. *Biol. Forum Int. J.* 14, 464–469.

Nagar, G., Abraham, T., and Kumar, D. (2016). Effect of tillage and Farm Yard Manure on growth and yield of soybean. *Adv. Res. J. Crop Improv.* 7, 56–59.

ParvathiSugumari, M., Maragatham, S., Santhi, R., and SwarnaPriya, R. (2021). Development of soil test crop response based fertilizer prescriptions through integrated plant nutrition system for aggregatum onion (*Allium cepa* L.) under drip fertigation. *J. Appl. Nat. Sci.* 13, 1094–11101.

Polara, K. B., Hadiyal, T. M., Babariya, N. B., Sakavadia, H. L., and Parmar, K. B. (2012). Soil test based fertilizer recommendation for onion (*Allium cepa*L.) in Saurashtra region of Gujarat. *Asian J. Soil Sci.* 7, 345–349.

Raghav, R. S., Singh, Y. V., Kumar, M., PradipDey,, and Dubey, S. (2019). STCR based nutrient management in soybean (Glycine max) for higher productivity and profitability. *Indian J. Agric. Sci.* 89, 1660–1663. doi: 10.56093/ijas.v89i10.94603

Ramamoorthy, B., Narasimham, R. L., and Dinesh, R. S. (1967). Fertilizer application for specific yield target of sonara64 wheat. *Indian Farming* 17, 43–45.

Rao, S., and Srivastava, S. (2000). Soil test based fertilizer use-A must for sustainable agriculture. *Fertil. News* 45, 25–38.

Santhi, R., Bhaskaran, A., and Natesan, R. (2011). Integrated Fertilizer Prescriptions for Beetroot through Inductive cum targeted Yield model on an Alfisol. *Commun. Soil Sci. Plant Anal.* 42, 1905–1912. doi: 10.1080/00103624.2011.591466

Santhi, R., Natesan, R., and Selvakumari, G. (2005). Effect of soil fertility and integrated plant nutrition system on yield, response and nutrient uptake by aggregatum onion. *Indian J. Agric. Res.* 39, 213–216.

Santhi, R., Sellamuthu, K. M., Maragatham, S., Natesan, R., Arulmozhiselvan, K., Kumar, K., et al. (2017). *Soil test and yield target based fertiliser prescriptions for crops-an overview of outreach activities in tribal villages of Tamil Nadu (in Tamil)* (Coimbatore: AICRP-STCR, Department of Soil Science and Agricultural Chemistry, Tamil Nadu Agricultural University), 641003.

Santhi, R., Selvakumari, G., and Perumal, R. (1999). Soil test-based fertilizer recommendation under integrated plant nutrition system for rice-rice-pulse cropping sequence. *J. Indian Soc Soil Sci.* 47, 288–294.

Sellamuthu, K. M., Santhi, R., Maragatham, S., and Dey, P. (2015). Balanced fertiliser prescription for glory lily through inductive cum targeted yield model on an Alfisol. *Res. Crops* 16, 555–561. doi: 10.5958/2348-7542.2015.00079.0

Sellamuthu, K. M., Santhi, R., Maragatham, S., and Dey, P. (2019). Balanced fertilizer prescription for big onion through inductive cum targeted yield model on an Alfisol. *Madras Agric. J.* 4, 10–12.

Singh, S., and Chauhan, S. (2016). Effect of integrated nutrient management on pearl millet crop grown in semi-arid climate. *Adv. J. Multidiscip.* 5, 54–57.

Singh, V. P., Gautam, P., Nanda, G., Dhaliwal, S. S., Pramanick, B., Meena, S. S., et al. (2021). Soil test based fertilizer application improves productivity, profitability and nutrient use efficiency of rice (Oryzasativa L.) under direct seeded condition. *Agronomy* 11, 1756–1769.

Singh, V. K., Gautam, P., Singh, S., Pareek, N., and V.P. Singh, V. P. (2020). Evalution of soil fertility gradient experiment on the basis of crop yield, Nutrient uptake and soil fertility. *Int. J. Curr. Microbiol. Appl. Sci.* 9, 2435–2440. doi: 10.20546/ijcmas.2020.902.278

Singh, D. P., Kumar, S., Sutanu, M., and Vijay, P. K. (2017). Studies on integrated nutrient management on growth, yield and quality of carrot (*Daucuscarota* L.). *Int. J. Agric. Sci.* 51, 2187–2188.

Singh, Y. V., Singh, P., and Pal, A. K. (2019). Fertilizer recommendation based on soil testing for the targeted yield of coriander (Coriandrumsativum L.) in an Inceptisol. *Ann. Plant Soil Res.* 21, 356–360.

Singh, Y. V., Singh, S. K., Srivastava, D. K., Singh, P., and Jatav, H. S. (2018). Fertilizer dose recommendation through soil test crop response study with integrated plant nutrient management system for fennel in an Inceptisol. *Int. J. Seed Spices* 8, 36–41.

Sipai, A., Jat, J., Nakrani, B., and Gadhavi, S. (2014). Integrated nutrient management in bajra. *Asian J. Soil Sci.* 9, 155–157.

Smitha John, K. (2004). Soil test crop response correlation studies under integrated plant nutrition system for cabbage (Brassica oleracea l. var capitata) on inceptisols. M.Sc. (Ag.) thesis Tamil Nadu Agric. University India.

Stanford, S., and English, L. (1949). Use of flame photometer in rapid soil tests of K and Ca. *Agron. J.* 41, 446. doi: 10.2134/agronj1949.00021962004100090012x

Subbiah, B. V., and Asija, G. L. (1956). A rapid procedure for determination of available nitrogen in soil. *Curr. Sci.* 25, 259–260.

Tovihoudji, G. P., Djogbenou, C. P., Akponikpe, P. B. I., Kpadonou, E., Agbanga, C. E., and Dagbenonbakin, D. G. (2015). Response of jute mallow (*Corchorusolitorius* L.) to organic manure and inorganic fertilizer on a ferruginous soil in North Eastern Benin. *J. Appl. Biosci.* 92, 8610–8861. doi: 10.4314/jab.v92i1.5

Udayakumar, S., and Santhi, R. (2016). Effect of integrated plant nutrition system (IPNS) and initial soil fertility on yield and NPK uptake by pearl millet on Inceptisol. *Int. J. Agric. Sci.* 8, 3020–3024.

Udayakumar, S., and Santhi, R. (2017). Impact of artificial soil fertility gradient strategy on soil fertility, nutrient uptake and fodder yield of sorghum. *Int. J. Curr. Microbiol. App. Sci.* 6, 938–944. doi: 10.20546/ijcmas.2017.603.111

Umadevi, R. (2005). Soil test crop response correlation studies under integrated plant nutrition system for Carrot on Alfisols. M.Sc. (Ag.) thesis. TNAU, Tamil Nadu, India.

Vamshi, M., Maragatham, S., Santhi, R., Kalarani, M. K., Sankari, A., Goplakrishnan, M., et al. (2023). Evaluation on the development of soil fertility gradient with nutrient exhaustive crop (Sorghum bicolor) regard to N,P, and K in Inceptisols in semi-arid regions of tamilnadu. *J. Appl. Nat. Sci.* 15, 1061–1070. doi: 10.31018/jans.v15i3.4788

Velayutham, M., Reddy, K. C. K., and MaruthiSankar, G. R. (1985). All India Co-ordinated Research Project on Soil Test Crop Response correlation and its impact on agricultural production. Fert. News 30(4), 81–95.

Verma, M., Singh, Y. V., Ajay, B., Sudhanshu, V., Meena, R., and Sahi, S. K. (2014). Soil test crop response based gradient experiment on rice (Oryzasativa L.) to fertilisers in the alluvial soil. *Indian J. Agric. Allied Sci.* 1, 51–53.

Waugh, D. L., and Fitts, J. W. (1966). *Soil test interpretation studies: Laboratory and potted plant* Vol. 3 (North Carolina State University Agricultural Experiment Station).

Wold, S., Esbensen, K., and Geladi, P. (1987). Principal component analysis. *Chemometrics Intelligent Lab. Syst.* 2, 37–52. doi: 10.1016/0169-7439(87)80084-9

Zannat, N. E. A., Sultana, A. K. M., Amin, R., Ruhul, P., Bithy, C. P., and Alam, I. (2020). Influence of organic and inorganic fertilizers on the yield of blackgram. *Int. J. Biosci.* 16, 79–89.